

Variations in climatic conditions from the Cayman Islands through stable isotope and element analyses from corals and sediment cores; a 500,000 year record

by

Simone Booker

A thesis submitted in partial fulfillment of the requirements for the degree of

Doctor of Philosophy

Department of Earth and Atmospheric Sciences

University of Alberta

© **Simone Booker**, 2020

## ABSTRACT

The Caribbean region is particularly important to understanding global climate change and feedback systems because the tropics are the primary source of heat and water vapor for the atmosphere. The Caribbean region, however, is a relatively understudied area in terms of tracking climate change through time. The Cayman Islands, specifically, have little documentation of climate change before the 1980's, apart from anecdotal records of past storms. Climate change has been increasingly studied in recent years due to the current and proposed future impacts of such changes on global environments. Numerous proxies ( $\delta^{18}\text{O}$ ,  $\delta^{13}\text{C}$ , Sr/Ca, Mg/Ca, U/Ca, Sr-U, Li/Ca, Li/Mg, Mg/Li, Ba/Ca,  $\text{B}^{11}/\text{Ca}$ , trace and rare earth elements) for past environmental conditions (sea surface temperature (SST), salinity, photosynthetic light activity, water depth, upwelling, riverine run-off, atmospheric moisture variability) have been developed for use with coral skeletons and sediment cores. The application of these proxies, however, is complicated as many factors that may control the incorporation of these proxies into the geologic records (vital effects, geographic location, sampling analytics) are still debated. Interpretations based on geochemical proxies (stable isotope, element/Ca ratios, and elemental concentrations) derived from sediment cores and modern and fossil corals (*Orbicella annularis* and *Montastrea cavernosa*) from the Cayman Islands over the last 500,000 years record alternating cool (SST < 28.5°C; current average water temperature for Grand Cayman) and warm (SST > 28.5°C) periods in the Caribbean Sea.

Coral skeletons from Grand Cayman and Cayman Brac are the baseline for the development of an oxygen isotope geothermometer that accurately reconstructs SST within the range of measured Caribbean water temperatures. Using this  $\delta^{18}\text{O}$ -geothermometer, these coral skeletons record two cool periods, one warm period, and one mild period over the last ~540 years around the Cayman Islands. These temperature periods correlate with climate change in the wider Caribbean region. Oxygen isotopes compositions and elemental concentrations from sediment cores in North Sound,

Grand Cayman's largest lagoon, record five periods of climate (SST and atmospheric moisture variability) change over the last ~6000 years. These climate periods correlate to phases of climatic variability in the Caribbean and at higher latitudes in the Northern Hemisphere. The global nature of these climate periods can be related to the movements of the Intertropical Convergence Zone and the phase of the North Atlantic Oscillation.

Although it has been shown that modern corals can reliably reconstruct SST, application to older corals is more complicated. Determination of SST from older corals is only possible if their aragonitic skeletons have undergone little to no diagenetic alteration. For corals from the Pleistocene Ironshore Formation (Units A-F; 80 to 500 ka), SST calculations are only viable if the coral skeleton has >95wt% aragonite, no cements, Mg/Ca ratios <12.0 mmol/mol, Sr/Ca ratios >8.0 mmol/mol,  $\delta^{18}\text{O}_{\text{VSMOW}}$  values >25.1‰, and  $\delta^{13}\text{C}_{\text{VPDB}}$  values >-3.0‰. Based on these criteria the corals from Units A-C (229 to 500 ka) cannot be used, whereas those from Units D-F (125 to 80 ka) produce reliable SST records. The temperature profiles developed from Units D-F correlate with temperature reconstructions from other localities during the Pleistocene (e.g., the Caribbean, North Atlantic, Coral Sea, South China Sea, and Antarctica). This work is significant as tracking changes in climate from the past may provide indicators for future climate trends.

## PREFACE

This thesis is the original work completed by Simone Booker, with the assistance of Dr. Brian Jones. The overall theme of this thesis was initially outlined by Dr. Jones and then developed through discussions between the two of us. Chapters three and five of this thesis were published as the following two papers:

Booker, S., Jones, B., Chacko, T., Li, L., 2019. Insights into sea surface temperatures from the Cayman Islands from corals over the last ~540 years. *Sedimentary Geology*, 389, 218-240.

The samples and measured water temperature data for this paper came from the Department of Environment, Cayman Islands. For this paper, I undertook the data analysis and produced the initial drafts of the manuscript, which were extensively edited by Dr. Jones. Co-authors provided valuable feed-back throughout the preparation of this manuscript.

Booker, S., Jones, B., Li, L., 2020. Diagenesis in Pleistocene corals (80 to 500 ka) corals from the Ironshore Formation: implications for paleoclimate reconstructions. *Sedimentary Geology*, 399.

This paper was based on samples collected by Dr. Jones over the last 30 years. I performed the data analysis and produced the initial drafts of the manuscript, which were extensively edited by Dr. Jones. The co-author provided valuable feed-back throughout the preparation of this manuscript.

Chapter two: Assessing the applicability of nine element/Ca proxies for paleotemperature reconstructions using modern tropical corals: insights into the future of element/Ca geothermometry.

The samples and measured water temperature data used in this chapter came from the Department of Environment, Cayman Islands. For this paper, I undertook the data analysis and produced the initial drafts of the manuscript, which were extensively edited by Dr. Jones.

Chapter four: A 6000 year record of change from stable isotopes and rare earth elements from sediment cores from North Sound lagoon, Grand Cayman, B.W.I.

The samples used in this chapter were collected by Dr. Jones in the 1980's. I performed the data analysis and produced the initial drafts of the manuscript, which were edited by Dr. Jones.

All papers reflect the fact that all authors were actively involved in their development and writing.

## ACKNOWLEDGEMENTS

There are many people I would like to thank for helping and supporting me throughout this thesis research.

I am grateful to my supervisor Dr. Brian Jones for his advice, encouragement, constructive criticism, patience, innumerable hours of editing, allowing me to go on many trips to expand my scientific knowledge, and for helping me build up my rhinoceros' skin. Without his help I would not have been able to complete this thesis!

As well as T. Austin and G. Ebanks-Petrie, the Department of Environment, Cayman Islands who collected the corals that were used in this study and imported them to the University of Alberta with a CITES Export Permit; The Water Authority and Department of Environment of the Cayman Islands, who provided and gave permission to use the water temperature data from Grand Cayman.

I would also like to thank Dr. Long Li for providing his laboratory for the stable isotope analyses, Dr. Thomas Chacko for his help in developing the oxygen-isotope geothermometer used in this study, Drs. Duane Froese and Dr. Alberto Reyes for help interpreting the carbon-14 dates used in this study, Dr. Murray Gingras for providing his X-Ray machine, Dr. Andy DuFrane and Mr. Guangecheng Chen for providing the laboratory and running the ICP-MS analyses, Dr. Nathan Gerein, who took the SEM photomicrographs, Mrs. Diana Caird, who ran the XRD analyses, Mr. Mark Labbe for cutting the coral specimens, Mr. Mark van Dollen and Mr. Walter Harley for making the thin sections, Ms. Kathrine Snihur who did the element water analyses, and Mrs. Shanna Cameron, Innotech Alberta, who operated the CT scanner used in this study.

Thanks must also be given to the Natural Science Sciences and Engineering Research Council of Canada (Grant A635 to Jones) for providing the funding for this research.

Lastly, I would like to thank my family for the constant support and encouragement over the course of my project!

## TABLE OF CONTENTS

<b>CHAPTER 1: INTRODUCTION</b>	<b>1</b>
1. Introduction	1
2. Study area and methods	6
2.1. Study area	6
2.2. Samples	11
2.3. Methods	11
2.3.1. Coral samples	11
2.3.2. Sediment cores	12
2.3.3. Water samples	13
3. Previous work	14
3.1. Geochemical proxies	14
3.2. Corals	15
3.3. Sediment cores	16
3.4. Ironshore Formation	17
4. Objectives	18
References	20
<b>CHAPTER 2: REVIEW OF ELEMENT/CA PROXIES FOR DERIVING PALEOTEMPERATURES FROM MODERN TROPICAL CORALS: INSIGHTS INTO THE FUTURE OF ELEMENT/CA GEOTHERMOMETRY</b>	<b>30</b>
1. Introduction	30
2. Datasets	32
3. Element/Ca geothermometers	34

3.1. Sr/Ca ratios	35
3.2. Mg/Ca ratios	36
3.3. U/Ca ratios	37
3.4. Sr-U	38
3.5. Li/Ca ratios	39
3.6. Li/Mg and Mg/Li ratios	40
3.7. Ba/Ca ratios	40
3.8. B <sup>11</sup> /Ca ratios	42
4. Vital effects	42
4.1. Interspecies and intraspecies differences	43
4.2. Size, age, and growth rate	44
4.3. Corals microstructure	46
4.4. Rayleigh fractionation	47
4.5. Temporal change in vital effects	48
5. Geographic variability	49
6. Sampling analytics	50
6.1. Instrument measured water temperatures	50
6.2. Methodology	50
7. Calculated water temperature	55
7.1. Sr/Ca geothermometry	55
7.2. Mg/Ca geothermometry	55
7.3. U/Ca geothermometry	59
7.4. Sr-U geothermometry	59
7.5. Li/Ca geothermometry	61
7.6. Li/Mg and Mg/Li geothermometry	61
7.7. Ba/Ca geothermometry	62
7.8. B <sup>11</sup> /Ca geothermometry	62
8. Cayman coral temperature reconstruction	62
8.1. Sr/Ca geothermometry	64



8.2. Mg/Ca geothermometry	64
8.3. U/Ca geothermometry	64
8.4. Sr-U geothermometry	67
8.5. Li based geothermometry	67
8.6. B <sup>11</sup> /Ca geothermometry	68
8.7. The ‘best’ equation	68
9. Discussion	69
10. Conclusions	72
References	74

**CHAPTER 3: INSIGHTS INTO SEA SURFACE TEMPERATURES FROM THE  
CAYMAN ISLANDS FROM CORALS OVER THE LAST ~540  
YEARS 98**

1. Introduction	98
2. Terminology	99
3. Geographic setting	101
4. Samples	103
5. Methodology	104
5.1. Mineralogy determination	104
5.1.1. X-Ray Diffraction (XRD)	104
5.1.2. Thin section analysis	104
5.1.3. Scanning Electron Microscopy (SEM)	104
5.2. Age determination	105
5.3. X-Ray images	105
5.4. Computer Tomography (CT) scan production and analysis	106
5.5. Elemental analysis	106
5.6. Stable C and O isotope analysis	111
5.7. Water temperature and isotopic composition	112

6. Results	113
6.1. Mineralogy	113
6.2. Growth patterns- grey values	113
6.3. Coral ages	117
6.3.1. Carbon-14 dating and U/Th dating	117
6.3.2. Correlation to calendar years	124
6.3.3. Growth bands	124
6.3.4. Growth rate	124
6.4. Water isotope compositions	125
6.5. Derivation of $\delta^{18}\text{O}_{\text{water}}$ from elemental concentrations	125
6.5.1. Elemental analyses	125
6.5.2. Sr/Ca equation	125
6.5.3. $\delta^{18}\text{O}_{\text{water}}$ determination	127
6.6. Stable isotope compositions	128
7. Interpretations	128
7.1. Coral age	128
7.2. Growth band thickness	131
7.3. Geochemistry	132
7.3.1. Rates of growth	132
7.3.2. Conversion of $\delta^{18}\text{O}_{\text{coral}}$ values to temperature	135
7.3.3. Calculated temperatures and trends through time	139
8. Discussion	143
9. Conclusions	147
References	149

**CHAPTER 4: A 6000-YEAR RECORD OF CLIMATE CHANGE FROM STABLE  
ISOTOPE AND RARE EARTH ELEMENT ANALYSES OF  
SEDIMENT CORES FROM NORTH SOUND LAGOON, GRAND  
CAYMAN, BRITISH WEST INDIES**

1. Introduction	166
2. Geographic setting	167
3. Samples	170
4. Methodology	170
4.1. X-Ray Diffraction (XRD)	170
4.2. Age dating	172
4.2.1. $^{14}\text{C}$ dating	172
4.2.2. Age-depth model	172
4.3. Elemental analysis	174
4.4. Seawater analysis	175
4.5. Sediment and foraminifera stable isotope analysis	176
5. Results	177
5.1. Facies	177
5.2. Mineralogy	177
5.3. Dating	183
5.4. Elemental concentrations	185
5.5. Seawater analysis	195
5.6. Stable isotopes	197
6. Interpretations	197
6.1. Facies	197
6.2. Element distributions	200
6.3. Geothermometers for calculating SST	202
6.3.1. Sr/Ca equations	204
6.3.2. Mg/Ca equations	204
6.3.3. $\delta^{18}\text{O}$ equations	206
7. Discussion	208
7.1. Climate change over the last ~6000 years	208
7.2. Atmospheric moisture and SST in North Sound	212

7.3. Caribbean correlations	216
7.4. Global correlations	221
8. Conclusions	225
References	227

**CHAPTER 5: DIAGENESIS IN PLEISTOCENE (80 TO 500 KA) CORALS FROM  
THE IRONSHORE FORMATION: IMPLICATIONS FOR  
PALEOCLIMATE RECONSTRUCTION** **241**

1. Introduction	241
2. Geographic setting	246
3. Samples	247
4. Methodology	247
4.1. X-ray and computer tomography scan production and analysis	247
4.2. Mineralogy determination	252
4.2.1. X-ray diffraction	252
4.2.2. Thin section analyses	252
4.2.3. Scanning electron microscopy	252
4.3. Elemental analysis	252
4.4. Stable isotope analysis	253
5. Results	255
5.1. Indication of diagenetic change	255
5.1.1. Mineral composition	255
5.1.2. Petrographic analyses	255
5.2. Elemental concentrations	257
5.3. Stable isotopes	261
6. Discussion	261
6.1. Diagenesis	261

6.2. Paleoclimate applications	269
6.2.1. Pleistocene paleotemperatures	273
7. Conclusions	277
References	279
<b>CHAPTER 6: CONCLUSIONS</b>	<b>287</b>
References	292
<b>REFERENCES</b>	<b>293</b>
<b>APPENDICES</b>	<b>348</b>
Supplementary Table 2.1	349
Supplementary Table 2.2	366
Supplementary Table 2.3	368
Supplementary Table 2.4	370
Supplementary Table 2.5	371
Supplementary Table 2.6	372
Supplementary Table 2.7	373
Supplementary Table 2.8	374
Supplementary Table 3.1	375
Supplementary Table 3.2	378
Supplementary Table 3.3	383
Supplementary Table 3.4	388
Supplementary Table 3.5	392
Supplementary Table 3.6	400
Supplementary Table 3.7	406
Supplementary Table 3.8	410
Supplementary Table 4.1	411
Supplementary Table 4.2	412

Supplementary Table 4.3	421
Supplementary Table 5.1	426
Supplementary Table 5.2	434
Supplementary Table 5.3	438

**LIST OF TABLES**

Table 2.1	44
Table 3.1	107
Table 3.2	120
Table 3.3	121
Table 3.4	122
Table 3.5	129
Table 4.1	173
Table 4.2	178
Table 4.3	187
Table 4.4	191
Table 4.5	196
Table 4.6	199
Table 5.1	246
Table 5.2	248
Table 5.3	256

**LIST OF FIGURES**

Fig. 1.1	2
Fig. 1.2	4
Fig. 1.3	5
Fig. 1.4	8
Fig. 1.5	9
Fig. 1.6	10
Fig. 2.1	34
Fig. 2.2	56
Fig. 2.3	58
Fig. 2.4	60
Fig. 2.5	63
Fig. 2.6	65
Fig. 2.7	66
Fig. 3.1	100
Fig. 3.2	102
Fig. 3.3	114
Fig. 3.4	116
Fig. 3.5	118
Fig. 3.6	119
Fig. 3.7	123
Fig. 3.8	130
Fig. 3.9	133
Fig. 3.10	134
Fig. 3.11	136
Fig. 3.12	140
Fig. 3.13	141
Fig. 3.14	142



Fig. 3.15	145
Fig. 4.1	168
Fig. 4.2	169
Fig. 4.3	171
Fig. 4.4	182
Fig. 4.5	184
Fig. 4.6	186
Fig. 4.7	190
Fig. 4.8	198
Fig. 4.9	203
Fig. 4.10	205
Fig. 4.11	206
Fig. 4.12	207
Fig. 4.13	211
Fig. 4.14	213
Fig. 4.15	217
Fig. 4.16	219
Fig. 4.17	223
Fig. 5.1	243
Fig. 5.2	244
Fig. 5.3	257
Fig. 5.4	258
Fig. 5.5	260
Fig. 5.6	262
Fig. 5.7	264
Fig. 5.8	265
Fig. 5.9	267
Fig. 5.10	270
Fig. 5.11	272

Fig. 5.12

275

Fig. 5.13

276

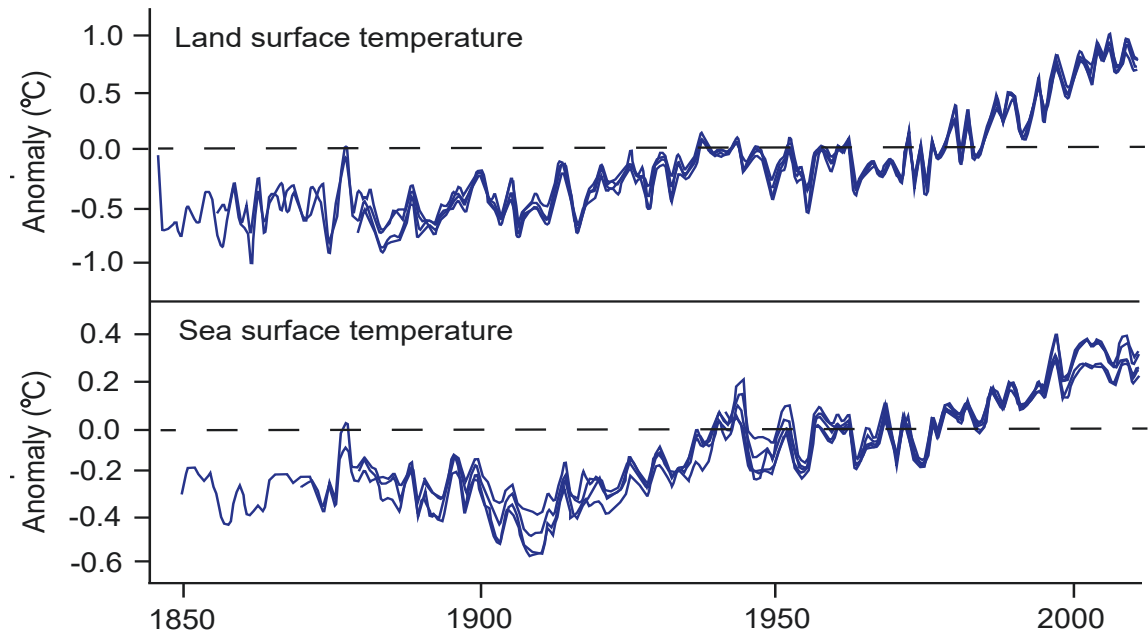
## CHAPTER 1

### INTRODUCTION

#### 1. Introduction

Climate change has been the focus of considerable research in recent years due to the current and proposed impacts of these changes on global environments. The last three decades have been successively warmer at the Earth's surface than during any preceding decade since 1850 (Fig. 1.1; Intergovernmental Panel on Climate Change (IPCC), 2014). Recently, numerous locations globally have experienced extreme climate phenomenon such as heat waves (western/central Europe, India, and Pakistan 2019), droughts (Zimbabwe, Somaliland 2019), floods (Midwestern USA, India 2019), cyclones (North India 2019, Bay of Bengal and Australia 2018, Central America, Eastern USA, Eastern Canada 2018), and wildfires (Northern Alberta 2019, 2016, California 2018, Australia 2018, 2019, 2020). With the IPCC Fifth Assessment Report concluding that, since the 1950's, many of the observed changes in the climate system have been unprecedented over decadal to millennial time scales, with the atmosphere and oceans having warmed, the amount of snow and ice diminished, and a global rise in sea level. The oceans are particularly vulnerable to increased warming, as 90% of global energy storage accumulates in these environments (IPCC, 2014). There is, therefore, increased focus from the scientific community on the impact of climate change, the causes, and possible remediation tools (Hasen et al., 2018; IPCC, 2018).

In order to better understand the future impacts of climate change, known intervals of climatic instability over the last 200,000 years have been investigated using environmental proxies derived from sediment cores (e.g., Hodell et al., 1991; Gregory et al., 2015), speleothems (e.g., Fensterer et al., 2012; Arienzo et al., 2015a), ice cores (e.g., Fegyveresi et al., 2016), and modern and fossil corals (e.g., Winter et al., 2003; Kuffner et al., 2017; Flannery et al., 2018). Such data have, for example, provided information



Anomalies are relative to 1986-2005 period

**Fig. 1.1.** (A) Land surface and (B) sea surface temperature anomalies from 1850 to 2010.

Anomalies are relative to the period 1986-2005. Blue lines were taken from IPCC (2014).

on past Sea Surface Temperature (SST), sea surface salinity (SSS), sea level rise or upwelling, amounts of precipitation/evaporation, the occurrence of El Niño/Southern Oscillation events, and the movement of regional water-air masses (i.e., Western Pacific Warm Pool, Intertropical Convergence Zone, the North American Oscillation; Kilbourne et al., 2007; Flannery et al., 2018).

Geochemical proxies within coral skeletons have become a powerful tool for paleoclimate determinations with the potential to provide a decadal to centennial scale high-resolution record of many aspects of climate. These samples, however, can only be used if their skeletons have not been altered by diagenesis. As such, few studies have analyzed corals that grew more than 20,000 years ago (e.g., Guilderson et al., 1994;

McCulloch et al., 1999; Gagan et al., 2000; Winter et al., 2003; Felis et al., 2015; Brocas et al., 2016). Nevertheless, isotopic and elemental proxies ( $\delta^{18}\text{O}$ ,  $\delta^{13}\text{C}$ , Sr/Ca, Mg/Ca, U/Ca, Sr-U, Ba/Ca, Li/Ca, Li/Mg, Mg/Li, B<sup>11</sup>/Ca) from coral skeletons have been used to gain insight into past SST, SSS, photosynthetic activity of the symbiotic zooxanthellae that live in the coral tissues, sun light availability, nutrient level, water depth, metabolic processes, precipitation, riverine input, and upwelling.

In this study, corals and sediment cores from the Cayman Islands have been used to establish changes in SST over the last 125,000 years. The Caribbean is a relatively understudied region, especially when compared to the tropical Pacific (e.g., Gagan et al., 2000) or higher latitude locations. Given that paleoclimate research in the Caribbean has primarily focused on the northern Caribbean-Gulf of Mexico area and the west-southwestern regions of the Caribbean Sea (Fig. 1.2), there is a lack of paleoclimate information from the central part of the Caribbean Sea, where the Cayman Islands are located (Fig. 1.3). Even though there are few Caribbean studies, the climatic interpretations from this region are highly variable (Goreau et al., 1992; Frich et al., 2002; Black et al., 2004; Hetzinger et al., 2010; Kuffner et al., 2015), therefore, highlighting the need for more high resolution climate reconstructions in the Caribbean. As such the Cayman Islands provide a unique opportunity for paleoclimate reconstructions because they are (1) located in the central Caribbean, a relatively understudied region where little paleoclimate work has been produced, (2) are not affected by riverine input, and (3) have prolific coral growth, both today and during the Pleistocene.

The general theme of this thesis is climate, specifically how has SST and atmospheric moisture around the Cayman Islands changed through time as recorded in coral skeletons and sediment cores. In order to answer this question, the methods commonly used for paleoclimate research in corals need to be thoroughly assessed. The calibrations used to determine past SST (i.e., the geothermometric equations that convert geochemical proxies such as isotopic and element/Ca ratios to temperature), and the

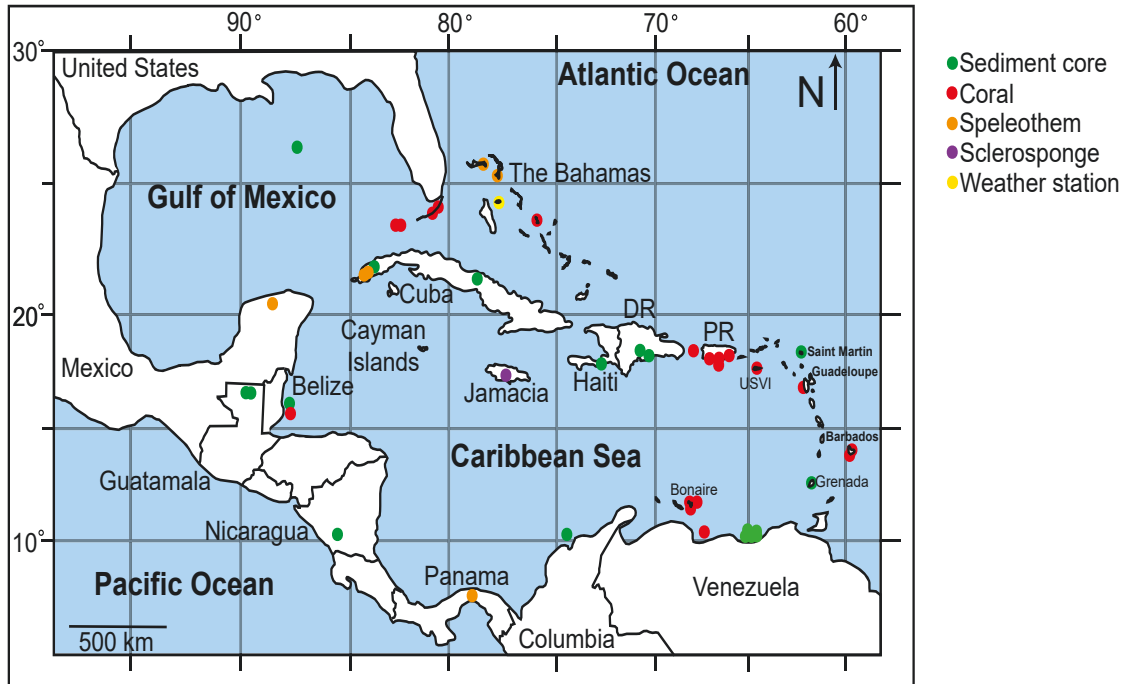


**Fig. 1.2.** Map of the Caribbean-Gulf of Mexico region showing the distribution of temperature related studies using proxies and instrument measured data.

procedure for determining the presence of diagenetic alteration are evaluated. This study is unique in terms of paleoclimate research using corals and sediment cores because it:

- Utilizes numerous well-preserved coral specimens, which is rare as many coral reefs are currently experiencing elevated levels of bleaching due to increased stress from high SST, ocean acidification, and pollution. As such, many locations that have coral reefs, like the Cayman Islands, are highly protected, and sampling of corals has become extremely regulated.
- Examines an extended time period (modern to Pleistocene), in order to determine a baseline temperature for the Cayman Islands today that can be compared to mid to late Holocene and Pleistocene climate.
- A diagenetic framework is developed for determining if a fossil coral can be used for paleoclimate reconstruction.

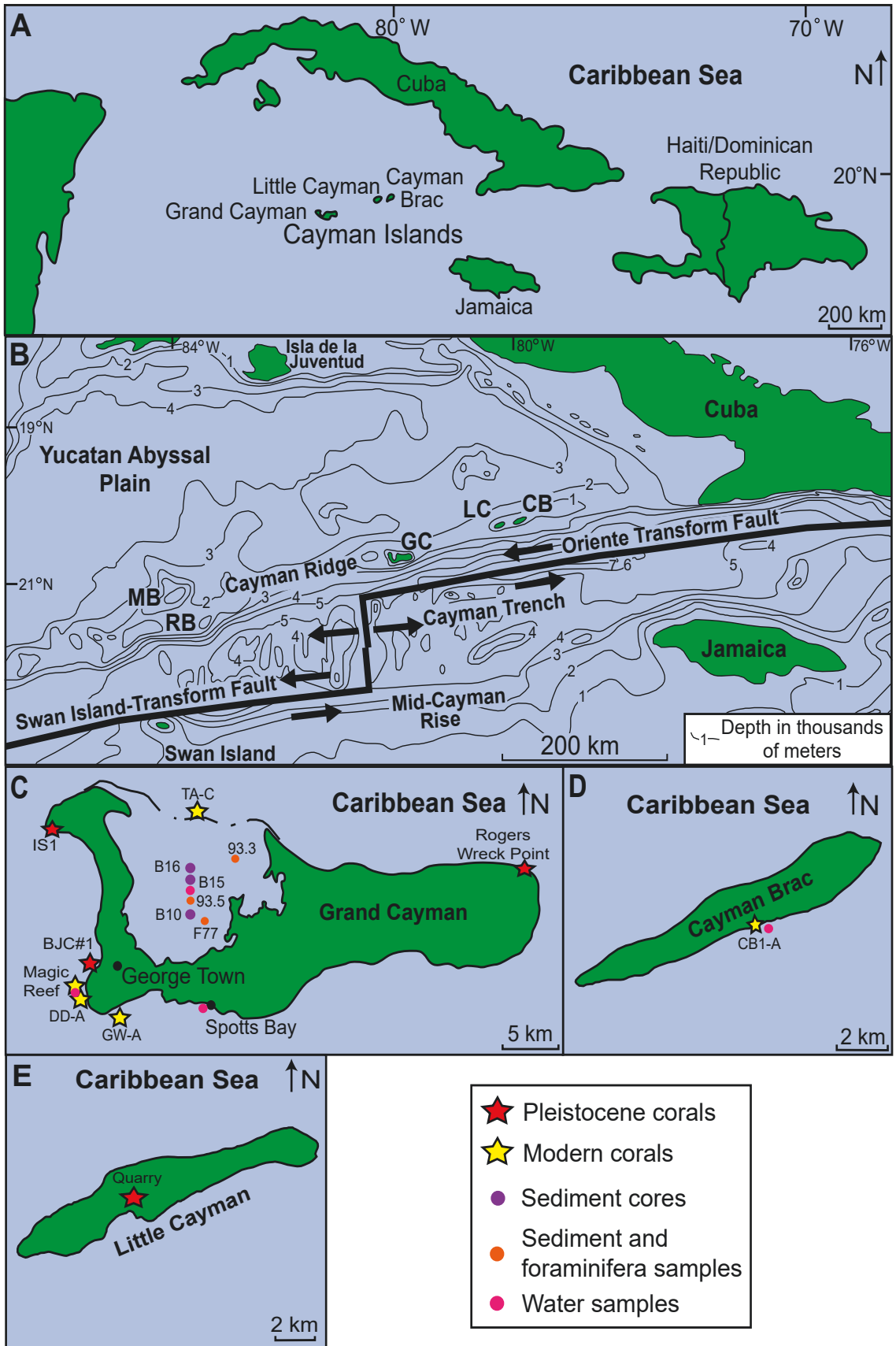


**Fig. 1.3.** Map of the study area. (A) Map of the Caribbean Sea, showing the location of the Cayman Islands. (B) Tectonic and bathymetric setting of the Cayman Islands (Grand Cayman (GC), Cayman Brac (CB), Little Cayman (LC)) on the Cayman Ridge. MB- Mysteriosa Bank, RB- Rosario Bank (modified from Jones, 1994 and based on maps from MacDonald and Holcombe, 1978 and Perfit and Heezen, 1978). (C) Map of Grand Cayman showing the location of coral specimens, sediment cores, surface sediment and foraminifera samples, and water samples used in this study. (D) Map of Cayman Brac showing the location of coral and water samples used in this study. (E) Map of Little Cayman showing the location of coral samples used in this study.

---

## 2. Study area and methods

### 2.1. Study area

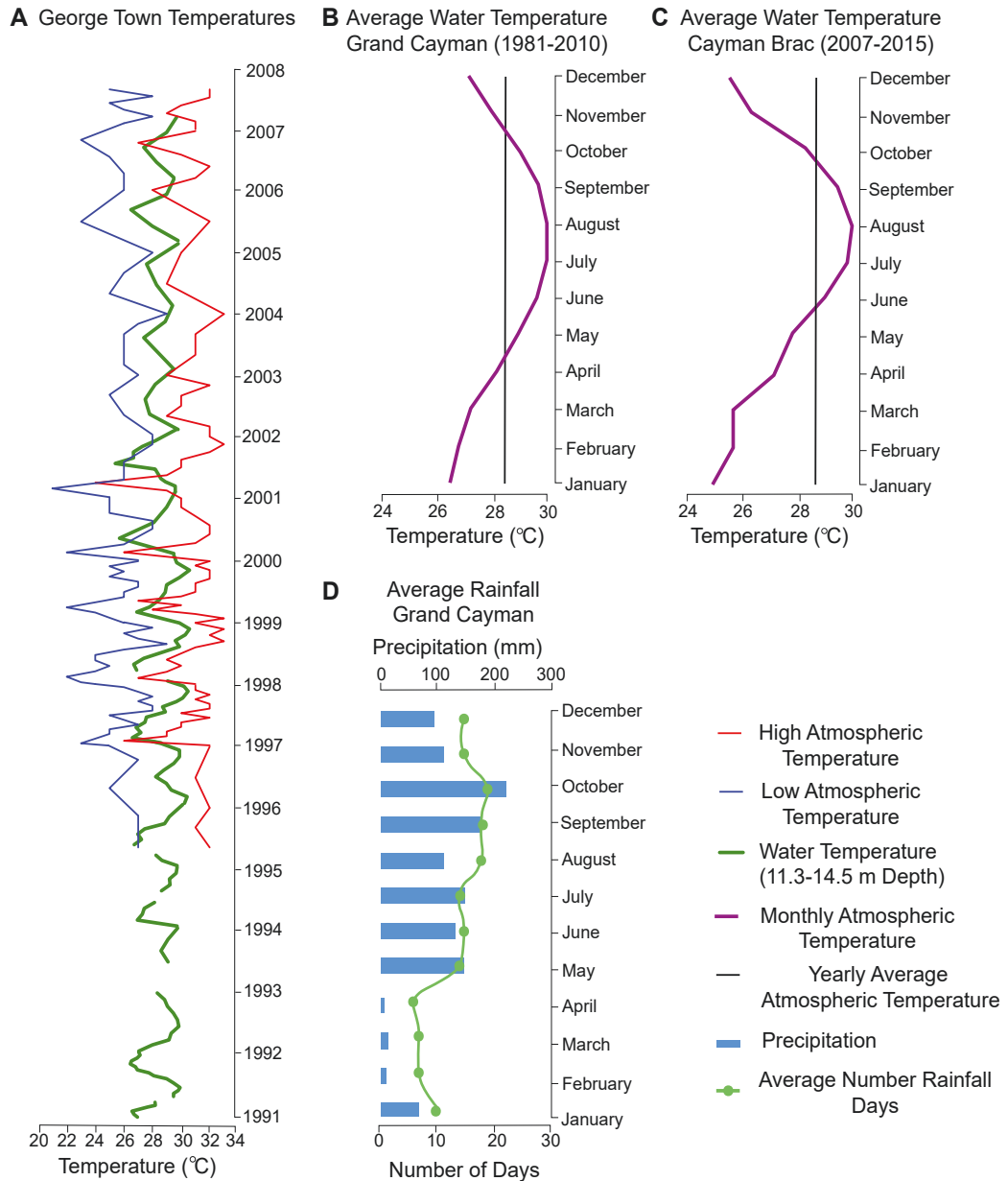
The Cayman Islands, which includes Grand Cayman, Cayman Brac, and Little Cayman, are located in the Caribbean Sea, 240 km south of Cuba and 280 km northwest of Jamaica (Fig. 1.3A). These islands are high points on the Cayman Ridge, a submarine mountain range that extends from the Sierra Maestra Range of Cuba to the base of the British Honduras Continental Slope (Fahlquist and Davies, 1971; Perfit and Heezen, 1978; Fig. 1.3B). The Cayman Ridge marks the southern boundary of the North American Plate and the northern boundary of the Cayman Trench. The Cayman Trench and the associated left lateral Oriente and Swan Island Transform Faults, which began developing during the Early Tertiary, were formed by the eastward movement of the Caribbean Plate relative to the North American Plate (Perfit and Heezen, 1978).

Grand Cayman, the largest of the Cayman Islands, is ~35 km long and 6 to 14 km wide with an area of 196 km<sup>2</sup> and an elevation of up to 24 m above sea level (m asl), but most of Grand Cayman is less than 3 m asl (Fig. 1.3C). Cayman Brac, ~145 km north-east of Grand Cayman, is ~19 km long and 2 km wide with an area of 32 km<sup>2</sup> and an

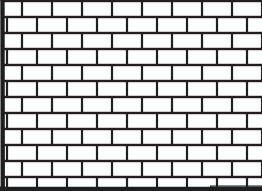
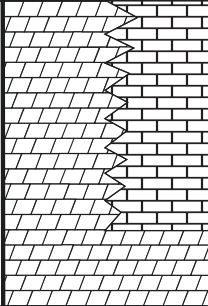
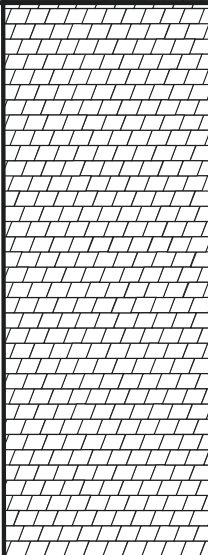
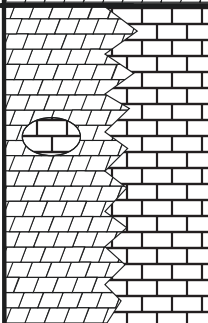


elevation of up to 43 m asl (Fig. 1.3D). Little Cayman, ~8 km west of Cayman Brac, is ~16 km long and 1.6 km wide with an area of ~28 km<sup>2</sup> and an elevation of up to 40 m asl (Fig. 1.3E). Today, the Cayman Islands experiences a humid sub-tropical climate that is dominated by the moisture-laden air masses of the North-East Trade Wind System (Blanchon, 1995). Today, Grand Cayman has air temperatures ranging from 21° to 33°C and the ocean temperatures (0–14.5 m depth) range from 25.3° to 30.8°C, with an average of 28.5°C (Goreau et al., 1992; NOAA, 2018; Fig. 1.4A and B). The average rainfall is 1,220 mm/year with the wet season from May to October and the dry season from November to April (Fig. 1.4D) with rainfall being the heaviest on the western part of the island (Ng, 1990). Cayman Brac has air temperatures of 26.6° to 30.6°C (2007 to 2015), with an average of 28.7°C (Fig. 1.4C) and receives an average of 860 mm/year rainfall (NOAA, 2018).

The Cayman Islands are composed of a dolostone and limestone core that belongs to the Oligocene-Pliocene Bluff Group (Brac Formation, Cayman Formation, Pedro Castel Formation), which are unconformably overlain and overlapped by limestones that belong to the Pleistocene Ironshore Formation (Fig. 1.5; Matley, 1926; Rigby and Roberts, 1976; Jones, 1994; Vezina et al., 1999; Coyne et al., 2007). The Ironshore Formation, found in outcrop and subsurface, is up to 19 m thick, encompasses six depositional units (A-F) that are separated from each other by unconformities (Fig. 1.6; Hunter and Jones, 1988; 1995; Vezina et al., 1999; Coyne et al., 2007; Li and Jones, 2013a; 2013b). U/Th dating of the well-preserved corals and conches in this formation, which developed during successive highstands of the Pleistocene, indicate that Unit A formed >500 ka, Unit B ~346 ka, Unit C ~229 ka, Unit D ~125 ka, Unit E ~101 ka, and Unit F ~80 ka (Vezina, 1997; Coyne, 2003; Li and Jones, 2014). Units A to F of the Ironshore Formation can be correlated to Marine Isotope Stages 11, 9, 7, 5e, 5c, and 5a, respectively (Vezina et al., 1999; Coyne et al., 2007).



**Fig. 1.4.** Climatic conditions for Grand Cayman and Cayman Brac between 1981 to 2015. (A) Atmospheric and water temperatures (11.3-14.5 m water depth) between 1991 and 2008 from offshore George Town, Grand Cayman. (B) Water temperatures (surface) for Grand Cayman between 1981 and 2010 (temperature derived from NOAA daily records). (C) Water temperatures (surface) for Cayman Brac between 2007 and 2015 (temperature derived from NOAA daily records). (D) Yearly rainfall for Grand Cayman between 2000 and 2012. (<http://www.worldweatheronline.com/george-town-weather-averages/ky.aspx>).

Age	Lithotype	Unit	Lithology	Biota
Pleistocene		Ironshore Formation Unconformity	Limestone	Corals (VC) Bivalves (VC) Gastropods (VC)
Pliocene		Pedro Castle Formation Unconformity	Dolostone, dolomitic limestone, and limestone	Foraminifera (VC) Corals (C) Gastropods (C) Red algae (C) <i>Halimeda</i> (R)
M. Miocene		Cayman Formation Unconformity	Dolostone	Corals (VC) Bivalves (LC) Rhodolites (LC) Gastropods (R) Red algae (LC) Foraminifera (LC) <i>Halimeda</i> (R)
L. Oligocene		Brac Formation	Limestone, sucrosic dolostone with pods of limestone	Bivalves (VC) Gastropods (C) Foraminifera (VC) Red algae (R)

**Fig. 1.5.** Stratigraphic column of the formations of the Cayman Islands (modified after Jones, 1994). VC- very common, C- common, LC- locally common, R- rare.

Age (ka)	Unit	Lithology	Biota	Sea level elevation (m)
80	F	Cross-bedded ooid grainstones, coral floatstone, <i>Halimeda</i> floatstone	Head and branching corals, <i>Halimeda</i>	+3.0 to +5.0
101	E	Coral floatstones	Head corals	+2.0 to +5.0
125	D	Grainstones	Head and branching corals	+2.5 to +6.0
229	C	Rudstones, packstones, grainstones, bafflestones	Head and branching corals	-2.5 to +1.0
346	B	Packstones, grainstones, minor wackstones	Head and branching corals	-3.0 to +0.5
>500	A	Grainstones	Head and branching corals	-9.0 to -5.5

**Fig. 1.6.** Internal stratigraphy of the Ironshore Formation on the Cayman Islands. Ages and sea levels (relative to modern sea level) from Vezina et al. (1999) and Coyne et al. (2007).

## 2.2. *Samples*

The samples used in this study came from (1) whole corals collected at Magic Reef, southwest coast of Grand Cayman, (2) cores drilled through the reefs at Gary's Wall and Dan's Dive, southwest coast of Grand Cayman, (3) cores drilled through the reefs at Tarpon Alley, North Sound fringing reef, Grand Cayman, (4) a whole coral from a storm rubble ridge, southeast coast of Cayman Brac, (5) sediment cores from the central part of North Sound lagoon, Grand Cayman, containing marine and marginal-marine material (6) cores from Rogers Wreck Point (RWP), east coast of Grand Cayman, (7) a whole coral from Unit D outcrop (IS1), northeast coast of Grand Cayman, (8) cores from George Town Harbor (GTH), offshore west coast of Grand Cayman, and (9) whole corals from Little Cayman Quarry, central Little Cayman (Fig. 1.3C-E). Water samples from Magic Reef, Spotts Bay, central North Sound, and the southeast coast of Cayman Brac were also collected for this study (Fig. 1.3C-E).

## 2.3. *Methodology*

### 2.3.1. *Coral samples*

All the coral samples analyzed in this study were subject to the same set of analyses to (1) image the bi-annual growth bands and produce a density map of the coral skeletal structure, (2) determine the degree of diagenetic alteration, and (3) analyze the elemental and isotopic compositions of the coral skeletons with the aims of producing paleoclimate reconstructions for each specimen. Detailed information about the methods used can be found in chapters 2, 3, and 5.

The ages of the corals were determined using; (1)  $^{14}\text{C}$  dating, (2) U/Th dating, (3) growth band counting, and (4) calculations based on average growth rates. The Cayman corals were imaged using a portable SY-31-100P X-ray machine and/or using an Aquilion ONE helical computer tomographic (CT) scanner at InnoTech Alberta (Edmonton, Alberta). These images highlight the corals bi-annual growth bands and were used to

measure and map the individual growth bands for elemental and isotopic analyses and to determine the lifespan of the corals by counting growth band couplets.

Mineralogy was confirmed by (1) X-Ray Diffraction (XRD) analyses, (2) thin section analyses, and (3) Scanning Electron Microscopy (SEM). XRD analyses were produced using a Rigaku Geigerflex Powder Diffractometer, the percentages of aragonite and calcite were determined by the method used by Li and Jones (2013b). Standard (27 x 46 mm) thin sections from the samples were used to verify the mineralogy of the corals, examine the growth banding, and the degree of diagenetic alteration. SEM photomicrographs of the samples were produced using a Zeiss Sigma Field Emission SEM. The SEM photomicrographs were used for assessment of the micro-scale fabrics and determination of any diagenetic alteration.

Elemental concentrations were determined in the Radiogenic Isotope Facility at the University of Alberta using two methods. Concentrations of Mg, Sr, and Ca were produced from powdered samples of the coral growth bands using a Thermo Fisher iCAP-Q Inductively Coupled Plasma Mass Spectrometer (ICP-MS). Additional elemental analysis of Ca, Sr, Mg, Li, Ba, B<sup>11</sup>, and U for a coral from Magic Reef were obtained using a New Wave UP-213 laser ablation system linked to a Thermo Fisher iCAP-Q ICP-MS. Numerous samples from individual growth bands from all corals were collected using a Dremel 8200 drill from the central part of each coral parallel to the maximum growth direction along the thecal walls of the coral skeleton.  $\delta^{13}\text{C}$  and  $\delta^{18}\text{O}$  values were determined using a Gasbench II system coupled with a Thermo MAT 253 Isotope Ratio Mass Spectrometer (IRMS).

### 2.3.2. *Sediment cores*

All of the samples from the sediment cores obtained from North Sound were subject to the same analyses to determine (1) mineralogy, (2) age, and (3) elemental and isotopic compositions with the aim of evaluating paleoclimate during deposition of the

North Sound sediments. Detailed information about the methods used can be found in chapter 4.

Radiocarbon dating analyses on material from the base and throughout the sediment cores were derived using conventional radiocarbon dating analysis at the Isotrace Laboratory, Toronto, Ontario (MacKinnon and Jones, 2001). Additional samples were analyzed by the A.E. Lalonde AMS Laboratory at the University of Ottawa in 2017. The radiocarbon ages were converted to calendar years using Calib 7.10. All marine samples were calibrated against the MARINE13 calibration curve and a local (Caribbean) reservoir effect ( $\Delta R$ ) of -28, as calculated within the program OxCal was applied. All non-marine samples were calibrated using the INTCAL13 calibration curve (Reimer et al., 2013).

The mineralogy of these samples was determined by XRD analyses using a Rigaku Geigerflex Powder Diffractometer at the University of Alberta. Element concentrations (Mg, Ca, Sr, Li, Be, B, Na, Al, P, K, Ti, V, Cr, Fe, Mn, Co, Ni, Zn, Ga, Ge, As, Se, Rb, Zr, Nb, Mo, Ru, Pd, Ag, Cd, Sn, Sb, Te, Cs, Ba, Hf, W, Re, Ir, Pt, Tl, Pb, Th, U and REE, including yttrium (Y)) were determined using a Thermo Fisher iCAP-Q ICP-MS.  $\delta^{13}\text{C}$  and  $\delta^{18}\text{O}$  values were determined using a Finnigan MAT, DeltaPlus XL IRMS at Isotope Tracer Technologies Inc, Waterloo, Ontario.

### 2.3.3. *Water samples*

The Department of Environment and the Water Authority Cayman Islands monitored the surface seawater temperature around Grand Cayman between 1991 to 2007. These records and satellite data from 1980 to 2015 (Goreau et al., 1992; NOAA, 2018) are combined and used to establish a baseline temperature record for comparison with the temperatures determined from the Cayman samples. Water samples from Grand Cayman and Cayman Brac (Fig. 1.2C, D) were analyzed for the oxygen isotope compositions by Isotope Tracer Technologies Ltd., Ontario, Canada, using a Thermo

Delta Plus Advantage linked to a Gasbench I via a GC PAL autosampler. Two seawater samples from Grand Cayman and one from Cayman Brac were analyzed for the metal concentrations using an Inductively Coupled Plasma- tandem Mass Spectrometer (ICP-MS/MS) at the University of Alberta. Detailed information about the methods used can be found in chapters 3 and 4.

### **3. Previous work**

#### *3.1. Geochemical proxies*

Carbonate samples (i.e., corals and sediment cores) are useful tools for geochemical analyses because climate proxies can be recorded in their skeletal material (Leder et al., 1996; Bryan et al., 2008), they are easily dated, and varying scales of high-resolution paleoenvironmental information can be determined (McCulloch et al., 1999; Kilbourne et al., 2007, Flannery et al., 2018). Geochemical proxies for determining paleoclimate conditions from carbonates have been used for many decades. This technique was first developed by Urey (1947), who showed that there is a detectable isotopic fractionation based on the relative abundances of two stable isotopes of oxygen ( $^{16}\text{O}$  and  $^{18}\text{O}$ ) in a body of water that is related to formation water temperatures of carbonates. Since that discovery numerous geochemical proxies have been applied to coral skeletons and sediment cores in order to determine past environmental conditions. These include (1)  $\delta^{18}\text{O}$ , clumped isotopes, Sr/Ca, Mg/Ca, U/Ca, Sr-U, Ba/Ca, Li/Ca, Li/Mg, and  $\text{B}^{11}/\text{Ca}$  for temperature determination (e.g., Watanabe et al., 2001; Quinn and Sampson, 2002; Alibert and Kinsley, 2008; Felis et al., 2009), (2)  $\delta^{18}\text{O}$ , Ba/Ca, Fe, Ti concentrations, and rare earth elements (REE) for salinity and/or precipitation/evaporation determinations (e.g., Haug et al., 2001; Allison and Finch, 2007; Kilbourne et al., 2007; Doherty et al., 2012), (3)  $\delta^{13}\text{C}$  for photosynthetic light activity of the symbiotic zooxanthellae that live in the coral tissues, sun light availability, water depth, nutrient levels, and metabolic processes (e.g., Erez, 1977; 1978), and (4) REE concentrations



of fine grained carbonate sediments to facilitate provenance studies (Muhs et al., 2007; Muhs and Budahn, 2009).

Although oxygen isotope geothermometry has been widely used for paleoclimate reconstructions, it is complicated by the influence of both the carbonate oxygen isotope composition, which is a function of temperature, and the oxygen isotopes composition of seawater, which is a function of salinity. In order to separate the influence of salinity on temperature, many oxygen isotope geothermometers incorporate a  $\delta^{18}\text{O}_{\text{water}}$  factor into the equation. The  $\delta^{18}\text{O}_{\text{water}}$  value, however, is commonly difficult to determine, especially for ancient samples. This issue can be circumvented by (1) using a value of 0‰ (value for modern seawater) as the residence time of oxygen in the world's oceans is thought to have remained relatively uniform throughout geological time (Muehlenbachs and Clayton, 1976), (2) applying a value derived from the SPECMAP curve of Imbrie and McIntyre (2006), or (3) using other elements in the skeleton to determine the  $\delta^{18}\text{O}_{\text{water}}$  value (e.g., Beck et al., 1992; Fallon et al., 2003; Kilbourne et al., 2010; Flannery et al., 2018). Other geothermometers have been developed using element/Ca ratios (Sr, Mg, U, Li, Ba, B<sup>11</sup>), which are believed to be unaffected by salinity. These geothermometers are a function of the element/Ca activity ratio of seawater and the distribution coefficient between aragonite and water for the specific element, which is dependent on temperature (e.g., Beck et al., 1992; Dietzel et al., 2004; Gaetani and Cohen, 2006).

### 3.2. Corals

Two species of coral are used in this study, *Orbicella annularis* and *Montastrea cavernosa*. Recently, Budd et al. (2012) reclassified Montastraeidae based on morphological criteria and molecular analysis (DNA, cellular definition, aggression, and protein sequestration). On this basis, Budd et al. (2012; their Table 2) transferred the *M. annularis* complex into Merulinidae and assigned it to the genus *Orbicella* Dana (1846). *M. cavernosa*, however, remains in Montastraeidae. Budd et al. (2012) then divided the

*M. annularis* complex, into *O. annularis*, *O. faveolata*, and *O. franksi*, which follows the names used by Vaughan (1918).

Modern scleractinian corals, that live in tropical environments and contain symbiotic zooxanthella, require a specific set of environmental conditions in order to grow, namely (1) water temperatures between 18° to 36°C, but preferably 25° to 29°C, (2) salinity between 22 to 40‰, but preferably 25 to 35‰, (3) low amounts of nutrients and suspended sediments, and (4) shallow water depths to remain within the photic zone (James and Jones, 2015; NOAA, 2016). Based on these specific growth parameters, corals are commonly used to assess past environmental conditions such as (1) depositional environment and water depth (e.g., Hunter and Jones, 1988; 1995; Jones and Hunter, 1990), (2) SST and SSS (e.g., Watanabe et al., 2001; Kilbourne et al., 2007; 2010), and (3) sea level change (e.g., Blanchon et al., 2009; Webb et al., 2016).

In order for coral skeletons to be used for paleoclimate interpretations, the growth bands in the skeletons are commonly analyzed and related to specific time periods. As such, Knutson et al. (1972), and Moore and Krishnaswami (1974), showed that coral skeletons are composed of layers of different densities that reflect seasonal growth. The density bands are visible on X-Ray or CT images, with the densest material being lighter in color (white) than the less dense material (Buddermeier et al., 1974; Moore and Krishnaswami, 1974). These growth bands reflect different periods of time and have been linked to yearly, monthly and daily growth (Knutson et al., 1972; Winter and Sammarco, 2010). In turn, these growth bands have been used to answer questions about the length of the day, year and lunar month in the geological record (e.g., Wells, 1963; Runcorn, 1966; Weber et al., 1975a, 1975b).

### 3.3. *Sediment cores*

Carbonate sediments that accumulate at the base of bodies of water are archives of the environmental changes that have taken place since the depositional systems were first

established and can provide a wealth of information about the environmental conditions. As such, large time scales (thousands of years) can be investigated. Geochemical proxies such as  $\delta^{18}\text{O}$ ,  $\delta^{13}\text{C}$ , element/Ca ratios, and elemental concentrations (Fe, Ti, REE) have the potential of providing detailed insights into the manner in which the lagoon responded to short-term sea level oscillations and climate change (Haug et al., 2001; Black et al., 2004; Muhs et al., 2007; Gregory et al., 2015). Sediment cores have also been used to provide evidence for Milankovitch cycles (Hays et al., 1976) and to establish Pleistocene (Imbrie and McIntyre, 2006) and Tertiary  $\delta^{18}\text{O}$  sea level curves (Shackleton and Kennett, 1975a; 1975b).

### 3.4. Ironshore Formation

The Ironshore Formation has been thoroughly studied in terms of its fossil assemblages, stratigraphy, lithology, relation to relative sea level changes during the Pleistocene, depositional history, paleogeography, and diagenetic alteration (Matley, 1926; Rehder, 1962; Burnt et al., 1973; Woodroffe et al., 1980; Hunter and Jones, 1988; 1995; Jones and Hunter, 1990; 1995; Rehman et al., 1994; Vezina et al., 1999; Coyne et al., 2007; Li and Jones, 2013a; 2013b; 2014). The depositional environments of the Ironshore Formation were first determined by Burnt et al. (1973), who divided the Ironshore Formation into the (1) reef facies dominated by *Acropora* and *Porites*, (2) back-reef facies with massive corals, (3) lagoonal facies or marl with diverse molluscan fauna, (4) a shoal facies characterized by cross-bedded oolitic sands, and (5) subaerial beach facies. Jones and Hunter (1990; 1995) established the paleogeographic framework of Grand Cayman ~125 ka based on rock type, sedimentary structures, fossil content, and trace fossil assemblages. Unit D of the Ironshore Formation was deposited in a large lagoon (Ironshore Lagoon) that covered the central and western part of Grand Cayman. The lagoonal sediments are overlain by limestones that were deposited in a high-energy, prograding beach-like environment (Jones and Hunter, 1990).

Subsurface drilling on the east coast of Grand Cayman showed that the Ironshore Formation is comprised of four unconformity-bound units (Units A-D) composed of rudstones, grainstones, and packstones-wackestones-mudstones (Vezina et al., 1999). These units were deposited on a high-energy narrow shelf, which was developed by marine erosion of the underlying Cayman Formations (Vezina et al., 1999). Additional offshore drilling in the western part of Grand Cayman showed two previously unrecognized younger units of the Ironshore Formation (Units E and F), as well as Unit D (Coyne et al., 2007). The offshore west coast cores contain head coral floatstones, branching coral floatstones, mixed coral floatstones, *Halimeda* floatstone-rudstones, and skeletal grainstone-packstone-wackestones, which were deposited in a marine setting below fair-weather wave base (Coyne et al., 2007). Surface exposures of the Ironshore Formation in the western part of Grand Cayman are formed of skeletal packstone-grainstones, coral floatstone-rudstones, and ooid grainstones (Coyne et al., 2007). Unit F is formed of sediments that were either deposited in tidal channels (Jones and Pemberton, 1989) or under hurricane conditions (Coyne et al., 2007). Diagenetic research on the Ironshore Formation has focused on the inversion of aragonite to calcite in the fossil components, borings, isotopic and trace metal concentrations, and the development of the calcrete crusts in terms of diagenetic fabric evolution, fluid flow, and relation to intervals of subaerial exposure (Jones and Pemberton, 1989; Jones and Hunter, 1990; Rehman et al., 1994; Li and Jones, 2013a; 2013b; 2014).

#### **4. Objectives**

The main objective of this thesis is to track climate change, specifically SST and atmospheric moisture in the Caribbean through time (0 to 125 ka) from multiple coral skeletons and sediment cores. This thesis provides a better understanding of climate dynamics in the central Caribbean, an understudied area in the tropical Atlantic Ocean, over an extended time period when compared to other coral based paleoclimate

reconstructions (Buddermeier et al., 1974; Weber et al., 1975a; Guilderson et al., 1994; Gagan et al., 2000; Watanabe et al., 2001; Winter et al., 2003; Kilbourne, 2007; 2010; Hetzinger et al., 2010; Winter and Sammarco, 2010; Felis et al., 2015; Brocas et al., 2016).

This thesis is 'paper based'. Collectively, these papers examine SST and moisture changes through time (0 to 125 ka) in the central Caribbean and examine the applicability of using geochemical proxies for paleoclimate reconstruction. These papers are incorporated into this thesis as Chapters 2, 3, 4 and 5.

**Chapter 2-** Review of element/Ca proxies for deriving paleotemperatures from modern tropical corals: insights into the future of element/Ca geothermometry.

**Chapter 3-** Insights into sea surface temperatures from the Cayman Islands from corals over the last ~540 years. A version of this chapter has been published.

**Chapter 4-** A 6000-year record of climate change from stable isotope and rare earth element analyses of sediment cores from North Sound lagoon, Grand Cayman, British West Indies

**Chapter 5-** Diagenesis in Pleistocene (80 to 500 ka) corals from the Ironshore Formation: implications for paleoclimate reconstruction. A version of this paper has been published.

**Chapter 6-** Conclusion. This chapter summarized the entire thesis.

## REFERENCES

- Alibert, C., Kinsley, L., 2008. A 170-year Sr/Ca and Ca/Ca coral record from the western Pacific warm pool: 1. What can we learn from an unusual coral record? *Journal of Geophysical Research- Oceans* 113. doi:10.1029/2006JC003979.
- Allison, N., Finch, A.A., 2007. High temporal resolution Mg/Ca and Ba/Ca records in modern *Porites lobata* corals. *Geochemistry Geophysics Geosystems* 8. doi:10.1029/2006GC001477.
- Arienzo, M.M., Swart, P.K., Pourmand, A., Board, K., Clement, A.C., Murphy, L.N., Vonhof, H.B., Kakuk, B., 2015. Bahamian speleothem reveals temperature decrease associated with Heinrich stadials. *Earth and Planetary Science Letters* 430, 377-386.
- Beck, J.W., Edwards, L., Ito, E., Taylor, F.W., Recy, J., Rougerie, F., Joannot, P., Henin, C., 1992. Sea-surface temperatures from coral skeletal strontium/calcium ratios. *Science* 257, 644-649.
- Black, D.E., Thunell, R.C., Kaplan, A., Peterson, L.C., Tappa, E.J., 2004. A 2000-year record of Caribbean and tropical North Atlantic hydrographic variability. *Paleoceanography* 19, 1-11.
- Blanchon, P.A., Jones, B., 1995. Marine-planation terrances on the shelf of Grand Cayman: a result of stepped Holocene sea-level rise. *Journal of Coastal Research* 11, 1-33.
- Blanchon, P.A., Eisenhauer, A., Fietzke, J., Liebetrau, V., 2009. Rapid sea-level rise and reef back-stepping at the close of the last interglacial highstand. *Nature: Letters* 458, 881-885.
- Brocas, W.M., Felis, T., Obert, J.C., Gierz, P., Lohmann, G., Scholz, D., Kolling, M., Scheffers, S.R., 2016. Last interglacial temperature seasonality reconstructed from tropical Atlantic corals. *Earth and Planetary Science Letters* 449, 418-429.
- Bryan, S.P., Marchitto, T.M., 2008. Mg/Ca-temperature proxy in benthic foraminifera:

- new calibrations from the Florida Straits and a hypothesis regarding Mg/Li. *Paleoceanography* 23, 1-17.
- Budd, A.F., Fukami, H., Smith, N.D., Knowlton, N., 2012. Taxonomic classification of the reef coral family Mussidae (Cnidaria: Anthozoa: Scleractinia). *Zoological Journal of the Linnean Society* 166, 465-529.
- Buddermeier, R.W., Maragos, J.E., Knutson, D.K., 1974. Radiographic studies of reef coral exoskeletons: rates and patterns of growth. *Journal of Experimental Marine Biology and Ecology* 14, 179-200.
- Burnt, M.A., Giglioli, M.E.C., Mather, J.D., Piper, D.J.W., Richards, H.G., 1973. The Pleistocene rocks of the Cayman Islands. *Geological Magazine* 110, 209-304.
- Coyne, M.K., Jones, B., Ford, D., 2007. Highstands during marine isotope stage 5: evidence from the Ironshore Formation of Grand Cayman, British West Indies. *Quaternary Science Reviews* 26, 536-559.
- Crann, C.A., Murseli, S., St-Jean, G., Zhao, X., Clark, I.D., Kieser, W.E., 2017. First status report on radiocarbon sample preparation techniques at the A.E. Lalonde AMS Laboratory (Ottawa, Canada). *Radiocarbon* 59, 695-704.
- Dana, J.D., 1846. Structure and classification of zoophytes. U.S. Exploring Expedition 1838-1842, 7. Lea and Blanchard, Philadelphia, 740 pp.
- Dietzel, M., Gussone, N., Eisenhauer, A., 2004. Co-precipitation of Sr<sup>2+</sup> and Ba<sup>2+</sup> with aragonite by membrane diffusion of CO<sub>2</sub> between 10 and 50°C. *Chemical Geology* 203, 139-151.
- Doherty, O.M., Riemer, N., Hameed, S., 2012. Control of Saharan mineral dust transport to Barbados in winter by the Intertropical Convergence Zone over West Africa. *Journal of Geophysical Research* 117. doi:10.1029/2012JD017767.
- Erez, J., 1977. Influence of symbiotic algae on the stable isotope composition of hermatypic corals: a radioactive tracer approach. In: Taylor, D.L. (Ed.), *Third International Coral Reef Symposium*. Rosenstiel School of Marine and

- Atmospheric Sciences, Miami, Florida, pp. 564-569.
- Erez, J., 1978. Vital effect on stable-isotopes composition seen in foraminifera and coral skeletons. *Nature* 273, 199-202.
- Fahlquist, D.A., Davies, D.K., 1971. Fault block origin of the western Cayman Ridge, Caribbean Sea. *Deep Sea Research* 18, 243-253.
- Fallon, S.J., McCulloch, M., Alibert, C., 2003. Examining water temperature proxies in *Porites* corals from the Great Barrier Reef: a cross-shelf comparison. *Coral Reefs* 22, 389-404.
- Fegyveresi, J.M., Alley, R.B., Fitzpatrick, J.J., Cuffey, K.M., McConnell, J.R., Voigt, D.E., Spencer, M.K., Stevens, N.T., 2016. Five millennia of surface temperatures and ice core bubble characteristics from the WAIS Divide deep core, West Antarctica. *Paleoceanography* 31, 416-433.
- Felis, T., Suzuki, A., Kuhnert, H., Dima, M., Lohmann, G., Kawahata, H., 2009. Subtropical coral reveals abrupt early-twentieth-century freshening in the western North Pacific Ocean. *Geology* 37, 527-530.
- Felis, T., Giry, C., Scholz, D., Lohmann, G., Pfeiffer, M., Patzold, J., Kolling, M., Scheffers, S.R., 2015. Tropical Atlantic temperature seasonality at the end of the last interglacial. *Nature: Communications*, 6. doi: 10.1038/ncomms7159.
- Fensterer, C., Scholz, D., Hoffmann, D.L., Spotl, C., Pajon, J.M., Mangini, A., 2012. Cuban stalagmite suggests relationship between Caribbean precipitation and the Atlantic Multidecadal Oscillation during the past 1.3ka. *Holocene* 22, 1405-1412.
- Flannery, J.A., Richey, J.N., Toth, L.T., Kuffner, I.B., Poore, R.Z., 2018. Quantifying uncertainty in Sr/Ca-based estimates of SST from the coral *Orbicella faveolata*. *Paleoceanography and Paleoclimatology* 33, 958-973.
- Gaetani, G.A., Cohen, A.L., 2006. Element partitioning during precipitation of aragonite from seawater: a framework for understanding paleoproxies. *Geochimica et Cosmochimica Acta* 70, 4617-4634.



- Gagan, M.K., Ayliffe, L.K., Beck, J.W., Cole, J.E., Druffel, E.R.M., Dunbar, R.B., Schrag, D.P., 2000. New views of tropical paleoclimates from corals. *Quaternary Science Reviews* 19, 45-64.
- Goreau, T.J., Hayes, R.L., Clark, J.W., Basta, D.J., Robertson, C.N., 1992. Elevated satellite sea surface temperatures correlate with Caribbean coral reef bleaching. In: Geyer, R.A. (Ed.), *A Global Warming Forum: Scientific, Economic, and Legal Overview*. CRC Press, Florida, USA, pp. 225-255.
- Gregory, B.R.B., Peros, M., Reinhardt, E.G., Donnelly, J.P., 2015. Middle-late Holocene Caribbean aridity inferred from foraminifera and elemental data in sediment cores from two Cuban lagoons. *Palaeogeography, Palaeoclimatology, Palaeoecology* 426, 239-241.
- Guilderson, T.P., Fairbanks, R.D., Rubenstone, J.L., 1994. Tropical temperature variations since 20,000 years ago: modulating interhemispheric climate change. *Science* 263, 663-665.
- Hasen, J., Sato, M., Russell, G., Kharecha, P., 2018. Climate sensitivity, sea level and atmospheric carbon dioxide. *Philosophical Transactions of the Royal Society A*.
- Haug, G.H., Hughen, K.A., Sigman, D.M., Peterson, L.C., Rohl, U., 2001. Southward migration of the Intertropical Convergence Zone through the Holocene. *Science* 293, 1304-1310.
- Hays, J.D., Imbrie, J., Shackleton, N.J., 1976. Variations in the Earth's orbit: pacemaker of the Ice Ages. *Science* 194, 1121-1132.
- Hetzinger, S., Pfeiffer, M., Dullo, W., Garbe-Schonberg, D., Halfar, J., 2010. Rapid 20th century warming in the Caribbean and impact of remote forcing on climate in the northern tropical Atlantic as recorded in a Guadeloupe coral. *Palaeogeography, Palaeoclimatology, Palaeoecology* 296, 111-124.
- Hodell, D.A., Curtis, J.H., Jones, G.A., Higuera-Gundy, A., Brenner, M., Binford, M.W., Dorsey, K.T., 1991. Reconstruction of Caribbean climate change over the past

- 10,500 years. *Nature: Letters* 352, 790-794.
- Hunter, I.G., Jones, B., 1988. Corals and paleogeography of the Pleistocene Ironshore Formation of Grand Cayman, Proceedings of the Sixth International Coral Reef Symposium, Townsville, Australia, pp. 431-435.
- Hunter, I.G., Jones, B., 1995. Coral associations of the Pleistocene Ironshore Formation, Grand Cayman. *Coral Reefs* 15, 249-267.
- Imbrie, J., McIntyre, A., 2006. SPECMAP time scale developed by Imbrie et al., 1984 based on normalized planktonic records (normalized O-18 vs time, specmap.017).
- IPCC, 2014. Climate change 2014: synthesis report. Contribution of working groups I, II and III to the Fifth Assessment Report of the Intergovernmental Panel on Climate Change, Geneva, Switzerland.
- IPCC, 2018. Summery for policymakers, World Meteorological Organization, Geneva, Switzerland.
- James, N.P., Jones, B., 2015. Origin of carbonate sedimentary rocks. John Wiley & Sons, 464 pp.
- Jones, B., 1994. Geology of the Cayman Islands. The Cayman Islands: Natural history and biogeography. Kluwer Academic Publishers, The Netherlands, pp. 13-49.
- Jones, B., Pemberton, S.P., 1989. Sedimentology and ichnology of a Pleistocene unconformity bounded, shallowing upward carbonate sequence: the Ironshore Formation, Salt Creek, Grand Cayman. *Palaios* 4, 343-355.
- Jones, B., Hunter, I.G., 1990. Pleistocene paleogeography and sea levels on the Cayman Islands, British West Indies. *Coral Reefs* 9, 81-91.
- Kilbourne, K.H., Quinn, T.M., Guilderson, T.P., Webb, R.S., Taylor, F.W., 2007. Decadal-to interannual-scale source water variations in the Caribbean Sea recorded by Puerto Rican coral radiocarbon. *Climate Dynamics* 29, 51-62.
- Kilbourne, K.H., Quinn, T.M., Webb, R., Guilderson, T., Nyberg, J., Winter, A., 2010. Coral windows onto seasonal climate variability in the northern Caribbean since

1479. *Geochemistry Geophysics Geosystems* 11. doi: 10.1029/2010GC003171.
- Knutson, D.W., Buddermeier, R.W., Smith, S.V., 1972. Coral chronometers: seasonal growth bands in reef corals. *Science* 177, 270-272.
- Kuffner, I.B., Lidz, B., Hudson, J.H., Anderson, J.S., 2015. A century of ocean warming on Florida Keys coral reefs: historic in situ observations. *Estuaries and Coasts* 38, 1085-1096.
- Kuffner, I.B., Roberts, H.H., Flannery, J.A., Morrison, J.M., Richey, J.N., 2017. Fidelity of Sr/Ca proxy in recording ocean temperature in the western Atlantic coral *Siderastrea siderea*. *Geochemistry Geophysics Geosystems* 18, 178-188.
- Leder, J.J., Swart, P.K., Szmant, A.M., Dodge, R.E., 1996. The origin of variations in the isotopic record of scleractinian corals: I. Oxygen. *Geochimica et Cosmochimica Acta* 60, 2857-2870.
- Li, R., Jones, B., 2013a. Temporal and spatial variations in the diagenetic fabrics and stable isotopes of Pleistocene corals from the Ironshore Formation of Grand Cayman, British West Indies. *Sedimentary Geology* 286-287, 58-72.
- Li, R., Jones, B., 2013b. Heterogeneous diagenetic patterns in Pleistocene Ironshore Formation of Grand Cayman, British West Indies. *Sedimentary Geology* 294, 251-265.
- Li, R., Jones, B., 2014. Calcareous crusts on exposed Pleistocene limestones: a case study from Grand Cayman, British West Indies. *Sedimentary Geology* 299, 88-105.
- Linsley, B.K., Zhang, P., Kaplan, A., Howe, S.S., Wellington, G.M., 2008. Interdecadal-decadal climate variability from multicoral oxygen isotope records in the South Pacific Convergence Zone region since 1650 A.D. *Paleoceanography* 23. doi: 10.1029/2007PA001539.
- MacDonald, K.C., Holcombe, T.L., 1978. Inversion of magnetic anomalies and sea-floor spreading in the Cayman Trough. *Earth and Planetary Science Letters* 40, 407-414.

- MacKinnon, L., Jones, B., 2001. Sedimentological evolution of North Sound, Grand Cayman: a freshwater to marine carbonate succession driven by Holocene sea-level rise. *Journal of Sedimentary Research* 71, 568-580.
- Matley, C.A., 1926. The geology of the Cayman Islands (British West Indies), and their relations to the Barlett Trough. *Quarterly Journal of the Geological Society of London* 82, 352-386.
- Moore, W.S., Krishnaswami, S., 1974. Correlation of X-Radiography revealed banding in corals with radiometric growth rates. In: Cameron, A.M., Cambell, B.M., Cribb, A.B., Endean, R., Jell, J.S., Jones, O.A., Mather, P., Talbot, F.H. (Eds.), *Proceeding of the Second International Coral Reef Symposium 2*. Great Barrier Reef Committee, Brisbane, pp. 269-276.
- Muehlenbachs, K., Clayton, R.N., 1976. Oxygen isotope composition of the oceanic crust and its bearing on seawater. *Journal of Geophysical Research* 81, 4365-4369.
- Muhs, D.R., Budahn, J.R., 2009. Geochemical evidence for African dust and volcanic ash inputs to terra rossa soils on carbonate reef terraces, northern Jamaica, West Indies. *Quaternary International* 196, 13-35.
- Muhs, D.R., Budahn, J.R., Prospero, J.M., Carey, S.N., 2007. Geochemical evidence for African dust inputs to soils of western Atlantic islands: Barbados, the Bahamas, and Florida. *Journal of Geophysical Research* 112.
- Ng, K., 1990. Diagenesis of the Oligocene-Miocene Bluff Formation of the Cayman Islands: a petrographic and hydrogeological approach., Unpublished. Ph.D., University of Alberta, Edmonton, Alberta, Canada, 343 pp.
- NOAA, 2018, World Sea Temperatures. <https://www.seatemperature.org/>.
- NOAA, 2016, In what types of water do corals live? <https://oceanservice.noaa.gov/facts/coralwaters.html>.
- Perfit, M.R., Heezen, B.C., 1978. The geology and the evolution of the Cayman Trench. *Geological Society of America Bulletin* 89, 1155-1174.

- Quinn, T.M., Sampson, D.E., 2002. A multiproxy approach to reconstructing sea surface conditions using coral skeleton geochemistry. *Paleoceanography* 17. doi:10.1029/2000PA000528.
- Rehder, H.A., 1962. The Pleistocene molluscs of Grand Cayman Islands, with notes on the geology of the island. *Journal of Paleontology* 36, 583-585.
- Rehman, J., Jones, B., Hagan, T.H., Coniglio, M., 1994. The influence of sponge borings on aragonite-to-calcite inversion in Late Pleistocene *Strombus gigas* from Grand Cayman, British West Indies. *Journal of Sedimentary Research* 64, 174-179.
- Reimer, P.J., Bard, E., Bayliss, A., Beck, J.W., Blackwell, P.G., Ramsey, C.B., Buck, C.E., Cheng, H., Edwards, R.L., Friedrich, M., Grootes, P.M., Guilderson, T.P., Haffidason, H., Hajdas, I., Hatte, C., Heaton, T.J., Hoffmann, D.L., Hogg, A.G., Hughen, K.A., Kaiser, K.F., Kromer, B., Manning, S.W., Niu, M., Reimer, R.W., Richardson, D.A., Scott, E.M., Southon, J., Staff, R.A., Turney, C.S.M., van der Plicht, J., 2013. IntCal13 and Marine13 radiocarbon age calibration curves 0-50,000 years cal BP. *Radiocarbon* 55, 1869-1887.
- Rigby, J.K., Roberts, H.H., 1976. Grand Cayman Island: geology, sediments, and marine communities. Brigham Young University Geology Studies: Special Publication, 4. Brigham Young University, Dept. of Geology, Utah, pp. 122.
- Runcorn, S.K., 1966. Corals as paleontological clocks. *Scientific America* 215, 26-33.
- Shackleton, N.J., Kennett, J.P., 1975a. Late Cenozoic oxygen and carbon isotopic changes at DSDP site 284: implications for glacial history of the northern hemisphere and Antarctica, Initial Reports of the Deep Sea Drilling Project. U.S. Government Printing Office, Washington, D.C., pp. 801.
- Shackleton, N.J., Kennett, J.P., 1975b. Paleotemperature history of the Cenozoic and the initiation of Antarctic glaciation: oxygen and carbon isotope analyses in DSDP sites 277, 279, 281, Initial Reports of the Deep Sea Drilling Project. U.S. Government Printing Office, Washington, D.C., pp. 743.

- Urey, H.C., 1947. The thermodynamic properties of isotopic substances. *Journal of the Chemical Society of London*, 562-581.
- Vaughan, T.W., 1918. Some shoal-water from Murray Island (Australia), Coco-Keelin Islands, and Fanning Island, Papers Department of Marine Biology, Carnegie Institute of Washington, 9, pp. 49-234.
- Veizina, J.L., Jones, B., Ford, D., 1999. Sea level highstands over the last 500,000 years: evidence from the Ironshore Formation on Grand Cayman, British West Indies. *Journal of Sedimentary Research* 69, 317-327.
- Watanabe, T., Winter, A., Oba, T., 2001. Seasonal changes in sea surface temperatures and salinity during the Little Ice Age in the Caribbean Sea deduced from Mg/Ca and  $^{18}\text{O}/^{16}\text{O}$  ratios in corals. *Marine Geology* 173, 21-35.
- Webb, G.E., Nothdurft, L.D., Zhao, J., Opdyke, B., Price, G., 2016. Significance of shallow core transects for reef models and sea-level curves, Heron Reef, Great Barrier Reef. *Sedimentology* 63, 1396-1424.
- Weber, J.N., White, E.W., Weber, P.H., 1975a. Correlation of density banding in reef coral skeletons with environmental parameters: the basis for interpretation of chronological records preserved in the coralla of corals. *Paleobiology* 1, 137-149.
- Weber, J.N., Deines, P., Weber, P.H., Baker, P.A., 1975b. Depth related changes in the  $^{13}\text{C}/^{12}\text{C}$  ratio of skeletal carbonate deposited by the Caribbean reef-frame building coral *Montastrea annularis*: further implications of a model from stable isotope fractionation by scleractinian corals. *Geochimica et Cosmochimica Acta* 40, 31-39.
- Wells, J.W., 1963. Coral growth and geochronometry. *Nature* 197, 948-950.
- Winter, A., Sammarco, P.W., 2010. Lunar banding in the scleractinian coral *Montastraea faveolata*: fine-scale structures and influences of temperature. *Journal of Geophysical Research* 115. doi: 10.1029/2009JG001264.
- Winter, A., Paul, A., Nyberg, J., Oba, T., Lundberg, J., Schrag, D.P., Taggart, B., 2003.

Orbital control of low-latitude seasonality during the Eemian. *Geophysical Research Letters* 30. doi:10.1029/2002GL016275.

Woodroffe, C.D., Stoddart, D.R., Giglioli, M.E.C., 1980. Pleistocene patch reefs and Holocene swamp morphology, Grand Cayman Island, West Indies. *Journal of Biogeography* 7, 103-113.

Yu, W., Tian, L., Risi, C., Yao, T., Ma, Y., Zhao, H., Zhu, H., He, Y., Xu, B., Zhang, H., Qu, D., 2016.  $\delta^{18}\text{O}$  records in water vapor and an ice core from the eastern Pamir Plateau: implications for paleoclimate reconstructions. *Earth and Planetary Science Letters* 456, 146-156.

## CHAPTER 2

### REVIEW OF ELEMENT/CA PROXIES FOR DERIVING PALEOTEMPERATURES FROM MODERN TROPICAL CORALS: INSIGHTS INTO THE FUTURE OF ELEMENT/CA GEOTHERMOMETRY

#### 1. Introduction

Paleoclimate models pertaining to the last 800,000 years are commonly based on environmental proxies from modern and fossil corals (e.g., Weber, 1977; Winter et al., 2003; Kuffner et al., 2017; Flannery et al., 2018; Booker et al., 2019; 2020), sediment cores (e.g., Hodell et al., 1991; Gregory et al., 2015), speleothems (e.g., Fensterer et al., 2012; Arienzo et al., 2015), and ice cores (e.g., Fegyveresi et al., 2016; Yu et al., 2016) from many different locations throughout the world. Much of this work has focused on past seawater temperature because that is considered a good measure of climate change (Gagan et al., 2000; Felis et al., 2015; Brocas et al., 2016). The calcium carbonate skeletons of many marine organisms, including corals, have commonly been used for determining climate change because various chemical proxies in their skeletons can be used to detect changes in environmental conditions through time.

Tropical corals have become one of the primary tools for determining climate change in low latitude regions because the chemical proxies (e.g.,  $\delta^{18}\text{O}$ ,  $\delta^{13}\text{C}$ , Sr/Ca, Mg/Ca, U/Ca, Sr-U, Ba/Ca, Li/Ca, Li/Mg,  $\text{B}^{11}/\text{Ca}$ ) in their skeletons can provide high resolution climatic information over decadal to centennial time scales. These proxies have, for example, been used to reconstruct past seawater temperature, sea surface salinity, photosynthetic activity, nutrient level, water depth, metabolic processes, precipitation, riverine input, and upwelling throughout geological time (e.g., Evans et al., 1999; Marshall and McCulloch, 2001; Watanabe et al., 2001; Quinn and Sampson, 2002; McCulloch et al., 2003; Montaggioni et al., 2006; Kilbourne et al., 2007; Alibert and Kinsley, 2008; Felis et al., 2009; Horta-Puga and Carriquiry, 2012; Booker et al., 2019;



2020). There is, however, considerable debate regarding the results obtained from the chemical proxies because the processes that govern incorporation of those proxies into the coral skeleton are poorly understood.

Oxygen isotope geothermometry has commonly been used to determine paleotemperatures. Nevertheless, it is difficult to use this geothermometer in fossil corals because both the  $\delta^{18}\text{O}$  of the carbonate material and  $\delta^{18}\text{O}$  of the surrounding seawater are required.  $\delta^{18}\text{O}_{\text{water}}$ , however, is difficult to determine for fossil samples (Hart and Cohen, 1996). The use of element/Ca ratios arose because they were deemed to be controlled solely by water temperature. The use of these temperature proxies, however, is not straightforward because the incorporation of these elements into the coral skeletons is commonly influenced by vital effects and/or other external environmental factors (e.g., Alibert and McCulloch, 1997; Boiseau et al., 1997; Sinclair et al., 1998; Marshall and McCulloch, 2002; Fallon et al., 2003; Goodkin et al., 2005; Yu et al., 2005; Corregge, 2006; Allison and Finch, 2007; Case et al., 2010; Kilbourne et al., 2010; DeLong et al., 2011; DeCarlo et al., 2015; Xu et al., 2015; von Reumont et al., 2016; Gonnee et al., 2017; Flannery et al., 2018).

There are at least 302 published element/Ca equations that have been developed for modern tropical corals. This paper reviews the theory behind the development and use of nine element/Ca geothermometers (e.g., Sr/Ca, Mg/Ca, U/Ca, Sr-U, Ba/Ca, Li/Ca, Li/Mg, Mg/Li,  $\text{B}^{11}/\text{Ca}$ ), highlights the causes of variability between the different equations that have been developed, and evaluates these equations in terms of their ability to produce ‘realistic’ temperatures. In most cases, the temperature derived from the coral skeletons are deemed acceptable if they fall in the range of local water temperatures in the area where they grew or the temperatures recorded during growth of the corals under controlled aquarium conditions. For the purpose of this review, the temperature range defined by the modern tropical coral growth window is used because it provides a global temperature range. The multifaceted growth window for modern tropical corals is

defined by clear waters with low turbidity that allows maximum light penetration, low-nutrient conditions, temperatures of 18° to 36°C with an ideal range of 25° to 29°C, and salinity between 22‰ and 40‰ but preferably 25‰ to 35‰ (James and Jones, 2015; NOAA, 2016).

The applicability of element/Ca temperature calibrations is herein examined and assessed by using (1) a dataset that is based on the full range of element/Ca ratios that have been reported from various tropical corals in the literature, and (2) a dataset derived from a specimen of *Orbicella annularis* from Grand Cayman (central Caribbean). Use of these datasets allows a thorough evaluation of the element/Ca equations that have been used to determine seawater temperatures. This information provides an assessment of the usefulness and applicability of each of the element/Ca geothermometers. By examining the current state of coral based element/Ca geothermometry recommendations about the direction of future research are established.

## 2. Datasets

Two sets of data (I and II) were used to test the applicability of the 302 published element/Ca equations. The results of the application of dataset I are used to determine which of the published equations produce seawater temperatures in the temperature range of the modern tropical coral growth window (18° to 36°C). Using the element/Ca ratios from a coral from Grand Cayman, Dataset II tests the ‘best’ equations, as determined by dataset I, against local instrument measured water temperatures (25° to 31°C) to assess the applicability of those calibrations.

- Dataset I was generated from published element/Ca ratios for 12 species of modern warm water hermatypic corals (*Porites*, *Siderastrea*, *Acropora*, *Orbicella*, *Diploastrea*, *Diploria*, *Montipora*, *Pollicipora*, *Panovia*, *Goniopora*, *Astrangia*, *Favia*) from various locations throughout the world. This dataset includes: (1) 28 Sr/Ca ratios from 7.3 to 10.0 millimole/mole (mmol/mol; Shen et al., 1996;

Sinclair et al., 1998; Quinn and Sampson, 2002; Fallon et al., 2003; Ourbak et al., 2006; Kilbourne et al., 2010; Flannery et al., 2018; Booker et al., 2018), (2) 38 Mg/Ca ratios from 2.5 to 6.3 mmol/mol (Sinclair et al., 1998; Watanabe et al., 2001; Quinn and Sampson, 2002; Fallon et al., 2003; Ourbak et al., 2006; Booker et al., 2018), (3) 8 U/Ca ratios from 0.7 to 1.4 micromole/mole ( $\mu\text{mol/mol}$ ; Sinclair et al., 1998; Quinn and Sampson, 2002; Fallon et al., 2003; Ourbak et al., 2006;), (4) 7 Sr-U values from 8.8 to 9.4 (DeCarlo et al., 2016; Alpert et al., 2017), (5) 63 Li/Ca ratios from 6.0 to 12.2  $\mu\text{mol/mol}$  (Marriott et al., 2004; Hathorne et al., 2013), (6) 6 Mg/Li ratios from 0.4 to 0.9 mol/mmol (Hathorne et al., 2013; Fowell et al., 2016), (7) 13 Li/Mg ratios from 1.0 to 2.2 for mmol/mol (Hathorne et al., 2013; Fowell et al., 2016), (8) 90 Ba/Ca ratios from 3 to 12  $\mu\text{mol/mol}$  (Gonneea et al., 2017), and (9) 31  $\text{B}^{11}$ /Ca ratios from 0.3 to 0.6 mmol/mol (Sinclair et al., 1998; Fallon et al., 2003). For each ratio, artificial increases between the minimum and maximum values of 0.1 mmol/mol for Sr/Ca, Mg/Ca, Li/Mg, and  $\text{B}^{11}$ /Ca, 0.1  $\mu\text{mol/mol}$  for U/Ca and Ba/Ca, 0.1 for Sr-U, and 0.1 mol/mmol for Mg/Li were generated so a complete range of values could be used.

- Dataset II is from a modern specimen of *O. annularis* that came from Magic Reef, which is located offshore George Town, on the southwest corner of Grand Cayman at a water depth of 20 m. This coral, 40 cm high with three broad (6 to 9 cm wide) branches, was selected because its aragonitic skeleton has not been altered and the younger part of the coral grew during a period (1996 to 2002) for which instrument measured water temperatures are available (NOAA, 2018; Booker et al., 2019). Three thin sections (one from each branch; Fig. 2.1) were made so that they corresponded to the growth period for which the instrument measured water temperatures are available. Analyses obtained using a New Wave UP-213 laser ablation and analyzed with an Inductively Coupled Plasma Mass Spectrometer (University of Alberta) yielded (1) Sr/Ca ratios from 7.1 to 11.7

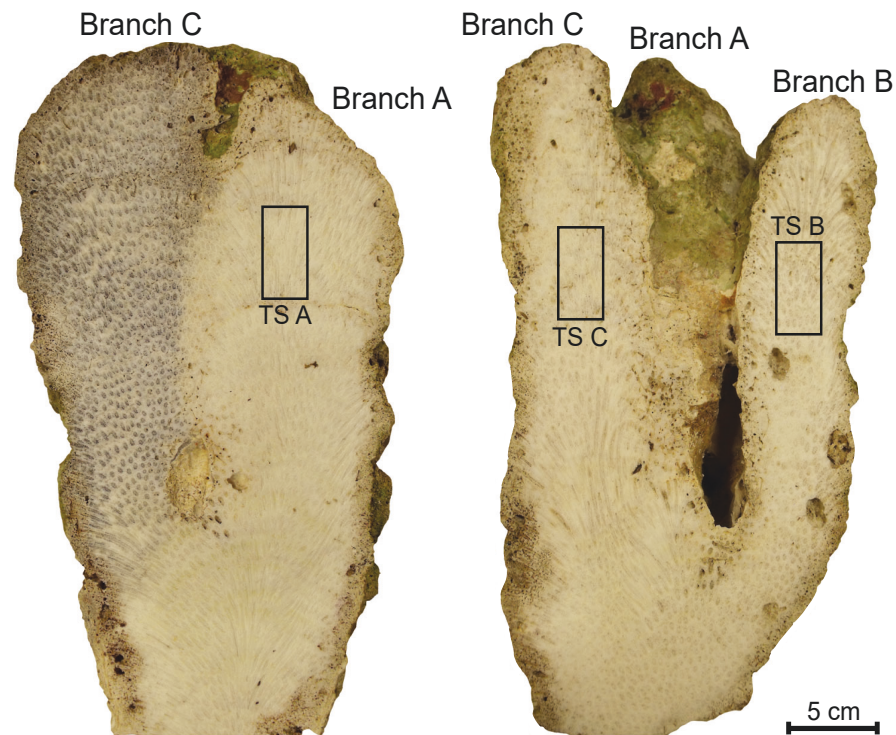


**Fig. 2.1.** Cayman coral, *O. annularis*, showing the three branches (A, B, C) and the location where the three thin sections (TS) were taken from (black rectangles). The element/Ca ratios in Dataset II were generated from these thin sections.

mmol/mol, (2) Mg/Ca ratios from 4.4 to 13.7 mmol/mol, (3) U/Ca ratios from 0.6 to 1.3  $\mu\text{mol/mol}$ , (4) Sr-U values from 8.8 to 10.0, (5) Ba/Ca ratios from 5 to 13  $\mu\text{mol/mol}$ , and (6)  $\text{B}^{11}$ /Ca ratios from 0.3 to 0.6 mmol/mol. Analytical uncertainty ( $2\sigma$ ), based on the standard deviations of two internal standards (NIST612 and MACS) run every 10 samples, is  $\pm 0.4$  ppm for Mg and  $\text{B}^{11}$ ,  $\pm 0.8$  ppm for Sr and Ba, and  $\pm 1.9$  ppm for U. Li concentrations were below detection limits.

### 3. Element/Ca geothermometers

The use of element/Ca ratios for determining seawater temperature is based on the premise that the quantity of an element incorporated into the coral skeleton is directly related to the ambient water temperature. Following the successful application of the Sr/

Ca geothermometer (Weber, 1973; Houck et al., 1977; Smith et al., 1979; Beck et al., 1992), other element/Ca proxies, including Mg/Ca, U/Ca, Sr-U, Li/Ca, Li/Mg, Mg/Li, Ba/Ca, and B<sup>11</sup>/Ca, were used to determine seawater temperatures from coral skeletons (e.g., Marshall and McCulloch, 2001; Watanabe et al., 2001; Quinn and Sampson, 2002; McCulloch et al., 2003; Kilbourne et al., 2007; Alibert and Kinsley, 2008; Felis et al., 2009). Although much of this information has been derived from corals grown in aquariums under carefully monitored environmental conditions (e.g., Houck et al., 1977; Smith et al., 1979; Inoue et al., 2007; Reynaud et al., 2007; Armid et al., 2011; Montagna et al., 2014; Gonnee et al., 2017), additional information came from natural corals that grew in areas where seawater temperature had been recorded (e.g., Fallon et al., 2003; Kilbourne et al., 2010; Gagan et al., 2012; Fowell et al., 2016; Alpert et al., 2017).

### 3.1. Sr/Ca ratio

Kinsman and Holland (1969) proposed that the incorporation of Sr and Ca into inorganically precipitated aragonite is a function of water temperature. Subsequently, Weber (1973) highlighted the paleoclimate applications of the Sr/Ca ratio in corals when he showed that there was an inverse relationship between the skeletal Sr/Ca ratio and water temperature. Although the processes responsible for the incorporation of Sr into the coral skeleton are poorly understood (Allison et al., 2011), it may be related to the (1) Sr/Ca activity ratio of seawater, and (2) Sr/Ca distribution coefficient between aragonite and seawater, which is dependent on water temperature (McIntire, 1963; Smith et al., 1979; Beck et al., 1992).

Temporal variations in the Sr/Ca ratio of seawater can generally be ignored because the residence times of Sr and Ca in the oceans are long (Broecker and Peng, 1982), with the Sr/Ca ratio being relatively constant over the last 100,000 years (Beck et al., 1992; Marshall and McCulloch, 2002). The use of Sr/Ca geothermometry is therefore based on the assumption that the Sr/Ca ratio of seawater has remained constant through

time. de Villiers et al. (1994, 1995), however, showed that seawater Sr/Ca ratios can vary locally in response to upwelling, remineralization of organic matter, and the production and dissolution of biogenic  $\text{CaCO}_3$  and celestite. Salinity, however, does not seem to influence the Sr/Ca ratios in coral skeletons (Moreau et al., 2015).

The Sr/Ca geothermometer is based on the notion that during periods of low water temperature, Sr is incorporated into the coral skeleton in preference to Mg (Weber, 1973; Marshall and McCulloch, 2002; Storz et al., 2013). Other studies, however, have argued that the incorporation of Sr into the aragonitic skeleton can also be influenced by photosynthetic activity of the symbionts (Cohen et al., 2001; 2002) and/or the rate of calcification (Ferrier-Pages et al., 2002) that causes changes in the Sr/Ca ratios during a day-night cycle that are not related to water temperature (Meibom et al., 2004). Thus, it has been argued that the calcification/growth rate is a primary factor in the incorporation of Sr into the coral skeleton and must therefore be factored into thermometric calibrations (e.g., Goodkin et al., 2005; 2007; Saenger et al., 2008; Kilbourne et al., 2010). Nevertheless, Sr/Ca geothermometry remains one of the most commonly used paleotemperature proxies.

### 3.2. Mg/Ca ratio

Chave (1954) suggested that the Mg/Ca ratios in the skeletons of many marine organisms, including corals, are positively correlated with water temperature. Subsequently, Oomori et al. (1982) showed that the Mg/Ca ratios along the maximum growth axis of *Porites* showed systematic variations that reflect seasonal changes. This was later confirmed by Hart and Cohen (1996), Mitsuguchi et al. (1996), and Watanabe et al. (2001), for various species of coral, by showing that the Mg/Ca ratios are not affected by other parameters such as salinity and water chemistry.

The factors that control Mg incorporation into coral skeletons are poorly understood (Allison et al., 2011; Gaetani et al., 2011; Fowell et al., 2016). Politi et al.

(2010) and Montagna et al. (2014) suggested that Mg substitutes for Ca, whereas Finch and Allison (2008) argued that an organic binding agent or amorphous calcium carbonate influences Mg incorporation. Although water temperature seems to influence Mg/Ca incorporation into the coral skeleton, the Mg/Ca ratio is strongly influenced by microscale skeletal heterogeneity (Meibom et al., 2004). Ion microprobe imaging has shown that the distribution of Mg varies over scales of  $<10\ \mu\text{m}$ , which corresponds to the layering/build-up of the skeletal fibers (Meibom et al., 2004; 2008). This has, in turn, been attributed to the rate of calcification that is indirectly controlled by water temperature (Reynaud et al., 2007). It has also been argued that Mg is required by the coral to control skeletal growth processes (Cuiff and Dauphin, 2004; Meibom et al., 2004; Inoue et al., 2007). This indicates that Mg incorporation is not a passive process driven simply by changes in the thermodynamic equilibrium between the coral skeleton and the surrounding seawater (Reynaud et al., 2007). Subsequently, Allison and Finch (2007) showed that the Mg/Ca ratio in the coral skeletal is controlled primarily by biological processes that may not be correlated with water temperature. Thus, the use of the Mg/Ca ratio in paleotemperature applications remains questionable (Armid et al., 2011; Siriananskul et al., 2012; Hathorne et al., 2013).

### 3.3. *U/Ca ratio*

Min et al. (1995) demonstrated that the mechanism of U incorporation into the coral skeleton is similar to inorganically precipitated marine aragonite, which is known to incorporate U and Ca as a function of water temperature. Accordingly, Min et al. (1995) developed a U/Ca equation, based on *Porites* collected from New Caledonia, that is based on the inverse relationship between U/Ca and water temperature. Subsequently, Shen and Dunbar (1995) strengthened the application of this geothermometer by demonstrating that U/Ca ratios in multiple hermatypic coral skeletons from Pacific and Caribbean locations displayed annual cyclicality.



Uranium substitution for Ca in the coral skeleton is difficult because of the large differences in ionic radii and valence states between U and Ca (Quinn and Sampson, 2002). Accordingly, it has been argued that U enters the coral skeleton as a complex anion, potentially  $\text{UO}_2(\text{CO}_3)_2^{2-}$  (Swart and Hubbard, 1982; Min et al., 1995; Shen and Dunbar, 1995) or  $\text{UO}_2(\text{CO}_3)_3^{4-}$  (Reeder et al., 2000). The differences in U speciation and crystallographic location in the aragonitic coral skeleton may result in the U/Ca geothermometer being sensitive to water temperature, pH, differences in coral species, extension rates, seawater carbonate concentration/chemistry ( $\text{CO}_3^{2-}$ ,  $\text{CO}_2$ , U/Ca ratio, U concentration), and/or salinity (Min et al., 1995; Shen and Dunbar, 1995; Cardinal et al., 2001; DeCarlo et al., 2015). Nevertheless, the use of U/Ca ratios from coral skeletons has, in some cases, produced ‘good’ paleotemperature reconstructions (Ourbak et al., 2006; Felis et al., 2009).

#### 3.4. Sr-U

Sr-U geothermometry, developed by DeCarlo et al. (2016), is a relatively new method of determining paleotemperatures from coral skeletons. They showed that the combination of Sr/Ca and U/Ca ratios from 14 specimens of *Porites* from the Pacific Ocean produced accurate temperature reconstructions. This is based on the positive correlations that have been reported between Sr/Ca and U/Ca ratios from various coral species (Cardinal et al., 2001; Quinn and Sampson, 2002; Sinclair et al., 2006; Jones et al., 2015). This correlation, however, has not been reported in experimentally precipitated abiogenic aragonite. For inorganically precipitated aragonite, the Sr/Ca ratio is controlled by temperature and is unaffected by the fluid carbonate ion concentration, whereas the U/Ca ratio is controlled by the fluid carbonate ion concentration and not temperature (DeCarlo et al., 2015). Therefore, biomineralization processes, such as Rayleigh fractionation and modification of the calcifying fluid concentrations, are deemed responsible for the correlations between Sr/Ca and U/Ca ratios found in coral skeletons



at a given temperature (DeCarlo et al., 2016). The application of Sr-U geothermometry is believed to reduce the impact of vital effects (specifically Rayleigh fractionation) on the temperature dependence of the Sr/Ca and U/Ca ratios (DeCarlo et al., 2016; Alpert et al., 2017). The effects of interspecies variability in reconstructing water temperature also seems to be reduced by using Sr-U geothermometry (Alpert et al., 2017). Applying Sr-U geothermometry to five species of Pacific and Atlantic corals, Alpert et al. (2017) produced a Sr-U equation that resulted in identical temperature reconstructions to that of the *Porites* based Sr-U equation from DeCarlo et al. (2016). Given that this proxy has only recently been proposed, more research is needed to fully verify the applicability of this geothermometer.

### 3.5. *Li/Ca ratio*

Delaney et al. (1985) suggested that Li/Ca geothermometry could be applied to calcitic foraminifera because the biogenic Li/Ca ratio is negatively correlated with water temperature. The application of this geothermometer has since been expanded to other marine organisms, including corals and brachiopods (e.g., Delaney et al., 1989; Hall and Chan, 2004; Marriott et al., 2004a; 2004b; Hathorne et al., 2013). The fact that Li is conservative in seawater with a residence time of ~1 million years (Edmond et al., 1979; Stoffyn-Egli and Mackenzie, 1984) and is generally not involved in biological activity or particle scavenging (Stoffyn-Egli and Mackenzie, 1984) strengthens its potential use in paleothermometry.

The mechanisms that control Li incorporation into the coral skeleton are poorly understood (Montagna et al., 2014; Fowell et al., 2016). Inorganic aragonite precipitation experiments have shown that Li<sup>+</sup> is incorporated by heterovalent substitution of Ca<sup>2+</sup> into the CaCO<sub>3</sub> structure (Okumura and Kitano, 1986; Marriott et al., 2004b), which may also be the case for the aragonite in coral skeletons. The incorporation of Li/Ca into coral skeletons has been related to water temperature, the internal pH of the calcifying fluid

(Adkins et al., 2003; McCulloch et al., 2012; Hathorne et al., 2013), calcification/growth rates (Thebault et al., 2009), and seawater carbonate ion concentration (Marriott et al., 2004a; 2004b; Thebault et al., 2009; Hathorne et al., 2013; Fowell et al., 2016). Salinity does not seem to affect the Li/Ca ratio (Marriott et al., 2004b). Li/Ca calibrations based on corals have, however, produced reliable paleotemperature reconstructions (Marriott et al., 2004a; Hathorne et al., 2013).

### 3.6. *Li/Mg and Mg/Li ratios*

Li/Mg and Mg/Li geothermometry was originally developed from foraminifera and ahermatypic corals because these ratios appeared to have a better correlation with water temperature than either the Mg/Ca or Li/Ca ratios (Bryan and Marchitto, 2008; Case et al., 2010; Raddatz et al., 2013). Bryan and Marchitto (2008) suggested that the use of Li/Mg and Mg/Li ratios can account for some of the influences that the physiological and/or saturation states have on the Mg/Ca and Li/Ca ratios in foraminifera. The seawater temperature dependence of the Li/Mg and Mg/Li ratios has been further tested and confirmed in various coral species (Case et al., 2010; Hathorne et al., 2013; Raddatz et al., 2013; Montagna et al., 2014; Fowell et al., 2016).

The mechanisms that control the incorporation of Li and Mg into the coral skeleton are poorly understood (Montagna et al., 2014; Fowell et al., 2016). Given that Li and Mg have similar ionic radii and partitioning coefficients, it is possible that these elements may be incorporated into coral skeletal aragonite in a similar manner (Hathorne et al., 2013; Montagna et al., 2014; Fowell et al., 2016). Despite some problems, these equations have been used to reconstruct seawater temperatures from corals (Hathorne et al., 2013; Fowell et al., 2016).

### 3.7. *Ba/Ca ratio*

Hart and Cohen (1996) were the first to investigate the application of the Ba/

Ca ratio for coral geothermometry. In their analysis of *Porites* from South Africa, however, they found that the seasonal variability in the Ba/Ca ratio was amplified, when compared to other proxies, and that the summer samples recorded large spikes in the Ba/Ca ratio. Erroneous Ba/Ca ratios, such as those recorded by Hart and Cohen (1996), have been attributed to non-skeletally bound Ba (Hart and Cohen, 1996), Ba-rich organic matter in the coral skeleton (Pingitore et al., 1988; Tudhope et al., 1996; Quinn and Sampson, 2002), periods of intense upwelling (Lea et al., 1989; Tudhope et al., 1996; Alibert and Kinsley, 2008), river flood plumes (McCulloch et al., 2003), and/or plankton effects driven by summer nutrient influx (Saha et al., 2019). In order to use the Ba/Ca ratios from coral skeletons for paleotemperature reconstructions, the Ba composition of seawater (Cohen and Gaetani, 2010; Gonnee et al., 2017) and all additional sources of Ba must be known (Dietzel et al., 2004). Accounting for the primary solution Ba composition, Dietzel et al. (2004) and Gaetani and Cohen (2006) demonstrated that the Ba/Ca distribution coefficient of inorganic aragonite is negatively correlated with water temperature, and therefore argued that this ratio could be used for coral-based paleothermometry.

The mechanism of Ba<sup>2+</sup> incorporation into aragonite is poorly understood (Kitano et al., 1971; Bath et al., 2000; Dietzel et al., 2004; Gaetani and Cohen, 2006; Gonnee et al., 2017; Mavromatis et al., 2018). Ourbak et al. (2006), Horta-Puga and Carriquiry (2012), and Gonnee et al. (2017) argued for a simple Ca-substitution mechanism based on the similar ionic radii of Ba and Ca. Other studies, however, have shown that the Ba/Ca ratio may also be influenced by the coral growth rate, aragonite saturation state of the calcifying fluid, and partial pressure of CO<sub>2</sub> (Al-Horani et al., 2003; Gaetani et al., 2011; Venn et al., 2013; Gonnee et al., 2017; Allison et al., 2018; Mavromatis et al., 2018). Although the incorporation of Ba/Ca in the coral skeleton can be influenced by many natural factors, this proxy has still been used for paleotemperature determinations (Gonnee et al., 2017).

### 3.8. $B^{11}/Ca$ ratio

Hart and Cohen (1996) demonstrated the presence of seasonal cycles in the  $B^{11}/Ca$  ratios in coral skeletons that seemed to be related to water temperature fluctuations. This was later confirmed by Sinclair et al. (1998) who identified an inverse relationship between coral  $B^{11}/Ca$  ratios and water temperature that they then used to develop  $B^{11}/Ca$  calibrations that produced good agreements between measured water temperature and seasonal variations. The use of this ratio was strengthened by Fallon et al. (1999, 2003) when they demonstrated that the  $B^{11}/Ca$  ratio was unaffected by microscale variability in the skeletal structure of *Porites*.

Boron may be incorporated into the coral skeleton as boric acid ( $B(OH)_3$ ) due to its electrostatic attraction to  $CaCO_3$  (Ichikuni and Kikuchi, 1972; Lahann, 1978; Given and Wilkinson, 1985). The speciation of boron in seawater, however, is influenced by water temperature, alkalinity, salinity, coral biology, and/or various kinetic factors (Vengosh et al., 1991; Hemming and Hanson, 1992; Gaillardet and Allegre, 1995; Fallon et al., 2003). Elevated water temperature and/or pH can increase the proportion of boric acid to borate in the seawater, which in turn affects the borate to carbonate ratio (Hershey et al., 1986; Hemming and Hanson, 1992). Altering the borate to carbonate ratio in seawater can affect the incorporation of  $B^{11}/Ca$  in the coral skeleton and, therefore, the resulting calibration. Regardless of the potential effect of the boron species on the incorporation of  $B^{11}/Ca$  in the coral skeleton, this proxy has been shown to produce ‘good’ reconstructions of water temperature (Fallon et al., 2003).

## 4. Vital effects

Vital effects are commonly invoked to explain the differences between many element/ $Ca$  equations that utilize the same proxies (Siegel, 1960; Weber, 1973; Marshall and McCulloch, 2002; Swart et al., 2002; Meibom et al., 2003; Gallup et al., 2006; Sadler et al., 2016a). This issue becomes increasingly prevalent when the same coral species

from similar environments have given rise to different calibrations (e.g., Quinn and Sampson, 2002; Fallon et al., 2003). Many studies have tried to accommodate the impact that vital effects have on the temperature dependence of element incorporation into the coral skeleton by (1) using multiple coral species and/or multiple specimens of the same species (Siegel, 1960; Cohen et al., 2002; Gallup et al., 2006; Alpert et al., 2016; 2017), (2) determining the most applicable skeletal structure to sample (de Villiers et al., 1994; Alibert and McCulloch, 1997; Allison and Finch, 2004; Gallup et al., 2006; Sinclair et al., 2006; DeLong et al., 2007; Saenger et al., 2008; Cohen and Gaetani, 2010; Brahmī et al., 2012; Sadler et al., 2016a), (3) empirically regressing temperature to a variety of elements to reduce coral-element specific modifications (Quinn and Sampson, 2002; DeCarlo et al., 2016; Alpert et al., 2017), (4) factoring in the effects of coral growth rate (Goodkin et al., 2005; Saenger et al., 2008; Kilbourne et al., 2010), (5) replicating time series with multiple corals from similar and/or the same environment (Cahyarini et al., 2009; Pfeiffer et al., 2009; DeLong et al., 2013; Grove et al., 2013; Flannery et al., 2018), and (6) conducting aquarium studies with corals grown under controlled conditions (Houck et al., 1977; Smith et al., 1979; Inoue et al., 2007; Reynaud et al., 2007; Armid et al., 2011; Montagna et al., 2014; Gonnee et al., 2017). There are, however, still many uncertainties regarding the controls on element uptake in coral skeletons and more research is needed to determine if temperature is truly the primary signal being recorded.

#### *4.1. Interspecies and intraspecies differences*

Interspecies differences between corals have been the primary driving force behind the development of species-specific equations (Table 2.1; e.g., Siegel, 1960; Cohen et al., 2002; Gallup et al., 2006; Alpert et al., 2016). Most calibrations (300/302) are developed as simple linear equations ( $y = mx + b$ ) where the gradient value ( $m$ ) is a function of the rate of change between the element/Ca ratio and water temperature and the intercept value ( $b$ ) represents coral specific conditions (i.e., vital effects,

**Table 2.1.** Number of papers using each coral species to develop the 302 element/Ca geothermometers.

Sample type	Sr/Ca	Sr-U	Mg/Ca	U/Ca	Li/Ca	Li/Mg	Mg/Li	Ba/Ca	B <sup>11</sup> /Ca
<i>Porites</i>	148	2	21	21	5		2	3	3
<i>Siderastrea</i>	12						1		
<i>Acropora</i>	11		1						
<i>Orbicella/</i>	13		1						
<i>Montastrea</i>									
<i>Diploastrea</i>	4								
<i>Diploria</i>	38								
<i>Montipora</i>	1								
<i>Pollicipora</i>	2								
<i>Panova</i>	4								
<i>Goniopora</i>	1								
<i>Astrangia</i>	1								
<i>Favia</i>								1	
<i>Lophelia</i>	1				1		1		
Multiple coral species	2	1				3		3	

environmental variability). Other calibrations (2/302), however, have been developed in exponential form ( $y = be^{mx}$ ) with the gradient and intercept values representing the same parameters as in a linear equation. The fact that there are so few calibrations in the exponential form strengthens the idea that water temperature and element/Ca concentrations in the coral skeleton are linearly correlated.

As might be expected, linear equations developed for different species commonly have different gradients. Different calibrations have also been produced from element/Ca proxies from coral skeletons of the same species (i.e., the >140 *Porites* Sr/Ca equations), which commonly have gradients with similar values but different intercepts (Rosenthal and Linsley, 2006). In these cases, differences in the intercepts have been variously attributed to differences in the age of the coral, size, growth rate, the exact location where the coral grew in the reef, and/or unknown vital effects (Marshall and McCulloch, 2002; Quinn and Sampson, 2002; Fallon et al., 2003; Ourbak et al., 2006; Kilbourne et al., 2010; Grove et al., 2013).

#### 4.2. Size, age, and growth rate

Marshall and McCulloch (2002) suggested that the size of a coral used for paleotemperature calibration is a critical issue because geochemical samples obtained from a small (<20 cm high) coral may result in a different Sr/Ca equation than when a larger coral of the same species is used. Ourbak et al. (2008) illustrated this notion, using two *Porites* specimens from the Republic of Vanuatu that were collected 34 km apart, when they showed that the smaller (~22 cm high) *Porites* had elevated Sr/Ca ratios (indicating cooler water temperatures) relative to the larger (~140 cm high) counterpart. They argued that the geochemistry of the skeleton of the smaller coral was different than the larger specimen due to ‘unknown’ biological processes, possibly related to the age when sexual maturity is reached. Potentially, this issue has significant ramifications for inferring paleotemperatures from fossil corals (Ourbak et al., 2008).

The influence of growth rates on element incorporation into a coral skeleton has long been debated (Weber, 1973; Houck et al., 1977; Smith et al., 1979). Many studies have argued that there is a clear linear relationship between water temperature and the element/Ca content of coral skeletons that is independent of growth rate (Houck et al., 1977; Smith et al., 1979; Shen et al., 1996; Alibert and McCulloch, 1997). Other studies, however, have recognized that the growth rate is an important parameter given that faster growth rates are commonly associated with higher element/Ca ratios and therefore contributes to the variability between equations (Swart, 1981; de Villiers et al., 1994; Mitsuguchi et al., 1996; Ferrier-Pages et al., 2002; Reynaud et al., 2007; Kuffner et al., 2012; Grove et al., 2013). The growth rate of corals has also been linked to the rate of aragonite precipitation (Allison and Finch, 2007), symbiont activity as a function of photosynthesis (Cohen et al., 2001; 2002), modification of the calcifying fluid (Allison and Finch, 2007), and/or 'bio-smoothing' (i.e., the progressive thickening of the coral skeleton throughout the tissue layer (Barnes and Lough, 1993; Gagan et al., 2012), and/or the incorporation of multiple skeletal elements due to shingle-style deposition (Sadler et al., 2015; 2016a)). These factors can affect the incorporation of elements in the coral skeleton, which in turn will impact the geothermometric calibration. Some studies have included a growth rate parameter in their calibrations in order to account for this variability (e.g., Goodkin et al., 2005; Saenger et al., 2008; Kilbourne et al., 2010).

#### *4.3. Coral microstructure*

The sampling path and the type of coral skeletal microstructure used for geothermometric analysis can greatly affect the calculated paleotemperatures (de Villiers et al., 1994; Alibert and McCulloch, 1997; Allison and Finch, 2004; Gallup et al., 2006; Sinclair et al., 2006; DeLong et al., 2007; Nothdurth and Webb, 2007; Saenger et al., 2008; Case et al., 2010; Cohen and Gaetani, 2010; Giry et al., 2010; Brahmi et al., 2012; Raddatz et al., 2013; Sadler et al., 2016a). Microscale compositional variability in trace element content has been documented in many different corals (Allison, 1996; Hart and



Cohen, 1996; Sinclair et al., 1998; Cohen et al., 2001; Meibom et al., 2006; Case et al., 2010; Raddatz et al., 2013; Jones et al., 2015). This variability is commonly related to the type of coral microstructure sampled, for example, centers of calcification have been shown to be significantly enriched in Mg, Ba, and Sr relative to the surrounding skeletal material (Allison and Tudhope, 1992; Allison, 1996; Allison et al., 2001; 2005; Allison and Finch, 2004; Meibom et al., 2004; 2008; Gaetani and Cohen, 2006; Gagnon et al., 2007; Holcomb et al., 2009). Variability has also been attributed to the presence of non-aragonitic mineral phases (i.e., strontianite, barite, witherite) in the coral skeleton that are enriched in trace elements and/or organic materials that contain elevated Sr (Nothdurft et al., 2007), U (Amiel et al., 1973; Min et al., 1995), Ba (Pingitore et al., 1988; Allison and Tudhope, 1992; Hart and Cohen, 1996; Tudhope et al., 1996; Quinn and Sampson, 2002; Sinclair et al., 2006), and/or Mg (Buddemeier et al., 1981).

Sinclair et al. (1998) and Meibom et al. (2004) showed that there is considerable heterogeneity in the coral skeleton due to the shape of the coral calyx. This heterogeneity is exacerbated by the effects of ‘bio-smoothing’, which can result in different material being deposited in the same location but at different times (Cuiff and Dauphin, 2005; Sadler et al., 2015; 2016a). Temporal offsets between the instrument measured water temperatures used for geothermometric calibrations and the deposition of the skeletal material (‘bio-smoothing’) can produce erroneous water temperature reconstructions. It has therefore been argued that samples must be taken from a single type of skeletal material (thecal walls) along the major growth axis of the coral skeleton (Mitsuguchi et al., 1996; Shen et al., 1996; Alibert and McCulloch, 1997; DeLong et al., 2013; Sadler et al., 2015; 2016a).

#### *4.4. Rayleigh fractionation*

Rayleigh fractionation is the discrimination against or preferential incorporation of trace elements into the coral skeleton relative to calcium (Elderfield et al., 1996). In

coral skeletons, this process occurs during the precipitation of aragonite in the calcifying fluid and affects the elements as a function of their partition coefficients (Cohen and McConnaughey, 2003; Gaetani and Cohen, 2006; Allison and Finch, 2007; Gagnon et al., 2007; Case et al., 2010; Cohen and Gaetani, 2010; Hathorne et al., 2013; Raddatz et al., 2013; Fowell et al., 2016; Marchitto et al., 2018) that are, in turn, a function of water temperature (Marriott et al., 2004a; 2004b; 2006; Gaetani et al., 2011). The physiological processes that control the modification of the calcifying fluid are unknown. Gattuso et al. (1998) suggested that enzymes (Ca-ATPase) and ion channels in the basal epithelium significantly alter the composition of the calcifying fluid by actively selecting or rejecting different elements from entering the coral tissue. Elements with comparable ionic radii to Ca may be similar enough for the Ca-ATPase or ion channels to allow those elements into the cell membrane, whereas elements with large ionic radii may be precluded (Cohen et al., 2001; Yu et al., 2004; Gaetani and Cohen, 2006). Conversely, Al-Horani et al. (2003) argued that protein-controlled proton pumping is responsible for modifying the composition of the calcifying fluid. Modification of the elemental composition in the calcifying fluid from that of seawater can potentially affect the element/Ca proxies' ability to reflect external seawater temperatures (Ferrier-Pages et al., 2002).

#### *4.5. Temporal changes in the vital effects*

Temporal changes (daily to seasonal) in the vital effects (Sinclair, 2005; 2006; Alpert et al., 2017), such as changes in symbiont activity (Cohen et al., 2002), coral behaviour (i.e., metabolism and sexual reproduction (Meibom et al., 2003; Reynaud et al., 2007)), or stress (Marshall and McCulloch, 2001) can alter the element/Ca ratios in coral skeletons. Variations in the vital effects themselves have been identified in symbiotic and asymbiotic corals in shallow and deep waters (Sinclair, 2005; 2006). These temporal changes may affect the relationship between the element/Ca ratios and water temperature.

## 5. Geographic variability

Calibrations based on the same proxy and developed for the same coral species on different reefs have commonly produced different equations that reflect different environmental conditions (e.g., Quinn and Sampson, 2002; Fallon et al., 2003; Zinke et al., 2004; Goodkin et al., 2005; Linsley et al., 2006; Saenger et al., 2008; Cahyarini et al., 2009; Pfeiffer et al., 2009). Water temperatures calculated using the same coral skeletal element/Ca proxies from the same reef have also produced contradictory results between corals (Grove et al., 2013) and/or to instrument measured water temperatures (Nurhati et al., 2011; Carilli et al., 2014). This inconsistency is commonly attributed to environmental variability due to the complex array of micro-environments that exist in reef systems (Linsley et al., 2004; Xu et al., 2015; Alpert et al., 2016; Fowell et al., 2016).

The geographic location of the coral used to develop the geothermometric calibrations is critical because the element/Ca ratios are not only affected by water temperature but also by (1) pH/salinity (Min et al., 1995; Shen and Dunbar, 1995; Tanaka et al., 2015), (2) element concentrations in the seawater (de Villiers et al., 1994; Shen and Dunbar, 1995; Swart et al., 2002; Fallon et al., 2003; Sun et al., 2005; Yu et al., 2005; Xu et al., 2015), (3) nutrient levels/water clarity/light availability (Marshall and McCulloch, 2002; Sun et al., 2005; Reynaud et al., 2007), (4) upwelling/tidal pumping (Smith et al., 2006), (5) precipitation/river run-off (Smith et al., 2006; Mitsuguchi et al., 2008; Gonneea et al., 2017), (6) local reef ecology (Quinn and Sampson, 2002; Reynaud et al., 2007), and/or (7) trace element vital effects (Sinclair, 2005; 2006). These parameters should be incorporated into the equation (Dietzel et al., 2004; Gaetani and Cohen, 2006), ruled as insignificant in altering the temperature signal (Watanabe et al., 2001; Marriott et al., 2004b; Moreau et al., 2015), and/or identified as possible causes of extreme element/Ca ratios that must be removed from the dataset before developing the calibration (Shen and Dunbar, 1995; Tudhope et al., 1996; Shaw et al., 1998; Sinclair and McCulloch, 2004; Prouty et al., 2010; Gonneea et al., 2017). Accordingly, the production

of a 'good' calibration requires a detailed characterization of all aspects of the geographic variability as close to the coral as possible. This will ensure that any variability recorded by the element/Ca proxies can be directly correlated to seawater temperature and will not be influenced by other environmental factors that could affect the resultant equation.

## **6. Sampling analytics**

Different analytical procedures have commonly been cited as the underlying reason for variability between coral calibrations that used the same proxy, especially when the calibrations are developed for the same coral species from similar environments. Variations in analytical procedures such as instrument measured water temperatures, coral sampling, and/or methods used to process the data, can also cause substantial differences between the resultant equations.

### *6.1. Instrument measured water temperatures*

The method used to obtain instrument measured water temperatures and the scale of measurement can cause substantial discrepancies between measured water temperature and coral derived water temperature (e.g., Scott et al., 2010, for a review). Water temperature measurements used for calibrations are commonly at a coarse resolution (e.g., satellite 1° x 1° gridded data, near-by monitoring/weather stations >1 km away), at extended time intervals (e.g., ship based monitoring >1 month between observation), and/or are unavailable at remote reef sites (Casey and Cornillon, 1999). Satellite, ship based, and/or near-by weather station data with a coarse resolution, may not represent the water temperatures where the coral actually grew (Pfeiffer et al., 2009; Alpert et al., 2016).

### *6.2. Methodology*

Different studies commonly result in different equations because of the methods used to develop them (Quinn and Sampson, 2002; Swart et al., 2002; Goodkin et al.,

2005; Yu et al., 2005; Correge, 2006; Ourbak et al., 2006; Smith et al., 2006; Reynaud et al., 2007; Saenger et al., 2008; Hathorne et al., 2013). These differences have been related to any of the following issues:

- Sample pre-treatment, where certain cleaning procedures have been shown to cause leaching of specific elements that, in turn, leads to erroneous temperature derivations (Mitsuguchi et al., 2001; Watanabe et al., 2001; Quinn and Sampson, 2002; Elderfield et al., 2006).
- Different methods used to collect the samples, which may vary from micromilling, freezing microtome techniques, to laser aided drilling (e.g., Alibert and McCulloch, 1997; Watanabe et al., 2001; Cohen and Gaetani, 2010b) can significantly impact the resultant equation. Each collection method has advantages and disadvantages depending on the desired sampling resolution, time, and costs involved. Micromilling is typically the most cost-effective technique, as only an automated drill with a computer-controlled positioning system is required to sample the coral skeleton at fixed increments. The freezing microtome technique is less commonly used as it requires a cold room and relies on the coral samples being frozen numerous times during the sampling process. Although laser aided drilling is the most expensive method the fact that the samples can be generated and measured for elemental concentrations at the same time with very high precision makes it the most time efficient.
- The size of the sample varies depending on the width of the coral growth bands and the desired sampling resolution. Typically, studies that use the micromilling or freezing microtome techniques generate samples that are 2 to 5 mm in diameter and 1 to 2 mm deep. Studies that use laser aided drilling typically generate samples with much smaller diameters (<80  $\mu\text{m}$ ) and a higher frequency based on beam size. Sampling at fixed increments is a common practice in element/Ca proxy studies, where samples are usually taken at 0.5 to 2 mm intervals, in

accordance with the desired sampling resolution. This type of fixed sampling, however, can result in growth rate biases (summer vs winter growth) that can lead to over/under sampling specific growth bands. Discrepancies between the size and spacing between samples can result in skewed geochemical signals (de Villiers et al., 1994; Mitsuguchi et al., 1996; Allison and Finch, 2004; Goodkin et al., 2005; Smith et al., 2006; Giry et al., 2010; Sadler et al., 2016a).

- Sample frequency in different studies have varied from fortnightly to yearly. A reduced number of samples used to develop an equation can cause smoothing of the geochemical signal so that it can no longer reflect the fluctuations in yearly seawater temperature (Swart et al., 2002; Sadler et al., 2015). Therefore, Swart et al. (2002) and Sadler et al. (2015) argued that increasing the number of samples per year can reduce the effects of signal smoothing.
- The sampling path and the type of skeletal element used to generate the element/Ca ratios are the most critical aspects of sampling a coral skeleton for geothermometry. These samples should be taken along the maximum growth axis from a single type of skeletal material. Deviation from the major growth axis can lead to the incorporation of different types of skeletal material that do not have element/Ca ratios consistent with the ambient water temperature. Thecal walls are the best skeletal structure to sample for geochemical analysis (Barnes and Lough, 1993; Watanabe et al., 2001) because the element/Ca ratios from these structures most accurately reflects seawater temperature (Mitsuguchi et al., 1996; Shen et al., 1996; Alibert and McCulloch, 1997; DeLong et al., 2013; Sadler et al., 2015; 2016a).
- The type of correlation and regression (i.e., correlation of extremes, correlation between known dates, linear interpolation, exponential interpolation) used to fit the element/Ca proxy data to the measured water temperatures can impact the resulting equation (Sinclair et al., 1998; Cardinal et al., 2001; Swart et al., 2002;

Lough, 2004; Cahyarini et al., 2009; Nurhati et al., 2011; Xu et al., 2015). The most reliable type of correlation is one that pairs known dates from the instrument measured water temperatures and the element/Ca data based on the location of the samples throughout each of the coral growth bands. This method ensures that the measured water temperatures are being correlated with an element/Ca ratio from the same time period. Correlation of extremes relies on the assumption that the extreme values recorded from the measured temperatures relate to those from the element/Ca ratios. This, however, is not always the case (e.g., Hart and Cohen, 1996; Sinclair et al., 1998; 2005) and can lead to asynchronous element/Ca-temperature signals. Linear interpolation is the most common type of regression used, as it has been shown that the incorporation of elements into the coral skeleton may be primarily a function of water temperature (Chave, 1954; Weber, 1973; Min et al., 1995; Hart and Cohen, 1996; Fowell et al., 2016).

- The analytical techniques, such as ICP-MS, ICP-AES, TIMS, SIMS, LA-ICPMS will influence the generation and precision of the geochemical data (Correge, 2006; Ourbak et al., 2006; Alibert and Kinsley, 2008). ICP-MS analyses, for example, show more variability in the element/Ca ratios than the analyses obtained from ICP-AES, and data from TIMS and SIMS offer higher precision than data from LA-ICPMS (Correge, 2006; Ourbak et al., 2006; Alibert and Kinsley, 2008; Giry et al., 2010). In order to use coral skeletal element/Ca proxies for paleotemperature reconstructions, high-precision analytical instruments (i.e., SIMS, TIMS, LA-ICPMS) with the ability to target specific regions of the coral microstructure and produce accurate measurements of the elements with small associated errors (<0.1 wt%) should be used (Beck et al., 1992; de Villiers et al., 1994; McCulloch et al., 1994; Alibert and McCulloch, 1997).
- The interlaboratory standards used for various element analyses of coral skeletons can impede direct comparisons between different studies. Some studies have used

the Davies Reef Coral Standard (DRCS) developed from *Porites mayeri* (Sinclair et al., 1998), the Amedee Island Coral Standard (AICS) developed from *Porites lutea* (Quinn and Sampson, 2002), the New Caledonia Coral Standard (NC20) developed from *Porites* (Correge et al., 2000), and/or an inorganic in-house standard. As there are no universally applied well-characterized interlaboratory coral standards for elemental analysis, discrepancies have resulted from the use of different standard material (Quinn and Sampson, 2002; Ourbak et al., 2006).

Many studies have tried to mitigate the problems that arise from the variability that can be incorporated into the coral based calibration by sampling analytics. Well developed element/Ca equations generally result from analytical protocols, such as laser aided drilling along the maximum growth axis of the thecal walls at fixed increments. This allows for the highest possible resolution (smallest distance between samples) using a high-precision analytical instrument (i.e., SIMS, TIMS, LA-ICPMS) to generate the elemental concentrations from the coral skeleton. Once the element/Ca ratios are generated, they should be correlated to measured temperature based on known dates and then linearly regressed to produce the equation. Additionally, comparisons with other proxy types, multiple corals, and/or replicate time series can reduce coral/location specific variability and result in a more robust equation (Smith et al., 1979; Alibert and McCulloch, 1997; Crowley et al., 1999; Quinn and Sampson, 2002; Stephans et al., 2004; Goodkin et al., 2007; Cahyarini et al., 2009; Pfeiffer et al., 2009; DeLong et al., 2011; 2013; Grove et al., 2013; DeCarlo et al., 2016; Alpert et al., 2017; Flannery et al., 2018). Consistency between studies should be maintained in terms of the (1) sample pre-treatment, resolution, and protocols (Swart et al., 2002; Goodkin et al., 2005; Yu et al., 2005; Smith et al., 2006; Reynaud et al., 2007; Saenger et al., 2008), (2) analytical techniques used (Beck et al., 1992; de Villiers et al., 1994; McCulloch et al., 1994; Alibert and McCulloch, 1997; Correge, 2006; Ourbak et al., 2006; Alibert and Kinsley, 2008), and (3) method of calibration/regression (Sinclair et al., 1998; Cardinal et al., 2001; Swart et al., 2002; Lough, 2004; Cahyarini et al., 2009; Nurhati et al., 2011; Xu



et al., 2015). Using consistent sampling analytics will negate the variability imposed by different methodologies.

## 7. Calculated water temperatures

Three hundred and two published equations, based on the nine most commonly used element/Ca proxies (Supplementary Table 2.1-2.8), were applied to dataset I in order to assess the calculated temperature ( $T_{cal}$ ) generated by each of those equations. Assessment was based on comparisons of the range of  $T_{cal}$  relative to the 18° to 36°C temperature range that is favored by modern corals. An equation is considered applicable if it generates  $T_{cal}$  values that are within the coral growth window temperature (CGT) range and/or if less than 10% of the  $T_{cal}$  values are  $\pm 1^\circ\text{C}$  outside of the CGT range (i.e., 17° to 37°C).

### 7.1. Sr/Ca geothermometry

Sr/Ca geothermometry has been widely applied to corals, with at least 228 Sr/Ca equations being proposed (Supplementary Table 2.1). Although based on various coral species, most were derived from *Porites* (148/228). Application of these equations to the Sr/Ca ratios in dataset I yielded  $T_{cal}$  from  $-507^\circ$  to  $+860^\circ\text{C}$  (Figs. 2.2. 2.3A) with many values significantly outside of the CGT range. The equations of Weber (1973;  $K(\text{Sr}/\text{Ca})$  (distribution coefficient) =  $1.0732 + 0.0024 * \text{SST} - 0.0175 * \text{growth rate (mm/yr)}$ ) with  $T_{cal}$  from 29° to 31°C developed from *Acropora*, Boiseau et al. (1997;  $\text{Sr}/\text{Ca} = 18.20 - 0.330 * \text{SST}$ ) with  $T_{cal}$  from 25° to 33°C developed from *Acropora*, and Cahyarini et al. (2009;  $\text{Sr}/\text{Ca} = 12.82 - 0.150 * \text{SST}$ ) with  $T_{cal}$  from 19° to 37°C developed from *Porites* produced temperatures in the CGT range (Fig. 2.2).

### 7.2. Mg/Ca geothermometry

Application of twenty-two Mg/Ca equations, developed from *Porites*, *Acropora*,

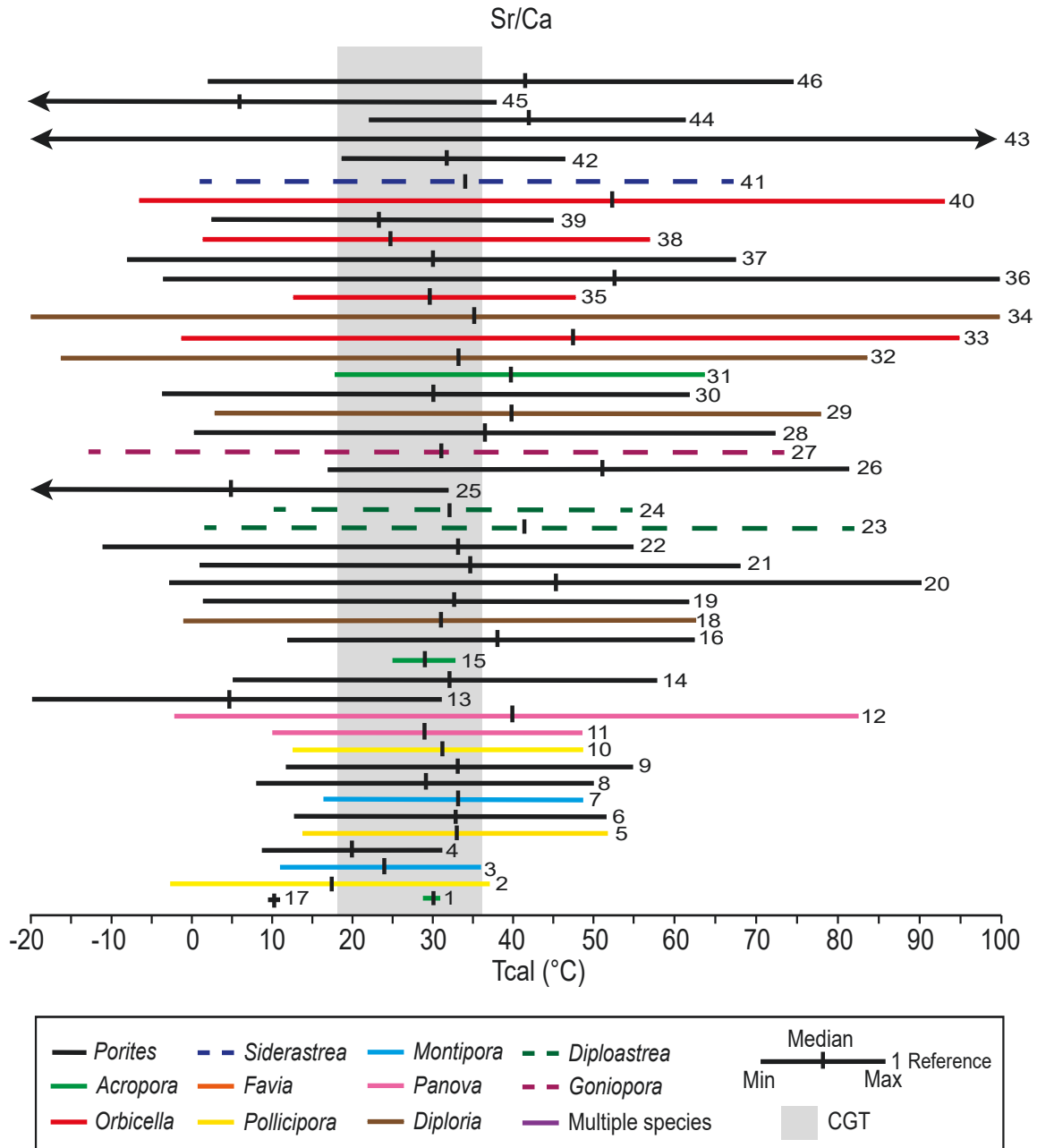


**Fig. 2.2.** Comparison between the calculated temperatures from Dataset I derived from the published Sr/Ca equations and the modern coral growth window temperature range (CGT; shown in grey). Numbers with more than one reference indicate that these equations yielded the same calculated temperature range. Equations from 1- Weber (1973); 2 to 4- Houck et al. (1977); 5 to 7- Smith et al. (1979); 8- Beck et al. (1992); (1994); DeLong et al. (2010); 9- de Villiers et al. (1994); Fallon et al. (1999); Nurhati et al. (2009); 10 and 11- de Villiers et al. (1994); 12- de Villiers et al. (1995); 13- Min

et al. (1995); 14- Mitsuguchi et al. (1996); Shen et al. (1996); Alibert and McCulloch (1997); Bessat (1997); Heiss et al. (1997); Gagan et al. (1998); Sinclair et al. (1998); McCulloch et al. (1999); Correge et al. (2000); Linsley et al. (2000); McCulloch and Esat (2000); Marshall and McCulloch (2001); Correge et al. (2001); Marshall and McCulloch (2002); DeLong et al. (2007); Inoue et al. (2007); Felis et al. (2012); Gagan et al. (2012); Bolton et al. (2014); 15- Boiseau et al. (1997); 16- Schrag (1999); Linsley et al. (2000); Ramos et al. (2017); 17- Wei et al. (2000); Nurhati et al. (2011); Carilli et al. (2014); 18- Cardinal et al. (2001); 19- Quinn and Sampson (2002); Swart et al. (2002); Felis et al. (2004); Stephans et al. (2004); Sun et al. (2005); Correge (2006); Pfeiffer et al. (2006); Mitsuguchi et al. (2008); Flannery et al. (2018); 20- Cohen et al. (2002); Giry et al. (2012); Alpert et al. (2016); 21- Fallon et al. (2003); Calvo et al. (2007); DeLong et al. (2014); Kuffner et al. (2017); 22- Allison and Finch (2004); 23- Bagnato et al. (2004); 24- Correge et al. (2004); 25- Kilbourne et al. (2004); 26- Linsley et al. (2004); 27- Yu et al. (2004); 28- Zinke et al. (2004); 29- Goodkin et al. (2005); Seo et al. (2013); 30- Yu et al. (2005); Cahyarini et al. (2008); Deng et al. (2009); Hetzinger et al. (2006); 31- Ourbak et al. (2006); 32- Gallup et al. (2006); 33- Smith et al. (2006); Flannery and Poore (2013); 35- Goodkin et al. (2007); 36- Saenger et al. (2008); 37- Cahyarini et al. (2009); 38- Pfeiffer et al. (2009); 39- Armid et al. (2011); 40 and 41- DeLong et al. (2011); 42- Siriananskul et al. (2012); Siriananskul and Pumijumnong (2014); Alpert et al. (2016); 43- Grove et al. (2013); von Reumont et al. (2016); 44- Xu et al. (2015); 45- Sadler et al. (2016a); 46- Murty et al. (2018). Arrows indicate values that extend off the scale. All equations are available in Supplementary Table 2.1.

---

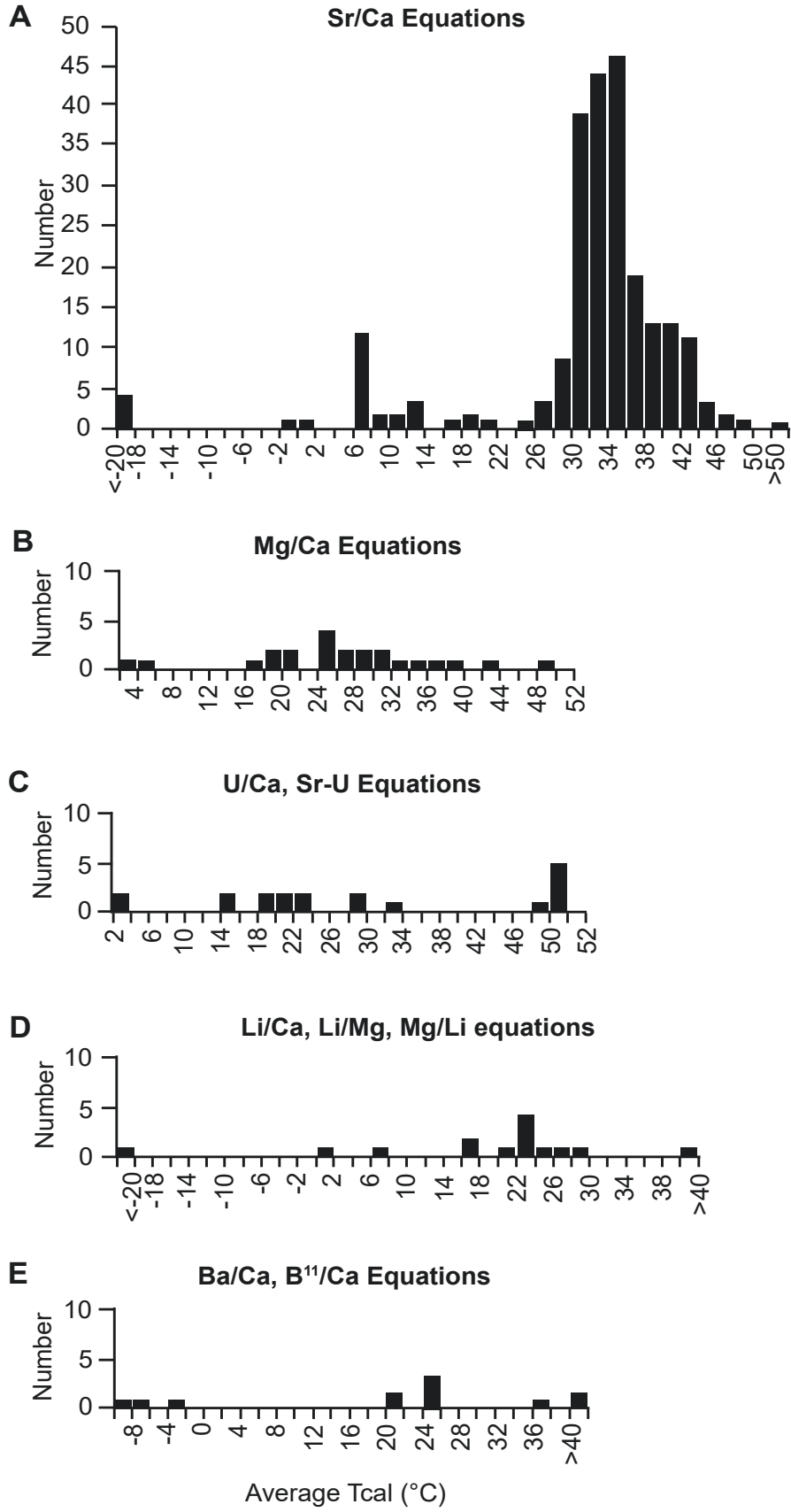


**Fig. 2.3.** Histograms of the average calculated temperatures produced by the 302 published element/Ca equations using Dataset I. (A) Sr/Ca equations. (B) Mg/Ca equations. (C) U/Ca and Sr-U equations. (D) Li/Ca, Li/Mg, and Mg/Li equations. (E) Ba/Ca and B<sup>11</sup>/Ca equations.

---

and *Orbicella* (Supplementary Table 2.2) to dataset I yielded  $T_{\text{cal}}$  from -13° to +69°C (Figs. 2.3B, 2.4A). Only the equation proposed by Watanabe et al. (2001;  $\text{Mg/Ca} = -3.24 + 0.280 * \text{SST}$ ), developed from *Orbicella*, produced  $T_{\text{cal}}$  in the CGT range with values from 21° to 34°C (Fig. 2.4A).

### 7.3. U/Ca geothermometry

Application of the twenty-one U/Ca equations developed from *Porites* (Supplementary Table 2.3) to dataset I yielded  $T_{\text{cal}}$  from 2° to 141°C (Figs. 2.3C, 2.4B). Eight equations resulted in  $T_{\text{cal}}$  in the CGT range, including four equations from Min et al. (1995;  $\text{U/Ca} = 2.23 - 0.047 * \text{SST}$ ;  $\text{U/Ca} = 2.27 - 0.047 * \text{SST}$ ;  $\text{U/Ca} = 2.45 - 0.054 * \text{SST}$ ;  $\text{U/Ca} = 2.11 - 0.043 * \text{SST}$ ) with  $T_{\text{cal}}$  from 17° to 36°C, one equation from Sinclair et al. (1998;  $\text{U/Ca} = 2.24 - 0.046 * \text{SST}$ ) with  $T_{\text{cal}}$  from 18° to 33°C, one equation from Fallon et al. (1999;  $\text{U/Ca} = 2.26 - 0.044 * \text{SST}$ ) with  $T_{\text{cal}}$  from 20° to 35°C, and two equations from Quinn and Sampson (2002;  $\text{U/Ca} = 2.19 - 0.044 * \text{SST}$ ;  $\text{U/Ca} = 2.31 - 0.046 * \text{SST}$ ) with  $T_{\text{cal}}$  from 18° to 35°C (Fig. 2.4B).

### 7.4. Sr-U geothermometry

Three Sr-U equations, developed for *Porites* and various other coral species (Supplementary Table 2.4), when applied to dataset I yielded  $T_{\text{cal}}$  from 23° to 40°C (Figs. 2.3C, 2.4C). Although most calculated temperatures are in the CGT range, one equation from DeCarlo et al. (2016;  $T = -11 * (\text{Sr-U} - 9) + 28.1$ ), developed from *Porites*, and the

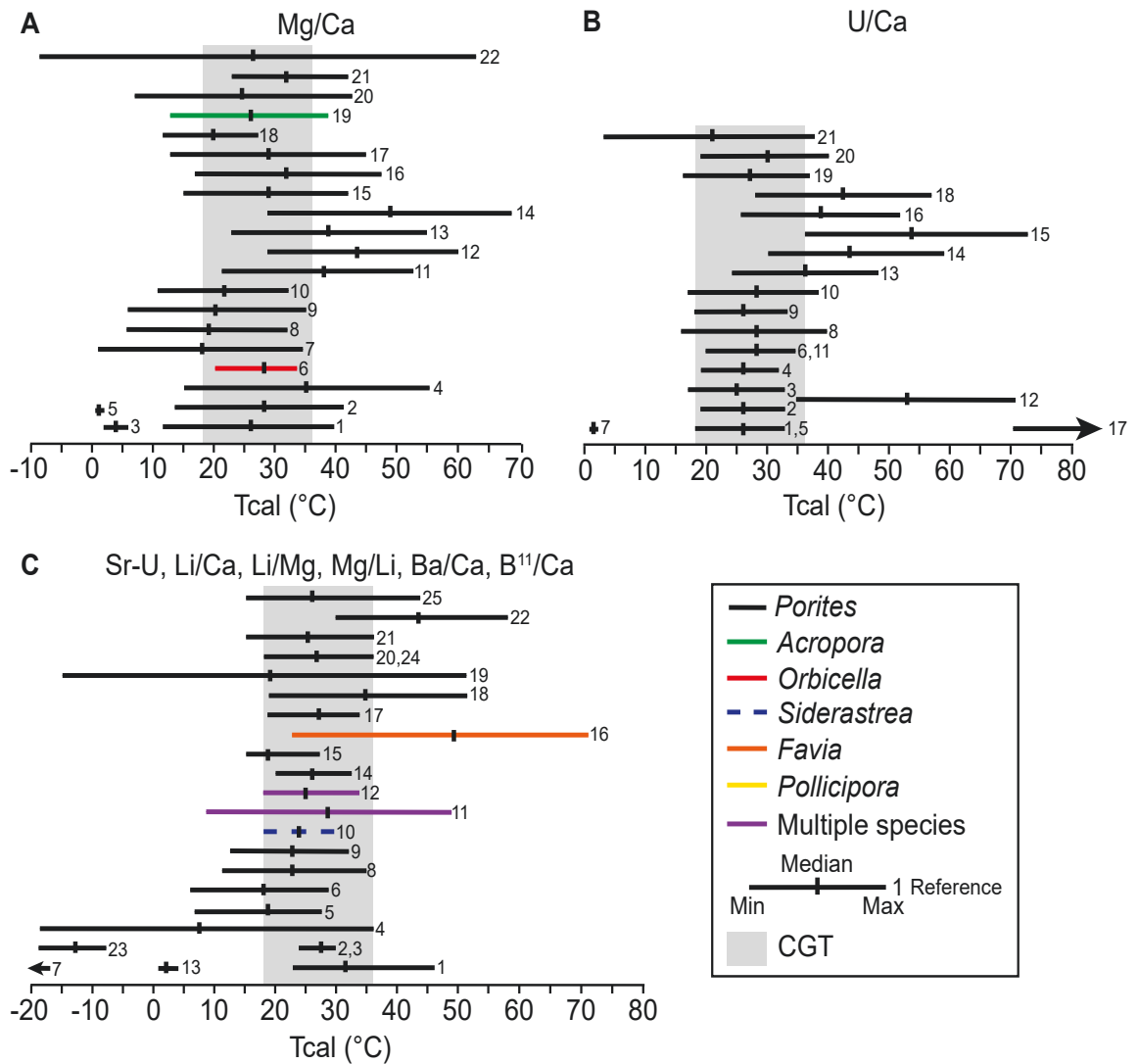


**Fig. 2.4.** Comparison between the calculated temperatures from Dataset I derived from the published element/Ca equations and the modern coral growth window temperature range (CGT; shown in grey). (A) Mg/Ca equations: 1- Mitsuguchi et al. (1996); 2- Mitsuguchi et al. (2001); 3- Sinclair et al. (1998); 4- Fallon et al. (1999); 5- Wei et al. (2000); 6- Watanabe et al. (2001); 7 to 10- Quinn and Sampson (2002); 11 to 16- Fallon et al. (2003); 17- Yu et al. (2005); 18- Ourbak et al. (2006); 19- Reynaud et al. (2007); 20-Armid et al. (2011); 21- Siriananskul et al. (2012); 22- Hathorne et al. (2013). (B) U/Ca equations: 1 to 4- Min et al. (1995); 5- Sinclair et al. (1998); 6- Fallon et al. (1999); 7- Wei et al. (2000); 8 to 11- Quinn and Sampson (2002); 12 to 18- Fallon et al. (2003); 19- Ourbak et al. (2006); 20- Felis et al. (2009); 21- Armid et al. (2011). (C)

Sr-U equations; 1 and 2- DeCarlo et al. (2016); 3- Alpert et al. (2017); Li/Ca equations: 4 to 7- Hathorne et al. (2013); Li/Mg equations: 8 and 9- Hathorne et al. (2013); 10 to 12- Fowell et al. (2016); Mg/Li equations: 13 to 15- Hathorne et al. (2013); Ba/Ca equation: 16- Gonnee et al. (2017); B<sup>11</sup>/Ca equations: 18- Sinclair et al. (1998); 19- Fallon et al. (1999); 20 to 25- Fallon et al. (2003). Arrows indicate values that extend off the scale. All equations are available in Supplementary Tables 2.2 to 2.8.

---

equation from Alpert et al. (2017;  $T = -11 * (\text{Sr-U}) + 126.98$ ), developed from 5 species of Pacific and Atlantic corals, produced  $T_{\text{cal}}$  from 24° to 30°C (Fig. 2.4C).

#### 7.5. Li/Ca geothermometry

Application of five Li/Ca equations, developed using *Porites* (Supplementary Table 2.5), to dataset I resulted in  $T_{\text{cal}}$  from -79° to +155°C (Figs. 2.3D, 2.4C). Given that all of these equations produced  $T_{\text{cal}}$  outside of the CGT range, this geothermometer is not considered further.

#### 7.6. Li/Mg and Mg/Li geothermometry

The eight equations that use Li and Mg ratios to determine SST were developed from *Porites*, *Siderastrea*, and various other coral species (Supplementary Table 2.6). Application to dataset I yielded  $T_{\text{cal}}$  of 9° to 49°C for Li/Mg and 1° to 33°C for Mg/Li (Figs. 2.3D, 2.4C). Two of the Li/Mg equations from Fowell et al. (2016;  $\text{Li/Mg} = -0.10 * \text{SST} + 3.962$ ;  $\text{Li/Mg} = 5.405e-0.05\text{SST}$ ) developed from various coral species produced  $T_{\text{cal}}$  from 18° to 34°C. One of the Mg/Li equations from Hathorne et al. (2013;  $\text{Mg/Li} = -0.40 + 0.04 * \text{SST}$ ) developed from *Porites* produced  $T_{\text{cal}}$  from 20° to 33°C (Fig. 2.4C).

### 7.7. Ba/Ca geothermometry

The only Ba/Ca equation, developed from laboratory grown *Favia* (Supplementary Table 2.7), when applied to dataset I yielded  $T_{\text{cal}}$  of 23° to 71°C (Figs. 2.3E, 2.4C), values that are at the upper end or above the CGT range (Fig. 2.4C). Given that this equation produced  $T_{\text{cal}}$  outside of the CGT range, this geothermometer is not considered further.

### 7.8. B<sup>11</sup>/Ca geothermometry

Six B<sup>11</sup>/Ca equations have been developed from *Porites* (Supplementary Table 2.8) when applied to dataset I yielded  $T_{\text{cal}}$  from -15° to +56°C (Figs. 2.3E, 2.4C). Three equations resulted in  $T_{\text{cal}}$  in the CGT range, including one equation from Sinclair et al. (1998;  $B^{11}/Ca = 1000 - 20.60 * SST$ ) with  $T_{\text{cal}}$  from 19° to 34°C and two equations from Fallon et al. (2003;  $B^{11}/Ca = 9093 - 17.07 * SST$ ,  $B^{11}/Ca = 8952 - 16.50 * SST$ ) with  $T_{\text{cal}}$  from 18° to 36°C (Fig. 2.4C).

## 8. Cayman coral temperature reconstruction

Of the 302 element/Ca equations listed in the Supplementary files, the 17 that resulted in temperatures in the CGT range (17° to 37°C) for dataset I were then applied to dataset II (Fig. 2.2). Dataset II consists of element/Ca ratios from one specimen of *O. annularis* that was collected from offshore George Town, Grand Cayman, at a water depth of 20 m. This coral, 42 cm high and 28 cm in diameter, is characterized by three branches that are 6 to 9 cm wide and up to 18 cm long. Based on growth band counting from the known death year, this coral grew between 1962 and 2014 (Booker et al., 2019). One thin section from each branch of the coral (Fig. 2.1), included the skeleton that grew between 1996 and 2002 and therefore corresponds to the time span for which instrument measured water temperatures are available (NOAA, 2018; Booker et al., 2019). During



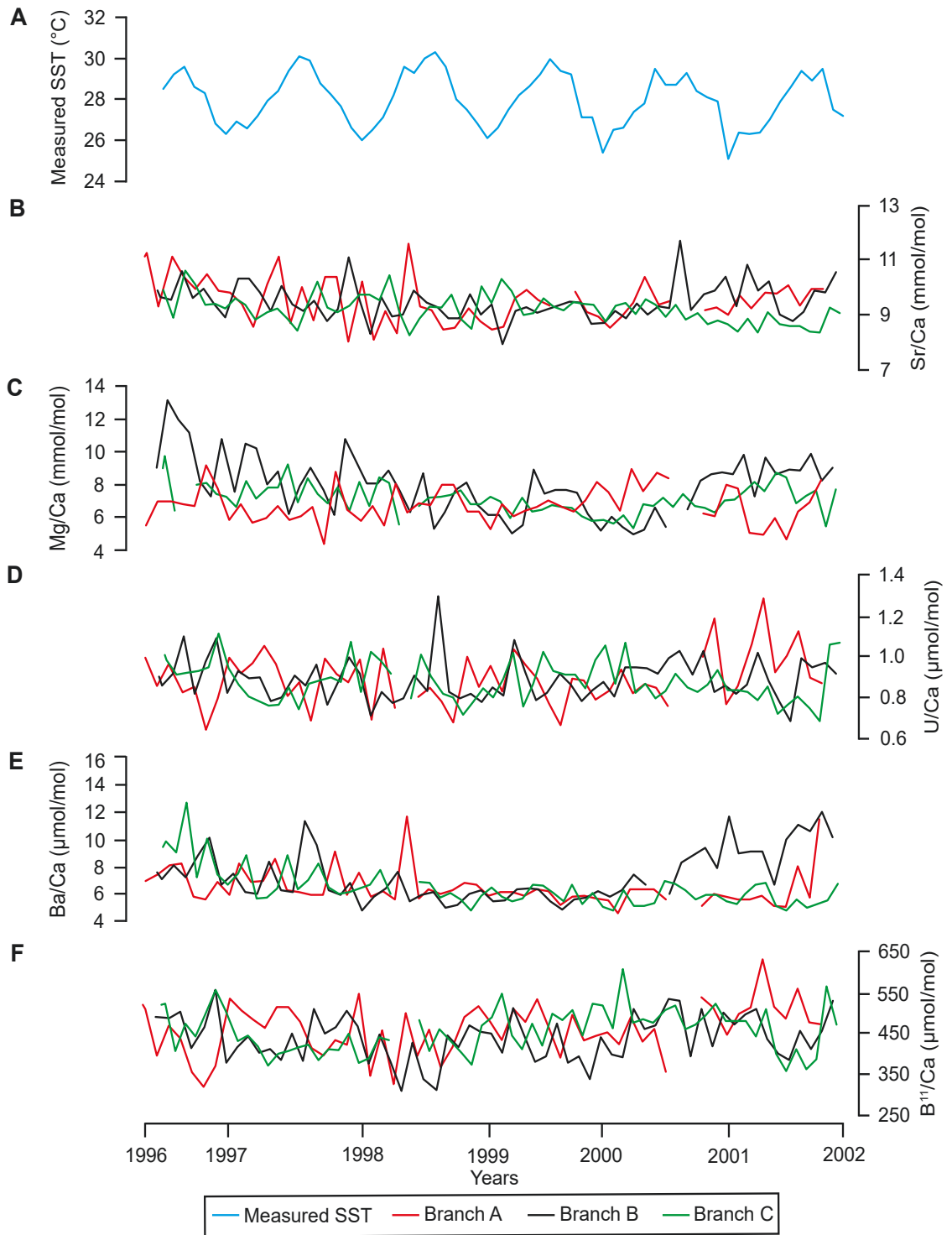


**Fig. 2.5.** (A) Measured water temperatures (1 m water depth) from offshore George Town, near Magic Reef. (B) Sr/Ca ratios, (C) Mg/Ca ratios, (D) U/Ca ratios, (E) Ba/Ca ratios, and (F) B<sup>11</sup>/Ca ratios from branches A, B, and C of the Cayman coral. Seasonal cycles are clearly developed in the Sr/Ca, U/Ca, and B<sup>11</sup>/Ca ratios.

this period T varied from 25° to 31°C with an average of 28°C.

### 8.1. Sr/Ca geothermometry

Application of the three viable Sr/Ca equations (i.e., Weber, 1973; Boisseau et al., 1997; Cahyarini et al., 2009) to dataset II yielded  $T_{cal}$  of 8° to 33°C (Fig. 2.6). The equation from Cahyarini et al. (2009) produced  $T_{cal}$  (8° to 33°C) that extended below the CGT range and the measured SST from Grand Cayman. Although the equation from Weber (1973) produced  $T_{cal}$  from 28° to 31°C, these temperatures do not include values that corresponded to the full SST range for the area where the coral grew. The equation of Boisseau et al. (1997) yielded  $T_{cal}$  from 20° to 31°C with an average of 27°C, which are consistent with the measured SST for the area (Fig. 2.7).

### 8.2. Mg/Ca geothermometry

Applying the one viable Mg/Ca equation (i.e., Watanabe et al., 2001) to dataset II yielded  $T_{cal}$  of 27° to 61°C, with most temperatures at the upper end or above the CGT range and the measured  $T_{cal}$  from Grand Cayman. This equation also resulted in the highest degree of variability between the three coral branches when compared to the other element/Ca proxies (Fig. 2.6). It is not surprising that the Mg/Ca calibration did not produce realistic  $T_{cal}$ , as it has been shown that the incorporation of the Mg into the coral skeleton is biologically mediated and not solely related to SST (Sinclair et al., 2006; Allison and Finch, 2007; Montagna et al., 2014). Accordingly, this equation is not considered any further.

### 8.3. U/Ca geothermometry

Application of the eight viable U/Ca equations (i.e., Min et al., 1995; Sinclair et al., 1998; Fallon et al., 1999; Quinn and Sampson, 2002) to dataset II yielded  $T_{cal}$  of 19° to 37°C, values which are consistent with the CGT range. The  $T_{cal}$  derived from the three

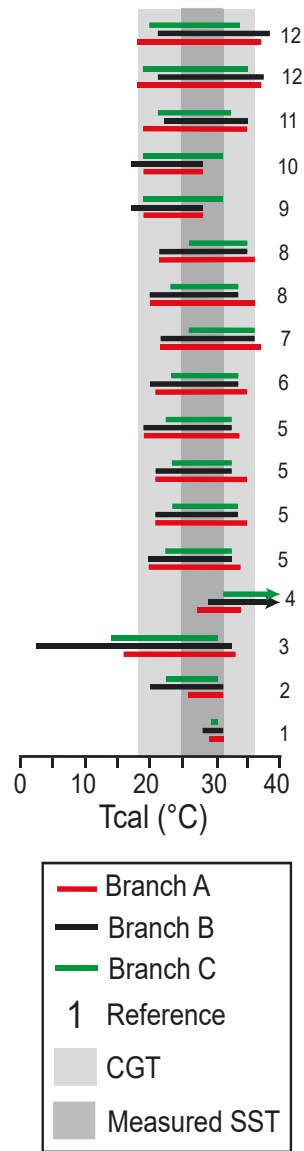


**Fig. 2.6.** Comparison between the calculated temperatures from Dataset II (Cayman coral branches A, B, and C) using the 17 ‘best’ equations as determined from Dataset I. Equations from: 1-Weber (1973); 2- Boiseau et al. (1997); 3- Cahyarini et al. (2009); 4- Watanabe et al. (2001); 5- Min et al. (1995); 6- Sinclair et al. (1998); 7- Fallon et al. (1999); 8- Quinn and Sampson (2002); 9- DeCarlo et al. (2016); 10- Alpert et al. (2017); 11- Sinclair et al. (1998); 12- Fallon et al. (2003). Dark grey shading represents the measured SST from Grand Cayman and the light grey shading represents the coral growth window temperature range (CGT). Arrows indicate values that extend off the scale.

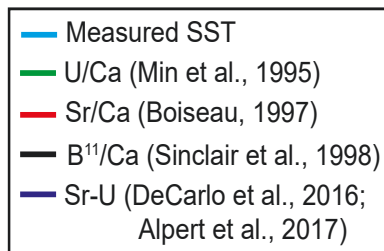
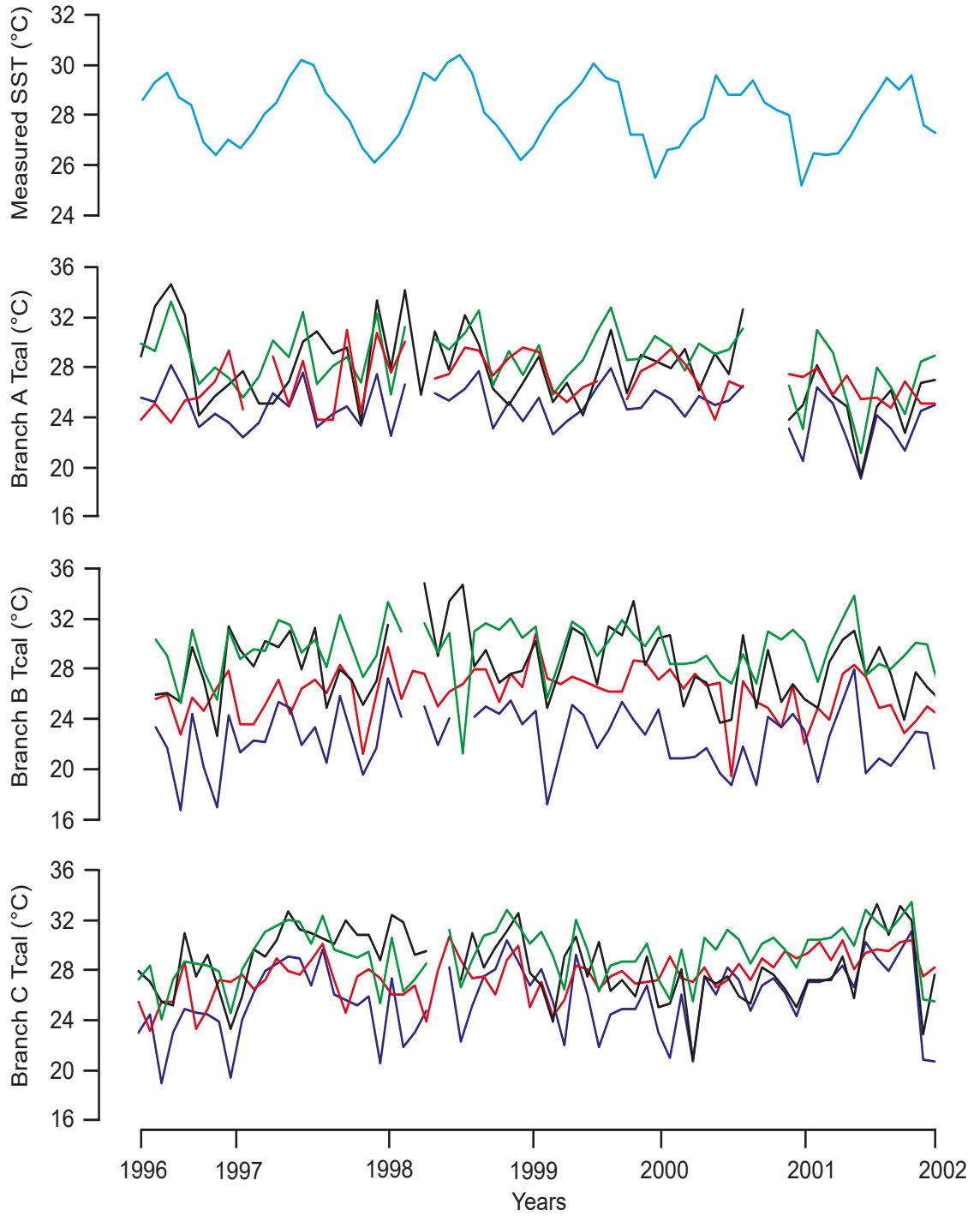


**Fig. 2.7.** (A) Measured water temperatures (1 m water depth) from offshore George Town, near Magic Reef. (B) Calculated temperatures for Cayman coral branch A. (C) Calculated temperatures for Cayman coral branch B. (D) Calculated temperatures for Cayman coral branch C. The coral branches show broadly seasonal cycles, with those from branch A displaying the most consistent cyclicity. Red line indicates the temperatures calculated using the Sr/Ca equation of Boisseau (1997). Green line indicates the temperatures calculated using the U/Ca equation of Min et al. (1995). Black line indicates the temperatures calculated using the B<sup>11</sup>/Ca equation of Sinclair et al. (1998). Blue line indicates the temperatures calculated using the Sr-U equations of DeCarlo et al. (2016) and Alpert et al. (2017).

---

coral branches were consistent with each other (Fig. 2.6). The equations from Sinclair et al. (1998), Fallon et al. (1999), and Quinn and Sampson (2002) resulted in slightly higher  $T_{\text{cal}}$  (20° to 37°C), whereas three equations from Min et al. (1995) produced slightly lower  $T_{\text{cal}}$  (19° to 34°C). The other equation from Min et al. (1995;  $U/Ca = 2.45 - 0.054 * SST$ ) resulted in  $T_{\text{cal}}$  from 21° and 33°C with an average of 29°C, values that are consistent with the measured SST from Grand Cayman (Fig. 2.7).

#### 8.4. Sr-U geothermometry

The two viable Sr-U equations (i.e., DeCarlo et al., 2016; Alpert et al., 2017) yielded  $T_{\text{cal}}$  of 17° to 31°C (average of 27°C), with similar values between the two equations for each coral branch (Fig. 2.6). Both equations produced temperatures that are consistent with the measured SST from Grand Cayman and the CGT range (Fig. 2.7).

#### 8.5. Li based geothermometry

The three Li based equations could not be tested with the Cayman coral data

because Li was below detection limits.

### 8.6. $B^{11}/Ca$ geothermometry

Applying the three  $B^{11}/Ca$  equations (i.e., Sinclair et al., 1998; Fallon et al., 2003) to dataset II yielded  $T_{cal}$  of 18° to 38°C (Fig. 2.6). The two equations from Fallon et al. (2003) resulted in  $T_{cal}$  that extended beyond the CGT range, whereas the equation of Sinclair et al. (1998) yielded  $T_{cal}$  from 19° to 35°C with an average of 27°C. The  $B^{11}/Ca$  temperature profiles derived from the three branches of the Cayman coral, are highly variable when compared to the measured SST from Grand Cayman (Fig. 2.7). This discrepancy may be due to the fact that the  $B^{11}/Ca$  ratio is not only responsive to the SST but also to the alkalinity and salinity of the surrounding seawater (Sinclair et al., 1998).

### 8.7. The 'best' equations

Application of 302 published element/Ca equations to dataset I and then applying the 17 viable equations to dataset II indicates that the equations from Boiseau et al. (1997) for Sr/Ca, Min et al. (1995) for U/Ca, DeCarlo et al. (2016) and Alpert et al. (2017) for Sr-U, and Sinclair et al. (1998) for  $B^{11}/Ca$  produced temperatures that were in the CGT range (17° to 37°C) and measured SST (25° to 31°C) from Grand Cayman. The temperature profiles from each of the coral branches display somewhat seasonal cycles similar to the measured SST from Grand Cayman. There are, however, some differences between the  $T_{cal}$  calculated from the three coral branches. The Sr/Ca and Sr-U equations record generally cool  $T_{cal}$  (20° to 31°C and 17° to 31°C, respectively) whereas the  $B^{11}/Ca$  equation records generally warm  $T_{cal}$  (19° to 35°C) when compared to the other equations (Figs. 2.6, 2.7). The U/Ca equation, however, yielded  $T_{cal}$  (21° to 33°C) that are not only in the CGT range and measured SST from Grand Cayman, but also resulted in the most consistent  $T_{cal}$  profiles between the three coral branches and the measured SST in terms of seasonal fluctuations (Fig. 2.7). Slight variations in  $T_{cal}$  between the three coral branches

may be related to (1) differences in growth rates and/or tissue thickness of the three branches (Weber, 1973; de Villiers et al., 1994; Gallup et al., 2006; Alibert and Kinsley, 2008; Cohen and Gaetani, 2010; Sadler et al., 2016a), (2) use of different elemental standards (Quinn and Sampson, 2002; Ourbak et al., 2006), (3) under sampling of the elemental data (Swart et al., 2002; Goodkin et al., 2005; Smith et al., 2006), (4) differences between the water temperature the coral experienced and the measured SST (Marshall and McCulloch, 2002; Goodkin et al., 2005; Cahyarini et al., 2009; Pfeiffer et al., 2009), and/or (5) uncertainties associated with the element data that contributes to an overestimation of  $T_{cal}$  (Alpert et al., 2017).

Underpinning the studies by Min et al. (1995), Boiseau et al. (1997), Sinclair et al. (1998), DeCarlo et al. (2016), and Alpert et al. (2017) that produced the ‘best’ equations was a thorough characterization of the environmental conditions that influenced the coral growth. These parameters included local daily SST and salinity measurements, analyses of the seawater elemental and isotopic concentrations at the reef site, and the influence of tidal/fresh-water exchange. These studies also used similar methodologies with continuous sampling along the maximum growth axis of the coral, similar sampling resolutions (by-monthly to monthly), comparison of the elemental proxy to at least one other temperature proxy and coral specimen, and use of similar high precision analytical techniques (TIMS and/or LA-ICP-MS).

## **9. Discussion**

Long term monitoring of the temperature regimes in the tropical oceans is critical to understanding how these oceans will respond to global warming. Such long-term records, however, are sparse, at low resolution, and/or semi-continuous in temporal coverage (Barnett et al., 1992). The development of element/Ca geothermometry from coral skeletons, as opposed to the traditional method of oxygen isotope geothermometry, has produced a suite of geothermometers that are generally regarded as being reliable

for determining past SST in tropical regions. Many studies have used element/Ca geothermometry in conjunction with  $\delta^{18}\text{O}$  geothermometry to calculate  $\delta^{18}\text{O}_{\text{water}}$  values, which can be used as a measure of sea surface salinity, from modern and fossil corals (e.g., Kilbourne et al., 2004; 2007; 2010; Ayling et al., 2006; Correge, 2006; Booker et al., 2019; 2020). Geochemical analyses of corals have commonly been used to reconstruct SST because of the large array of elements that are incorporated in their aragonitic skeletons. Corals are ideal for this purpose because they can grow for up to 1000 years and therefore have the potential of yielding long-term high-resolution SST records. In contrast, other organisms such as foraminifera, brachiopods, and fish, that have also been used for this purpose, are limited by their short life spans, mobile lifestyles, and their skeletal structures that are highly susceptible to diagenetic alteration. Corals have therefore become one of the most valuable archives for paleoclimate information in remote tropical locations where instrument measured temperatures are rare or non-existent (Gagan et al., 2000; Correge, 2006; Felis et al., 2015; Brocas et al., 2016; Alpert et al., 2017). Accordingly, coral-based element/Ca geothermometry has been widely used to reconstruct past SST records (Guilderson et al., 1994; Beck et al., 1997; Sinclair et al., 1998; McCulloch et al., 1999; 2000; Correge et al., 2001; Watanabe et al., 2001; Hendy et al., 2002; Quinn and Sampson, 2002; Fallon et al., 2003; Correge et al., 2004; Felis et al., 2004; 2009; Ourbak et al., 2006; Kilbourne et al., 2007; Hathorne et al., 2013).

Numerous element/Ca equations have been developed for modern tropical corals. The excessively high number of equations, however, brings into question the validity of element/Ca geothermometry for corals. This is especially true for fossil corals that have no modern analogs. Without reference to modern counterparts, it becomes difficult to determine if the calculated temperatures are truly representative of 'real' temperature fluctuations (Gaetani and Cohen, 2006). Equations used with fossil coral data, however, require an equation produced from a modern coral that is considered to be essentially



the same as the fossil coral (i.e., same species and similar environmental settings; DeLong et al., 2010). Many studies, however, have successfully reconstructed SST using modern corals (e.g., Sinclair et al., 1998; Fallon et al., 1999; 2003; Cardinal et al., 2001; Quinn and Sampson, 2002; Swart et al., 2002; DeLong et al., 2007; Goodkin et al., 2007; Sadler et al., 2016a; Alpert et al., 2017). These well developed modern coral element/Ca calibrations have also been successfully applied to fossil corals as far back as the Pleistocene (e.g., Gagan et al., 1998; McCulloch et al., 1999; Correge et al., 2000; 2001; 2004; Felis et al., 2004; 2015; Kilbourne et al., 2004; Yu et al., 2004; Goodkin et al., 2005; Deng et al., 2009; DeLong et al., 2010; 2012; 2013; Flannery and Poore, 2013; Brocas et al., 2016; Sadler et al., 2016b; 2017; Booker et al., 2020). That only 17 of the 302 element/Ca equations produced  $T_{cal}$  in the CGT range may, in part, reflect the fact that the total range of element/Ca ratios used in Dataset I exceeds the range of values for which specific equations were developed. In many cases use of a narrower range of element/Ca ratios to calculate temperatures leads to the production of ‘realistic’ temperature (Figs. 2.4, 2.5). Many of the published equations, therefore, should only be used to reconstruct SST from corals that have similar element/Ca ratios to those used in the original calibration. Well developed element/Ca equations for a specific modern coral specimen and/or location are underpinned by (1) a thorough assessment of the environmental conditions, (2) a high sampling frequency of the coral growth bands, (3) samples from multiple coral specimens, use of replicate time series, and multiple temperature proxies ( $\delta^{18}O$  and/or element/Ca ratios) from the same sampling transect, and (4) high precision analytical techniques that generate accurate element/Ca ratios.

Although it has been suggested that a ‘universal geothermometer’ cannot be produced due to the innumerable factors that influence the element/Ca signal (Yu et al., 2005), analysis of the data used in this study indicates that some of the published element/Ca equations have the potential of being widely applied. Application of the 302 published element/Ca equations to Dataset I and the 17 viable equations to Dataset II

identified five published element/Ca equations (Boiseau et al. (1997) for Sr/Ca, Min et al. (1995) for U/Ca, DeCarlo et al. (2016) and Alpert et al. (2017) for Sr-U, Sinclair et al. (1998) for B<sup>11</sup>/Ca) that can produce ‘realistic’ temperatures for various species of corals. Therefore, it seems appropriate that future paleoclimate studies that are based on coral skeleton element/Ca geothermometry should attempt to utilize one of these five published element/Ca equations for calculating the SST.

## 10. Conclusions

Modern tropical corals are one of the most valuable paleoclimate archives due to the extensive range of geothermometers that can be used to determine past SST from the element/Ca ratios in their aragonitic skeletons. Given that the tropical oceans are the primary contributor to global climate variability over various time scales, it is critical to understand how the climate in these dynamic regions changes in response to global climate variability. A review of the theory used to develop the element/Ca geothermometers, the causes of variability between the published equations, and an assessment of the calculated temperatures relative to the coral growth window has produced the following important conclusions:

- The results produced from applying the element/Ca ratios derived from published values from 12 species of modern tropical coral (Dataset I) indicate that 17 of the 302 published equations yield temperatures within the coral growth window range.
- Application of the 17 ‘best’ equations to the element/Ca ratios from a modern *O. annularis* from Grand Cayman (Dataset II) identified five equations (Boiseau et al. (1997) for Sr/Ca, Min et al. (1995) for U/Ca, DeCarlo et al. (2016) and Alpert et al. (2017) for Sr-U, Sinclair et al. (1998) for B<sup>11</sup>/Ca) that yielded  $T_{\text{cal}}$  that were consistent with measured SST.
- Some of the published element/Ca equations can be widely applied to various

coral species and it is recommended that priority should be given to these element/Ca equations for calculating the SST in future paleoclimate studies based on coral skeleton element/Ca geothermometry.

In an ideal situation, the only element/Ca equation that should be used for calculating SST is one that utilizes an element/Ca ratio that is solely a function of water temperature. There are, however, still numerous unanswered questions with respect to element/Ca geothermometry. In many cases it is difficult to prove that the variability in the element/Ca ratios is dependent solely on temperature. The most critical questions in this respect are those that relate to the mechanisms that control the uptake of elements into the coral skeleton and how that affects the element/Ca ratio that is used to calculate temperature. Future research should therefore focus on (1) the factors that control element incorporation into the coral skeleton, (2) the reasons why elements are not uniformly incorporated into different skeletal structures, and (3) what causes the differences between corals of the same species (i.e., the effect of coral size, age, and growth rate) and different species.

## REFERENCES

- Adkins, J.F., Boyle, E.A., Curry, W.B., Lutringer, A., 2003. Stable isotopes in deep-sea corals and a new mechanism for “vital effects”. *Geochimica et Cosmochimica Acta* 67, 1129-1143.
- Al-Horani, F., Al-Moghrabi, S.M., De Beer, D., 2003. The mechanism of calcification and its relation to photosynthesis and respiration in scleractinian coral *Glaxea fascicularis*. *Marine Biology* 142, 419-426.
- Alibert, C., McCulloch, M.T., 1997. Strontium/calcium ratios in modern *Porites* corals from the Great Barrier Reef as a proxy for sea surface temperature: calibration of the thermometer and monitoring of ENSO. *Paleoceanography* 12, 345-363.
- Alibert, C., Kinsley, L., 2008. A 170-year Sr/Ca and Ba/Ca coral record from the western Pacific warm pool: 1. What can we learn from an unusual coral record? *Journal of Geophysical Research- Oceans* 113. doi:10.1029/2006JC003979.
- Allison, N., 1996. Geochemical anomalies in coral skeletons and their possible implications for paleoenvironmental analyses. *Marine Chemistry* 55, 367-379.
- Allison, N., Tudhope, A.W., 1992. Nature and significance of geochemical variations in coral skeletons as determined by ion microprobe analysis, 7th International Coral Reef Symposium. 1, pp. 173-178.
- Allison, N., Finch, A.A., 2004. High-resolution Sr/Ca records in modern *Porites lobata* corals: effects of skeletal extension rate and architecture. *Geochemistry Geophysics Geosystems* 5, doi:10.1029/2004GC000696.
- Allison, N., Finch, A.A., 2007. High temporal resolution Mg/Ca and Ba/Ca records in modern *Porites lobata* corals. *Geochemistry Geophysics Geosystems* 8. doi:10.1029/2006GC001477.
- Allison, N., Finch, A.A., Sutton, S.R., Newville, M., 2001. Strontium heterogeneity and speciation in coral aragonite: implications for the strontium paleothermometer. *Geochimica et Cosmochimica Acta* 65, 2669-2676.
- Allison, N., Finch, A.A., Newville, M., Sutton, S.R., 2005. Strontium in coral aragonite: 3.

- Sr coordination and geochemistry in relation to skeletal architecture. *Geochimica et Cosmochimica Acta* 69, 3801-3811.
- Allison, N., Cohen, I., Finch, A.A., Erez, J., EMIF, 2011. Controls on Sr/Ca and Mg/Ca in scleractinian corals: the effects of Ca-ATPase and transcellular Ca channels on skeletal chemistry. *Geochimica et Cosmochimica Acta* 75, 6350-6360.
- Allison, N., Cole, C., Hintz, C., Hintz, K., Finch, A.A., 2018. Influences of coral genotype and seawater pCO<sub>2</sub> on skeletal Ba/Ca and Mg/Ca in cultured massive *Porites* spp. corals. *Palaeogeography, Palaeoclimatology, Palaeoecology* 505, 351-358.
- Alpert, A.E., Cohen, A.L., Oppo, D.W., DeCarlo, T.M., Gove, J., Young, C., 2016. Comparison of equatorial Pacific sea surface temperature variability and trends with Sr/Ca records from multiple corals. *Paleoceanography* 31, 252-265.
- Alpert, A.E., Cohen, A.L., Oppo, D.W., DeCarlo, T.M., Gaetani, G.A., Hernandez-Delgado, E.A., Winter, A., Gonneea, M.E., 2017. Twentieth century warming of the tropical Atlantic captured by Sr-U paleothermometry. *Paleoceanography* 32, 146-160.
- Amiel, A.J., Friedman, G.M., Miller, D.S., 1973. Distribution and nature of incorporation of trace elements in modern aragonitic corals. *Sedimentology* 20, 47-64.
- Arienzo, M.M., Swart, P.K., Pourmand, A., Board, K., Clement, A.C., Murphy, L.N., Vonhof, H.B., Kakuk, B., 2015. Bahamian speleothem reveals temperature decrease associated with Heinrich stadials. *Earth and Planetary Science Letters* 430, 377-386.
- Armid, A., Asami, R., Fahmiati, T., Sheikh, M.A., Fujimura, H., Higuchi, T., Taira, E., Shinjo, R., Oomori, T., 2011. Seawater temperature proxies based on D<sub>Sr</sub>, D<sub>Mg</sub>, and D<sub>U</sub> from culture experiments using the branching coral *Porites cylindrica*. *Geochimica et Cosmochimica Acta* 75, 4273-4285.
- Ayling, B.F., McCulloch, M., Gagan, M.K., Stirling, C.H., Andersen, M.B., Blake, S.G., 2006. Sr/Ca and δ<sup>18</sup>O seasonality in a *Porites* coral from the MIS 9 (339-303 ka) interglacial. *Earth and Planetary Science Letters* 248, 462-475.
- Bagnato, S., Linsley, B.K., Howe, S.S., Wellington, G.M., Salinger, J., 2004. Evaluating

the use of massive coral *Diploastrea heliopora*. *Paleoceanography* 19.

doi:10.1029/2003PA000935.

- Barnes, D.J., Lough, J.M., 1993. On the nature and causes of density banding in massive coral skeletons. *Journal of Experimental Marine Biology and Ecology* 167, 91-108.
- Barnett, T.P., Delgenio, A.D., Ruedy, R.A., 1992. Unforced decadal fluctuations in a coupled model of the atmosphere and ocean mixed layer. *Journal of Geophysical Research-Oceans* 97, 7341-7354.
- Bath, G.E., Thorrold, S.R., Jones, C.M., Campana, S.E., McLaren, J.W., Lam, J.W.H., 2000. Strontium and barium uptake in aragonite otoliths of marine fish. *Geochimica et Cosmochimica Acta* 64, 1705-1714.
- Beck, J.W., Recy, J., Taylor, F., Edwards, L.R., Cabioch, G., 1997. Abrupt changes in early Holocene tropical sea surface temperature derived from coral records. *Nature* 385, 705-707.
- Beck, J.W., Edwards, L., Ito, E., Taylor, F.W., Recy, J., Rougerie, F., Joannot, P., Henin, C., 1992. Sea-surface temperatures from coral skeletal strontium/calcium ratios. *Science* 257, 644-649.
- Beck, J.W., Edwards, R.L., Ito, E., Taylor, F.W., Recy, J., Rougerie, F., Joannot, P., Isdale, P.J., 1994. Erratum. *Science* 264, 891.
- Bessat, F., 1997. Variabilite hydro-climatique et croissance co-rallienne en Polynesie francaise: exemples de l'ile de Moorea et de l'atoll de Mururoa, Paris. Ph.D., University Paris I et EPHE.
- Boiseau, M., Cornu, H., Turpin, L., Juillet-Leclerc, A., 1997. Sr/Ca and  $\delta^{18}\text{O}$  ratios measured from *Acropora nobilis* and *Porites lutea*: is Sr/Ca paleothermometry always reliable? *Earth and Planetary Science Letters* 325, 747-752.
- Bolton, A., Goodkin, N.F., Hughen, K.A., Ostermann, D.R., Vo, S.T., Phan, H.K., 2014. Paired *Porites* coral Sr/Ca and  $\delta^{18}\text{O}$  from the western South China Sea: proxy calibration of sea surface temperatures and precipitation. *Palaeogeography, Palaeoclimatology,*

- Palaeoecology 410, 233-243.
- Booker, S.D., Jones, B., Li, L., 2020. Diagenesis in Pleistocene (80 to 500 ka) corals from the Ironshore Formation: implications for paleoclimate reconstruction. *Sedimentary Geology* 399, doi: 10.1016/j.sedgeo.2020.105615.
- Booker, S.D., Jones, B., Chacko, T., Li, L., 2019. Insights into sea surface temperatures from the Cayman Islands from corals over the last ~540 years. *Sedimentary Geology* 389, 218-240.
- Brahmi, C., Kopp, C., Domart-Coulon, I., Stolarski, J., Meibom, A., 2012. Skeletal growth dynamics linked to trace-element composition in the scleractinian coral *Pocillopora damicornis*. *Geochimica et Cosmochimica Acta* 99, 146-158.
- Brocas, W.M., Felis, T., Obert, J.C., Gierz, P., Lohmann, G., Scholz, D., Kolling, M., Scheffers, S.R., 2016. Last interglacial temperature seasonality reconstructed from tropical Atlantic corals. *Earth and Planetary Science Letters* 449, 418-429.
- Broecker, W.S., Peng, T., 1982. Tracers in the sea. Eldigio Pree, Lamont Doherty Geological Observatory, New York, pp. 702.
- Bryan, S.P., Marchitto, T.M., 2008. Mg/Ca-temperature proxy in benthic foraminifera: new calibrations from the Florida Straits and a hypothesis regarding Mg/Li. *Paleoceanography* 23. doi:10.1029/2007PA001553.
- Buddemeier, R.W., Schneider, R.C., Smith, S.V., 1981. The alkaline earth chemistry of corals, *Proceedings of the 4th International Coral Reef Symposium*, pp. 81-85.
- Cahyarini, S.Y., Pfeiffer, M., Dullo, W., 2009. Improving SST reconstructions from coral Sr/Ca records: multiple corals from Tahiti (French Polynesia). *International Journal of Earth Sciences (Geol Rundsch)*, doi: 10.1007/s00531-008-0323-2.
- Cahyarini, S.Y., Pfeiffer, M., Timm, O., Dullo, W., Garbe-Schonberg, D., 2008. Reconstructing seawater  $\delta^{18}\text{O}$  from paired  $\delta^{18}\text{O}$  and Sr/Ca ratios: methods, error analysis and problems, with examples from Tahiti (French Polynesia) and Timor (Indonesia). *Geochimica et Cosmochimica Acta* 72, 2841-2853.

- Calvo, E., Marshall, J.F., Pelegero, C., McCulloch, M., Gagan, M.K., Lough, J.M., 2007. Interdecadal climate variability in the Coral Sea since 1708 A.D. *Palaeogeography, Palaeoclimatology, Palaeoecology* 248, 109-201.
- Cardinal, D., Hamelin, B., Bard, E., Patzold, J., 2001. Sr/Ca, U/Ca and  $\delta^{18}\text{O}$  records in recent massive corals from Bermuda: relationships with sea surface temperature. *Chemical Geology* 176, 213-233.
- Carilli, J.E., McGregor, H.V., Gaudry, J.J., Donner, S.D., Gagan, M.K., Stevenson, S., Wong, H., Fink, D., 2014. Equatorial Pacific coral geochemical records show recent weakening of the Walker Circulation. *Paleoceanography* 29, 1031-1045.
- Case, D.H., Robinson, L.F., Auro, M.E., Gagnon, A.C., 2010. Environmental and biological controls on Mg and Li in deep-sea scleractinian corals. *Earth and Planetary Science Letters* 300, 215-225.
- Casey, K.S., Cornillon, P., 1999. A comparison of satellite and in situ-based sea surface temperature climatologies. *Journal of Climate* 12, 1848-1863.
- Chave, K.E., 1954. Aspects of the biogeochemistry of magnesium 1. Calcareous marine organisms. *Journal of Geology* 62, 266-283.
- Cohen, A.L., McConnaughey, T.A., 2003. Geochemical perspectives on coral mineralization. In: Dove, P.M., Yorer, J.J.D., Weiner, S. (Eds.), *Biom mineralization*. Mineralogy Society of America, Washington, DC, pp. 37.
- Cohen, A.L., Gaetani, G.A., 2010. Ion partitioning and the geochemistry of coral skeletons: solving the mystery of the vital effect. In: Prieto, M., Stoll, H.M., *Mineralogy, European Mineralogy Union Notes in* (Eds.), *Ion partitioning in ambient-temperature aqueous systems*. European Mineralogy Union, Vienna, pp. 377-397.
- Cohen, A.L., Layne, G.D., Hart, S.R., Lobel, P.S., 2001. Kinetic control of skeletal Sr/Ca in a symbiotic coral: implications for the paleotemperature proxy. *Paleoceanography* 16, 20-26.
- Cohen, A.L., Owens, K.E., Layne, G.D., Shimizu, N., 2002. The effect of algal symbionts on the



- accuracy of Sr/Ca paleotemperatures from coral. *Science* 296, 331-333.
- Correge, T., 2006. Sea surface temperature and salinity reconstruction from coral geochemical tracers. *Palaeogeography, Palaeoclimatology, Palaeoecology* 232, 408-428.
- Correge, T., Deleroix, T., Recy, J., Beck, W.C., Cabioch, G., Le Cornec, F., 2000. Evidence for stronger El Nino-Southern Oscillation (ENSO) events in a mid-Holocene massive coral. *Paleoceanography* 15, 465-470.
- Correge, T., Quinn, T., Delcroix, T., Le Cornec, F., Recy, J., Cabioch, G., 2001. Little Ice Age sea surface temperature variability in the southwest tropical Pacific. *Geophysical Research Letters* 28, 3477-3480.
- Correge, T., Gagan, M.K., Beck, J.W., Burr, G.S., Cabloch, G., Le Cornec, F., 2004. Interdecadal variation in the extent of South Pacific tropical waters during the Younger Dryas event. *Nature* 428, 927-929.
- Crowley, T.J., Quinn, T.M., Hyde, W.T., 1999. Validation of coral temperature calibrations. *Paleoceanography* 14, 605-615.
- Cuiff, J., Dauphin, Y., 2004. Associated water and organic compounds in coral skeletons: quantitative thermogravimetry coupled to infrared absorption spectrometry. *Geochemistry Geophysics Geosystems* 5. doi:10.1029/2004GC000783.
- Cuiff, J., Dauphin, Y., 2005. The environment recording unit in coral skeletons- a synthesis of structural and chemical evidences for a biochemically driven, stepping-growth process in fibers. *Biogeosciences* 2, 61-73.
- de Villiers, S., Shen, G.T., Nelson, B.K., 1994. The Sr/Ca-temperature relationship in coralline aragonite: influence of variability in  $(\text{Sr}/\text{Ca})_{\text{seawater}}$  and skeletal growth parameters. *Geochimica et Cosmochimica Acta* 58, 197-208.
- de Villiers, S., Nelson, B.K., Chivas, A.R., 1995. Biological controls on coral Sr/Ca and  $\delta^{18}\text{O}$  reconstructions of sea surface temperatures. *Science* 269, 1247-1250.
- DeCarlo, T.M., Gaetani, G.A., Holcomb, M., Cohen, A.L., 2015. Experimental determination of factors controlling U/Ca of aragonite precipitated from seawater: implications for

- interpreting coral skeleton. *Geochimica et Cosmochimica Acta* 162, 151-165.
- DeCarlo, T.M., Gaetani, G.A., Cohen, A.L., Foster, G.L., Alpert, A.E., Stewart, J.A., 2016. Coral Sr-U thermometry. *Paleoceanography* 31, 626-638.
- Delaney, M.L., Be, A.W.H., Boyle, E.A., 1985. Li, Sr, Mg, and Na in foraminiferal calcite shells from laboratory culture, sediment traps, and sediment cores. *Geochimica et Cosmochimica Acta* 49, 1327-1341.
- Delaney, M.L., Popp, B.N., Lepzelter, C.G., Anderson, T.F., 1989. Lithium-to-calcium ratios in modern, Cenezoic, and Paleozoic articulate brachiopod shells. *Paleoceanography* 4, 681-691.
- DeLong, K.L., Quinn, T.M., Taylor, F.W., 2007. Reconstructing twentieth-century sea surface temperature variability in the southwest Pacific: a replication study using multiple coral Sr/Ca records from New Caledonia. *Paleoceanography* 22. doi:10.1029/2007PA001444.
- DeLong, K.L., Quinn, T.M., Shen, C., Lin, K., 2010. A snapshot of climate variability at Tahiti at 9.5 ka using a fossil coral from IODP Expedition 310. *Geochemistry Geophysics Geosystems* 11. doi:10.1029/2009GC002758.
- DeLong, K.L., Flannery, J.A., Maupin, C.R., Poore, R.Z., Quinn, T.M., 2011. A coral Sr/Ca calibration and replication study of two massive corals from the Gulf of Mexico. *Palaeogeography, Palaeoclimatology, Palaeoecology* 307, 117-128.
- DeLong, K.L., Quinn, T.M., Taylor, F.W., Shen, C., Lin, K., 2013. Improving coral-based paleoclimate reconstructions by replicating 350 years of coral Sr/Ca variations. *Palaeogeography, Palaeoclimatology, Palaeoecology* 373, 6-24.
- DeLong, K.L., Flannery, J.A., Poore, R.Z., Quinn, T.M., Maupin, C.R., Lin, K., She, C., 2014. A reconstruction of sea surface temperature variability in the southeastern Gulf of Mexico from 1734 to 2008 C.E. using cross-dated Sr/Ca records from the coral *Siderastrea siderea*. *Paleoceanography* 29, 403-422.
- Deng, W., Liu, X., Wei, G., Zeng, T., Xie, L., Zhao, J., 2017. A comparison of the climates of the Medieval Climate Anomaly, Little Ice Age, and Current Warm Period reconstructed

- using coral records from the northern South China Sea. *Journal of Geophysical Research: Oceans* 122, 264-275.
- Deng, W., Wei, G., Li, X., Yu, K., Zhao, J., Sun, W., Lui, Y., 2009. Paleoprecipitation record from coral Sr/Ca and  $\delta^{18}\text{O}$  during the mid Holocene in the northern South China Sea. *The Holocene* 19, 811-821.
- Dietzel, M., Gussone, N., Eisenhauer, A., 2004. Co-precipitation of  $\text{Sr}^{2+}$  and  $\text{Ba}^{2+}$  with aragonite by membrane diffusion of  $\text{CO}_2$  between 10 and  $50^\circ\text{C}$ . *Chemical Geology* 203, 139-151.
- Edmond, J.M., Measures, C., McDuff, R.E., Chan, L.H., Collier, R., Grant, B., Gordon, L.I., Corliss, J.B., 1979. Ridge crest hydrothermal activity and the balances of the major and minor elements in the ocean: the Galapagos data. *Earth and Planetary Science Letters* 46, 1-18.
- Elderfield, H., Bertram, C.J., Erez, J., 1996. Biomineralization model for the incorporation of trace elements into foraminiferal calcium carbonate. *Earth and Planetary Science Letters* 142, 409-423.
- Elderfield, H., Yu, J., Anand, P., Kiefer, T., Nyland, B., 2006. Calibrations for benthic foraminiferal Mg/Ca paleothermometry and the carbonate ion hypothesis. *Earth and Planetary Science Letters* 250, 633-649.
- Evans, M.N., Fairbanks, R.G., Rubenstone, J.L., 1999. The thermal oceanographic signal of El Niño reconstructed from a Kiritimati Island coral. *Journal of Geophysical Research* 104, 409-421.
- Fallon, S.J., McCulloch, M., Alibert, C., 2003. Examining water temperature proxies in *Porites* corals from the Great Barrier Reef: a cross-shelf comparison. *Coral Reefs* 22, 389-404.
- Fallon, S.J., McCulloch, M., van Woesik, R., Sinclair, D.J., 1999. Corals at their latitudinal limits: laser ablation trace element systematics in *Porites* from Shirigai Bay, Japan. *Earth and Planetary Science Letters* 172, 221-238.
- Fegyveresi, J.M., Alley, R.B., Fitzpatrick, J.J., Cuffey, K.M., McConnell, J.R., Voigt, D.E., Spencer, M.K., Stevens, N.T., 2016. Five millennia of surface temperatures and

- ice core bubble characteristics from the WAIS Divide deep core, West Antarctica. *Paleoceanography* 31, 416-433.
- Felis, T., Suzuki, A., Kuhnert, H., Dima, M., Lohmann, G., Kawahata, H., 2009. Subtropical coral reveals abrupt early-twentieth-century freshening in the western North Pacific Ocean. *Geology* 37, 527-530.
- Felis, T., Lohmann, G., Kuhnert, H., Lorenz, S.J., Scholz, D., Patzold, J., Al-Rousan, S., Al-Moghrabi, S.M., 2004. Increased seasonality in Middle East temperatures during the last interglacial period. *Nature* 429, 164-168.
- Felis, T., Giry, C., Scholz, D., Lohmann, G., Pfeiffer, M., Patzold, J., Kolling, M., Scheffers, S.R., 2015. Tropical Atlantic temperature seasonality at the end of the last interglacial. *Nature: Communications* 6, doi: 10.1038/ncomms7159.
- Felis, T., Merkel, U., Asami, R., Deschamps, P., Hathorne, E., Kolling, M., Bard, E., Cabioch, G., Durand, N., Prange, M., 2012. Pronounced interannual variability in tropical South Pacific temperatures during Heinrich Stadial 1. *National Communication* 3. doi: 10.1038/ncomms1973.
- Fensterer, C., Scholz, D., Hoffmann, D.L., Spotl, C., Pajon, J.M., Mangini, A., 2012. Cuban stalagmite suggests relationship between Caribbean precipitation and the Atlantic Multidecadal Oscillation during the past 1.3ka. *Holocene* 22, 1405-1412.
- Ferrier-Pages, C., Boisson, F., Allemand, D., Tambutte, E., 2002. Kinetics of strontium uptake in the scleractinian coral *Stylophora pistillata*. *Marine Ecology - Progress Series* 245, 93-100.
- Finch, A.A., Allison, N., 2008. Mg structural state in coral aragonite and implications for the paleoenvironmental proxy. *Geophysical Research Letters* 35. doi:10.1029/2008GL033543.
- Flannery, J.A., Poore, R.Z., 2013. Sr/Ca proxy sea-surface temperature reconstructions from modern and Holocene *Montastrea faveolata* specimens from the Dry Tortugas National Park, Florida, U.S.A. *Journal of Coastal Research* 63, 20-31.

- Flannery, J.A., Richey, J.N., Toth, L.T., Kuffner, I.B., Poore, R.Z., 2018. Quantifying uncertainty in Sr/Ca-based estimates of SST from the coral *Orbicella faveolata*. *Paleoceanography and Paleoclimatology* 33, 958-973.
- Fowell, S.E., Sandford, K., Stewart, J.A., Castillo, K.D., Ries, J.B., Foster, G.L., 2016. Intrareef variations in Li/Mg and Sr/Ca sea surface temperature proxies in the Caribbean reef-building coral *Siderastrea siderea*. *Paleoceanography* 31, 1315-1329.
- Gaetani, G.A., Cohen, A.L., 2006. Element partitioning during precipitation of aragonite from seawater: a framework for understanding paleoproxies. *Geochimica et Cosmochimica Acta* 70, 4617-4634.
- Gaetani, G.A., Cohen, A.L., Wang, Z., Crusius, J., 2011. Rayleigh-based, multi-element coral thermometry: a biomineralization approach to developing climate proxies. *Geochimica et Cosmochimica Acta* 75, 1920-1932.
- Gagan, M.K., Dunbar, G.B., Suzuki, A., 2012. The effect of skeletal mass accumulation in *Porites* on coral Sr/Ca and  $\delta^{18}\text{O}$  paleothermometry. *Paleoceanography* 27. doi:10.1029/2011PA002215.
- Gagan, M.K., Ayliffe, L.K., Beck, J.W., Cole, J.E., Druffel, E.R.M., Dunbar, R.B., Schrag, D.P., 2000. New views of tropical paleoclimates from corals. *Quaternary Science Reviews* 19, 45-64.
- Gagan, M.K., Ayliffe, L.K., Hopley, D., Cali, J.A., Mortimer, G.E., Chappell, J., McCulloch, M., Head, M.J., 1998. Temperature and surface-ocean water balance of the Mid-Holocene tropical western Pacific. *Science* 279, 1014-1018.
- Gagnon, A.C., Adkins, J.F., Fernandez, D.P., Robinson, L.F., 2007. Sr/Ca and Mg/Ca vital effects correlated with skeletal architecture in a scleractinian deep-sea coral and the role of Rayleigh fractionation. *Earth and Planetary Science Letters* 261, 280-295.
- Gaillardet, J., Allegre, C.J., 1995. Boron isotopic composition of corals: seawater or diagenesis record? *Earth and Planetary Science Letters* 136, 665-676.
- Gallup, C.D., Olson, D.M., Edwards, L.R., Gruhn, L.M., Winter, A., Taylor, B., 2006. Sr/Ca-sea

- surface temperature calibration in the branching Caribbean coral *Acropora palmata*. Geophysical Research Letters 33. doi: 10.1029/2005GL024935.
- Gattuso, J.P., Frankignoulle, M., Bourge, I., Romaine, S., Buddemeier, R.W., 1998. Effect of calcium carbonate saturation of seawater on coral calcification. Global and Planetary Change 18, 37-46.
- Giry, C., Felis, T., Kolling, M., Scheffers, S., 2010. Geochemistry and skeletal structure of *Diploria strigosa*, implications for coral-based climate reconstruction. Paleogeography. doi: 10.1016/j.palaeo.2010.10.022.
- Giry, C., Felis, T., Kolling, M., Scholz, D., Wei, W., Lohmann, G., Scheffers, S.R., 2012. Mid- to late Holocene changes in tropical Atlantic temperature seasonality and interannual to multidecadal variability documented in southern Caribbean corals. Earth and Planetary Science Letters 331-332, 187-200.
- Given, R.K., Wilkinson, B.H., 1985. Kinetic control of morphology, composition and mineralogy of abiogenic sedimentary carbonates. Journal of Sedimentary Petrology 55, 109-119.
- Gonneea, M.E., Cohen, A.L., DeCarlo, T.M., Charette, M.A., 2017. Relationship between water and aragonite barium concentrations in aquaria reared juvenile corals. Geochimica et Cosmochimica Acta 209, 123-134.
- Goodkin, N.F., Hughen, K.A., Cohen, A.L., 2007. A multicoral calibration method to approximate a universal equation relating Sr/Ca and growth rate to sea surface temperature. Paleoceanography 22. doi:10.1029/2006PA001312.
- Goodkin, N.F., Hughen, K.A., Cohen, A.L., Smith, S.R., 2005. Record of Little Ice Age sea surface temperatures at Bermuda using a growth-dependent calibration of coral Sr/Ca. Paleoceanography 20. doi:10.1029/2005PA001140.
- Gregory, B.R.B., Peros, M., Reinhardt, E.G., Donnelly, J.P., 2015. Middle-late Holocene Caribbean aridity inferred from foraminifera and elemental data in sediment cores from two Cuban lagoons. Palaeogeography, Palaeoclimatology, Palaeoecology 426, 239-241.
- Grove, C.A., Brummer, G.A., Kasper, S., Zinke, J., Pfeiffer, M., Garbe-Schonberg, D., 2013.

- Confounding effects of coral growth and high SST variability on skeletal Sr/Ca: implications for coral paleothermometry. *Geochemistry, Geophysics, Geosystems* 14, 1277-1294.
- Guilderson, T.P., Fairbanks, R.D., Rubenstone, J.L., 1994. Tropical temperature variations since 20,000 years ago: modulating interhemispheric climate change. *Science* 263, 663-665.
- Hall, J.M., Chan, L.H., 2004. Li/Ca in multiple species of benthic and planktonic foraminifera: thermocline, latitudinal, and glacial-interglacial variations. *Geochimica et Cosmochimica Acta* 66, 1955-1967.
- Hart, S.R., Cohen, A.L., 1996. An ion probe study of annual cycles of Sr/Ca and other trace elements in corals. *Geochimica et Cosmochimica Acta* 60, 3075-3084.
- Hathorne, E.C., Felis, T., Suzuki, A., H., K., Cabioch, G., 2013. Lithium in the aragonite skeletons of massive *Porites* corals: a new tool to reconstruct tropical sea surface temperatures. *Paleoceanography* 28, 143-152.
- Heiss, G.A., Camoin, G.F., Eisenhauer, A., Wischow, D., Dullo, W., Hasen, B., 1997. Stable isotopes and Sr/Ca-signals in corals from the Indian Ocean, 8th International Coral Reef Symposium, pp. 1713-1718.
- Hemming, N.G., Hanson, G.N., 1992. Boron isotopic composition and concentration in modern marine carbonates. *Geochimica et Cosmochimica Acta* 56, 537-543.
- Hendy, E.J., Gagan, M.K., Albert, C.A., McCulloch, M.T., Lough, J.M., Isdale, P.J., 2002. Abrupt decrease in tropical Pacific sea surface salinity at the end of the Little Ice Age. *Science* 295, 1511-1514.
- Hershey, J.P., Fernandez, M., Milne, P.J., Millero, F.J., 1986. The ionization of boric acid in NaCl, Na-Ca-Cl and Na-Mg-Cl solutions at 25°C. *Geochimica et Cosmochimica Acta* 50, 143-148.
- Hetzinger, S., Pfeiffer, M., Dullo, W., Ruprecht, E., Garbe-Schonberg, D., 2006. Sr/Ca and  $\delta^{18}\text{O}$  in a fast-growing *Diploria strigosa* coral: evaluation of a new climate archive for the tropical Atlantic. *Geochemistry Geophysics Geosystems* 7. doi: 10.1029/2006GC001347.

- Hodell, D.A., Curtis, J.H., Jones, G.A., Higuera-Gundy, A., Brenner, M., Binford, M.W., Dorsey, K.T., 1991. Reconstruction of Caribbean climate change over the past 10,500 years. *Nature: Letters* 352, 790-794.
- Holcomb, M., Cohen, A.L., Gabitov, R.I., Hutter, J.L., 2009. Compositional and morphological features of aragonite precipitated experimentally from seawater and biogenically by corals. *Geochimica et Cosmochimica Acta* 73, 4166-4179.
- Horta-Puga, G., Carriquiry, J.D., 2012. Coral Ba/Ca molar ratios as a proxy of precipitation in the northern Yucatan Peninsula, Mexico. *Applied Geochemistry* 27, 1579-1586.
- Houck, J.E., Buddemeier, R.W., Smith, S.V., Jokiel, P.I., 1977. The response of coral growth rate and skeletal strontium content to light intensity and water temperature. In: Taylor, D.L. (Ed.), *Third International Coral Reef Symposium*, Rosenstiel School of Marine and Atmospheric Sciences. University of Miami, Miami, pp. 425-431.
- Ichikuni, M., Kikuchi, K., 1972. Retention of boron by travertines. *Chemical Geology* 9, 13-21.
- Inoue, M., Suzuki, A., Nohara, M., Hibino, K., Kawhata, H., 2007. Empirical assessment of coral Sr/Ca and Mg/Ca ratios as climate proxies using colonies grown at different temperatures. *Geophysical Research Letters* 34. doi:10.1029/2007GL029628.
- James, N.P., Jones, B., 2015. *Origin of carbonate sedimentary rocks*. Wiley, pp. 464.
- Jones, J.P., Carricart-Ganivet, J.P., Prieto, R.I., Enriquez, S., Ackerson, M., Gabitov, R.I., 2015. Microstructural variation in oxygen isotopes and elemental calcium ratios in the coral skeleton of *Orbicella annularis*. *Chemical Geology* 419, 192-199.
- Kilbourne, K.H., Quinn, T.M., Taylor, F.W., 2004. A fossil coral perspective on western tropical Pacific climate ~350 ka. *Paleoceanography* 19. doi:10.1029/2003PA000944.
- Kilbourne, K.H., Quinn, T.M., Guilderson, T.P., Webb, R.S., Taylor, F.W., 2007. Decadal-to interannual-scale source water variations in the Caribbean Sea recorded by Puerto Rican coral radiocarbon. *Climate Dynamics* 29, 51-62.
- Kilbourne, K.H., Quinn, T.M., Webb, R., Guilderson, T., Nyberg, J., Winter, A., 2010. Coral windows into seasonal climate variability in the northern Caribbean since 1479.



- Geochemistry Geophysics Geosystems 11. doi: 10.1029/2010GC003171.
- Kinsman, D.J.J., Holland, H.D., 1969. The co-precipitation of cations with  $\text{CaCO}_3$ -IV. The co-precipitation of  $\text{Sr}^{2+}$  with aragonite between 16 and 96°C. *Geochimica et Cosmochimica Acta* 33, 1-17.
- Kitano, Y., Kanamori, N., Oomori, T., 1971. Measurements of distribution coefficients of strontium and barium between carbonate precipitate and solution: abnormally high values of distribution coefficients measured at early stages of carbonate formation. *Geochemical Journal* 4, 183-206.
- Kuffner, I.B., Jokiel, P.I., Rodgers, K.S., Anderson, A.J., Mackenzie, F.T., 2012. An apparent “vital effect” of calcification rate on the Sr/Ca temperature proxy in the reef coral *Montipora capitata*. *Geochemistry Geophysics Geosystems* 13. doi: 10.1029/2012GC004128.
- Kuffner, I.B., Roberts, H.H., Flannery, J.A., Morrison, J.M., Richey, J.N., 2017. Fidelity of Sr/Ca proxy in recording ocean temperature in the western Atlantic coral *Siderastrea siderea*. *Geochemistry Geophysics Geosystems* 18, 178-188.
- Lahann, R.W., 1978. A chemical model for calcite crystal growth and morphology control. *Journal of Sedimentary Petrology* 48, 337-344.
- Lea, D.W., Shen, G.T., Boyle, E.A., 1989. Coralline barium records temporal variability in equatorial Pacific upwelling. *Nature* 340, 373-376.
- Linsley, B.K., Wellington, G.M., Schrag, D.P., 2000. Decadal sea surface temperature in the subtropical South Pacific from 1726 to 1997 A.D. *Science* 290, 1145-1148.
- Linsley, B.K., Wellington, G.M., Schrag, D.P., Ren, L., Salinger, M.J., Tudhope, A.W., 2004. Geochemical evidence from corals for changes in the amplitude and spatial pattern of South Pacific interdecadal climate variability over the last 300 years. *Climate Dynamics* 22. doi: 10.1007/s00382-003-0364-y.
- Linsley, B.K., Kaplan, A., Gouriou, Y., Salinger, J., deMenocal, P.B., Wellington, G.M., Howe, S.S., 2006. Tracking the extent of the South Pacific Convergence Zone since the early

- 1600s. *Geochemistry Geophysics Geosystems* 7. doi:10.1029/2005GC001115.
- Lough, J.M., 2004. A strategy to improve the contribution of coral data to high-resolution paleoclimatology. *Palaeogeography, Palaeoclimatology, Palaeoecology* 204, 115-143.
- Marchitto, T.M., Bryan, S.P., Doss, W., McCulloch, M., Montagna, P., 2018. A simple biomineralization model to explain Li, Mg, and Sr incorporation into aragonitic foraminifera and corals. *Earth and Planetary Science Letters* 481, 20-29.
- Marriott, C.S., Henderson, G.H., Belshaw, N.S., Tudhope, A.W., 2004a. Temperature dependence of  $\delta^7\text{Li}$ ,  $\delta^{44}\text{Ca}$  and Li/Ca during growth of calcium carbonate. *Earth and Planetary Science Letters* 22, 615-624.
- Marriott, C.S., Henderson, G.H., Crompton, R., Staubwasser, M., Shaw, S., 2004b. Effect of mineralogy, salinity, and temperature on Li/Ca and Li isotope composition of calcium carbonate. *Chemical Geology* 212, 5-15.
- Marshall, J.F., McCulloch, M., 2001. Evidence of El Nino and the Indian Ocean Dipole from Sr/Ca derived SSTs from modern corals at Christmas Island, eastern Indian Ocean. *Geophysical Research Letters* 28, 3453-3456.
- Marshall, J.F., McCulloch, M.T., 2002. An assessment of the Sr/Ca ratio in shallow water hermatypic corals as a proxy for sea surface temperature. *Geochimica et Cosmochimica Acta* 66, 3263-3280.
- Mavromatis, V., Goetschl, K.E., Grengg, C., Konrad, F., Purgstaller, B., Dietzel, M., 2018. Barium partitioning in calcite and aragonite as a function of growth rate. *Geochimica et Cosmochimica Acta* 237, 65-78.
- McCulloch, M., Falter, J., Trotter, J., Montagna, P., 2012. Coral resilience to ocean acidification and global warming through pH up-regulation. *Nature Letters- Climate Change* 2, doi: 10.1038/NCLIMATE1473.
- McCulloch, M., Fallon, S., Wyndham, T., Hendy, E., Lough, J., Barnes, D., 2003. Coral record of increased sediment flux to the inner Great Barrier Reef since European settlement. *Nature* 421, 727-730.

- McCulloch, M.T., Esat, T., 2000. The coral record of last interglacial sea levels and sea surface temperatures. *Chemical Geology* 169, 107-129.
- McCulloch, M.T., Gagan, M.K., Mortimer, G.E., Chivas, A.R., Isdale, P.J., 1994. A high-resolution Sr/Ca and  $\delta^{18}\text{O}$  coral record from the Great Barrier Reef, Australia, and the 1982-1983 El Nino. *Geochimica et Cosmochimica Acta* 58, 2747-2754.
- McCulloch, M.T., Tudhope, A.W., Esat, T.M., Mortimer, G.E., Chappell, J., Pillans, B., Chivas, A.R., Omura, A., 1999. Coral record of equatorial sea-surface temperatures during the Penultimate Deglaciation at Huon Peninsula. *Science* 283, 202-204.
- McIntire, W.L., 1963. Trace element partition coefficients- a review of theory and applications to geology. *Geochimica et Cosmochimica Acta* 27, 1209-1264.
- Meibom, A., Cuiff, J., Houlbreque, F., Mostefaoui, S., Dauphin, Y., Meibom, K.L., Dunbar, R.B., 2008. Compositional variations at ultra-structure length scales in coral skeleton. *Geochimica et Cosmochimica Acta* 72, 1555-1569.
- Meibom, A., Cuiff, J., Hillion, F., Constantz, B.R., Juillet-Leclerc, A., Dauphin, Y., Watanabe, T., Dunbar, R.B., 2004. Distribution of magnesium in coral skeleton. *Geophysical Research Letters* 31. doi:10.1029/2004GL021313.
- Meibom, A., Stage, M., Wooden, J., Constantz, B.R., Dunbar, R.B., Owen, A., Grumet, N., Bacon, C.R., Chamberlin, C.P., 2003. Monthly strontium/calcium oscillations in symbiotic coral aragonite: biological effects limiting the precision of paleotemperature proxy. *Geophysical Research Letters* 30. doi:10.1029/2002GL016864.
- Meibom, A., Yurimoto, H., Cuiff, J., Domart-Coulon, I., Houlbreque, F., Constantz, B., Dauphin, Y., Tambutte, E., Tambutte, S., Allemand, D., Dunbar, R.B., 2006. Vital effects in coral skeletal composition display strict three-dimensional control. *Geophysical Research Letters* 33. doi: 10.1029/2006GL025968.
- Min, G.R., Edwards, R.L., Taylor, F.W., Recy, J., Gallup, C.D., Beck, J.W., 1995. Annual cycles of U/Ca in coral skeletons and U/Ca thermometry. *Geochimica et Cosmochimica Acta* 59, 2025-2042.

- Mitsuguchi, T., Matsumoto, E., Abe, O., Uchida, T., Isdale, P.J., 1996. Mg/Ca thermometry in coral skeletons. *Science* 274, 961-963.
- Mitsuguchi, T., Uchida, T., Matsumoto, E., Isdale, P.J., Kawana, T., 2001. Variations in Mg/Ca, Na/Ca, and Sr/Ca ratios of coral skeletons with chemical pretreatments: implications for carbonate geochemistry. *Geochimica et Cosmochimica Acta* 65, 2865-2874.
- Mitsuguchi, T., Dang, P.X., Kitagawa, H., Uchida, T., Shibata, Y., 2008. Coral Sr/Ca and Mg/Ca records in Con Dao Island off the Mekong Delta: assessment of their potential for monitoring ENSO and East Asian monsoon. *Global and Planetary Change* 63, 341-352.
- Montaggioni, L.F., Le Cornec, F., Correge, T., Cabioch, G., 2006. Coral barium/calcium record of mid-Holocene upwelling activity in New Caledonia, South-West Pacific. *Paleogeography, Paleoclimatology, Paleoecology* 237, 436-455.
- Montagna, P., McCulloch, M., Douville, E., Lopez Correa, M., Trotter, J., Rodolfo-Metalpa, R., Dissard, D., Ferrier-Pages, C., Frank, N., Freiwald, A., Goldstein, S., Mazzoli, C., Reynaud, S., Ruggeberg, A., Russo, S., Taviani, M., 2014. Li/Mg systematics in scleractinian corals: calibration of the thermometer. *Geochimica et Cosmochimica Acta* 132, 288-310.
- Moreau, M., Correge, T., Dassies, E.P., Le Cornec, F., 2015. Evidence for the non-influence of salinity variability on the *Porites* coral Sr/Ca palaeothermometer. *Climate of the Past* 11, 523-532.
- Murty, S.A., Bernstein, W.N., Ossolinski, J.E., Davis, R.S., Goodkin, N.F., Hughen, K.A., 2018. Spatial and temporal robustness of the Sr/Ca-SST calibrations in Red Sea corals: evidence for influence of mean annual temperature on calibration slopes. *Paleoceanography and Paleoclimatology* 33, 443-456.
- NOAA, 2016, In what types of water do corals live? <https://oceanservice.noaa.gov/facts/coralwaters.html>.
- NOAA, 2018, World Sea Temperatures. <https://www.seatemperature.org/>.
- Nothdurft, L.D., Webb, G.E., Bostrom, T., Rintoul, L., 2007. Calcite-filled borings in the most

- recently deposited skeleton in live-collected *Porites* (Scleractinia): implications for trace element archives. *Geochimica et Cosmochimica Acta* 71, 5423-5438.
- Nurhati, I.S., Cobb, K.M., Di Lorenzo, E., 2011. Decadal-scale SST and salinity variations in the central tropical Pacific: signatures of natural and anthropogenic climate change. *Journal of Climate* 24, 3294-3308.
- Nurhati, I.S., Cobb, K.M., Charles, C.D., Dunbar, R.B., 2009. Late 20th century warming and freshening in the central tropical Pacific. *Geophysical Research Letters* 36. doi: 10.1029/2009GL040270.
- Okumura, M., Kitano, Y., 1986. Coprecipitation of alkali metal ions with calcium carbonate. *Geochimica et Cosmochimica Acta* 50, 49-58.
- Oomori, T., Kaneshima, K., Nakamura, Y., Kitano, Y., 1982. Seasonal variation of minor elements in coral skeletons. *Galaxea* 1, 77-86.
- Ourbak, T., Correge, T., Malaize, B., Le Cornec, F., Charlier, K., Peypouquet, J.P., 2006. A high-resolution investigation of temperature, salinity, and upwelling activity proxies in corals. *Geochemistry Geophysics Geosystems* 7. doi:10.1029/2005GC001064.
- Ourbak, T., DeLong, K.L., Correge, T., Malaize, B., Kilbourne, H., Cawuineau, S., Hollander, D., 2008. The significance of geochemical proxies in corals; does size (age) matter?, *Proceedings of the 11th International Coral Reef Symposium*, Ft. Lauderdale, Florida, pp. 82-86.
- Pfeiffer, M., Timm, O., Dullo, W., Garbe-Schonberg, D., 2006. Paired coral Sr/Ca and  $\delta^{18}\text{O}$  records from the Chagos Archipelago: late twentieth century warming affects rainfall variability in the tropical Indian Ocean. *Geology* 34, 1069-1072.
- Pfeiffer, M., Dullo, W., Zinke, J., Garbe-Schonberg, D., 2009. Three monthly coral Sr/Ca records from the Chagos Archipelago covering the period of 1950-1995 A.D.: reproducibility and implication for quantitative reconstructions of sea surface temperature variations. *International Journal of Earth Sciences* 98, 53-66.
- Pingitore, N.E., Rangel, Y., Kwarteng, A., 1988. Barium variation in *Acropora palmata* and

- Montastrea annularis*. Coral Reefs 8, 31-36.
- Politi, Y., Batchelor, D.R., Zaslansky, P., Chmelka, B.F., Weaver, J.C., Sagi, I., Weiner, S., Addadi, L., 2010. Role of magnesium ion stabilization of biogenic amorphous calcium carbonate: a structure-function investigation. *Chemistry of Materials* 22, 161-166.
- Prouty, N.G., Field, M.E., Stock, J.D., Jupiter, S.D., McCulloch, M., 2010. Coral Ba/Ca records of sediment input to the fringing reef of the southshore of Moloka'i, Hawai'i over the last several decades. *Marine Pollution Bulletin* 60, 1822-1835.
- Quinn, T.M., Sampson, D.E., 2002. A multiproxy approach to reconstructing sea surface conditions using coral skeleton geochemistry. *Paleoceanography* 17, doi:10.1029/2000PA000528.
- Raddatz, J., Liebetrau, V., Rüggeberg, A., Hathorne, E., Krabbenhoft, A., Eisenhauer, A., Böhm, F., Vollstaedt, H., Fietzke, J., Lopez Correa, M., Freiwald, A., Dullo, W., 2013. Stable Sr-isotope, Sr/Ca, Mg/Ca, Li/Ca and Mg/Li ratios in the scleractinian cold-water coral *Lophelia pertusa*. *Chemical Geology* 352, 143-152.
- Ramos, R.D., Goodkin, N.F., Siringan, F.P., Hughen, K.A., 2017. *Diploastrea heliopora* Sr/Ca and  $\delta^{18}\text{O}$  records from northeast Luzon, Philippines: an assessment of interspecies coral proxy calibrations and climate controls of sea surface temperature and salinity. *Paleoceanography* 32, 424-438.
- Reeder, R.J., Nugent, M., Lamble, G.M., Drew, C., Morris, D.E., 2000. Uranyl incorporation into calcite and aragonite: XAFS and luminescence studies. *Environmental Science Technology* 34, 634-644.
- Reynaud, S., Ferrier-Pages, C., Meibom, A., Mostefaoui, S., Mortlock, R., Fairbanks, R., Allemand, D., 2007. Light and temperature effects on Sr/Ca and Mg/Ca ratios in the scleractinian coral *Acropora* sp. *Geochimica et Cosmochimica Acta* 71, 354-362.
- Rosenthal, Y., Linsley, B., 2006. Mg/Ca and Sr/Ca paleothermometry from calcareous marine fossils, *Encyclopedia of Quaternary Sciences*. Elsevier Ltd, pp. 24.
- Sadler, J., Webb, G.E., Nothdurft, L.D., 2015. Structure and palaeoenvironmental implications of

- inter-branch coenosteum-rich skeleton in corymbose *Acropora* species. *Coral Reefs* 34, 201-213.
- Sadler, J., Nguyen, A.D., Leonard, N.D., Webb, G.E., Nothdurft, L.D., 2016a. *Acropora* interbranch skeleton Sr/Ca ratios: evaluation of a potential new high-resolution paleothermometer. *Paleoceanography* 31, 505-517.
- Sadler, J., Webb, G.E., Leonard, N.D., Nothdurft, L.D., Clark, T.R., 2016b. Reef core insights into mid-Holocene water temperatures of the southern Great Barrier Reef. *Paleoceanography* 31, 1395-1408.
- Saenger, C., Cohen, A.L., Oppo, D.W., Hubbard, D., 2008. Interpreting sea surface temperature from strontium/calcium ratios in *Montastrea* corals: link with growth rate and implications for proxy reconstructions. *Paleoceanography* 23. doi:10.1029/2007PA001572.
- Saha, N., Webb, G.E., Zhao, J., Nguyen, A.D., Lewis, S.E., Lough, J.M., 2019. Coral-based high-resolution rare earth element proxy for terrestrial sediment discharge affecting coastal seawater quality, Great Barrier Reef. *Geochimica et Cosmochimica Acta* 254, 173-191.
- Schrag, D.P., 1999. Rapid analysis of high-precision Sr/Ca ratios in corals and other marine carbonates. *Paleoceanography* 14, 97-102.
- Scott, R.B., Holland, C.L., Quinn, T.M., 2010. Multidecadal trends in instrumental SST and coral proxy Sr/Ca records. *Journal of Climate* 23, 1017-1033.
- Seo, I., Lee, Y.I., Watanabe, T., Yamano, H., Shimamura, M., Yoo, C.M., Hyeong, K., 2013. A skeletal Sr/Ca record preserved in *Dipsastraea* (*Favia*) *speciosa* and implications for coral Sr/Ca thermometry in mid-latitude regions. *Geochemistry Geophysics Geosystems* 14, 2873-2885.
- Shaw, T.J., Moore, W.S., Kloepfer, J., Sochaski, M.A., 1998. The flux of barium to the coastal waters of the southeaster USA: the importance of submarine groundwater discharge. *Geochimica et Cosmochimica Acta* 62, 3047-3054.
- Shen, C., Lee, T., Chen, C., Wang, C., Dai, C., Li, A., 1996. The calibration of  $D_{(Sr/Ca)}$  versus sea

- surface temperature relationship for *Porites* coral. *Geochimica et Cosmochimica Acta* 60, 3849-3858.
- Shen, G.T., Dunbar, R.B., 1995. Environmental controls on uranium in reef corals. *Geochimica et Cosmochimica Acta* 59, 2009-2024.
- Siegel, F.R., 1960. The effects of strontium on the aragonite-calcite ratios of Pleistocene corals. *Journal of Sedimentary Petrology* 30, 297-304.
- Sinclair, D.J., 2005. Correlated trace element 'vital effects' in tropical corals: a new tool for probing biomineralization chemistry. *Geochimica et Cosmochimica Acta* 69, 3265-3284.
- Sinclair, D.J., McCulloch, M., 2004. Corals record low mobile barium concentrations in the Burdekin River during the 1974 flood: evidence for limited Ba supply to rivers? *Palaeogeography, Palaeoclimatology, Palaeoecology* 214, 155-174.
- Sinclair, D.J., Kinsley, L.P.J., McCulloch, M.T., 1998. High resolution analysis of trace elements in corals by laser ablation ICP-MS. *Geochimica et Cosmochimica Acta* 62, 1889-1901.
- Sinclair, D.J., Williams, B., Risk, M., 2006. A biological origin for climate signals in corals- trace element 'vital effects' are ubiquitous in scleractinian coral skeletons. *Geophysical Research Letters* 33. doi: 10.1029/2006GL027183.
- Siriananskul, W., Pumijumnong, N., 2014. A preliminary study of Sr/Ca thermometry in Chang Islands, Gulf of Thailand. *Songklanakarin Journal of Science and Technology* 36, 583-589.
- Siriananskul, W., Pumijumnong, N., Mitsuguchi, T., Puchakarn, S., Boontanon, N., 2012. Mg/Ca and Sr/Ca ratios in a coral from Koh Chuek, Surat Thani, Thailand. *Journal of Coral Reef Studies* 14, 63-72.
- Smith, J.M., Quinn, T.M., Helmle, K.P., Halley, R.B., 2006. Reproducibility of geochemical and climatic signals in the Atlantic coral *Montastrea faveolata*. *Paleoceanography* 21. doi: 10.1029/2005PA001187.
- Smith, S.R., Buddemeier, R.W., Redale, R., Houck, J.E., 1979. Strontium-calcium thermometry in coral skeletons. *Science* 204, 404-406.



- Stephans, C.L., Quinn, T.M., Taylor, F.W., Corregge, T., 2004. Assessing the reproducibility of coral-based climate records. *Geophysical Research Letters* 31. doi:10.1029/2004GL020343.
- Stoffyn-Egli, P., Mackenzie, F.T., 1984. Mass balance oceans of dissolved lithium. *Geochimica et Cosmochimica Acta* 48, 859-872.
- Storz, D., Gischler, E., Fiebig, J., Eisenhauer, A., Garbe-Schonberg, D., 2013. Evaluation of oxygen isotope and Sr/Ca ratios from a Maldivian scleractinian coral from reconstruction of climate variability in the Northwestern Indian Ocean. *Palaios* 28, 42-55.
- Sun, Y., Sun, M., Lee, T., Nie, B., 2005. Influence of seawater Sr content on coral Sr/Ca and Sr thermometry. *Coral Reefs* 24, 23-29.
- Swart, P.K., 1981. The strontium, magnesium, and sodium composition of recent scleractinian coral skeletons as standards for palaeoenvironmental analysis. *Palaeogeography, Palaeoclimatology, Palaeoecology* 34, 115-136.
- Swart, P.K., Hubbard, J.A.E.B., 1982. Uranium in scleractinian coral skeletons. *Coral Reefs* 1, 13-19.
- Swart, P.K., Elderfield, H., Greaves, M.J., 2002. A high-resolution calibration of Sr/Ca thermometry using the Caribbean coral *Montastrea annularis*. *Geochemistry Geophysics Geosystems* 3. doi: 10.1029/2002GC000306.
- Tanaka, K., Holcomb, M., Takahashi, A., Kurihara, H., Asami, R., Shinjo, R., Sowa, K., Rankenburg, K., Watanabe, T., McCulloch, M., 2015. Response of *Acropora digitifera* to ocean acidification: constraints from  $\delta^{11}\text{B}$ , Sr, Mg, and Ba composition of aragonitic skeletons cultured under variable seawater pH. *Coral Reefs* 34, 1139-1149.
- Thebault, J., Schone, B.R., Hallmann, N., Barth, M., Nunn, E.V., 2009. Investigation of Li/Ca variations in aragonitic shells of the ocean quahog *Arctica islandica*, northeast Iceland. *Geochemistry Geophysics Geosystems* 10. doi: 10.1029/2009GC002789.
- Tudhope, A.W., Lea, D.W., Shimmield, G.B., Chilcott, C.P., Head, S., 1996. Monsoon climate and Arabian Sea coastal upwelling recorded in massive corals from southern Oman.

PALAIOS 11, 347-361.

- Vengosh, A., Kolodny, Y., Starinsky, A., Chivas, A.R., McCulloch, M.T., 1991. Coprecipitation and isotopic fractionation of boron in modern carbonates. *Geochimica et Cosmochimica Acta* 55, 2901-2910.
- Venn, A.A., Tambutte, E., Holcomb, M., Laurent, J., Allemand, D., Tambutte, S., 2013. Impact of seawater acidification on pH at the tissue-skeleton interface and calcification on coral reefs. *Geochimica et Cosmochimica Acta* 68, 1473-1488.
- von Reumont, J., Hetzinger, S., Garbe-Schonberg, D., Manfrino, C., Dullo, W., 2016. Impact of warming events on reef-scale temperature variability as captured in two Little Cayman coral Sr/Ca records. *Geochemistry Geophysics Geosystems* 17. doi: 10.1002/2015GC006194.
- Watanabe, T., Winter, A., Oba, T., 2001. Seasonal changes in sea surface temperatures and salinity during the Little Ice Age in the Caribbean Sea deduced from Mg/Ca and  $^{18}\text{O}/^{16}\text{O}$  ratios in corals. *Marine Geology* 173, 21-35.
- Weber, J.N., 1973. Incorporation of strontium into reef coral skeletal carbonate. *Geochimica et Cosmochimica Acta* 37, 2173-2190.
- Weber, J.N., 1977. Use of corals in determining glacial-interglacial changes in temperature and isotopic composition of seawater: reef biota. In: Frost, S. H., Weiss, M. P., Saunders, J. B. (Eds.), *Reefs and Related Carbonates - Ecology and Sedimentology*. American Association of Petroleum Geologists Special Volumes, 4, pp. 289-295.
- Wei, G., Sun, M., Li, X., Nie, B., 2000. Mg/Ca, Sr/Ca and U/Ca ratios of a *Porites* coral from Sanya Bay, Hainan Island, South China Sea and their relationship to sea surface temperature. *Palaeogeography, Palaeoclimatology, Palaeoecology* 162, 59-74.
- Winter, A., Paul, A., Nyberg, J., Oba, T., Lundberg, J., Schrag, D.P., Taggart, B., 2003. Orbital control of low-latitude seasonality during the Eemian. *Geophysical Research Letters* 30. doi:10.1029/2002GL016275.
- Xu, Y., Pearson, S., Kilbourne, K.H., 2015. Assessing coral Sr/Ca-SST calibration techniques

- using the species *Diploria strigosa*. *Palaeogeography, Palaeoclimatology, Palaeoecology* 440, 353-362.
- Yu, K., Zhao, J., Liu, T., Wei, G., Wang, P., Collerson, K.D., 2004. High-frequency winter cooling and reef coral mortality during the Holocene climatic optimum. *Earth and Planetary Science Letters* 224, 143-155.
- Yu, K., Zhao, J., Wei, G., Cheng, X., Chen, T., Felis, T., Wang, P., Liu, T., 2005.  $\delta^{18}\text{O}$ , Sr/Ca and Mg/Ca records of *Porites lutea* corals from Leizhou Peninsula, northern South China Sea, and their applicability as paleoclimatic indicators. *Palaeogeography, Palaeoclimatology, Palaeoecology* 218, 57-73.
- Yu, W., Tian, L., Risi, C., Yao, T., Ma, Y., Zhao, H., Zhu, H., He, Y., Xu, B., Zhang, H., Qu, D., 2016.  $\delta^{18}\text{O}$  records in water vapor and an ice core from the eastern Pamir Plateau: implications for paleoclimate reconstructions. *Earth and Planetary Science Letters* 456, 146-156.
- Zinke, J., Dullo, W., Heiss, G.A., Eisenhauer, A., 2004. ENSO and Indian Ocean subtropical dipole variability is recorded in a coral record off southwest Madagascar for the period 1659 to 1995. *Earth and Planetary Science Letters* 228, 177-194.

## CHAPTER 3

### INSIGHTS INTO SEA SURFACE TEMPERATURES FROM THE CAYMAN ISLANDS FROM CORALS OVER THE LAST ~540 YEARS

#### 1. Introduction

Long-term global temperature reconstructions, based on data from speleothems, corals, ice cores, and/or sediment cores, have pointed to an overall global warming since 1850 (e.g., Trenberth et al., 2007; Chollett et al., 2012a; Tiernery et al., 2017). Other studies, however, have suggested global cooling (0.1 to 0.9°C/century) between 1950 and 1989 or periods with little or no change in temperature between 1854 and 1950 (Atwood et al., 1992; Glynn, 1992). Similarly, it has been suggested that the Caribbean region experienced significant climatic changes over this time period that included, for example, an increase in rainfall and the number of high-temperature days since the 1950's (Frich et al., 2002; Peterson et al., 2002), rapid warming (0.1°C/year) since the early 1980's (Strong, 1989; McWilliams et al., 2005), warming of ~0.51°C/decade in Guadeloupe (Hetzinger et al., 2010), warming of ~0.8°C in the Florida Keys since the 1800's (Kuffner et al., 2015), cooling in the Western Atlantic from 1825-1834 and warming from 1995 to 2004 (Tierney et al., 2015), and warming in the Cayman Islands (~0.5°C) between 1980 and 1990 (Goreau et al., 1992). In contrast, cooling has been highlighted in the Cariaco Basin from 1-1990 A.D. (Black et al., 2004) and no change in temperature since 1914 in the Gulf of Mexico and the Caribbean region (Atwood et al., 1992).

Geochemical data from growth bands in corals have long been used as environmental proxies (Buddermeier et al., 1974; Moore and Krishnaswami, 1974; Baker and Weber, 1975; Dunbar et al., 1994; McCulloch et al., 1994; Linsley et al., 2008).

Oxygen isotope compositions of corals have, for example, been used to trace temperature

---

A version of this chapter has been published as: Booker, S., Jones, B., Chacko, T., Li, L., 2019. Insights into sea surface temperatures from the Cayman Islands from corals over the last ~540 years, *Sedimentary Geology*, 389, 218-240.

and salinity variations (Epstein et al., 1953; Weber and Woodhead, 1972; Cole et al., 1993; Abram et al., 2007; Peros et al., 2007; Linsley et al., 2008; Bolton et al., 2014), whereas carbon isotope compositions have been used to gain insight into nutrient levels, photosynthetic activity, water depth, and metabolic processes (Fairbanks and Dodge, 1979; Swart, 1983; Gagan et al., 2000; Grotoli and Eakin, 2007).

The present study focuses on decadal-scale Surface Seawater Temperature (SST) changes from 1470 CE to present as derived from oxygen and carbon isotope data from corals from Grand Cayman and Cayman Brac (Fig. 3.1). These data indicate that the central Caribbean has experienced four periods of temperature change and an overall  $\sim 3^{\circ}\text{C}$  temperature increase since 1815. These temperature trends are consistent with other Caribbean records. The conclusions derived from this study provide important constraints on the historical SST changes for a part of the Caribbean that has, up to now, been largely ignored in terms of its temperature record.

## 2. Terminology

The terminology used to denote and describe periods of time that are characterized by different seawater temperatures and/or trends in temperature change is prodigious and commonly invoked without clear definitions of how such terms are derived and applied. In many cases, confusion arises simply because of the poor usage of terms that have not been clearly defined or that are used interchangeably with words of varying meanings. Accordingly, the terms used in this paper are defined as follows.

*Cool Period:* The majority of the calculated temperatures ( $T_{\text{cal}}$ ) are lower than the present-day average seawater temperature at the location of study. This follows the definition of Chenoweth (1998).

*Warm Period:* The majority of the  $T_{\text{cal}}$  are higher than the present-day average seawater temperature at the location of study. This follows the definition of Chenoweth (1998).

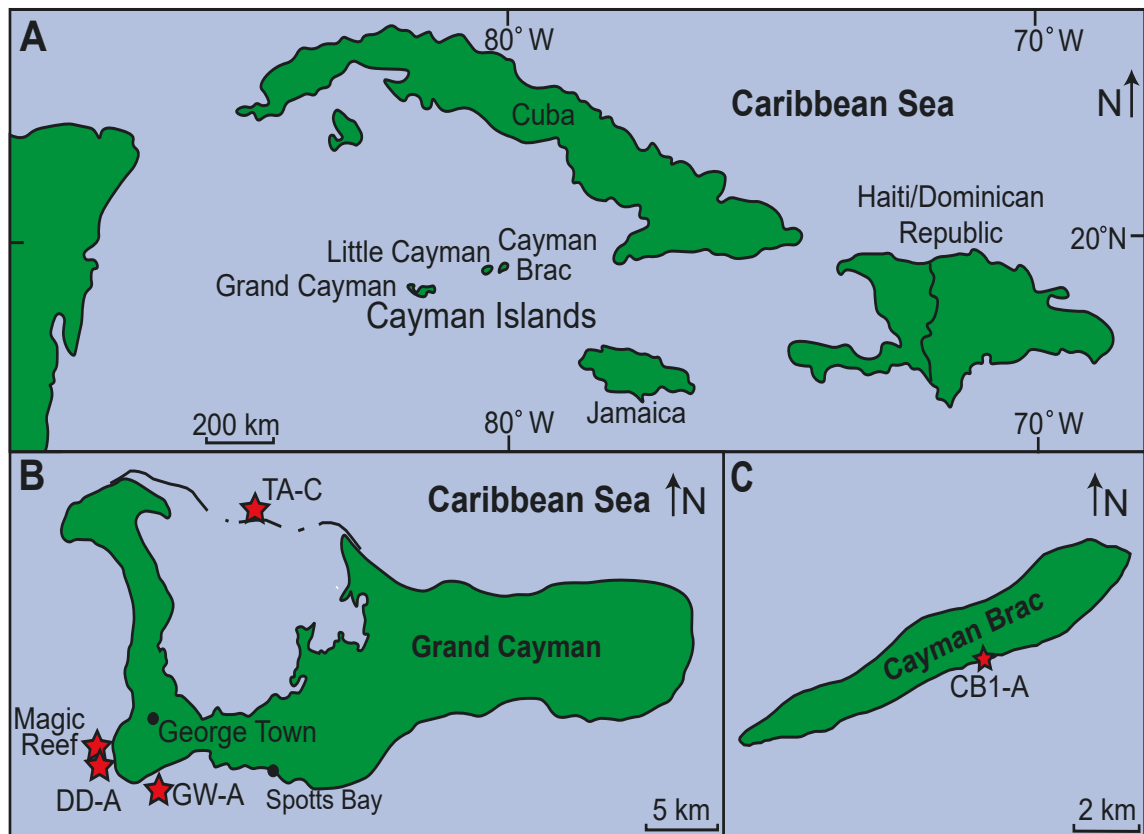


**Fig. 3.1.** Location maps. (A) Map showing location of Grand Cayman and Cayman Brac. (B) Location of Magic Reef, Gary's Wall, Dans Dive, and Tarpon Alley on Grand Cayman (red stars). (C) Location of storm rubble ridge on Cayman Brac (red star).

*Mild Period:* The majority of the  $T_{cal}$  are consistent with the present-day average seawater temperature in the location of study, allowing for seasonal fluctuations of  $\pm 1^\circ\text{C}$ . This usage is akin to that proposed by Saenger et al. (2009).

*Cool Interval:* This denotes an interval of time during which the  $T_{cal}$  is lower than the preceding time interval, but remains within the range of temperatures that define either the encompassing Cool Period or Warm Period.

*Warm Interval:* This denotes an interval of time during which the  $T_{cal}$  is higher than the preceding time interval, but remains within the range of temperatures that define either the encompassing Cool Period or Warm Period.

*Trend*: This term is used as an indicator of the direction of temperature (T) change, e.g., a warming trend signifies an increase in T, whereas a cooling trend signifies a decrease in T. This usage of ‘trend’ is similar to that of Goreau et al. (1992), Corderio et al. (2014), and Alpert et al. (2017).

With this terminological scheme, the cool and warm periods represent a longer time duration than the cool and warm intervals.

### 3. Geographic Setting

The Cayman Islands, which includes Grand Cayman, Cayman Brac, and Little Cayman (Fig. 3.1A), are high points on the Cayman Ridge, which extends from the Sierra Maestra Range of Cuba to the base of the British Honduras Continental Slope (Fahlquist and Davies, 1971; Perfit and Heezen, 1978). The Caribbean Sea around the Cayman Islands is characterized by warm, clear waters with normal salinity (Chollett et al., 2012b). These islands are characterized by narrow shelves and numerous lagoons with thriving coral growth. Among the 44 species of corals identified from the waters around Grand Cayman (Hunter, 1994), various species of *Orbicella* and *Montastrea* dominate.

The Cayman Islands enjoy a humid sub-tropical climate, dominated by the moisture-laden air masses of the North-East Trade Wind System (Blanchon, 1995). For Grand Cayman, air temperature ranges from 21°C–33°C, and the ocean temperatures (0–14.5 m depth) range from 25.3°C–30.8°C, with an average of 28.5°C (Goreau et al., 1992; Chollett et al., 2012b; NOAA, 2018; Fig. 3.2). The average rainfall is 1,220 mm/year with the wet season from May to October and the dry season from November to April (Fig. 3.2D). From 2007 to 2015, Cayman Brac experienced air temperatures of 26.6°C–30.6°C, with an average of 28.7°C (Fig. 3.2C) and received an average of 860 mm/year rainfall (NOAA, 2018). The wet season is characterized by high cloud cover, which results in a lower number of sunlight hours than during the dry season.

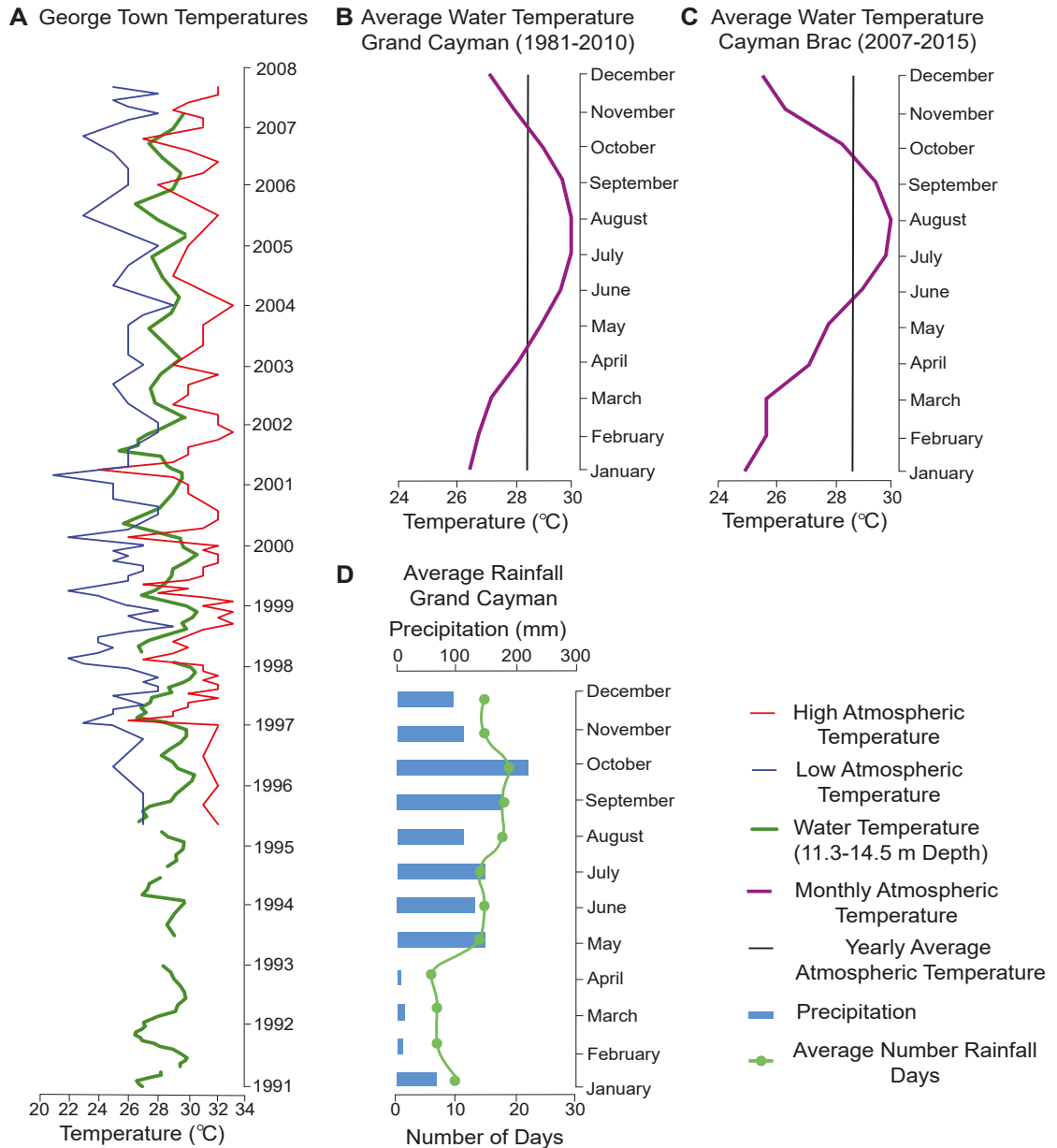


**Fig. 3.2.** Climatic conditions for Grand Cayman and Cayman Brac between 1981 and 2015.

(A) Atmospheric and water temperatures (11.3-14.5 m depth) on Grand Cayman between 1991 and 2008. Data from the Department of Environment and the Water Authority, Cayman Islands. (B) Water temperatures (surface) for Grand Cayman between 1981 and 2010 (T derived from NOAA daily records). (C) Water temperatures (surface) for Cayman Brac between 2007 and 2015 (T derived from NOAA daily records). (D) Yearly rainfall for Grand Cayman between 2000 and 2012. (<http://www.worldweatheronline.com/george-town-weather-averages/ky.aspx>).



#### 4. Samples

The coral reefs around the Cayman Islands are highly protected with the collection of corals prohibited. The samples used in this research were obtained with the help and permission of the Department of Environment, Cayman Islands. Five specimens of *Orbicella annularis* (formally *Montastrea annularis*, four from Grand Cayman, one from Cayman Brac) and two specimens of *Montastrea cavernosa* (from Grand Cayman) were used in this study. Three corals came from Magic Reef (Fig. 3.1B), with a reef top depth of 20 m, that is located off the southwest coast of Grand Cayman. A cruise ship dragged its anchor across the reef in December 2014 and uprooted many corals. The samples used in this study, collected in 2015, came from those uprooted corals. Sample ER#30-C is a 19.5 cm high hemispherical *M. cavernosa*. ER#31-A is a 48 cm high hemispherical *O. annularis*. ER#32-A is a 40 cm high *O. annularis* with three broad branches.

Cores (9.5 cm diameter) were obtained from three corals on the fringing reef around Grand Cayman (Fig. 3.1B) in 1987 during the installation of boat moorings by the Department of Environment (Blanchon, 1995; Blanchon and Jones, 1995; Blanchon et al., 1997). These corals came from: Gary's Wall (GW-A) a 57 cm long *O. annularis* collected at 25 m water deep, Dan's Dive (DD-A) a 54 cm long *O. annularis* collected at 19.8 m water depth, Tarpon Alley (TA-C) a 35 cm long *M. cavernosa* collected at 15.8 m water depth from the forereef of the fringing reef on the north margin of North Sound (Fig. 3.1B).

The coral from Cayman Brac (CB1-A) is a 49.8 cm *O. annularis* that was collected from the coral rubble ridge (~1.5 m high, ~ 10 m wide) that stretches along the south coast of the island (Fig. 3.1C). This ridge was created in 1932 by Hurricane Cuba (Rigby and Roberts, 1976), a category 5 hurricane with wind speeds up to 320 km/h, 16 m high waves, and a storm surge up to 10 m (Sauer, 1982; Fenner, 1993; Markoff, 2012). No other hurricanes of this magnitude have affected Cayman Brac since 1932 (Markoff,

2015). Eye-witnesses reported large boulders and ships being thrown on-shore and into buildings (Sauer, 1982; Markoff, 2012; 2015). Importantly, the Oxford Expedition photographed the existence of this ridge in 1934 (sourced from the National Archives, Cayman Islands), shortly after it formed. Thus, the death date of the Cayman Brac ridge coral is well established as 1932.

## **5. Methodology**

### *5.1. Mineralogy determination*

#### *5.1.1. X-Ray Diffraction (XRD)*

Mineralogy was confirmed by XRD analyses using a Rigaku Geigerflex Powder Diffractometer. Seven samples, each weighing ~1 g, were taken from the base and bored margins of each coral, and ground into a fine powder using a mortar and pestle. Thirty-five micro-samples, each ~300 mg, came from different growth bands in each coral. The percentages of aragonite and calcite were determined by the method used by Li and Jones (2013).

#### *5.1.2. Thin section analysis*

Standard (27 x 46 mm) thin sections (1 from ER#30-C, 2 from ER#31-A, 4 from ER#32-A, 3 from CB1-A, 6 from TA-C), made from each coral, were used to verify the mineralogy of the corals and to examine the growth banding.

#### *5.1.3. Scanning Electron Microscopy (SEM)*

SEM photomicrographs of the corals were produced using a Zeiss Sigma Field Emission SEM with an accelerating voltage of 10 kV. Two samples from each coral were taken from the base and top of corals ER#31-A, ER#32-A, CB1-A, GW-A, DD-A, and TA-C and from the right and left sides of ER#30-C. These samples were mounted on SEM stubs with conductive glue and sputter coated with carbon. The SEM

photomicrographs were used to determine if the corals had been altered in any way.

### 5.2. Age determination

Given that the death year of the corals from Magic Reef (2014) and Cayman Brac (1932) are known, the basal ages of each coral were determined by (1)  $^{14}\text{C}$  dating, (2) U/Th dating, (3) growth band counting, and (4) calculations based on average growth rates.

Carbon-14 dating of the base of the corals from Magic Reef, CB1-A, and DD-A was done at the A.E. Lalonde AMS Laboratory, University of Ottawa. Pre-treatment following Crann et al. (2017) involved physical cleaning by manual abrasion and etching with 0.2N HCl. Graphite targets for accelerator mass spectrometry were prepared from  $\text{CO}_2$  liberated by sample dissolution in anhydrous  $\text{H}_3\text{PO}_4$  overnight at room temperature. Carbon-14 dating of the base of corals GW-A and TA-C, was performed using conventional gas-proportional counting as outlined by Blanchon (1995).

U/Th dating for samples from the base of corals ER#31-A, GW-A, DD-A, and TA-C, and the base and top of coral CB1-A were done at the GEOTOP-UQAM Laboratory, University of Quebec in Montreal. These samples were powdered and dissolved in nitric acid, a  $^{233}\text{U}$ - $^{236}\text{U}$ - $^{239}\text{Th}$  calibration spike was added, and the mixture was evaporated to dryness before being dissolved once again in 7N  $\text{HNO}_3$  and ~10 mg of an iron carrier and left overnight for spike-sample equilibrium. U and Th measurements were performed using a multicollector inductively coupled plasma mass spectrometer (MC-ICP-MS).

### 5.3. X-Ray images

X-Ray images were produced at the University of Alberta using a portable SY-31-100P X-Ray machine with scans generated at 70kV for 0.8 to 1.2 second scan times, depending on slab thickness. On these images, the light-colored bands (white) represent the densest material whereas the dark bands represent less dense material (cf., Buddermeier et al., 1974; Moore and Krishnaswami, 1974; Hudson et al., 1976). Growth band thickness was measured from the X-Ray images.

#### *5.4. Computer Tomography (CT) scan production and analysis*

CT scans, produced on an Aquilion ONE helical CT scanner at InnoTech Alberta (Edmonton, Alberta), were used to produce high-resolution density maps of each coral (cf., Bosscher, 1992; Chan et al., 2017). Each CT scan, which has a 0.5 mm voxel depth and 0.47 mm pixel width, is a compilation of numerous slices through the coral that are perpendicular to the maximum growth axis (763 slices for ER#30-C; 883 slices for ER#31-A; 758 slices for ER#32-A; 1064 slices for CB1-A; 1277 slices for GW-A; 1085 slices for DD-A; 548 slices for TA-C). ImageJ was used to map and determine the grey values along the growth axis of each coral. This calibration was performed using an 8-bit grey value step table, with 20 steps (changes in grey values); black was assigned a grey value of 0 and white a value of 252.

For each coral, a greyscale curve was produced using ERDAS Imagine. The greyscale values range from 0–252, with each coral having its own minimum and maximum value, to allow direct comparison between the corals. The original ERDAS Imagine graphs were smoothed using a 6-point moving average (or 3 years of coral growth).

#### *5.5. Elemental analysis*

Powdered samples, weighing 19-68 mg (3 from ER#30-C, 32 from ER#31-A, 6 from ER#32-A, 10 from CB1-A, 11 from GW-A, 12 from DD-A, 6 from TA-C) were analyzed for their Mg, Ca, and Sr concentrations (Table 3.1). A section of coral ER#31-A was analyzed for elemental concentration corresponding to the instrument measured water temperatures (1991-2004). All other coral samples were taken at random positions along the maximum growth axis of the coral skeletons. A Thermo Fisher iCAP-Q ICP-MS at the University of Alberta was used for these analyses. The samples were dissolved in 2 mL 50% HNO<sub>3</sub>. Then, 0.1 mL of this solution was added to 0.1 mL HNO<sub>3</sub>, 0.1 mL

**Table 3.1.** Elemental concentrations from the Cayman coral growth bands.

Coral	Sample location (cm from coral base)	Sample age (CE) <sup>1</sup>	Mg (ppm)	Sr (ppm)	Ca (ppm)	Sr/Ca (mmol/mol)
ER#30-C	4.5	1990	1084	7302	373544	8.9
(N = 3)	10.1	2000	1065	7041	365475	8.8
	15.2	2008	1035	7423	385664	8.8
ER#31-A	2.5	1962	1687	7213	364055	9.1
(N = 32)	6.0	1968	1391	7007	367997	8.7
	10.2	1973	1682	6935	364399	8.7
	16.9	1980	1338	7117	361410	9.0
	21.5	1987	1360	7141	366165	8.8
	23.3	1991	1346	7261	386462	8.6
	23.6	1991	1526	7145	374267	8.7
	24.6	1992	1626	7666	404089	8.7
	24.7	1992	1402	7272	379847	8.8
	25.4	1993	1413	7247	389790	8.5
	26.0	1993	1859	7536	391112	8.8
	26.4	1994	1725	7400	392564	8.6
	26.6	1994	2001	6890	353680	8.9
	27.1	1995	1509	7044	372074	8.5
	27.5	1995	1772	7085	366523	8.8
	28.0	1996	1623	6862	367415	8.5
	28.8	1997	1577	7069	352708	9.2
	29.4	1997	1679	6992	370061	8.6
	30.0	1998	1637	7413	394635	8.6
	20.8	1998	1589	7210	388592	8.5

Coral	Sample location (cm from coral base)	Sample age (CE) <sup>1</sup>	Mg (ppm)	Sr (ppm)	Ca (ppm)	Sr/Ca (mmol/mol)
ER#31-A	31.4	1999	2025	6953	381159	8.3
	31.8	1999	1830	7446	395201	8.6
	32.1	2000	1578	6750	362234	8.5
	32.4	2000	1961	7595	407722	8.5
	32.8	2001	2164	7347	385997	8.7
	33.1	2001	1618	6799	364127	8.5
	33.9	2002	1628	7151	382482	8.6
	34.5	2002	1925	7878	415544	8.7
	34.9	2003	1700	6963	357940	8.9
	35.2	2003	2120	7048	373134	8.6
	35.6	2004	1590	7056	380725	8.5
	35.9	2004	2238	7265	387160	8.6
ER#32-A	6.2 (left branch)	1974	2505	6792	355053	8.7
(N = 6)	13.0 (left branch)	1985	1932	7184	376921	8.7
	18.1 (left branch)	1993	1382	7076	367249	8.8
	23.5 (left branch)	2006	1230	7172	372040	8.8
	21.9 (right branch)	1989	1225	7132	372626	8.8
	46.9 (right branch)	2001	1520	6298	331656	8.7
CB1-A	4.9	1877	1505	7157	371591	8.8
(N = 10)	10.0	1884	1151	6749	351313	8.8
	15.3	1890	1218	6947	363351	8.7
	20.2	1896	1202	6944	361027	8.8
	24.8	1902	1146	6942	355073	8.9

Coral	Sample location (cm from coral base)	Sample age (CE) <sup>1</sup>	Mg (ppm)	Sr (ppm)	Ca (ppm)	Sr/Ca (mmol/mol)
CB1-A	32.8	1911	1259	7294	380029	8.8
	36.8	1916	1093	7134	362542	9.0
	41.1	1921	1216	7379	372207	9.1
	45.5	1925	1271	7003	362149	8.8
	49.3	1930	1207	7173	368704	8.9
GW-A	3.6	1822	1575	7160	378489	8.7*
(N = 11)	7.1	1828	1219	5848	300472	8.9
	11.5	1834	1508	5672	277656	9.3
	4.1	1841	1394	5884	295664	9.1
	12.7	1857	1374	5359	348303	8.8
	18.4	1864	1637	7103	359973	9.0
	4.4	1872	1560	5672	297273	9.1
	8.0	1877	1342	6990	347238	9.2
	12.8	1887	1639	7071	354788	9.1
	15.5	1893	1898	5732	284033	9.2
	19.4	1900	1472	6766	352765	8.8*
	DD-A	5.8	1824	1850	7361	353807
(N = 12)	10.0	1829	1466	7220	343987	9.6
	14.4	1835	1862	5943	286649	9.5
	25.2	1849	1480	7269	351795	9.5
	29.4	1854	1756	6016	297765	9.2
	32.5	1859	1706	7175	356850	9.2
	36.5	1865	1710	6973	352952	9.0
	37.8	1866	1853	5996	293650	9.3

Coral	Sample location (cm from coral base)	Sample age (CE) <sup>1</sup>	Mg (ppm)	Sr (ppm)	Ca (ppm)	Sr/Ca (mmol/mol)
DD-A	41.7	1872	1536	6875	346018	9.1
	49.3	1883	1516	6754	340681	9.1
	50.0	1884	1850	7361	353807	9.5
	51.9	1887	1406	6305	311996	9.2
TA-C (N = 7)	1.4	1476	1875	6683	339153	9.0
	6.8	1487	1743	5885	299595	9.0
	8.9	1490	1478	6802	33537	9.3
	13.4	1497	1844	7399	380149	8.9*
	16.5	1501	1876	5865	300959	8.9*
	19.8	1506	1367	7086	353661	9.2
	23.0	1507	1447	6958	369003	8.6*

1. Ages based on growth band counting

\* These values have been removed from the data set, as outliers, due to inconsistent (low) Sr concentrations relative to the proportion of Ca in the coral skeletons.



100 ppb internal standards (Sc, In, and Bi), and 9.7 mL deionized water. The samples were analyzed using a 4-point calibration curve (0, 0.001, 0.002, and 0.004 ppm for Sr, 0, 0.05, 0.1, and 0.2 ppm for Mg and Ca), with typical count rates for 1 ppb between 300000 to 400000 cps. Detection limits were 0.52, 10.41, and 0.005 ppb for Mg, Ca, and Sr, respectively.

### 5.6. *Stable C and O isotope analysis*

Each sample came from a different growth band that was accurately delineated by placing the CT scan on a 2–4 cm thick slab that had been cut from the central part of each coral parallel to the maximum growth direction. Samples were taken from the thecal walls of the coral skeleton (cf., Leder et al., 1996; Watanabe et al., 2001; Kilbourne et al., 2010). A Dremel 8200 drill with a 0.89 to 1.6 mm round bit (inner diameter) was used for sample collection depending on growth band thickness. Only samples with >95 wt% aragonite (as confirmed by XRD) with no evidence of cement/alteration and/or borings were used for analyses (cf., McGregor and Gagan, 2003; Quinn and Taylor, 2006; Hendy et al., 2007; Sadler et al., 2014). The basal and upper 0.5 to 5 cm (or 1 to 10 years) of each coral were not analyzed because they had been altered by boring organisms. The following samples were collected:

- Coral ER#30-C: 63 samples (33 light and 30 dark bands) at 2 to 4 mm spacing.
- Coral ER#31-A: 78 samples (40 light and 38 dark bands) at 2 to 7 mm spacing.
- Coral ER#32-A: 114 samples (57 light and 57 dark bands) at 2 to 4 mm spacing.

Two branches from this coral were analyzed.

- Coral CB1-A: 120 samples (61 light and 59 dark bands) at 2 to 7 mm spacing.
- Coral GW-A: 186 samples (91 light and 95 dark bands) at 1 to 8 mm spacing
- Coral DD-A: 134 samples (67 light and 67 dark bands) at 3 to 8 mm spacing
- Coral TA-C: 77 samples (39 light and 38 dark bands) at 1 to 4 mm spacing

The  $\delta^{13}\text{C}$  and  $\delta^{18}\text{O}$  values were determined using a Gasbench II system coupled

with a Thermo MAT 253 Isotope Ratio Mass Spectrometer (IRMS) at the University of Alberta. Powdered samples, each weighing  $0.23 \pm 0.06$  mg, were held at a constant temperature of  $72^\circ\text{C}$  over the course of the analyses. A high purity helium stream was introduced to each vial to flush for 10 minutes to remove air. Subsequently, 0.1 mL of 100% phosphoric acid at  $72^\circ\text{C}$  was reacted with a sample for at least 1 hour. Produced  $\text{CO}_2$  was then carried by a helium stream to the IRMS for  $^{18}\text{O}/^{16}\text{O}$  and  $^{13}\text{C}/^{12}\text{C}$  measurements. During every run sequence, calcite international standard NBS-18 ( $\delta^{13}\text{C} = -5.0\text{‰}$ ,  $\delta^{18}\text{O}_{\text{VPDB}} = -23.0\text{‰}$ ) and two in-house calcite lab standards (LSC-1:  $\delta^{13}\text{C} = -51.3\text{‰}$ ,  $\delta^{18}\text{O}_{\text{VPDB}} = -16.1\text{‰}$  and LSC-2:  $\delta^{13}\text{C} = -22.0\text{‰}$ ,  $\delta^{18}\text{O}_{\text{VPDB}} = -34.6\text{‰}$ ) were measured throughout the sequence to establish a calibration curve, monitor data quality, and long-term instrument performance. Analytical uncertainties ( $2\sigma$ ) are  $\pm 0.16\text{‰}$  for  $\delta^{18}\text{O}$  and  $\pm 0.15\text{‰}$  for  $\delta^{13}\text{C}$ . The C and O isotope compositions are reported using the  $\delta$  notation relative to VPDB (Vienna Pee Dee Belemnite) and VSMOW (Vienna Standard Mean Ocean Water) standards, respectively. The  $\delta^{18}\text{O}$  values were converted from VPDB to VSMOW using Equation 2.21 ( $\delta^{18}\text{O}_{\text{VSMOW}} = 1.0309[\delta^{18}\text{O}_{\text{VPDB}}] + 30.91$ ) from Sharp (2007).

Given that the samples are composed of aragonite whereas the laboratory standards used for the calibration curve are calcite, a correction factor of  $-0.38\text{‰}$  (from Kim et al., 2007; 2015) was made to the  $\delta^{18}\text{O}$  values to account for the difference in the phosphoric acid fractionation of these two minerals at the temperature used for carbonate dissolution ( $72^\circ\text{C}$ ). It should be noted, however, that not all published  $\delta^{18}\text{O}$  values for corals (e.g., Weber, 1977; Leder et al., 1996; Watanabe et al., 2001) have had this correction applied.

### 5.7. Water temperature and isotopic composition

From 1991 to 2007, the Department of Environment and the Water Authority Cayman Islands monitored seawater temperature at various locations around Grand

Cayman at the sea surface (0.9–1.2 m depth) and at depth (11.3–14.5 m). This included George Town, which is close to Magic Reef (Fig. 1B, 2A). These records and satellite data from 1980 to 1990 (Goreau et al., 1992), 1993 to 2008 (Chollett et al., 2012b), and 1981 to 2015 (NOAA, 2018), are combined and used herein.

Two samples of seawater, one from the surface above Magic Reef and the other from beside the reef at a depth of 18.3 m, were collected by the Department of Environment in May 2016. A seawater sample from the east end of Cayman Brac was collected in October 2018. Their oxygen isotope compositions were determined by Isotope Tracer Technologies Ltd., Ontario, Canada, using a Thermo Delta Plus Advantage linked to a Gasbench I via a GC PAL autosampler.  $\delta^{18}\text{O}_{\text{water}}$  values are reported relative to the VSMOW standard.

## 6. Results

### 6.1. Mineralogy

Samples from the base of the corals and their bored margins contain <95 wt% aragonite, whereas samples from individual growth bands in the rest of the coral contained >95 wt% aragonite. Thin section and SEM analyses confirmed that the aragonite skeletons had not been altered (Figs. 3.3, 3.4). Only very minor amounts of cement were found in isolated pores in ER#32-A and CB1-A.

### 6.2. Growth patterns - grey values

The growth bands evident in the CT scans are largely characterized by uniform and consistent grey levels within each light and dark band. Some growth bands in corals ER#31-A, ER#32-A, and DD-A, however, are characterized by 4 to 12 thin (0.2 to 1.1 mm), alternating light and dark microbands. Designation of these heterogeneous growth bands as light or dark reflects the dominant shade that is present.

Corals ER#30-C, CB1-A, GW-A, and TA-C are characterized by homogeneous



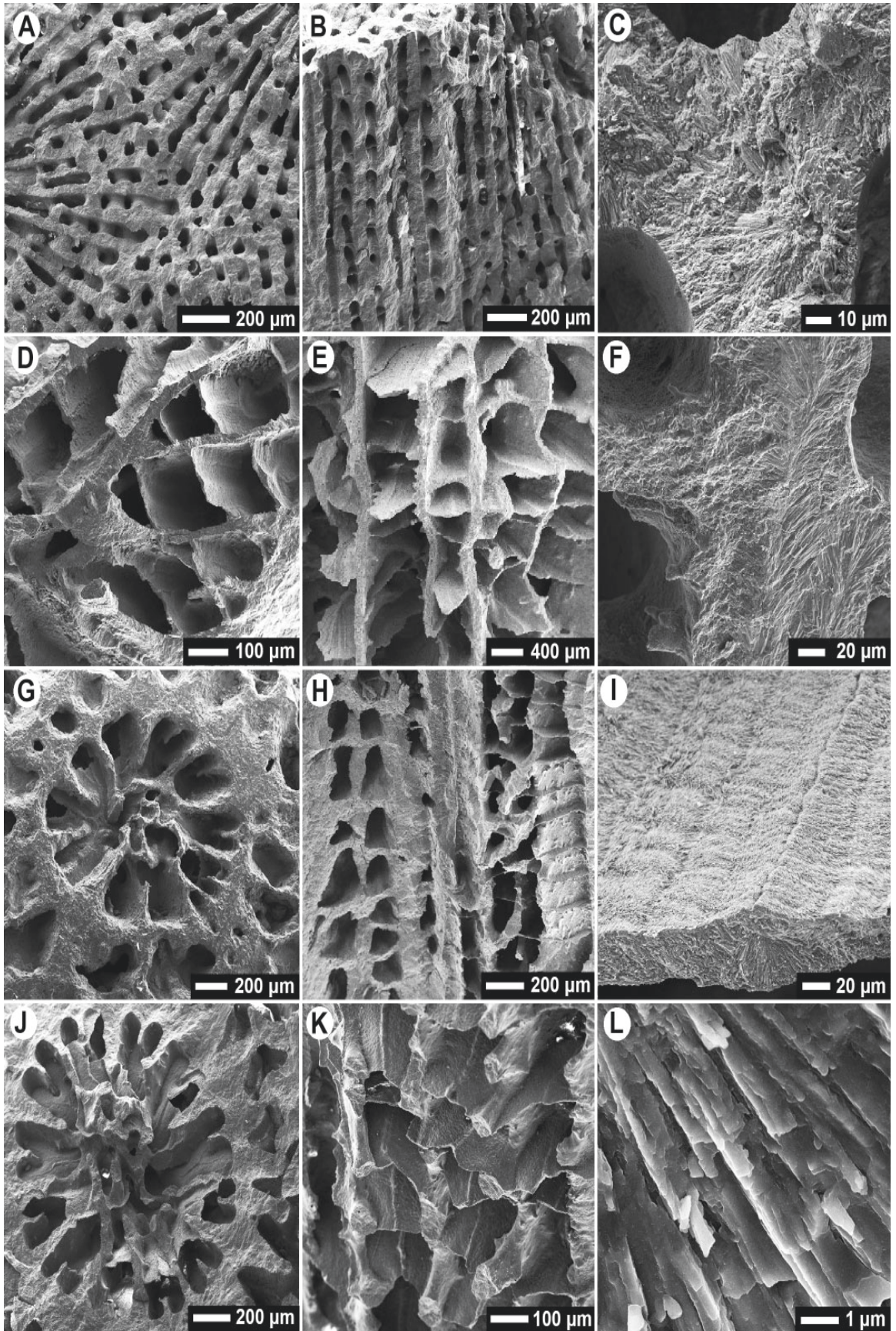


**Fig. 3.3.** SEM images from the Cayman corals. (A) Intersection of three corallites in ER#30-C, displaying well-developed coenosteum and septal structures. (B) Theca structure from ER#30-C, displaying thecal walls and endothelial dissepiments. (C) Close up image of costae from ER#30-C, showing well-developed aragonite needle bundles. (D) Oblique view of a corallite from ER#31-A, displaying open pore spaces. (E) Theca structure from ER#31-A, displaying thecal walls and endothelial dissepiments. (F) Close up image of thecal wall from ER#31-A, showing well-developed aragonite needle bundles. (G) Corallite from ER#32-A, showing open pore spaces and well-developed septa. (H) Theca structure from ER#32-A, displaying thecal walls and endothelial dissepiments. (I) Close up image of endothelial dissepiment from ER#32-A, showing well-developed sclerodermites formed of aragonite needle bundles. (J) Corallite from CB1-A, showing open pore spaces and well-developed septa. (K) Theca structure from CB1-A, displaying thecal walls and endothelial dissepiments. (L) Aragonite needles from CB1-A. All images display open pore spaces and are devoid of cements.

---

growth bands that are 1 to 8 mm thick (Fig. 3.5). In coral CB1-A, however, there are four light growth bands that are significantly thicker (>7 mm) than the other growth bands. The grey level curves range from 3 to 211, with a smooth curve characterized by regular fluctuations that correspond to the growth bands (Fig. 3.6).

Corals ER#31-A, ER#32-A, and DD-A are characterized by homogenous and heterogenous growth bands that are 1 to 9.5 mm thick (Fig. 3.7). Coral ER#31-A contains five light and one dark growth band that are >8 mm thick and ER#32-A contains one light and one dark growth bands that are >6 mm thick. The grey level curves range from 12 to 219, with small-scale variations that are superimposed on the large-scale fluctuations (Fig. 3.6).



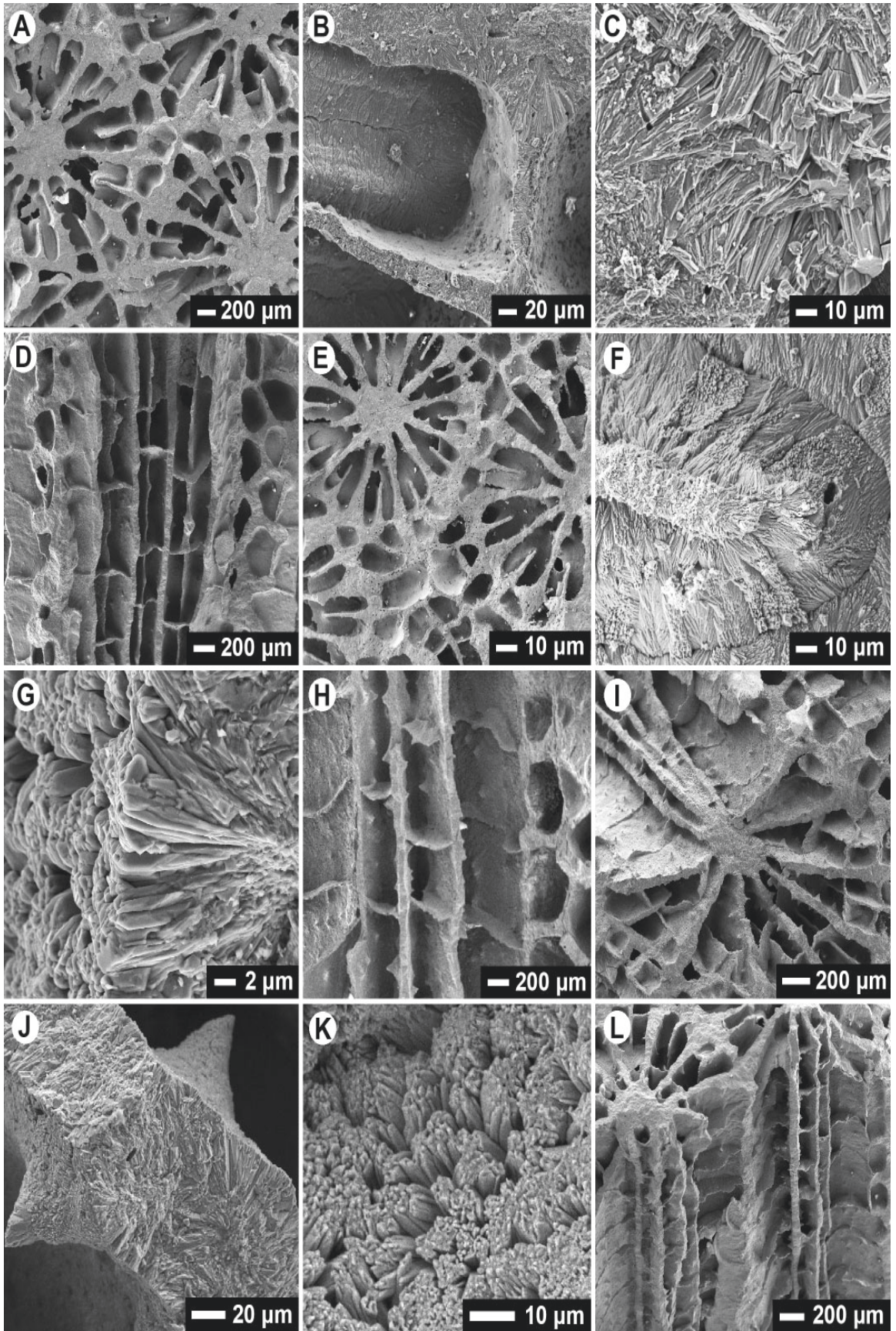


**Fig. 3.4.** SEM images from the Cayman corals. (A) Intersection of three corallites in GW-A, displaying well-developed coenosteum and septal structures. (B) Close up of septal sides and margin from GW-A. (C) Aragonite needle bundles from GW-A. (D) Theca structure from GW-A, displaying thecal walls and endothecal dissepiments. (E) Intersection of four corallites in DD-A, displaying well-developed coenosteum and septal structures. (F) Close up image of septal margin and floor from ER#31-A, showing well-developed aragonite needle bundles. (G) Aragonite needle bundles from DD-A. (H) Theca structure from DD-A, displaying thecal walls and endothecal dissepiments. (I) Oblique view of a corallite from TA-C, showing open pore spaces and well-developed structures. (J) Close up image of a dentate septal from TA-C, showing well-developed aragonite needle bundles. (K) Aragonite needle bundles from TA-C. (L) Oblique view of theca structure from TA-C, displaying thecal walls, endothecal dissepiments, and corallites. All images display open pore spaces and are devoid of cements.

---

### 6.3. Coral ages

#### 6.3.1. Carbon-14 dating and U/Th dating

The  $^{14}\text{C}$  and U/Th date for the basal parts of the corals and the upper part of CB1-A are variable and open to debate (Tables 3.2, 3.3). The basal ages as determined by U/Th dating are used in preference to the  $^{14}\text{C}$  ages for corals GW-A and DD-A because the (1)  $^{14}\text{C}$  ages are unreliable because the corals are too young and error margins are too large for reliable age determination, (2)  $^{14}\text{C}$  probability distribution for DD-A is multi-modal, (3) U/Th dates have smaller uncertainties, (4) samples contain no evidence of internal  $^{230}\text{Th}$  (e.g., Cobb et al., 2003), and (5) U/Th dates do not require the application of a reservoir correction. For coral TA-C, no U/Th age was produced because the

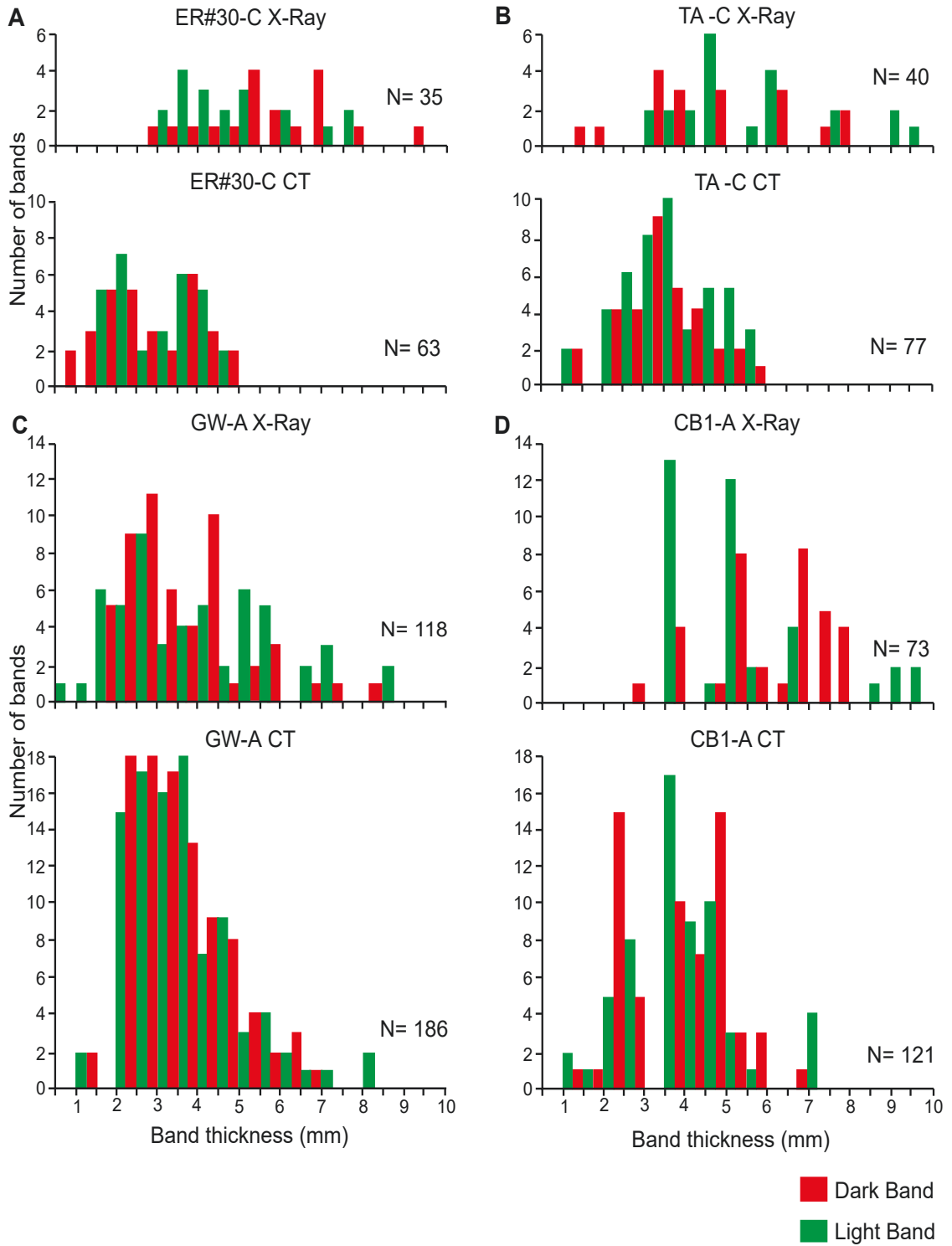


**Fig. 3.5.** Histograms of coral growth band thickness, showing the contrast in band thickness as determined from X-Ray images and CT scans. (A) ER#30-C, (B) TA-C, (C) GW-A, and (D) CB1-A. Light (green) and dark (red) growth bands as identified on X-Ray and CT scan.



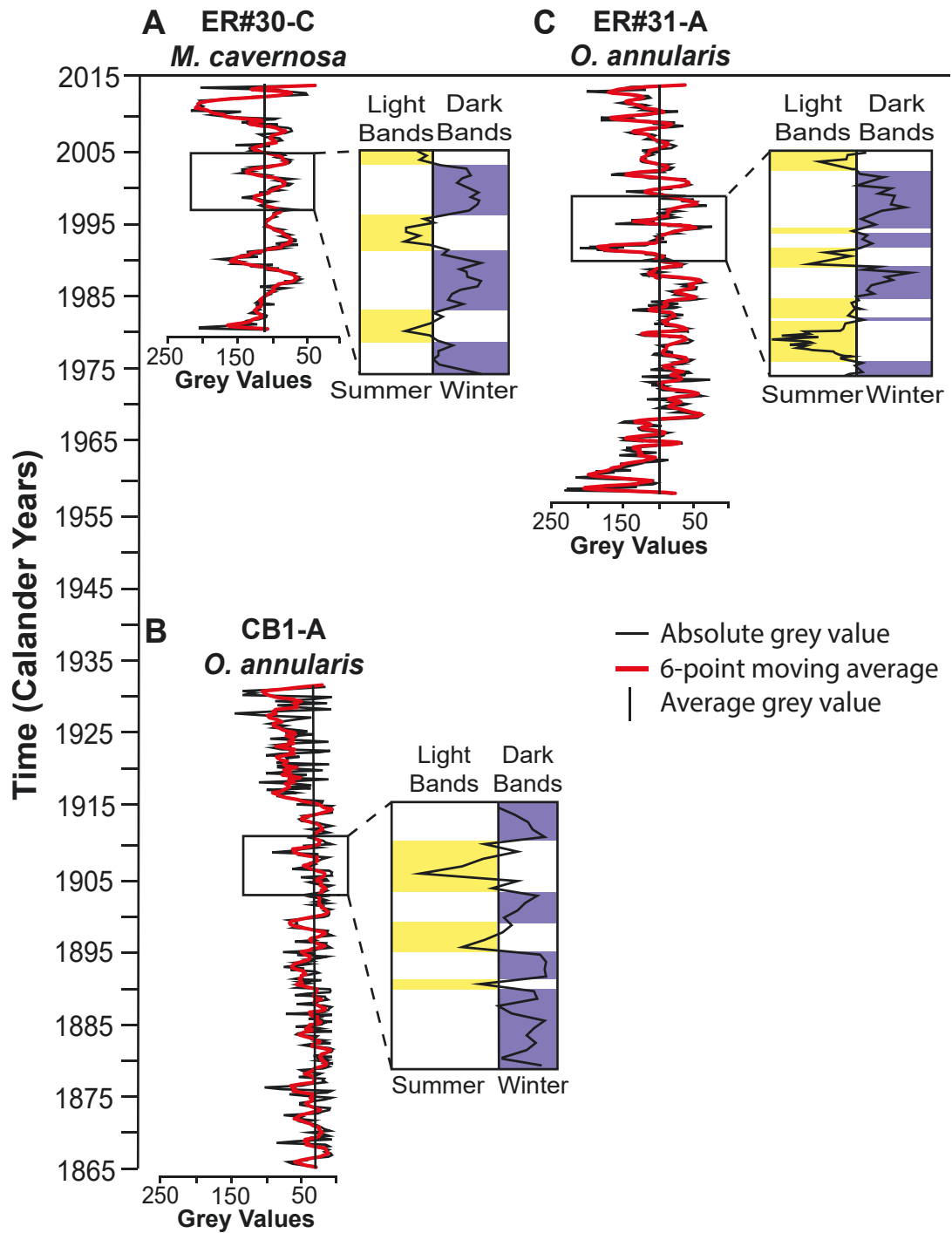


**Fig. 3.6.** Pattern of growth banding in corals (A) ER#30-C, (B) CB1-A, and (C) ER#31-A, based on skeletal density as identified by grey levels on the CT scans relative to the average grey values of each coral. CT scan for (C) displays homogenous and heterogeneous (microbands highlighted) growth banding and (A and B) displays homogeneous growth only.

**Table 3.2.**  $^{14}\text{C}$  dating information. Calibration was performed using the MARINE13 calibration curve (Reimer et al., 2013). Calendar years for the coral samples were calibrated using Calib 7.10 (Reimer et al., 2013). Samples ER#30-C, ER#31-A, and ER#32-A were analyzed September 21, 2016. Samples CB1-A and DD-A were analyzed March 20, 2017. Samples GW-A and TA-C were analyzed October 11, 1990. All errors are reported at the  $1\sigma$  level.

Coral ID	Sample ID	Weight (mgC)	$\delta^{13}\text{C}$ (‰)	Fraction of $^{14}\text{C}$	Conventional $^{14}\text{C}$ age (BP)	Reservoir correction (‰)	Reservoir corrected age (BP)	$\Delta^{14}\text{C}$	Calendar year CE
ER#30-C	UOC-2669	1.29	-1.45 $\pm 0.15$	0.9564 $\pm 0.0027$	358 $\pm$ 22	-28	95 $\pm$ 22	-43.6	Too young
ER#31-A	UOC-2670	1.31	-1.73 $\pm 0.15$	0.9426 $\pm 0.0026$	475 $\pm$ 22	-28	240 $\pm$ 22	-57.5	Too young
ER#32-A	UOC-2671	1.39	-1.25 $\pm 0.15$	0.9524 $\pm 0.0027$	391 $\pm$ 22	-28	113 $\pm$ 22	-47.6	Too young
CB1-A	UOC-4023	1.39	-0.16 $\pm 0.15$	0.9451 $\pm 0.0035$	453 $\pm$ 29	-28	143 $\pm$ 29	-54.8	Too young
GW-A	1260Cc	n.d.	+0.20 $\pm 0.15$	0.9815	150 $\pm$ 90	-28	Modern	-19.5	Too young
DD-A	UOC-4022	1.31	+0.39 $\pm 0.15$	0.9419 $\pm 0.0032$	481 $\pm$ 27	-28	129 $\pm$ 27	-58.1	1862 CE (1835–1889)
TA-C	1267Cc	n.d.	-2.40 $\pm 0.15$	0.9018	830 $\pm$ 90	-28	476 $\pm$ 90	-99.0	1474 CE (1384–1564)



**Table 3.4.** General coral characteristics.

	ER#30-C	ER#31-A	ER#32-A	CB1-A	GW-A	DD-A	TA-C
Species <sup>1</sup>	<i>M. cavernosa</i>	<i>O. annularis</i>	<i>O. annularis</i>	<i>O. annularis</i>	<i>O. annularis</i>	<i>O. annularis</i>	<i>M. cavernosa</i>
Water Depth (m)	20	20	20	20	25	19.8	15.8
Location	Magic Reef, Grand Cayman	Magic Reef, Grand Cayman	Magic Reef, Grand Cayman	S coast Cayman Brac	SW Grand Cayman	SW Grand Cayman	North Sound, Grand Cayman
Size- Height (cm)	19.5	48.0	42.0	50.0	57.0	54.0	35.0
Diameter (cm)	36.0	24.0	28.0	36.5	9.5	9.5	9.5
Age <sup>2</sup>	1980-2014	1959-2014	1962-2014	1865-1932	1815-1908	1822-1889	1474-1512
# Growth Couplets <sup>3</sup>	34	55	52	67	93	67	38
Growth Rate vs Size <sup>4</sup>	44	80	70	83	95	90	59
<sup>14</sup> C (Calendar years)	358 ±22	475 ±22	391 ±22	453 ±29	150 ±90	481 ±27	830 ±90
U/Th		198 ±9		42 ±16	203 ±20	196 ±25	
Growth Band Style	Homogeneous	Homogeneous Heterogeneous	Homogeneous Heterogeneous	Homogeneous	Homogeneous	Homogeneous Heterogeneous	Homogeneous
Calculated T <sup>5</sup>							
Range (°C)	24.9 to 33.0	22.7 to 31.4	22.3 to 35.1	22.0 to 31.5	19.6 to 30.5	17.6 to 27.4	21.0 to 28.9
Average (°C)	28.3	26.9	28.5	27.4	23.5	21.9	25.1

1. Genus and species classification as defined by Budd et al. (2012),
2. Number of growth couplets determined from CT scans, corroborated by grey level and density values (converted to calendar years).
3. Age determinations based on growth band counting.
4. Age based on average growth rates versus coral height.
5. Calculated temperatures determined from the Cayman Island oxygen isotope geothermometer.

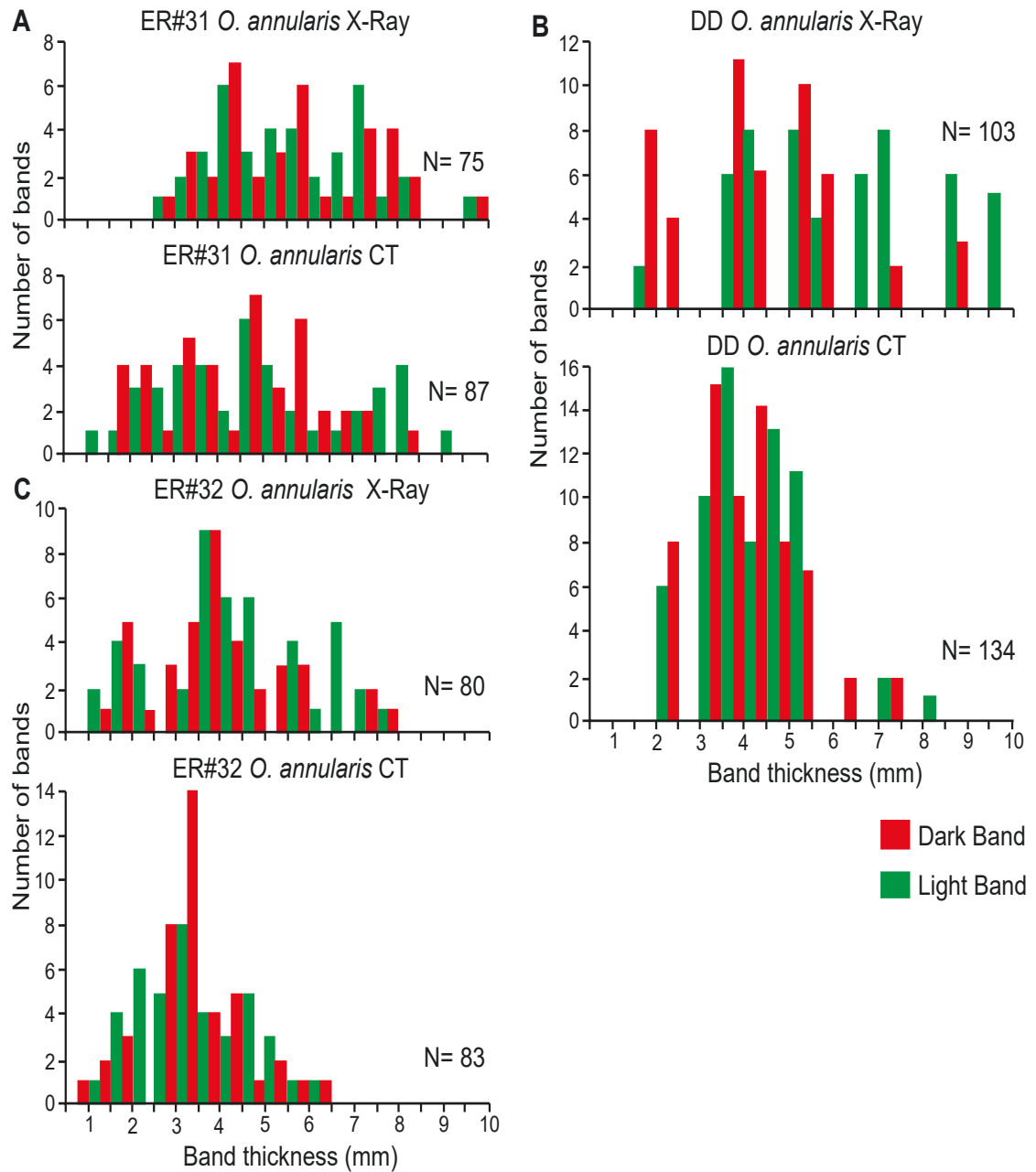


**Fig. 3.7.** Histograms of coral growth band thickness, showing the contrast in band thickness as determined from X-Ray images and CT scans. (A) ER#31-A, (B) ER#32-A, and (C) DD-A. Light (green) and dark (red) growth bands as identified on X-Ray and CT scan.

concentration of  $^{230}\text{Th}$  could not be measured accurately and it had a uranium isotopic composition that is higher than sea water. Accordingly, the  $^{14}\text{C}$  date is used for this coral.

### 6.3.2. Correlation to calendar years

The basal ages for corals GW-A, DD-A, and TA-C were converted into approximate calendar years using Calib 7.10 for the  $^{14}\text{C}$  dates and by subtracting the U/Th ages from 2018. Given the uncertainties associated with these dates, comparisons between the  $T_{\text{cal}}$  records from the different corals were also used to substantiate their ages. For example, corals GW-A and DD-A, which both came from the southwest coast of Grand Cayman, have similar basal ages, and  $T_{\text{cal}}$  records characterized by three high  $T_{\text{cal}}$  peaks that are separated by intervals with lower  $T_{\text{cal}}$ .

### 6.3.3. Growth bands

Given that each light and dark growth couplet represents one year of growth (cf., Knutson et al., 1972; Buddermeier et al., 1974; Dodge and Thomason, 1974; Hudson et al., 1976; Winter and Sammarco, 2010) the duration of coral growth can be determined from the high-resolution CT scans (Table 3.4).

### 6.3.4. Growth rates

Using average growth rates of 6.0 mm/year for *Orbicella* (ER#31-A, ER#32-A, CB1-A, GW-A, DD-A; Baker and Weber, 1975; Hudson 1981; Carricart-Ganivet et al., 1994; Carricart-Ganivet and Merino, 2001; Carricart-Ganivet, 2004) and 4.4 mm/year for *M. cavernosa* (ER#30-C, TA-C; Highsmith et al., 1983), the lifespans of the corals can be determined (Table 3.4). The fact that these ages are higher than those based on growth band counts probably reflects the fact that growth rate calculations are based on average growth rates from elsewhere in the Caribbean and may not be the same for the Cayman corals.

#### 6.4. Water isotope compositions

Water samples from Magic Reef yielded  $\delta^{18}\text{O}_{\text{water}}$  values of  $+0.75 \pm 0.18\text{‰}$  (surface) and  $+0.79 \pm 0.06\text{‰}$  (depth 18.3 m) that are consistent with the oxygen isotope compositions obtained from numerous seawater samples collected from Spotts Bay, Grand Cayman (Fig. 3.1B) over the last 20 years (Ren and Jones, 2017). Herein, the  $\delta^{18}\text{O}_{\text{water}}$  value from beside Magic Reef at a depth of 18.3 m ( $+0.8\text{‰}$ ) is used in the paleotemperature calculations for the corals from the southwest corner of Grand Cayman. The water sample from the east end of Cayman Brac yielded a  $\delta^{18}\text{O}_{\text{water}}$  value of  $-0.09 \pm 0.1\text{‰}$ .

#### 6.5. Derivation of $\delta^{18}\text{O}_{\text{water}}$ from elemental concentrations

##### 6.5.1. Elemental analyses

Eighty samples from the Cayman corals yielded Ca concentrations of 277656 to 415544 ppm, Sr concentrations of 5672 to 7878 ppm, Mg concentrations of 1035 to 2505 ppm, and Sr/Ca ratios of 8.3 to 9.6 mmol/mol (Table 3.1). The Sr/Ca ratios are similar to those reported for modern corals, including 8.9 – 9.2 mmol/mol for *Diploria strigosa* from Little Cayman (von Reumont et al., 2016), 8.5 – 9.5 mmol/mol for *O. faveolata* from St. Croix (Saenger et al., 2008), 9.1 – 9.3 mmol/mol for *A. danai* and *A. formosa* (Ribaud-Laurenti et al., 2001) from Reunion Island (Western Indian Ocean) and the Great Barrier Reef (Australia), and 8.9 – 9.5 mmol/mol for *Porites lutea* from New Caledonia (DeLong et al., 2007).

##### 6.5.2. Sr/Ca equation

There are more than 80 coral Sr/Ca geothermometer calibrations that are based on the negative correlation that exists between water temperature and the Sr/Ca ratio (e.g., Weber, 1973; Storz et al., 2013). Some incorporate the coral growth rate into the temperature formulation (e.g., Goodkin et al., 2005; Saenger et al., 2008, Kilbourne et

al., 2010), whereas others do not (e.g., Smith et al., 1979; Beck et al., 1992; de Villiers et al., 1994; Shen et al., 1996; Albert and McCulloch, 1997; Heiss et al., 1997; Gagan et al., 1998; Fallon et al., 1999; Correge et al., 2000; Swart et al., 2002; Smith et al., 2006; DeLong et al., 2007; Maupin et al., 2008; DeLong et al., 2011; Flannery and Poore, 2013; von Reumont et al., 2016; Kuffner et al., 2017).

In order to determine an appropriate Sr/Ca seawater temperature equation for the Cayman corals, the Sr/Ca data from the corals from Magic Reef were applied to all equations that have been developed for *Orbicella* (e.g., Swart et al., 2002; Smith et al., 2006; Saenger et al., 2008; Kilbourne et al., 2010; DeLong et al., 2011; Flannery and Poore, 2013; Flannery et al., 2018). Given that no Sr/Ca equation has been developed specifically for *M. cavernosa*, the equation developed from *Orbicella* is used. For the Magic Reef corals, the calculated water temperatures range from 14.9° to 57.4°C. For equations that incorporate growth rate, average values of 5.7, 8.7, and 8.1 mm/year (values derived by comparing the height of the coral with its age) were used for ER#30-C, ER#31-A, and ER#32-A, respectively. The Kilbourne et al. (2010) equation, which incorporates growth rate, yielded the lowest  $T_{\text{cal}}$  (16.0° to 23.8°C), with most  $T_{\text{cal}}$  being at the lower end of temperature spectrum preferred by *Orbicella* (15° to 32°C; Hunter, 1994). In contrast,  $T_{\text{cal}}$  derived from the Swart et al. (2002), Smith et al. (2006), Kilbourne et al. (2010; no growth rate), DeLong et al. (2011), Flannery and Poore (2013), and Flannery et al. (2018) equations yielded  $T_{\text{cal}}$  values at or above the upper end of the growth temperature spectrum. Herein, the equation from Saenger et al. (2008) ( $\text{Sr/Ca} = 11.82 - 0.058 * \text{extension rate (mm/yr)} - 0.092 * \text{SST}$ ) is used because the  $T_{\text{cal}}$  values obtained from the Magic Reef corals, from 23.3° to 32.3°C  $\pm$  0.1°C (average of 28.4°C) are within the T spectrum of *Orbicella* and are close to the measured water temperatures (T-test:  $p < 0.05$ ). Using this equation with the Sr/Ca ratios from corals CB1-A, GW-A, DD-A, and TA-C yielded  $T_{\text{cal}}$  of 19.0° to 30.6°C  $\pm$  0.1°C.



### 6.5.3. $\delta^{18}\text{O}_{\text{water}}$ determination

Oxygen isotope geothermometry requires knowledge of the  $\delta^{18}\text{O}$  value of both the coral and the water from which that coral precipitated. The  $\delta^{18}\text{O}_{\text{water}}$  value during coral growth can be determined from the Sr/Ca ratios of the coral skeleton and the corresponding  $\delta^{18}\text{O}_{\text{carbonate}}$  values. Although the current  $\delta^{18}\text{O}_{\text{water}}$  value for Magic Reef is known, the values for the coral from Cayman Brac and the older corals (GW-A, DD-A, TA-C) are unknown. The Sr/Ca ratios from the Magic Reef corals yielded temperatures of  $19^\circ$  to  $32^\circ\text{C} \pm 0.1^\circ\text{C}$  that, in turn, yielded  $\delta^{18}\text{O}_{\text{water}}$  values of  $-0.9$  to  $+1.7\text{‰}$  (Standard Deviation SD:  $0.6\text{‰}$ ), with an average of  $+0.8\text{‰}$ , the same as the present-day  $\delta^{18}\text{O}_{\text{water}}$  value from Magic Reef (T-test:  $p < 0.05$ ).

Coral CB1-A yielded  $\delta^{18}\text{O}_{\text{water}}$  values of  $-0.7$  to  $+0.6\text{‰}$  (SD:  $0.4\text{‰}$ ), with an average value of  $-0.04\text{‰}$ , which is similar to the current  $\delta^{18}\text{O}_{\text{water}}$  value from the east end of Cayman Brac ( $-0.09\text{‰}$ , T-test:  $p < 0.05$ ). Corals GW-A and DD-A yielded  $\delta^{18}\text{O}_{\text{water}}$  values of  $-0.9$  to  $+2.3\text{‰}$  (SD:  $0.8\text{‰}$ ), with an average of  $+1.0\text{‰}$ . Coral TA-C yielded  $\delta^{18}\text{O}_{\text{water}}$  values of  $+0.7$  to  $+1.7\text{‰}$  (SD:  $0.5\text{‰}$ ), with an average of  $+1.4\text{‰}$ . For the corals from Magic Reef (ER#30-C, ER#31-A, ER#32-A), GW-A, and DD-A, the average calculated  $\delta^{18}\text{O}_{\text{water}}$  value ( $+0.8\text{‰}$ ) is in accordance with the current measured water value from Magic Reef. The southwest corner of Grand Cayman is characterized as the leeward coast with minimal mixing, resulting in a more enriched  $\delta^{18}\text{O}$  value than the global seawater ( $0.0\text{‰}$ ). The coral from Cayman Brac, however, was collected on the exposed windward coast of the island, which is a well mixed environment, resulting in a measured and calculated  $\delta^{18}\text{O}_{\text{water}}$  value that is very similar to the global average. Herein, average  $\delta^{18}\text{O}_{\text{water}}$  value of  $+0.8$ , will be used for the corals from Magic Reef (ER#30-C, ER#31-A, ER#32-A), GW-A, and DD-A, and  $0.0\text{‰}$  for CB1-A for temperature calculations ( $1\sigma \pm 0.3\text{‰}$  for all corals).

Coral TA-C was collected from North Sounds exposed fringing reef at a water depth of  $15.8$  m, the calculated  $\delta^{18}\text{O}_{\text{water}}$  value, however, does not support a well mixed

environment. The calculated  $\delta^{18}\text{O}_{\text{water}}$  (+1.4‰) is enriched, which may, in part, be related to the age of this coral (1474-1512), which grew during the Little Ice Age (LIA). The LIA may have caused more seasonal variability in the Caribbean (Watanabe et al., 2001), potentially contributing to a more enriched  $\delta^{18}\text{O}_{\text{water}}$ . Since the  $\delta^{18}\text{O}_{\text{water}}$  value of the Caribbean is unknown during this time, the average value calculated from TA-C (+1.4‰  $\pm$  0.3‰) will be used in the temperature calculations.

### 6.6. *Stable isotope compositions*

The isotopic compositions of the Cayman corals, with  $\delta^{13}\text{C}_{\text{VPDB}}$  values of  $-4.9$  to  $+2.0$ ‰ and  $\delta^{18}\text{O}_{\text{coral}}$  values of  $+25.4$  to  $+29.5$ ‰ (Table 3.5, Supplementary Tables 3.1-3.7), are similar (slightly enriched) to the ranges reported for other corals globally (e.g., Keith and Weber, 1965; Weber and Woodhead, 1970; Swart, 1983; Fig. 3.8). The isotopic compositions of the corals from Grand Cayman are enriched in  $\delta^{18}\text{O}$  when compared to those from Cayman Brac (Fig. 3.8), corresponding to the more  $^{18}\text{O}$ -enriched seawater from Grand Cayman.

## 7. Interpretations

### 7.1. *Coral age*

The four methods used to determine the ages of the corals from Magic Reef and Cayman Brac produced different dates (Table 3.4). Growth band couplet counting gives a minimum age because it cannot account for periods of no growth (Carricart-Ganivet, 2011), and errors may arise from bands that are not evident or are artifacts of the X-Ray or CT images (Barnes et al., 1989; Barnes and Taylor, 1993). The Cayman corals, however, do not display any evidence of stress banding (cf., Worum et al., 2007) or internal abrasion resulting from periods of no growth.

Age calculations based on average growth rate assume that growth was continuous and the growth rate constant (cf., Hudson et al., 1981; Carricart-Ganivet, 2004; DeLong et al., 2010). For the Cayman corals, this yielded lifespan estimates that

**Table 3.5.** Range and average isotope compositions of successive growth bands from Cayman corals.

Sample	$\delta^{13}\text{C}_{\text{VPDB}}$ (‰)	$\delta^{18}\text{O}_{\text{VSMOW}}$ (‰)	$\delta^{18}\text{O}_{\text{VPDB}}$ (‰)
ER#30-C	-3.0 to 0.0, -1.5	26.7 to 28.0, 27.3	-4.5 to -2.8, -3.5
CB1-A	-4.9 to +2.0, -0.1	25.8 to 27.8, 26.7	-4.9 to -3.1, -4.1
Homogeneous light band	-1.5 to +1.7, -0.2	26.0 to 26.7, 26.2	-4.1 to -3.4, -4.4
Homogeneous dark band	+0.3 to +0.9, +0.6	26.3 to 26.9, 26.5	-4.5 to -3.9, -4.3
GW-A	-4.4 to +0.1, -0.6	26.7 to 29.1, 28.2	-5.1 to -1.8, -2.6
TA-C	-4.5 to +0.6, -0.7	25.4 to 29.4, 28.3	-5.3 to -1.5, -2.3
ER#31-A	-2.6 to +0.3, -1.2	26.6 to 28.4, 27.6	-4.2 to -2.4, -3.2
Heterogenous light band			
Vertical sampling	-2.0 to +0.1, -1.4	26.9 to 27.9, 27.3	-3.9 to -2.9, -3.5
Horizontal sampling	-0.3 to -1.3, -1.0	26.1 to 28.1, 27.1	-4.7 to -2.7, -3.7
Heterogeneous dark band			
Vertical sampling	-2.1 to -0.1, -1.4	27.2 to 28.1, 27.6	-3.6 to -2.7, -3.2
Horizontal sampling	-0.5 to +1.9, -1.2	26.8 to 27.8, 27.2	-4.0 to -3.0, 3.6
ER#32-A	-0.5 to -3.8, -2.3	25.8 to 28.5, 26.8	-4.9 to -2.3, -3.6
DD-A	-4.9 to +0.8, -0.2	25.8 to 29.5, 28.6	-5.0 to -1.4, -2.3

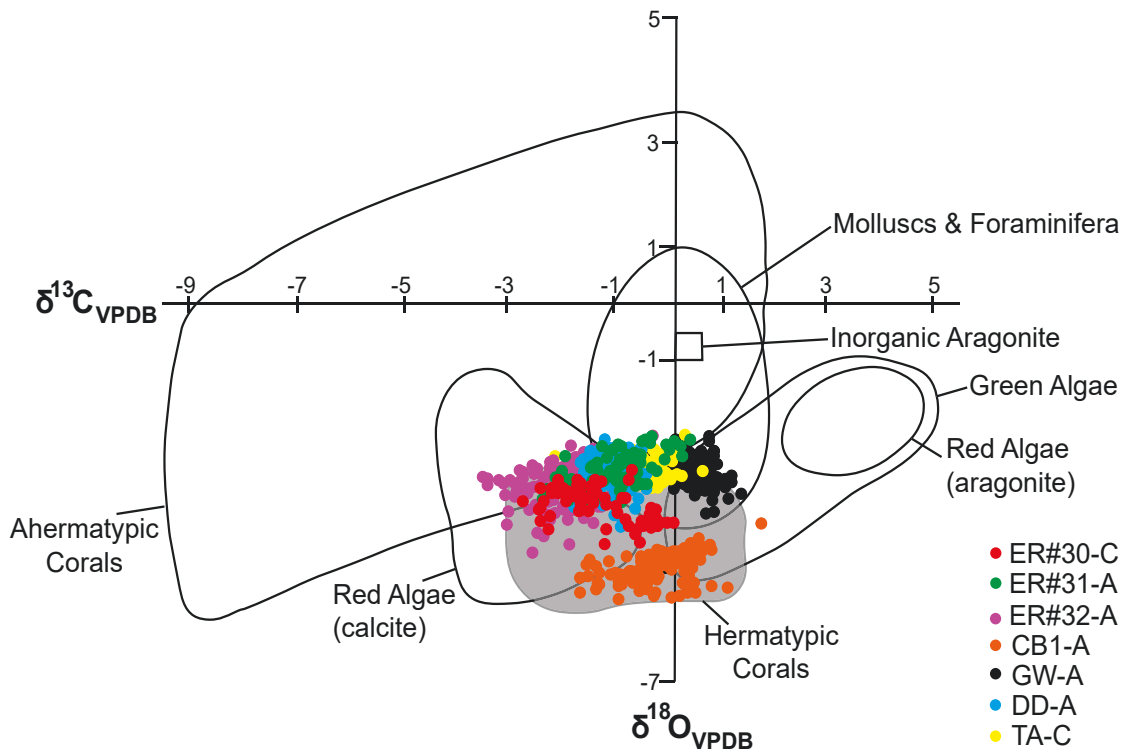


**Fig. 3.8.** Carbon and oxygen isotope compositions of the Cayman corals compared with those from other calcareous organisms (data from Swart, 1983). Grey shaded area indicates range of stable isotope compositions for hermatypic corals, showing an overlap between the Cayman values and previously reported coral values.

are 10 to 25 years longer than those based on growth band counts. This discrepancy may be a function of the average growth rate that was used.

The ages obtained from radiocarbon dating for the corals from Magic Reef and Cayman Brac are questionable because of the large propagated uncertainties when the measured radiocarbon years are converted to calendar years using the CALIB marine calibration curve (Stuiver et al., 2018) for corals less than 200 years old. The marine reservoir correction for the Cayman Islands is unknown, and  $\Delta R$  values from Cuba ( $\Delta R = -46$  to  $+222$ , Diaz et al., 2017), Florida ( $\Delta R = -11$  to  $+207$ , Druffel, 1997; Hadden and Cherkinsky, 2015), Venezuela ( $\Delta R = +13$  to  $+33$ , Hughen et al., 2004), Puerto Rico ( $\Delta$

R = -27, Kilbourne, 2007), and the Florida Keys ( $\Delta R = -54$  to  $-64$ , Toth et al., 2017) are highly variable.

For young corals, U/Th dating can, in principle, provide more precise ages than  $^{14}\text{C}$  dating (Cobb et al., 2003). For the corals from Magic Reef and Cayman Brac, however, the derived ages are inconsistent with those obtained from other methods. The U/Th age of  $198 \pm 9$  years for the base of coral ER#31-A, for example, is more than three times the age determined from growth band counting (55 years) and twice that determined from growth rates (80 years). The U/Th age for the base of coral CB1-A ( $217 \pm 14$  years) is also much older than that obtained by band counting (167 year difference) and growth rate calculation (165 year difference). For the top of coral CB1-A, however, the U/Th age of  $175 \pm 8$  years, implies that the lifespan of this coral was  $42 \pm 16$  years, which is much less than the lifespan based on growth band counting (67 years) and growth rate (83 years). These age discrepancies may be due to the presence of variable amounts of non-radiogenic  $^{230}\text{Th}$  in the corals (e.g., Cobb et al., 2003; Shen et al., 2008). This initial  $^{230}\text{Th}$  may have been brought into the Caribbean Basin as wind blown African dust (Trapp et al., 2010; Prospero and Mayol-Bracero, 2013) and incorporated into the coral skeleton during growth. Herein, the growth band counting ( $\pm 5$  years) method based on the high-resolution CT scans is used for the corals from Magic Reef and Cayman Brac because it gives the most accurate delineation of the growth bands, and hence the corals' age (Table 3.4).

## 7.2. Growth band thickness

The Cayman corals are characterized by growth bands that are 0.8 to  $9.5 \pm 0.05$  mm thick (Figs. 3.5, 3.7, 3.9). The light growth bands, indicative of growth during the dry season when the Cayman Islands experience warmer temperatures and increased solar radiation (cf., Buddemeier et al., 1975; Fairbanks and Dodge, 1979; Winter and Sammarco, 2010), are generally thicker than the dark bands that grew during the wet

season when increased cloud cover led to a reduction in sunlight, increased precipitation, and cooler temperatures (cf., Buddemeier et al., 1974; Fairbanks and Dodge, 1979; Winter and Sammarco, 2010). Unusually thick (>6 mm) light growth bands in corals ER#31-A, ER#32-A, and CB1-A may reflect prolonged dry seasons. Similar dry versus wet seasonal growth patterns have been reported for corals from the Pacific Ocean and the Atlantic Ocean (cf., Buddemeier et al., 1974; Moore and Krishnaswami, 1974; Buddemeier and Kinzie, 1976; Fairbanks and Dodge, 1979; Knowlton et al., 1992; Delong et al., 2011; Flannery and Poore, 2013; Sadler et al., 2016; Fig. 3.9).

The growth band thicknesses for *O. annularis* and *M. cavernosa* from the Cayman Islands are similar to those found in other Caribbean corals (Fairbanks and Dodge, 1979; Hudson, 1981; Knowlton et al., 1992; Delong et al., 2011; Flannery and Poore, 2013; Fig. 3.9). The greater ranges of thicknesses found in the Cayman corals may be a reflection of the methods used because CT scans provide higher resolution than the X-Ray images (Figs. 3.5, 3.7, 3.9) that have been used in many studies (e.g., Buddemeier et al., 1974; Hudson, 1981; Knowlton et al., 1992; DeLong et al., 2011; Sadler et al., 2016). For the Cayman coral, the higher resolution CT scans allow identification of the thinner growth bands that are not evident on the X-Ray images (cf., Saenger et al., 2009).

### 7.3. Geothermometry

#### 7.3.1. Rates of growth

Comparison of the thick (>6 mm) homogeneous and heterogeneous light and dark growth bands in ER#31-A and CB1-A (both *O. annularis*) shows variations in the stable isotope compositions and densities that reflect differences in their growth histories (Figs. 3.6, 3.10). In ER#31-A, the  $\delta^{18}\text{O}_{\text{coral}}$  values from sampling horizontally along light and dark heterogeneous growth bands (26.9 to 28.1‰) are relatively constant (SD = 0.4‰), whereas those from sampling vertically across the growth bands are more variable (SD = 0.7‰; Fig. 3.10. Table 3.5). In contrast, the light and dark thick homogeneous bands in

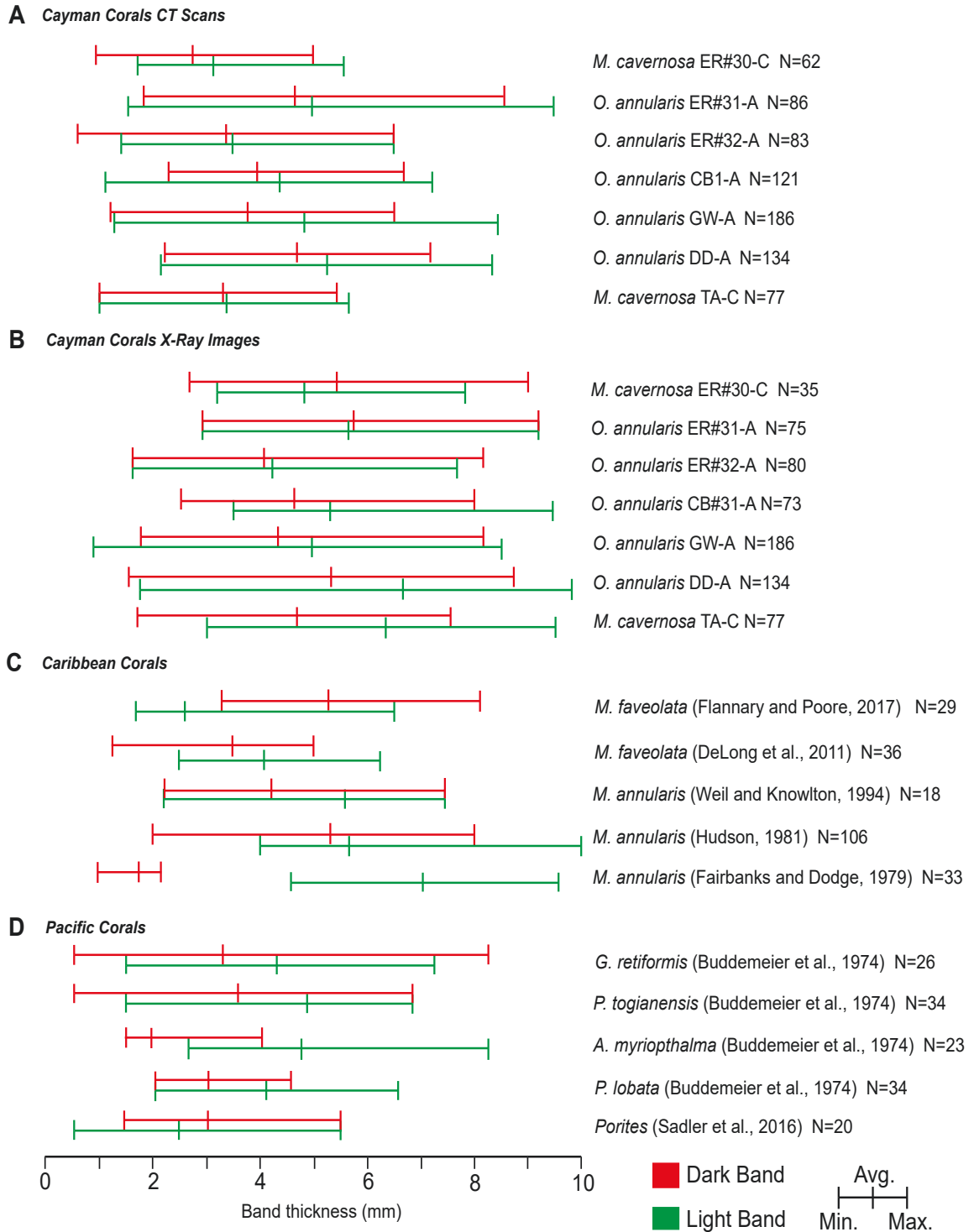


**Fig. 3.9.** Graphs showing range of growth band thicknesses between (A) Cayman coral CT scans, (B) Cayman coral X-Ray images, (C) Caribbean corals (X-Ray), and (D) Pacific Corals (X-Ray). Light (green) and dark (red) growth bands as identified on either X-ray or CT scans.

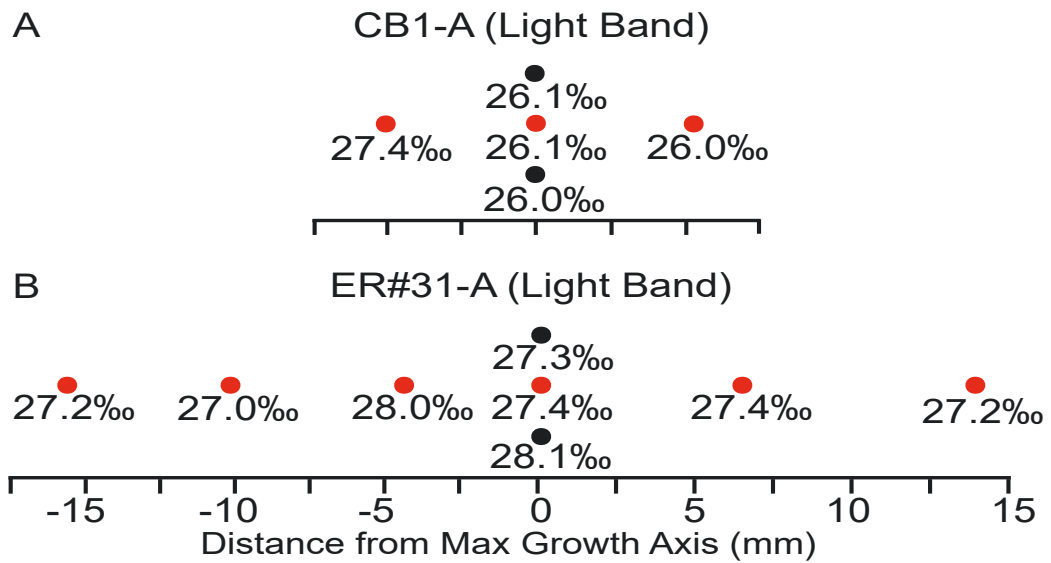


**Fig. 3.10.** Vertical and lateral variations in the  $\delta^{18}\text{O}_{\text{coral}}$  compositions from light growth bands in corals (A) CB1-A and (B) ER#31-A.

CB1-A are characterized by vertical and horizontal  $\delta^{18}\text{O}_{\text{coral}}$  values (26.0 to 26.7‰, SD = 0.3‰) that are more consistent (Fig. 3.10, Table 3.5). On the basis of meso- and micro-scale structures in skeletal growth bands, Winter and Sammarco (2010) suggested that corals may record yearly, monthly, and daily growth patterns. For the Cayman corals, the homogenous growth bands represent seasonal (~6 months) growth, whereas, the heterogenous thick growth bands represent seasonal growth and the microbands represent shorter, possibly monthly growth periods (Fig. 3.6). This suggestion is supported by the fact that there are, on average, six microbands per larger growth band.

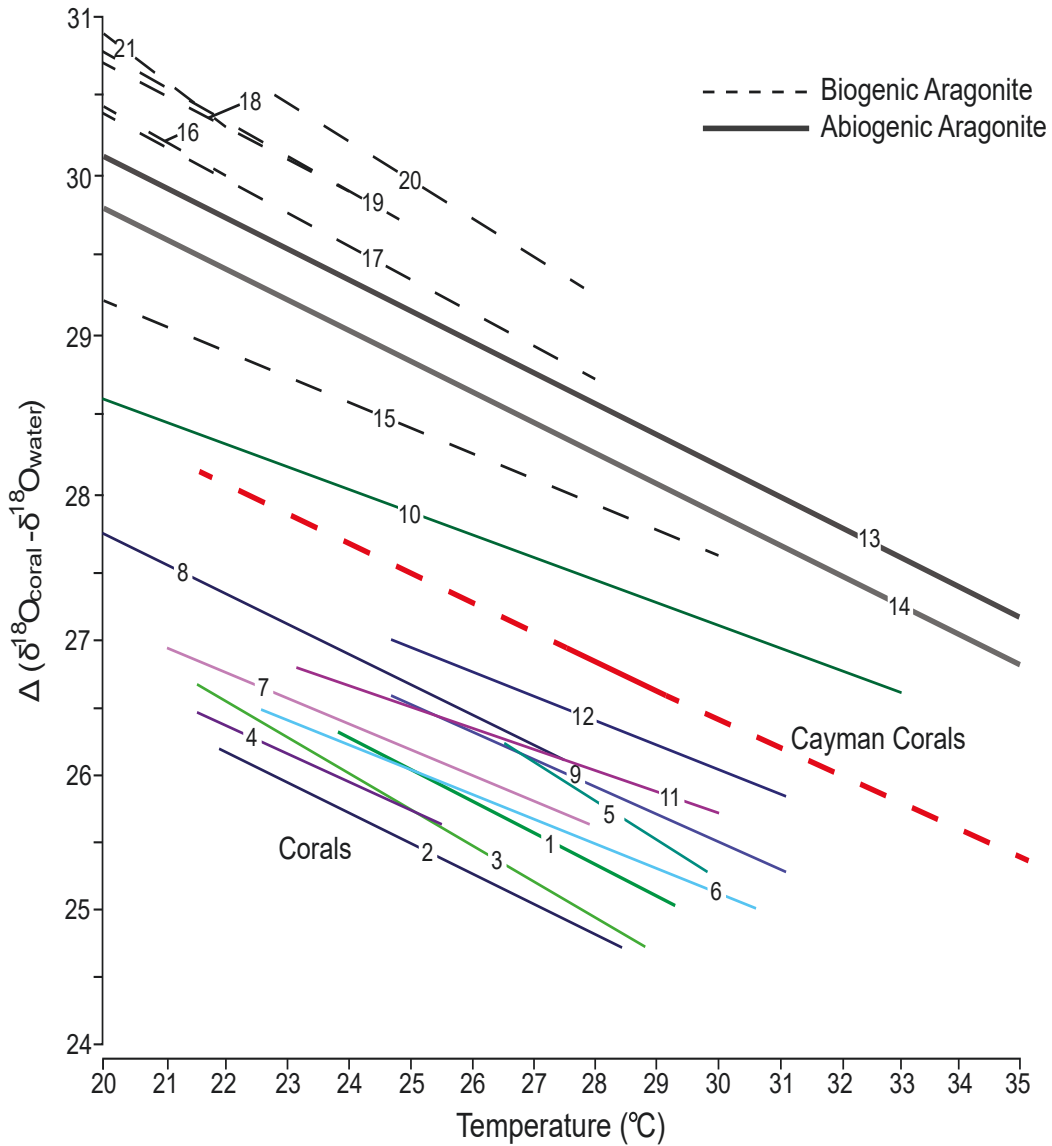
The fact that multiple rates of growth are evident in the *Orbicella* samples but not in the *M. cavernosa* suggests that the different growth scales may be species-specific. This, however, does not explain why the multiple growth scales are not evident in *O. annularis* from Cayman Brac or GW-A. The differences evident between these corals maybe related to the overall growth rate. Corals ER#31-A, ER#32-A, and DD-A have faster average growth rates than ER#30-C, CB1-A, GW-A, and TA-C, which resulted



in increased skeletogenesis that may account for the smaller scales of growth and the associated changes in microstructure and isotope compositions. Rapid skeletogenesis causes a strong kinetic disequilibrium that can alter the isotopic fractionation of the coral that may potentially enhance the sub-seasonal variations, as is apparent in corals ER#31-A, ER#32-A, and DD-A (cf., Land et al., 1975; Erez, 1977, 1978; Weil et al., 1981; McConnaughey, 1988).

### 7.3.2. Conversion of $\delta^{18}O_{coral}$ values to temperature

There are many different equations for calculating water temperature from the oxygen isotope compositions of calcium carbonate minerals. For corals, the critical calibrations involve the aragonite-water fractionations, which includes those known from biogenic and abiogenic aragonite (Fig. 3.11). The biogenic group includes those derived for corals (Weber, 1977; Dunbar and Wellington, 1981; Weil et al., 1981; McConnaughey, 1988; Chakraborty and Ramesh, 1993; Leder et al., 1996; Wellington et al., 1996; Cardinal et al., 2001; Watanabe et al., 2001; Felis et al., 2004; Smith et al., 2006; Kilbourne et al., 2010; Supplementary Table 3.8) and those derived for other organisms (Aharon and Chappell, 1983; Grossman and Ku, 1986; Hudson and Anderson, 1989; Patterson et al., 1993; Thorrold et al., 1997; White et al., 1999; Bohm et al., 2000). The abiogenic aragonite-water calibrations are based either on laboratory experiments (Kim et al., 2007) or theoretical calculations (Chacko and Deines, 2008). These two independent methods give similar results, which suggests that both methods reflect the true equilibrium oxygen isotope fractionation between aragonite and water (Fig. 3.11). The general similarity between these abiogenic fractionations and many of the biogenic aragonite-water fractionation curves (Fig. 3.11) suggest that many marine organisms form their skeletons in near isotopic equilibrium with the parent water (cf., Kim et al., 2007; Grossman, 2012). In stark contrast, corals yield aragonite-water fractionations that, at a given temperature, are typically 1.5 to 2‰ lower than those of abiogenic or



- Cayman Corals  
*O. annularis* and *M. cavernosa*
- 1- Weber (1977) *Galaxea* spp.
- 2- Weil et al., (1981) *Pocillopora damicornis*
- 3- Dunbar and Wellington (1981) *Pocillopora damicornis*
- 4- McConnaughey (1988) *Porites lobata*
- 5- Chakraborty and Ramesh (1993) *Porites*
- 6- Leder et al., (1996) *Orbicella annularis*
- 7- Wellington et al., (1996) *Porites lobata*
- 8- Cardinal et al., (2001) *Diploria Labyrinthiformis*
- 9- Watanabe et al., (2001) *Orbicella faveolata*
- 10- Felis et al., (2004) *Porites*
- 11- Smith et al., (2006) *Orbicella faveolata*
- 12- Kilbourne et al., (2011) *Orbicella faveolata*
- 13- Chacko and Deines (2008) Synthetic Aragonite
- 14- Kim et al., (2007) Synthetic Aragonite
- 15- Patterson et al., (1993) Fresh Water Otoliths
- 16- Grossman and Ku (1986) Marine Organisms
- 17- Bohm et al., (2000) Marine Coralline Sponges
- 18- White et al., (1999) Marine Molluscs
- 19- Thorrold et al., (1997) Marine Otoliths
- 20- Aharon and Chappell (1983) *Tridacna*
- 21- Husdon and Anderson (1989) Marine Organisms

**Fig. 3.11.** Comparison of oxygen isotope geothermometer equations, showing coral-based, biogenic aragonite-based, and abiogenic aragonite-based geothermometers relative to the Cayman geothermometer used in this study, which is based on  $\delta^{18}\text{O}$  values that are equivalent to calcite, as used in previous studies. The length of each line represents the range of temperature covered by each equation. The red dashed line shows the projection of the Cayman coral equation to a wider temperature range. The geothermometers for biogenic (non-coral) and abiogenic aragonite were developed for temperatures from 0 to 40°C.

---

non-coral biogenic aragonite (cf., McConnaughey, 1988; Cardinal et al., 2001; Kilbourne et al., 2010; Fig. 3.11). Clearly, coral biology has a profound influence on the isotope fractionation (e.g., Grossman, 2012). The aragonite-water geothermometers developed specifically for corals have been derived from different coral species throughout the world (Fig. 3.11; Supplementary Table 3.8).

Applying each coral equation, temperatures were calculated using the  $\delta^{18}\text{O}_{\text{coral}}$  values from the upper part (23.3 to 35.6 cm) of Cayman coral ER#31-A, which represents the 25-year span (1990-2014) for which measured water temperatures are available (Fig. 3.2A). A  $\delta^{18}\text{O}_{\text{water}}$  value of +0.8‰ was used because that is the value obtained from the water sample collected beside Magic Reef in 2016. Temperatures calculated ( $T_{\text{cal}}$ ) from various equations ranged from ~10° to 39°C with many being outside the range of the measured water temperatures. Given that these equations are based on different coral species, their slope and intercepts are influenced by different ‘vital effects’, such as growth rates (e.g., McConaughy, 1988; Crowley et al., 1999; Felis et al., 2003), water depth (e.g., Weber and Woodhead, 1970; Erez, 1978; Fairbanks and Dodge, 1979), and/or local effects such as seasonal rainfall (Dunbar and Wellington, 1981), upwelling (e.g., Weil et al., 1981; Smith et al., 2006), and reef ecology (Marshall and McCulloch, 2002;

Meibom et al., 2003). Although the slopes (0.16 to 0.32) are similar, the intercepts vary from 30.5° to 34.2°C and a wide range of  $T_{cal}$ . Additional factors, such as the method used to derive the equation, sampling errors, analytical uncertainties, differences in the sampling procedures, and the number of samples can also affect the calibration of these equations (Weil et al., 1981; Swart et al., 1996; Cardinal et al., 2001; Swart et al., 2002; Smith et al., 2006; Reynaud et al., 2007).

If meaningful temperatures are to be derived from the isotopic data for the Cayman corals, the geothermometric equation must be adjusted to reflect Cayman conditions (Fig. 3.11). The range of measured Cayman seawater temperatures is too narrow to allow accurate derivation of the relationship between temperature and isotope fractionation. Thus, an average temperature dependence (slope) for the coral-water fractionations derived from all of the published coral equations was used with the assumption that the equation must pass through the point defined by mean measured seawater temperature for Grand Cayman and the mean  $\Delta^{18}\text{O}$  ( $\delta^{18}\text{O}_{coral} - \delta^{18}\text{O}_{water}$ ) values for the last 25 years of growth of ER#31-A.

For the Cayman corals, two temperature equations based on  $\delta^{18}\text{O}_{coral}$  and  $\delta^{18}\text{O}_{water}$  values (both at VSMOW scale), were derived with equation (1) based on coral  $\delta^{18}\text{O}$  values that have been corrected by  $-0.38\text{‰}$  to account for the difference between the aragonite and calcite acid fractionation factors (Kim et al., 2007; 2015), and equation (2) based on coral  $\delta^{18}\text{O}$  values that assume that the aragonite and calcite acid fractionation factors are identical.

$$\Delta^{18}\text{O}_{coral-water} (\delta^{18}\text{O}_{coral} - \delta^{18}\text{O}_{water}) = -0.21(\pm 0.05) * T(^{\circ}\text{C}) + 32.40 \quad (1)$$

$$\Delta^{18}\text{O}_{coral-water} (\delta^{18}\text{O}_{coral} - \delta^{18}\text{O}_{water}) = -0.21(\pm 0.05) * T(^{\circ}\text{C}) + 32.78 \quad (2)$$

Using equation (1) and the analytical and biological uncertainties on the oxygen isotope composition from the corals ( $1\sigma = \pm 0.25\text{‰}$ ) results in a propagated standard error of  $\pm 0.49^{\circ}\text{C}$  for  $T_{cal}$  for any single analysis. In the temperature profiles produced from the Cayman corals, with a 6-point moving average, the 95% confidence level on the

standard error is  $\pm 0.95^{\circ}\text{C}$ . For the upper part of coral ER#31-A, equation (1) yielded  $T_{\text{cal}}$  of  $26.3^{\circ}$  to  $31.3^{\circ}\text{C}$  and an average of  $28.6^{\circ}\text{C}$ , which is similar to the current average water temperature ( $28.5^{\circ}\text{C}$ ; T-test:  $p < 0.05$ ) for Grand Cayman (Goreau et al., 1992; Chollett et al., 2012b; NOAA, 2018).

### 7.3.3. Calculated temperatures and trends through time

The  $T_{\text{cal}}$  from the Cayman corals (1474 to 2014) ranged from  $19^{\circ}$  to  $35^{\circ}\text{C}$  and show a T increase of  $\sim 3^{\circ}\text{C}$  from 1815 to 2014 (Fig. 3.12). Overall, the  $T_{\text{cal}}$  record between 1474 to 1512 (Fig. 3.13) and 1815 to 2014 (Fig. 3.14) embodies two cool periods, one warm period, and one mild period. Warm and cool intervals occurred within these periods. For the Cayman corals, the overall temperature trends recorded by each coral are consistent with one another, the absolute temperatures, however, may not be the same (Fig. 3.14). Individual corals may have been influenced by factors such as biological/metabolic differences, water depth, sunlight availability, and/or micro-scale reef ecology differences (cf., Weber and Woodhead, 1970; Weber and Woodhead, 1972; Land et al., 1975; Erez, 1978; Fairbanks and Dodge, 1979; Aharon and Chappell, 1983; McConaughey, 1988; Marshall and McCulloch, 2002; Meibom et al., 2003; Lough, 2004; Flannery et al., 2018) that may have been responsible for the discrepancies in the absolute  $T_{\text{cal}}$ . Since multiple corals were used in this study (cf., Flannery et al., 2018) and the overall trends recorded by these corals show correlated fluctuations in temperature, decadal-scale changes in SST for the Cayman Islands can be confidently assessed.

- Cool Period 1 (1474-1512), was characterized by  $T_{\text{cal}}$  of  $21^{\circ}$  to  $29^{\circ}\text{C}$  (average  $25.1^{\circ} \pm 0.95^{\circ}\text{C}$ ), which is significantly lower (T-test:  $p < 0.01$ ) than the current average seawater T (Fig. 3.13).
- Cool Period 2 (1815-1924), was characterized by  $T_{\text{cal}}$  of  $18^{\circ}$  to  $31^{\circ}\text{C}$  (average  $23.9 \pm 0.95^{\circ}\text{C}$ ), which is significantly lower (T-test:  $p < 0.01$ ) than the current average seawater T (Fig. 3.14). During that period there were two cool intervals

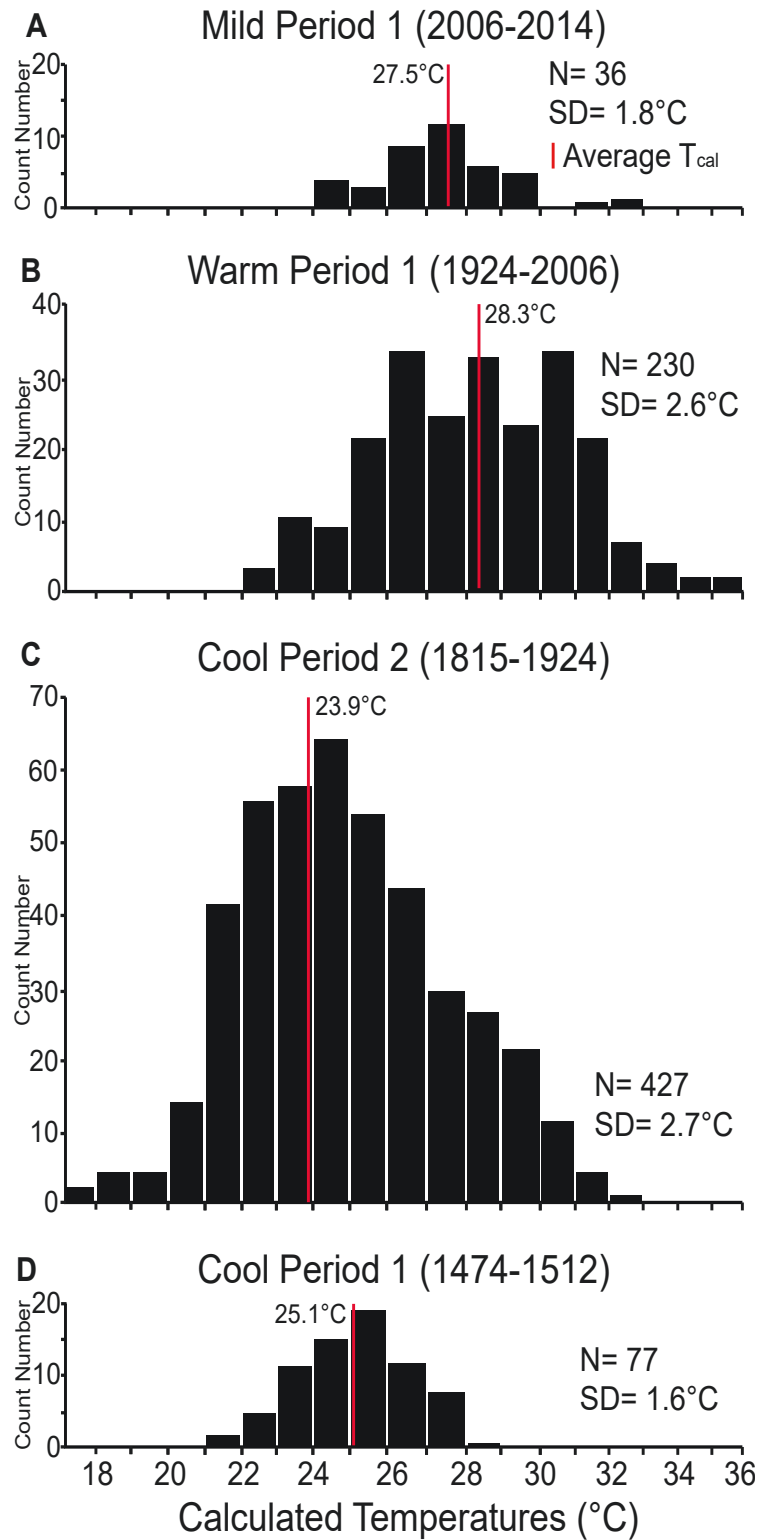


**Fig. 3.12.** Histograms of the  $T_{cal}$  from the Cayman corals. (A)  $T_{cal}$  for Mild Period 1, (B)  $T_{cal}$  for Warm Period 1, (C)  $T_{cal}$  for Cool Period 2, and (D)  $T_{cal}$  for Cool Period 1. N = number of data points. SD = standard deviation.

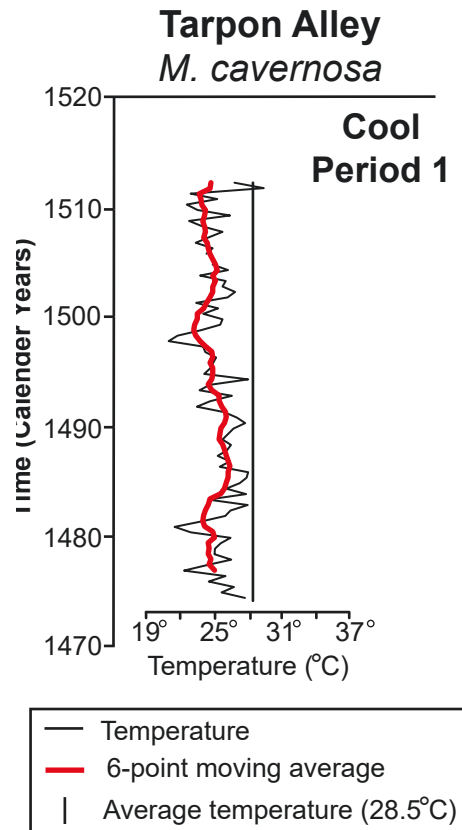


**Fig. 3.13.**  $T_{\text{cal}}$  trends derived from TA-C from 1474 to 1512.  $T_{\text{cal}}$  determined using the Cayman Island oxygen isotope geothermometer, with  $\delta^{18}\text{O}_{\text{water}}$  value of +1.4‰.

(CI 1: 1815-1861, CI 2: 1896-1924) that were separated by a warm interval (WI 1: 1861-1896). The cool intervals are characterized by an overall decrease of  $\sim 4^{\circ}\text{C}$ , when comparing the beginning  $T_{\text{cal}}$  of this interval with the end, whereas the warm interval was characterized by an overall increase of  $\sim 5^{\circ}\text{C}$ .

- Warm Period 1 (1924-2006), was characterized by  $T_{\text{cal}}$  from  $23^{\circ}$  to  $35^{\circ}\text{C}$  (average  $28.3^{\circ} \pm 0.95^{\circ}\text{C}$ ), which is similar to the current seawater T for Grand Cayman and significantly warmer than CP 2 (T-test:  $p < 0.01$ ; Fig. 3.14). During this period there were two warm intervals (WI 2: 1924-1932, WI 3: 1972-1993) and two cool intervals (CI 3: 1960-1972, CI 4: 1993-2006). The warm intervals

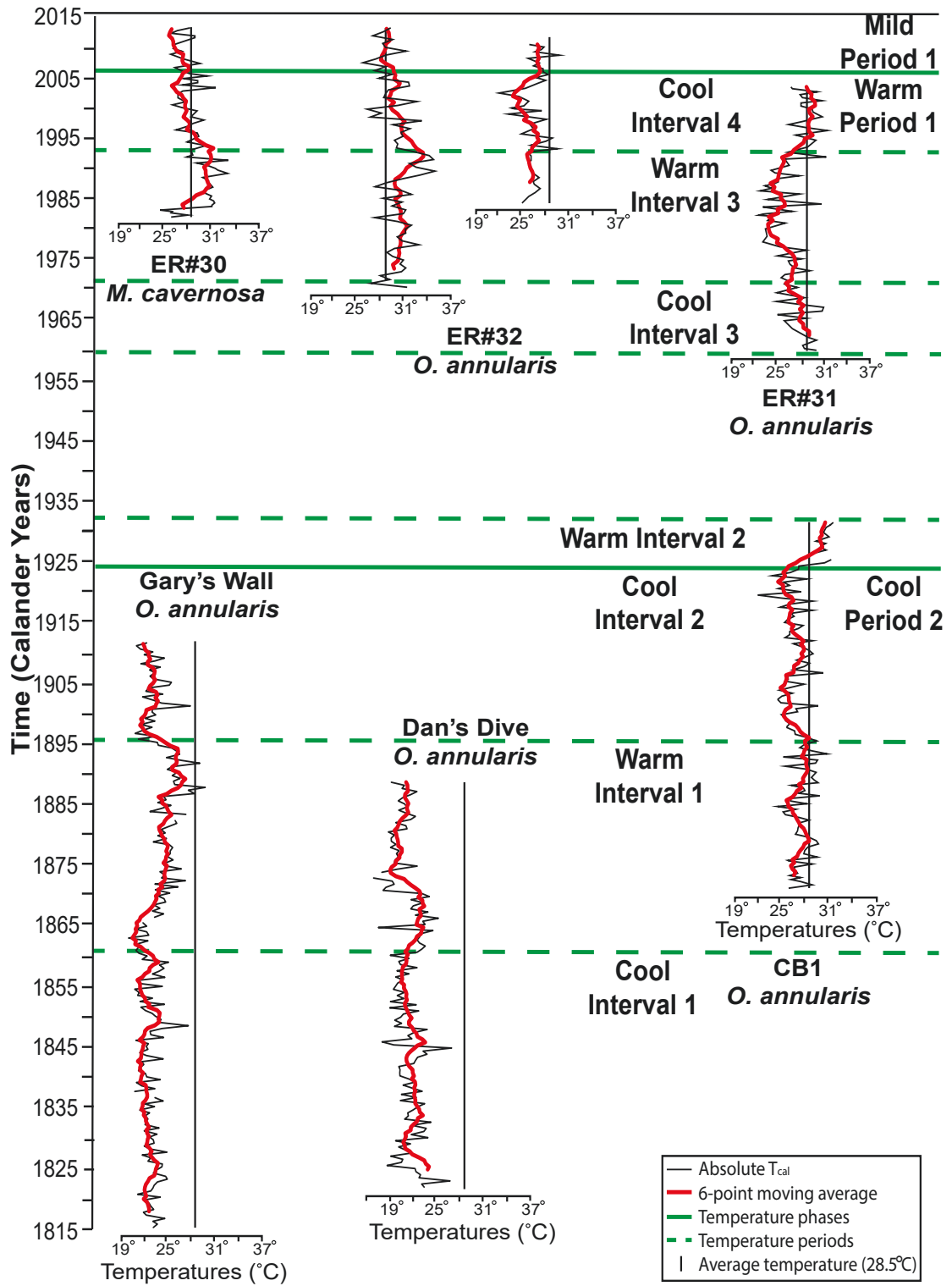


**Fig. 3.14.**  $T_{cal}$  trends derived from Cayman corals from 1815 to 2014.  $T_{cal}$  determined using the Cayman Island oxygen isotope geothermometer, with  $\delta^{18}O_{water}$  value of +0.8‰ for the corals from Magic Reef, GW-A, and DD-A, and 0.0‰ for coral CB1-A respectively.



are characterized by an increase in  $T_{cal}$  of  $\sim 5^{\circ}$ - $7^{\circ}$ C. The cool intervals are characterized by a decrease of  $\sim 4^{\circ}$ - $5^{\circ}$ C.

- Mild Period 1 (2006-2014), was characterized by  $T_{cal}$  of  $25^{\circ}$  to  $33^{\circ}$ C (average  $27.5^{\circ} \pm 0.95^{\circ}$ C) which is similar to the current average seawater T for Grand Cayman (T-test:  $p < 0.01$ ; Fig. 3.14).

Over the last 35 years, coral bleaching events around Grand Cayman, which were triggered by high temperature anomalies occurred in 1982, 1987-1988, 1990, 1995, 1998, and 2009 (Bruckner, 2010). On the  $T_{cal}$  profiles, these events coincide with a slightly elevated  $T_{cal}$ , these values, however, are not extremes (Fig. 3.14). During bleaching events, high temperatures result in the loss of zooxanthellae (Swart, 1983) that causes reduced vertical growth and lateral thickening of the coral skeleton, which in turn may cause a  $^{18}\text{O}$  enrichment (Gagan et al., 1994). The ‘true’ high-temperature signal, therefore, is not reliably captured by the corals due to the lag time caused by their reduced vertical growth during the bleaching events (Arthur, 2000; Rodrigues and Grottoli, 2006; Grottoli and Eakin, 2007; Bruckner, 2010; Carricart-Ganivet, 2011). The temperature recorded by the subsequent growth band, may represent re-established vertical growth when temperatures were more conducive to coral growth but still high relative to the norm for that period (Porter et al., 1989; Webster et al., 1999; Rodrigues and Grottoli, 2006; Ahmed et al., 2011).

## 8. Discussion

Calculated and measured T from other areas in the Caribbean ( $14^{\circ}$  to  $34^{\circ}$ C; e.g., Atwood et al., 1992; Goreau et al., 1992; Chenoweth, 1998; Winter et al., 1998; Haase-Schramm et al., 2003; Maupin et al., 2008; Hetzinger et al., 2010; Giry et al., 2012; Corderio et al., 2014; Alpert et al., 2017; Flannery et al., 2017) are similar to those derived from the Cayman corals. Direct comparison of those T records, however, is complicated by inconsistent terminology, with terms such as “cool period” or “warm

period” being used without precise definitions (e.g., Hetzinger et al., 2008; Maupin et al., 2008; Saenger et al., 2009; Alpert et al., 2017). Atwood et al. (1992), Chenoweth (1993), and Flannery et al. (2017), for example, used different boundary T of 29°, 24°, and 30°C, respectively, as the boundaries between their warm and cool periods. This ambiguity is exacerbated when the terms such as “warming” and “cooling” refer to different magnitudes of T change (0.3 to 2.1°C; e.g., Gagan et al., 2000; Black et al., 2004; Saenger et al., 2009; Hetzinger et al., 2010; Corderio et al., 2014). In other cases, a value of 0 has been assigned to the average annual T with anomalies defined relative to that baseline (e.g., Goreau et al., 1992; Maupin et al., 2008; Hetzinger et al., 2010). In many cases, however, the temperature used to define the baseline is not specified (e.g., Haase-Schramm et al., 2003; Hetzinger et al., 2008; Giry et al., 2012).

Temperature changes from 1815 to 2014, indicated by the Cayman corals are similar to those derived from other parts of the Caribbean (Florida to Brazil) with a cooling trend evident from 1815-1924 (Fig. 3.15) that may be related to the end of the LIA (cf., Dunbar et al., 1994; Trenberth et al., 2007; Abahazi, 2009; Cronin et al., 2010; Chollett et al., 2012a; Carlson, 2017). During that time span, however, there were two mild periods (Jamaica; Haase-Schramm et al., 2003 and Florida; Flannery et al., 2017) and one warm period (Brazil; Corderio et al., 2014), that may have been related to local climate factors. The warming trend from 1965 to 2014 recorded by the Cayman corals and evident throughout the Caribbean (Fig. 3.15), is consistent with global T increases since the 1970’s (Strong et al., 1989; Goreau et al., 1992; McWilliams et al., 2005; Hansen et al., 2006; Trenberth et al., 2007; Hetzinger et al., 2010; Chollett et al., 2012a; Kuffner et al., 2015; Tierney et al., 2015). In the Bahamian records, however, there are exceptions (cool periods) to this overall warming trend (Chenoweth, 1998; Saenger et al., 2009) that reflect local factors.

Over the last 155 years there has been an increase of 1°– 3°C in global SST that resulted from an increase of ~0.04°C/decade between 1850 and 2005, and an increase of

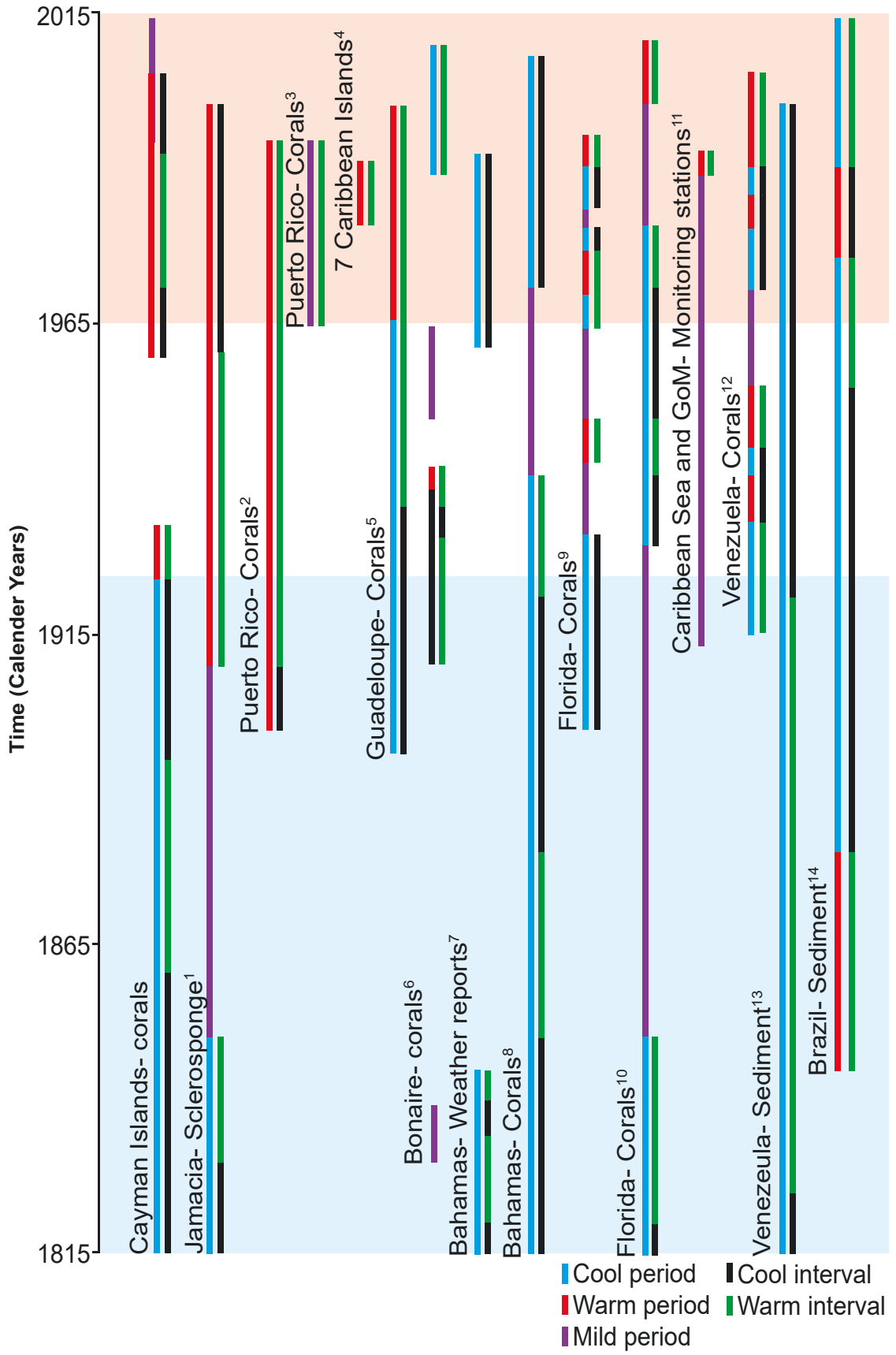


**Fig. 3.15.** Comparison of temperature profiles derived from the Cayman corals with those developed from other parts of the Caribbean. Warm, cool, and mild periods and warm and cool intervals for the other Caribbean profiles were determined based on the terminology outlined in this study. 1- Haase-Schramm et al., 2003. 2- Aplert et al., 2017. 3- Winter et al., 1998. 4- Goreau et al., 1992. 5- Hetzinger et al., 2010. 6- Girya et al., 2012. 7- Chenoweth, 1998. 8- Saenger et al., 2009. 9- Maupin et al., 2008. 10- Flannery et al., 2017. 11- Atwood et al., 1992. 12- Hetzinger et al., 2008. 13- Black et al., 2004. 14- Corderio et al., 2014.

---

0.13° – 0.51°C/decade since 1970 (Hansen et al., 2006; Trenberth et al., 2007; Hetzinger et al., 2010; Chollett et al., 2012a; Tierney et al., 2015). The Caribbean region has experienced an air T increase of 0.6°C over the last 150 years and an increase of 0.1°C/decade over recent decades (Nurse and Sem, 2001; Day, 2010). The increase in SST of ~3°C from 1815 to 2014, as determined from the Cayman corals, is consistent with global trends.

Differences in the SST records between the Cayman Islands and other areas of the Caribbean may be due to the fact that rates of T change commonly vary due to local conditions (Trenberth et al., 2007; Chollett et al., 2012a; Gregory et al., 2015; Tierney et al., 2015). Changes in the local SST can, for example, be caused by increased cloud cover due to high storm frequency (Swart, 1983), the influence of intense and frequent cold-air fronts from North America (Roberts et al., 1982; Chenoweth, 1998; Melo-Gonzalez et al., 2000; Chollett et al., 2012a), a reduction in the size and/or the intensity of the Atlantic Warm Pool (Enfield et al., 2001; Flannery et al., 2017), shifts in the phase of the Atlantic Multidecadal Oscillation (Enfield et al., 2001; Kilbourne et al., 2007; Flannery et al., 2017; Toth et al., 2017), weakening of the Cayman Basin current (Centurioni and Niiler, 2003), micro-scale reef variability (Marshall and McCulloch,

2002; Meibom et al., 2003; Lough, 2004; Flannery et al., 2018), and/or volcanism (Chenoweth, 1998; Gagan et al., 2000). Further problems can arise from the methods used to calculate the SST, the type of physical record and geochemical proxy used, measurement resolution, and the incorporation of site-specific climatic parameters (e.g., Weil et al., 1981; Atwood et al., 1992; Cardinal et al., 2001). Identifying which temperature changes are caused by local factors, as opposed to global-scale events, is difficult due to the lack of available long-term climate data for the Cayman Islands and Caribbean region, as well as the superimposition of global events on the local signal. The record from the Cayman corals, however, are consistent with other Caribbean T reconstructions, capturing a general trend of lower T from 1815-1924 and higher T from 1965-2014.

## 9. Conclusions

This study has produced the first surface seawater temperature profile from the Cayman Islands from 1474 to 2014, and thereby increases our knowledge of temperature changes in the Caribbean region during this time. Detailed analyses of the growth patterns and oxygen isotope compositions of seven corals (*O. annularis* and *M. cavernosa*) from the Cayman Islands, have yielded the following important conclusions:

- The Cayman corals are characterized by clearly defined seasonal growth banding and, in some cases, possibly monthly growth.
- The oxygen isotope geothermometer calibration determined using the Cayman coral data and published geothermometers can be applied to various coral species that grow within the temperature range typical of the central Caribbean.
- Oxygen isotope temperatures calculated from the Cayman corals, show that there have been two cool periods, one warm period, and one mild period in surface seawater temperatures between 1474 to 2014. These trends are consistent with other Caribbean temperature records.

- For the Cayman Islands, the  $\sim 3^{\circ}\text{C}$  increase in the SST from 1815 to 2014 is consistent with general global increases in SST.
- Variations between the SST determined from the Cayman Islands and other areas may be due to local differences in factors such as changing atmospheric circulation patterns, evaporation/precipitation, increased cloud cover, and/or micro-scale reef habitats. Determining the exact cause of these variations, however, is difficult because of the paucity of long-term climate monitoring in this region.

## REFERENCES

- Abahazi, M.A., 2009. Tropical North Atlantic sea surface temperature reconstruction for the last 800 years using Mg/Ca ratios in planktonic foraminifera, Unpublished M.Sc., University of Akron, Ohio, USA, 117 pp.
- Abram, N.J., Gagan, M.K., Liu, Z., Hantoro, W.S., McCulloch, M.T., Suwargadi, B.W., 2007. Seasonal characteristics of the Indian Ocean dipole during the Holocene epoch. *Nature* 445, 299-302.
- Aharon, P., Chappell, J., 1983. Carbon and oxygen isotope probes of reef environment histories. In: Barner, D.J. (Ed.), *Perspectives on Coral Reefs*. Australian Institute of Marine Science, pp. 1-10.
- Ahmed, S.M., Padmakumari, V.M., Raza, W., Venkatesham, K., Suseela, G., Sagar, N., Chamoli, A., Rajan, R.S., 2011. High-resolution carbon and oxygen isotope records from a scleractinian (*Porites*) coral of Lakshadweep Archipelago. *Quaternary International* 238, 107-114.
- Albert, C., McCulloch, M.T., 1997. Strontium/calcium ratios in modern *Porites* corals from the Great Barrier Reef as a proxy for sea surface temperature: calibration of the thermometer and monitoring of ENSO. *Paleoceanography* 12, 345-363.
- Alpert, A.E., Cohen, A.L., Oppo, D.W., DeCarlo, T.M., Gaetani, G.A., Hernandez-Delgado, E.A., Winter, A., Gonneea, M.E., 2017. Twentieth century warming of the tropical Atlantic captured by Sr-U paleothermometry. *Paleoceanography* 32, 146-160.
- Arthur, R., 2000. Coral bleaching and mortality in three Indian reef regions during an El Niño southern oscillation event. *Current Science* 79, 1723-1729.
- Atwood, D.K., Hendee, J.C., Mendez, A., 1992. An assessment of global warming stress on Caribbean coral reef ecosystems. *Bulletin of Marine Science* 51, 118-130.
- Baker, P.A., Weber, J.N., 1975. Coral growth rate: variation with depth. *Earth and Planetary Science Letters* 27, 57-61.
- Barnes, D.J., Lough, J.M., Tobin, B.J., 1989. Density measurements and the interpretation of

- X-radiographic images of slices of skeleton from the colonial hard coral *Porites*. *Journal of Experimental Marine Biology and Ecology* 131, 45-60.
- Barnes, D.J., Taylor, R.B., 1993. On corallites apparent in X-radiographs of skeletal slices of *Porites*. *Journal of Experimental Marine Biology and Ecology* 173, 123-131.
- Beck, J.W., Edwards, L., Ito, E., Taylor, F.W., Recy, J., Rougerie, F., Joannot, P., Henin, C., 1992. Sea-surface temperatures from coral skeletal strontium/calcium ratios. *Science* 257, 644-649.
- Black, D.E., Thunell, R.C., Kaplan, A., Peterson, L.C., Tappa, E.J., 2004. A 2000-year record of Caribbean and tropical North Atlantic hydrographic variability. *Paleoceanography* 19. doi: 10.1029/2003PA000982.
- Blanchon, P.A., 1995. Controls on modern reef development around Grand Cayman, Unpublished Ph.D., University of Alberta, Edmonton, Alberta, Canada, 200 pp.
- Blanchon, P.A., Jones, B., 1995. Marine-planation terraces on the shelf of Grand Cayman: a result of stepped Holocene sea-level rise. *Journal of Coastal Research* 11, 1-33.
- Blanchon, P.A., Jones, B., Kalbfleisch, W., 1997. Anatomy of a fringing reef around Grand Cayman: storm rubble, not coral framework. *Journal of Sedimentary Research* 67, 1-16.
- Bohm, F., Joachimski, M.M., Dullo, W., Eisenhauer, A., Lehnert, H., Reitner, J., Worheide, G., 2000. Oxygen isotope fractionation in marine aragonite of coralline sponges. *Geochimica et Cosmochimica Acta* 64, 1695-1703.
- Bolton, A., Goodkin, N.F., Hughen, K.A., Ostermann, D.R., Vo, S.T., Phan, H.K., 2014. Paired *Porites* coral Sr/Ca and  $\delta^{18}\text{O}$  from the western South China Sea: proxy calibration of sea surface temperatures and precipitation. *Palaeogeography, Palaeoclimatology, Palaeoecology* 410, 233-243.
- Bosscher, H., 1992. Computer tomography and skeletal density of coral skeletons. *Coral Reefs* 12, 97-103.
- Bruckner, A., 2010, Cayman Islands coral reef health and resilience assessment. <https://www.livingoceansfoundation.org/publication/cayman-islands-coral-reef-health-and-resilience->



assessments/ (Accessed August 2016).

- Buddemeier, R.W., Maragos, J.E., Knutson, D.K., 1974. Radiographic studies of reef coral exoskeletons: rates and patterns of growth. *Journal of Experimental Marine Biology and Ecology* 14, 179-200.
- Buddemeier, R.W., Kinzie, R.A., 1976. Coral growth. *Oceanography, Marine Biology Annual Review* 14, 183-225.
- Cardinal, D., Hamelin, B., Brad, E., Patzold, J., 2001. Sr/Ca, U/Ca and  $\delta^{18}\text{O}$  records in recent massive corals from Bermuda: relationships with sea surface temperature. *Chemical Geology* 176, 213-233.
- Carlson D., 2017. A comparison of Holocene Climate Optimum Periods: are they as warm as the Post-Little Ice Age Periods and are greenhouse gas concentrations similar? *Gulf Coast Association of Geological Societies Transactions* 67, 39-78.
- Carricart-Ganivet, J.P., 2004. Sea surface temperature and the growth of the West Atlantic reef-building coral *Montastraea annularis*. *Journal of Experimental Marine Biology and Ecology* 302, 249-260.
- Carricart-Ganivet, J.P., 2011. Coral skeletal extension rate: an environmental signal or a subject to inaccuracies? *Journal of Experimental Marine Biology and Ecology* 405, 73-79.
- Carricart-Ganivet, J.P., Merino, M., 2001. Growth responses of the reef-building coral *Montaster annularis* along a gradient of continental influence in the Southern Gulf of Mexico. *Bulletin of Marine Science* 68, 133-146.
- Centurioni, L.R., Niiler, P.P., 2003. On the surface currents of the Caribbean Sea. *Geophysical Research Letters* 30, doi 10.1029/2002GL016231.
- Chacko, T., Deines, P., 2008. Theoretical calculation of oxygen isotope fractionation factors in carbonate systems. *Geochimica et Cosmochimica Acta* 72, 3642-3660.
- Chakraborty, S., Ramesh, R., 1993. Monsoon-induced sea surface temperature changes recorded in Indian corals. *Terra Nova* 5, 545-551.
- Chan, P., Halfar, J., Norley, C.J.D., Pollmann, S.I., Adey, W., Holdsworth, D.W., 2017. Micro-

- computed tomography: applications for high-resolution skeletal density determinations: an example using annually banded crustose coralline algae. *Geochemistry Geophysics Geosystems* 18, 3542-3553.
- Chenoweth, M., 1998. The early 19<sup>th</sup> century climate of the Bahamas and a comparison with 20<sup>th</sup> century averages. *Climate Change* 40, 577-603.
- Chollett, I., Muller-Karger, F.E., Heron, S.F., Skirving, W., Mumby, P.J., 2012a. Seasonal and spatial heterogeneity of recent sea surface temperature trends in the Caribbean Sea and southeast Gulf of Mexico. *Marine Pollution Bulletin* 64, 956-965.
- Chollett, I., Mumby, P.J., Muller-Karger, F.E., Hu, C., 2012b. Physical environments of the Caribbean Sea. *Limnology and Oceanography* 57, 1233-1244.
- Cobb, K.M., Charles, C.D., Cheng, H., Kastner, M., Edwards, R.L., 2003. U/Th-dating living and young fossil corals from the central tropical Pacific. *Earth and Planetary Science Letters* 210, 91-103.
- Cole, J.E., Fairbanks, R.G., Shen, G.T., 1993. Variability in the Southern Oscillation: isotopic results from a Tarawa Atoll coral. *Science* 260, 1790-1793.
- Corderio, L.G.M.S., Belem, A.L., Rangel, B., Sifeddine, A., Capilla, R., Albuquerque, A.L.S., 2014. Reconstruction of southwestern Atlantic sea surface temperatures during the last century: Cabo Frio continental shelf (Brazil). *Palaeogeography, Palaeoclimatology, Palaeoecology* 415, 225-232.
- Correge, T., Deleroix, T., Recy, J., Beck, W.C., Cabioch, G., Le Cornec, F., 2000. Evidence for stronger El Nino-Southern Oscillation (ENSO) events in a mid-Holocene massive coral. *Paleoceanography* 15, 465-470.
- Crann, C.A., Murseli, S., St-Jean, G., Zhao, X., Clark, I.D., Kieser, W.E., 2017. First status report on radiocarbon sample preparation techniques at the A.E. Lalonde AMS Laboratory (Ottawa, Canada). *Radiocarbon* 59, 695-704.
- Cronin, T.M., Hayo, K., Thunell, R.C., Dwyer, G.S., Saenger, C., Willard, D.A., 2010. The Medieval Climate Anomaly and Little Ice Age in Chesapeake Bay and the North Atlantic

- Ocean. *Palaeogeography, Palaeoclimatology, Palaeoecology* 291, 299-310.
- Crowley, T.J., Quinn, T.M., Hyde, W.T., 1999. Validation of coral temperature calibrations. *Paleoceanography* 14, 605-615.
- Day, M., 2010. Challenges to sustainability in the Caribbean karst. *Geologia Croatia* 63, 149-154.
- Diaz, M., Macario, K.D., Gomes, P.R.S., Alvarez-Lajonchere, L., Aguilera, O., Alves, E.Q., 2017. Radiocarbon marine reservoir effects on the northwestern coast of Cuba. *Radiocarbon* 59, 333-341.
- de Villiers, S., Shen, G.T., Nelson, B.K., 1994. The Sr/Ca-temperature relationship in coralline aragonite: influence of variability in  $(\text{Sr}/\text{Ca})_{\text{seawater}}$  and skeletal growth parameters. *Geochimica et Cosmochimica Acta* 58, 197-208.
- DeLong, K.L., Quinn, T.M., Taylor, F.W., 2007. Reconstructing twentieth-century sea surface temperature variability in the southwest Pacific: a replication study using multiple coral Sr/Ca records from New Caledonia. *Paleoceanography* 22. doi:10.1029/2007PA001444.
- DeLong, K.L., Flannery, J.A., Maupin, C.R., Poore, R.Z., Quinn, T.M., 2011. A coral Sr/Ca calibration and replication study of two massive corals from the Gulf of Mexico. *Palaeogeography, Palaeoclimatology, Palaeoecology* 307, 117-128.
- Dodge, R.E., Thomason, J., 1974. The natural radiochemical and growth records in contemporary hermatypic corals from the Atlantic and Caribbean. *Earth and Planetary Science Letters* 23, 313-322.
- Druffel, E.R.M., 1997. Pulses of rapid ventilation in the north Atlantic surface ocean during the past century. *Science* 275, 1454-1457.
- Dunbar, R.B., Wellington, G.M., 1981. Stable isotopes in a branching coral monitor seasonal temperature variation. *Nature* 293, 453-455.
- Dunbar, R.B., Wellington, G.M., Colgan, M.W., Glynn, P.W., 1994. Eastern Pacific sea surface temperature since 1600 A.D.: the  $\delta^{18}\text{O}$  record of climate variability in Galapagos corals. *Paleoceanography* 9, 291-315.
- Enfield, D.B., Mestas-Nunez, A.M., Trimble, P.J., 2001. The Atlantic multidecadal oscillation

- and its relation to rainfall and river flows in the continental U.S. *Geophysical Research Letters* 28, 2077-2080.
- Epstein, S., Buchsbaum, R., Lowenstam, H., Urey, H.C., 1953. Revised carbonate-water isotopic temperature scale. *Geological Society of America Bulletin* 64, 1315-1325.
- Erez, J., 1977. Influence of symbiotic algae on the stable isotope composition of hermatypic corals: a radioactive tracer approach. In: Taylor, D.L. (Ed.), *Third International Coral Reef Symposium*. Rosenstiel School of Marine and Atmospheric Sciences, Miami, Florida, 564-569.
- Erez, J., 1978. Vital effect on stable-isotopes composition seen in foraminifera and coral skeletons. *Nature* 273, 199-202.
- Fahlquist, D.A., Davies, D.K., 1971. Fault block origin of the western Cayman Ridge, Caribbean Sea. *Deep Sea Research* 18, 243-253.
- Fairbanks, R.D., Dodge, R.E., 1979. Annual periodicity of the  $^{18}\text{O}/^{16}\text{O}$  and  $^{13}\text{C}/^{12}\text{C}$  ratios in the coral *Montastrea annularis*. *Geochimica et Cosmochimica Acta* 43, 1009-1020.
- Fallon, S.J., McCulloch, M., van Woesik, R., Sinclair, D.J., 1999. Corals at their latitudinal limits: laser ablation trace element systematics in *Porites* from Shirigai Bay, Japan. *Earth and Planetary Science Letters* 172, 221-238.
- Felis, T., Patzold, J., Loya, Y., 2003. Mean oxygen-isotope signatures in *Porites* sp. corals: inter-colony variability and correction for extension-rate effects. *Coral Reefs* 22, 328-336.
- Felis, T., Lohmann, G., Kuhnert, H., Lorenz, S.J., Scholz, D., Patzold, J., Al-Rousan, S., Al-Moghrabi, S.M., 2004. Increased seasonality in Middle East temperatures during the last interglacial period. *Nature* 429, 164-168.
- Flannery, J.A., Poore, R.Z., 2013. Sr/Ca proxy sea-surface temperature reconstructions from modern and Holocene *Montastrea faveolata* specimens from the Dry Tortugas National Park, Florida, U.S.A. *Journal of Coastal Research* 63, 20-31.
- Flannery, J.A., Richey, J.N., Thirumalai, K., Poore, R.Z., Della-Marta, P., 2017. Multi-species coral Sr/Ca-based sea-surface temperature reconstruction using *Orbicella faveolata*

- and *Sideratrea siderea* from the Florida Straits. *Palaeogeography, Palaeoclimatology, Palaeoecology*. 466, 100-109.
- Flannery, J.A., Richey, J.N., Toth, L.T., Kuffner, I.B., Poore, R.Z., 2018. Quantifying uncertainty in Sr/Ca-based estimates of SST from the coral *Orbicella faveolata*. *Paleoceanography and Paleoclimatology* 33, 958-973.
- Fenner, D.P., 1993. Some reefs and corals of Roatan (Honduras), Cayman Brac, and Little Cayman. *Atoll Research Bulletin* 388, 1-32.
- Frich, P.L., Alexander, V., Della-Marta, P., Gleason, B., Haylock, M., Tank, A.K., Peterson, T.C., 2002. Global changes in climatic extremes during the 2<sup>nd</sup> half of the 20<sup>th</sup> century. *Climate Resources* 19, 193-212.
- Gagan, M.K., Chivas, A.R., Isdale, P.J., 1994. High-resolution isotopic records from corals using ocean temperature and mass-spawning chronometers. *Earth and Planetary Science Letters* 121, 549-558.
- Gagan, M.K., Ayliffe, L.K., Hopley, D., Cali, J.A., Mortimer, G.E., Chappell, J., McCulloch, M., Head, M.J., 1998. Temperature and surface-ocean water balance of the Mid-Holocene tropical western Pacific. *Science* 279, 1014-1018.
- Gagan, M.K., Ayliffe, L.K., Beck, J.W., Cole, J.E., Druffel, E.R.M., Dunbar, R.B., Schrag, D.P., 2000. New views of tropical paleoclimates from corals. *Quaternary Science Reviews* 19, 45-64.
- Giry, C., Felis, T., Kolling, M., Scholz, D., Wei, W., Lohmann, G., Scheffers, S.R., 2012. Mid- to late Holocene changes in tropical Atlantic temperature seasonality and interannual to multidecadal variability documented in southern Caribbean corals. *Earth and Planetary Science Letters* 331-332, 187-200.
- Glynn, P.W., 1992. Coral reef bleaching: ecological perspectives. *Coral Reefs* 12, 1-17.
- Goodkin, N.F., Hughen, K.A., Cohen, A.L., Smith, S.R., 2005. Record of Little Ice Age sea surface temperatures at Bermuda using a growth-dependent calibration of coral Sr/Ca. *Paleoceanography* 20, doi:10.1029/2005PA001140,.

- Goreau, T.J., Hayes, R.L., Clark, J.W., Basta, D.J., Robertson, C.N., 1992. Elevated satellite sea surface temperatures correlate with Caribbean coral reef bleaching. In: Geyer, R.A. (Ed.), *A Global Warming Forum: Scientific, Economic, and Legal Overview*. CRC Press, Florida, USA, pp. 225-255.
- Gregory, B.R.B., Peros, M., Reinhardt, E.G., Donnelly, J.P., 2015. Middle-late Holocene Caribbean aridity inferred from foraminifera and elemental data in sediment cores from two Cuban lagoons. *Palaeogeography, Palaeoclimatology, Palaeoecology* 426, 239-241.
- Grossman, E.L., 2012. Applying oxygen isotope paleothermometry in deep time. *Paleontological Society Papers* 18, 39-67.
- Grossman, E.L., Ku, T.L., 1986. Oxygen and carbon isotope fractionation in biogenic aragonite: temperature effects. *Chemical Geology* 59, 59-74.
- Grottoli, A.G., Eakin, C.M., 2007. A review of modern coral  $\delta^{18}\text{O}$  and  $\Delta^{14}\text{C}$  proxy records. *Earth Science Reviews* 81, 67-91.
- Haase-Schramm, A., Bohm, F., Eisenhauer, A., Dullo, W., Joachimski, M.M., Hansen, B., Reitner, J., 2003. Sr/Ca ratios and oxygen isotopes from sclerosponges: temperature history of the Caribbean mixed layer and thermocline during the Little Ice Age. *Paleoceanography* 10. doi:10.1029/2002PA000830.
- Hadden, C.S., Cherkinsky, A., 2015.  $^{14}\text{C}$  variations in pre-bomb nearshore habitats of the Florida panhandle USA. *Radiocarbon* 57, 469-491.
- Hansen, J., Sato, M., Ruedy, R., K., L., Lea, D.W., Medina-Elizalde, M., 2006. Global temperature change. *Proceedings of the National Academy of Science of the USA* 106, 14288-14293.
- Heiss, G.A., Camoin, G.F., Eisenhauer, A., Wischow, D., Dullo, C., Hasen, B., 1997. Stable isotopes and Sr/ Ca-signals in corals from the Indian Ocean. In: Lessios, H.A., Macintyre, I.G. (Ed.), *Proceedings of the 8th International Coral Reef Symposium*, vol. 2. Smithsonian Tropical Research Institute, Panama. pp. 1713-1718.
- Hendy, E.J., Gagan, M.K., Lough, J.M., McCulloch, M., deMenocal, P., 2007. Impact of skeletal

- dissolution and secondary aragonite on trace element and isotopic climate proxies in *Porites* corals. *Paleoceanography* 22. doi: 10.1029/2007PA001462.
- Hetzinger, S., Pfeiffer, M., Dullo, W., Keenlyside, N., Latif, M., Zinke, J., 2008. Caribbean coral tracks Atlantic Multidecadal Oscillation and past hurricane activity. *Geology* 36, 11-14.
- Hetzinger, S., Pfeiffer, M., Dullo, W., Garbe-Schonberg, D., Halfar, J., 2010. Rapid 20<sup>th</sup> century warming in the Caribbean and impact of remote forcing on climate in the northern tropical Atlantic as recorded in a Guadeloupe coral. *Palaeogeography, Palaeoclimatology, Palaeoecology* 296, 111-124.
- Highsmith, R.C., Lueptow, R.L., Schonberg, S.C., 1983. Growth and bioerosion of three massive corals in the Belize barrier reef. *Marine Ecology - Progress Series* 13, 261-271.
- Hudson, J.H., Shinn, E.A., Halley, R.B., Lidz, B., 1976. Sclerochronology: tool for interpreting past environments. *Geology* 4, 361-364.
- Hudson, J.H., 1981. Growth rates in *Montastraea annularis*: a record of environmental change in Key Largo coral reef marine sanctuary, Florida. *Bulletin of Marine Science* 2, 444-459.
- Hudson, J.D., Anderson, T.F., 1989. Ocean temperatures and isotopic compositions through time. *Transactions of the Royal Society of Edinburgh: Earth Science* 80, 183-192.
- Hughen, K.A., Southon, J.R., Bertrand, C.J.H., Frantz, B., Zermeno, P., 2004. Cariaco Basin calibration update: revisions to calendar and <sup>14</sup>C chronologies for core PI07-58PC. *Radiocarbon* 46, 1161-1187.
- Hunter, I.G., 1994. Modern and ancient coral association of the Cayman Islands, Unpublished Ph.D., University of Alberta, Edmonton, Alberta, Canada, 345 pp.
- Keith, M.L., Weber, J.N., 1965. Carbon and oxygen composition of selected limestones and fossils. *Geochimica et Cosmochimica Acta* 28, 1787-1816.
- Kilbourne, K.H., 2006. Tropical Atlantic and Caribbean climate variations during the past eight centuries. Unpublished Ph.D., University of South Florida, Florida, USA, 188 pp.
- Kilbourne, K.H., Quinn, T.M., Guilderson, T.P., Webb, R.S., Taylor, F.W., 2007. Decadal-to interannual-scale source water variations in the Caribbean Sea recorded by Puerto Rican

- coral radiocarbon. *Climate Dynamics*, 29, 51-62.
- Kilbourne, K.H., Quinn, T.M., Webb, R.S., Guilderson, T.P., Nyberg, J., Winter, A., 2010. Coral windows into seasonal climate variability in the northern Caribbean since 1479. *Geochemistry Geophysics Geosystems* 11, doi 10.1029/2010GC003171.
- Kim, S., O'Neil, J.R., Hillaire-Marcel, C., Mucci, A., 2007. Oxygen isotope fractionation between synthetic aragonite and water: influence of temperature and  $Mg^{2+}$  concentration. *Geochimica et Cosmochimica Acta* 71, 4704-4715.
- Kim, S., Coplen, T.B., Horita, J., 2015. Normalization of stable isotope data for carbonate minerals: implementation of IUPAC guidelines. *Geochimica et Cosmochimica Acta* 158, 276-289.
- Knowlton, N., Weil, E., Weigt, L.A., Guzman, H.M., 1992. Sibling species in *Montastrea annularis*, coral bleaching, and the coral climate record. *Science* 255, 330-333.
- Knutson, D.W., Buddermeier, R.W., Smith, S.V., 1972. Coral chronometers: seasonal growth bands in reef corals. *Science* 177, 270-272.
- Kuffner, I.B., Lidz, B., Hudson, J.H., Anderson, J.S., 2015. A century of ocean warming on Florida Keys coral reefs: historic in situ observations. *Estuaries and Coasts* 38, 1085-1096.
- Kuffner, I.B., Roberts, H.H., Flannery, J.A., Morrison, J.M., Richey, J.N., 2017. Fidelity of Sr/Ca proxy in recording ocean temperature in the western Atlantic coral *Siderastrea siderea*. *Geochemistry Geophysics Geosystems* 18, 178-188.
- Land, L.S., Lang, J.C., Barnes, D.J., 1975. Extension rate: a primary control on the isotopic composition of West Indian (Jamaican) scleractinian reef coral skeletons. *Marine Biology* 33, 221-233.
- Leder, J.J., Swart, P.K., Szmant, A.M., Dodge, R.E., 1996. The origin of variations in the isotopic record of scleractinian corals: I. Oxygen. *Geochimica et Cosmochimica Acta* 60, 2857-2870.
- Li, R., Jones, B., 2013. Temporal and spatial variations in the diagenetic fabrics and stable



- isotopes of Pleistocene corals from the Ironshore Formation of Grand Cayman, British West Indies. *Sedimentary Geology* 286-287, 58-72.
- Linsley, B.K., Zhang, P., Kaplan, A., Howe, S.S., Wellington, G.M., 2008. Interdecadal-decadal climate variability from multicoloral oxygen isotope records in the South Pacific Convergence Zone region since 1650 A.D. *Paleoceanography* 23. doi 10.1029/2007PA001539.
- Lough, J.M., 2004. A strategy to improve the contribution of coral data to high-resolution paleoclimatology. *Palaeogeography Paleoclimatology Palaeoecology* 204, 115-143.
- Markoff, A., 2012. Terror came to Cayman 80 years ago. *Cayman Compass*. Pinnacle Media Ltd., Cayman Islands, November 9, 2012.
- Markoff, A., 2015, Cayman's stormy hurricane history. <http://hurricanes.ky/caymans-stormy-hurricane-history/> (Accessed March 2016).
- Marshall, J.F., McCulloch, M.T., 2002. An assessment of the Sr/Ca ratio in shallow water hermatypic corals as a proxy for sea surface temperature. *Geochimica et Cosmochimica Acta* 66, 3263-3280.
- Maupin, C.R., Quinn, T.M., Halley, R.B., 2008. Extracting a climate signal from the skeletal geochemistry of the Caribbean coral *Siderastrea siderea*. *Geochemistry Geophysics Geosystems* 9. doi: 10.1029/2008GC002106.
- McConnaughey, T., 1988.  $^{13}\text{C}$  and  $^{18}\text{O}$  isotopic disequilibrium in biological carbonates: I. Patterns. *Geochimica et Cosmochimica Acta* 53, 151-162.
- McCulloch, M.T., Gagan, M.K., Mortimer, G.E., Chivas, A.R., Isdale, P.J., 1994. A high-resolution Sr/Ca and  $\delta^{18}\text{O}$  coral record from the Great Barrier Reef, Australia, and the 1982-1983 El Niño. *Geochimica et Cosmochimica Acta* 58, 2747-2754.
- McGregor, H.V., Gagan, M.K., 2003. Diagenesis and geochemistry of *Porites* corals from Papua New Guinea: implications for paleoclimate reconstruction. *Geochimica et Cosmochimica Acta* 67, 2147-2156.
- McWilliams, J.P., Cote, I.M., Gill, J.A., Sutherland, W.J., Watkinson, A.R., 2005. Accelerating

impacts of temperature-induced coral bleaching in the Caribbean. *Ecology* 86, 2055-2060.

- Meibom, A., Stage, M., Wooden, J., Constantz, B.R., Dunbar, R.B., Owen, A., Grumet, N., Bacon, C.R., Chamberlin, C.P., 2003. Monthly strontium/calcium oscillations in symbiotic coral aragonite: biological effects limiting the precision of paleotemperature proxy. *Geophysical Research Letters* 30, doi 10.1029/2002GL016864.
- Melo-Gonzalez, N.M., Muller-Karger, F.E., Cerdeira-Estrada, S., Perez de los Reyes, R., Victoria del Rio, I., Cardenas-Perez, P., Mitrani-Arenal, I., 2000. Near-surface phytoplankton distribution in the western Intra-Americas Sea: the influence of El Nino and weather events. *Journal of Geophysical Research* 105, 14029-14043.
- Moore, W.S., Krishnaswami, S., 1974. Correlation of X-radiography revealed banding in corals with radiometric growth rates. In: Cameron, A.M., Cambell, B.M. Cribb, A.B. Endean, R. Jell, J.S. Jones, O.A. Mather, P. Talbot, F.H. (Eds.), *Proceeding of the Second International Coral Reef Symposium 2*. Great Barrier Reef Committee, Brisbane, pp. 269-276.
- NOAA, 2018, World Sea Temperatures. <https://www.seatemperature.org/>.
- Nurse, L.A., Sem, G., 2001. Small island states. In: McCarth, J.J., Canziani, O.F., Leary, N.A., Dokken, D.J., White, K.S. (Ed.), *Climate change 2001: impacts, adaptations and vulnerability*. Cambridge University Press. pp. 843-875.
- Patterson, W.P., Smith, G.R., Lohmann, K.C., 1993. Continental paleothermometry and seasonality using the isotopic composition of aragonitic otoliths of freshwater fishes. In: Swart, P.K., Lohman, K.C., McKenzie, J., Savin, S. (Eds.), *Climate Change in Continental Isotopic Records*. Geophysical Monograph Series. American Geophysical Union, Washington, D.C., 78, 191-202.
- Perfit, M.R., Heezen, B.C., 1978. The geology and the evolution of the Cayman Trench. *Geological Society of America Bulletin* 89, 1155-1174.
- Peros, M.C., Reinhardt, E.G., Schwarcz, H.P., Davis, A.M., 2007. High-resolution paleosalinity

- reconstruction from Laguna de la Leche, north coastal Cuba, using Sr, O, and C isotopes. *Palaeogeography, Palaeoclimatology, Palaeoecology* 245, 535-550.
- Peterson, T.C., Taylor, M.A., Demeritte, R., Duncombe, D.L., Burton, S., Thompson, F., Porter, A., Mercedes, M., Villegas, E., Fils, R.S., Tank, A.K., Martis, A., Warner, R., Joyette, A., Mills, W., Gleason, B., 2002. Recent changes in climate extremes in the Caribbean region. *Journal of Geophysical Research* 107, doi: 10.1029/2002JD002251.
- Porter, J.W., Fitt, W.K., Spero, H.J., Rogers, C.S., White, M.W., 1989. Bleaching in reef corals: physiological and stable isotopic responses. *Ecology* 86, 9342-9346.
- Prospero, J.M., Mayol-Bracero, O.L., 2013. Understanding the transport and impact of African dust on the Caribbean Basin. *American Meteorological Society*, 1329-1338.
- Quinn, T.M., Taylor, F.W., 2006. SST artifacts in coral proxy records produced by early marine diagenesis in a modern coral from Rabaul, Papua New Guinea. *Geophysical Research Letters* 35, 1-4.
- Reynaud, S., Ferrier-Pages, C., Meibom, A., Mostefaoui, S., Mortlock, R., Fairbanks, R., Allemand, D., 2007. Light and temperature effects on Sr/Ca and Mg/Ca ratios in the scleractinian coral *Acropora* sp. *Geochimica et Cosmochimica Acta* 71, 354-362.
- Ribaud-Laurenti, A., Hamelin, B., Montaggioni, L., Cardinal, D., 2001. Diagenesis and its impacts on Sr/Ca ratio in Holocene *Acropora* corals. *International Journal of Earth Sciences* 90, 438-451.
- Rigby, J.K., Roberts, H.H., 1976. Grand Cayman Island: geology, sediments, and marine communities. *Brigham Young University Geology Studies: Special Publication*, 4. Brigham Young University, Department of Geology, Utah, 122 pp.
- Ren, M., Jones, B., 2017. Spatial variations in the stoichiometry and geochemistry of Miocene dolomite from Grand Cayman: implications for the origins of island dolostone. *Sedimentary Geology* 348, 69-93.
- Roberts, H.H., Rouse, L.J., Walker, S.E., Hudson, J.H., 1982. Cold-water stress in Florida Bay and northern Bahamas: a product of winter cold-air outbreaks. *Journal of Sedimentary*

Research 52, 145-155.

- Rodrigues, L.J., Grottoli, A.G., 2006. Calcification rate and the stable carbon, oxygen, and nitrogen isotopes in the skeleton, host tissue, and zooxanthellae of bleached and recovering Hawaiian corals. *Geochimica et Cosmochimica Acta* 70, 2781-2789.
- Sadler, J., Webb, G.E., Nothdurft, L.D., Dechnik, B., 2014. Geochemistry-based coral paleoclimate studies and the potential of 'non-traditional' (non-massive *Porites*) coral: recent developments and future progression. *Earth Science Reviews* 139, 291-316.
- Sadler, J., Nguyen, A.D., Leonard, N.D., Webb, G.E., Nothdurft, L.D., 2016. *Acropora* interbranch skeleton Sr/ Ca ratios: evaluation of a potential new high-resolution paleothermometer. *Paleoceanography* 31, 505-517.
- Saenger, C., Cohen, A.L., Oppo, D.W., Hubbard, D., 2008. Interpreting sea surface temperature from strontium/calcium ratios in *Montastrea* corals: link with growth rate and implications for proxy reconstructions. *Paleoceanography* 23. doi 10.1029/2007PA001572.
- Saenger, C., Cohen, A.L., Oppo, D.W., Halley, R.B., Carilli, J.E., 2009. Surface-temperature trends and variability in the low-latitude North Atlantic since 1552. *Nature Geoscience Letters* 2, 492-946.
- Sauer, J.D., 1982. Cayman Islands seashore vegetation. A study in comparative biogeography. University of California Press, London, England. 25, 161 pp.
- Sharp, Z., 2007. Principles of stable isotope geochemistry. Pearson/Prentice Hall, Upper Saddle River, New Jersey, 334 pp.
- Shen, C., Lee, T., Chen, C., Wang, C., Dai, C., Li, A., 1996. The calibration of  $D_{(Sr/Ca)}$  versus sea surface temperature relationship for *Porites* coral. *Geochimica et Cosmochimica Acta* 60, 3849-3858.
- Shen, C., Li, K., Sieh, K., Natawidjaja, D., Cheng, H., Wang, X., Edwards, R.L., Lam, D.D., Hsieh, Y., Fan, T., Meltzner, A.J., Taylor, F.W., Quinn, T.M., Chiang, H., Kilbourne, K.H., 2008. Variation of initial  $^{230}\text{Th}/^{232}\text{Th}$  and limits of high precision U-Th dating of shallow-

- water corals. *Geochimica et Cosmochimica Acta* 7, 4201-4223.
- Smith, S.R., Buddemeier, R.W., Redale, R., Houck, J.E., 1979. Strontium-calcium thermometry in coral skeletons. *Science* 204, 404-406.
- Smith, J.M., Quinn, T.M., Helmle, K.P., Halley, R.B., 2006. Reproducibility of geochemical and climatic signals in the Atlantic coral *Montastrea faveolata*. *Paleoceanography* 21, doi 10.1029/2005PA001187.
- Storz, D., Gischler, E., Fiebig, J., Eisenhauer, A., Garbe-Schonberg, D., 2013. Evaluation of oxygen isotope and Sr/Ca ratios from a Maldivian scleractinian coral from reconstruction of climate variability in the Northwestern Indian Ocean. *Palaios* 28, 42-55.
- Strong, A.E., 1989. Greater global warming revealed by satellite-derived sea-surface temperature trends. *Nature* 338, 642-645.
- Stuiver, M., Reimer, P.J., Reimer, R.W., 2019, CALIB 7.1 {WWW program}.
- Swart, P.K., 1983. Carbon and oxygen isotope fractionation in scleractinian corals: a review. *Earth Science Reviews* 19, 51-80.
- Swart, P.K., Elderfield, H., Greaves, M.J., 2002. A high-resolution calibration of Sr/Ca thermometry using the Caribbean coral *Montastraea annularis*. *Geochemistry Geophysics Geosystems* 3, doi 10.1029/2002GC000306.
- Thorrold, S.R., Campana, S.E., Jones, C.M., Swart, P.K., 1997. Factors determining  $\delta^{13}\text{C}$  and  $\delta^{18}\text{O}$  fractionation in aragonitic otoliths of marine fish. *Geochimica et Cosmochimica Acta* 61, 2909-2919.
- Tierney, J.E., Abram, N.J., Anchukaitis, K.J., Evans, M.N., Giry, C., Kilbourne, K.H., Saenger, C., Wu, H.C.,
- Zinke, J., 2015. Tropical sea surface temperatures for the last four centuries reconstructed from coral archives. *Paleoceanography* 30, 226-252.
- Toth, L.T., Cheng, H., Edwards, L.R., Ashe, E., Richey, J.N., 2017. Millennial-scale variability in the local radiocarbon reservoir age of south Florida during the Holocene. *Quaternary Geochronology* 42, 130-143.

- Trapp, J.M., Millero, F.J., Prospero, J.M., 2010. Temporal variability of the elemental composition of African dust measured in trade wind aerosoles at Barbados and Maimi. *Marine Chemistry* 120, 71-82.
- Trenberth, K.E., Jones, P.D., Ambenje, P., Bojariu, R., Easterling, D., Klein Tank, A., Parker, D., Rahimzadeh, F., Renwick, J.A., Rusticucci, M., Soden, B., Zhai, P., 2007. Observations: surface and atmospheric climate change. In: Solomon, S., Qin, D., Manning, M., Chen, Z., Marquis, M., Averyt, K.B., Tignor, M., Miller, H.L. (Eds.), *Climate Change 2007: The Physical Science Basis. Contribution of Working Group I to the Fourth Assessment Report of the Intergovernmental Panel on Climate Change* Cambridge University Press, Cambridge, United Kingdom, 102 pp.
- van Hengstum, P.J., Donnelly, J.P., Kingston, A.W., Williams, B.E., Scott, D.B., Reinhardt, E.G., Little, S.N., Patterson, W.P., 2015. Low-frequency storminess signal at Bermuda linked to cooling events in the North Atlantic region. *Paleoceanography* 30, 52-76.
- von Reumont, J., Hetzinger, S., Garbe-Schonberg, D., Manfrino, C., Dullo, W., 2016. Impact of warming events on reef-scale temperature variability as captured in two Little Cayman coral Sr/Ca records. *Geochemistry Geophysics Geosystems* 17. doi: 10.1002/2015GC006194.
- Watanabe, T., Winter, A., Oba, T., 2001. Seasonal changes in sea surface temperatures and salinity during the Little Ice Age in the Caribbean Sea deduced from Mg/Ca and  $^{18}\text{O}/^{16}\text{O}$  ratios in corals. *Marine Geology* 173, 21-35.
- Weber, J.N., 1973. Incorporation of strontium into reef coral skeletal carbonate. *Geochimica et Cosmochimica Acta* 37, 2173-2190.
- Weber, J.N., 1977. Use of corals in determining Glacial-Interglacial changes in temperature and isotopic composition of seawater: reef biota. In: Frost, S. H., Weiss, M.P., Saunders, J.B. (Eds.), *Reefs and Related Carbonates - Ecology and Sedimentology*. American Association of Petroleum Geologists Special Volumes, 4, 289-295.
- Weber, J.N., Woodhead, P.M.J., 1970. Carbon and oxygen isotope fractionation in the skeletal

- carbonate of reef-building corals. *Chemical Geology* 6, 93-117.
- Weber, J.N., Woodhead, P.M.J., 1972. Temperature dependence of oxygen-18 concentration in reef coral carbonates. *Journal of Geophysical Research* 77, 463-474.
- Webster, P.J., Moore, A.M., Loschnigg, J.P., Leben, R.R., 1999. Coupled ocean-atmosphere dynamics in the Indian Ocean during 1997-1998. *Nature* 401, 356-360.
- Weil, S.M., Buddemeier, R.W., Smith, S.V., Kroopnick, P.M., 1981. The stable isotopic composition of coral skeletons: control by environmental variables. *Geochimica et Cosmochimica Acta* 45, 1147-1153.
- Weil, E., Knowlton, N., 1994. A multi-character analysis of the Caribbean coral *Montastrea annularis* (Ellis and Solander, 1786) and its two sibling species, *M. faveolata* (Ellis and Solander, 1786) and *M. franksi* (Gregory, 1895). *Bulletin of Marine Science* 55, 151-175.
- Wellington, G.M., Dunbar, R.B., Merlen, G., 1996. Calibration of stable oxygen isotope signatures in Galapagos corals. *Paleoceanography* 11, 467-480.
- White, R.M.P., Dennis, P.F., Atkinson, T.C., 1999. Experimental calibration and field investigation of the oxygen isotopic fractionation between biogenic aragonite and water. *Rapid Communications in Mass Spectrometry* 13, 1242-1247.
- Winter, A., Appeldoorn, R.S., Bruckner, A., Williams, E.H., Goenaga, C., 1998. Sea surface temperatures and coral reef bleaching off La Parguera, Puerto Rico (northeastern Caribbean Sea). *Coral Reefs* 17, 377-382.
- Winter, A., Sammarco, P.W., 2010. Lunar banding in the scleractinian coral *Montastraea faveolata*: fine-scale structures and influences of temperature. *Journal of Geophysical Research* 115. doi: 10.1029/2009JG001264.
- Worum, F.P., Carricart-Ganivet, J.P., Benson, L., Golicher, D., 2007. Simulation and observations of annual density banding in skeletons of *Montastrea* (Cnidaria: Scleractinia) growing under thermal stress associated with ocean warming. *Limnology and Oceanography* 52, 2317-2323.

## CHAPTER 4

### A 6000-YEAR RECORD OF CLIMATE CHANGE FROM STABLE ISOTOPE AND RARE EARTH ELEMENT ANALYSES OF SEDIMENT CORES FROM NORTH SOUND LAGOON, GRAND CAYMAN, BRITISH WEST INDIES

#### 1. Introduction

Vertical successions of sediments in tropical lagoons are archives of environmental changes that have been laid down in these dynamic depositional environments. As such, they provide records of temporal changes in depositional architecture that may reflect sea level oscillations and/or climate changes (Bracco et al., 2005; Switzer and Jones, 2008; Marco-Barba et al., 2013). At a smaller and more detailed scale, analyses of the carbonate components in lagoonal facies may reflect temporal changes in ecology (Lane et al., 2009; 2011) and/or water conditions such as salinity and water depth (Culver, 1990; Debenay et al., 1998; Anthony et al., 2009), whereas geochemical proxies such as  $\delta^{18}\text{O}$ ,  $\delta^{13}\text{C}$ , Sr/Ca and Mg/Ca ratios, and rare earth elements (REE) can be used to track short-term changes (100-1000s of years) in sea level oscillations and/or climate (Haug et al., 2001; Black et al., 2004; Muhs et al., 2007; Lane et al., 2009; Gregory et al., 2015).

Barnett et al. (1992) argued that climate between 30 °S and 30 °N latitudes has a primary control on global atmospheric circulation and sea surface temperatures (SST). The sparse record of pre-industrial climate variability for low resolution, semi-continuous, and poor spatial coverage in these low latitudes, however, makes correlations to regional and global-scale climates difficult (Holmgren et al., 1999). For the Caribbean region, examples of climatological studies include Hodell et al. (1991) who used oxygen isotope compositions of ostracod shells in sediment cores from a brackish-water lake in Haiti to ascertain tropical climate changes since the late Pleistocene (last 10 ka). Similarly, Hodell et al. (1995) used sediment composition (gypsum/calcite ratios) and



$\delta^{18}\text{O}$  values from ostracod and gastropod shells in a carbonate sediment core from a brackish-water lake in Mexico to reconstruct precipitation/evaporation cycles over the last ~3000 years. Nyberg et al. (2001) used three sediment cores from offshore Puerto Rico to determine climate changes over the last ~2000 years using a multi-proxy approach that included geochemical and magnetic susceptibility measurements of the sediment. Lane et al. (2009) used sediment cores from two freshwater lakes in the Dominican Republic to decipher paleoenvironmental changes over the last ~3000 years using a multi-proxy approach that involved sediment characteristics and the isotopic composition of the shells and sediment. Similarly, Gregory et al. (2015) used foraminifera assemblages and element analyses of foraminifera and carbonate sediment from cores in fully marine coastal lagoons in Cuba to determine regional climate change over the last ~4000 years.

This study, based on three sediment cores from North Sound, Grand Cayman (Fig. 1), uses a multi-proxy approach that includes analysis of facies, carbonate components, elemental concentrations, and stable isotope compositions to reconstruct centennial-scale climate changes over the last ~6000 years. The reconstruction of climate change around Grand Cayman is based on element concentrations (REE, Ti, Fe) for atmospheric variability (dry and wet periods) and oxygen isotope compositions for paleotemperatures (cool, mild, and warm periods). Together, these parameters are used to assess the behaviour of atmospheric pressure regimes that affect the tropics such as the ITCZ and the phase of the NAO. This Grand Cayman record is compared to regional and global climate fluctuations, such comparisons are essential to deciphering the timing, effects, and causes of large-scale climate change in the Caribbean region and globally over the last ~6000 years.

## **2. Geological setting**

Grand Cayman (Fig. 4.1) is located on the Cayman Ridge, which is an uplifted

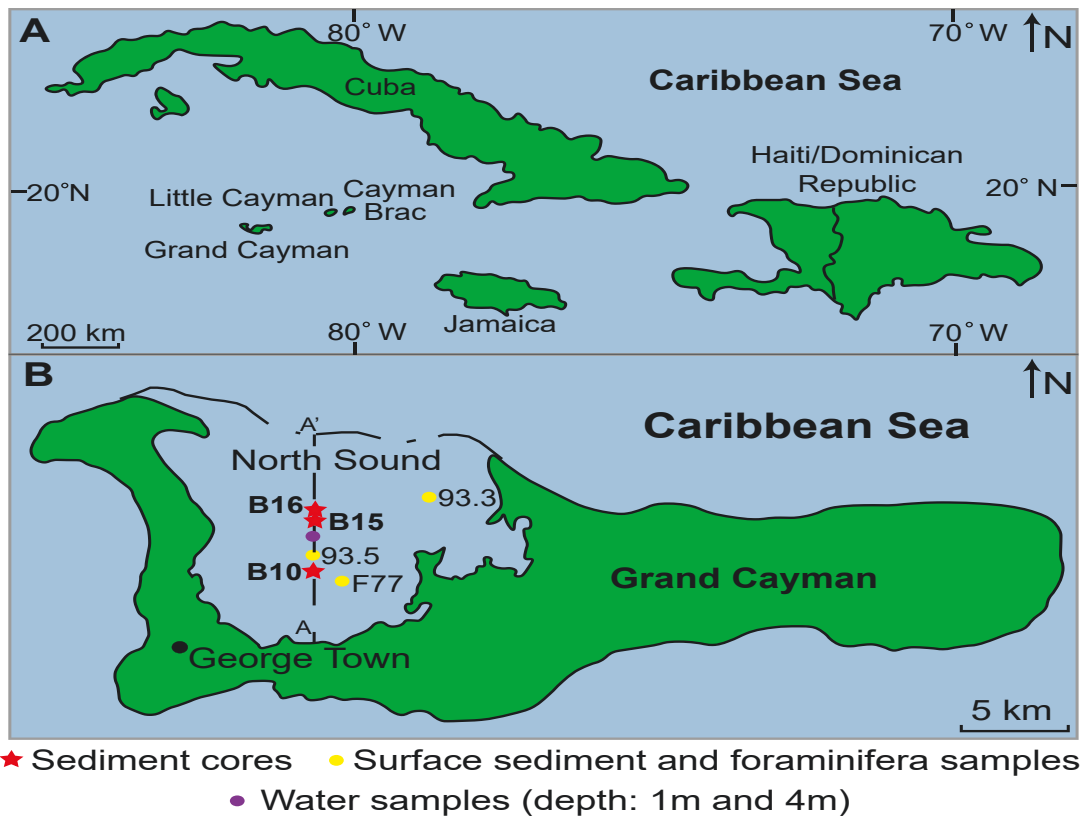


**Fig. 4.1.** Location maps. (A) Map showing location of the Cayman Islands. (B) Map of Grand Cayman. Red stars indicate location of sediment cores. Yellow circles indicate location of surface sediment and foraminifera samples. Purple circle indicates location of water samples. Line A to A' represents the location of the profile in figure 4.3.

fault block that extends from the Sierra Maestra Range (Cuba) to the base of the British Honduras Continental Slope (Fahlquist and Davies, 1971; Perfit and Heezen, 1978). Although located in a tectonically active area, this island does not appear to have undergone any vertical movement during the last 125 ka (Emery, 1981; Jones and Hunter, 1990; Jones, 1994).

The coastal areas of the island are characterized by narrow shelves and lagoons formed by fringing reefs that stretch from headland to headland. Present-day ocean temperatures off the west coast of Grand Cayman range from 25° to 31°C, with an

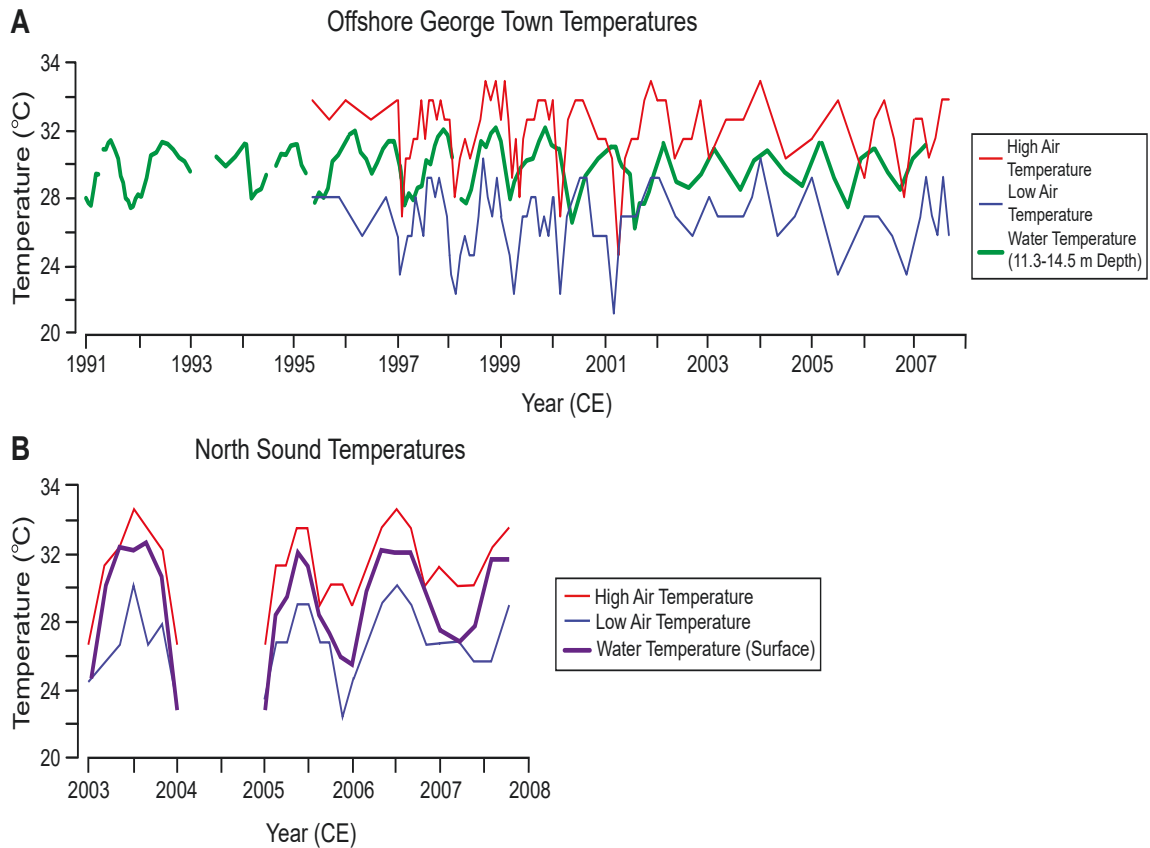


**Fig. 4.2.** Air and ocean water temperatures for Grand Cayman. (A) Atmospheric and water temperatures (11.3-14.5 m water depth) between 1991 and 2008 from offshore George Town. (B) Atmospheric and water temperatures (surface) between 2003 and 2008 from North Sound. Data from the Department of Environment and the Water Authority, Cayman Islands.

average of 28.5°C (Goreau et al., 1992; Department of Environment and the Water Authority, Cayman Islands, 1991 and 2008; Chollett et al., 2012; NOAA, 2018; Fig. 4.2A). North Sound, the largest lagoon on Grand Cayman (Fig. 4.1B), is 9 km long and 7 km wide with water up to 6 m deep (MacKinnon, 2000; MacKinnon and Jones, 2001). A fringing reef on its north margin separates North Sounds from the open ocean. Water temperatures in this lagoon, measured from 1991-2008, have a seasonal range from 22° to 32°C, with an average of 28°C (Fig. 4.2B; Department of Environment and the Water

Authority, Cayman Islands, 1991 and 2008).

### 3. Samples

This study is based on three 4 cm diameter sediment cores (B10, B15, B16) from North Sound that provide a record of sedimentation over the last ~6000 years (MacKinnon, 2000; MacKinnon and Jones, 2001). All cores terminate at bedrock, and thus represent sedimentation prior to and during the last transgressive cycle (MacKinnon and Jones, 2001). Core B10 is 2.23 m long, core B15 is 2.4 m long, and core B16 is 1.65 m long (Fig. 4.1B). MacKinnon (2000) and MacKinnon and Jones (2001) divided the surface and subsurface sediments of North Sound into the Composite Grain, Gastropod, Bivalve, and Peat Facies that developed in fresh to brackish waters, and the *Halimeda*, *Halimeda*-Benthic Foraminifera-Bivalve, and Bivalve-*Halimeda* Facies that formed in fully marine conditions (Fig. 4.3).

In addition to the samples from the cores, three bulk surface sediment samples (~1 g) from North Sound, collected in the center (samples F77 and 93.5) and northeast corner of the lagoon (sample 93.3; Fig. 4.1B) were analyzed for elemental and isotopic composition. The foraminifera, *Archaias angulatus* and *Amphistegina gibbosa* were picked out of the surface samples in three sediment-based size classes (6, 16, 26 mm diameter). Two 10 ml samples of seawater from the center of North Sound (Fig. 4.1B) at surface and depth (4 m water depth), collected by the Department of Environment (Cayman Islands) in August 2019, were analyzed for their elemental and isotopic composition.

### 4. Methodology

#### 4.1. X-ray diffraction

Sediment mineralogy was determined by X-ray diffraction (XRD) using a Rigaku Geigerflex Powder Diffractometer at the University of Alberta. Twenty-one bulk samples

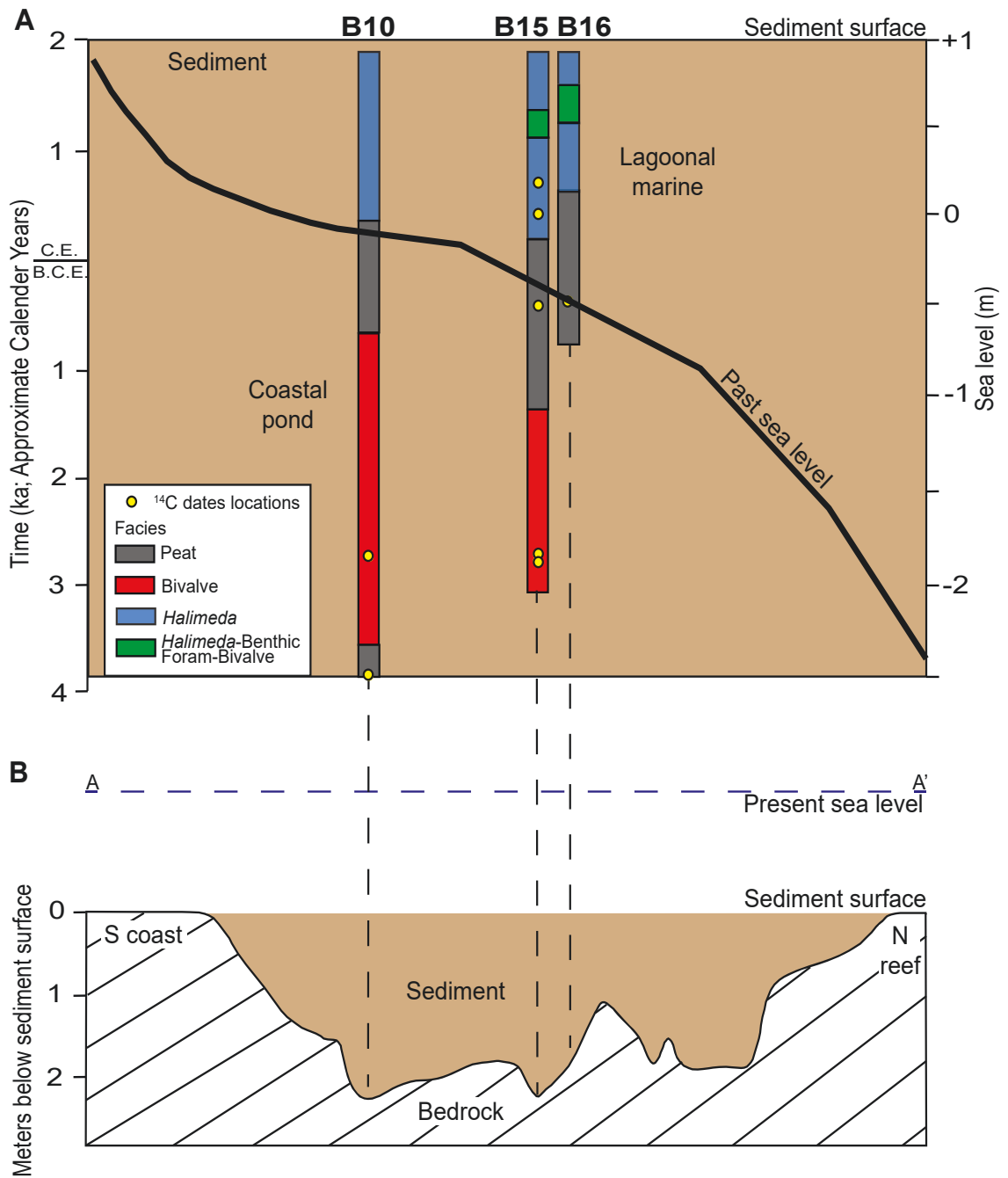


**Fig. 4.3.** Sea level curve modified from Fleming et al. (1998) and Miline et al. (2005). (A)

Facies distribution from MacKinnon, (2000) and MacKinnon and Jones, (2001) of the North Sound cores B10, B15, and B16 superimposed on sea level curve, showing the transition of sediment deposition and facies type associated with deposition in a coastal pond setting to a fully marine lagoonal setting during the last transgressive cycle. (B) Location of the North Sound cores. Location of line A to A' shown on figure 4.1B.

(~1 g) at 10 cm intervals were analyzed from core B10, 23 bulk samples (10 cm intervals) from core B15, and 16 bulk samples (10 cm intervals) from core B16. The mineralogy of the foraminifera samples was also determined. The percentage of aragonite and calcite in each sample was determined following the approach of Li and Jones (2013).

## 4.2. Age dating

### 4.2.1. $^{14}\text{C}$ dating

Previously published  $^{14}\text{C}$  dates from cores B10, B15, and B16 were obtained by conventional radiocarbon dating analysis (MacKinnon, 2000; MacKinnon and Jones, 2001) using the following technique. The shell material was pretreated by leaching with HCl to remove the outer 20-40% before hydrolysis and the basal peat samples were treated three times with hot HCl extraction prior to radiocarbon analysis. Two additional  $^{14}\text{C}$  dates were obtained from core B15 in order to maximum the dating resolution as dictated by the availability of large well-preserved shells. The additional  $^{14}\text{C}$  dates from core B15 were produced by the A.E. Lalonde AMS Laboratory at the University of Ottawa in 2017. These samples were pretreated following the method of Crann et al. (2017). Briefly, samples were physically cleaned by manual abrasion and etched with 0.2N HCl. Graphite targets for accelerator mass spectrometry were prepared from  $\text{CO}_2$  liberated by sample dissolution in anhydrous  $\text{H}_3\text{PO}_4$  overnight at room temperature.

### 4.2.2. Age-depth model

The radiocarbon ages were converted to calendar years using CALIB 7.10 (Stuiver et al., 2020). All marine samples were calibrated using the MARINE13 calibration curve (Reimer et al., 2013) and a local (Caribbean) reservoir effect ( $\Delta\text{R}$ ) of -28 (Table 4.1). Non-marine samples were calibrated using the INTCAL13 calibration curve (Table 4.1). The age-depth model for core B15 was developed using the BACON package ('rbacon'; Blaauw and Christen, 2011) in R (R Core Team, 2013). BACON reconstructs age-

**Table 4.1.**  $^{14}\text{C}$  dating information. Calibration was performed with CALIB 7.10 (Stuiver et al., 2020), using the MARINE13 calibration curve (Reimer et al., 2013) and a local reservoir correction ( $\Delta\text{R}$ ) of -28 for all marine samples. Non-marine samples are calibrated using the INTCAL13 calibration curve. Calendar years are given as the median probability and  $2\sigma$  of calibrated ages, rounded to the nearest tenth year.

Sample (Lab ID)	Core Depth	Sample type	$^{14}\text{C}$ year BP	Fraction of $^{14}\text{C}$ in sample	Calendar year ( $2\sigma$ calibrated range)
Peat (TO-8948)	B10 2.23 m	Non-marine	$5060 \pm$ 80	n.d.	3850 BCE (4030-3660 BCE)
<i>Mytilopsis</i> <i>domingensis</i> (TO-7501)	B10 1.65 m	Marine	$4160 \pm$ 40	n.d.	2750 BCE (2880-2620 BCE)
<i>Mytilopsis</i> <i>domingensis</i> (TO-7502)	B15 2.39 m	Non-marine	$3770 \pm$ 40	n.d.	2190 BCE (2330 to 2040 BCE)
Peat (TO-8949)	B15 2.37 m	Non-marine	$4140 \pm$ 80	n.d.	2720 BCE (2900 to 2490 BCE)
<i>Anodontina alba</i> (TO-7503)	B15 1.96 m	Marine	$2520 \pm$ 30	n.d.	280 BCE (360 to 180 BCE)
<i>Anadara floridana?</i> (UOC-2672)	B15 1.4 m	Marine	$1948 \pm$ 22	$0.7846 \pm$ 0.0022	410 CE (340 to 510 CE)
<i>Cerithium</i> <i>eburneum</i> (UOC-2673)	B15 0.6 m	Marine	$1584 \pm$ 22	$0.8211 \pm$ 0.0023	760 CE (700 to 850 CE)
Bivalve fragments (TO-7504)	B16 1.15 m	Marine	$2600 \pm$ 40	n.d.	370 BCE (480 to 220 BCE)

depth relationships using a Bayesian approach with prior assumptions about sediment accumulation rates and their variability together with Markov Chain Monte Carlo analysis. Default values for section thickness, the shape and mean parameters for the accumulation rate gamma distribution, and the accumulation rate autocorrelation between sections were used. The calendar age for the top of the core was set to 1980 CE, the year the core was collected. Since North Sound is a small lagoon characterized by laterally continuous facies and the three cores were collected close to one another, the age-depth model from core B15 was extrapolated to cores B10 and B16.

#### 4.3. Elemental analyses

Sixty-seven powdered samples (< 200 mg) of the sediments from core B10 and B15 were analyzed for 45 elements (Mg, Ca, Sr, Li, Be, B, Na, Al, P, K, Ti, V, Cr, Fe, Mn, Cu, Co, Ni, Zn, Ga, Ge, As, Se, Rb, Zr, Nb, Mo, Ru, Pd, Ag, Cd, Sn, Sb, Te, Cs, Ba, Hf, W, Re, Ir, Pt, Tl, Pb, Th, U) and 15 REE (La, Ce, Pr, Nd, Sm, Eu, Gd, Tb, Dy, Ho, Er, Tm, Yb, Lu, including yttrium (Y)). Determination limits (DL) ranged from 0.02 to 62 ppm, elements that are below DL are not considered further. For the remaining 30 elements that are above DL, only the major element (>10000 ppm) Ca, the minor elements (1000 to 10000 ppm) Mg, Sr, Fe, Al, and the trace elements (<100 ppm) Ti and REE+Y are utilized because these elements are (1) commonly used for paleotemperature determination (e.g., Ca, Mg, Sr), (2) display contrasts in concentrations that reflect the change from coastal pond to marine facies (e.g., Mg, Sr, Fe, Al, Ti), and (3) can be used to assess climatic variability (e.g., Fe, Ti, REE+Y). Only the Mg, Ca, and Sr concentrations were determined for the three surface sediment samples and the six foraminifera samples, as these elements are typically used to calculate SST. Analytical uncertainties ( $2\sigma$ ) are  $\pm 4000$  ppm for Ca,  $\pm 40$  ppm for Mg and Sr,  $\pm 20$  ppm for Al,  $\pm 5$  ppm for Fe,  $\pm 2$  ppm for Ti, and  $\pm 0.05$  ppm for the REE+Y.

A Thermo Fisher iCAP-Q inductively coupled plasma mass spectrometer



(ICP-MS) at the University of Alberta was used for elemental analysis. The samples were dissolved in 2 mL 50% HNO<sub>3</sub>, from this 0.1 mL was added to 9.7 mL deionized water, 0.1 mL HNO<sub>3</sub>, and 0.1 mL of internal standard solution at 100 ppb concentration for Sc, In, and Bi. Typical count rates for 1 ppm were 300000 to 400000 cps. REE concentrations were normalized to chondrite (CN; McLennan, 1989) and plotted on logarithmic scales against atomic number (cf., McLennan, 1989). The REE are divided into light REE (LREE; La, Ce, Pr, Nd, Pm), middle REE (MREE; Sm, Eu, Gd, Dy), and heavy REE (HREE; Ho, Er, Tm, Yb, Lu) following standard conventions (Kuss et al., 2001; Muhs and Budahn, 2009). The scale of the Eu anomaly is given by  $Eu_{(CN)}/Eu^*$ , where  $Eu^*$  is  $(Sm_{(CN)} * Gd_{(CN)})^{0.5}$  (Muhs et al., 2007). Differences in the abundances of LREE relative to HREE are given by  $La_{(CN)}/Yb_{(CN)}$ , where high  $La_{(CN)}/Yb_{(CN)}$  values indicate LREE enrichment, and  $Gd_{(CN)}/Yb_{(CN)}$ , where high  $Gd_{(CN)}/Yb_{(CN)}$  indicates significant HREE depletion (Muhs et al., 2007).

#### 4.4. Seawater analyses

The seawater samples from the center of North Sound (Fig. 4.1B) were analysed for metal concentrations at the University of Alberta using an inductively coupled plasma-tandem mass spectrometer (ICP-MS/MS). For all elements, except Na, the samples and standards were prepared in a matrix of 2% HNO<sub>3</sub> with 2000 ppm NaCl and then diluted to 1:15 sample to matrix. For Na, samples were diluted to 1:200 sample to matrix. The standards covered a range of 0.0005-120 ppm in three tiers to accommodate varying concentrations. Various collision/reaction gases (He, H<sub>2</sub>, and O<sub>2</sub>) were used for ICP-MS/MS analysis, with In as an internal standard to account for instrument drift.

The oxygen isotope compositions of these water samples were determined by Isotope Tracer Technologies Ltd., Ontario, Canada, using a Thermo Delta Plus Advantage linked to a Gasbench I via a GC PAL autosampler.  $\delta^{18}O_{\text{water}}$  values are reported relative to the VSMOW standard and have an analytical uncertainty ( $2\sigma$ ) of  $\pm 0.2\%$ .

#### 4.5. Sediment and foraminifera stable isotope analyses

$\delta^{13}\text{C}$  and  $\delta^{18}\text{O}$  values of the bulk sediment and foraminifera samples were determined using a Finnigan MAT DeltaPlus XL isotope ratio mass spectrometer (IRMS) at Isotope Tracer Technologies Inc, Waterloo, Ontario. Twenty-one 5 g samples collected at 10 cm spacing were taken from core B10, 46 samples collected at 5 cm spacing were taken from core B15, and 16 samples collected at 10 cm spacing were taken from core B16. The three surface sediment samples and six foraminifera samples (6-26 mm size fractions) were also analyzed. Powdered samples, each weighing <100 mg, were evacuated with ultrapure helium and held at a constant temperature of 50°C over the course of the analysis. Samples were digested with 100% phosphoric acid and allowed to react for 2 hours. During each run sequence, two international calcite standards NBS-18 and NBS-19 and an in-house calcite lab standard were measured repeatedly. The C and O isotope compositions are reported using the  $\delta$  notation relative to VPDB (Vienna Pee Dee Belemnite) and VSMOW (Vienna Standard Mean Ocean Water) standards, respectively. The  $\delta^{18}\text{O}$  values were converted from VPDB to VSMOW using Equation 2.21 ( $\delta^{18}\text{O}_{\text{VSMOW}} = 1.0309[\delta^{18}\text{O}_{\text{VPDB}}] + 30.91$ ) from Sharp (2007). Analytical uncertainties ( $2\sigma$ ) are  $\pm 0.2\text{‰}$  for  $\delta^{18}\text{O}$  and  $\delta^{13}\text{C}$ .

Given that the cores are composed mostly of aragonite and the laboratory standards are calcite, a correction factor was applied to all the  $\delta^{18}\text{O}$  values to account for the difference in the acid fractionations between these two minerals at 50°C (from Kim et al., 2007; 2015). Due to the fact that the sediments in the North Sound cores are not composed entirely of aragonite, the correction factor was modified to reflect the proportion of aragonite and calcite in the samples. Specifically, correction factors varied from  $-0.20$  in samples with nearly 50% calcite to  $-0.38\text{‰}$  in samples with 100% aragonite.

## 5. Results

### 5.1. Facies

Although MacKinnon (2000) and MacKinnon and Jones (2001) divided the sediments in North Sound into seven facies, only the (1) Bivalve, (2) Peat, (3) *Halimeda*, and (4) *Halimeda*-Benthic Foraminifera-Bivalve Facies are found in the cores used in this study.

- Bivalve Facies: This facies is formed of disarticulated and fragmented *Mytilopsis domigensis* shells (~90%) that are intermixed with fine-grained organic material (~10%).
- Peat Facies: This facies consists largely of dark brown to black organic-rich sediment that contains scattered wood fragments and rare bivalve shells.
- *Halimeda* Facies: This facies is dominated by *Halimeda* plates (~40-50%), micritized grains (~30%), scattered benthic foraminifera (~5-10%) and rare bivalve, gastropod, coral fragments, and composite grains (~10-25%).
- *Halimeda*-Benthic Foraminifera-Bivalve Facies: This facies consists of *Halimeda* plates (~30-65%), benthic foraminifera (~5-35%), bivalves (~5-10%), and rare composite grains, gastropods, red algae, coral fragments, and fragmentary echinoderms (<~5%).

### 5.2. Mineralogy

The North Sound cores are formed primarily of aragonite, with the samples from core B10 containing 53 to 100 wt% aragonite, core B15 from 71 to 97 wt% aragonite, and core B16 from 83 to 98 wt% aragonite (Table 4.2). These samples also contain calcite and trace amounts of quartz and gypsum. There is a marked decrease in the percentages of aragonite towards the top of core B10 (Fig. 4.4). For cores B15 (Fig. 4.5) and B16, apart from minor deviations there is only a slight decrease in the percentages of aragonite towards the top of cores. The foraminifera samples are composed primarily of

**Table 4.2.** Cores B10, B15, and B16 aragonite weight percentages and stable isotopic compositions.

Core	Distance (m)	Aragonite wt%	$\delta^{13}\text{C}_{\text{VPDB}}$ (‰)	$\delta^{18}\text{O}_{\text{VPDB}}$ (‰)	$\delta^{18}\text{O}_{\text{VSMOW}}$ (‰)
B10-A	2.2	96	-7.0	+0.2	31.1
B10-B	2.1	100	-7.9	-0.1	30.8
B10-C	2.0	97	-7.3	+0.3	31.2
B10-D	1.9	93	-7.3	0.0	31.0
B10-E	1.8	92	-7.6	+0.5	31.4
B10-F	1.7	97	-6.9	+1.3	32.2
B10-G	1.6	92	-6.8	+1.0	32.0
B10-H	1.5	92	-6.1	+1.6	32.6
B10-I	1.4	95	-6.4	+0.9	31.9
B10-J	1.3	86	-5.8	+0.6	31.6
B10-K	1.2	59	-2.1	-1.8	29.0
B10-L	1.1	65	0.0	-1.0	29.9
B10-M	1.0	70	+0.8	-1.0	29.9
B10-N	0.9	80	+1.8	-1.8	29.1
B10-O	0.8	84	+2.1	-1.2	29.6
B10-P	0.7	61	+2.5	+0.3	31.2
B10-Q	0.6	78	+3.0	+0.3	31.2
B10-R	0.5	53	+3.3	-1.1	29.8
B10-S	0.4	77	+2.9	-0.3	30.6
B10-T	0.3	53	+3.1	+1.0	32.0
B10-U	0.2	55	+2.8	-0.9	30.0
B15-A	2.35	97	-7.4	0.0	30.9

Core	Distance (m)	Aragonite wt%	$\delta^{13}\text{C}_{\text{VPDB}}$ (‰)	$\delta^{18}\text{O}_{\text{VPDB}}$ (‰)	$\delta^{18}\text{O}_{\text{VSMOW}}$ (‰)
B15-01	2.30	87	-7.6	-0.1	30.8
B15-B	2.25	77	-4.8	+0.1	31.0
B15-02	2.20	86	-1.0	-1.8	29.0
B15-C	2.15	95	-0.5	-1.2	29.7
B15-03	2.10	84	+0.9	-1.5	29.4
B15-D	2.05	73	+0.7	-1.2	29.7
B15-04	2.00	82	+1.1	-1.1	29.8
B15-05	1.95	82	+1.0	-1.0	29.9
B15-E	1.90	91	+1.2	-0.9	30.0
B15-06	1.85	91	+1.8	-1.2	29.7
B15-F	1.80	90	+1.9	-0.6	30.2
B15-07	1.75	88	+2.0	-1.3	29.6
B15-G	1.70	85	+2.5	-1.4	29.5
B15-08	1.65	87	+3.1	-1.5	29.3
B15-H	1.60	89	+3.3	-1.6	29.2
B15-09	1.55	89	+3.2	-1.3	29.5
B15-I	1.50	89	+3.1	-1.8	29.1
B15-10	1.45	88	+3.1	-1.5	29.3
B15-J	1.40	88	+2.9	-1.7	29.1
B15-11	1.35	89	+2.8	-1.5	29.4
B15-K	1.30	89	+3.5	-1.7	29.2
B15-12	1.25	89	+2.8	-1.2	29.6
B15-L	1.20	88	+3.4	-1.1	29.7
B15-13	1.15	89	+3.1	-1.4	29.4
B15-M	1.10	90	+3.3	-1.2	29.7

Core	Distance (m)	Aragonite wt%	$\delta^{13}\text{C}_{\text{VPDB}}$ (‰)	$\delta^{18}\text{O}_{\text{VPDB}}$ (‰)	$\delta^{18}\text{O}_{\text{VSMOW}}$ (‰)
B15-14	1.05	90	+2.9	-1.1	29.8
B15-N	1.00	89	+3.1	-1.2	29.6
B15-15	0.95	89	+3.2	-1.6	29.3
B15-O	0.90	88	+3.2	-1.2	29.7
B15-16	0.85	87	+3.2	-1.2	29.7
B15-P	0.80	85	+3.5	-1.2	29.6
B15-17	0.75	85	+3.4	-1.4	29.4
B15-Q	0.70	85	+3.3	-1.3	29.6
B15-18	0.65	82	+3.4	-1.4	29.5
B15-R	0.60	79	+3.3	-1.1	29.7
B15-19	0.55	79	+3.3	-1.3	29.5
B15-S	0.50	78	+3.3	-1.0	29.9
B15-20	0.45	77	+3.4	-1.1	29.7
B15-T	0.40	76	+3.3	-0.9	30.0
B15-21	0.35	75	+3.1	-0.7	30.2
B15-U	0.30	73	+2.6	-0.9	30.0
B15-22	0.25	77	+2.9	-1.2	29.7
B15-V	0.20	81	+3.2	-1.2	29.7
B15-23	0.15	77	+2.2	-0.6	30.3
B15-W	0.10	74	+3.0	-1.2	29.7
B16-A	1.6	97	+1.7	-0.9	29.6
B16-B	1.5	98	+1.5	-2.0	28.8
B16-C	1.4	96	+2.0	-2.2	28.6
B16-D	1.3	95	+1.6	-1.9	29.0

Core	Distance (m)	Aragonite wt%	$\delta^{13}\text{C}_{\text{VPDB}}$ (‰)	$\delta^{18}\text{O}_{\text{VPDB}}$ (‰)	$\delta^{18}\text{O}_{\text{VSMOW}}$ (‰)
B16-E	1.2	97	+1.5	-1.2	29.3
B16-F	1.1	98	+1.3	-1.9	28.9
B16-G	1.0	92	+0.8	-1.4	29.4
B16-H	0.9	95	+1.6	-1.4	29.4
B16-I	0.8	90	+2.0	-1.7	29.2
B16-J	0.7	93	+2.4	-0.6	30.2
B16-K	0.6	89	+2.7	-1.0	29.9
B16-L	0.5	89	+2.8	-1.4	29.5
B16-M	0.4	88	+2.6	-1.3	29.6
B16-N	0.3	83	+3.0	-1.7	29.2
B16-O	0.2	86	+2.8	-1.9	29.0
B16-P	0.1	88	+2.9	-1.2	29.7

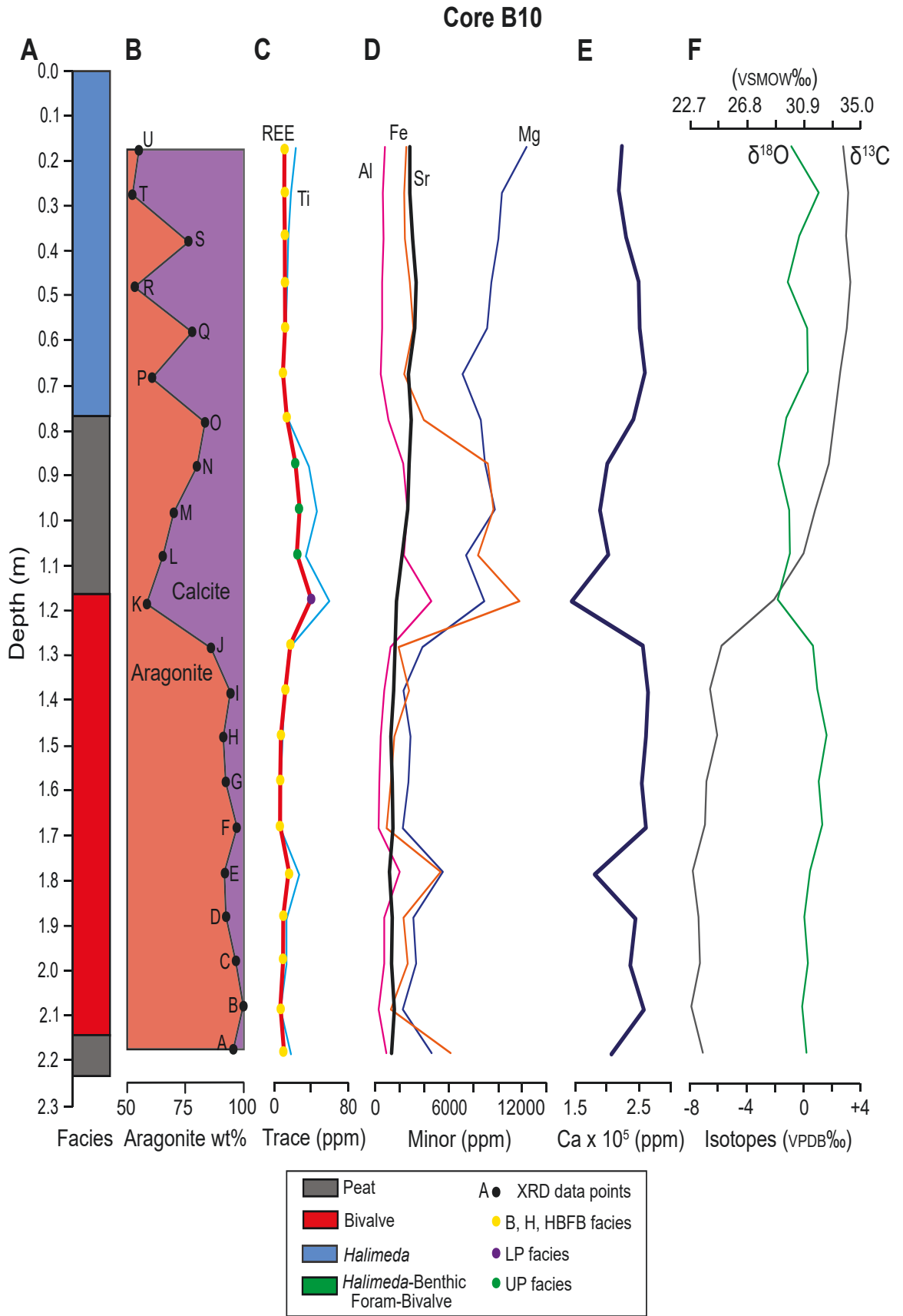




**Fig. 4.4.** Sedimentological and chemical components of core B10. (A) Facies distribution from MacKinnon, (2000) and MacKinnon and Jones, (2001). (B) Aragonite weight percentages, black circles indicate samples analyzed for XRD, letters correspond to sample ID, at 10 cm spacing. (C) Rare earth element group divisions, yellow circles indicate REE+Y for the sediments from the Bivalve, *Halimeda*, *Halimeda*- Benthic Foraminifera- Bivalve (B, H, HBFB) facies, the purple circles indicate REE for the sediment from the lower Mangrove peat (LM) facies, and the green indicate circles REE for the sediment from the upper Mangrove peat (UM) facies. (D) Elemental concentrations of selected minor elements. (E) Stable isotopic ( $\delta^{13}\text{C}$  and  $\delta^{18}\text{O}$ ) concentrations.

---

high Mg-calcite, with trace amounts of aragonite.

### 5.3. $^{14}\text{C}$ Dating

$^{14}\text{C}$  dating of samples from the sediment cores yielded radiocarbon ages from  $1584 \pm 40$  to  $5060 \pm 80$   $^{14}\text{C}$  years BP (Table 4.1). The associated calibrated “calendar” ages for these samples, as determined using the radiocarbon calibration software CALIB 7.10, range between ~4000 BCE to 500 CE (Table 4.1). The accuracy and precision of the age-depth model is influenced by the uncertainties associated with (1)  $^{14}\text{C}$  date analytical uncertainty ( $\pm 22$ -80  $^{14}\text{C}$  years), (2) choice of the  $^{14}\text{C}$  marine reservoir correction value ( $\Delta R$ ), which is poorly known for the Caribbean and unknown for Grand Cayman (Booker et al., 2019), (3) uncertainties in the calibration curve, and (4) assumptions in the BACON age-depth modeling software. The BACON age-depth modeling routine calculates 1 and  $2\sigma$  confidence intervals from millions of age model iterations (Fig. 4.6) and suggests a general  $\pm 200$  years uncertainty in the age model.

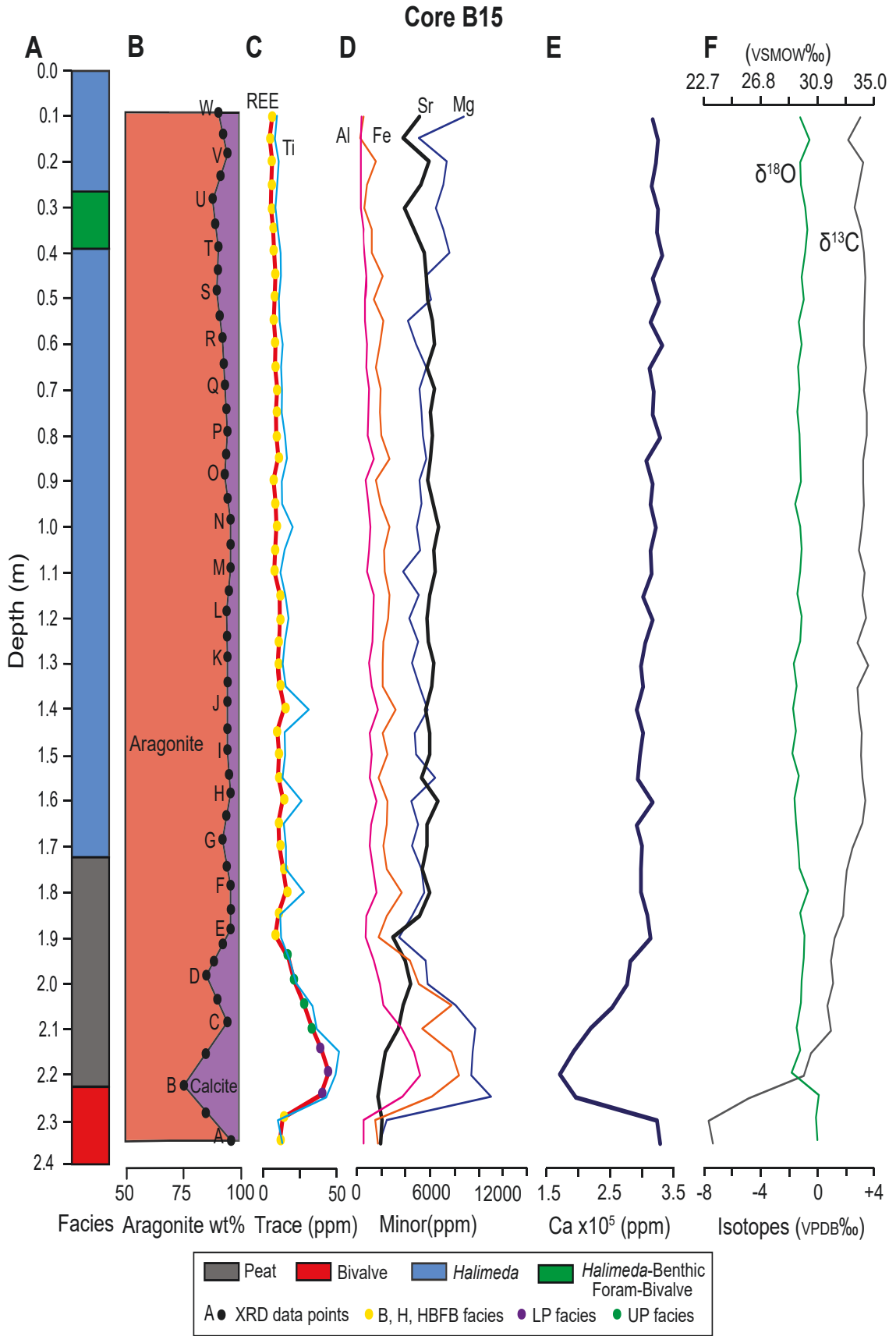


**Fig. 4.5.** Sedimentological and chemical components of core B15. (A) Facies distribution from MacKinnon, 2000 and MacKinnon and Jones, 2001. (B) Aragonite weight percentages, black circles indicate samples analyzed by XRD, letters correspond to sample ID, at 10 cm spacing. (C) Rare earth element group divisions, yellow circles indicate REE+Y for the sediments from the Bivalve, *Halimeda*, *Halimeda*- Benthic Foraminifera- Bivalve (B, H, HBFB) facies, the purple circles indicate REE for the sediment from the lower Mangrove peat (LM) facies, and the green circles indicate REE for the sediment from the upper Mangrove peat (UM) facies. (D) Elemental concentrations of selected minor element. (E) Stable isotopic ( $\delta^{13}\text{C}$  and  $\delta^{18}\text{O}$ ) concentrations.

---

#### 5.4. Elemental concentrations

Analyses of 67 bulk sediment samples from core B10 and B15 yielded concentrations of major (Ca), minor (Mg, Sr, Fe, Al), and trace (Ti, RRE+Y) elements (Tables 4.3, 4.4. Figs. 4.4, 4.5, 4.7) that are linked, to varying degrees, to the sedimentary facies.

- Bivalve Facies: The elemental concentrations in this facies (10 samples from core B10; 2 from core B15) range from 170221 to 322118 ppm Ca, 300 to 5516 ppm minor elements, 5.8 to 27.0 ppm Ti, and 0.1 to 5.6 ppm REE+Y (Tables 4.3, 4.4). Plotted against depth, the Ca, Mg, Sr, Fe, Al, Ti, and REE+Y concentrations display generally uniform curves apart from minor fluctuations (Figs. 4.4, 4.5). None of these samples have detectible concentrations of Tb, Tm, or Lu, 8 samples do not have detectable levels of Eu, Ho, or Yb, and 5 samples do not have detectable levels of Er (Fig. 4.7). These samples do not display Eu or Gd anomalies (Fig. 4.7).
- Peat Facies: Based on the elemental concentrations (4 samples from core B10; 11 from core B15), this facies is divided into the Lower Peat Facies and the Upper

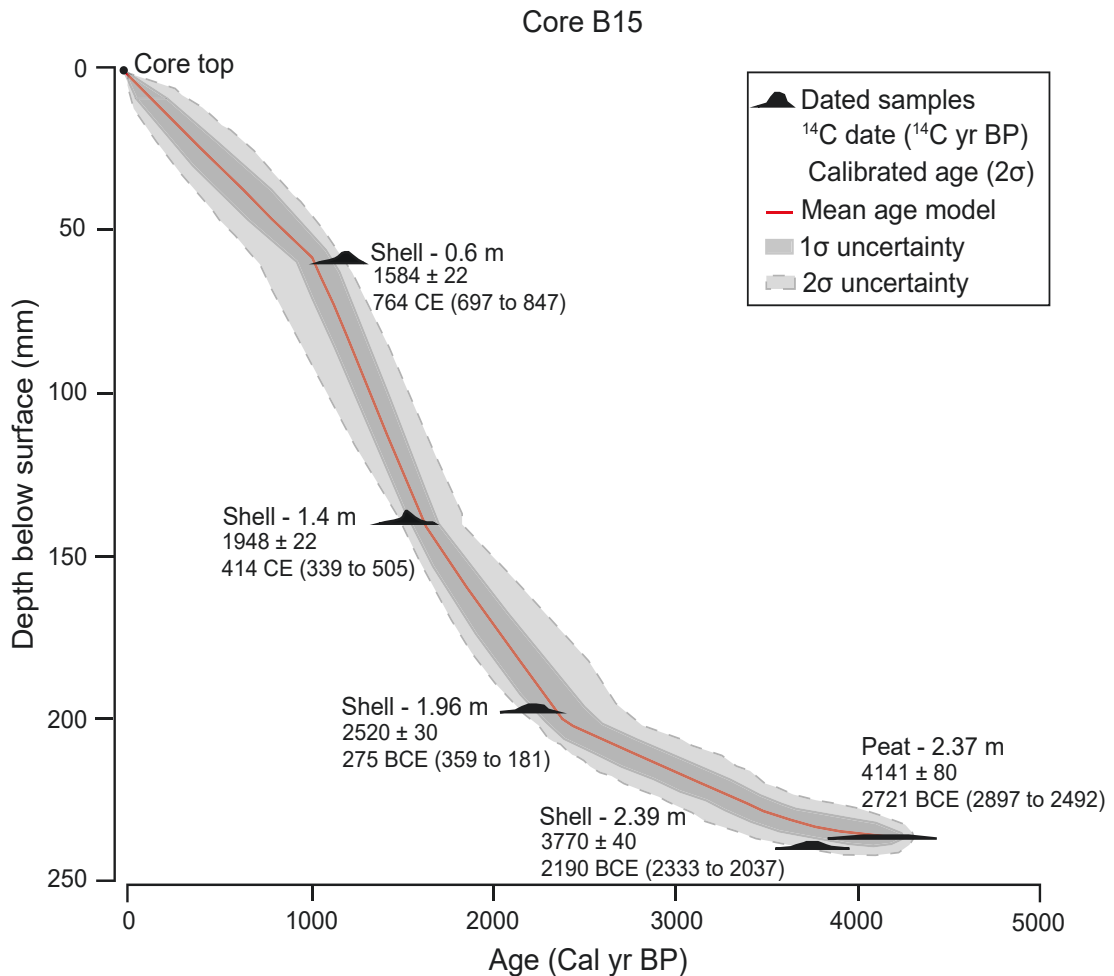


**Fig. 4.6.** Age-depth model for core B15, produced using BACON (Blaauw and Christen, 2011).  $^{14}\text{C}$  dates for individual samples calibrated with Calib 7.10 (Stuiver et al., 2020). All marine samples calibrated using the MARINE13 calibration curve (Reimer et al., 2013) with local reservoir correction of -28. Non-marine samples calibrated using the INTCAL13 calibration curve.

Peat Facies. The four Lower Peat Facies contains 21795 to 280481 ppm Ca, 460 to 11783 ppm minor elements, 57.9 to 70.9 ppm Ti, and 0.1 to 14.3 ppm REE+Y (Tables 4.3, 4.4). The Ca, Sr, Mg, Al, Fe, Ti, and REE+Y contents increase up core (Figs. 4.4, 4.5). The four samples in the Lower Peat Facies contain all the

**Table 4.3.** Major and minor element concentrations. All concentrations in ppm.

<b>Core</b>	<b>Ca</b>	<b>Mg</b>	<b>Sr</b>	<b>Fe</b>	<b>Al</b>	<b>K</b>
B10-A	217495	4543	1287	6123	944	1051
B10-B	261813	2227	1489	1232	310	631
B10-C	244016	3278	1268	2588	741	839
B10-D	250641	3038	1356	2264	774	605
B10-E	194814	5516	1106	5294	2013	1118
B10-F	264617	2209	1383	884	303	413
B10-G	259296	2667	1323	1196	351	441
B10-H	264654	2844	1188	1531	484	344
B10-I	267821	2263	1447	2714	741	332
B10-J	260860	3800	1549	1870	1272	480
B10-K	162378	8925	1658	11783	4604	1157
B10-L	213841	7406	2141	8352	2343	863
B10-M	201072	9766	2623	9641	2667	920
B10-N	212217	8980	2732	9193	2297	877
B10-O	247893	8602	2920	3959	1088	468
B10-P	263817	7136	2663	2291	479	334
B10-Q	256448	9102	3200	3055	576	535
B10-R	255421	9451	3276	2793	609	333
B10-S	238170	10040	3006	2371	698	513
B10-T	227947	10352	2802	2339	631	773
B10-U	231305	12381	2786	2497	840	917
B15-A	327395	1827	1939	1728	542	300
B15-01	322118	2471	2067	1503	555	485
B15-B	195281	11013	1733	6134	3743	1350

<b>Core</b>	<b>Ca</b>	<b>Mg</b>	<b>Sr</b>	<b>Fe</b>	<b>Al</b>	<b>K</b>
B15-02	170221	9402	2014	8415	5185	1234
B15-C	190940	9497	2343	7804	4698	1148
B15-03	217954	9758	3377	5374	3686	922
B15-D	252328	8123	3785	7757	2162	728
B15-04	275290	5818	4415	5071	1867	608
B15-05	280481	5637	3988	4349	1393	628
B15-E	312473	3465	2926	1780	710	460
B15-06	306937	4535	5153	2447	780	623
B15-F	296947	5538	5955	3672	1590	618
B15-07	298412	5312	5379	2471	1308	747
B15-G	298738	4523	5784	2184	1050	615
B15-08	291432	5033	5762	2452	1156	749
B15-H	316668	4453	6650	2513	1605	470
B15-09	293239	6420	5330	1778	1041	637
B15-I	296494	4885	5966	2509	1204	697
B15-10	300963	4774	5993	2084	1047	700
B15-J	290601	5801	5661	3199	1714	442
B15-11	300772	5165	6149	2099	1187	741
B15-K	297139	4501	6326	2112	1004	617
B15-12	303669	5036	5877	2181	1291	654
B15-L	315380	4307	5757	2552	1332	561
B15-13	300799	5073	6008	2659	1385	643
B15-M	315093	3818	6438	2271	801	510
B15-14	312723	5169	6311	2226	981	564
B15-N	321176	4928	6724	2662	1082	418

---

<b>Core</b>	<b>Ca</b>	<b>Mg</b>	<b>Sr</b>	<b>Fe</b>	<b>Al</b>	<b>K</b>
B15-15	312955	5291	6277	1923	924	532
B15-O	315793	5160	5801	1523	708	436
B15-16	305577	5675	6037	2657	1378	584
B15-P	328716	5448	6182	1984	872	405
B15-17	315488	5335	6017	1888	931	488
B15-Q	318513	5165	6388	1932	995	490
B15-18	310475	5698	5746	1537	773	532
B15-R	331670	4883	6359	1872	804	386
B15-19	312728	4189	6210	2153	622	473
B15-S	326986	6107	5805	1363	656	342
B15-20	316424	5668	5678	2094	769	418
B15-T	330551	7600	5527	1217	591	378
B15-21	323261	7096	4688	1212	553	381
B15-U	324428	6486	3885	613	335	394
B15-22	314592	7130	5236	829	320	468
B15-V	321834	7401	5902	1536	333	388
B15-23	325099	5111	3804	284	287	345
B15-W	315505	8799	5123	552	375	501

---

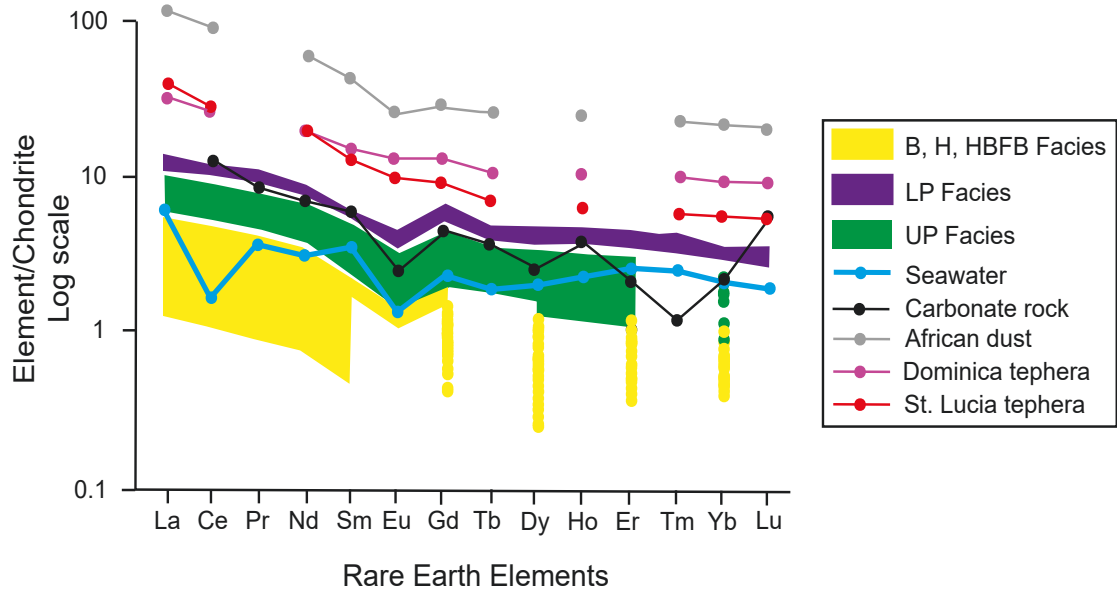


**Fig. 4.7.** Rare earth element concentrations from cores B10 and B15 normalized to Chondrite.

REE groups based on facies distributions. Seawater REE concentrations from Mysteriosa Bank at 10 m water depth multiplied by a factor of  $10^8$  from the data of Osborne et al. (2015), average carbonate rock REE concentrations (black) from Turekian and Wedepohl (1961), and African dust (grey), Dominica tephra (fuchsia), and St. Lucia tephra REE concentrations (red) from Muhs et al. (2007) and Muhs and Budahn (2009), for comparison.

rare earth elements. All of the  $REE_{(CN)}$  profiles exhibit negative Eu anomalies and displays positive Gd anomalies (Fig. 4.7). The Upper Peat Facies contains 1623 to 303669 ppm Ca, 615 to 5955 ppm minor elements, 11.4 to 48.5 ppm Ti, and 0.1 to 4.5 ppm REE+Y (Tables 4.3, 4.4). The Mg, Al, Fe, Ti, and REE+Y values decrease up core, whereas the Ca and Sr content increases up core (Figs. 4.4, 4.5). The  $REE_{(CN)}$  profiles exhibit negative Eu anomalies and positive Gd anomalies (Fig. 4.7). None of these samples have detectable concentrations of Tm and Lu, and one sample does not have detectable Tb.



**Table 4.4.** Trace element concentrations. All concentrations in ppm. <DL indicate elements that are below determination limits.

Core	Ti	La	Ce	Pr	Nd	Sm	Eu	Gd	Tb	Dy	Ho	Er	Tm	Yb	Lu	Y
B10-A	17.8	0.9	2.2	0.3	1.2	0.3	<DL	0.4	<DL	0.3	<DL	0.21	<DL	0.2	<DL	2.6
B10-B	6.2	0.5	1.3	0.2	0.7	0.1	<DL	0.2	<DL	0.1	<DL	<DL	<DL	<DL	<DL	0.9
B10-C	12.7	0.9	2.1	0.3	1.1	0.3	<DL	0.3	<DL	0.2	<DL	0.1	<DL	0.1	<DL	2.0
B10-D	12.6	0.9	2.2	0.3	1.1	0.2	<DL	0.3	<DL	0.2	<DL	0.2	<DL	0.1	<DL	2.1
B10-E	27.0	1.4	3.5	0.4	1.9	0.5	0.1	0.6	<DL	0.5	0.1	0.3	<DL	0.3	<DL	4.7
B10-F	5.8	0.5	1.2	0.1	0.6	0.1	<DL	0.1	<DL	0.1	<DL	<DL	<DL	<DL	<DL	0.8
B10-G	6.0	0.5	1.3	0.1	0.6	0.1	<DL	0.1	<DL	0.1	<DL	<DL	<DL	<DL	<DL	0.9
B10-H	8.6	0.6	1.5	0.2	0.7	0.2	<DL	0.1	<DL	0.1	<DL	<DL	<DL	<DL	<DL	1.2
B10-I	10.5	1.4	3.5	0.4	1.7	0.4	<DL	0.4	<DL	0.2	<DL	0.1	<DL	0.1	<DL	2.1
B10-J	15.8	2.1	5.6	0.6	2.5	0.5	0.1	0.6	<DL	0.4	<DL	0.2	<DL	0.2	<DL	3.3
B10-K	60.5	4.1	10.4	1.3	5.5	1.3	0.3	1.8	0.3	1.6	0.4	1.0	0.2	0.8	0.1	12.9
B10-L	34.2	2.6	6.6	0.8	3.6	0.8	0.2	0.9	0.1	0.8	0.2	0.5	<DL	0.4	<DL	6.6
B10-M	46.7	3.0	7.3	0.9	3.8	0.9	0.2	1.1	0.2	1.0	0.2	0.6	<DL	0.5	<DL	8.0
B10-N	37.7	2.5	6.0	0.7	3.2	0.7	0.2	0.9	0.1	0.8	0.2	0.5	<DL	0.4	<DL	6.4
B10-O	14.8	1.4	3.2	0.4	1.8	0.4	<DL	0.5	<DL	0.4	<DL	0.3	<DL	0.2	<DL	3.5
B10-P	7.84	0.8	1.9	0.2	1.1	0.2	<DL	0.3	<DL	0.2	<DL	0.2	<DL	0.1	<DL	2.1

Core	Ti	La	Ce	Pr	Nd	Sm	Eu	Gd	Tb	Dy	Ho	Er	Tm	Yb	Lu	Y
B10-Q	11.9	1.1	2.7	0.3	1.5	0.3	<DL	0.4	<DL	0.3	<DL	0.2	<DL	0.2	<DL	2.9
B10-R	13.6	1.1	2.5	0.3	1.4	0.3	<DL	0.4	<DL	0.3	<DL	0.2	<DL	0.2	<DL	3.0
B10-S	14.7	1.1	2.4	0.3	1.3	0.3	<DL	0.4	<DL	0.3	<DL	0.2	<DL	0.2	<DL	2.9
B10-T	17.6	1.0	2.2	0.3	1.3	0.3	<DL	0.4	<DL	0.3	<DL	0.2	<DL	0.2	<DL	2.8
B10-U	23.1	1.0	2.3	0.3	1.2	0.3	<DL	0.3	<DL	0.4	<DL	0.2	<DL	0.2	<DL	2.8
B15-A	13.5	1.6	4.0	0.5	1.9	0.4	<DL	0.4	<DL	0.2	<DL	0.1	<DL	<DL	<DL	1.8
B15-01	9.0	1.9	4.5	0.5	2.4	0.5	0.1	0.5	<DL	0.3	<DL	0.1	<DL	<DL	<DL	2.0
B15-B	57.9	4.0	9.9	1.3	5.6	1.3	0.3	1.6	0.2	1.4	0.3	0.9	0.1	0.7	0.1	11.8
B15-02	67.4	4.6	10.7	1.4	6.1	1.3	0.4	1.9	0.3	1.7	0.4	1.0	0.1	0.8	0.1	14.3
B15-C	70.9	4.4	10.1	1.3	5.7	1.3	0.3	1.7	0.2	1.5	0.3	0.9	0.1	0.7	0.1	11.4
B15-03	48.5	3.6	8.3	1.0	4.6	1.1	0.3	1.3	0.2	1.3	0.3	0.7	<DL	0.6	<DL	10.0
B15-D	44.1	3.2	7.5	1.0	4.3	0.9	0.2	1.1	0.2	1.0	0.2	0.6	<DL	0.4	<DL	7.1
B15-04	27.7	2.6	6.0	0.7	3.2	0.7	0.2	0.8	0.1	0.6	0.1	0.4	<DL	0.3	<DL	5.3
B15-05	21.1	2.2	5.2	0.6	2.7	0.5	0.1	0.6	<DL	0.5	0.1	0.3	<DL	0.2	<DL	3.9
B15-E	12.4	1.0	2.3	0.3	1.3	0.2	<DL	0.3	<DL	0.3	<DL	0.2	<DL	<DL	<DL	1.8
B15-06	11.4	1.4	3.3	0.4	1.6	0.4	<DL	0.3	<DL	0.3	<DL	0.2	<DL	0.1	<DL	2.2
B15-F	35.4	2.0	4.5	0.6	2.4	0.5	0.1	0.6	<DL	0.5	<DL	0.3	<DL	0.3	<DL	3.6

Core	Ti														Y	
	La	Ce	Pr	Nd	Sm	Eu	Gd	Tb	Dy	Ho	Er	Tm	Yb	Lu		
B15-07	17.2	1.6	3.7	0.5	2.0	0.5	0.1	0.5	<DL	0.4	<DL	0.2	<DL	0.2	<DL	3.2
B15-G	17.2	1.4	3.1	0.4	1.6	0.4	<DL	0.4	<DL	0.3	<DL	0.2	<DL	0.2	<DL	2.4
B15-08	15.0	1.3	2.9	0.4	1.5	0.3	<DL	0.4	<DL	0.3	<DL	0.2	<DL	0.1	<DL	2.5
B15-H	33.0	1.6	3.6	0.4	2.0	0.4	0.1	0.5	<DL	0.4	<DL	0.3	<DL	0.2	<DL	3.5
B15-09	13.7	1.2	2.7	0.3	1.4	0.3	<DL	0.4	<DL	0.3	<DL	0.2	<DL	0.2	<DL	2.7
B15-I	16.4	1.2	2.9	0.4	1.5	0.3	<DL	0.4	<DL	0.4	<DL	0.2	<DL	0.2	<DL	2.7
B15-10	15.9	1.2	2.7	0.3	1.4	0.3	<DL	0.3	<DL	0.3	<DL	0.2	<DL	0.2	<DL	2.2
B15-J	40.3	1.6	3.7	0.5	2.1	0.5	0.1	0.6	<DL	0.5	<DL	0.3	<DL	0.3	<DL	3.8
B15-11	17.1	1.4	3.1	0.4	1.6	0.4	<DL	0.4	<DL	0.3	<DL	0.2	<DL	0.2	<DL	2.7
B15-K	14.0	1.2	2.7	0.3	1.5	0.3	<DL	0.4	<DL	0.3	<DL	0.2	<DL	0.2	<DL	2.4
B15-12	16.2	1.2	2.9	0.4	1.5	0.4	<DL	0.4	<DL	0.3	<DL	0.2	<DL	0.2	<DL	2.9
B15-L	19.9	1.4	3.1	0.4	1.7	0.3	<DL	0.4	<DL	0.4	<DL	0.2	<DL	0.2	<DL	2.7
B15-13	16.7	1.3	3.0	0.4	1.6	0.4	<DL	0.4	<DL	0.3	<DL	0.2	<DL	0.2	<DL	2.8
B15-M	11.7	0.9	2.0	0.2	1.0	0.2	<DL	0.3	<DL	0.2	<DL	0.1	<DL	0.1	<DL	1.8
B15-14	15.9	1.0	2.1	0.3	1.1	0.3	<DL	0.3	<DL	0.3	<DL	0.2	<DL	0.1	<DL	2.1
B15-N	24.1	1.0	2.3	0.3	1.3	0.3	<DL	0.4	<DL	0.3	<DL	0.2	<DL	0.2	<DL	2.3
B15-15	13.3	1.0	2.2	0.3	1.2	0.3	<DL	0.3	<DL	0.2	<DL	0.2	<DL	0.1	<DL	2.0

Core	Ti	La	Ce	Pr	Nd	Sm	Eu	Gd	Tb	Dy	Ho	Er	Tm	Yb	Lu	Y
B15-O	13.0	0.8	1.9	0.2	0.9	0.2	<DL	0.2	<DL	0.2	<DL	0.1	<DL	<DL	<DL	1.7
B15-16	18.3	1.2	2.8	0.4	1.4	0.3	<DL	0.4	<DL	0.3	<DL	0.2	<DL	0.2	<DL	2.5
B15-P	16.3	1.0	2.3	0.3	1.3	0.2	<DL	0.3	<DL	0.3	<DL	0.2	<DL	0.1	<DL	2.2
B15-17	13.0	1.0	2.3	0.3	1.2	0.3	<DL	0.3	<DL	0.3	<DL	0.2	<DL	0.1	<DL	2.2
B15-Q	13.3	1.2	2.5	0.3	1.3	0.3	<DL	0.4	<DL	0.3	<DL	0.2	<DL	0.2	<DL	2.4
B15-18	12.3	1.0	2.1	0.3	1.1	0.3	<DL	0.3	<DL	0.2	<DL	0.2	<DL	0.1	<DL	1.9
B15-R	13.9	1.0	2.2	0.3	1.1	0.3	<DL	0.4	<DL	0.3	<DL	0.2	<DL	0.2	<DL	2.0
B15-19	10.8	0.9	2.0	0.3	1.1	0.2	<DL	0.3	<DL	0.2	<DL	0.1	<DL	<DL	<DL	1.6
B15-S	10.1	0.9	2.0	0.3	1.1	0.2	<DL	0.3	<DL	0.2	<DL	0.2	<DL	0.1	<DL	2.0
B15-20	12.2	1.0	2.2	0.3	1.1	0.3	<DL	0.3	<DL	0.3	<DL	0.2	<DL	0.1	<DL	1.9
B15-T	11.9	0.8	1.9	0.2	1.0	0.2	<DL	0.3	<DL	0.2	<DL	0.1	<DL	0.1	<DL	1.8
B15-21	9.1	0.7	1.7	0.2	0.9	0.2	<DL	0.2	<DL	0.2	<DL	0.1	<DL	<DL	<DL	1.7
B15-U	6.6	0.6	1.2	0.2	0.7	0.2	<DL	0.2	<DL	0.1	<DL	0.1	<DL	<DL	<DL	1.3
B15-22	8.4	0.6	1.4	0.2	0.7	0.2	<DL	0.2	<DL	0.2	<DL	<DL	<DL	<DL	<DL	1.3
B15-V	9.9	0.7	1.5	0.2	0.8	0.2	<DL	0.2	<DL	0.2	<DL	0.1	<DL	<DL	<DL	1.5
B15-23	6.1	0.5	1.1	0.1	0.6	0.1	<DL	0.1	<DL	0.1	<DL	<DL	<DL	<DL	<DL	1.0
B15-W	8.1	0.7	1.5	0.2	0.9	0.2	<DL	0.2	<DL	0.2	<DL	0.1	<DL	<DL	<DL	1.6

- *Halimeda* Facies: This facies (7 samples from core B10, 31 from core B15) contains 190940 to 330551 ppm Ca, 287 to 12381 ppm minor elements, 6.1 to 40.3 ppm Ti, and 0.1 to 3.8 ppm REE+Y (Tables 4.3, 4.4). The Ca content initially increases before decreasing up core, whereas the Mg content increases up core, and the other elements (Sr, Fe, Al, Ti, REE+Y) remain relatively constant throughout the core (Figs. 4.4, 4.5). None of these samples contain detectible concentrations of Tb, Ho, Tm, or Lu, most (36) of the samples do not have detectible Eu or Yb, and two samples do not contain detectible Er (Fig. 4.7). The two samples that contain Eu display a negative Eu anomaly and a positive Gd anomaly (Fig. 4.7).
- *Halimeda*-Benthic Foraminifera-Bivalve Facies: This facies (2 samples from core B15) contains 326486 to 331670 ppm Ca, 381 to 7096 ppm minor elements, 8.4 to 10.0 ppm Ti, and 0.1 to 1.7 ppm REE+Y (Tables 4.3, 4.4). All element concentrations decrease slightly up core (Figs. 4.4, 4.5). None of the samples contain detectible concentrations of Eu, Tb, Ho, Er, Tm, Yb, or Lu (Fig. 4.7). These samples do not display Eu or Gd anomalies (Fig. 4.7).

The three surface sediment samples yielded 325396 to 352356 ppm Ca, 4063 to 6548 ppm Sr, 5284 to 7120 ppm Mg, Sr/Ca ratios of 5.7 to 8.6 mmol/mol, and Mg/Ca ratios of 2.5 to 3.3 mmol/mol (Table 4.5). The foraminifera samples yielded 309494 to 352356 ppm Ca, 1415 to 2640 ppm Sr, 11121 to 28078 ppm Mg, Sr/Ca ratios of 2.3 to 4.6 mmol/mol, and Mg/Ca ratios of 10.2 to 14.6 mmol/mol (Table 4.5). The surface sediment samples contain consistently higher Mg and Ca, and lower Sr concentrations than the foraminifera samples (Fig. 4.8A-C).

#### 5.4. Seawater analyses

The two seawater samples (surface and 4 m water depth) from the center of North Sound yielded similar elemental concentrations (Table 4.6). The B, Mg, K, Br, Sr, Mo,

**Table 4.5.** Surface sediment and foraminifera isotopic and elemental concentrations.

Sample	$\delta^{13}\text{C}_{\text{VPDB}}$ (‰)	$\delta^{18}\text{O}_{\text{VPDB}}$ (‰)	$\delta^{18}\text{O}_{\text{VPSMOW}}$ (‰)	Mg (ppm)	Sr (ppm)	Ca (ppm)	Sr/Ca (mmol/mol)	Mg/Ca (mmol/mol)
F77 Bulk	+1.4	-0.4	30.5	5967	4063	325396	5.7	30.2
<i>A. angulatus</i>								
16 mm	+2.7	-2.1	28.7	25908	1686	309494	2.5	138.0
93.3 Bulk	+5.2	+0.9	31.8	5284	6548	347698	8.6	25.1
<i>A. gibbosa</i>								
6 mm	+4.3	-2.2	28.6	23304	3422	339355	3.5	113.2
16 mm	+4.6	-3.2	27.6	20478	3348	330996	4.6	102.0
26 mm	+4.6	-2.6	28.2	28012	2542	336205	4.6	137.4
93.5 Bulk	+3.0	-1.4	29.5	7120	5175	352356	6.7	33.3
<i>A. angulatus</i>								
16 mm	+3.5	+0.6	31.5	27704	1678	312835	2.3	146.0
26 mm	+3.3	-0.6	30.3	28078	1603	316345	2.5	146.4

and U concentrations are, within error, the same for the two samples. In contrast, the S and Ca concentrations differ by 18 and 60 ppm, respectively, between samples, with these elements being elevated in the 4 m water sample. The Na concentrations in the surface sample is 500 ppm higher than that of the 4 m water depth sample. Li, Al, Si, P, Ti, Cr, Mn, Fe, Co, Ni, Cu, Zn, As, Cd, Ba, and Pb were all below DL.

These samples yielded  $\delta^{18}\text{O}_{\text{water}}$  values of +0.30 and +0.37‰ for the surface and 4 m depth samples, respectively. Additionally, two water samples that were collected from the northwest corner of North Sound in 1987, yielded  $\delta^{18}\text{O}_{\text{water}}$  values of +1.20 and +1.21‰ (Ng, 1990).

### 5.5. Stable isotopes

The carbonate sediments in core B10 yielded  $\delta^{13}\text{C}_{\text{VPDB}}$  values from -7.9 to +3.3‰ and  $\delta^{18}\text{O}_{\text{VSMOW}}$  values from 29.1 to 32.6‰ (Table 4.2. Fig. 4.4). Sediments in core B15 yielded  $\delta^{13}\text{C}$  values from -7.6 to +3.5‰ and  $\delta^{18}\text{O}$  values from 29.1 to 31.0‰ (Table 4.2. Fig. 4.5). Core B16 yielded  $\delta^{13}\text{C}$  values from +0.5 to +3.0‰ and  $\delta^{18}\text{O}$  values from 28.6 to 30.3‰ (Table 4.2). The stable isotopes display minor fluctuations throughout the cores, with the exception of the Peat Facies, which are different (~1 to 2‰ for  $\delta^{18}\text{O}$  and ~2 to 7‰ for  $\delta^{13}\text{C}$ ) from the other facies. The three surface sediment samples yielded  $\delta^{13}\text{C}$  values from +1.4 to +5.2‰ and  $\delta^{18}\text{O}$  values from 29.5 to 31.8‰. The six foraminifera samples yielded  $\delta^{13}\text{C}$  values from +2.7 to +4.6‰ and  $\delta^{18}\text{O}$  values from 27.6 to 31.5‰. There appears to be no pattern in the isotopic compositions between the surface sediment samples and the foraminifera samples (Fig. 4.8D, E).

## 6. Interpretations

### 6.1. Facies

MacKinnon (2000) and MacKinnon and Jones (2001) divided the sediment succession in North Sound into fresh to brackish water coastal ponds and marine facies

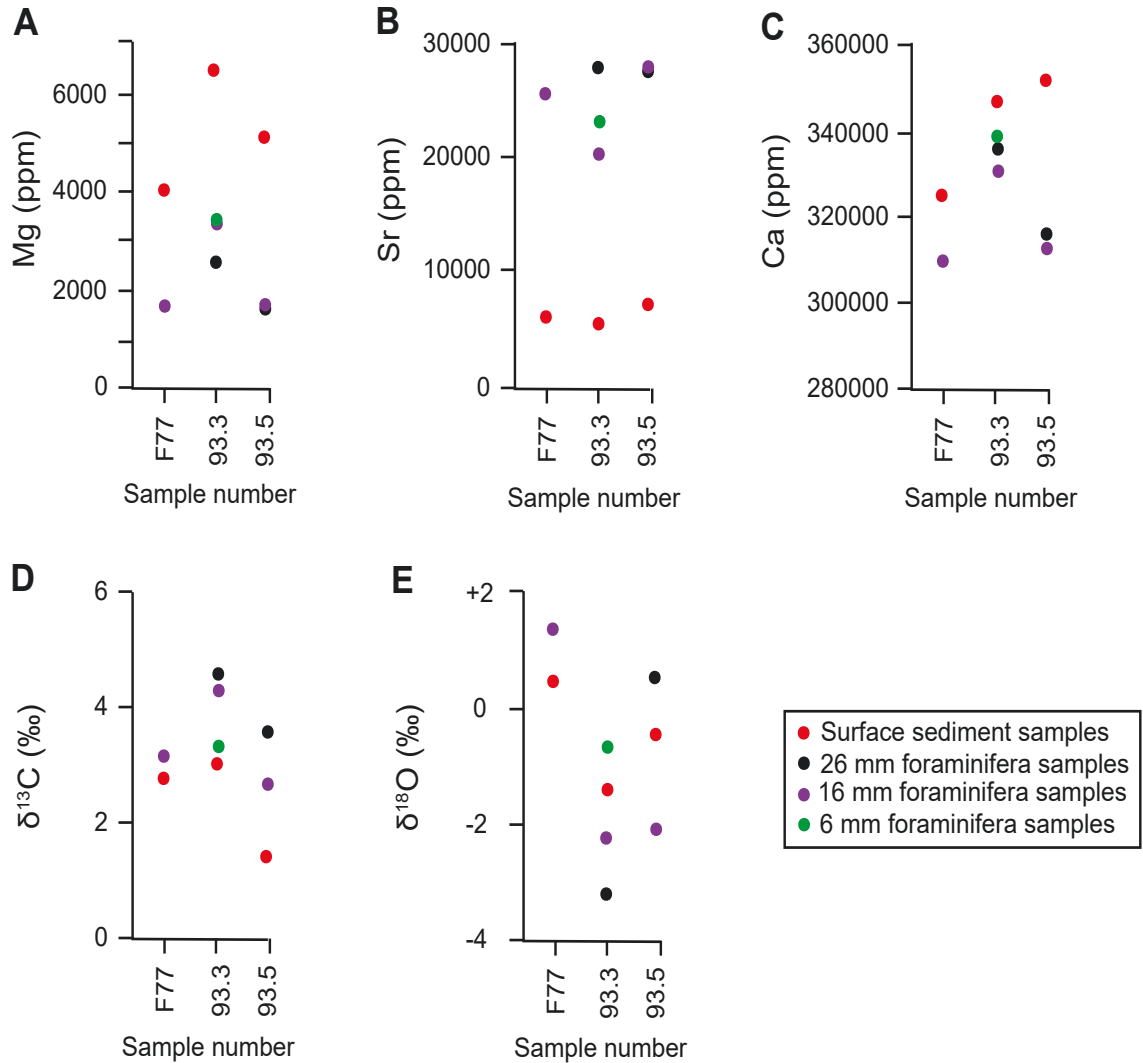


**Fig. 4.8.** Elemental (A) Mg, (B) Sr, (C) Ca and isotopic (D)  $\delta^{13}\text{C}$  and (E)  $\delta^{18}\text{O}$  concentrations of the surface sediment and foraminifera samples from North Sound.

that were related to sea level rise and creation of North Sound. For the three cores used in this study the Bivalve and Peat Facies formed in the fresh to brackish water coastal ponds, whereas the *Halimeda* and *Halimeda*-Benthic Foraminifera-Bivalve Facies developed in marine environments (Fig. 4.3). The Peat Facies overlies bedrock throughout most of the lagoon, with the exception of core B15 where there is a thin layer of the Bivalve Facies between the bedrock and the Peat Facies. The *Halimeda* Facies,



**Table 4.6.** Elemental concentration of North Sound seawater. All concentrations in mg/L. <DL indicates elements below determination limits.

<b>Samples</b>	<b>B</b>	<b>Na</b>	<b>Mg</b>	<b>S</b>	<b>K</b>	<b>Ca</b>	<b>Br</b>	<b>Sr</b>	<b>Mo</b>	<b>U</b>
Surface (1m)	3.5	11300	1326	1070	42.6	417	65.3	7.6	<DL	0.01
Depth (4m)	3.5	10800	1281	1130	42.6	435	63.4	7.6	0.01	0.01

with interlayers of the *Halimeda*-Benthic Foraminifera-Bivalve Facies, commonly overlies the Peat Facies. The division between the Peat and *Halimeda* Facies marks the transition from the coastal pond to marine environment, which based on  $^{14}\text{C}$  dating in core B15, is congruent with sea level rise  $\sim 3000$  years ago (Fig. 4.3).

## 6.2. Element distributions

Given that most sediments in North Sound accumulated in shallow marine waters, their  $\text{REE}_{(\text{CN})}$  profiles are compared to a seawater  $\text{REE}_{(\text{CN})}$  profile (Fig. 4.7) for a sample from 10 m below sea level on the Mysteriosa Bank, which is located  $\sim 400$  km west of Grand Cayman on the Cayman Ridge (Osborne et al., 2015, their Supplementary Data Table 2, station 164-1). Although the  $\text{REE}_{(\text{CN})}$  profile for the Peat Facies is similar to the  $\text{REE}_{(\text{CN})}$  seawater profile from Mysteriosa Bank (Fig. 4.7) the negative Ce anomaly evident in most marine carbonates (Taylor and McLennan, 1985) is not present in the Peat Facies samples. For the marine facies in North Sound, only the LREE segment of the  $\text{REE}_{(\text{CN})}$  profile is similar to the seawater profile from Mysteriosa Bank, apart from the negative Ce anomaly seen in the seawater profile that is lacking in the marine facies. Differences between the North Sound  $\text{REE}_{(\text{CN})}$  profiles and the seawater profile from Mysteriosa Bank may be related to the organic matter found in those facies given that organic particles in seawater can preferentially absorb elements, including REE, onto their surfaces (Byrne and Kim, 1990; Sholkovitz et al., 1994; Byrne and Sholkovitz, 1996; Alibo and Nozaki, 1999; Kuss et al., 2001; Osborne et al., 2015). It has been shown, experimentally, that LREE are more readily incorporated into carbonate minerals as metal oxides (iron oxyhydroxide) or onto the surfaces of marine particulates (Fe(III) complexes with organic ligands), when compared to HREE that form strong complexes with carbonate anions and remain in seawater (Cantrell and Byrne, 1987; Koeppenkastrop et al., 1991; Nozaki et al., 1997; Moraetis and Mouslopoulou, 2013). The preferential incorporation of Mg, Sr, Fe, Al, Ti, and REE+Y in the Peat Facies of North Sound was

probably related to the organic matter in that facies (Figs. 4.4, 4.5, 4.7). The elevated concentrations of Fe in the Peat Facies are critical to understanding the increased concentrations of the other elements. In seawater, 99% of the dissolved Fe(III) forms complexes with organic ligands, like those found in the leaf litter of mangrove trees (Hinokidani and Nakanishi, 2019), which facilitate the sorption of elements (especially LREE) onto these surfaces, and may be responsible for the different elemental patterns in the North Sound sediments relative to the seawater from Mysteriosa Bank.

Comparison of the North Sound sediment  $REE_{(CN)}$  profiles against the average carbonate rock  $REE_{(CN)}$  values of Turekian and Wedepohl (1961) shows that the  $REE_{(CN)}$  profiles for the sediment are more consistent with the carbonate rock profile than the seawater profile from the Mysteriosa Bank (Fig. 4.7). Both the North Sound sediment and the carbonate rock  $REE_{(CN)}$  profiles are LREE dominated, display similar shapes and elemental concentrations, and have a positive Ce anomaly. Additional fractionation between the LREE and HREE that may have taken place at the sediment-water interface in the restricted lagoon caused the relatively flat  $REE_{(CN)}$  pattern and the positive Ce anomaly that characterizes the North Sound sediments (cf., Lerche and Nozaki, 1998; Alibo and Nozaki, 1999). This supports the notion that the differences between the  $REE_{(CN)}$  profiles from the North Sound sediment and the seawater profile from Mysteriosa Bank may reflect differences in the behaviour of the REE in open ocean water as opposed to a restricted lagoon.

The four possible sources for the REE+Y found in Caribbean carbonate sediments are (1) weathering of insoluble material from the underlying carbonate bedrock, (2) fluvial transport of detrital materials from surrounding highlands, (3) wind-blown volcanic ash, and/or (4) wind-blown aerosols from distant regions (Muhs et al., 1987; 2007; Muhs and Budahn, 2009). For the North Sound sediments, derivation from the underlying bedrock, which may be part of the Pedro Castle Formation based on drill cores from the west coast of North Sound (Wignall, 1995), is unlikely due to the paucity

of clays and other insoluble residues in those limestones. A detrital origin is impossible due to the lack of rivers and siliciclastic material on Grand Cayman (Jones, 2019). Therefore, the most probably origin of these REE+Y is from fine grained wind-blown aerosols and/or volcanic ash that came from other localities distant from the Cayman Islands (cf., Jones, 2019).

Comparison of the North Sound sediment  $REE_{(CN)}$  profiles with those derived from African dust and Dominica/St. Lucia tephra from Muhs et al. (2007), suggests that most of the REE probably came from the Sahara Desert, as the North Sound sediment  $REE_{(CN)}$  profiles are more consistent in terms of shape to the African dust  $REE_{(CN)}$  profiles than the tephra profile (Fig. 4.7). Conversely, the  $Eu_{(CN)}/Eu^*$  vs  $La_{(CN)}/Yb_{(CN)}$  plots (Fig. 4.9A) indicate that the REE in North Sound may have been derived from Sahara Desert dust and/or Dominica/St. Lucia volcanic ash. In contrast, a plot of  $Eu_{(CN)}/Eu^*$  vs  $Gd_{(CN)}/Yb_{(CN)}$  (Fig. 4.9B; cf., Muhs et al., 2007; Muhs and Budahn, 2009) indicates that the REE originated from the Saharan Desert dust.

### 6.3. Geothermometers for calculating SST

Past seawater temperatures have commonly been calculated from the Sr/Ca ratios, Mg/Ca ratios, or  $\delta^{18}O$  values of carbonate material (e.g., Shackleton, 1974; Black et al., 2007; Cleroux et al., 2008; Abahazi, 2009) using geothermometers derived from (1) abiogenic carbonates, (2) biogenic calcite, and/or (3) biogenic aragonite. Given that at least 132 different equations (Supplementary Tables 4.1-4.3) have been developed for this purpose, their viability was first tested by comparing the calculated temperatures ( $T_{cal}$ ) derived from the surface sediment and the foraminifera samples from North Sound that have accumulated over recent years for which measured water temperatures of 22° to 32°C (1991 to 2008) are known.  $T_{cal}$  derived from those modern samples are considered viable if they are within the 22° to 32°C temperature range. Those equations are then used to derive  $T_{cal}$  for the sediments in core B15, the  $T_{cal}$  are deemed suitable if they are

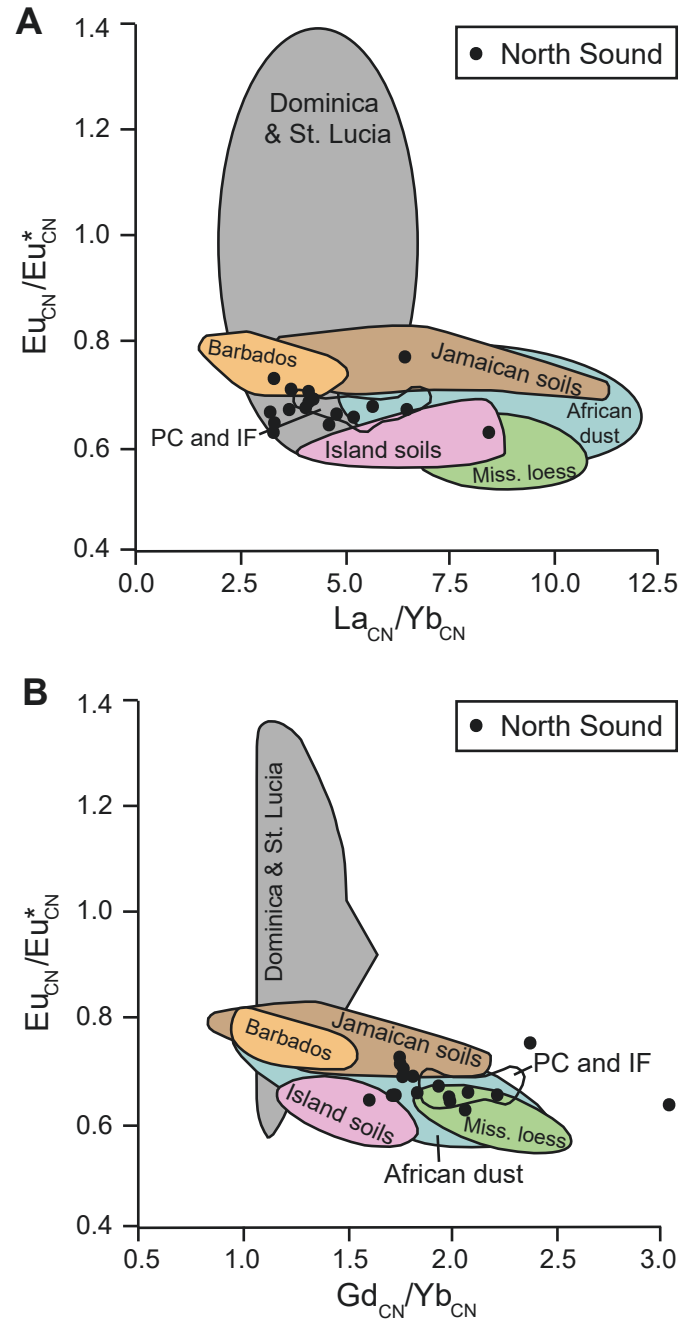


**Fig. 4.9.** Comparison of North Sound core B10 and B15 sediment samples (black circles) with tephhera from Dominica and St. Lucia, Barbados soils, various island (Florida Key and Bahamas) soils, Mississippi loess, and African dust (Muhs et al., 2007, their Fig. 19a), Jamaican soils (Muhs and Budahn, 2009, their Fig. 15), and Pedro Castle (PC) and Ironshore Formation (IF) terra rossa from Little Cayman (Jones, 2019, their Fig. 19), based on (A)  $Eu_{CN}/Eu^*_{CN}$  versus  $La_{CN}/Yb_{CN}$  and (B)  $Eu_{CN}/Eu^*_{CN}$  versus  $Gd_{CN}/Yb_{CN}$ .

within  $\pm 5^\circ\text{C}$  of the  $22^\circ$  to  $32^\circ\text{C}$  temperature range to account for temperature variability over the last  $\sim 6000$  years.

### 6.3.1. Sr/Ca equations

Application of the 9 published Sr/Ca geothermometers (Supplementary Table 4.1) to the Sr/Ca ratios derived from the surface sediment and foraminifera samples produced  $T_{\text{cal}}$  of  $+127^\circ$  to  $+441^\circ\text{C}$  and  $+31^\circ$  to  $+206^\circ\text{C}$ , respectively (Fig. 4.10). These temperatures are significantly higher than the measured range of  $22^\circ$  to  $32^\circ\text{C}$  for North Sound. In some cases, it has been shown that the Sr/Ca ratios from foraminifera are independent of temperature (Delaney et al., 1985) and controlled primarily by past seawater Sr/Ca ratios and/or  $\text{CO}_3^{2-}$  concentrations in the seawater (Graham et al., 1982; Stoll et al., 1999; Rosenthal et al., 2006), calcification rates, and/or changes in pH and salinity (Elderfield et al., 2000; Mortyn et al., 2005; Cleroux et al., 2008). Herein, these equations are not used because of these issues.

### 6.3.2. Mg/Ca equations

The 82 published Mg/Ca geothermometers (Supplementary Table 4.2) yielded  $T_{\text{cal}}$  of  $-130^\circ$  to  $+77^\circ\text{C}$  and  $-85^\circ$  to  $+465^\circ\text{C}$  from the surface sediment and foraminifera samples, respectively (Fig. 4.10). Although most equations produced  $T_{\text{cal}}$  values that are significantly outside the temperature range for North Sound, the equations developed by Rosenthal and Lohman (2002), Anand et al. (2003), Mekik et al. (2007), Bryan and Marchitto (2008), Cleroux et al. (2008), and two equations from Elderfield et al. (2006), yielded  $T_{\text{cal}}$  from  $23^\circ$  to  $33^\circ\text{C}$  when applied to the surface sediment and foraminifera samples. Use of these seven Mg/Ca equations for the sediments in core B15 yielded  $T_{\text{cal}}$  from  $-24^\circ$  to  $+112^\circ\text{C}$  (Figs. 4.11, 4.12A). The  $T_{\text{cal}}$  that are outside the  $17^\circ$  to  $37^\circ\text{C}$  range may be due to the mixture of carbonate components in the sediment samples (c.f., Rosenthal and Linsley, 2006; Wejnert et al., 2013; Evans et al., 2015; Reghellin et

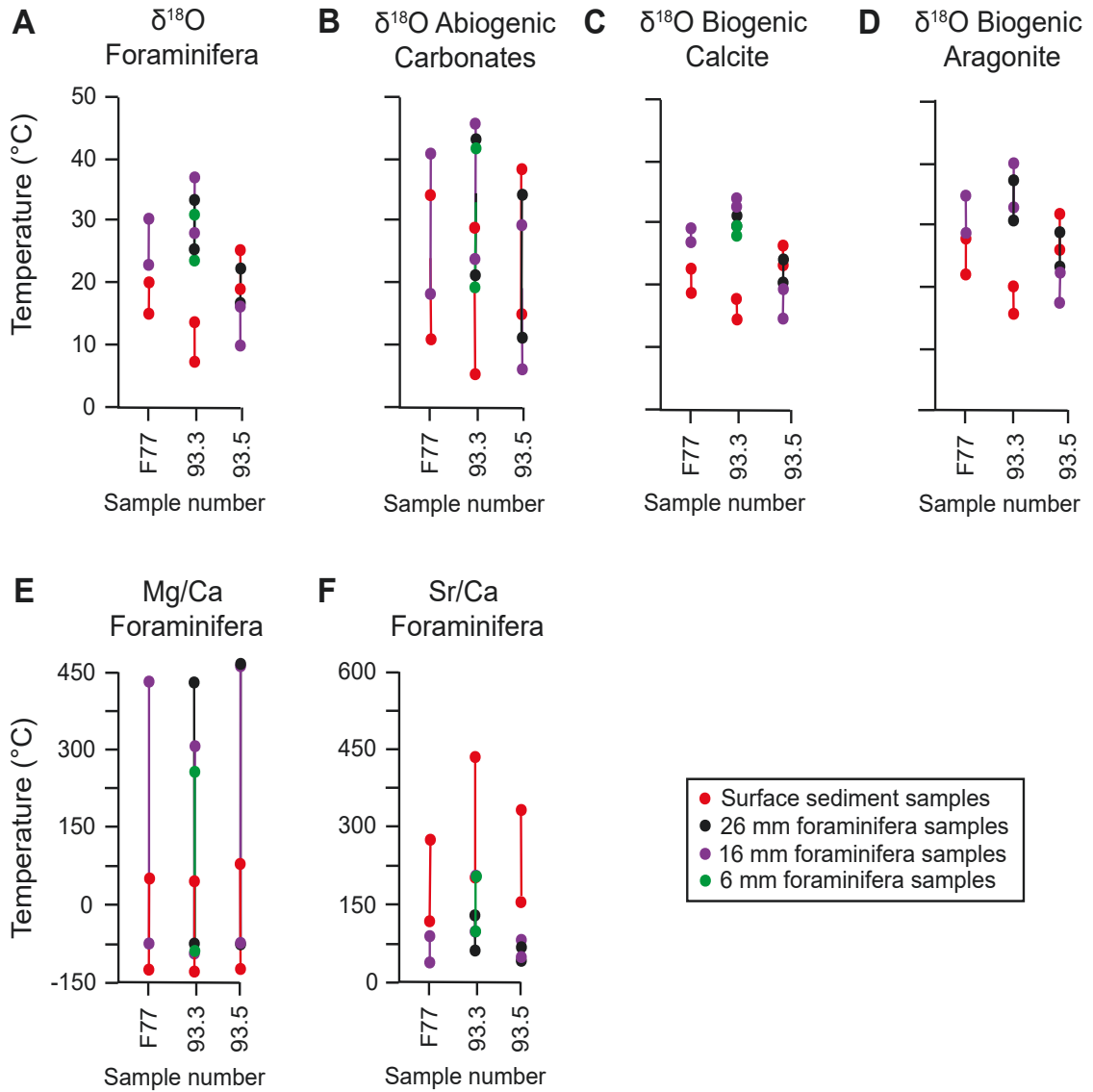


**Fig. 4.10.** Comparison of the calculated temperatures from the surface sediment and foraminifera samples using (A)  $\delta^{18}\text{O}$ -geothermometers developed specifically from foraminifera, (B)  $\delta^{18}\text{O}$ -geothermometers developed from abiogenic carbonates, (C)  $\delta^{18}\text{O}$ -geothermometers developed from biogenic calcite, (D)  $\delta^{18}\text{O}$ -geothermometers developed from biogenic aragonite, (E) Mg/Ca-geothermometers developed from foraminifera, and (F) Sr/Ca-geothermometers developed from foraminifera.

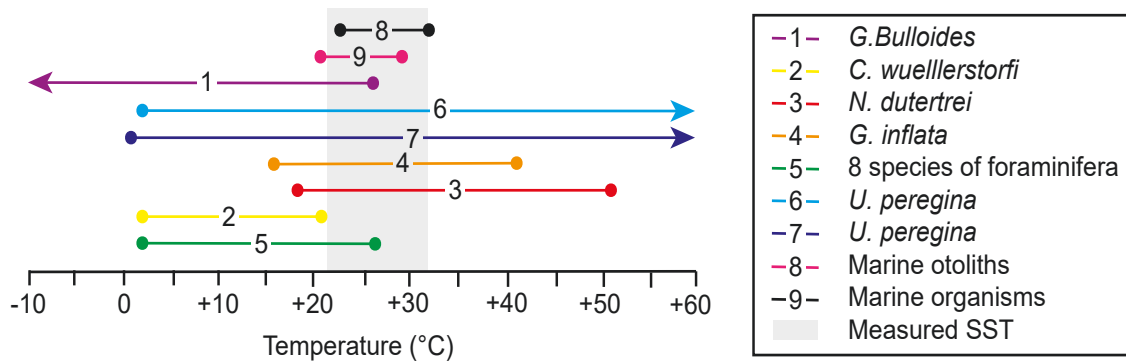


**Fig. 4.11.** Comparison of the calculated temperatures from sediment core B15 using the 7 ‘best’ Mg/Ca and 2 ‘best’  $\delta^{18}\text{O}$ -geothermometers based on the foraminifera and surface sediment samples to the measured temperatures from North Sound. Grey shading shows the current instrument measured water temperature for North Sound. 1- Cleroux et al. (2008); 2- Elderfield et al. (2006); 3- Mekik et al. (2007); 4- Anand et al. (2003); 5- Rosenthal and Lohman (2002); Bryan and Marchitto (2008); 7- Elderfield et al. (2006); 8- Thorrold et al. (1997); 9- Hudson and Anderson (1989).

al., 2015) and/or effects of the seawater  $\text{CO}_3^{2-}$  concentration on the Mg/Ca ratios (Bryan and Marchitto, 2008). Given these uncertainties, these equations are not considered further for deriving temperatures from the sediment cores.

### 6.3.3. $\delta^{18}\text{O}$ equations

The  $\delta^{18}\text{O}$  of carbonate components is a function of the ambient seawater temperature at the time of calcification and the  $\delta^{18}\text{O}_{\text{water}}$  value (Craig, 1965). Herein, a  $\delta^{18}\text{O}_{\text{water}}$  value of +0.4‰ is used in applying these O-isotope geothermometers because that value came from a water sample that was collected from the center of North Sound at a depth of 4 m, where the water is well-mixed. It was chosen in preference to the  $\delta^{18}\text{O}_{\text{water}}$  value of +1.2‰ that Ng (1990) reported from the NW corner of North Sound



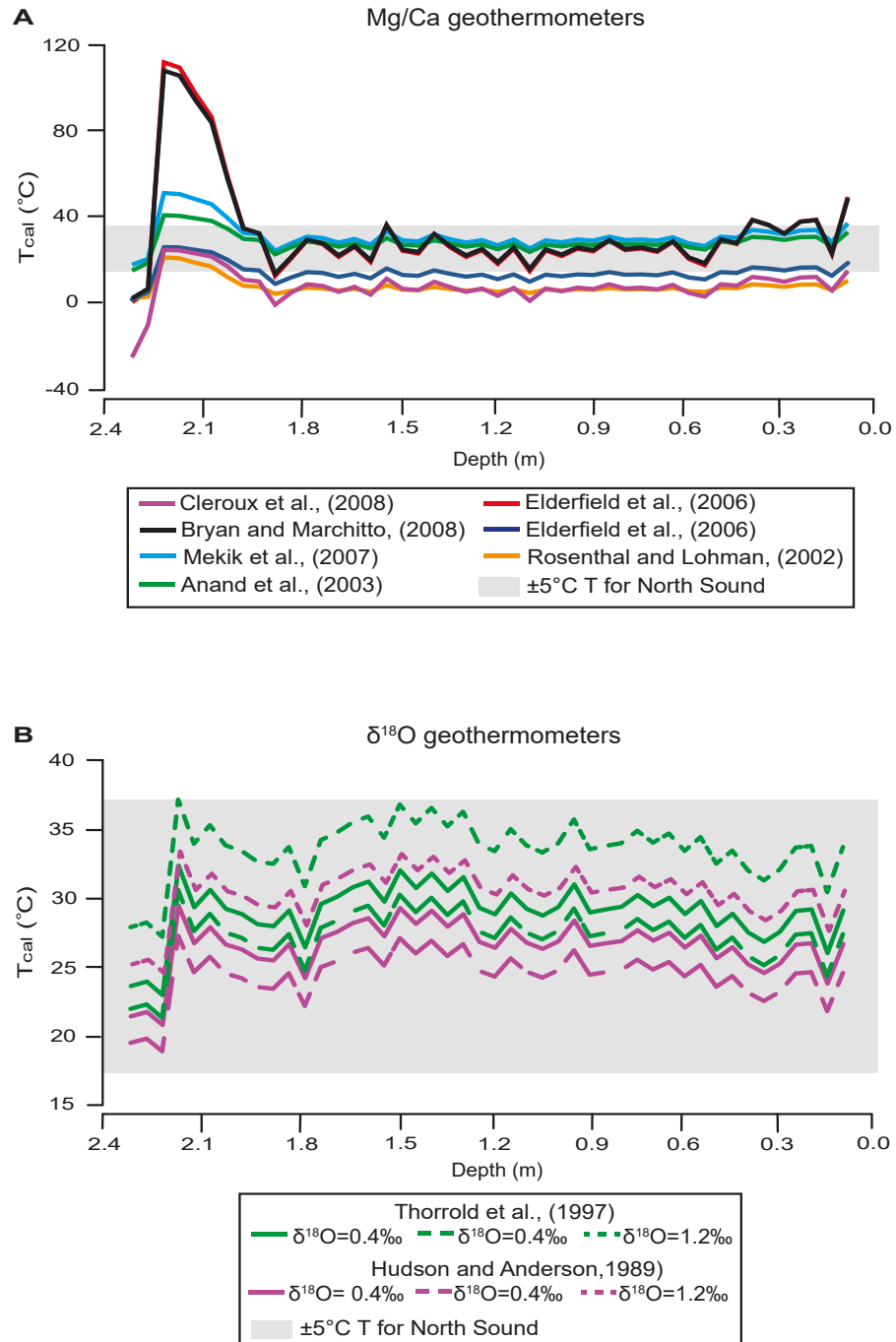


**Fig. 4.12.** Comparison of the calculated temperatures from sediment core B15 using (A) the 7 ‘best’ Mg/Ca geothermometers as determined by the modern samples and (B) the 2 ‘best’  $\delta^{18}\text{O}$ -geothermometers based on the modern samples to the measured temperatures from North Sound using different  $\delta^{18}\text{O}_{\text{water}}$  values. Note the shapes of the different lines are maintained regardless of the choice of  $\delta^{18}\text{O}_{\text{water}}$  value.  $\pm 5^{\circ}\text{C}$  of the 22° to 32°C temperature range for North Sound shown in grey.

because that sample came from a sheltered, shallow water environment that is prone to elevated water temperatures and enhanced evaporation. Use of the 41 published  $\delta^{18}\text{O}$ -geothermometers (Supplementary Table 4.3) with the  $\delta^{18}\text{O}$  values derived from the surface sediment and foraminifera samples produced  $T_{\text{cal}}$  of +5° to +36°C and +6° to +45°C, respectively (Fig. 4.10). Although many of these  $T_{\text{cal}}$  values are within the measured range of water temperatures from North Sound, most (39) equations produced some  $T_{\text{cal}}$  values that are outside of this range. The equations proposed by Hudson and Anderson (1989), based on various species of foraminifera, gastropods, and scaphopods, and Thorrold et al. (1997), based on aragonitic marine otoliths, yielded  $T_{\text{cal}}$  from 19° to 30°C, values that are consistent with the modern range of water temperatures in North Sound. Use of these two thermometer equations for the sediments in core B15 yielded  $T_{\text{cal}}$  from +21° to +32°C (Fig. 4.11), the geothermometer of Hudson and Anderson (1989;  $T = 19.7 - (4.34 * (\delta^{18}\text{O}_{\text{carbonate}} - \delta^{18}\text{O}_{\text{water}}))$ ) is used in preference to that of Thorrold et al. (1997) because it was derived from organisms that are akin to those found in the North Sound sediment.

## 7. Discussion

### 7.1. Climate change over the last ~6000 years

Facies changes, facies components, and/or their geochemical (Ca, Mg, Sr, Al, Fe, Ti, REE+Y,  $\delta^{18}\text{O}$ ,  $\delta^{13}\text{C}$ ) composition have the potential of providing critical information about past environmental and climatic variability that underpinned their evolution. Sediments in North Sound on Grand Cayman, for example, reflect climate changes over the past ~6000 years that included the transgression that began ~3000 years ago when the environmental setting changed from coastal ponds and mangrove swamps to a marine lagoon (Fig. 4.3). The inundation of North Sound with seawater was associated with global sea level rise (cf., Fleming et al., 1998; Milne et al., 2005) and increased SST at that time. Subsequent sedimentation in North Sound remained relatively constant as

various types of carbonate sediments continued to accumulate.

The concentrations of minor elements (Mg, Sr, Fe, Al) and trace elements (Ti, REE+Y) in carbonate sediments have been related to periods of atmospheric moisture variability (Prospero and Lamb, 2003; Doherty et al., 2012; Prospero and Mayol-Bracero, 2013). The concentrations of Fe and Ti in carbonate sediments in the Caribbean have, for example, been used to indicate changes in precipitation and the position of the Intertropical Convergence Zone (ITCZ). Low metal concentrations have been associated with reduced rainfall and a southward displacement of the ITCZ, whereas high metal concentrations point to enhanced rainfall and a northward displacement of the ITCZ (Haug et al., 2001; Black et al., 2004; 2007). Additionally, increasing REE+Y levels in the atmosphere of the Caribbean region have been linked to dry atmospheric conditions, enhanced trade wind speeds, southward displacement of the ITCZ, and increased African dust transportation (Nyberg et al., 2001; Prospero and Lamb, 2003; Mahowald et al., 2006; Muhs et al., 2007; Doherty et al., 2012; Prospero and Mayol-Bracero, 2013). Conversely, decreasing REE+Y concentrations have been linked to periods characterized by wet atmospheric conditions, diminished trade wind speeds, northward displacement of the ITCZ, and reduced African dust transportation. Today in the Caribbean, large plumes of African dust typically move through the region during the dry season (Prospero et al., 1970; Doherty et al., 2012; Donegan, 2019).

The possibility that the distribution of the minor and trace elements in carbonate sediments may reflect climate conditions must be treated with caution because depositional processes may modify those signals. The elevated minor (710 to 11783 ppm; Mg, Sr, Al, Fe) and trace element concentrations (8 to 71 ppm; Ti, REE) in the Peat Facies (Figs. 4.4, 4.5), for example, may reflect (1) the preferential absorption of the Fe and REE+Y by the organic matter in that facies (cf., Cantrell and Byrne, 1987; Byrne and Kim, 1990; Byrne and Sholkovitz, 1996; Osborne et al., 2015), (2) climate change that led to increased precipitation over Grand Cayman, and/or (3) climate change that

increased the frequency of dust storms that originated from the Sahara Desert. Relative to the Peat Facies, the carbonate facies with their lower organic matter content also have lower concentrations of the minor (303 to 3959 ppm) and trace elements (4 to 40 ppm). Thus, changes in the trends in the Fe, Ti, and  $\Sigma\text{REE}+\text{Y}$  depth profiles may reflect regional atmospheric moisture variability (Mahowald et al., 2006; Doherty et al., 2012). Increasing  $\Sigma\text{REE}+\text{Y}$  values and low Fe and Ti concentrations in the depth profiles, may correlate to enhanced mobilization and export of African dust to the Caribbean region during periods of reduced atmospheric moisture (cf., Haug et al., 2001; Nyberg et al., 2001). In contrast, decreasing  $\Sigma\text{REE}+\text{Y}$  values and elevated Fe and Ti concentrations in the depth profiles, may be related to periods of increased atmospheric moisture and reduced influxes of African dust (cf., Haug et al., 2001; Nyberg et al., 2001). Given this, changes in the relative concentrations of Fe and Ti, and the shape of the  $\Sigma\text{REE}+\text{Y}$  depth profiles may provide evidence for dry and wet conditions over the last ~6000 years in North Sound (Fig. 4.13).

The stable isotope depth profiles in the North Sound sediments are characterized by fluctuations in the  $\delta^{13}\text{C}$  and  $\delta^{18}\text{O}$  values. The Peat Facies is characterized by elevated  $\delta^{13}\text{C}$  values (2 to 7‰) and reduced  $\delta^{18}\text{O}$  values (1 to 2‰) when compared to the Bivalve Facies. The high  $\delta^{13}\text{C}$  values are probably related to the enhanced proportion of organic carbon that accumulated when the mangroves were thriving (cf., Gonneea et al., 2004; Bouillon et al., 2008). The  $\delta^{18}\text{O}$  values, however, are not affected by organic matter accumulation or facies changes as shown by the small differences in  $\delta^{18}\text{O}$  values (< 5‰) between all the facies. Thus, the differences in the  $\delta^{18}\text{O}$  values may reflect variability in the SST (Oppo et al., 1998; Richey, 2007; Cronin et al., 2010) that affected North Sound during the deposition of the carbonate components. Both temperature and salinity influence the  $\delta^{18}\text{O}$  values of carbonate material (Black et al., 2004; 2007; Lane et al., 2009; 2011), therefore, it is important to stress that discussions involving the temperatures fluctuations derived from these  $\delta^{18}\text{O}$  values are established in relation

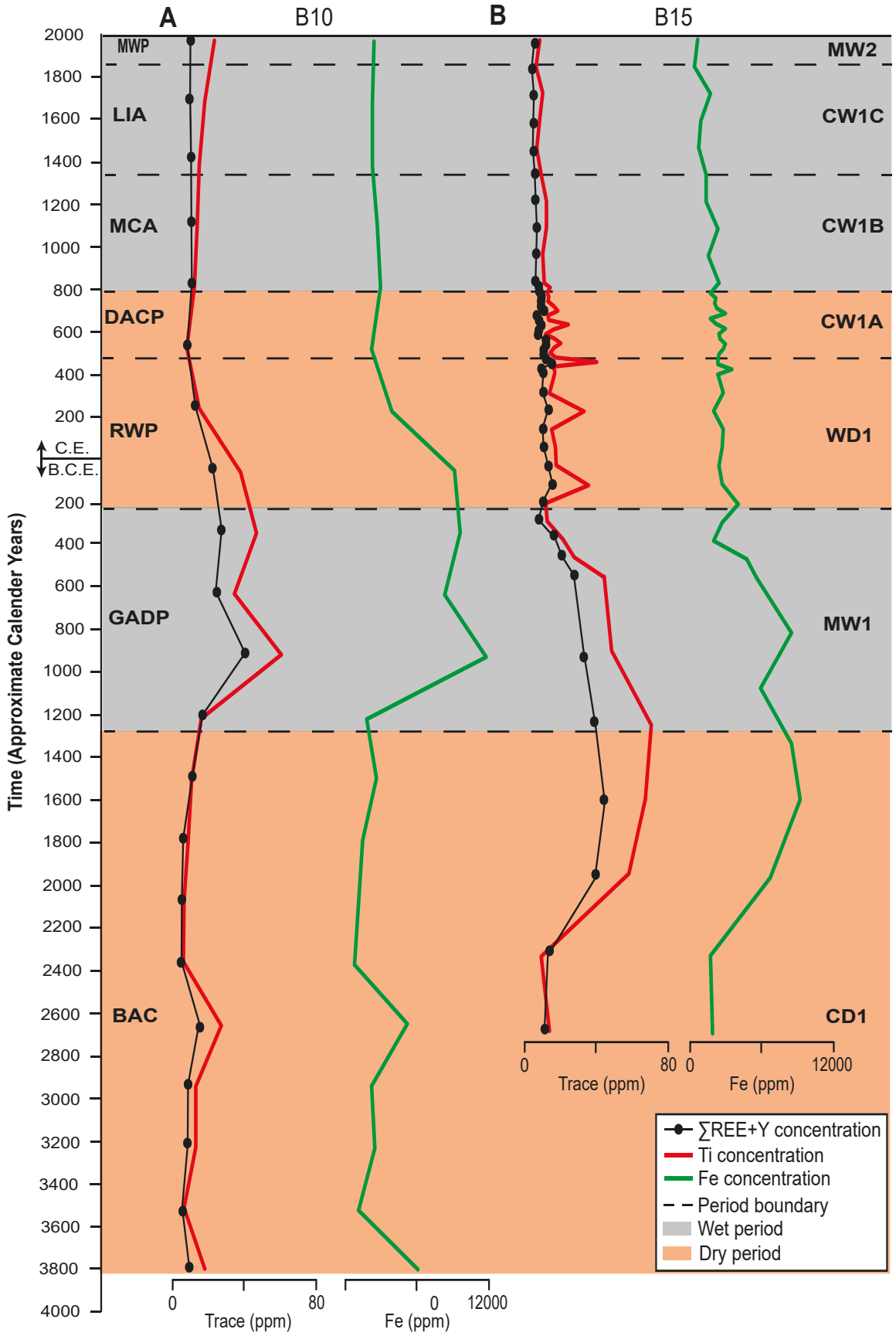


**Fig. 4.13.** Comparison between the trace element ( $\Sigma\text{REE}+\text{Y}$  and Ti) and Fe concentration depth profiles of core (A) B10 and (B) B15. Orange shaded regions represent dry periods and grey shaded regions represents wet periods. Dashed lines separate periods. Time scale in calendar years ( $\pm 200$  years) based on the conversion of  $^{14}\text{C}$  dates. BAC- Bronze Age Collapse, GADP- Greek Age Dark Period, RWP- Roman Warm Period, DACP- Dark Ages Cool Period, MCA- Medieval Climate Anomaly, LIA- Little Ice Age, MWP- Modern Warm Period.

---

to the current average water temperature ( $28^\circ\text{C}$ ) for North Sound and reflect relative temperature fluctuations as opposed to absolute values (cf., Black et al., 2007). As such, the  $\delta^{18}\text{O}$  values can be correlated to warm, mild, and cool periods that have affected North Sound over the last  $\sim 6000$  years (Fig. 4.14).

Herein, periods are considered dry if the  $\Sigma\text{REE}+\text{Y}$  depth profiles display increasing values and reduced Fe and Ti concentrations relative to the preceding data points and wet if opposite trends are evident. Additionally, warm periods are defined by O-isotope temperatures that are elevated relative to the modern average SST of North Sound ( $28^\circ\text{C}$ ; Fig. 4.2), mild periods are defined by O-isotope temperatures consistent with the present-day average seawater temperature in North Sound, allowing for seasonal fluctuations of  $\pm 1^\circ\text{C}$ , and cool periods are defined by the O-isotope temperatures lower than the current average water temperature for North Sound (cf., Booker et al., 2019).

## 7.2. Atmospheric moisture and SST in North Sound

Based on the trends displayed in the Fe, Ti, and  $\Sigma\text{REE}+\text{Y}$  depth profiles and changes in the  $\delta^{18}\text{O}$  derived temperatures relative to the modern average SST value, the record from the North Sound cores indicates that North Sound has experienced the following changes in climatic conditions over the last  $\sim 6000$  years (Figs. 4.13, 4.14).

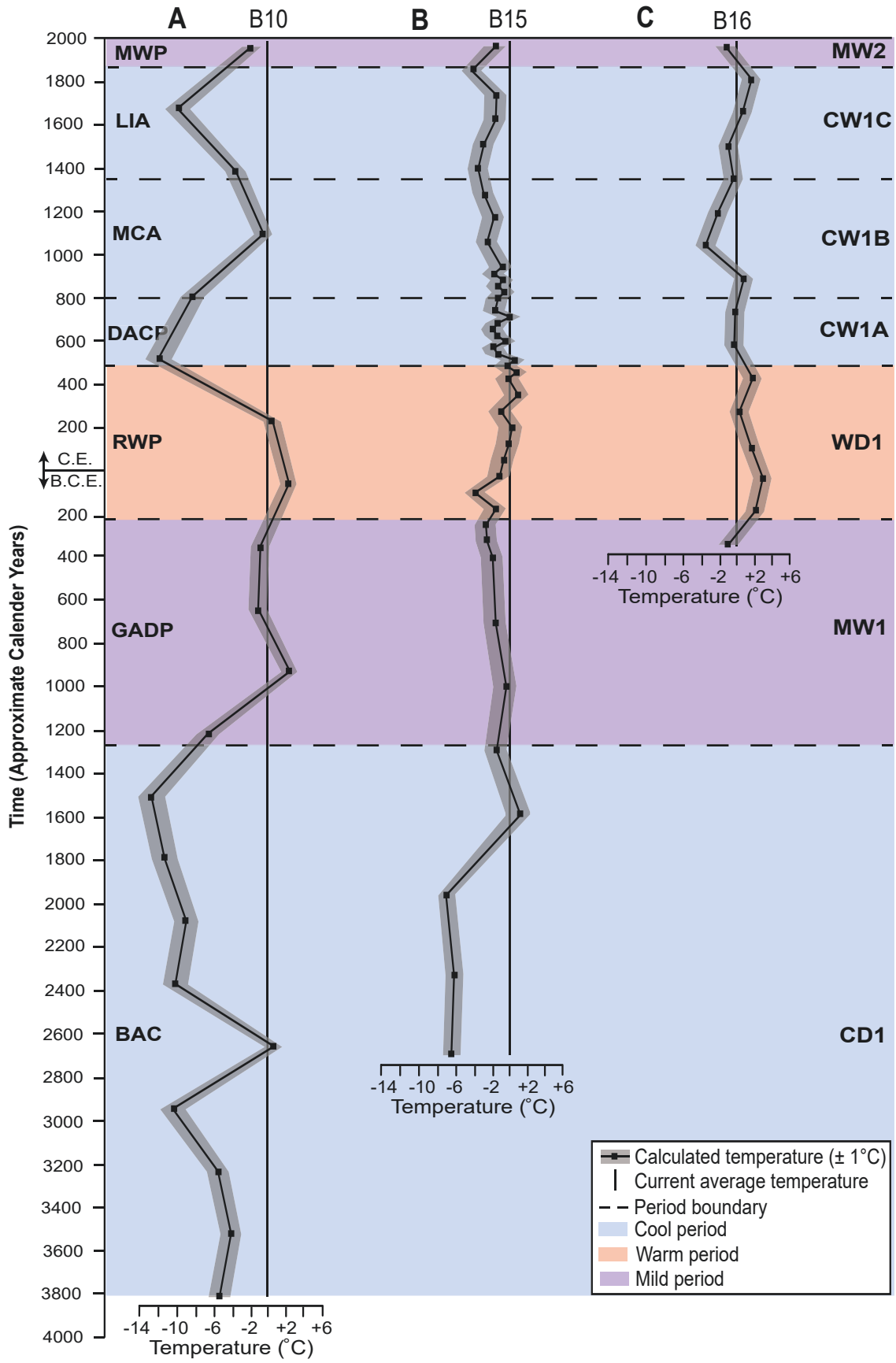


**Fig. 4.14.** Calculated temperature profiles for North Sound cores (A) B10, (B) B15, and (C) B16. Calculated temperatures determined using the  $\delta^{18}\text{O}$ -geothermometer of Hudson and Anderson (1989) with a  $\delta^{18}\text{O}_{\text{water}}$  value of +0.4‰. Grey bars indicate  $\pm 1^\circ\text{C}$  error in SST. Red shaded regions represent warm periods, purple shaded regions represent mild periods, blue shaded regions represent cool periods. Dashed lines separate periods. Time scale in calendar years ( $\pm 200$  years) based on the conversion of  $^{14}\text{C}$  dates. BAC- Bronze Age Collapse, GADP- Greek Age Dark Period, RWP- Roman Warm Period, DACP- Dark Ages Cool Period, MCA- Medieval Climate Anomaly, LIA- Little Ice Age, MWP- Modern Warm Period.

---

- **Cool-Dry period 1** (CD1: ~3850 to 1280 BCE): Deposition of the Bivalve Facies during this period was associated with  $\Sigma\text{REE}+\text{Y}$  depth profiles with two trends of generally increasing values through time, the first between ~3850 to 2400 BCE when the  $\Sigma\text{REE}+\text{Y}$  increased from 4 to 14 ppm and the second between ~2400 to 1280 BCE when the  $\Sigma\text{REE}+\text{Y}$  increased from 4 to 45 ppm (Fig. 4.13). These increases may be indicative of dry conditions. The Fe and Ti concentrations also record two trends, with generally low concentrations (884 to 6123 ppm and 6 to 27 ppm, respectively) between ~3850 to 2100 BCE and elevated concentrations (1196 to 8415 ppm and 6 to 67 ppm, respectively) between ~2100 to 1280 BCE (Fig. 4.13). This suggests initially dry conditions that transitioned to a wetter climate. The O-isotope temperatures, which are up to  $13^\circ\text{C}$  cooler than the current average water temperature for North Sound, decreased between ~3850 to 1600 BCE. Between ~1600 to 1280 BCE the temperatures increased by up to  $2^\circ\text{C}$  relative to the previous temperature (Fig. 4.14).
- **Mild-Wet period 1** (MW1: ~1280 to 200 BCE): The Bivalve and Lower and



Upper Peat Facies, which accumulated during this period, have  $\Sigma\text{REE+Y}$  depth profiles characterized by decreasing values (42 to 8 ppm) and elevated Fe and Ti concentrations (1780 to 11783 ppm and 11 to 71 ppm, respectively; Fig. 4.13). This may indicate that wet conditions were the norm. These sediments developed when there was an initial increase in  $T_{\text{cal}}$  of  $\sim 6^{\circ}\text{C}$  relative to CD1. The temperatures then remained  $\sim 28^{\circ}\text{C}$ , values that are consistent with the current water temperatures in North Sound, for the next  $\sim 800$  years (Fig. 4.14).

- **Warm-Dry period 1 (WD1:  $\sim 200$  BCE to 480 CE):** The Upper Peat and *Halimeda* Facies accumulated during this period was characterized by  $\Sigma\text{REE+Y}$  values that decreased from 23 to 9 ppm and low Fe and Ti concentrations (1178 to 9193 ppm and 14 to 40 ppm, respectively; Fig. 4.13), which may indicate a dry but variable climate. The temperatures during this period are up to  $3^{\circ}\text{C}$  warmer than the current average water temperature for North Sound (Fig. 4.14). Although temperatures during this period were higher than the current average water temperature for North Sound, there was an overall decrease in  $T_{\text{cal}}$ .
- **Cool-Wet period 1 (CW1:  $\sim 480$  to 1850 CE):** The deposition of the *Halimeda* and *Halimeda*-Benthic Foraminifera-Bivalve Facies was accompanied by  $\Sigma\text{REE+Y}$  values that decreased from 11 to 4 ppm, Fe and Ti concentrations that increased from 284 to 3055 ppm and 6 to 18 ppm, respectively, and temperatures that fluctuated by up to  $12^{\circ}\text{C}$  relative to the current average water temperature for North Sound (Figs. 4.13, 4.14). This period is divided into: (1) CW1A:  $\sim 480$  to 800 CE that was characterized by low  $T_{\text{cal}}$  ( $-12^{\circ}$  to  $+1^{\circ}\text{C}$  relative to the current average water temperature for North Sound),  $\Sigma\text{REE+Y}$  that increased from 7 to 10 ppm, and Fe and Ti that increased from 1523 to 3199 ppm and 12 to 24 ppm, respectively, which collectively may indicate dry conditions, (2) CW1B:  $\sim 800$  to 1350 CE that was characterized by an overall increasing trend in  $T_{\text{cal}}$  that was up to  $1^{\circ}\text{C}$  warmer than the current average water temperature in North Sound,

$\Sigma$ REE+Y values that decreased slightly from 9 to 7 ppm, and Fe and Ti that increased from 1217 to 3055 ppm and 10 to 14 ppm, respectively, which may indicate wet conditions, and (3) CW1C: ~1350 to 1850 CE that was characterized by generally low temperatures as much as 10°C cooler than the current average water temperature for North Sound, apart from a 100-year period at ~1600 CE with increasing  $T_{\text{cal}}$  of up to 2°C relative to the current average water temperature for North Sound,  $\Sigma$ REE+Y that slightly decreased from 9 to 4 ppm, and Fe and Ti that increased from 284 to 2339 ppm and 6 to 18 ppm, respectively, which may indicate wet conditions.

- **Mild-Wet period 2** (MW2: ~1850 to 1980 CE): Deposition of the *Halimeda* Facies with  $\Sigma$ REE+Y that decreased slightly from 9 to 6 ppm and Fe and Ti that increased from 552 to 2497 ppm and 8 to 23 ppm, respectively (Fig. 4.13). This may suggest wet conditions during this period. The temperature fluctuations varied by 1°C relative to the current average water temperature for North Sound, values that are consistent with mild conditions (Fig. 4.14).

### 7.3. Caribbean correlations

The climate periods derived from the cores from North Sound on Grand Cayman are broadly consistent with those evident in other climate records from the Cayman Islands and elsewhere in the Caribbean-Gulf of Mexico region (Figs. 4.15, 4.16). Coral skeletons collected from open ocean reefs from Grand Cayman and Cayman Brac, which grew between ~1474 to 1512 CE and ~1815 to 2014 CE, provided evidence of systematic climate changes over the last ~540 years (Booker et al., 2019). The Grand Cayman corals came from a reef on the southwest corner of the island and from North Sound's fringing reef that are 9.5 km and 6 km from the North Sound cores, respectively. The Cayman Brac coral came from a locality that is 170 km from the North Sound cores. Although the SST records derived from the corals and North Sound cores are broadly in agreement,

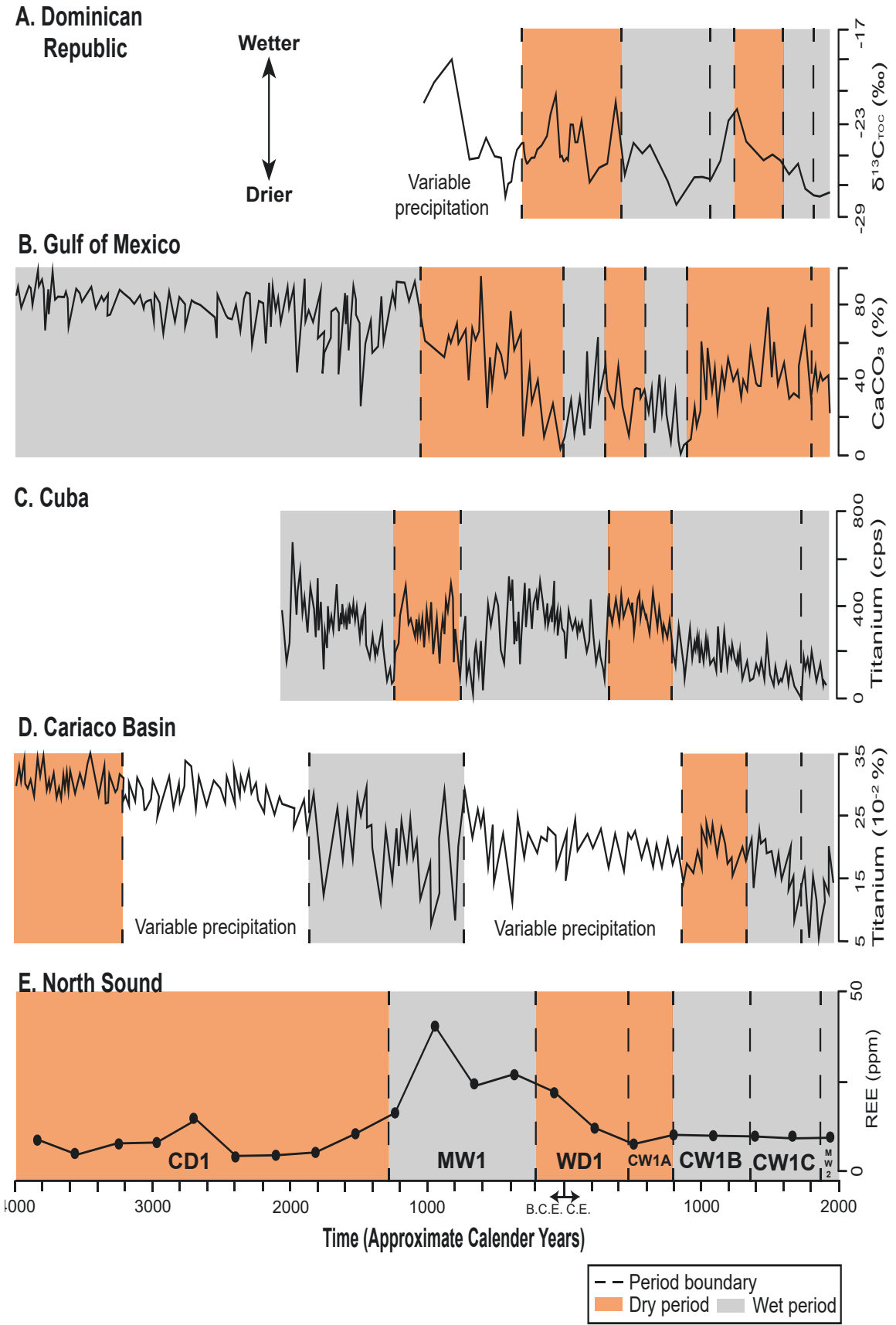


**Fig. 4.15.** Comparison between atmospheric moisture reconstructions from Grand Cayman and other localities: (A)  $\delta^{13}\text{C}_{\text{TOC}}$  of bulk sediments from a core in Laguna Castilla, Dominican Republic (Lane et al., 2009, their Fig. 8), (B)  $\text{CaCO}_3$  content from a sediment core in Lake Chichancanba, Gulf of Mexico (Hodell et al., 1995, their Fig. 2), (C) 5 point running mean of Ti content from sediments in a core from Playa Bilen, Cuba (Gregory et al., 2015, their Fig. 10), (D) bulk Ti content of sediments from ODP Site 1002 in the Cariaco Basin (Haug et al., 2001, their Fig. 3), and (E) Ti and  $\Sigma\text{REE}+\text{Y}$  concentrations from core B10 in North Sound, Grand Cayman (this study). Grey shaded regions represent wet periods and orange shaded regions represent dry periods ( $\pm 200$  years).

---

there are minor differences with respect to the upper part of cool period 2 (~1896 to 1924 CE), as derived from the Cayman corals (low and decreasing temperatures of  $29^\circ$  to  $21^\circ\text{C}$ ), and the North Sound cores (mild temperatures around  $28^\circ\text{C}$ ) over the same time period. This discrepancy may be a function of (1) the fact that today, the water in North Sound is generally  $1^\circ$  to  $2^\circ\text{C}$  warmer than in the open ocean around the Cayman Islands due to differences in circulation patterns, and (2) the smaller scale sampling resolution for the corals relative to the sediment core. Although the North Sound cores provide records of climate variability on the centennial scale, decadal scale changes like those obtained from the corals cannot be resolved from the sediment cores. Nevertheless, the Cayman coral-based SST records show similar trends in warming and cooling to those from the North Sound cores.

Climatic cycles in the tropics have generally been attributed to changes in the positions of the Intertropical Convergence Zone (ITCZ) and North Atlantic Oscillation (NAO) that both influence the temperature and precipitation regimes (Haug et al., 2001; Nyberg et al., 2001; Lane et al., 2009; Gregory et al., 2015). Inferences about the

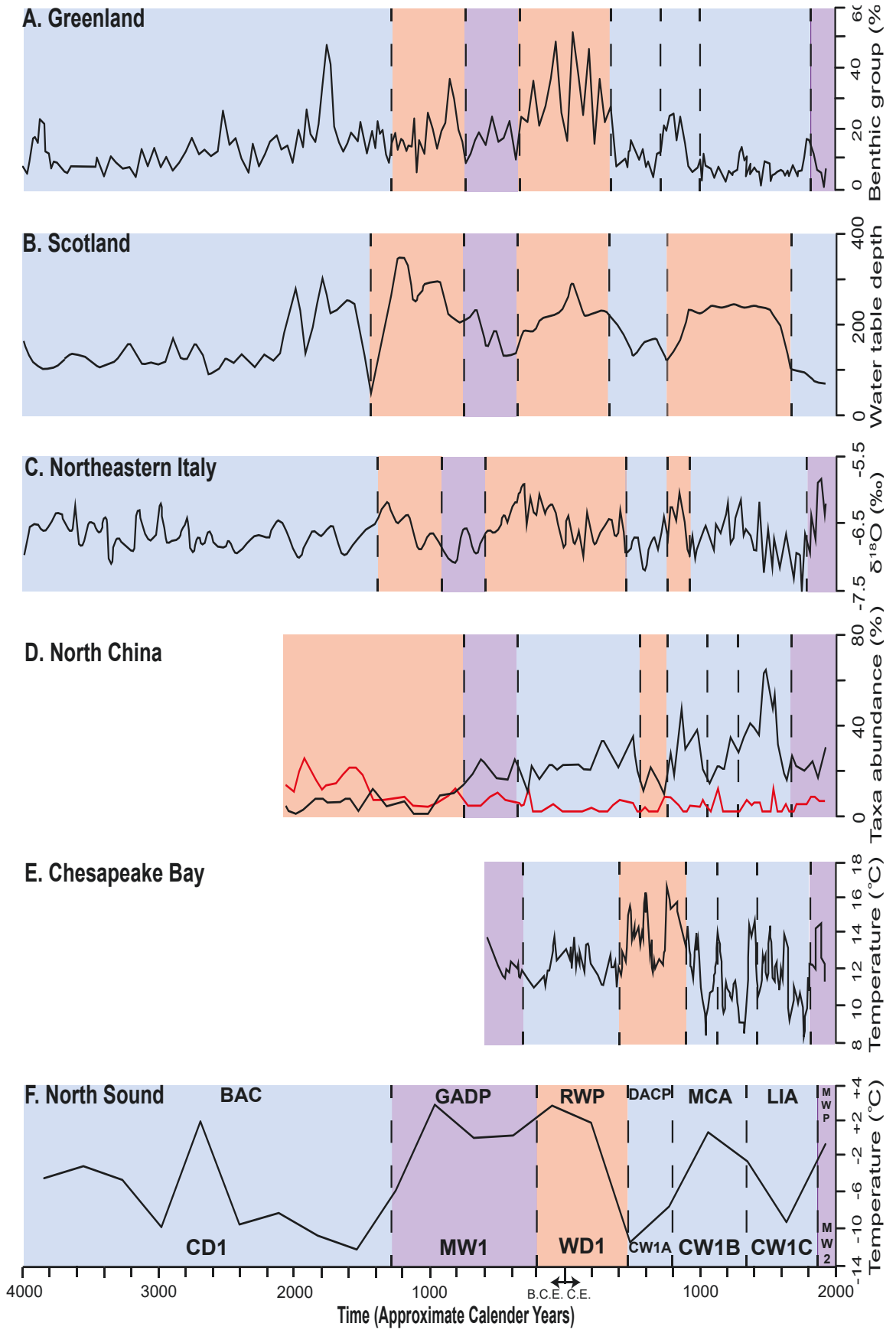


**Fig. 4.16.** Comparison between temperature reconstructions from Grand Cayman and other localities: (A) abundance of benthic chilled Atlantic foraminifera from the East Greenland Shelf (Kolling et al., 2017, their Fig. 2), (B) reconstructed water table depth from Temple Hill Moss, Scotland (Langdon et al., 2003, their Fig. 8), (C)  $\delta^{18}\text{O}$  values from a stalagmite in northeastern Italy (Finne et al., 2011, their Fig. 3, after Frisia et al., 2005), (D) chironomid cold (black) and warm-preferring (red) taxa abundances from Gonghai Lake, Northern China (Wang et al., 2018, their Fig. 4), (E)  $\delta^{18}\text{O}$  derived temperatures from sediment cores in Chesapeake Bay (Cronin et al., 2010, their Fig. 4), and (F)  $\delta^{18}\text{O}$  derived temperatures from core B10 North Sound, Grand Cayman (this study). Red shaded regions represent warm periods, purple shaded regions represent mild periods, and blue shaded regions represent cool periods ( $\pm 200$  years). BAC- Bronze Age Collapse, GADP- Greek Age Dark Period, RWP- Roman Warm Period, DACP- Dark Ages Cool Period, MCA- Medieval Climate Anomaly, LIA- Little Ice Age, MWP- Modern Warm Period.

---

past movements and positions of these atmospheric pressure regimes are commonly developed based on records of atmospheric moisture variability (Hodell et al., 1991; 1995; Haug et al., 2001; Nyberg et al., 2001; Lane et al., 2009; 2011; Stansell et al., 2013; Gregory et al., 2015). If true, the climate regimes deduced from the North Sound cores (Figs. 4.13, 4.14) should correlate with the atmospheric moisture and temperature variability that have been established for other areas in the Caribbean.

The dry conditions during CD1 (~3850 to 1280 BCE), WD1 (~200 BCE to 480 CE), and CW1A (~480 to 800 CE) detected from the North Sound cores can be correlated (Fig. 4.15) with similar periods recognized in Cuba (Fensterer et al., 2012; Gregory et al., 2015), the Cariaco Basin (Hodell et al., 1991; Haug et al., 2001), the Dominican Republic (Lane et al., 2009; 2011), and the Gulf of Mexico (Hodell et al.,

1991). Similarly, the wet conditions that characterized MW1 (~1280 to 200 BCE), CW1B (~800 to 1350 CE), CW1C (~1350 to 1850 CE), and MW2 (~1850 to 1980 CE) in North Sound (Fig. 4.15) can be linked to wet phases interpreted from records from the Cariaco Basin (Haug et al., 2001; 2003), the Gulf of Mexico/Yucatan Peninsula (Hodell et al., 1991; 1995; 2005; Bernal et al., 2011), Florida (Wang et al., 2013), Cuba (Gregory et al., 2015), the Dominican Republic (Lane et al., 2009; 2011), and Puerto Rico (Nyberg et al., 2001). Slight discrepancies in the timing and/or duration between the record from North Sound and elsewhere in the Caribbean region can be attributed to the (1) type of samples (sediment core, speleothem, coral), proxies (REE, Ti, Fe, CaCO<sub>3</sub> content,  $\delta^{18}\text{O}$ ), and methods used by different studies, (2) differences in data resolution between different studies and age depth models used to develop the chronologies, (3) differential deposition rates or compaction, and/or (4) the position of the ITCZ relative to the study area (Haug et al., 2001; Gregory et al., 2015).

The warm, mild, and cool periods recognized in the North Sound cores can be correlated to temperature changes throughout the Caribbean-Gulf of Mexico region (Fig. 4.16). The decrease in temperatures that characterized CD1, CW1A, and CW1C have also been identified in Bonaire (Felis et al., 2015), Puerto Rico (Kilbourne, 2006), Bermuda (van Hengstum et al., 2015), and the Cariaco Basin (Wurtzel et al., 2013). Elevated temperatures, like those during periods WD1 and CW1B, have been recognized in the Cariaco Basin (Black et al., 2004), and Nicaragua (Stansell et al., 2013). The mild temperatures during MW1 and MW2, are akin to those from Puerto Rico (Winter et al., 1998; Alpert et al., 2017), Jamaica (Haase-Schramm et al., 2003), and the Cariaco Basin (Abahazi, 2009).

#### *7.4. Global correlations*

The climate periods derived from the North Sound cores correlate to various climate records from the Caribbean region and higher latitudes (Figs. 4.15, 4.16). The

cool, dry conditions of CD1 (~3850 to 1280 BCE) and CW1A (~480 to 800 CE) in North Sound are akin to those evident in records from the North Atlantic (Bond et al., 1997), Scotland (Anderson, 1998; Tipping et al., 2008), and Greenland (Kolling et al., 2017). The warm, wet climates of CW1B (~800 to 1350 CE) in North Sound also correlate with similar climate phases derived from Chesapeake Bay (Cronin et al., 2010), eastern Canada (Finkenbinder et al., 2016), the Mediterranean (Finne et al., 2011), and China (Deng et al., 2017; Wang et al., 2018). The mild and wet conditions of MW1 (~1280 to 200 BCE) and MW2 (~1850 to 1980 CE) correspond to temperature and moisture variability in the Galapagos (Dunbar et al., 1994), Chesapeake Bay (Cronin et al., 2010), the Mediterranean (Finne et al., 2011), northern China (Wang et al., 2018), and Scotland (Wang et al., 2012). The warm and dry conditions of WD1 (~200 BCE to 480 CE) are similar to those identified in the Mediterranean (Finne et al., 2011), Scotland (Wang et al., 2012), and Greenland (Kolling et al., 2017). The cool and wet conditions that characterized CW1C (~1350 to 1850 CE) in North Sound are similar to those noted for North America (Trouet et al., 2013) and Greenland (Kolling et al., 2017) and the slight warming during this interval (~1600 to 1700 CE) is similar to that detected elsewhere (Saenger et al., 2009; Wanner et al., 2011; Jaume-Santero et al., 2016).

Major changes in temperature and atmospheric moisture regimes on a global scale over the last ~6000 years may have resulted in the climate variability documented in North Sound in terms of the timing, duration, and type of climate change (Figs. 4.14, 4.15, 4.16, 4.17). Variance between the timing and duration of the North Sound climate periods and those from other locations (Fig. 4.17) could be attributed to (1) latitudinal differences/local variability (Bengtsson et al., 2006; Cronin et al., 2010; Marcott et al., 2013; IPCC, 2014), (2) the position of the ITCZ relative to the study area (Haug et al., 2001; Gregory et al., 2015), with an associated temporal lag between low and high latitude locations, (3) volcanic activity (Mayewski et al., 2004; Wanner et al., 2011; Helama et al., 2017), (4) errors associated with age determinations (deMenocal et al.,



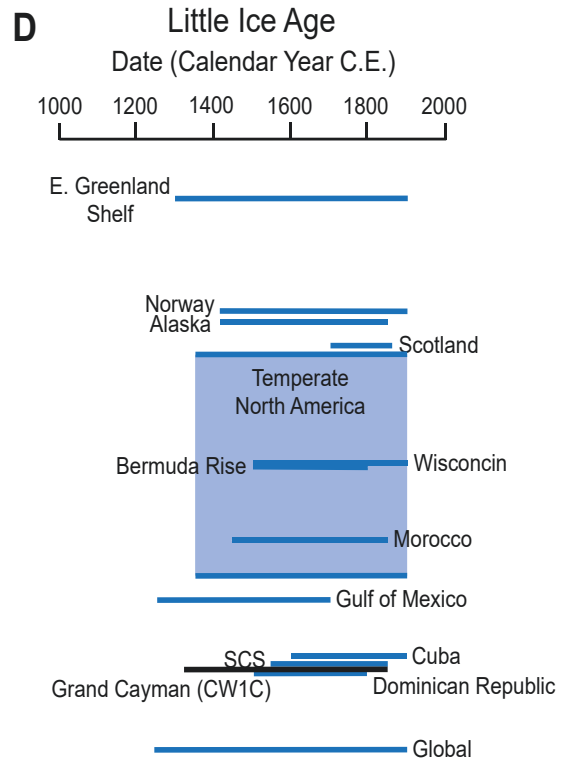
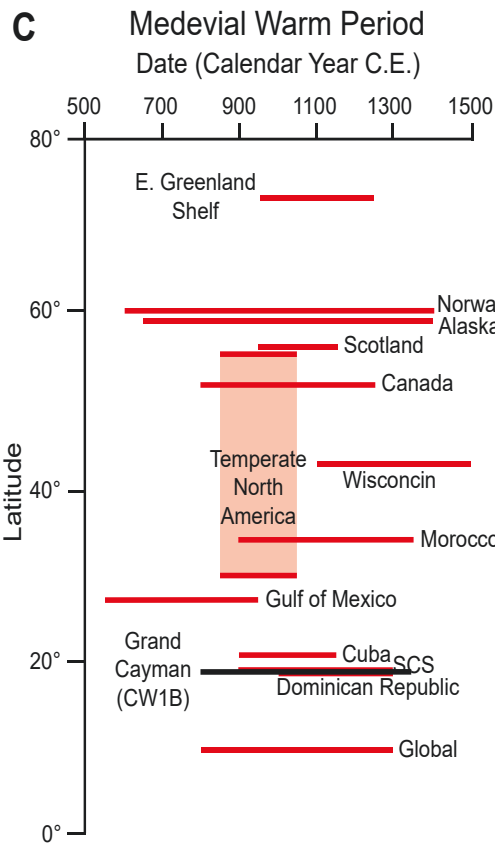
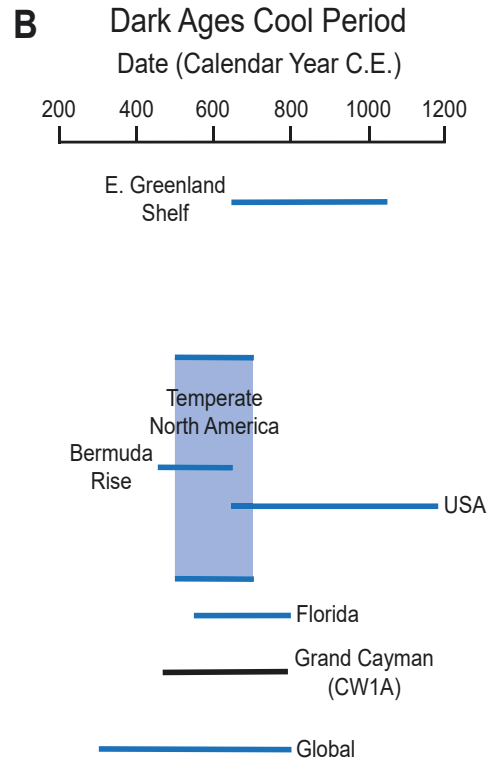
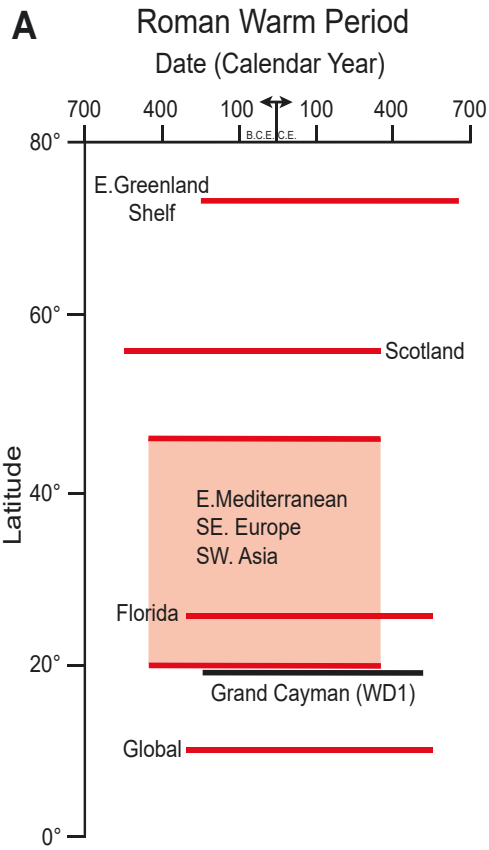


**Fig. 4.17.** Comparison of “known” climate period to those identified in the North Sound cores.

(A) Roman Warm Period; East Greenland Shelf (Kolling et al., 2017), Scotland (Wang et al., 2012), eastern Mediterranean, southwest Europe, and southeast Asia (Finne et al., 2011), Florida (Wang et al., 2013), and globally (Ljungqvist, 2009). (B) Dark Ages Cool Period; East Greenland Shelf (Kolling et al., 2017), temperate North America (Trouet et al., 2013), Bermuda Rise (Keigwin and Pickart, 1999), Florida (Wang et al., 2013), and globally (Ljungqvist, 2009; Wanner et al., 2011; Helama et al., 2017). (C) Medieval Climate Anomaly; East Greenland Shelf (Kolling et al., 2017), Norway (Nesje et al., 1991), Alaska (Rothlisberger, 1986), Scotland (Wang et al., 2012), Canada (Osborn and Luckman, 1988), temperate North America (Trouet et al., 2013), Wisconsin (Wahl et al., 2012), Morocco (Wassenburg et al., 2013), Gulf of Mexico (Richey, 2007), Cuba (Fensterer et al., 2012), South China Sea (SCS; Deng et al., 2017), Dominican Republic (Lane et al., 2009), and globally (Ljungqvist, 2009). (D) Little Ice Age; East Greenland Shelf (Kolling et al., 2017), Norway (Nesje et al., 1991), Alaska (Rothlisberger, 1986), Scotland (Wang et al., 2012), temperate North America (Trouet et al., 2013), Wisconsin (Wahl et al., 2012), Bermuda Rise (Keigwin and Pickart, 1999), Morocco (Wassenburg et al., 2013), Gulf of Mexico (Richey, 2007), Cuba (Fensterer et al., 2012), South China Sea (SCS; Deng et al., 2017), Dominican Republic (Lane et al., 2009), and globally (Ljungqvist, 2009; Wanner et al., 2011; Marcott et al., 2013).

---

2000; Charman et al., 2006; Finne et al., 2011), and/or (5) the methods and proxies used for climate reconstructions (Kemp et al., 2011; Trouet et al., 2013).

Varying amounts of solar output (Abahazi, 2009; Finne et al., 2011; Wanner et al., 2011; Helama et al., 2017; Kolling et al., 2017) and the movements of the ITCZ (Haug et al., 2001; Nyberg et al., 2001; Lane et al., 2009; Stansell et al., 2013) are commonly

invoked as the underlying driving forces of climate variability on a global scale. It has been suggested that changes in solar activity affect the tropical hydrological cycles by influencing salinity balances, thermocline circulation, and ocean heat transport in the North Atlantic, which effects trade wind variability and the movements of the ITCZ and NAO (Broecker, 1991; Rind and Overpeck, 1993; Black et al., 1999; Nyberg et al., 2001). A more northerly position of the ITCZ and/or a negative phase of the NAO facilitates the movement of warm air masses, increases precipitation, and reduces the transport of African dust to the Caribbean region (Nyberg et al., 2001; Lane et al., 2009; Doherty et al., 2012). This configuration of the atmospheric pressure regimes may have caused the elevated  $T_{cal}$ , decreasing  $\Sigma REE+Y$  values, and increasing Fe and Ti concentrations evident in the North Sound cores during MW1, CW1B, and MW2. In contrast, cooler SST, dry atmospheric conditions, and increased transport of African dust to the Caribbean region would occur when the ITCZ was displaced to the south, was in a stationary position, and/or when NAO was in a positive phase (Nyberg et al., 2001; Lachniet et al., 2009; Lane et al., 2009; 2011). This may have produced the low  $T_{cal}$ , increasing  $\Sigma REE+Y$  concentrations, and decreasing Fe and Ti concentrations recorded in North Sound during CD1, WD1, and CW1A. The configuration of these atmospheric pressure regimes is difficult to determine during CW1C, as this interval does not correspond to the general SST and atmospheric moisture patterns. It has been shown, however, that disturbances in the northeastern trade winds can cause climate states to be out of phase with the general patterns of precipitation in the Caribbean region (Broecker, 1991; Nyberg et al., 2001). More records, therefore, from the early-mid Holocene in the Caribbean region are necessary to fully verify the movements of the ITCZ and the phase of the NAO, in order to determine their role in global climate change.

## 8. Conclusions

Integration of data from three sediment cores from North Sound, Grand Cayman,

has provided a detailed atmospheric moisture and SST record for the central Caribbean over the last ~6000 years. Examination of the moisture and temperature profiles from these sediments resulted in the following important conclusions.

- The transition from a coastal pond to a marine lagoon is accompanied by a distinct change in sediment type from the Bivalve and Peat Facies to the *Halimeda* and *Halimeda*-Benthic Foraminifera-Bivalve Facies, a decrease in elemental concentrations and organic material, and changes in the isotopic compositions.
- The North Sound cores recorded five periods of climate change, including one cool-dry period (~3850 and 1280 BCE), two mild-wet periods (~1280 to 200 BCE and ~1850 to 1980 CE), one warm-dry period (~200 BCE to 480 CE), and one cool-wet period (~480 and 1850 CE) that correlate to global climate phases.
- The movements of the Intertropical Convergence Zone (ITCZ) and the phase of the North Atlantic Oscillation (NAO) have been determined from the Fe, Ti,  $\Sigma$ REE+Y, and isotopic depth profiles of the North Sound cores. During MW1, CW1B, and MW2 the ITCZ was in a northerly position and/or the NAO in a negative phase, resulting in increased atmospheric moisture and elevated temperatures. In contrast, CD1, WD1, and CW1A, resulted from a southerly position of the ITCZ and/or a positive phase of the NAO, resulting in low temperatures and decreased atmospheric moisture.

The pronounced climatic periods, as evidenced from the North Sound cores, over the last ~6000 years around Grand Cayman correlate with climate changes recognized elsewhere in the Caribbean and higher latitude locations. Such correlations indicate the global nature of these changes.

## REFERENCES

- Abahazi, M.A., 2009. Tropical North Atlantic sea surface temperature reconstruction for the last 800 years using Mg/Ca ratios in planktic foraminifera, Unpublished. M.Sc., University of Akron, Ohio, USA, 117 pp.
- Alibo, D.S., Nozaki, Y., 1999. Rare earth elements in seawater: particle association, shale-normalization, and Ce oxidation. *Geochimica et Cosmochimica Acta* 63, 363-372.
- Alpert, A.E., Cohen, A.L., Oppo, D.W., DeCarlo, T.M., Gaetani, G.A., Hernandez-Delgado, E.A., Winter, A., Gonneea, M.E., 2017. Twentieth century warming of the tropical Atlantic captured by Sr-U paleothermometry. *Paleoceanography* 32, 146-160.
- Anand, P., Elderfield, H., Conte, M.H., 2003. Calibration of Mg/Ca thermometry in planktonic foraminifera from a sediment trap time series. *Paleoceanography* 18. doi:10.1029/2002PA000846.
- Anderson, D.E., 1998. A reconstruction of Holocene climatic changes from peat bogs in north-west Scotland. *Boreas* 27, 208-224.
- Anthony, A., Atwood, J., August, P., Byron, C., Cobb, S., Foster, C., Fry, C., Gold, A., Hagos, K., Heffner, L., Kellogg, D.Q., Lellis-Dibble, K., Opaluch, J.J., Oviatt, C., Pfeiffer-Herbert, A., Rohr, N., Smith, L., Smythe, T., Swift, J., Vinhateiro, N., 2009. Coastal lagoons and climate change: ecological and social ramifications in U.S. Atlantic and Gulf coast ecosystems. *Ecology and Society* 14.
- Barnett, T.P., Delgenio, A.D., Ruedy, R.A., 1992. Unforced decadal fluctuations in a coupled model of the atmosphere and ocean mixed layer. *Journal of Geophysical Research-Oceans* 97, 7341-7354.
- Bengtsson, L., Hodges, K.I., Roeckner, E., Brokopf, R., 2006. On the natural variability of the pre-industrial European climate. *Climate Dynamics* 27, 743-760.
- Bernal, J.P., Lachniet, M., McCulloch, M., Mortimer, G.E., Morales, P., Cienfuego, E., 2011. A speleothem record of Holocene climate variability from southwestern Mexico. *Quaternary Research* 75, 104-113.

- Blaauw, M., Christen, J.A., 2011. Flexible paleoclimate age-depth models using an autoregressive gamma process. *Bayesian Anal.* 6, 457-474.
- Black, D.E., Thunell, R.C., Kaplan, A., Peterson, L.C., Tappa, E.J., 2004. A 2000-year record of Caribbean and tropical North Atlantic hydrographic variability. *Paleoceanography* 19. 10.1029/2003PA000982.
- Black, D.E., Peterson, L.C., Overpeck, J.T., Kaplan, A., Evans, M.N., Kashgarian, M., 1999. Eight centuries of North Atlantic Ocean atmosphere variability. *Science* 286, 1709-1713.
- Black, D.E., Abahazi, M.A., Thunell, R.C., Kaplan, A., Tappa, E.J., Peterson, L.C., 2007. An 8-century tropical Atlantic SST record from the Cariaco Basin: baseline variability, twentieth-century warming, and Atlantic hurricane frequency. *Paleoceanography* 22, 4023-4034.
- Bond, G., Showers, W., Cheseby, M., Lotti, R., Almasi, P., deMenocal, P., Priore, P., Cullen, H., Hajads, I., Bonani, G., 1997. A pervasive millennial-scale cycle in North Atlantic Holocene and glacial climates. *Science* 278, 1257-1266.
- Booker, S.D., Jones, B., Chacko, T., Li, L., 2019. Insights into sea surface temperatures from the Cayman Islands from corals over the last ~540 years. *Sedimentary Geology* 389, 218-240.
- Bouillon, S., Connolly, R.M., S.Y., L., 2008. Organic matter exchange and cycling in mangrove ecosystems: recent insights from stable isotope studies. *Journal of Sea Research* 59, 44-58.
- Bracco, R., Inda, H., del Puerto, L., Castiñeira, C., Sprechmann, P., García-Rodríguez, F., 2005. Relationships between Holocene sea-level variations, trophic development, and climatic change in Negra Lagoon, Southern Uruguay. *Journal of Paleolimnology* 33, 253-263.
- Broecker, W.S., 1991. The great ocean conveyor. *Oceanography* 4, 79-89.
- Bryan, S.P., Marchitto, T.M., 2008. Mg/Ca-temperature proxy in benthic foraminifera: new calibrations from the Florida Straits and a hypothesis regarding Mg/Li. *Paleoceanography* 23. doi:10.1029/2007PA001553.

- Byrne, R., Sholkovitz, E., 1996. Marine chemistry and geochemistry of the lathanides. Handbook on the Physics and Chemistry of Rare Earths, 23. Elsevier, Amsterdam, pp. 497-593.
- Byrne, R.H., Kim, K., 1990. Rare earth elements scavenging in seawater. *Geochimica et Cosmochimica Acta* 54, 2645-2656.
- Cantrell, K.J., Byrne, R.H., 1987. Rare earth element complexation by carbonate and oxalate ions. *Geochimica et Cosmochimica Acta* 51, 597-605.
- Charman, D.J., Blundell, A., Chiverrell, R.C., Hendon, D., Langdon, P.G., 2006. Compilation of non-annually resolved Holocene proxy climate records: stacked Holocene peatland palaeo-water table reconstructions from northern Britain. *Quaternary Science Reviews* 25, 336-350.
- Cleroux, C., Cortijo, E., Anand, P., Labeyrie, L., Bassinot, F., Caillon, N., Duplessy, J.C., 2008. Mg/Ca and Sr/Ca ratios in planktonic foraminifera: proxies for upper water column temperature reconstruction. *Paleoceanography* 23. doi:10.1029/2007PA001505.
- Craig, H., 1965. The measurement of oxygen isotope paleotemperatures. In: E., Tongiorgi. (Ed.), *Stable Isotopes in Oceanographic Studies and Paleotemperatures*. Spoleto, Consiglio Nazionale delle Ricerche, Laboratorio de Geologica Nucleare, Pisa, pp. 161-182.
- Crann, C.A., Murseli, S., St-Jean, G., Zhao, X., Clark, I.D., Kieser, W.E., 2017. First status report on radiocarbon sample preparation techniques at the A.E. Lalonde AMS Laboratory (Ottawa, Canada). *Radiocarbon* 59, 695-704.
- Cronin, T.M., Hayo, K., Thunell, R.C., Dwyer, G.S., Saenger, C., Willard, D.A., 2010. The Medieval Climate Anomaly and Little Ice Age in Chesapeake Bay and the North Atlantic Ocean. *Palaeogeography, Palaeoclimatology, Palaeoecology* 291, 299-310.
- Culver, S.J., 1990. Benthic foraminifera of Puerto Rican mangrove-lagoon systems: potential for paleoenvironmental interpretations. *PALAIOS* 5, 34-51.
- Debenay, J., Eichler, B.B., Duleba, W., Bonetti, C., Eichler-Colho, P., 1998. Water stratification in coastal lagoons: its influence on foraminiferal assemblages in two Brazilian lagoons. *Marine Micropaleontology* 35, 67-89.

- Delaney, M.L., Be, A.W.H., Boyle, E.A., 1985. Li, Sr, Mg, and Na in foraminiferal calcite shells from laboratory culture, sediment traps, and sediment cores. *Geochimica et Cosmochimica Acta* 49, 1327-1341.
- deMenocal, P., Ortiz, J., Guilderson, T., Sarnthein, M., 2000. Coherent high and low-latitude climate variability during the Holocene warm period. *Science* 288, 2198-2202.
- Deng, W., Liu, X., Wei, G., Zeng, T., Xie, L., Zhao, J., 2017. A comparison of the climates of the Medieval Climate Anomaly, Little Ice Age, and Current Warm Period reconstructed using coral records from the northern South China Sea. *Journal of Geophysical Research: Oceans* 122, 264-275.
- Doherty, O.M., Riemer, N., Hameed, S., 2012. Control of Saharan mineral dust transport to Barbados in winter by the Intertropical Convergence Zone over West Africa. *Journal of Geophysical Research* 117. doi:10.1029/2012JD017767.
- Donegan, B., 2019. Saharan dust surges into Caribbean- here's what that means during hurricane season, The Weather Channel. TWC Product and Technology LLC.
- Dunbar, R.B., Wellington, G.M., Colgan, M.W., Glynn, P.W., 1994. Eastern Pacific sea surface temperature since 1600 A.D.: the  $\delta^{18}\text{O}$  record of climate variability in Galapagos corals. *Paleoceanography* 9, 291-315.
- Elderfield, H., Cooper, M., Ganssen, G., 2000. Sr/Ca in multiple species of planktonic foraminifera: implications for reconstructions of seawater Sr/Ca. *Geochemistry Geophysics Geosystems* 1. doi: 10.1029/1999GC000031.
- Elderfield, H., Yu, J., Anand, P., Kiefer, T., Nyland, B., 2006. Calibrations for benthic foraminiferal Mg/Ca paleothermometry and the carbonate ion hypothesis. *Earth and Planetary Science Letters* 250, 633-649.
- Emery, K.O., 1981. Low marine terraces of Grand Cayman Island. *Estuarine, Coastal and Shelf Science* 12, 569-578.
- Evans, D., Erez, J., Oron, S., Muller, W., 2015. Mg/Ca-temperature and seawater-test chemistry relationships in the shallow-dwelling large benthic foraminifera *Operculina ammonoides*.



- Geochimica et Cosmochimica Acta* 148, 325-342.
- Fahlquist, D.A., Davies, D.K., 1971. Fault block origin of the western Cayman Ridge, Caribbean Sea. *Deep Sea Research* 18, 243-253.
- Felis, T., Giry, C., Scholz, D., Lohmann, G., Pfeiffer, M., Patzold, J., Kolling, M., Scheffers, S.R., 2015. Tropical Atlantic temperature seasonality at the end of the last interglacial. *Nature: Communications* 6. doi:10.1038/ncomms7159.
- Fensterer, C., Scholz, D., Hoffmann, D.L., Spotl, C., Pajon, J.M., Mangini, A., 2012. Cuban stalagmite suggests relationship between Caribbean precipitation and the Atlantic Multidecadal Oscillation during the past 1.3ka. *Holocene* 22, 1405-1412.
- Finkenbinder, M.S., Abbot, M.B., Steinman, B.A., 2016. Holocene climate change in Newfoundland reconstructed using oxygen isotope analysis of lake sediment cores. *Global and Planetary Change* 143, 251-261.
- Finne, M., Holmgren, K., Sundqvist, H.S., Weiberg, E., Lindblom, M., 2011. Climate in the eastern Mediterranean, and adjacent regions, during the past 6000 years- a review. *Journal of Archaeological Science* 38, 3153-3173.
- Fleming, K., Johnston, P., Zwartz, D., Yokoyama, Y., Lambeck, K., Cchappell, J., 1998. Refining the eustatic sea-level curve since the Last Glacial Maximum using far- and intermediate-field sites. *Earth and Planetary Science Letters* 163, 327-342.
- Frisia, S., Borsato, A., Spotl, C., Villa, I., Cucchi, F., 2005. Climate variability in the SE Alps of Italy over the past 17 000 years reconstructed from a stalagmite record. *Boreas* 34, 445-455.
- Gonneea, M.E., Paytan, A., Herrera-Silveira, J.A., 2004. Tracing organic matter sources and carbon burial in mangrove sediments over the past 160 years. *Estuarine, Coastal and Shelf Science* 61, 211-227.
- Graham, D.W., Bender, M.L., Williams, D.F., Keigwin, L.D., 1982. Strontium-calcium ratios in Cenozoic planktonic foraminifera. *Geochimica et Cosmochimica Acta* 46, 1281-1292.
- Gregory, B.R.B., Peros, M., Reinhardt, E.G., Donnelly, J.P., 2015. Middle-late Holocene

- Caribbean aridity inferred from foraminifera and elemental data in sediment cores from two Cuban lagoons. *Palaeogeography, Palaeoclimatology, Palaeoecology* 426, 239-241.
- Haase-Schramm, A., Bohm, F., Eisenhauer, A., Dullo, W., Joachimski, M.M., Hansen, B., Reitner, J., 2003. Sr/Ca ratios and oxygen isotopes from sclerosponges: temperature history of the Caribbean mixed layer and thermocline during the Little Ice Age. *Paleoceanography* 10. doi:10.1029/2002PA000830.
- Haug, G.H., Hughen, K.A., Sigman, D.M., Peterson, L.C., Rohl, U., 2001. Southward migration of the Intertropical Convergence Zone through the Holocene. *Science* 293, 1304-1310.
- Haug, G.H., Gunther, D., Peterson, L.C., Sigman, D.M., Hughen, K.A., Aeschlimann, B., 2003. Climate and collapse of Maya civilization. *Science* 299, 1731-1735.
- Helama, S., Jones, P.D., Briffa, K.R., 2017. Dark Ages Cold Period: a literature review and directions for future research. *The Holocene* 27, 1601-1606.
- Hinokidani, K., Nakanishi, Y., 2019. Dissolved iron elution from mangrove ecosystem associated with polyphenols and a herbivorous snail. *Ecology and Evolution* 9, 6772-6784.
- Hodell, D.A., Curtis, J.H., Brenner, M., 1995. Possible role of climate in the collapse of Classic Maya civilization. *Letters to Nature* 375, 391-394.
- Hodell, D.A., Curtis, J.H., Jones, G.A., Higuera-Gundy, A., Brenner, M., Binford, M.W., Dorsey, K.T., 1991. Reconstruction of Caribbean climate change over the past 10,500 years. *Nature: Letters* 352, 790-794.
- Hodell, D.A., Brenner, M., Curtis, J.H., Medina-Gonzalez, R., Can, E.I.C., Albornaz-Pat, A., Guilderson, T.A., 2005. Climate change on the Yucatan Peninsula during the Little Ice Age. *Quaternary Research* 63, 109-121.
- Holmgren, K., Karlen, W., Lauritzen, S.E., Lee-Thorp, J.A., Partridge, T.C., Piketh, S., Repinshi, P., Stevenson, C., Svanered, O., Tyson, P.D., 1999. A 3000-year high-resolution stalagmite-based record of palaeoclimate for northeastern South Africa. *The Holocene* 9, 295-309.
- Hudson, J.D., Anderson, T.F., 1989. Ocean temperatures and isotopic compositions through time.

- Transactions of the Royal Society of Edinburgh: Earth Science 80, 183-192.
- IPCC, 2014. Climate change 2014: synthesis report. Contribution of working groups I, II and III to the Fifth Assessment Report of the Intergovernmental Panel on Climate Change, Geneva, Switzerland.
- Jaume-Santero, F., Pickler, C., Beltrami, H., Mareschal, J., 2016. North American regional climate reconstruction from ground surface temperature histories. *Climate of the Past* 12, 2181-2194.
- Jones, B., 1994. Geology of the Cayman Islands. The Cayman Islands: natural history and biogeography. Kluwer Academic Publishers, The Netherlands, pp. 13-49.
- Jones, B., 2019. Diagenetic processes associated with unconformities in carbonate successions on isolated oceanic islands: case study of the Pliocene to Pleistocene sequence, Little Cayman, British West Indies. *Sedimentary Geology* 386, 9-30.
- Jones, B., Hunter, I.G., 1990. Pleistocene paleogeography and sea levels on the Cayman Islands, British West Indies. *Coral Reefs* 9, 81-91.
- Keigwin, L.D., Pickart, R.S., 1999. Slope water current over the Laurentian Fan on interannual to millennial time scales. *Science* 286, 520-525.
- Kemp, A.C., Horton, B.P., Donnelly, J.P., Mann, M.E., Vermeer, M., Rahmstorf, S., 2011. Climate related sea-level variations over the past two millennia. *Proceedings of the National Academy of Science of the USA* 108, 11017-11022.
- Kilbourne, K.H., 2006. Tropical Atlantic and Caribbean climate variations during the past eight centuries, Unpublished. Ph.D., University of South Florida, Florida, USA, 188 pp.
- Kim, S., Mucci, A., Taylor, B., 2007. Phosphoric acid fractionation factors for calcite and aragonite between 25 and 75°C: revisited. *Chemical Geology* 246, 135-146.
- Kim, S., Coplen, T.B., Horita, J., 2015. Normalization of stable isotope data for carbonate minerals: implementation of IUPAC guidelines. *Geochimica et Cosmochimica Acta* 158, 276-289.
- Koeppenkastrop, D., DeCarlo, E.H., Roth, M., 1991. A method to investigate the interaction of

- rare earth elements in aqueous solution with metal oxides. *Journal of Radioanalytical and Nuclear Chemistry* 152, 337-346.
- Kolling, H.M., Stein, R., Fahl, K., Perner, K., Moros, M., 2017. Short-term variability in late Holocene sea ice cover on the East Greenland Shelf and its driving mechanisms. *Palaeogeography, Palaeoclimatology, Palaeoecology* 485, 336-350.
- Kuss, J., Garbe-Schonberg, C., Kremling, K., 2001. Rare earth elements in suspended particulate material of North Atlantic surface waters. *Geochimica et Cosmochimica Acta* 65, 187-199.
- Lachniet, M., Johnson, L., Asmerom, Y., Burns, S.J., Polyak, V., Patterson, W.P., Burt, L., Azouz, A., 2009. Late Quaternary moisture export across Central America and to Greenland: evidence for tropical rainfall variability from Costa Rican stalagmites. *Quaternary Science Reviews* 28, 3348-3360.
- Lane, C.S., Horn, S.P., Mora, C.I., Orvis, K.H., 2009. Late-Holocene paleoenvironmental change at mid-elevation on the Caribbean slope of the Cordillera Central, Dominican Republic: a multi-site, multi-proxy analysis. *Quaternary Science Reviews* 28, 2239-2260.
- Lane, C.S., Horn, S.P., Orvis, K.H., Thomason, J.M., 2011. Oxygen isotope evidence of Little Ice Age aridity on the Caribbean slope of the Cordillera Central, Dominican Republic. *Quaternary Research* 75, 461-470.
- Langdon, P.G., Barber, K.E., Hughes, P.D.M., 2003. A 7500-year peat-based palaeoclimate reconstruction and evidence for an 1100-year cyclicity in bog surface wetness from Temple Hill Moss, Pentland Hills, southeast Scotland. *Quaternary Science Reviews* 22, 259-274.
- Lerche, D., Nozaki, Y., 1998. Rare earth elements of sinking particulate matter in the Japan Trench. *Earth and Planetary Science Letters* 159, 71-86.
- Li, R., Jones, B., 2013. Temporal and spatial variations in the diagenetic fabrics and stable isotopes of Pleistocene corals from the Ironshore Formation of Grand Cayman, British West Indies. *Sedimentary Geology* 286-287, 58-72.

- Ljungqvist, F.C., 2009. Temperature proxy records covering the last two millennia: a tabular and visual overview. *Swedish Society of Anthropology and Geography* 91, 11-29.
- MacKinnon, L., 2000. Sedimentology of North Sound, Grand Cayman, British West Indies, Unpublished. M.Sc., University of Alberta, Edmonton, Alberta, Canada, 144 pp.
- MacKinnon, L., Jones, B., 2001. Sedimentological evolution of North Sound, Grand Cayman: a freshwater to marine carbonate succession driven by Holocene sea-level rise. *Journal of Sedimentary Research* 71, 568-580.
- Mahowald, N.M., Muhs, D.R., Levis, S., Rasch, P.J., Yoshioka, M., Zender, C.S., Luo, C., 2006. Change in atmospheric mineral aerosols in response to climate: last glacial period, preindustrial, modern, and double carbon dioxide climates. *Journal of Geophysical Research* 111. doi: 10.1029/2005JD006653.
- Marco-Barba, J., Holmes, J.A., Mesquita-Joanes, F., Miracle, M.R., 2013. The influence of climate and sea-level change on the Holocene evolution of a Mediterranean coastal lagoon: evidence from ostracod palaeoecology and geochemistry. *Geobios* 46, 409-421.
- Marcott, S.A., Shakun, J.D., Clark, P.U., Mix, A.C., 2013. A reconstruction of regional and global temperature for the past 11,300 years. *Science* 339, 1198-1201.
- Mayewski, P.A., Rohling, E.J., Stager, J.C., Karlen, W., Maasch, K.A., Meeker, L.D., Meyerson, E.A., Gasse, F., van Kreveld, S., Holmgren, K., 2004. Holocene climate variability. *Quaternary Research* 62, 243-255.
- McLennan, S.M., 1989. Rare earth elements in sedimentary rocks: influence of provenance and sedimentary processes. *Reviews in Mineralogy* 21, 169-200.
- Mekik, F., Francois, R., M, S., 2007. A novel approach to dissolution correction of Mg/Ca-based paleothermometry in the tropical Pacific. *Paleoceanography and Paleoclimatology* 22. doi: 10.1029/2007PA001504.
- Milne, G.A., Long, A.J., Bassett, S.E., 2005. Modelling Holocene relative sea-level observations from the Caribbean and South America. *Quaternary Science Reviews* 24, 1183-1202.
- Moraetis, D., Mouslopoulou, V., 2013. Preliminary results of REE-Y sorption on carbonate rocks.

Bulletin of the Geological Society of Greece 47, 843-851.

- Mortyn, P.G., Elderfield, H., Anand, P., Greavea, M., 2005. An evaluation of controls on planktonic foraminiferal Sr/Ca: comparison of water column and core-top data from a North Atlantic transect. *Geochemistry Geophysics Geosystems* 6. doi: 10.1029/2005GC001047.
- Muhs, D.R., Budahn, J.R., 2009. Geochemical evidence for African dust and volcanic ash inputs to terra rossa soils on carbonate reef terraces, northern Jamaica, West Indies. *Quaternary International* 196, 13-35.
- Muhs, D.R., Budahn, J.R., Prospero, J.M., Carey, S.N., 2007. Geochemical evidence for African dust inputs to soils of western Atlantic islands: Barbados, the Bahamas, and Florida. *Journal of Geophysical Research* 112. doi: 10.1029/2005JF000445.
- Muhs, D.R., Crittenden, R.C., Rosholt, J.N., Bush, C.A., Stewart, K.C., 1987. Genesis of marine terrace soils, Barbados, West Indies: evidence from mineralogy and geochemistry. *Earth Surface processes and Landforms* 12, 605-618.
- Nesje, A., Kvamme, M., Rye, N., Lovlie, R., 1991. Holocene glacial and climate history of the Jostedalsbreen Region, Western Norway: evidence from lake sediments and terrestrial deposits. *Quaternary Science Reviews* 10, 87-114.
- Ng, K., 1990. Diagenesis of the Oligocene-Miocene Bluff Formation of the Cayman Islands: a petrographic and hydrogeological approach., Unpublished. Ph.D., University of Alberta, Edmonton, Alberta, Canada, 343 pp.
- Nozaki, Y., Zhang, J., Amakawa, H., 1997. The fractionation between Y and Ho in the marine environment. *Earth and Planetary Science Letters* 148, 329-340.
- Nyberg, J., Kuijpers, A., Malmgren, B.A., Kunzendorf, H., 2001. Late Holocene changes in precipitation and hydrography recorded in marine sediments from the northeastern Caribbean Sea. *Quaternary Science Reviews* 56, 87-102.
- Oppo, D.W., McManus, J.F., Cullen, J.L., 1998. Abrupt climate events 500,000 to 340,000 years ago: evidence from subpolar North Atlantic sediments. *Science* 279, 1335-1338.

- Osborn, G., Luckman, B.H., 1988. Holocene glacier fluctuations in the Canadian Cordillera (Alberta and British Columbia). *Quaternary Science Reviews* 7, 115-128.
- Osborne, A.H., Haley, B.A., Hathorne, E.C., Plancherel, Y., Frank, M., 2015. Rare earth element distribution in Caribbean seawater: continental inputs versus lateral transport of distinct REE compositions in subsurface water masses. *Marine Chemistry* 177, 172-183.
- Perfit, M.R., Heezen, B.C., 1978. The geology and the evolution of the Cayman Trench. *Geological Society of America Bulletin* 89, 1155-1174.
- Prospero, J.M., Lamb, P.J., 2003. African droughts and dust transport to the Caribbean: climate change implications. *Science* 302, 1024-1029.
- Prospero, J.M., Mayol-Bracero, O.L., 2013. Understanding the transport and impact of African dust on the Caribbean Basin. *American Meteorological Society* 94, 1329-1338.
- Prospero, J.M., Bonatti, E., Schubert, C., Carlson, T.N., 1970. Dust in the Caribbean atmosphere traced to an African dust storm. *Earth and Planetary Science Letters* 9, 287-293.
- Reghellin, D., Coxall, H.K., Dickens, G.R., Backman, J., 2015. Carbon and oxygen isotopes of bulk carbonate in sediment deposited beneath the eastern equatorial Pacific over the last 8 million years. *Paleoceanography*, 30, 1261-1287.
- Reimer, P.J., Bard, E., Bayliss, A., Beck, J.W., Blackwell, P.G., Ramsey, C.B., Buck, C.E., Cheng, H., Edwards, R.L., Friedrich, M., Grootes, P.M., Guilderson, T.P., Hafliðason, H., Hajdas, I., Hatte, C., Heaton, T.J., Hoffmann, D.L., Hogg, A.G., Hughen, K.A., Kaiser, K.F., Kromer, B., Manning, S.W., Niu, M., Reimer, R.W., Richardson, D.A., Scott, E.M., Southon, J., Staff, R.A., Turney, C.S.M., van der Plicht, J., 2013. IntCal13 and Marine13 radiocarbon age calibration curves 0-50,000 years cal BP. *Radiocarbon* 55, 1869-1887.
- Richey, J.N., 2007. A 1400-year multi-proxy record of climate variability from the northern Gulf of Mexico, Unpublished. M.Sc., University of South Florida, Florida, USA, 66 pp.
- Rind, D., Overpeck, J.T., 1993. Hypothesized causes of decade-to-century climate variability: climate model results. *Quaternary Science Reviews* 12, 357-374.
- Rosenthal, Y., Lohman, K.C., 2002. Accurate estimation of sea surface temperatures using

- dissolution-corrected calibrations for Mg/Ca paleothermometry. *Paleoceanography* 17.  
doi: 10.1029/2001PA000749.
- Rosenthal, Y., Linsley, B., 2006. Mg/Ca and Sr/Ca paleothermometry from calcareous marine fossils, *Encyclopedia of Quaternary Sciences*. Elsevier Ltd., 24 pp.
- Rosenthal, Y., Lear, C.H., Oppo, D.W., Linsley, B.K., 2006. Temperature and carbonate ion effects on Mg/Ca and Sr/Ca ratios in benthic foraminifera: the aragonite species *Hoeglundina elegans*. *Paleoceanography* 21. doi: 10.1029/2005PA001158.
- Rothlisberger, F., 1986. 10000 Jahre Gletschergeschichte der Erde, mit einem Beitrag von M.A. Geyh. Sauerländer, Aarau und Frankfurt am Main, 416 pp.
- Saenger, C., Cohen, A.L., Oppo, D.W., Halley, R.B., Carilli, J.E., 2009. Surface-temperature trends and variability in the low-latitude North Atlantic since 1552. *Nature Geoscience Letters* 2, 492-946.
- Shackleton, N.J., 1974. Attainment of isotopic equilibrium between ocean water and the benthonic foraminifera genus *Uvigerina*: isotopic changes in the ocean during the last glacial. *Colloques Internationaux du Centre National de la Recherche Scientifique* 219, 203-210.
- Sholkovitz, E.R., Landing, W.M., Lewis, B.L., 1994. Ocean particle chemistry: the fractionation of rare earth elements between suspended particles and seawater. *Geochimica et Cosmochimica Acta* 58, 1567-1579.
- Stansell, N.D., Steinman, B.A., Abbot, M.B., Rubinov, M., Roman-Lacayo, M., 2013. Lacustrine stable isotope record of precipitation changes in Nicaragua during the Little Ice Age and Medieval Climate Anomaly. *Geology* 41, 151-154.
- Stoll, H.M., Schrag, D.P., Clemens, S.C., 1999. Are seawater Sr/Ca variations preserved in Quaternary foraminifera? *Geochimica et Cosmochimica Acta* 63, 3535-3547.
- Stuiver, M., Reimer, P.J., Reimer, R.W., 2020. CALIB 7.10 {WWW program} at <http://calib.org>.
- Switzer, A.D., Jones, B.G., 2008. Large-scale washover sedimentation in a freshwater lagoon from the southeast Australian coast: sea-level change, tsunami or exceptionally large



- storm? *The Holocene* 18, 787-803.
- Taylor, S.R., McLennan, S.M., 1985. *The continental crust: its composition and evolution*. Blackwell Scientific Publications, 312 pp.
- Team, R.C., 2013. R: a language and environment for statistical computing In: *Computing, R Foundation for Statistical (Ed.)*, Vienna, Austria.
- Thorrold, S.R., Campana, S.E., Jones, C.M., Swart, P.K., 1997. Factors determining  $\delta^{13}\text{C}$  and  $\delta^{18}\text{O}$  fractionation in aragonitic otoliths of marine fish. *Geochimica et Cosmochimica Acta* 61, 2909-2919.
- Tipping, R., Davies, A., McCulloch, R., Tisdall, E., 2008. Response to late Bronze Age climate change of farming communities in north east Scotland. *Journal of Archaeological Science* 35, 2379-2386.
- Trouet, V., Diaz, H.F., Wahl, E.R., Viau, A.E., Graham, R., Graham, N., Cook, E.R., 2013. A 1500-year reconstruction of annual mean temperature for temperate North America on decadal-to-multidecadal time scales. *Environmental Research Letters* 8. doi:10.1088/1748-9326/8/2/024008.
- Turekian, K.K., Wedepohl, K.H., 1961. Distribution of the elements in some major units of the Earth's crust. *Geological Society of America Bulletin* 72, 175-192.
- van Hengstum, P.J., Donnelly, J.P., Kingston, A.W., Williams, B.E., Scott, D.B., Reinhardt, E.G., Little, S.N., Patterson, W.P., 2015. Low-frequency storminess signal at Bermuda linked to cooling events in the North Atlantic region. *Paleoceanography* 30, 52-76.
- Wahl, E.R., Diaz, H.F., Ohlwein, C., 2012. A pollen-based reconstruction of summer temperature in central North America and implications for circulation patterns during medieval times. *Global and Planetary Change* 84-85, 66-74.
- Wang, H., Chen, J., Zhang, S., Zhang, D.D., Wang, Z., Xu, Q., Chen, S., Wang, S., Hang, S., Chen, F., 2018. A chironomid-based record of temperature variability during the past 4000 years in northern China and its possible societal implications. *Climate of the Past* 14, 383-396.

- Wang, T., Surge, D., Mithen, S., 2012. Seasonal temperature variability of the Neoglacial (3300-2500 BP) and Roman Warm Period (2500-1600 BP) reconstructed from oxygen isotope ratios of limpet shells (*Patella vulgata*), Northwest Scotland. *Palaeogeography, Palaeoclimatology, Palaeoecology* 317-318, 104-113.
- Wang, T., Surge, D., Walker, K.J., 2013. Seasonal climate change across the Roman Warm Period/Vandal Minimum transition using isotope sclerochronology in archaeological shells and otoliths, southwest Florida, USA. *Quaternary International* 308-309, 230-241.
- Wanner, H., Solomina, O., Grosjean, M., Ritz, S.P., Jetel, M., 2011. Structure and origin of Holocene cold events. *Quaternary Science Reviews* 30, 3109-3123.
- Wassenburg, J.A., Immenhauser, A., Richter, D.K., Niedermayr, A., Riechelmann, S., Fietzke, J., Scholz, D., Jochum, K.P., Fohlmeister, J., Schroder-Ritzrau, A., Sabaoui, A., Riechelmann, D.F.C., Schneider, L., Esper, J., 2013. Moroccan speleothem and tree ring records suggest a variable positive state of the North Atlantic Oscillation during the Medieval Warm Period. *Earth and Planetary Science Letters* 375, 291-302.
- Wejnert, K.E., Thunell, R.C., Astor, Y., 2013. Comparison of species-specific oxygen isotope paleotemperature equations: sensitivity analysis using planktonic foraminifera from the Cariaco Basin, Venezuela. *Marine Micropaleontology* 101, 76-88.
- Wignall, B., 1995. Sedimentology and diagenesis of the Cayman (Miocene) and Pedro Castle (Pliocene) Formations at Safe Haven, Grand Cayman. British West Indies, Edmonton, AB. M.Sc., University of Alberta, 110 pp.
- Winter, A., Appeldoorn, R.S., Bruckner, A., Williams, E.H., Goenaga, C., 1998. Sea surface temperatures and coral reef bleaching off La Parguera, Puerto Rico (northeastern Caribbean Sea). *Coral Reefs* 17, 377-382.
- Wurtzel, J.B., Black, D.E., Thunell, R.C., Peterson, L.C., Tappa, E.J., Rahman, S., 2013. Mechanisms of southern Caribbean SST variability over the last two millennia. *Geophysical Research Letters* 40, 5954-5958.

**CHAPTER 5**

**DIAGENESIS IN PLEISTOCENE (80 TO 500 KA) CORALS FROM THE  
IRONSHORE FORMATION: IMPLICATIONS FOR PALEOCLIMATE  
RECONSTRUCTIONS**

**1. Introduction**

Corals incorporate numerous isotopes and various elements from the surrounding seawater into their aragonite skeletons during growth. These chemical signatures can be used for dating through U-series techniques and for tracking climate change through time using temperature sensitive parameters (e.g.,  $\delta^{18}\text{O}$ , element/Ca ratios). These techniques, however, can only be used if the coral skeletons have not undergone diagenesis, which can occur rapidly upon coral death and becomes increasingly more likely as the age of the coral increases (Hendy et al., 2007; Webb et al., 2009). Applying such techniques to older corals is therefore limited by the fact that the skeletal aragonite of the coral is extremely susceptible to diagenesis that will commonly alter the mineralogy and chemistry of the skeletons (Muller et al., 2001; McGregor and Gagan, 2003; Allison et al., 2007; Nothdurft et al., 2007; Nothdurft and Webb, 2009; Cochran et al., 2010).

X-ray diffraction (XRD), thin section analysis, and/or scanning electron microscopy (SEM) are commonly used to demonstrate that coral skeletons have undergone little or no diagenetic change (e.g., Hendy et al., 2007; Nothdurft and Webb, 2007; McGregor and Abram, 2008). These techniques, however, cannot identify subtle chemical changes in the coral skeletons that may have taken place with little or no physical alteration of the aragonite (Cross and Cross, 1983; Bar-Matthews et al., 1993). As such, analysis of the elemental (Sr, Mg, Ca) and/or oxygen and carbon isotope composition of the coral skeleton should be used in conjunction with physical assessments to identify possible indicators of diagenetic alteration. Cross and Cross (1983) analyzed numerous *Montastrea annularis* and *Acropora palmata* skeletons from the modern, Holocene, and Pleistocene strata on Barbados and showed that there was a

progressive decrease in Mg and an increase in Sr as the pristine aragonitic skeletons were progressively altered under normal marine conditions. A similar trend was also evident in modern *Porites* from the Great Barrier Reef, where early marine diagenesis caused dissolution through incongruent leaching of the otherwise pristine aragonitic skeletons, resulting in elevated Sr/Ca ratios and reduced Mg/Ca ratios (Hendy et al., 2007). Hendy et al. (2007) also investigated the effects of early marine secondary aragonite cement in the skeletal voids of the corals, which also resulted in elevated Sr/Ca ratios and reduced Mg/Ca ratios. Pingitore (1978) and Martin et al. (1985), however, reported opposite trends in the proportion of Mg and Sr in Pleistocene *M. annularis* from Florida, such that late meteoric diagenesis caused the neomorphic calcitic skeletons to become enriched in Mg and depleted in Sr relative to their modern aragonitic counterparts. The mechanisms controlling the diagenetic trends (e.g., the degree of system openness; the volume and type of water flushed through the rock body) recorded in those studies can provide insights into the specific type of diagenetic alteration (meteoric vs marine) in corals.

Corals are common components of the biota in the Pleistocene Ironshore Formation (Units A-F) on the Cayman Islands (Fig. 5.1; Hunter and Jones, 1988, 1995; Hunter, 1994; Vezina et al., 1999; Coyne et al., 2007; Li and Jones, 2013a, 2013b). These corals grew during successive highstands (Fig. 5.2) at >400 ka (Unit A), 346 ka (Unit B), 229 ka (Unit C), 125 ka (Unit D), 101 ka (Unit E), and 80 ka (Unit F) based on U/Th radiometric dating of pristine coral skeletons and conches from each unit (Vezina et al., 1999; Coyne et al., 2007). The limestones in this formation have undergone differential diagenesis that is both geographically and temporally variable (Li and Jones, 2013a, 2013b). Coral skeletons from Units A to C in the Ironshore Formation have experienced moderate to extensive meteoric and/or marine diagenetic alteration, whereas corals in Units D to F underwent minimal diagenetic change. The reasons for this variable diagenesis have not been well established. Corals from this formation provide an ideal sample set for determining the impact of diagenesis on the mineralogy and isotopic



**Fig. 5.1.** Location maps. (A) Map showing location of the Cayman Islands. (B) Location of Pleistocene corals from Roger's Wreck Point (RWP), IS1, and George Town Harbor (BJC) shown by red star, and Magic Reef (modern corals) shown by yellow star on Grand Cayman. (C) Location of Little Cayman Quarry shown by red star on Little Cayman.

and elemental compositions of coral skeletons because well-preserved and altered corals from the same succession can be directly compared. Accordingly, this study assesses the diagenesis of the corals by using a combination of mineralogical (XRD, SEM, thin section) and elemental/isotopic (Sr, Mg, Ca,  $\delta^{18}\text{O}$ ,  $\delta^{13}\text{C}$ ) analyses to examine the type and

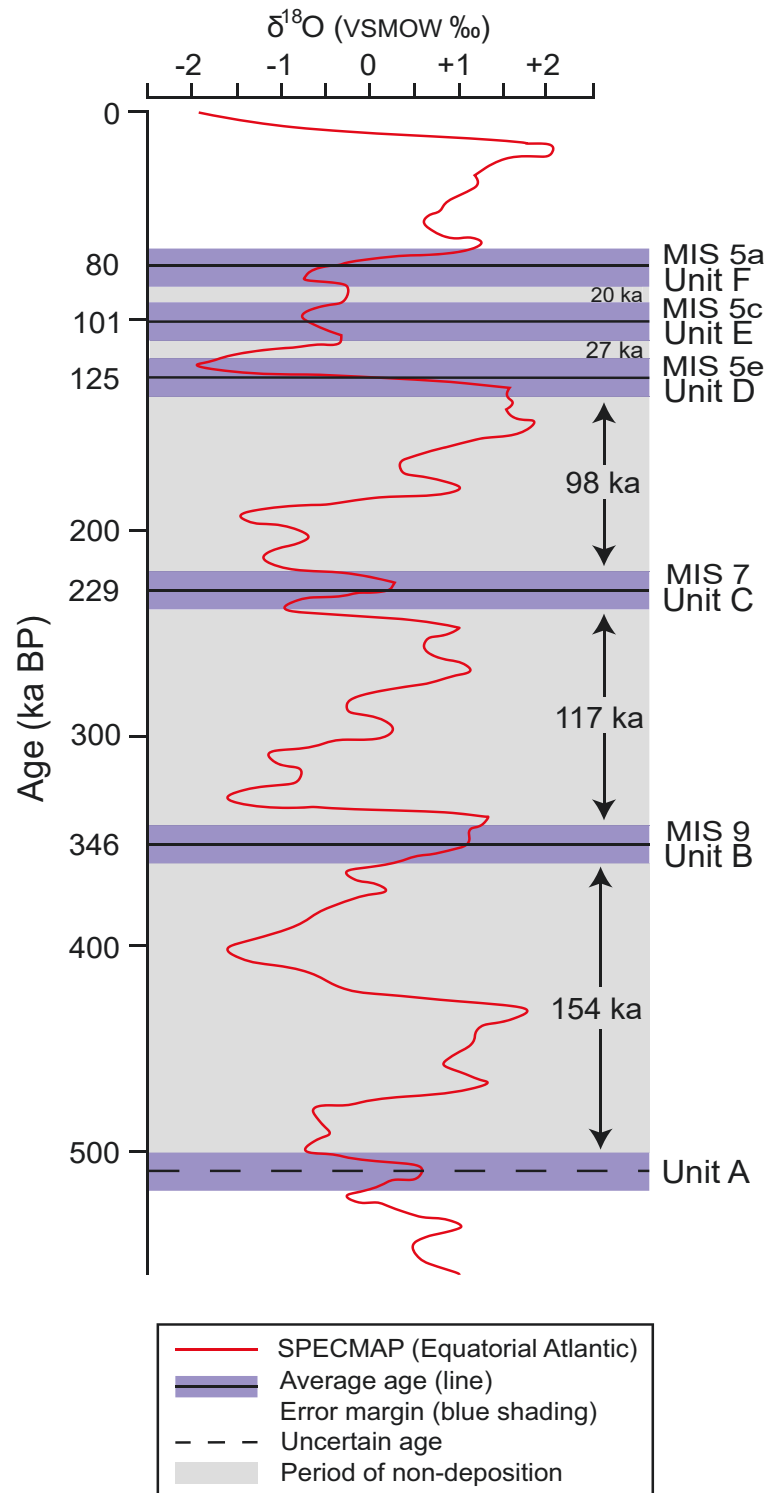


**Fig. 5.2.** SPECMAP- seawater oxygen isotopic composition of the Equatorial Atlantic Ocean through time (Imbrie and McIntyre, 2006). Ironshore Formation unit ages and period of non-deposition superimposed on curve.

controlling mechanisms of the diagenetic alteration. This process is calibrated against similar data obtained from modern corals collected from the west coast of Grand Cayman (Booker et al., 2019). This paper aims to illustrate how different types of meteoric and/or marine diagenesis (open or closed system) can alter coral skeletons, provides guidelines for assessing the degree of physical and chemical diagenetic change in corals, and highlights that with detailed diagenetic assessment of older fossil corals, reliable paleoclimate reconstructions can be developed.

## 2. Geological Setting

Grand Cayman and Little Cayman, the largest and smallest of the three Cayman Islands, respectively, are located in the Caribbean Sea (Fig. 5.1). Today, Grand Cayman experiences a humid sub-tropical climate, with ocean water temperatures from 25.3° to 30.5°C (average 28.5°C; Booker et al., 2019) and rainfall that is heaviest on the western parts of the islands (Ng, 1990).

On each of the Cayman Islands, Middle to Late Pleistocene limestones of the Ironshore Formation unconformably overlie Neogene limestones and dolostones of the Bluff Group (Jones and Hunter, 1990). The Ironshore Formation is divided into Units A-F based on their lithology and biota with the bounding unconformities commonly being highlighted by calcrete crusts (Vezina, 1997; Coyne, 2003). The stratigraphic framework used herein was established by Hunter and Jones (1988, 1995), Hunter (1994), Vezina (1997), Vezina et al. (1999), Coyne (2003), Coyne et al. (2007), and Li and Jones (2013b). Among the 33 coral species found in the Ironshore Formation, *Orbicella annularis*, *Montastrea cavernosa*, *Acropora palmata*, *A. cervicornis*, and *Porites porites* dominate (Table 5.1; Hunter and Jones, 1988, 1995; Hunter, 1994; Vezina, 1997; Coyne, 2003).

**Table 5.1.** Coral species of the Ironshore Formation.

Coral species	Unit A	Unit B	Unit C	Unit D	Unit E	Unit F
<i>Orbicella annularis</i>	○	●	○	●	●	○
<i>Montastrea cavernosa</i>				●	○	●
<i>Acropora</i> sp.		○		○		○
<i>Acropora palmata</i>	●		●	○	○	
<i>Acropora cervicornis</i>	○	○	●	○	○	
<i>Porites</i> sp.	○	○		○	○	○
<i>Porites porites</i>		○	●	○		
<i>Porites astreoides</i>		○		○		
<i>Siderastrea</i> sp.	○	○	○	●	○	
<i>Siderastrea sidera</i>				○		
<i>Diploria</i> sp.		○	○	○		○
<i>Diploria strigosa</i>	○	○		○	○	
<i>Diploria clivosa</i>		○		○	○	
<i>Diploria labyrinthiformis</i>				○	○	
<i>Agaricia</i> sp		○		○		
<i>Agaricia fragilis</i> (?)					○	
<i>Manicina</i> sp.					○	○
<i>Manicina areolata</i>				○		
<i>Dendrogyra cylindrus</i>		○		○		
<i>Dichocoenia stokesi</i> (?)		○		○		
<i>Favia fragrum</i>				○		
<i>Goniopora</i> (?)		○		○		
<i>Isophyllastrea rigada</i>				○		
<i>Eusmilia fastigata</i>				○		
<i>Mycectophillia ferox</i>				○		

Closed circles indicate the dominant species and open circles indicate that the species is present.



### 3. Samples

The distribution of the samples used in this study was controlled largely by coral availability. These samples included (1) a 16.4 cm high colony of *O. annularis* (IS1), from Unit D on the northwest corner of Grand Cayman (Fig. 5.1B), (2) two small (<10 cm high) *O. annularis* (LCQ2, LCQ5) from Unit D (Jones, 2019) in Little Cayman Quarry on the south-central part of Little Cayman (Fig. 5.1C), (3) four corals from cores from Rogers Wreck Point (4 cm diameter) on the northeast corner of Grand Cayman (Fig. 5.1B; RWP#13 (21 m long), RWP#14 (18.6 m long)) that included specimens from Units A to D, and (4) three corals from core BJC#1 (6 cm diameter, 10.8 m long) that came from a well drilled in water that was 14.5 m deep offshore George Town (west coast, Grand Cayman; Fig. 5.1B), that included specimens from Units D to F (Table 5.2).

### 4. Methodology

#### 4.1. X-ray and computer tomography scan production and analysis

Corals from Units C, D (west coast of Grand Cayman and Little Cayman), E, and F were imaged using a portable SY-31-100P X-ray machine with scans generated at 70kV for 0.8 second scan times. Corals from Units A, B, and D (east coast of Grand Cayman) were imaged using an Aquilion ONE helical computer tomographic (CT) scanner at InnoTech Alberta (Edmonton, Alberta). On those images, light-colored bands represent the densest material and the dark bands represent less dense material (Buddermeier et al., 1974; Moore and Krishnaswami, 1974). These images were used to determine the life span of the corals by counting growth band couplets, which have been shown to represent one year of coral growth (Knutson et al., 1972; Buddermeier et al., 1974). Grayscale curves from these images were produced using ERDAS Imagine, with values ranging from 0 – 252. The images and the corresponding gray level curves were used to produce maps of the coral growth bands for isotopic and elemental analysis.

**Table 5.2.** Data from growth bands in corals from Units A to F of the Ironshore Formation from Grand Cayman and Little Cayman. Meters below sea level (mbsl). Meters above sea level (masl).

Sample	Age (ka)	Location	Depth (mbsl)	Species	Height (cm)	Aragonite (wt%)	Mg (ppm)	Sr (ppm)	Ca (ppm)	Mg/Ca (mmol/mol)	Sr/Ca (mmol/mol)	$\delta^{13}\text{C}_{\text{VPDB}}$ (‰)	$\delta^{18}\text{O}_{\text{VPDB}}$ (‰)	$\delta^{18}\text{O}_{\text{VSMOW}}$ (‰)
Unit F	80	Offshore	13.7	<i>O.</i>	54.5									
		George Town core		<i>annularis</i>										
v					96	1746	5593	228807	10.3	9.2	-0.5	-2.8	28.0	
an		1			98	2075	5707	282486	12.1	9.2	+0.3	-2.6	28.2	
bl					98	2179	5741	306484	11.7	8.6	-0.2	-2.5	28.3	
do					93	1801	5771	282851	10.5	9.3	+0.2	-2.6	28.2	
ev					93	2559	5667	27176	15.5	9.5	-0.3	-2.5	28.3	
Unit E	101	Offshore	16.5	<i>O.</i>	45.0									
		George Town core		<i>annularis</i>										
n					90	1593	5829	293515	9.0	9.1	-1.2	-2.8	28.0	
ac		1			100	512	1858	93261	9.5	8.6	-0.5	-2.2	28.6	
br					100	1755	5697	303727	9.1	9.2	-1.2	-1.8	29.1	
cd					100	2126	5629	273014	12.8	9.4	-0.8	-2.1	28.8	
Unit D	125	Offshore	20.7	<i>M.</i>	28.0									
GTH-D		George Town core		<i>cavernosa</i>										
y		1			92	1269	6784	348800	6.0	8.9	+0.1	-3.0	27.8	
ai					89	1323	6590	358391	6.1	8.4	0.0	-3.6	27.2	
ar					92	1457	6688	363565	6.6	8.4	+0.5		27.8	



Sample	Age (ka)	Location	Depth	Species	Height (cm)	Aragonite (wt%)	Mg (ppm)	Sr (ppm)	Ca (ppm)	Mg/Ca (mmol/mol)	Sr/Ca (mmol/mol)	$\delta^{13}\text{C}_{\text{VPDB}}$ (‰)	$\delta^{18}\text{O}_{\text{VPDB}}$ (‰)	$\delta^{18}\text{O}_{\text{VSMOW}}$ (‰)
RWP-C	229	Roger's	4.9-	<i>O.</i>	11.3									
		Wreck	8.6	<i>annularis</i>										
		Point core	mbsl			80	2248	5819	430582	8.6	6.2	-2.4	-3.8	27.0
		13				76	2193	5893	442526	8.2	6.1	-2.9	-4.2	26.6
RWP-B	346	Roger's	8.6-	<i>O.</i>	69.7									
		Wreck	14.4	<i>annularis</i>										
		Point core	mbsl			0	3733	2528	375604	16.4	3.1	-6.7	-5.1	25.7
f						3	3695	2916	463320	13.2	2.9	-5.9	-4.6	26.2
n						4	3743	2828	56417	13.5	2.8	-6.3	-5.7	25.0
w						2	608	2467	326349	30.8	3.5	-5.4	-5.2	25.6
ar						2	3878	3119	457540	14.0	3.1	-3.3	-3.4	27.4
au						40	5852	3367	314653	30.7	4.9	-3.2	-5.7	25.0
bf						0	3748	3302	474661	13.0	3.2	-5.4	-5.7	25.0
bj						0	4506	3358	44825	16.6	3.4	-5.6	-5.6	25.1
bq						0	5693	2849	305780	30.7	4.3	-6.1	-5.7	25.0
ca						5	6304	4970	738999	14.1	3.0	-5.9	-5.4	25.3
ck						2	2374	1805	300315	13.0	2.8	-6.6	-5.2	25.6
cx														
du						11	3584	2637	462443	12.8	2.6	-5.8	-5.2	25.6
dz						85	5074	2289	294860	28.4	3.6	-6.6	-5.1	25.7
eq						0	4858	2446	437281	18.3	2.6	-4.5	-5.0	25.8
fa						63	4827	3768	292600	27.2	5.9	-6.9	-3.2	27.6
fk						60	3494	4726	928430	13.5	5.1	-2.0	-5.2	25.6
fp						0	3980	9345	427014	15.4	4.7	-0.6	-4.0	26.8

Sample	Age (ka)	Location	Depth	Species	Height (cm)	Aragonite (wt%)	Mg (ppm)	Sr (ppm)	Ca (ppm)	Mg/Ca (mmol/mol)	Sr/Ca (mmol/mol)	$\delta^{13}\text{C}_{\text{VPDB}}$ (‰)	$\delta^{18}\text{O}_{\text{VPDB}}$ (‰)	$\delta^{18}\text{O}_{\text{VSMOW}}$ (‰)
RWP-A	>500	Roger's	14.4-	<i>O.</i>	9.5									
		Wreck	18.4	<i>annularis</i>										
e		Point core	mbsl			97	4522	663	418595	17.8	7.3	0.0	-3.1	27.7
n		14				96	2882	6878	426079	11.2	7.4	+1.2	-3.4	27.4
x						99	4179	5477	289778	23.8	8.7	+2.0	-2.2	28.6
ah						98	2648	7048	437898	10.0	7.4	+2.0	-3.5	27.3
ap						33	8130	3763	285540	47.0	6.0	-0.5	-2.2	28.6

## *4.2. Mineralogy determination*

### *4.2.1. X-ray diffraction*

The mineralogy of 50 samples was determined by XRD analysis performed at the University of Alberta using a Rigaku Geigerflex Powder Diffractometer. Powdered microsamples (~300 µg) from corals in Units A (5 samples), B (17 samples), C (6 samples), D (15 samples), E (4 samples), and F (5 samples), taken from individual growth bands along the maximum growth axis of the corals were analyzed. The percentages of aragonite and calcite in each sample were determined following Li and Jones (2013a).

### *4.2.2 Thin section analyses*

Twenty-five standard (27 x 46 mm) thin sections were made from the matrix, well-preserved corals, and diagenetically altered corals found in cores from wells RWP#13, RWP#14, and BJC#1 (Coyne, 2003; Li and Jones, 2013a, 2013b). These thin sections were used to verify the mineralogy of the corals, examine the growth banding, and assess diagenetic alteration and cementation.

### *4.2.3 Scanning Electron Microscopy*

Fracture samples from selected corals from each unit were mounted on SEM stubs with conductive glue and sputter coated with carbon before being examined on a Zeiss Sigma Field Emission SEM with an accelerating voltage of 10 kV. Examination of the samples in this manner allowed microscale assessment of the fabrics and determination of any diagenesis that had affected the corals. Photoshop software was used to adjust the contrast of the SEM images used herein.

## *4.3. Elemental analysis*

Powdered samples (15-168 mg) of the individual coral growth bands, along the maximum growth axis (pristine and recrystallized), and the matrices of each unit

were analyzed for Mg, Ca, and Sr concentrations. The matrices surrounding the coral skeletons in the Ironshore Formation consists of low Mg-calcite (<4 wt% Mg; LMC) with *Halimeda*, foraminifera, and fragmentary mollusk and gastropod shells embedded in micrite (Li and Jones, 2013a, 2013b). Ten samples from Unit A included seven from individual coral growth bands and three from the matrices. Twenty samples from Unit B included 17 from individual coral growth bands and three from the matrices. Eight samples from Unit C included six from specific coral growth bands and two from the matrices. Eighteen samples from Unit D included 18 from specific coral growth bands and three from the matrices. Four samples from Unit E and five samples from Unit F were all from specific coral growth bands.

A Thermo Fisher iCAP-Q Inductively Coupled Plasma Mass Spectrometer (ICP-MS) in the Department of Earth and Atmospheric Science at the University of Alberta was used for elemental analysis. The samples were dissolved in 2 mL 50% HNO<sub>3</sub>, from which a 0.1 mL aliquot was added with 0.1 mL HNO<sub>3</sub> and 0.1 mL 100 ppb internal standards (Sc, In, and Bi) into 9.7 mL deionized water. The samples were analyzed using a 4-point calibration curve (0, 0.001, 0.002, and 0.004 ppm for Sr, and 0, 0.05, 0.1, and 0.2 ppm for Mg and Ca) with typical count rates of 300000 to 400000 cps for a 1 ppb concentration. Detection limits were 0.52, 10.41, and 0.005 ppb for Mg, Ca, and Sr, respectively.

#### 4.4. Isotope analysis

A Dremel 8200 drill with a 0.5 to 0.9 mm round (inner diameter) bit was used to obtain samples from the thecal walls along the maximum growth axis of the individual coral growth bands (Leder et al., 1996; Watanabe et al., 2001; Swart et al., 2002; Kilbourne et al., 2010; DeLong et al., 2011; Flannery et al., 2018) with spacing between each sample determined by the thicknesses of the growth bands. The following samples were collected:

- RWP-A: 5 samples
- RWP-B: 17 samples
- RWP-C: 6 samples
- RWP-D: 84 samples (42 light and dark bands) at 1 – 5 mm spacing
- IS1: 57 samples (29 light bands and 28 dark) at 1 – 5 mm spacing
- LCQ2: 3 samples
- LCQ5: 3 samples
- GTH-D: 46 samples (23 light and dark bands) at 1 – 5 mm spacing
- GTH-E: 88 samples (44 light and dark bands) at 1 – 5 mm spacing
- GTH-F: 166 samples (83 light and dark bands) at 1 – 6 mm spacing

The  $\delta^{13}\text{C}$  and  $\delta^{18}\text{O}$  values of each sample were determined using a Gasbench II system coupled with a Thermo MAT 253 Isotope Ratio Mass Spectrometer (IRMS) at the University of Alberta. Powdered samples, weighing 100-500  $\mu\text{g}$ , were put into a glass vial with a septum cap and held at a constant temperature of  $72^\circ\text{C}$ . A small amount (0.1 mL) of 100% phosphoric acid ( $72^\circ\text{C}$ ) was added to each sample to react for at least 1 hour. The resultant  $\text{CO}_2$  was then carried by a helium stream to the IRMS for  $^{18}\text{O}/^{16}\text{O}$  and  $^{13}\text{C}/^{12}\text{C}$  measurements. During each sequence, two in-house calcite lab standards (LSC-1:  $\delta^{13}\text{C} = -51.3\text{‰}$ ,  $\delta^{18}\text{O} = -16.1\text{‰}$  and LSC-2:  $\delta^{13}\text{C} = -22.0\text{‰}$ ,  $\delta^{18}\text{O} = -34.6\text{‰}$ ) and an international standard (NBS-18:  $\delta^{13}\text{C} = -5.0\text{‰}$ ,  $\delta^{18}\text{O} = -23.0\text{‰}$ ) were measured repeatedly. The C and O isotope compositions are reported using the  $\delta$  notation relative to VPDB (Vienna Pee Dee Belemnite) and VSMOW (Vienna Standard Mean Ocean Water) standards, respectively. The  $\delta^{18}\text{O}$  values were converted from VPDB to VSMOW using Equation 2.21 ( $\delta^{18}\text{O}_{\text{VSMOW}} = 1.0309[\delta^{18}\text{O}_{\text{VPDB}}] + 30.91$ ) from Sharp (2007). Analytical uncertainties ( $2\sigma$ ), relative to the standards are  $\pm 0.2\text{‰}$  for both  $\delta^{18}\text{O}$  and  $\delta^{13}\text{C}$ . Given that the samples used in this study are composed largely of aragonite and the laboratory standards are calcite, a correction of  $-0.38\text{‰}$  was made to the  $\delta^{18}\text{O}$  values following Kim et al. (2007; 2015).



## 5. Results

### 5.1. Indicators of diagenetic change

#### 5.1.1. Mineral composition

Coral growth bands from Units A, D (Grand Cayman and Little Cayman), E, and F generally contain >90 wt% aragonite, with most having >96 wt% aragonite, whereas corals from Unit C contain 54 to 98 wt% aragonite. Apart from one sample at the base of GTH-E that contained high-Mg calcite (HMC; 4-18 wt% Mg), all of the calcite is low Mg calcite (LMC: <4 wt% Mg). Samples from the base of Unit A contain LMC (<1 wt%) and dolomite (<3 wt%). Sample LCQ2 contains trace amounts of witherite. These analytical results are consistent with those provided by Li and Jones (2013a, 2013b).

Based on XRD analyses, Li and Jones (2013a, 2013b) showed that the matrices in the limestones from Units A-F of the Ironshore Formation contained 0-15 wt% aragonite in unit A, 0-10 wt% aragonite in unit B, 0-12 wt% aragonite in unit C, 0-30 wt% aragonite in unit D, 0-60 wt% aragonite in unit E, and 0-60 wt% aragonite in unit F (Table 5.3). The LMC and HMC in these units reflect the types of allochems that are present (Li and Jones, 2013a, 2013b).

#### 5.1.2. Petrographic analyses

The corals from Units A, C, D, E, and F exhibit varying degrees of skeletal preservation (Figs. 5.3, 5.4). Although largely devoid of cements, some corals from Units A, C, and D contain minor amounts of fibrous and/or finely crystalline cement in some of their pores. No cement was found in the corals from Units E and F. Isolated pores in some corals from Units E and F contain some biofragments of unknown origin. Overall, cements, biofragments, and/or borings are rare.

Many corals from Unit B with well-preserved external skeletons have been extensively replaced and their sclerodermite structures have been lost (Fig. 5.3). Although these corals have been recrystallized, most pores are open and contain only

**Table 5.3.** Data from the matrices from Units A to D in the Ironshore Formation at from Roger's Wreck Point on Grand Cayman.

Matrices	Aragonite (wt%)	Mg (ppm)	Sr (ppm)	Ca (ppm)	Mg/Ca (mmol/mol)	Sr/Ca (mmol/mol)	$\delta^{13}\text{C}$ (‰)	$\delta^{18}\text{O}_{\text{VPDB}}$ (‰)	$\delta^{18}\text{O}_{\text{VSMOW}}$ (‰)
Unit D	0 – 30	5803 – 9454	1088 – 4190	338751 – 349619	27.4 – 44.6	1.5 – 5.5	-6.3 to -6.0	-6.0 to -4.5	24.7 to 26.3
Unit C	0 – 12	4989 – 5757	1187 – 1303	340456 – 363705	24.2 – 26.1	1.5 – 1.7	-6.8 to -6.5	-5.5 to -3.9	25.2 to 26.9
Unit B	0 – 10	6734 – 10824	1222 – 1339	353060 – 353985	31.4 – 50.6	1.5 – 1.7	-6.9 to -5.3	-5.5 to -5.2	25.2 to 25.6
Unit A	0 – 15	5575 – 13941	914 – 4182	346108 – 356943	26.6 – 65.6	1.2 – 5.5	-7.2 to -5.5	-5.0 to -3.5	25.8 to 27.3

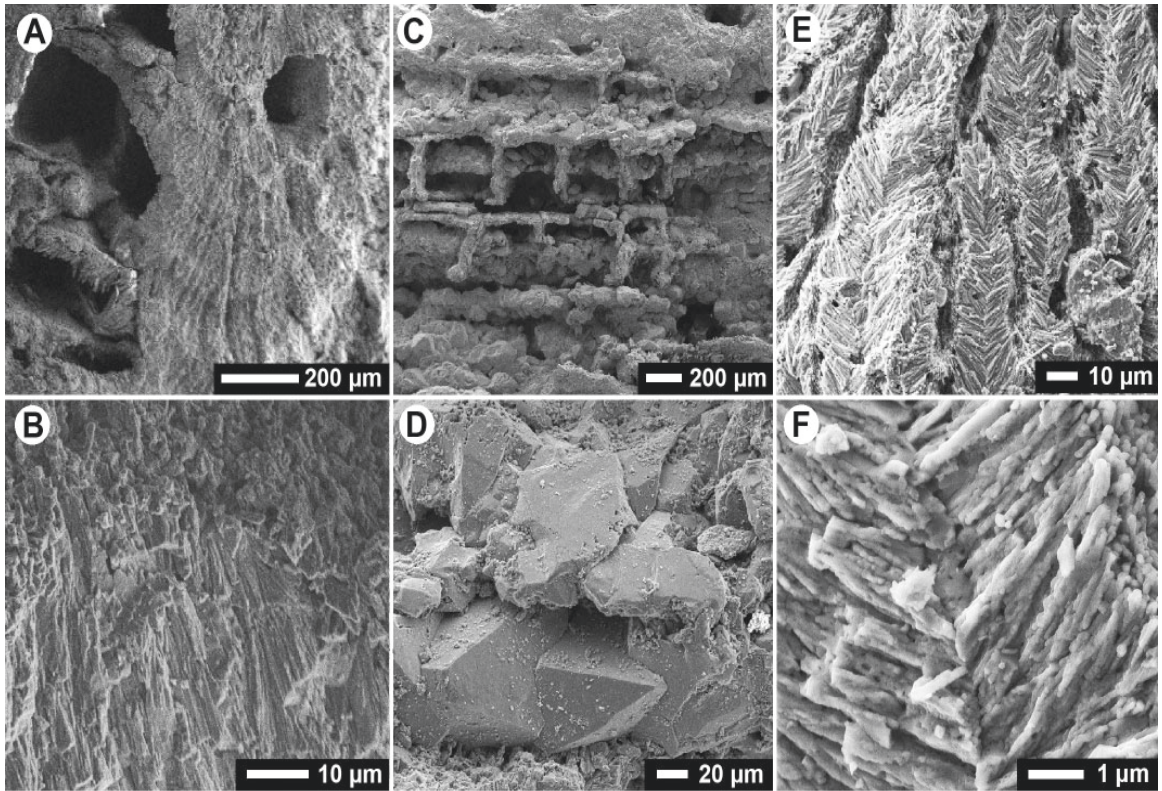


**Fig. 5.3.** SEM images from the Ironshore Formation corals. (A) Oblique view of theca structure in a coral from Unit A, displaying well developed thecal walls. (B) Aragonite needles along the thecal wall of a coral from Unit A. (C) Theca structure from a Unit B coral, displaying recrystallized thecal walls and endotheal dissepiments. (D) Close up image of replacive calcite rhombs from a coral in Unit B. (E) Sclerodermite structures in a coral from Unit C. (F) Close up of the sclerodermite structures showing aragonite needle bundles in a coral from Unit C.

minor amounts of finely crystalline cements.

### 5.2. Elemental concentrations

Analyses of 56 samples from summer and winter growth bands in 10 corals from Units A-F, yielded 93261 to 738999 ppm Ca, 1805 to 7252 ppm Sr, 512 to 8130 ppm Mg,



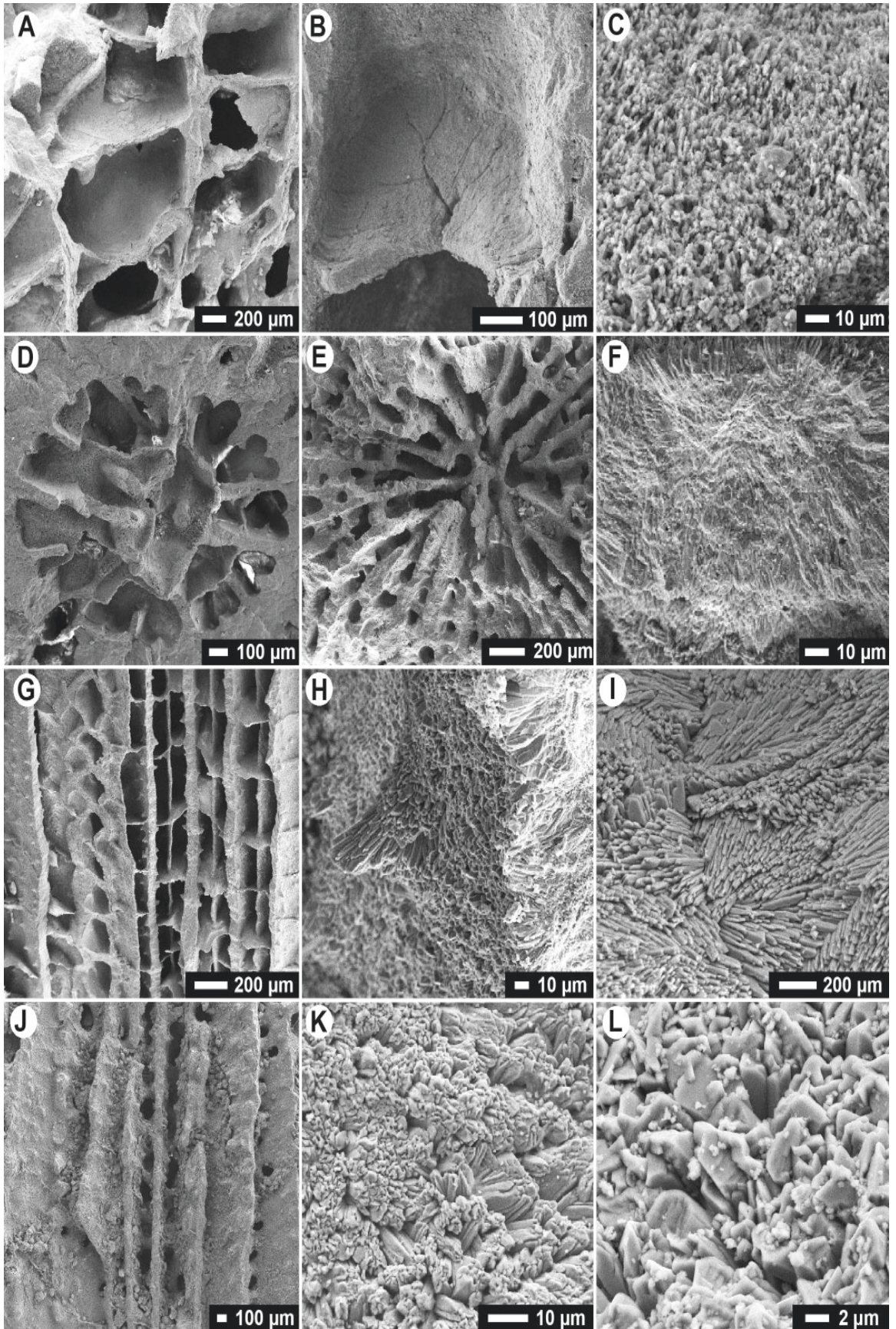


**Fig. 5.4.** SEM images from the Ironshore Formation corals. (A) Theca structure from a coral in Unit D (GTH), displaying well-preserved thecal walls, endothecal dissepiments, and open pore spaces. (B) Close up of thecal wall and endothecal dissepiment, displaying aragonite needle bundles from a coral in Unit D (GTH). (C) Close up of the endothecal dissepiment from (B) showing primary aragonite needles. (D) Corallite in a coral from Unit D (IS1), displaying well-developed coenosteum, septal structures, and open pore spaces. (E) Corallite from a coral in Unit D (RWP), displaying well-developed coenosteum, septal structures, and open pore spaces. (F) Close up of septa from (E) showing aragonite needles. (G) Theca structure from a coral in Unit E, displaying thecal walls, endothecal dissepiments, and open pore spaces. (H) Close up image of thecal wall from a coral in Unit E, displaying aragonite needle bundles. (I) Close up image of endothecal dissepiment from a coral in Unit E, displaying aragonite needle bundles. (J) Theca structure from a coral in Unit F, displaying thecal walls and endothecal dissepiments, some pores contain biofragments; of unknown origin. (K) Aragonite needle bundles from the thecal wall of a coral in Unit F. (L) Close up image of the aragonite needle bundles from (K), displaying bladed crystal shape. All images display open pore spaces and are devoid of cements.

---

Mg/Ca ratios of 3.2 to 47.0 mmol/mol, and Sr/Ca ratios of 2.6 to 9.5 mmol/mol (Fig. 5.5, Table 5.2). The highest Mg/Ca values (>15 mmol/mol) are from corals in Units A and B, whereas the lowest values (<6 mmol/mol) are from Unit D. The highest Sr/Ca values (>8 mmol/mol) are from Units D, E, and F, whereas the lowest values (<5 mmol/mol) are in Unit B (Fig. 5.5B).

The range of Mg/Ca ratios in corals from the Ironshore Formation (3.2 to 47.0 mmol/mol) is greater than that of the modern Cayman corals (4.4-11.6 mmol/mol; Booker et al., 2019; Fig. 5.5B). If the highest ratios from Units A and B (<50 wt% aragonite) are



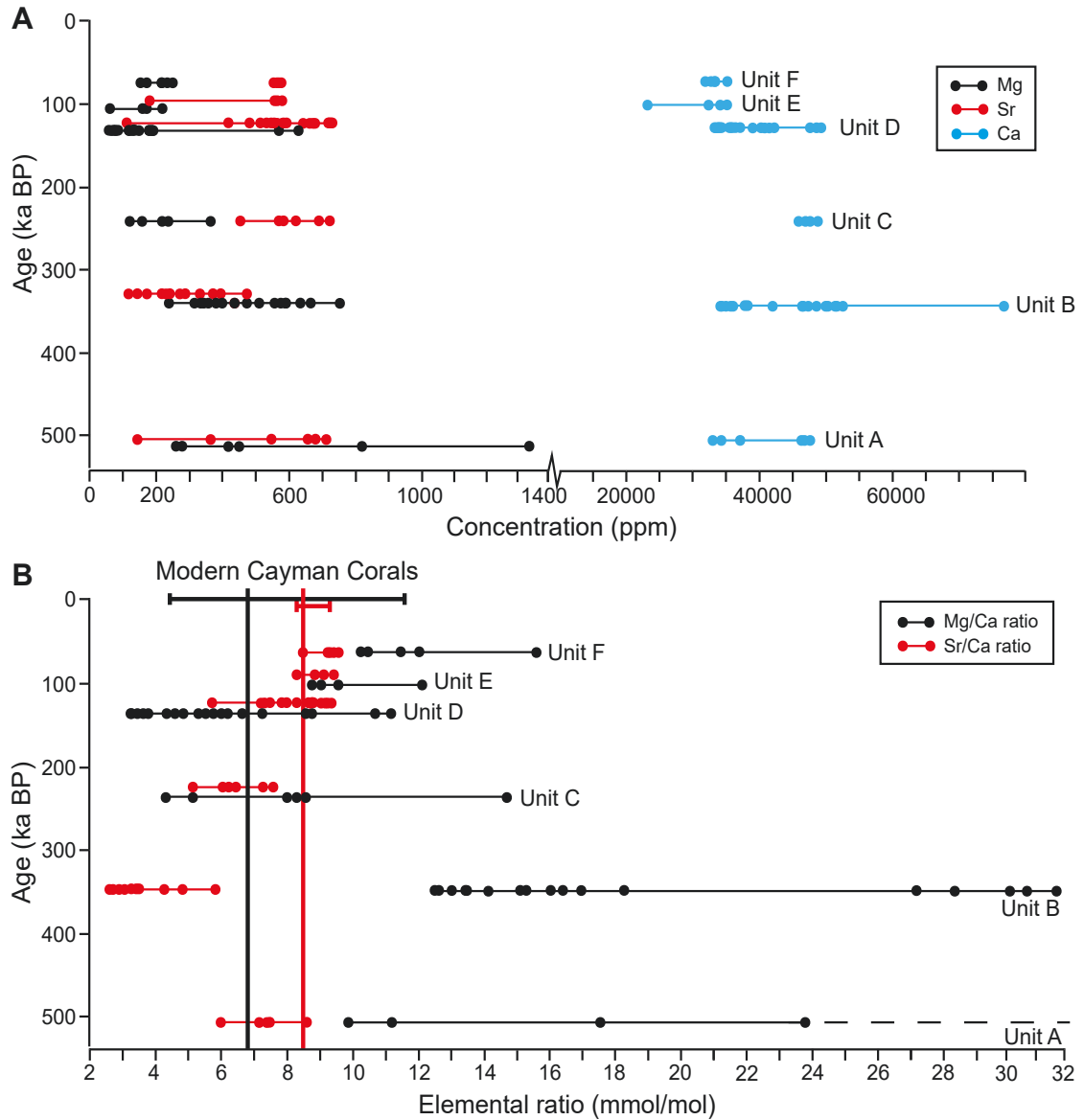


**Fig. 5.5.** (A) Comparison of the elemental concentrations (Mg (black), Sr (red), Ca (blue)) from the Ironshore Formation corals, separated by unit. Elevated Mg and lower Sr values in Units A and B, whereas the corals from Units C to E have lower Mg and higher Sr concentrations. (B) Comparison of the Mg/Ca ratios (black) and Sr/Ca ratios (red) from the Ironshore Formation corals, separated by unit. Elevated Mg/Ca and lowered Sr/Ca ratios in the corals from Unit A to C, whereas the corals from Units D to F have Sr/Ca and Mg/Ca ratios that are consistent with those of modern corals. Dashed line represents values that extend off the graph, 40.7 mmol/mol Mg/Ca for samples from Unit A.

removed from the data set, then the range of 3.2 to 15.5 mmol/mol for the corals from Units C, D, E, and F is more consistent with that of the modern corals. The same is true for the Sr/Ca ratios. Removing the samples from Units A and B (<50 wt% aragonite), results in values between 5.1 and 9.5 mmol/mol, which is consistent with modern Cayman corals (8.3-9.2 mmol/mol).

The matrices in Units A, B, C, and D yielded 338751 to 363705 ppm Ca, 914 to 4182 Sr, 4989 to 13941 ppm Mg, Mg/Ca ratios of 24.2 to 65.6 mmol/mol, and Sr/Ca ratios of 1.2 to 5.5 mmol/mol (Table 5.3). The Mg/Ca ratios from the matrices (>24.0 mmol/mol Mg/Ca) are significantly higher than those from the primary skeletal material (3.2 to 15.5 mmol/mol Mg/Ca). The Sr/Ca values for the matrices (<5.5 mmol/mol Sr/Ca) are lower than those from the primary skeletal material (5.1 to 9.5 mmol/mol Sr/Ca).

### 5.3. *Stable isotopes*

The  $\delta^{13}\text{C}$  values of the corals from the Ironshore Formation range from  $-6.9$  to  $+3.0\text{‰}$ . Corals with <85 wt% aragonite (e.g., Units B and C) have more negative  $\delta^{13}\text{C}$  values ( $-6.9$  to  $-1.9\text{‰}$ ) than those corals with higher percentages of aragonite ( $-1.8$  to  $+2.0\text{‰}$ ; Fig. 5.6A. Supplementary Tables 5.1-5.3). The  $\delta^{18}\text{O}$  values of corals from the Ironshore Formation range from 24.1 to 29.5‰. Corals with <85 wt% aragonite have lower  $\delta^{18}\text{O}$  values than those corals with higher aragonite content (<26.0‰; Fig. 5.6B Supplementary Tables 5.1-5.3).

## 6. Discussion

### 6.1. *Diagenesis*

Units A to D of the Ironshore Formation are separated from each other by unconformities that developed during sea level lowstands, which led to exposure of the older strata to diagenesis by meteoric waters for long periods of time (Fig. 5.2). Reliable paleoclimate reconstructions can only be obtained from the corals in these units if their

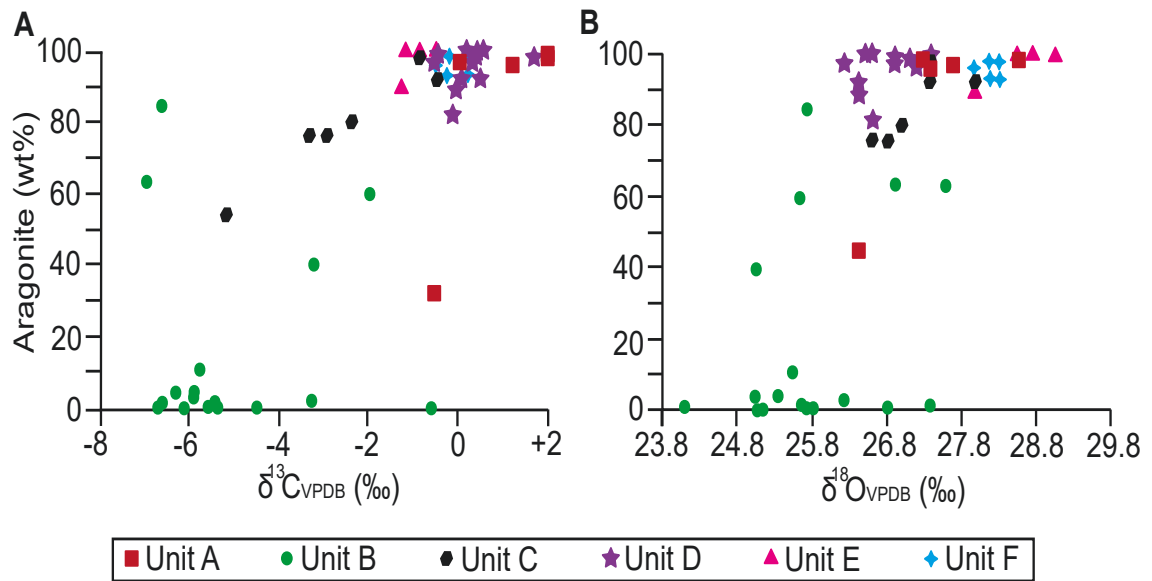


**Fig. 5.6.** Graphs showing the amount of aragonite in the corals from the Ironshore Formation relative to (A)  $\delta^{13}\text{C}$  values and (B)  $\delta^{18}\text{O}$  values.

aragonitic skeletons have retained their original isotopic and elemental compositions. Most coral skeletons in Units A, C, D, E, and F of the Ironshore Formation display minimal evidence of physical diagenetic alteration, whereas the coral skeletons from Unit B have clearly undergone extensive diagenetic alteration (Figs. 5.3, 5.4). For some coral skeletons from Units A and C, however, various geochemical parameters indicate that they have experienced some diagenetic alteration even though their aragonitic skeletons appear physically intact.

The mechanisms responsible for differential diagenesis in the coral skeletons from each unit of the Ironshore Formation can be assessed by considering the constituent units in terms of how open their systems were to diagenetic fluids. An open system has a high water/rock ratio, whereas a closed system has a low water/rock ratio (Kinsman, 1969; Pingitore, 1978; Veizer, 1983). In the context of carbonate successions, a system is considered open if (1) the  $\delta^{18}\text{O}$  values of the altered coral skeletons are consistent with



the  $\delta^{18}\text{O}$  values of the diagenetic fluid (e.g., meteoric water or seawater), (2)  $\delta^{13}\text{C}$  values of the coral skeletons are highly variable (Fig. 5.7), (3) distribution coefficients of Mg ( $K^{\text{Mg}}$ ) and Sr ( $K^{\text{Sr}}$ ) in the coral skeletons relative to the formation fluids are  $< 1$ , and (4) altered coral skeletons have a higher Mg content relative to the original aragonite (occurs as a result of meteoric alteration, Fig. 5.8; Kinsman, 1969; Pingitore, 1978; Brand and Veizer, 1983; Meyers and Lohman, 1983; Veizer, 1983; Martin et al., 1985). In this context, Pingitore (1978) defined alloenrichment as the precipitation of a diagenetic mineral from a liquid enriched in trace elements or isotopes from an external or in situ source before entering the diagenetic site. Conversely, he defined autodepletion as the preferential loss of trace elements at the diagenetic site due to high water flow rates relative to reaction rates.

Coral skeletons in Unit B are characterized by obvious diagenetic changes with most displaying clear evidence of recrystallization and various types of prismatic/blocky calcite cements in their pores (Li and Jones, 2013a, 2013b). The  $\delta^{18}\text{O}$  values of the individual growth bands in the coral skeletons range from 24.1 to 27.6‰, which indicates alteration by meteoric waters, which is depleted in  $^{18}\text{O}$  relative to ocean water (modern meteoric water on Grand Cayman:  $-1.6$  to  $-7.3$ ‰, average  $-4.3$ ‰; Ng, 1990). The  $\delta^{13}\text{C}$  values vary by  $\sim 6$ ‰ ( $-6.1$  to  $-0.6$ ‰), the  $K^{\text{Mg}}$  and  $K^{\text{Sr}}$  are  $< 1$ , and the Mg content of the altered coral skeletons (2374 to 6304 ppm, Fig. 5.8) is high relative to unaltered modern coral skeletons (1035 to 2505 ppm; Booker et al., 2019). These parameters clearly indicate that the coral skeletons in Unit B were altered in an open system where meteoric water was probably the primary diagenetic fluid (Fig. 5.9). Such diagenesis is consistent with the fact that Unit B is capped by an unconformity that developed over a period of  $\sim 67,000$  years (Fig. 5.2).

Although coral skeletons in Units A and C have largely retained their primary aragonite (90-100 wt%), their elemental and isotopic compositions indicate that subtle chemical diagenetic changes have taken place. The  $\delta^{18}\text{O}$  values of the coral skeletons

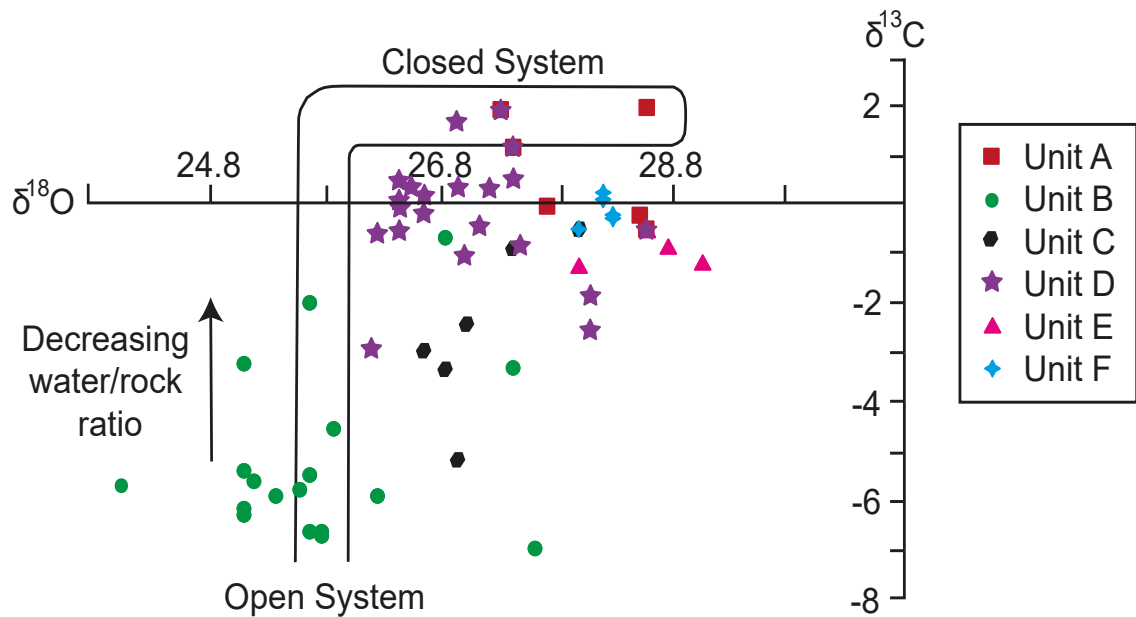


**Fig. 5.7.** Graph of the  $\delta^{18}\text{O}$  vs  $\delta^{13}\text{C}$  values showing the J-Shaped trend of Meyers and Lohman (1983) for the Ironshore Formation corals. The lower portion of the graph indicates an open system where diagenetic alteration was controlled by meteoric waters (narrow range of  $\delta^{18}\text{O}$  and variable  $\delta^{13}\text{C}$  values), whereas the top of the graph indicates a closed system (constant  $\delta^{13}\text{C}$  and varied  $\delta^{18}\text{O}$  values). This highlights the alteration styles in the Ironshore Formation corals, with Unit B being altered in an open system influenced by meteoric waters, Units A and C in a semi-open system influenced by seawater diluted by meteoric water, and Units D to F in closed systems.

(27.3 to 28.6‰ for Unit A, 26.6 to 28.0‰ for Unit C) indicate that the system was at least semi-closed relative to rainwater and seawater given that the  $\delta^{18}\text{O}$  seawater values for the equatorial Atlantic Ocean during the Pleistocene, as derived from the SPECMAP curve of Imbrie and McIntyre (2006), were  $-0.4$  to  $+1.8$ ‰ while the sediments of Unit A accumulated, and  $-1.0$  to  $+0.3$ ‰ when the sediments of Unit C accumulated (Fig. 5.2). The  $\delta^{13}\text{C}$  values of the coral skeletons from Unit A vary by  $\sim 3$ ‰ ( $-0.8$  to  $+2.0$ ‰), whereas those from Unit C vary by  $\sim 5$ ‰ ( $-5.1$  to  $-0.5$ ‰, Fig. 5.7). The  $K^{\text{Mg}}$  and  $K^{\text{Sr}}$

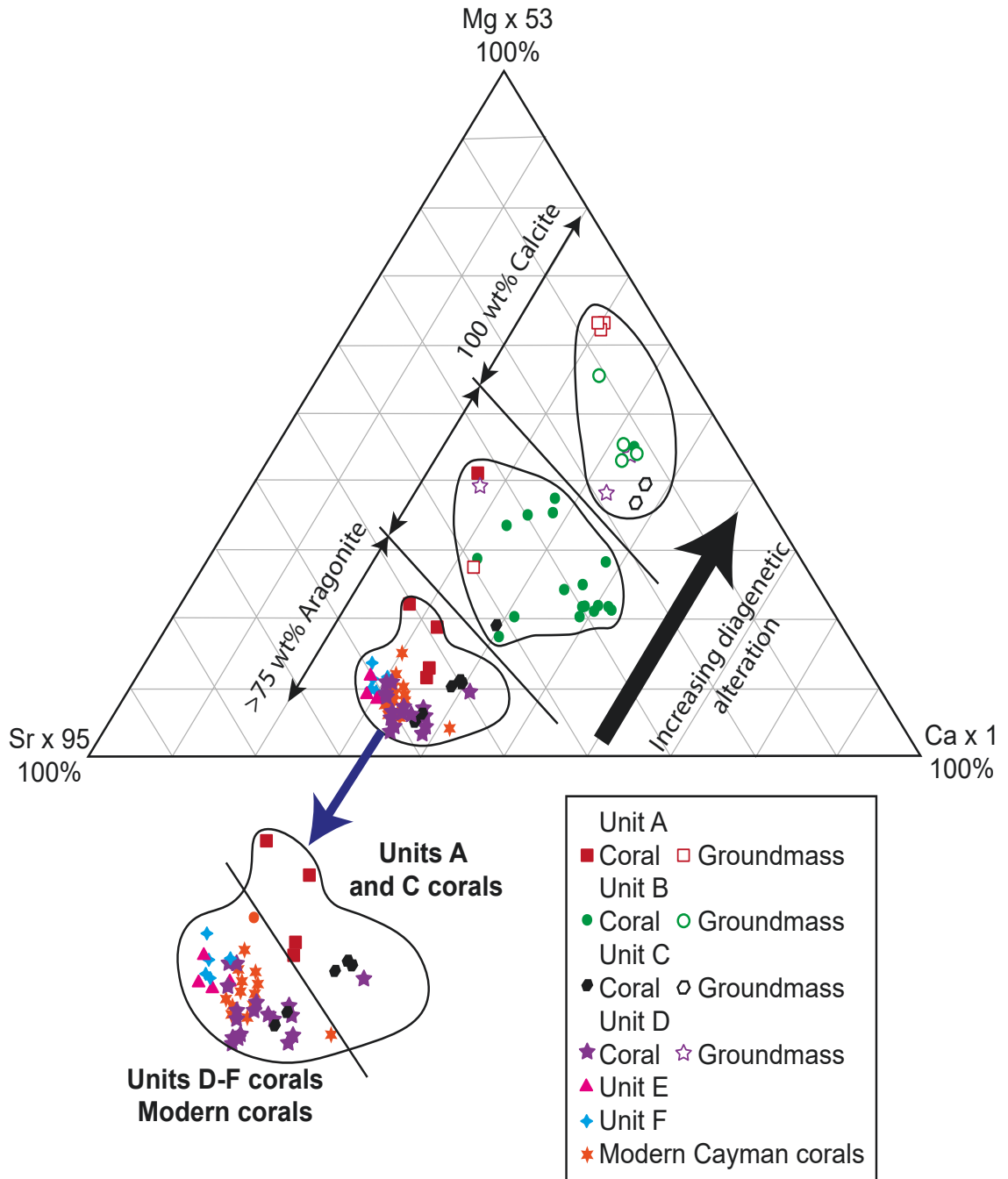


**Fig. 5.8.** Ternary diagram showing the relationship between the amount of aragonite and the elemental concentrations of the Ironshore Formation corals. Lower proportions of aragonite correspond to an increase in Mg and a reduction in Sr. Close up of corals with >75 wt% aragonite showing a clear division between the minimally altered corals from Units D to F and the modern Cayman corals, and the chemically altered corals of Units A and C. Sr and Mg concentrations are normalized to Ca concentration.

provide contradictory results, with Unit A having  $K^{Mg}$  and  $K^{Sr}$  values  $>1$  and Unit C having  $K^{Mg}$  and  $K^{Sr}$  values  $<1$ . The Mg content of the coral skeletons (2648 to 4522 ppm for Unit A, 1129 to 3727 ppm for Unit C) from these units is higher than that from pristine modern coral skeletons (Fig. 5.8). Collectively, these parameters indicate that diagenesis of the coral skeletons in Units A and C was probably mediated by seawater diluted by meteoric waters in a semi-open system, with Unit C having a more open system than Unit A (Fig. 5.9).

Evidence that the composition of the diagenetic fluids was modified (alloenrichment) comes from alteration of the matrix components found around the coral skeletons in Units A and C, which consist primarily of *Halimeda*, foraminifera, and fragmentary mollusk and gastropod shells. Originally composed of aragonite and HMC, these allochems are now largely dissolved and/or recrystallized to LMC (Li and Jones, 2013a, 2013b). The matrix components underwent more diagenesis relative to the corals because their higher surface area and roughness facilitated higher dissolution rates (Li and Jones, 2013a). Comparison of the elemental concentrations in the altered matrix to those of the original allochems (data from Martin et al. (1985) for mollusks, Delaney et al. (1996) for *Halimeda*, Toler et al. (2001) for foraminifera) shows that the aragonitic biofragments (mollusk, gastropod, *Halimeda*) replaced by calcite have higher Mg and lower Sr contents than the original aragonite. The foraminifera tests, however, have lost Mg, which led to an increase in the Mg content in the diagenetic fluid (e.g., Pingitore, 1976). Movement of the diagenetic fluids through the porous coral skeletons resulted in the loss of Sr from this material (autodepletion; Kinsman, 1969; Pingitore, 1976; Farfan et al., 2018). This reflects the fact that Mg ions are easily incorporated into the calcite crystal structure, whereas Sr is less compatible (Siegel, 1960; Finch and Allison, 2003; Sayani et al., 2011). Collectively, these processes altered the Mg/Ca (elevated) and Sr/Ca (reduced) ratios of the coral skeletons in Unit A and C without causing a change in their mineralogy.

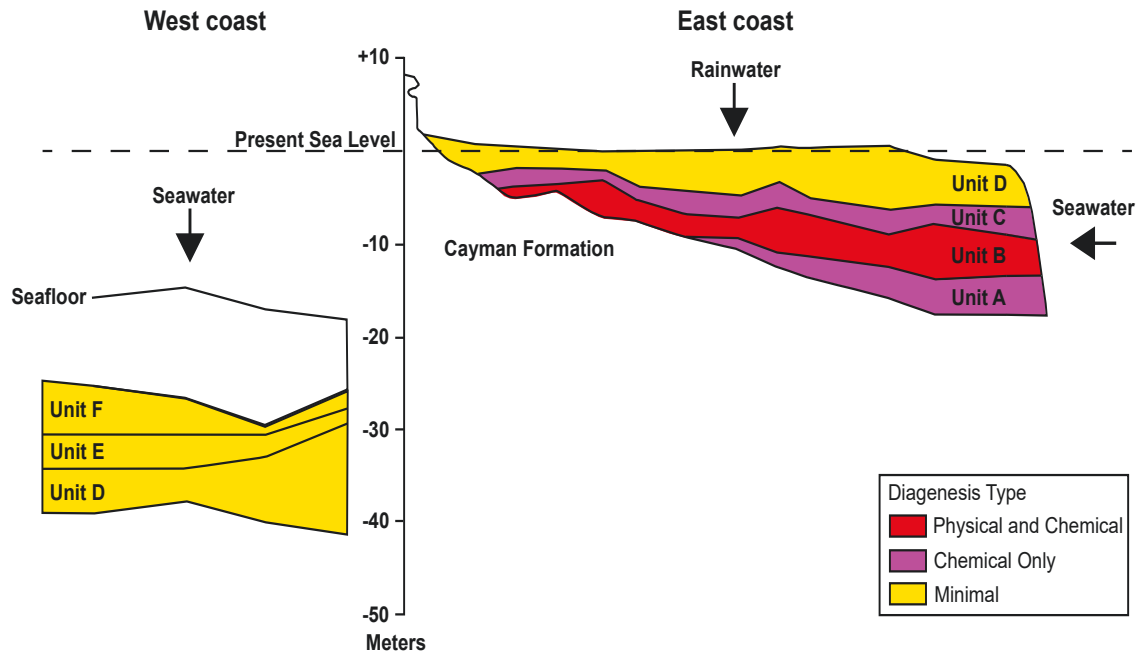


**Fig. 5.9.** Idealized cross-sections of the west (left) and east (right) coasts of Grand Cayman showing the types of diagenesis that affected the Ironshore Formation.

The coral skeletons in Units D, E, and F, which include the best preserved corals in the Ironshore Formation, are characterized by minimal physical and chemical alteration. The  $\delta^{18}\text{O}$  values for the coral skeletons in Units D (25.8 to 29.5‰), E (27.1 to 29.2‰), and F (27.1 to 29.1‰) have ranges that are generally higher than those of Units A-C, are different from those of modern meteoric water (−1.6 to −7.3‰, average −4.3‰; Ng, 1990), and the seawater that existed during their growth (Units D: −1.8 to +1.4‰, E: −0.6 to −0.4‰, F: −0.6 to +1.0‰ values from SPECMAP of Imbrie and McIntyre (2006)). The  $\delta^{13}\text{C}$  values vary by <1‰ (Fig. 5.7) and the  $K^{\text{Mg}}$  and  $K^{\text{Sr}}$  are >1 for Units D, E, and F. The coral skeletons in these units have Mg concentrations (512 to 2559 ppm) similar to those in pristine modern coral skeletons (Fig. 5.8). These lines of evidence indicate that these coral skeletons have not undergone significant diagenetic change (Fig. 5.9).

The progressive change from aragonite to calcite in the coral skeletons in the

Ironshore Formation is accompanied by an increase in the Mg content and a decrease in the Sr content (Fig. 5.8). Similar changes have been documented in Pleistocene corals from the Florida Keys (Siegel, 1960; Martin et al., 1985), Barbados (Pingitore, 1978), and mid-Holocene corals from the Huon Peninsula (McGregor and Gagan, 2003). The extensively altered coral skeletons in Unit B (<85 wt% aragonite), for example, have the highest Mg/Ca (up to 30.8 mmol/mol) and lowest Sr/Ca ratios (as low as 2.6 mmol/mol; Fig. 5.5B). This agrees with Pingitore (1978), Martin et al. (1985), McGregor and Gagan (2003), and Sayani et al. (2011) who showed that replacive calcite in coral skeletons typically has lower Sr/Ca ratios than the primary aragonite.

Pleistocene corals from Barbados (Cross and Cross, 1983) and modern corals from the Great Barrier Reef (Hendy et al., 2007) are characterized by an increase in Sr and a reduction in Mg as the aragonitic coral skeletons were altered by leaching and/or aragonite cements, which is a trend opposite to that found in other corals. Although Cross and Cross (1983) suggested that their study provided a baseline for assessing chemical diagenesis, this is only applicable for specimens that have undergone leaching. Pingitore (1976), however, suggested that the observed trends from a set of Pleistocene corals from Barbados were caused by closed system diagenesis in the vadose zone. Diagenetic changes, such as those documented by Pingitore (1976), Cross and Cross (1983), and Hendy et al. (2007), are not evident in the coral skeletons from Units A and C of the Ironshore Formation.

Given that diagenesis is more obvious and easier to discern from the elemental concentrations in coral skeletons than their isotopic concentrations (McGregor and Gagan, 2003; Sayani et al., 2011), the Mg/Ca and Sr/Ca ratios can be used to detect subtle diagenetic changes. Low Mg/Ca ratios and high Sr/Ca ratios in coral skeletons with >95 wt% aragonite, like those from Units D, E, and F, indicate that little or no diagenetic alteration has taken place (Fig. 5.8). Available information from multiple species of pristine modern coral skeletons (Fig. 5.10) indicates that a coral can be considered

viable for paleoclimatic studies providing that (1) the coral skeleton contains >95 wt% primary aragonite, (2) skeletal pores are devoid of cements, (3) Mg/Ca ratio is <12.0 mmol/mol, (4) Sr/Ca ratio is >8.0 mmol/mol, (5)  $\delta^{18}\text{O}$  values >25.1‰, and (6)  $\delta^{13}\text{C}$  values >-3.0‰ (Fig. 5.10). Although the above criteria act as guidelines for assessing the presence of physical and chemical diagenesis, it should be noted that coral skeletons are highly heterogeneous. Therefore, minimally altered portions of an otherwise well-preserved coral can skew the results and caution should always be used when interpreting geochemical proxy data from coral skeletons. Applying the suggested criteria to older fossil corals will ensure that the coral samples have been thoroughly checked for both physical and chemical diagenetic alteration. Based on these criteria, the Pleistocene corals from Units A, B, and C cannot be used for paleoclimate reconstruction, whereas the corals from Units D, E, and F have the potential of producing reliable paleoclimatic information.

## 6.2. Paleoclimate applications

Coral derived temperature calculations ( $T_{\text{cal}}$ ) using elemental (Sr/Ca and Mg/Ca ratios) and isotopic ( $\delta^{18}\text{O}$ ) concentrations are only viable if the coral has not been physically and chemically altered. Sr/Ca ratios derived from coral skeletons with secondary aragonite cements can lead to spuriously high temperature anomalies (Muller et al., 2001; Quinn and Taylor, 2006). In contrast, the use of Mg/Ca, Sr/Ca, and  $\delta^{18}\text{O}$ -geothermometers can lead to spuriously low temperature anomalies when secondary aragonite cements and/or dissolution of the primary aragonite skeleton has occurred (Enmar et al., 2000; Quinn and Taylor, 2006; Hendy et al., 2007).

For the coral skeletons from the Ironshore Formation, the effect that diagenesis had on the calculated paleotemperatures was tested by comparing the results derived from the Sr/Ca ratio (Swart et al., 2002; Smith et al., 2006; Saenger et al., 2008; Kilbourne et al., 2010; DeLong et al., 2011; Flannery and Poore, 2013; Alpert et al., 2017; Flannery et

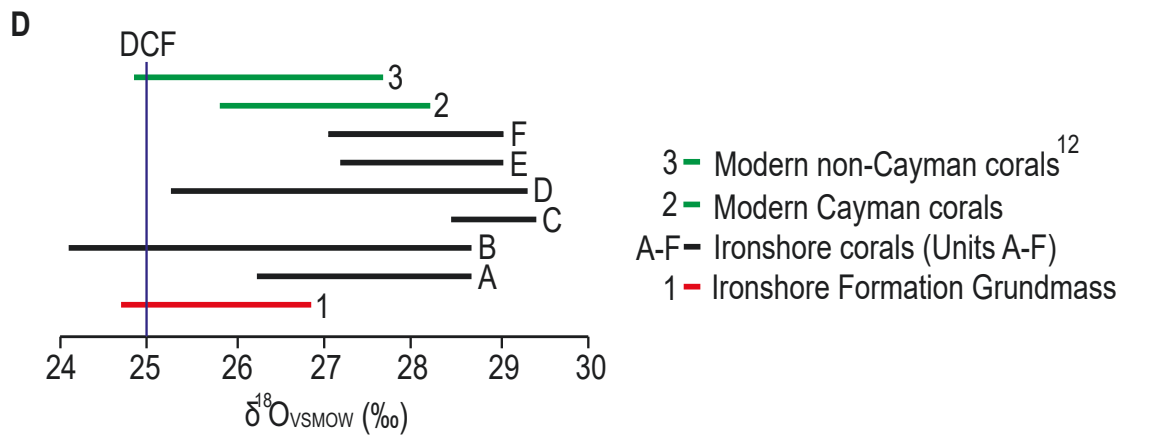
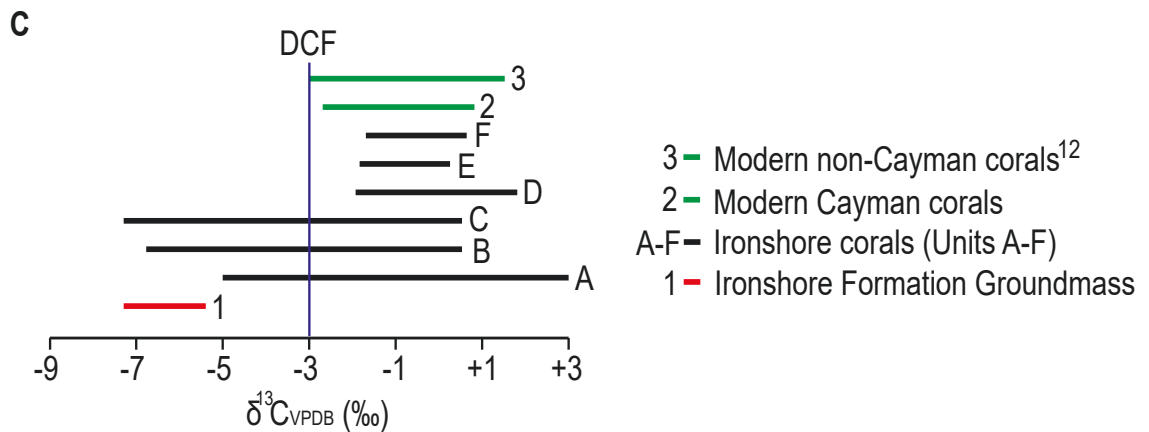
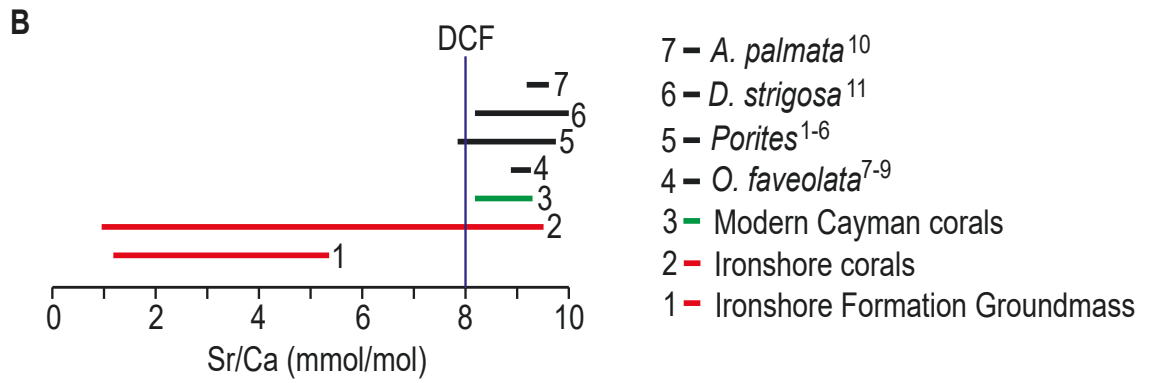
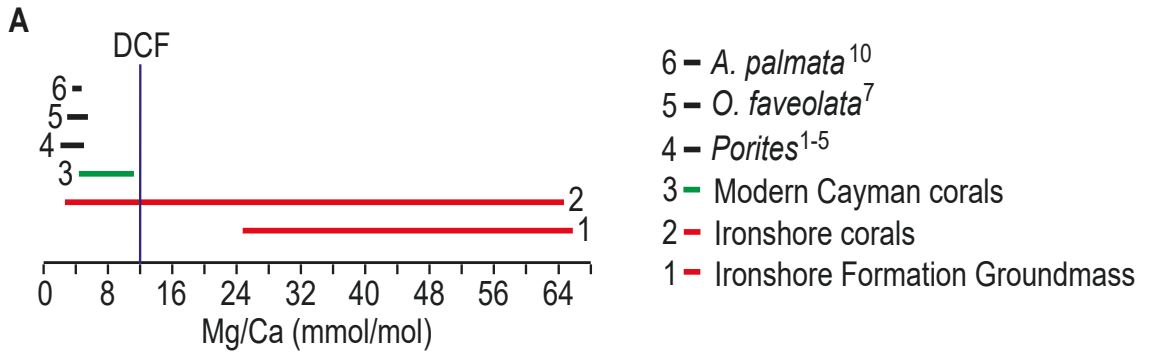




**Fig. 5.10.** Comparison of (A) Mg/Ca ratios, (B) Sr/Ca ratios, (C)  $\delta^{13}\text{C}$  values, and (D)  $\delta^{18}\text{O}$  values from the Ironshore Formation corals and others; Modern Cayman corals- Booker et al. (2019), 1- Mitsuguchi et al. (1996), 2- Sinclair et al. (1998), 3- Fallon et al. (2003), 4- Armid et al. (2011), 5- Sayani et al.(2011), 6- McCulloch et al. (1999), 7- Watanabe et al. (2001), 8- Saenger et al. (2008), 9- DeLong et al. (2007), 10- Reynaud et al. (2007), 11- von Reumont et al. (2016), 12- Swart (1983). Vertical blue lines indicate the cut off (DCF) values for corals that have been diagenetically altered.

---

al., 2018), the Mg/Ca ratio (Watanabe et al., 2001), and the  $\delta^{18}\text{O}$ -geothermometers (Leder et al., 1996; Watanabe et al., 2001; Smith et al., 2006; Kilbourne et al., 2010; Booker et al., 2019) that have been developed specifically for *Orbicella*. These  $T_{\text{cal}}$  were assessed relative to modern *Orbicella* that thrive in water temperatures of 15° to 32°C (Hunter, 1994), but prefer temperatures between 23° and 29°C (NOAA, 2016). Anomalously high temperatures are considered as  $T_{\text{cal}}$  higher than the max (29°C) value, whereas anomalously low temperatures are lower than the minimum (23°C) value. The extensively recrystallized coral skeletons in Unit B yielded  $T_{\text{cal}}$  from 52.7° to 271.5°C for Sr/Ca, 57.2° to 121.6°C for Mg/Ca, and 18.7° to 55.4°C for  $\delta^{18}\text{O}$  (Fig. 5.11). The Sr/Ca and Mg/Ca ratios produced anomalously high  $T_{\text{cal}}$  anomalies, whereas the  $\delta^{18}\text{O}$ -based  $T_{\text{cal}}$  yielded a wide range of values, which included temperatures within the coral growth window. These anomalous temperatures clearly reflect the extensive diagenesis that has taken place. The coral skeletons in Units A and C, which show subtle chemical diagenesis, yielded  $T_{\text{cal}}$  of 26.1° to 176.6°C for Sr/Ca, 27.0° to 179.3°C for Mg/Ca, and 10.5° to 32.1°C for  $\delta^{18}\text{O}$  (Fig. 5.11). The Sr/Ca and Mg/Ca thermometers generally produced anomalously high  $T_{\text{cal}}$ , whereas the  $\delta^{18}\text{O}$ -based  $T_{\text{cal}}$  are within to slightly below the modern coral growth window (15° to 32°C; Hunter, 1994).

The coral skeletons from Units D to F of the Ironshore Formation, which have

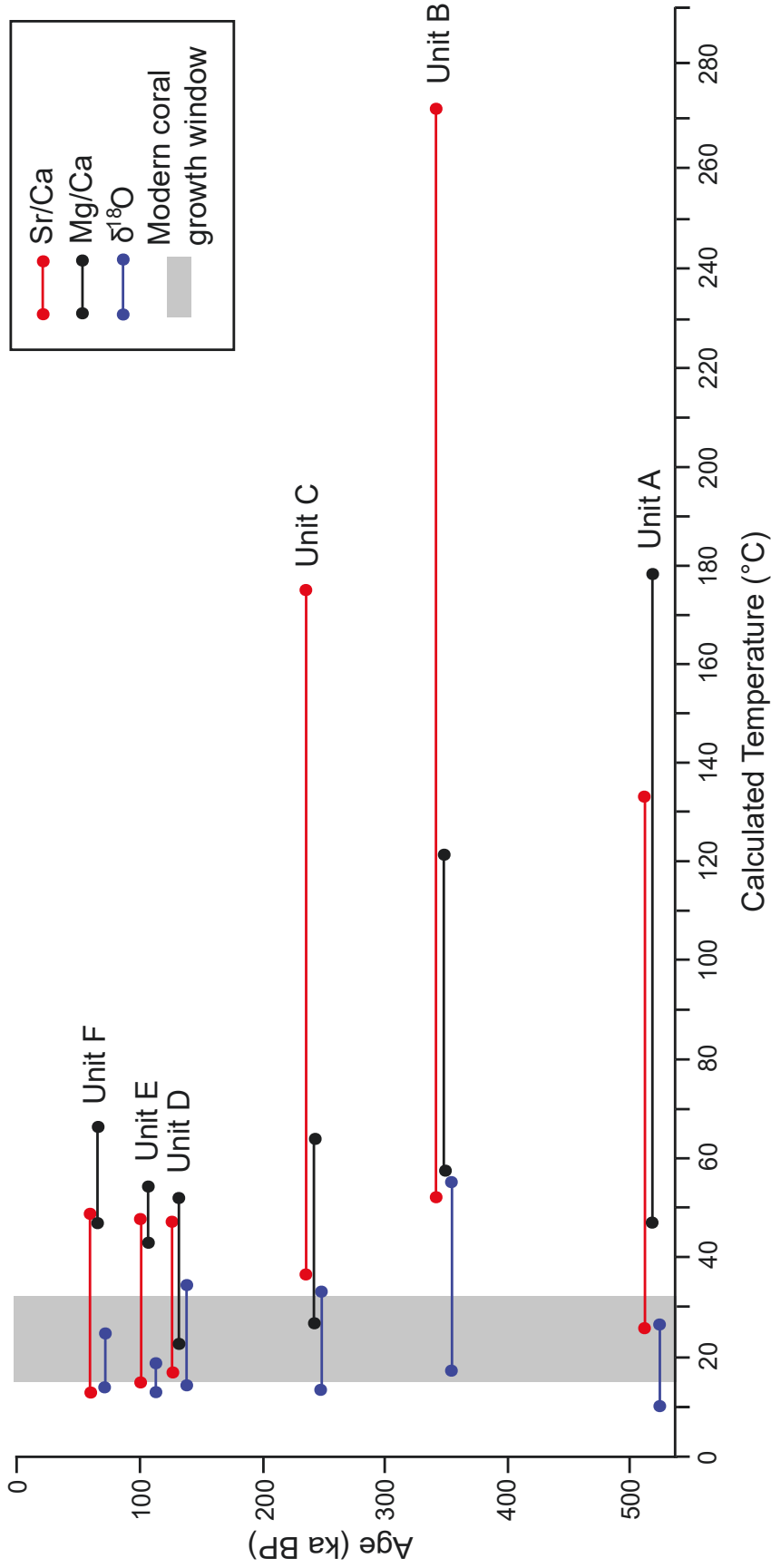


**Fig. 5.11.** Comparison of the Ironshore Formation coral Sr/Ca (red), Mg/Ca (black), and  $\delta^{18}\text{O}$  (blue) derived temperatures, using the Sr/Ca-geothermometers of Swart (2002), Smith et al. (2006), Saenger et al. (2008), Kilbourne et al. (2010), DeLong et al. (2011); Flannery and oore (2013), Alpert et al. (2017), and Flannery et al. (2018), the Mg/Ca-geothermometer of Watanabe et al. (2001), and the  $\delta^{18}\text{O}$ -geothermometers of Leder et al. (2001), Smith et al. (2006), Kilbourne et al. (2010), and Booker et al. (2019) for *Orbicella*, separated by unit. The modern coral growth window is shown in gray. The proxy-derived temperatures from the corals from Units A to C resulted in positive temperature anomalies (outside the preferred range of temperatures for *Orbicella*), whereas the  $\delta^{18}\text{O}$  and Sr/Ca ratios from the corals in Units D to F result in temperatures within the modern coral growth window.

experienced minimal diagenesis, have  $T_{\text{cal}}$  ranging from 12.6° to 49.7°C for Sr/Ca, 22.9° to 67.0°C for Mg/Ca, and 11.4° to 34.0°C for  $\delta^{18}\text{O}$  (Fig. 5.11). Most of the  $T_{\text{cal}}$  generated from the Sr/Ca and  $\delta^{18}\text{O}$ -geothermometers fall within the temperature range of *Orbicella* (15° to 32°C; Hunter, 1994). The  $T_{\text{cal}}$  generated from the Mg/Ca-geothermometers produced generally overestimated  $T_{\text{cal}}$ , which is probably because Mg/Ca ratios may not accurately reflect SST due to various biological processes, including the active incorporation of the biologically essential Mg ions into the coral skeleton (Allison and Finch, 2007; Inoue et al., 2007; Reynaud et al., 2007). This may be true for all Mg/Ca ratios. Although the Sr/Ca ratios and the  $\delta^{18}\text{O}$  values derived from the coral skeletons in these units generally produced  $T_{\text{cal}}$  within the *Orbicella* temperature range, there are also some abnormally high or low  $T_{\text{cal}}$ . These unusual  $T_{\text{cal}}$  may be attributed to differences between ‘vital effects’, coral growth rates, water depth, reef ecology, methods used to derive the equation, sampling errors, analytical uncertainties, differences in sampling procedures, and the number of samples used for calibration of these geothermometers used in these calculations (Booker et al., 2019).

### 6.2.1. Pleistocene paleotemperatures

Applying the oxygen isotope geothermometer developed by Booker et al. (2019) developed from modern *O. annularis* and *M. cavernosa* corals from the Cayman Islands, with the  $\delta^{18}\text{O}_{\text{coral}}$  values from the corals in Units D to F, paleotemperatures during growth of the Pleistocene Ironshore Formation corals were calculated.  $\delta^{18}\text{O}_{\text{water}}$  values of +0.1, -0.4, and +0.9‰ for Units D, E, and F, respectively, derived from the SPECMAP curve for the equatorial Atlantic Ocean during the Pleistocene (Imbrie and McIntyre, 2006) were used in the temperature calculations. These  $\delta^{18}\text{O}_{\text{water}}$  values are best estimates of the true  $\delta^{18}\text{O}_{\text{water}}$  values for the seawater that existed during deposition of those units, and it is important to stress that any modification of those values will result in temperatures that differ from those reported herein. The corals found in Unit D, which grew during

the ~12,000 year long Marine Isotope Stage (MIS) 5e ~125 ka (Siddall et al., 2007), gave  $T_{\text{cal}}$  of 17° to 32°C (average 25°C), which are consistent with the temperatures in which these corals live today. Specifically, the corals from the east coast of Grand Cayman (RWP-D) yielded  $T_{\text{cal}}$  of 21° to 31°C (average 27°C; Fig. 5.12A), whereas those from the west coast, yielded  $T_{\text{cal}}$  of 17° to 26°C (average 22°C; Fig. 5.12B) for GTH-D and  $T_{\text{cal}}$  of 24 to 32°C (average 28°C; Fig. 5.12C) for IS1. The record from the 6-point moving average of these corals displays overall warming in corals RWP-D and GTH-D, whereas coral IS1 displays overall cooling during coral growth. Differences in the  $T_{\text{cal}}$  between the west and the east coasts may reflect (1) species specific differences between *O. annularis* and *M. cavernosa*, (2) differences in the age of the corals, and/or (3) microenvironmental variations (Smith et al., 1979; de Villiers et al., 1995, de Villiers, 1999; Lear et al., 2003; Allison and Finch, 2007; Armid et al., 2011; Balter et al., 2011; Xu et al., 2015).

The coral in Unit E, which grew during the ~15,000 year long highstand of MIS 5c ~101 ka (Coyne et al., 2007), yielded  $T_{\text{cal}}$  of 14° to 23°C (average 18°C; Fig. 5.13A). The record from the 6-point moving average of this coral shows an overall decrease in  $T_{\text{cal}}$  (~3°C) during the 44 years of coral growth. The coral from Unit F, which grew during the ~14,000 year long highstand of MIS 5a ~80 ka (Coyne et al., 2007), yielded  $T_{\text{cal}}$  from 20° to 30°C (average 25°C; Fig. 5.13B). The 6-point moving average temperature profile for Unit F displays cycles of warming (1° – 4°C) and cooling (1° – 4°C), 5 to 45 years in length, superimposed on an overall decrease in  $T_{\text{cal}}$  of ~4°C during the 83 years of coral growth. Similar small-scale cycles superimposed on a larger trend have also been recorded from modern Cayman corals (Booker et al., 2019).

The corals from Units D and F record  $T_{\text{cal}}$  in the modern coral growth window. In contrast, the coral from Unit E yielded  $T_{\text{cal}}$  that are lower than those from Units D and F, and generally at the lower end of the modern growth window. This suggests that the climate during the deposition of Units D and F was similar to today's climate (Kukla et al., 1997). Similar conditions to those recorded by the corals in Unit D have also been

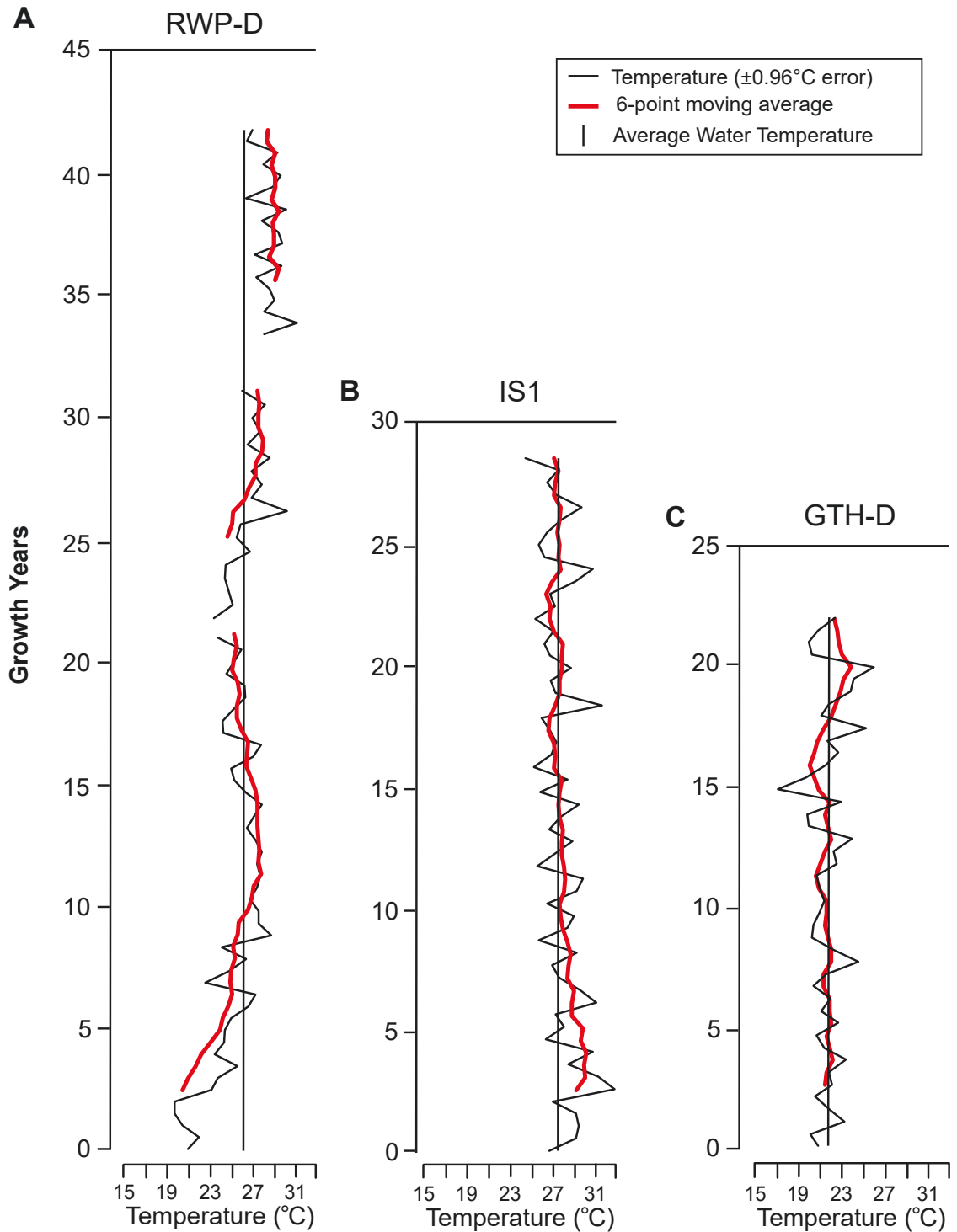


**Fig. 5.12.** Temperature profile of the Unit D corals of the Ironshore Formation; (A) RWP-D, (B) IS1, and (C) GTH-D. Temperatures determined using the oxygen isotope geothermometer of Booker et al. (2019) with a  $\delta^{18}\text{O}_{\text{water}}$  value of +0.1‰ as derived from the SPECMAP of Imbrie and McIntyre (2006) for the equatorial Atlantic.

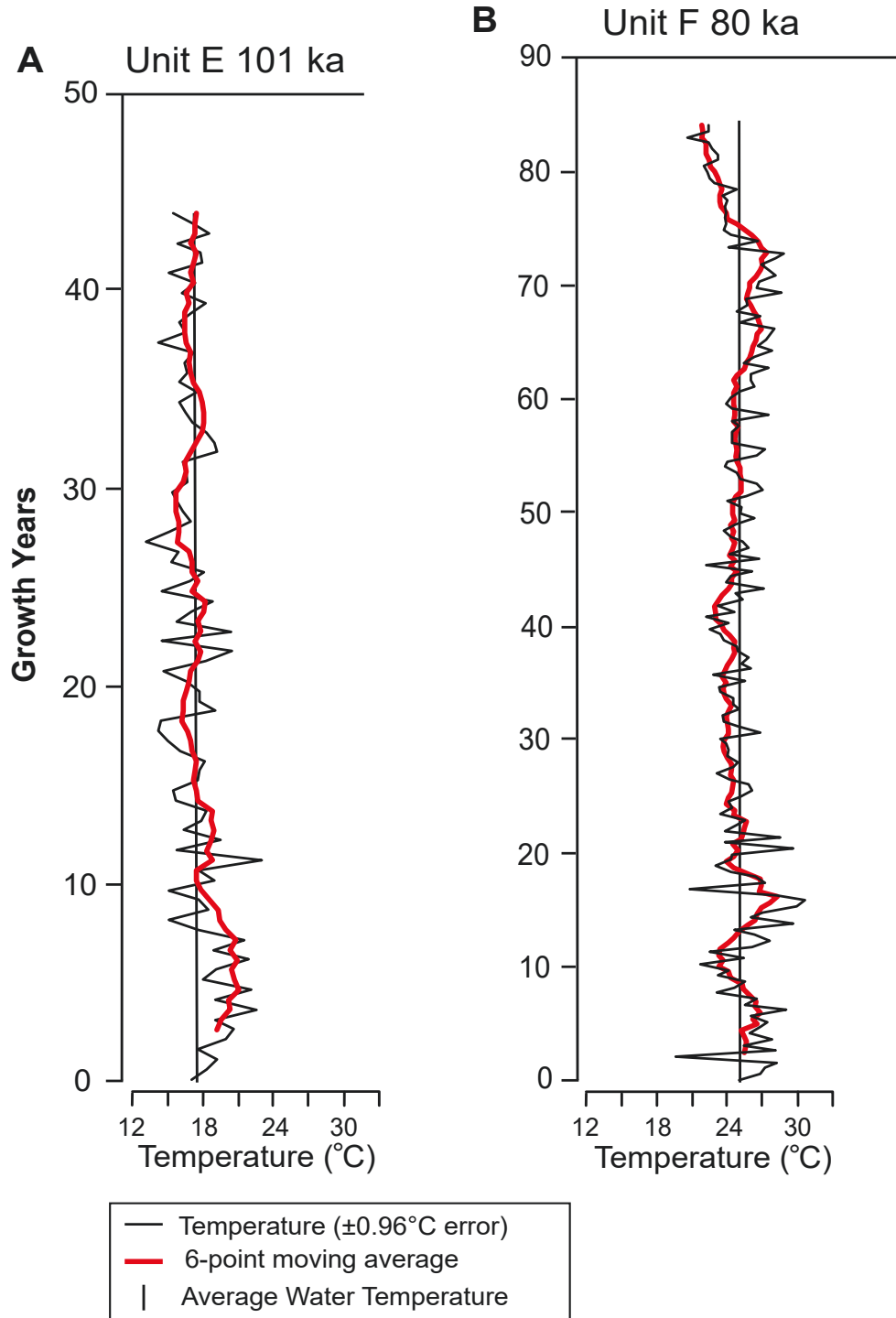


**Fig. 5.13.** Temperature profile of Ironshore Formation corals from (A) Unit E and (B) Unit F.

Temperature determined using the oxygen isotope geothermometer of Booker et al. (2019) with a  $\delta^{18}\text{O}_{\text{water}}$  value of  $-0.4\text{‰}$  for Unit E and  $+0.9\text{‰}$  for Unit F as derived from the SPECMAP of Imbrie and McIntyre (2006) for the equatorial Atlantic.

recorded from Isla de Mona, Northern Caribbean (Winter et al., 2003), Bonaire (Brocas et al., 2016), Death Valley, California (Lowenstein et al., 1999), the Timor Sea (Kawamura et al., 2006), and Antarctica (Rohling et al., 2009). From 125 to 132 ka, Crowley and Kim (1994) suggested an increase in summer temperatures of at least 1°C on all land masses, which is consistent with the slight  $T_{cal}$  increase recorded in RWP-D and GTH-D (Fig. 5.12).

Decreasing temperatures, such as that deduced from the coral in Units E, have been recognized in the North Atlantic, Arabian Sea, and Timor Sea (McManus et al., 1999; Prabhu et al., 2004; Kawamura et al., 2006). Cooling trends of up to 4°C, such as that recorded from the coral in Unit F, have also been identified in the North Atlantic, Arabian Sea, Timor Sea, Coral Sea, southern South China Sea, California, and Antarctica (Lowenstein et al., 1999; McManus et al., 1999; Chen et al., 2000; Prabhu et al., 2004; Kawamura et al., 2006; Rohling et al., 2009; Tachikawa et al., 2009). As cooling has been recorded in multiple locations globally during the deposition of both Unit E and F, these cooling trends may reflect global-scale events, such as a decrease in temperature following the peaks of interglacial MIS 5c and 5a, respectively. The records from the corals from Units D to F of the Ironshore Formation are consistent with global temperature trends during their growth.

## 7. Conclusions

Analysis of the corals in the Pleistocene Ironshore Formation (Units A-F) on Grand Cayman has produced the following important conclusions;

- Obvious (mineralogical change or cementation) diagenetic alteration of coral skeletons can be recognized in thin section, SEM imaging, and/or XRD analysis, but subtle chemical (elemental or isotopic) change may not be identified.

Therefore, the proposed screening methods (the coral skeleton contains >95 wt% primary aragonite, skeletal pores are devoid of cements, Mg/Ca ratio is

<12.0 mmol/mol, Sr/Ca ratio is >8.0 mmol/mol,  $\delta^{18}\text{O}$  values >25.1‰, and  $\delta^{13}\text{C}$  values >-3.0‰) can be used to thoroughly assess the suitability of corals for paleoclimatic interpretations.

- The progressive change from aragonite to calcite in the coral skeletons in the Ironshore Formation is accompanied by an increase in the Mg content and a decrease in the Sr content.
- The coral skeletons from Units A and C in the Ironshore Formation have retained their primary aragonitic skeletons, but have undergone chemical diagenesis resulting in altered Mg/Ca and Sr/Ca ratios. These corals were diagenetically altered in a semi-open system by seawater diluted with meteoric water. These corals cannot be used to calculate paleotemperatures.
- The coral skeletons in Unit B in the Ironshore Formation have been pervasively recrystallized, as these corals were altered in an open diagenetic system dominated by meteoric groundwaters. These corals cannot be used to reconstruct paleoclimate.
- The coral skeletons in Units D, E, and F in the Ironshore Formation have retained their primary aragonitic skeletons and isotopic/elemental compositions. These corals remained in a closed system, and therefore, experienced minimal physical and chemical alteration. These corals can be used to determine paleotemperatures.
- The unaltered corals from Unit D and F in the Ironshore Formation record temperatures that are consistent with today's climate. The coral from Unit E records low temperatures and overall cooling. These temperature reconstructions are consistent with regional and global paleoclimate interpretations during the deposition of these units.



## REFERENCES

- Allison, N., Finch, A.A., 2007. High temporal resolution Mg/Ca and Ba/Ca records in modern *Porites lobata* corals. *Geochemistry Geophysics Geosystems* 8. doi:10.1029/2006GC001477.
- Allison, N., Finch, A.A., Webster, J.M., Clague, D.A., 2007. Palaeoenvironmental records from fossil corals: the effects of submarine diagenesis on temperature and climate estimates. *Geochimica et Cosmochimica Acta* 71, 4693-4703.
- Alpert, A.E., Cohen, A.L., Oppo, D.W., DeCarlo, T.M., Gaetani, G.A., Hernandez-Delgado, E.A., Winter, A., Gonneea, M.E., 2017. Twentieth century warming of the tropical Atlantic captured by Sr-U paleothermometry. *Paleoceanography* 32, 146-160.
- Armid, A., Asami, R., Fahmiati, T., Sheikh, M.A., Fujimura, H., Higuchi, T., Taira, E., Shinjo, R., Oomori, T., 2011. Seawater temperature proxies based on  $D_{Sr}$ ,  $D_{Mg}$ , and  $D_U$  from culture experiments using the branching coral *Porites cylindrica*. *Geochimica et Cosmochimica Acta* 75, 4273-4285.
- Balter, V., Lecuyer, C., Barrat, J., 2011. Reconstructing seawater Sr/Ca during the last 70 My using fossil fish tooth enamel. *Palaeogeography, Palaeoclimatology, Palaeoecology* 310, 133-138.
- Bar-Matthews, M., Wasserburg, G.J., Chen, J.H., 1993. Diagenesis of fossil coral skeletons: correlation between trace elements, textures and  $^{234}U/^{238}U$ . *Geochimica et Cosmochimica Acta* 57, 257-276.
- Booker, S.D., Jones, B., Chacko, T., Li, L., 2019. Insights into sea surface temperatures from the Cayman Islands from corals over the last ~540 years. *Sedimentary Geology* 389, 218-240.
- Brand, U., Veizer, J., 1983. Origin of coated grains: trace element constraints. In: Peryt, T. (Ed.), *Coated Grains*. Springer-Verlag, Berlin Heidelberg New York Tokyo, pp. 9-26.
- Brocas, W.M., Felis, T., Obert, J.C., Gierz, P., Lohmann, G., Scholz, D., Kolling, M., Scheffers, S.R., 2016. Last interglacial temperature seasonality reconstructed from tropical Atlantic corals. *Earth and Planetary Science Letters* 449, 418-429.
- Buddermeier, R.W., Maragos, J.E., Knutson, D.K., 1974. Radiographic studies of reef coral exoskeletons: rates and patterns of growth. *Journal of Experimental Marine Biology and*

- Ecology 14, 179-200.
- Chen, M., Tu, X., Zheng, F., Yan, W., Tang, X., Lu, J., Wang, B., Lu, M., 2000. Relations between sedimentary sequence and paleoclimatic changes during last 200 ka in the southern South China Sea. Chinese Science Bulletin 45, 1334-1340.
- Cochran, J.K., Kallenberg, K., Landman, N.H., Harries, P.J., Weinreb, D., Turekian, K.K., Beck, A.J., Cobban, W.A., 2010. Effect of diagenesis on the Sr, O, and C isotope composition of Late Cretaceous mollusks from the Western Interior Seaway of North America. American Journal of Science 310, 69-88.
- Coyne, M.K., 2003. Transgressive-regressive cycles in the Ironshore Formation, Grand Cayman, British West Indies, Unpublished. M.Sc. Thesis, University of Alberta, Edmonton, Alberta, Canada, 98 pp.
- Coyne, M.K., Jones, B., Ford, D., 2007. Highstands during marine isotope stage 5: evidence from the Ironshore Formation of Grand Cayman, British West Indies. Quaternary Science Reviews 26, 536-559.
- Cross, T.S., Cross, B.W., 1983. U, Sr, and Mg in Holocene and Pleistocene corals *A. palmata* and *M. annularis*. Journal of Sedimentary Petrology 53, 587-594.
- Crowley, T.J., Kim, K., 1994. Milankovitch forcing of the last Interglacial sea level. Science 265, 1566-1568.
- de Villiers, S., 1999. Seawater strontium and Sr/Ca variability in the Atlantic and Pacific oceans. Earth and Planetary Science Letters 171, 623-634.
- de Villiers, S., Nelson, B.K., Chivas, A.R., 1995. Biological controls on coral Sr/Ca and  $\delta^{18}\text{O}$  reconstructions of sea surface temperatures. Science 269, 1247-1250.
- Delaney, M.L., Linn, L.J., Davies, P.J., 1996. Trace and minor element ratios in *Halimeda* aragonite from the Great Barrier Reef. Coral Reefs 15, 181-189.
- DeLong, K.L., Quinn, T.M., Taylor, F.W., 2007. Reconstructing twentieth-century sea surface temperature variability in the southwest Pacific: a replication study using multiple coral Sr/Ca records from New Caledonia. Paleoceanography 22. doi:10.1029/2007PA001444.
- DeLong, K.L., Flannery, J.A., Maupin, C.R., Poore, R.Z., Quinn, T.M., 2011. A coral Sr/Ca calibration and replication study of two massive corals from the Gulf of Mexico. Palaeogeography, Palaeoclimatology, Palaeoecology 307, 117-128.

- Enmar, R., Stein, M., Bar-Matthews, M., Sass, E., Katz, A., Lazar, B., 2000. Diagenesis in live corals from the Gulf of Aqaba. I. The effect on paleo-oceanography tracers. *Geochimica et Cosmochimica Acta* 64, 3123-3132.
- Fallon, S.J., McCulloch, M., Alibert, C., 2003. Examining water temperature proxies in *Porites* corals from the Great Barrier Reef: a cross-shelf comparison. *Coral Reefs* 22, 389-404.
- Farfan, G.A., Cordes, E.E., Waller, R.G., DeCarlo, T.M., Hansel, C.M., 2018. Mineralogy of deep-sea coral aragonites as a function of aragonite saturation state. *Frontiers in Marine Science* 5. doi: 10.3389/fmars.2018.00473.
- Finch, A.A., Allison, N., 2003. Strontium in coral aragonite: 2. Sr coordination and the long-term stability of coral environmental records. *Geochimica et Cosmochimica Acta* 67, 4519-4527.
- Flannery, J.A., Poore, R.Z., 2013. Sr/Ca proxy sea-surface temperature reconstructions from modern and Holocene *Montastrea faveolata* specimens from the Dry Tortugas National Park, Florida, U.S.A. *Journal of Coastal Research* 63, 20-31.
- Flannery, J.A., Richey, J.N., Toth, L.T., Kuffner, I.B., Poore, R.Z., 2018. Quantifying uncertainty in Sr/Ca-based estimates of SST from the coral *Orbicella faveolata*. *Paleoceanography and Paleoclimatology* 33, 958-973.
- Hendy, E.J., Gagan, M.K., Lough, J.M., McCulloch, M., deMenocal, P., 2007. Impact of skeletal dissolution and secondary aragonite on trace element and isotopic climate proxies in *Porites* corals. *Paleoceanography* 22. doi: 10.1029/2007PA001462.
- Hunter, I.G., 1994. Modern and ancient coral association of the Cayman Islands, Unpublished. Ph.D. Thesis, University of Alberta, Edmonton, Alberta, Canada, 345 pp.
- Hunter, I.G., Jones, B., 1988. Corals and paleogeography of the Pleistocene Ironshore Formation of Grand Cayman. *Proceedings of the Sixth International Coral Reef Symposium*, Townsville, Australia, pp. 431-435.
- Hunter, I.G., Jones, B., 1995. Coral associations of the Pleistocene Ironshore Formation, Grand Cayman. *Coral Reefs* 15, 249-267.
- Imbrie, J., McIntyre, A., 2006. SPECMAP time scale developed by Imbrie et al., 1984 based on normalized planktonic records (normalized O-18 vs time, specmap.017). PANGAEA. doi: 10.1594/PANGAEA.441706.

- Inoue, M., Suzuki, A., Nohara, M., Hibino, K., Kawhata, H., 2007. Empirical assessment of coral Sr/Ca and Mg/Ca ratios as climate proxies using colonies grown at different temperatures. *Geophysical Research Letters* 34. doi:10.1029/2007GL029628.
- Jones, B., 2019. Diagenetic processes associated with unconformities in carbonate successions on isolated oceanic islands: case study of the Pliocene to Pleistocene sequence, Little Cayman, British West Indies. *Sedimentary Geology* 386, 9-30.
- Jones, B., Hunter, I.G., 1990. Pleistocene paleogeography and sea levels on the Cayman Islands, British West Indies. *Coral Reefs* 9, 81-91.
- Kawamura, H., Holbourn, A., Kuhnt, W., 2006. Climate variability and land-ocean interactions in the Indo Pacific Warm Pool: a 460-ka palynological and organic geochemical record from the Timor Sea. *Marine Micropaleontology* 59, 1-14.
- Kilbourne, K.H., Quinn, T.M., Webb, R., Guilderson, T., Nyberg, J., Winter, A., 2010. Coral windows onto seasonal climate variability in the northern Caribbean since 1479. *Geochemistry Geophysics Geosystems* 11. doi: 10.1029/2010GC003171.
- Kim, S., Mucci, A., Taylor, B., 2007. Phosphoric acid fractionation factors for calcite and aragonite between 25 and 75°C: Revisited. *Chemical Geology* 246, 135-146.
- Kim, S., Coplen, T.B., Horita, J., 2015. Normalization of stable isotope data for carbonate minerals: implementation of IUPAC guidelines. *Geochimica et Cosmochimica Acta* 158, 276-289.
- Kinsman, D.J.J., 1969. Interpretation of Sr<sup>2+</sup> concentrations in carbonate minerals and rocks. *Journal of Sedimentary Petrology* 39, 486-508.
- Knutson, D.W., Buddermeier, R.W., Smith, S.V., 1972. Coral chronometers: seasonal growth bands in reef corals. *Science* 177, 270-272.
- Kukla, G., McManus, J.F., Rousseau, D.D., Chuine, I., 1997. How long and how stable was the last interglacial? *Quaternary Science Reviews* 16, 605-612.
- Lear, C.H., Elderfield, H., Wilson, P.A., 2003. A Cenozoic seawater Sr/Ca record from benthic foraminiferal calcite and its application in determining global weathering fluxes. *Earth and Planetary Science Letters* 208, 69-84.
- Leder, J.J., Swart, P.K., Szmant, A.M., Dodge, R.E., 1996. The origin of variations in the isotopic record of scleractinian corals: I. Oxygen. *Geochimica et Cosmochimica Acta* 60, 2857-

2870.

- Li, R., Jones, B., 2013a. Heterogeneous diagenetic patterns in Pleistocene Ironshore Formation of Grand Cayman, British West Indies. *Sedimentary Geology* 294, 251-265.
- Li, R., Jones, B., 2013b. Temporal and spatial variations in the diagenetic fabrics and stable isotopes of Pleistocene corals from the Ironshore Formation of Grand Cayman, British West Indies. *Sedimentary Geology* 286-287, 58-72.
- Lowenstein, T.K., Li, J., Brown, C., Roberts, S.M., Ku, T., Luo, S., Yang, W., 1999. 200 k.y. paleoclimate record from Death Valley salt core. *Geology* 27, 3-6.
- Martin, G.D., Wilkinson, B.H., Lohman, K.C., 1985. The role of skeletal porosity in aragonite neomorphism- *Strombus* and *Montastrea* from the Pleistocene Key Largo Limestone, Florida. *Journal of Sedimentary Petrology* 56, 194-203.
- McCulloch, M.T., Tudhope, A.W., Esat, T.M., Mortimer, G.E., Chappell, J., Pillans, B., Chivas, A.R., Omura, A., 1999. Coral record of equatorial sea-surface temperatures during the Penultimate Deglaciation at Huon Peninsula. *Science* 283, 202-204.
- McGregor, H.V., Gagan, M.K., 2003. Diagenesis and geochemistry of *Porites* corals from Papua New Guinea: implications for paleoclimate reconstruction. *Geochimica et Cosmochimica Acta* 67, 2147-2156.
- McGregor, H.V., Abram, N.J., 2008. Images of diagenetic textures in *Porites* corals from Papua New Guinea and Indonesia. *Geochemistry Geophysics Geosystems* 9, 1-17.
- McManus, J.F., Oppo, D.W., Cullen, J.L., 1999. A 0.5-million year record of millennial-scale climate variability in the North Atlantic. *Science* 283, 971-975.
- Meyers, W.J., Lohman, K.C., 1983. Isotope geochemistry of regionally extensive calcite cement zones and marine components in Mississippian limestones, New Mexico. In: Schneiderman, N., Harris, P.M. (Eds.), *Carbonate Cements*. The Society of Economic Paleontologists and Mineralogists Special Publication 36, pp. 223-239.
- Mitsuguchi, T., Matsumoto, E., Abe, O., Uchida, T., Isdale, P.J., 1996. Mg/Ca thermometry in coral skeletons. *Science* 274, 961-963.
- Moore, W.S., Krishnaswami, S., 1974. Correlation of X-Radiography revealed banding in corals with radiometric growth rates. In: Cameron, A.M., Cambell, B.M., Cribb, A.B., Edean, R., Jell, J.S., Jones, O.A., Mather, P., Talbot, F.H. (Eds.), *Proceeding of the Second*

- International Coral Reef Symposium 2. Great Barrier Reef Committee, Brisbane, pp. 269-276.
- Muller, A.D., Gagan, M.K., McCulloch, M.T., 2001. Early marine diagenesis in corals and geochemical consequences for paleoceanographic reconstructions. *Geophysical Research Letters* 28, 4471-4474.
- Ng, K., 1990. Diagenesis of the Oligocene-Miocene Bluff Formation of the Cayman Islands: a petrographic and hydrogeological approach., Unpublished. Ph.D. Thesis, University of Alberta, Edmonton, Alberta, Canada, 343 pp.
- NOAA, 2016, In what types of water do corals live? <https://oceanservice.noaa.gov/facts/coralwaters.html>.
- Nothdurft, L.D., Webb, G.E., 2007. Microstructure of common reef-building coral genera *Acropora*, *Pocillopora*, *Goniastrea* and *Porites*: constraints on spatial resolution in geochemical sampling. *Facies* 53. doi: 10.1007/s10347-006-0090-0.
- Nothdurft, L.D., Webb, G.E., Bostrom, T., Rintoul, L., 2007. Calcite-filled borings in the most recently deposited skeleton in live-collected *Porites* (Scleractinia): implications for trace element archives. *Geochimica et Cosmochimica Acta* 71, 5423-5438.
- Nothdurft, L.D., Webb, G.E., 2009. Earliest diagenesis in scleractinian coral skeletons: implications for palaeoclimate-sensitive geochemical archives. *Facies* 55, 161-201.
- Pingitore, N.E., 1976. Vadose and phreatic diagenesis: processes, products and their recognition in corals. *Journal of Sedimentary Petrology* 46, 985-1006.
- Pingitore, N.E., 1978. The behavior of Zn<sup>2+</sup> and Mn<sup>2+</sup> during carbonate diagenesis: theory and applications. *Journal of Sedimentary Petrology* 48, 799-814.
- Prabhu, C.N., Shankar, R., Anupama, K., Taieb, M., Bonnefille, R., Vidal, L., Prasad, S., 2004. A 200-ka pollen and oxygen-isotopic record from two sediment cores from the eastern Arabian Sea. *Palaeogeography, Palaeoclimatology, Palaeoecology* 214, 309-321.
- Quinn, T.M., Taylor, F.W., 2006. SST artifacts in coral proxy records produced by early marine diagenesis in a modern coral from Rabaul, Papua New Guinea. *Geophysical Research Letters* 35. doi: 10.1029/2005GL024972.
- Reynaud, S., Ferrier-Pages, C., Meibom, A., Mostefaoui, S., Mortlock, R., Fairbanks, R., Allemand, D., 2007. Light and temperature effects on Sr/Ca and Mg/Ca ratios in the

- scleractinian coral *Acropora* sp. *Geochimica et Cosmochimica Acta* 71, 354-362.
- Rohling, E.J., Grant, K., Bolshaw, M., Roberts, A.P., Siddall, M., Hemleben, C., Kucera, M., 2009. Antarctic temperature and global sea level closely coupled over past five glacial cycles. *Nature Geoscience Letters* 2, 500-504.
- Saenger, C., Cohen, A.L., Oppo, D.W., Hubbard, D., 2008. Interpreting sea surface temperature from strontium/calcium ratios in *Montastrea* corals: link with growth rate and implications for proxy reconstructions. *Paleoceanography* 23. doi: 10.1029/2007PA001572.
- Sayani, H.R., Cobb, K.M., Cohen, A.L., Elliott, W.C., Nurhati, I.S., Dunbar, R.B., Rose, K.A., Zaunbrecher, L.K., 2011. Effects of diagenesis on paleoclimate reconstructions from modern and young fossil corals. *Geochimica et Cosmochimica Acta* 75, 6361-6373.
- Siddall, M., Chappell, J., Potter, E.K., 2007. Eustatic sea level during past Interglacials. In: Sirocko, F., Claussen, M., Litt, T., Sanchez-Goni, M.F. (Eds.), *The Climate of Past Interglacials*. Elsevier Science, pp. 75-92.
- Siegel, F.R., 1960. The effects of strontium on the aragonite-calcite ratios of Pleistocene corals. *Journal of Sedimentary Petrology* 30, 297-304.
- Sinclair, D.J., Kinsley, L.P.J., McCulloch, M.T., 1998. High resolution analysis of trace elements in corals by laser ablation ICP-MS. *Geochimica et Cosmochimica Acta* 62, 1889-1901.
- Smith, J.M., Quinn, T.M., Helmle, K.P., Halley, R.B., 2006. Reproducibility of geochemical and climatic signals in the Atlantic coral *Montastrea faveolata*. *Paleoceanography* 21. doi: 10.1029/2005PA001187.
- Smith, S.R., Buddemeier, R.W., Redale, R., Houck, J.E., 1979. Strontium-calcium thermometry in coral skeletons. *Science* 204, 404-406.
- Swart, P.K., 1983. Carbon and oxygen isotope fractionation in scleractinian corals: a review. *Earth-Science Reviews* 19, 51-80.
- Swart, P.K., Elderfield, H., Greaves, M.J., 2002. A high-resolution calibration of Sr/Ca thermometry using the Caribbean coral *Montastraea annularis*. *Geochemistry Geophysics Geosystems* 3. doi: 10.1029/2002GC000306.
- Tachikawa, K., Vidal, L., Sonzogni, C., Brad, E., 2009. Glacial/interglacial sea surface temperature changes in the Southwest Pacific Ocean over the past 360 ka. *Quaternary*

- Science Reviews 28, 1160-1170.
- Toler, S.K., Hallock, P., Schijf, J., 2001. Mg/Ca ratios in stressed foraminifera, *Amphistegina gibbosa*, from the Florida Keys. *Marine Micropaleontology* 43, 199-206.
- Veizer, J., 1983. Chemical diagenesis of carbonates: theory and application of trace elements. In: Aruth, M.A. (Ed.), *Stable Isotopes in Sedimentary Geology*, 10, 100 pp.
- Veizina, J.L., 1997. Stratigraphy and sedimentology of the Pleistocene Ironshore Formation at Rogers Wreck Point, Grand Cayman: a 400 ka record of sea-level highstands, Unpublished. M.Sc. Thesis, University of Alberta, Edmonton, Alberta, Canada, 131 pp.
- Veizina, J.L., Jones, B., Ford, D., 1999. Sea level highstands over the last 500,000 years: evidence from the Ironshore Formation on Grand Cayman, British West Indies. *Journal of Sedimentary Research* 69, 317-327.
- von Reumont, J., Hetzinger, S., Garbe-Schonberg, D., Manfrino, C., Dullo, W., 2016. Impact of warming events on reef-scale temperature variability as captured in two Little Cayman coral Sr/Ca records. *Geochemistry Geophysics Geosystems* 17. doi: 10.1002/2015GC006194.
- Watanabe, T., Winter, A., Oba, T., 2001. Seasonal changes in sea surface temperatures and salinity during the Little Ice Age in the Caribbean Sea deduced from Mg/Ca and  $^{18}\text{O}/^{16}\text{O}$  ratios in corals. *Marine Geology* 173, 21-35.
- Webb, G.E., Nothdurft, L.D., Kamber, B.S., Kloprogge, J.T., Zhao, J., 2009. Rare earth element geochemistry of scleractinian coral skeleton during meteoric diagenesis: a sequence through neomorphism of aragonite to calcite. *Sedimentology* 56, 1433-1463.
- Winter, A., Paul, A., Nyberg, J., Oba, T., Lundberg, J., Schrag, D.P., Taggart, B., 2003. Orbital control of low-latitude seasonality during the Eemian. *Geophysical Research Letters* 30. doi:10.1029/2002GL016275.
- Xu, Y., Pearson, S., Kilbourne, K.H., 2015. Assessing coral Sr/Ca-SST calibration techniques using the species *Diploria strigosa*. *Palaeogeography, Palaeoclimatology, Palaeoecology* 440, 353-362.



## CHAPTER 6

### CONCLUSIONS

The impact of climate change has become increasingly prevalent around the world, with the last three decades being successively warmer than any preceding decade since 1850 (IPCC, 2014). This has sparked considerable research into the topic of climate change, with researchers looking to the past for insights on what the future may hold (Hasen et al., 2018; IPCC, 2018). To better understand the future impacts of climate change, known intervals of climatic instability, over the last 200,000 years have been investigated using geochemical proxies (e.g., Hodell et al., 1991; Fensterer et al., 2012; Arienzo et al., 2015; Kuffner et al., 2017; Flannery et al., 2018). These paleoclimate reconstructions have shown fluctuations in sea surface temperature (SST) and atmospheric moisture globally. Additionally, these studies have identified similar trends in diverse regions that highlight the importance of global climate dynamics.

Element-based proxies have become a promising avenue for reconstructing past climate changes, this is especially true for modern tropical corals where long-term instrument monitoring of the climate is rare. Numerous proxies have been developed ( $\delta^{18}\text{O}$ ,  $\delta^{13}\text{C}$ , Sr/Ca, Mg/Ca, U/Ca, Sr-U, Li/Ca, Li/Mg, Mg/Li, Ba/Ca,  $\text{B}^{11}/\text{Ca}$ , trace and rare earth elements) that provide insights into many aspects of environmental variability worldwide. A review of the theory used to develop the nine most commonly used elemental SST proxies and a comparison of the 302 published element-based equations to two datasets resulted in the following key conclusions.

- More research is required to better understand the factors controlling elemental uptake into the coral skeleton, specifically the mechanisms responsible for element incorporation, the role of the vital effects, the effect of different environmental parameters, and the influence of different sampling techniques. It is critical to understand if temperature is the truly the primary

control on the element/Ca signals used to interpret paleoclimate.

- This study suggests using (1) multiple coral species and/or multiple specimens of the same species, (2) replicating time series with multiple corals from similar and/or the same environment, (3) empirically regressing temperature to a variety of elements to reduce coral-element specific modifications, (4) detailed characterization of all aspects of geographic variability as close to the coral as possible, (5) laser aided drilling along the maximum growth axis of the thecal walls of the coral skeleton at fixed increments, (6) a high precision analytical instrument to generate the elemental concentrations from the coral skeleton, (7) correlation of the element/Ca ratios to temperature based on known dates, and (8) linear regression to produce the resultant equation.
- Five published equations produced calculated temperatures within the modern coral growth window temperature range (18° to 36°C) and the measured SST from Grand Cayman (25° to 31°C). The Sr/Ca equation of Boiseau et al. (1997), a U/Ca equation of Min et al. (1995), the Sr-U equations of DeCarlo et al. (2016) and Alpert et al. (2017), and the B<sup>11</sup>/Ca equation of Sinclair et al. (1998) yielded the most ‘realistic’ calculated temperatures for various species of corals. This suggests that future paleoclimate research dealing with coral-based element proxies should utilize one of these published equations for calculating temperature.

The first coral and sediment core-based SST profiles over the last ~540 years, ~6000 years, and 80,000 to 125,000 years from the Cayman Islands were developed in this study, thereby vastly increasing our knowledge of temperature changes in the Caribbean. The development of these SST profiles over the investigated time periods provides better constraints on past temperature variability in an understudied area. These windows in time record SST changes that are consistent with other recorded intervals of global climate change. Comparison of the SST profiles associated with the

Cayman coral skeletons (*O. annularis* and *M. cavernosa*; modern and Pleistocene) and sediment cores (~6000 year record) produced the following important conclusions.

- Temperatures calculated using oxygen isotopes from modern Cayman corals, indicate that there have been two cool periods (C1: 1474 to 1512 CE and C2: 1824 to 1924), one warm period (W1: 1924 to 2006), and one mild period (M1: 2006 to 2014 CE) in SST between ~1474 to 1512 CE and ~1815 to 2014 CE. These trends are consistent with other Caribbean temperature records. Global increases in SST since the Industrial Revolution, are highlighted by the ~3°C increase in SST from ~1815 to 2014 CE.
- Various types of data (facies, carbonate composition, stable isotope and elemental compositions) from the North Sound cores indicate that there have been five periods of climate change (temperature and atmospheric moisture), including one cool-dry period from ~3850 to 1280 BCE, two mild-wet periods from ~1280 to 200 BCE and ~1850 to 1980 CE, one warm-dry period from ~200 BCE to 480 CE, and one cool-wet period from ~480 to 1850 CE. These climate periods are consistent with records from the Caribbean and higher latitude locations. The global nature of these climate periods can be related to the movements of the Intertropical Convergence Zone (ITCZ) and the phase of the North Atlantic Oscillation (NAO). During MW1, MW2, and CW1B the ITCZ was in a northerly position and/or the NAO in a negative phase. In contrast, CD1, WD1, and CW1A, resulted from a southerly position of the ITCZ and/or a positive phase of the NAO.
- Corals from Units D (125 ka) and F (80 ka) of the Ironshore Formation (Pleistocene) record SST that are consistent with today's climate, whereas the coral from Unit E (101 ka) records low SST and overall cooling. These SST reconstructions are consistent with other paleoclimate records that were developed from samples deposited at the same time as these units.

The use of coral skeletons for paleoclimate reconstructions hinges on the preservation of the corals, where any diagenetic alteration to the coral's skeleton can skew the original geochemical conditions and therefore the environmental signals. The comparative study of mineralogical and geochemical changes in the coral skeletons from units A to F of the Ironshore Formation (Pleistocene) yielded the following critical conclusions.

- Visual determination of coral preservation (mineralogical change or cementation) using thin section, SEM imaging, and XRD analysis may not identify subtle (elemental or isotopic) changes.
- Coral samples that contain >95 wt% primary aragonite, lack cementation, Mg/Ca ratios <12.0 mmol/mol, Sr/Ca ratios >8.0 mmol/mol,  $\delta^{18}\text{O}$  values >25.1‰, and  $\delta^{13}\text{C}$  values >-3.0‰ will result in reliable temperature reconstructions for paleoclimate interpretations, as both obvious and subtle diagenesis has been assessed. Applying this set of criteria to fossil corals will reduce the potential inaccuracies in coral based SST reconstructions.
- The coral skeletons from Units A and C in the Ironshore Formation have retained their primary aragonitic skeletons but have undergone chemical diagenesis in a semi-open system by seawater diluted with meteoric water. The coral skeletons in Unit B have been pervasively recrystallized due to alteration in an open diagenetic system dominated by meteoric groundwaters. These corals (A-C) cannot be used to reconstruct paleoclimate. The coral skeletons in Units D, E, and F in the Ironshore Formation have retained their primary aragonitic skeletons and isotopic/elemental compositions and can be used for paleoclimate reconstructions.

In summary, the findings obtained from this study are important because (1) they provide insights into the future of element/Ca geothermometry, (2) include the first SST records from the Cayman Islands over a variety of time periods (modern to

Pleistocene), which are consistent with those from other studies globally and reinforce the implications of global climate dynamics as the driving force for climate change, (3) understanding mid to late Holocene and Pleistocene SST is critical to understanding how future climates will respond to global warming, (4) integration of the Cayman SST profiles to computer models may help to improve the predictive capabilities for future Caribbean climate change, and (5) they provide a criteria for assessing whether older fossil corals are viable candidates for paleoclimate reconstruction.

## REFERENCES

- Alpert, A.E., Cohen, A.L., Oppo, D.W., DeCarlo, T.M., Gaetani, G.A., Hernandez-Delgado, E.A., Winter, A., Gonneea, M.E., 2017. Twentieth century warming of the tropical Atlantic captured by Sr-U paleothermometry. *Paleoceanography* 32, 146-160.
- Arienzo, M.M., Swart, P.K., Pourmand, A., Board, K., Clement, A.C., Murphy, L.N., Vonhof, H.B., Kakuk, B., 2015. Bahamian speleothem reveals temperature decrease associated with Heinrich stadials. *Earth and Planetary Science Letters* 430, 377-386.
- Boiseau, M., Cornu, H., Turpin, L., Juillet-Leclerc, A., 1997. Sr/Ca and  $\delta^{18}\text{O}$  ratios measured from *Acropora nobilis* and *Porites lutea*: is Sr/Ca paleothermometry always reliable? *Earth and Planetary Science Letters* 325, 747-752.
- DeCarlo, T.M., Gaetani, G.A., Cohen, A.L., Foster, G.L., Alpert, A.E., Stewart, J.A., 2016. Coral Sr-U thermometry. *Paleoceanography* 31, 626-638.
- Fensterer, C., Scholz, D., Hoffmann, D.L., Spotl, C., Pajon, J.M., Mangini, A., 2012. Cuban stalagmite suggests relationship between Caribbean precipitation and the Atlantic Multidecadal Oscillation during the past 1.3ka. *Holocene* 22, 1405-1412.
- Flannery, J.A., Richey, J.N., Toth, L.T., Kuffner, I.B., Poore, R.Z., 2018. Quantifying uncertainty in Sr/Ca-based estimates of SST from the coral *Orbicella faveolata*. *Paleoceanography and Paleoclimatology* 33, 958-973.
- Hasen, J., Sato, M., Russell, G., Kharecha, P., 2018. Climate sensitivity, sea level and atmospheric carbon dioxide. *Philosophical Transactions of the Royal Society A*. doi: 371: 20120294.
- Hodell, D.A., Curtis, J.H., Jones, G.A., Higuera-Gundy, A., Brenner, M., Binford, M.W., Dorsey, K.T., 1991. Reconstruction of Caribbean climate change over the past 10,500 years. *Nature: Letters* 352, 790-794.
- IPCC, 2014. Climate change 2014: synthesis report. Contribution of working groups I, II and III to the Fifth Assessment Report of the Intergovernmental Panel on Climate Change, Geneva, Switzerland, 151 pp.
- IPCC, 2018. Summery for policymakers, World Meteorological Organization, Geneva,

Switzerland, 32 pp.

- Kuffner, I.B., Roberts, H.H., Flannery, J.A., Morrison, J.M., Richey, J.N., 2017. Fidelity of Sr/Ca proxy in recording ocean temperature in the western Atlantic coral *Siderastrea siderea*. *Geochemistry Geophysics Geosystems* 18, 178-188.
- Min, G.R., Edwards, R.L., Taylor, F.W., Recy, J., Gallup, C.D., Beck, J.W., 1995. Annual cycles of U/Ca in coral skeletons and U/Ca thermometry. *Geochimica et Cosmochimica Acta* 59, 2025-2042.
- Sinclair, D.J., Kinsley, L.P.J., McCulloch, M.T., 1998. High resolution analysis of trace elements in corals by laser ablation ICP-MS. *Geochimica et Cosmochimica Acta* 62, 1889-1901.

## REFERENCES

- Abahazi, M.A., 2009. Tropical North Atlantic sea surface temperature reconstruction for the last 800 years using Mg/Ca ratios in planktonic foraminifera, Unpublished M.Sc., University of Akron, Ohio, USA, 117 pp.
- Abram, N.J., Gagan, M.K., Liu, Z., Hantoro, W.S., McCulloch, M.T., Suwargadi, B.W., 2007. Seasonal characteristics of the Indian Ocean dipole during the Holocene epoch. *Nature* 445, 299-302.
- Adkins, J.F., Boyle, E.A., Curry, W.B., Lutringer, A., 2003. Stable isotopes in deep-sea corals and a new mechanism for “vital effects”. *Geochimica et Cosmochimica Acta* 67, 1129-1143.
- Aharon, P., Chappell, J., 1983. Carbon and oxygen isotope probes of reef environment histories. In: Barner, D.J. (Ed.), *Perspectives on Coral Reefs*. Australian Institute of Marine Science, pp. 1-10.
- Ahmed, S.M., Padmakumari, V.M., Raza, W., Venkatesham, K., Suseela, G., Sagar, N., Chamoli, A., Rajan, R.S., 2011. High-resolution carbon and oxygen isotope records from a scleractinian (*Porites*) coral of Lakshadweep Archipelago. *Quaternary International* 238, 107-114.
- Alibo, D.S., Nozaki, Y., 1999. Rare earth elements in seawater: particle association, shale-normalization, and Ce oxidation. *Geochimica et Cosmochimica Acta* 63, 363-372.
- Al-Horani, F., Al-Moghrabi, S.M., De Beer, D., 2003. The mechanism of calcification and its relation to photosynthesis and respiration in scleractinian coral *Glaxea fascicularis*. *Marine Biology* 142, 419-426.
- Alibert, C., Kinsley, L., 2008. A 170-year Sr/Ca and Ca/Ca coral record from the western Pacific warm pool: 1. What can we learn from an unusual coral record? *Journal of Geophysical Research- Oceans* 113. doi:10.1029/2006JC003979.
- Alibert, C., McCulloch, M.T., 1997. Strontium/calcium ratios in modern *Porites* corals from the Great Barrier Reef as a proxy for sea surface temperature: calibration of the thermometer and monitoring of ENSO. *Paleoceanography* 12, 345-363.



- Alibo, D.S., Nozaki, Y., 1999. Rare earth elements in seawater: particle association, shale-normalization, and Ce oxidation. *Geochimica et Cosmochimica Acta* 63, 363-372.
- Allison, N., 1996. Geochemical anomalies in coral skeletons and their possible implications for paleoenvironmental analyses. *Marine Chemistry* 55, 367-379.
- Allison, N., Tudhope, A.W., 1992. Nature and significance of geochemical variations in coral skeletons as determined by ion microprobe analysis, 7th International Coral Reef Symposium. 1, pp. 173-178.
- Allison, N., Finch, A.A., 2004. High-resolution Sr/Ca records in modern *Porites lobata* corals: effects of skeletal extension rate and architecture. *Geochemistry Geophysics Geosystems* 5, doi:10.1029/2004GC000696.
- Allison, N., Finch, A.A., Sutton, S.R., Newville, M., 2001. Strontium heterogeneity and speciation in coral aragonite: implications for the strontium paleothermometer. *Geochimica et Cosmochimica Acta* 65, 2669-2676.
- Allison, N., Finch, A.A., Newville, M., Sutton, S.R., 2005. Strontium in coral aragonite: 3. Sr coordination and geochemistry in relation to skeletal architecture. *Geochimica et Cosmochimica Acta* 69, 3801-3811.
- Allison, N., Finch, A.A., 2007. High temporal resolution Mg/Ca and Ba/Ca records in modern *Porites lobata* corals. *Geochemistry Geophysics Geosystems* 8. doi:10.1029/2006GC001477.
- Allison, N., Finch, A.A., Webster, J.M., Clague, D.A., 2007. Palaeoenvironmental records from fossil corals: the effects of submarine diagenesis on temperature and climate estimates. *Geochimica et Cosmochimica Acta* 71, 4693-4703.
- Allison, N., Cohen, I., Finch, A.A., Erez, J., EMIF, 2011. Controls on Sr/Ca and Mg/Ca in scleractinian corals: the effects of Ca-ATPase and transcellular Ca channels on skeletal chemistry. *Geochimica et Cosmochimica Acta* 75, 6350-6360.
- Allison, N., Cole, C., Hintz, C., Hintz, K., Finch, A.A., 2018. Influences of coral genotype and seawater pCO<sub>2</sub> on skeletal Ba/Ca and Mg/Ca in cultured massive *Porites* spp. corals.

- Palaeogeography, Palaeoclimatology, Palaeoecology 505, 351-358.
- Alpert, A.E., Cohen, A.L., Oppo, D.W., DeCarlo, T.M., Gove, J., Young, C., 2016. Comparison of equatorial Pacific sea surface temperature variability and trends with Sr/Ca records from multiple corals. *Paleoceanography* 31, 252-265.
- Alpert, A.E., Cohen, A.L., Oppo, D.W., DeCarlo, T.M., Gaetani, G.A., Hernandez-Delgado, E.A., Winter, A., Gonneea, M.E., 2017. Twentieth century warming of the tropical Atlantic captured by Sr-U paleothermometry. *Paleoceanography* 32, 146-160.
- Amiel, A.J., Friedman, G.M., Miller, D.S., 1973. Distribution and nature of incorporation of trace elements in modern aragonitic corals. *Sedimentology* 20, 47-64.
- Anand, P., Elderfield, H., Conte, M.H., 2003. Calibration of Mg/Ca thermometry in planktonic foraminifera from a sediment trap time series. *Paleoceanography* 18. doi:10.1029/2002PA000846.
- Anderson, T.F., Arthur, M.A., 1983. Stable isotopes of oxygen and carbon and their application to sedimentological and paleoenvironmental problems. *Stable Isotopes in Sedimentary Geology*. SEPM Short Course 10, 1-151.
- Anderson, D.E., 1998. A reconstruction of Holocene climatic changes from peat bogs in north-west Scotland. *Boreas* 27, 208-224.
- Anthony, A., Atwood, J., August, P., Byron, C., Cobb, S., Foster, C., Fry, C., Gold, A., Hagos, K., Heffner, L., Kellogg, D.Q., Lellis-Dibble, K., Opaluch, J.J., Oviatt, C., Pfeiffer-Herbert, A., Rohr, N., Smith, L., Smythe, T., Swift, J., Vinhateiro, N., 2009. Coastal lagoons and climate change: ecological and social ramifications in U.S. Atlantic and Gulf coast ecosystems. *Ecology and Society* 14.
- Arienzo, M.M., Swart, P.K., Pourmand, A., Board, K., Clement, A.C., Murphy, L.N., Vonhof, H.B., Kakuk, B., 2015. Bahamian speleothem reveals temperature decrease associated with Heinrich stadials. *Earth and Planetary Science Letters* 430, 377-386.
- Armid, A., Asami, R., Fahmiati, T., Sheikh, M.A., Fujimura, H., Higuchi, T., Taira, E., Shinjo, R., Oomori, T., 2011. Seawater temperature proxies based on  $D_{Sr}$ ,  $D_{Mg}$ , and  $D_U$  from culture

- experiments using the branching coral *Porites cylindrica*. *Geochimica et Cosmochimica Acta* 75, 4273-4285.
- Arthur, R., 2000. Coral bleaching and mortality in three Indian reef regions during an El Niño southern oscillation event. *Current Science* 79, 1723-1729.
- Atwood, D.K., Hendee, J.C., Mendez, A., 1992. An assessment of global warming stress on Caribbean coral reef ecosystems. *Bulletin of Marine Science* 51, 118-130.
- Ayling, B.F., McCulloch, M., Gagan, M.K., Stirling, C.H., Andersen, M.B., Blake, S.G., 2006. Sr/Ca and  $\delta^{18}\text{O}$  seasonality in a *Porites* coral from the MIS 9 (339-303 ka) interglacial. *Earth and Planetary Science Letters* 248, 462-475.
- Bagnato, S., Linsley, B.K., Howe, S.S., Wellington, G.M., Salinger, J., 2004. Evaluating the use of massive coral *Diploastrea heliopora*. *Paleoceanography* 19. doi:10.1029/2003PA000935.
- Baker, P.A., Weber, J.N., 1975. Coral growth rate: variation with depth. *Earth and Planetary Science Letters* 27, 57-61.
- Balter, V., Lecuyer, C., Barrat, J., 2011. Reconstructing seawater Sr/Ca during the last 70 My using fossil fish tooth enamel. *Palaeogeography, Palaeoclimatology, Palaeoecology* 310, 133-138.
- Bar-Matthews, M., Wasserburg, G.J., Chen, J.H., 1993. Diagenesis of fossil coral skeletons: correlation between trace elements, textures and  $^{234}\text{U}/^{238}\text{U}$ . *Geochimica et Cosmochimica Acta* 57, 257-276.
- Barnes, D.J., Lough, J.M., Tobin, B.J., 1989. Density measurements and the interpretation of X-radiographic images of slices of skeleton from the colonial hard coral *Porites*. *Journal of Experimental Marine Biology and Ecology* 131, 45-60.
- Barnes, D.J., Lough, J.M., 1993. On the nature and causes of density banding in massive coral skeletons. *Journal of Experimental Marine Biology and Ecology* 167, 91-108.
- Barnes, D.J., Taylor, R.B., 1993. On corallites apparent in X-radiographs of skeletal slices of *Porites*. *Journal of Experimental Marine Biology and Ecology* 173, 123-131.

- Barnett, T.P., Delgenio, A.D., Ruedy, R.A., 1992. Unforced decadal fluctuations in a coupled model of the atmosphere and ocean mixed layer. *Journal of Geophysical Research-Oceans* 97, 7341-7354.
- Bath, G.E., Thorrold, S.R., Jones, C.M., Campana, S.E., McLaren, J.W., Lam, J.W.H., 2000. Strontium and barium uptake in aragonite otoliths of marine fish. *Geochimica et Cosmochimica Acta* 64, 1705-1714.
- Beck, J.W., Recy, J., Taylor, F., Edwards, L.R., Cabioch, G., 1997. Abrupt changes in early Holocene tropical sea surface temperature derived from coral records. *Nature* 385, 705-707.
- Beck, J.W., Edwards, L., Ito, E., Taylor, F.W., Recy, J., Rougerie, F., Joannot, P., Henin, C., 1992. Sea-surface temperatures from coral skeletal strontium/calcium ratios. *Science* 257, 644-649.
- Beck, J.W., Edwards, R.L., Ito, E., Taylor, F.W., Recy, J., Rougerie, F., Joannot, P., Isdale, P.J., 1994. Erratum. *Science* 264, 891.
- Bemis, B.E., Spero, H.J., Bijma, J., Lea, D.W., 1998. Reevaluation of the oxygen isotopic composition of planktonic foraminifera: experimental results and revised paleotemperature equations. *Paleoceanography* 13, 150-160.
- Bengtsson, L., Hodges, K.I., Roeckner, E., Brokopf, R., 2006. On the natural variability of the pre-industrial European climate. *Climate Dynamics* 27, 743-760.
- Bernal, J.P., Lachniet, M., McCulloch, M., Mortimer, G.E., Morales, P., Cienfuegos, E., 2011. A speleothem record of Holocene climate variability from southwestern Mexico. *Quaternary Research* 75, 104-113.
- Bessat, F., 1997. Variabilité hydro-climatique et croissance co-rallienne en Polynésie française: exemples de l'île de Moorea et de l'atoll de Mururoa, Paris. Ph.D., University Paris I et EPHE.
- Billups, K., Schrag, D.P., 2002. Paleotemperatures and ice volume of the past 27 Myr revisited with paired Mg/Ca and  $^{18}\text{O}/^{16}\text{O}$  measurements on benthic foraminifera. *Paleoceanography*

17. doi: 10.1029/2000PA000567.

- Blaauw, M., Christen, J.A., 2011. Flexible paleoclimate age-depth models using an autoregressive gamma process. *Bayesian Anal.* 6, 457-474.
- Black, D.E., Abahazi, M.A., Thunell, R.C., Kaplan, A., Tappa, E.J., Peterson, L.C., 2007. An 8-century tropical Atlantic SST record from the Cariaco Basin: baseline variability, twentieth-century warming, and Atlantic hurricane frequency. *Paleoceanography* 22, 4023-4034.
- Black, D.E., Peterson, L.C., Overpeck, J.T., Kaplan, A., Evans, M.N., Kashgarian, M., 1999. Eight centuries of North Atlantic Ocean atmosphere variability. *Science* 286, 1709-1713.
- Black, D.E., Thunell, R.C., Kaplan, A., Peterson, L.C., Tappa, E.J., 2004. A 2000-year record of Caribbean and tropical North Atlantic hydrographic variability. *Paleoceanography* 19, 1-11.
- Blanchon, P.A., Jones, B., 1995. Marine-planation terraces on the shelf of Grand Cayman: a result of stepped Holocene sea-level rise. *Journal of Coastal Research* 11, 1-33.
- Blanchon, P.A., Jones, B., Kalbfleisch, W., 1997. Anatomy of a fringing reef around Grand Cayman: storm rubble, not coral framework. *Journal of Sedimentary Research* 67, 1-16.
- Blanchon, P.A., Eisenhauer, A., Fietzke, J., Liebetrau, V., 2009. Rapid sea-level rise and reef back-stepping at the close of the last interglacial highstand. *Nature: Letters* 458, 881-885.
- Bohm, F., Joachimski, M.M., Dullo, W., Eisenhauer, A., Lehnert, H., Reitner, J., Worheide, G., 2000. Oxygen isotope fractionation in marine aragonite of coralline sponges. *Geochimica et Cosmochimica Acta* 64, 1695-1703.
- Boiseau, M., Cornu, H., Turpin, L., Juillet-Leclerc, A., 1997. Sr/Ca and  $\delta^{18}\text{O}$  ratios measured from *Acropora nobilis* and *Porites lutea*: is Sr/Ca paleothermometry always reliable? *Earth and Planetary Science Letters* 325, 747-752.
- Bolton, A., Goodkin, N.F., Hughen, K.A., Ostermann, D.R., Vo, S.T., Phan, H.K., 2014. Paired *Porites* coral Sr/Ca and  $\delta^{18}\text{O}$  from the western South China Sea: proxy calibration of sea surface temperatures and precipitation. *Palaeogeography, Palaeoclimatology,*

- Palaeoecology 410, 233-243.
- Booker, S.D., Jones, B., Li, L., 2020. Diagenesis in Pleistocene (80 to 500 ka) corals from the Ironshore Formation: implications for paleoclimate reconstruction. *Sedimentary Geology* 399, doi: 10.1016/j.sedgeo.2020.105615.
- Booker, S.D., Jones, B., Chacko, T., Li, L., 2019. Insights into sea surface temperatures from the Cayman Islands from corals over the last ~540 years. *Sedimentary Geology* 389, 218-240.
- Bond, G., Showers, W., Cheseby, M., Lotti, R., Almasi, P., deMenocal, P., Priore, P., Cullen, H., Hajads, I., Bonani, G., 1997. A pervasive millennial-scale cycle in North Atlantic Holocene and glacial climates. *Science* 278, 1257-1266.
- Bosscher, H., 1992. Computer tomography and skeletal density of coral skeletons. *Coral Reefs* 12, 97-103.
- Bouillon, S., Connolly, R.M., S.Y., L., 2008. Organic matter exchange and cycling in mangrove ecosystems: recent insights from stable isotope studies. *Journal of Sea Research* 59, 44-58.
- Bouvier-Soumagnac, Y., Duplessy, J.C., 1985. Carbon and oxygen isotopic composition of planktonic foraminifera from laboratory culture, planktonic tows and recent sediment: implications for the reconstruction of paleoclimatic conditions and of the global carbon cycle. *Journal of Foraminiferal Research* 15, 302-320.
- Bracco, R., Inda, H., del Puerto, L., Castiñeira, C., Sprechmann, P., García-Rodríguez, F., 2005. Relationships between Holocene sea-level variations, trophic development, and climatic change in Negra Lagoon, Southern Uruguay. *Journal of Paleolimnology* 33, 253-263.
- Brahmi, C., Kopp, C., Domart-Coulon, I., Stolarski, J., Meibom, A., 2012. Skeletal growth dynamics linked to trace-element composition in the scleractinian coral *Pocillopora damicornis*. *Geochimica et Cosmochimica Acta* 99, 146-158.
- Brand, U., Veizer, J., 1983. Origin of coated grains: trace element constraints. In: Peryt, T. (Ed.), *Coated Grains*. Springer-Verlag, Berlin Heidelberg New York Tokyo, pp. 9-26.

- Brocas, W.M., Felis, T., Obert, J.C., Gierz, P., Lohmann, G., Scholz, D., Kolling, M., Scheffers, S.R., 2016. Last interglacial temperature seasonality reconstructed from tropical Atlantic corals. *Earth and Planetary Science Letters* 449, 418-429.
- Broecker, W.S., Peng, T., 1982. Tracers in the sea. Eldigio Pree, Lamont Doherty Geological Observatory, New York, pp. 702.
- Broecker, W.S., 1991. The great ocean conveyor. *Oceanography* 4, 79-89.
- Bruckner, A., 2010, Cayman Islands coral reef health and resilience assessment. <https://www.livingoceansfoundation.org/publication/cayman-islands-coral-reef-health-and-resilience-assessments/> (Accessed August 2016).
- Bryan, S.P., Marchitto, T.M., 2008. Mg/Ca-temperature proxy in benthic foraminifera: new calibrations from the Florida Straits and a hypothesis regarding Mg/Li. *Paleoceanography* 23, 1-17.
- Budd, A.F., Fukami, H., Smith, N.D., Knowlton, N., 2012. Taxonomic classification of the reef coral family Mussidae (Cnidaria: Anthozoa: Scleractinia). *Zoological Journal of the Linnean Society* 166, 465-529.
- Buddemeier, R.W., Maragos, J.E., Knutson, D.K., 1974. Radiographic studies of reef coral exoskeletons: rates and patterns of growth. *Journal of Experimental Marine Biology and Ecology* 14, 179-200.
- Buddemeier, R.W., Kinzie, R.A., 1976. Coral growth. *Oceanography, Marine Biology Annual Review* 14, 183-225.
- Buddemeier, R.W., Schneider, R.C., Smith, S.V., 1981. The alkaline earth chemistry of corals, *Proceedings of the 4th International Coral Reef Symposium*, pp. 81-85.
- Burnt, M.A., Giglioli, M.E.C., Mather, J.D., Piper, D.J.W., Richards, H.G., 1973. The Pleistocene rocks of the Cayman Islands. *Geological Magazine* 110, 209-304.
- Byrne, R., Sholkovitz, E., 1996. Marine chemistry and geochemistry of the lathanides. *Handbook on the Physics and Chemistry of Rare Earths*, 23. Elsevier, Amsterdam, pp. 497-593.
- Byrne, R.H., Kim, K., 1990. Rare earth elements scavenging in seawater. *Geochimica et*

- Cosmochimica Acta 54, 2645-2656.
- Cahyarini, S.Y., Pfeiffer, M., Dullo, W., 2009. Improving SST reconstructions from coral Sr/Ca records: multiple corals from Tahiti (French Polynesia). International Journal of Earth Sciences (Geol Rundsch), doi: 10.1007/s00531-008-0323-2.
- Cahyarini, S.Y., Pfeiffer, M., Timm, O., Dullo, W., Garbe-Schonberg, D., 2008. Reconstructing seawater  $\delta^{18}\text{O}$  from paired  $\delta^{18}\text{O}$  and Sr/Ca ratios: methods, error analysis and problems, with examples from Tahiti (French Polynesia) and Timor (Indonesia). Geochimica et Cosmochimica Acta 72, 2841-2853.
- Calvo, E., Marshall, J.F., Pelegero, C., McCulloch, M., Gagan, M.K., Lough, J.M., 2007. Interdecadal climate variability in the Coral Sea since 1708 A.D. Palaeogeography, Palaeoclimatology, Palaeoecology 248, 109-201.
- Cardinal, D., Hamelin, B., Bard, E., Patzold, J., 2001. Sr/Ca, U/Ca and  $\delta^{18}\text{O}$  records in recent massive corals from Bermuda: relationships with sea surface temperature. Chemical Geology 176, 213-233.
- Cantrell, K.J., Byrne, R.H., 1987. Rare earth element complexation by carbonate and oxalate ions. Geochimica et Cosmochimica Acta 51, 597-605.
- Carilli, J.E., McGregor, H.V., Gaudry, J.J., Donner, S.D., Gagan, M.K., Stevenson, S., Wong, H., Fink, D., 2014. Equatorial Pacific coral geochemical records show recent weakening of the Walker Circulation. Paleoceanography 29, 1031-1045.
- Carlson D., 2017. A comparison of Holocene Climate Optimum Periods: are they as warm as the Post-Little Ice Age Periods and are greenhouse gas concentrations similar? Gulf Coast Association of Geological Societies Transactions 67, 39-78.
- Carricart-Ganivet, J.P., 2004. Sea surface temperature and the growth of the West Atlantic reef-building coral *Montastraea annularis*. Journal of Experimental Marine Biology and Ecology 302, 249-260.
- Carricart-Ganivet, J.P., 2011. Coral skeletal extension rate: an environmental signal or a subject to inaccuracies? Journal of Experimental Marine Biology and Ecology 405, 73-79.



- Carricart-Ganivet, J.P., Merino, M., 2001. Growth responses of the reed-building coral *Montastrea annularis* along a gradient of continental influence in the Southern Gulf of Mexico. *Bulletin of Marine Science* 68, 133-146.
- Case, D.H., Robinson, L.F., Auro, M.E., Gagnon, A.C., 2010. Environmental and biological controls on Mg and Li in deep-sea scleractinian corals. *Earth and Planetary Science Letters* 300, 215-225.
- Casey, K.S., Cornillon, P., 1999. A comparison of satellite and in situ-based sea surface temperature climatologies. *Journal of Climate* 12, 1848-1863.
- Centurioni, L.R., Niiler, P.P., 2003. On the surface currents of the Caribbean Sea. *Geophysical Research Letters* 30, doi 10.1029/2002GL016231.
- Chacko, T., Deines, P., 2008. Theoretical calculation of oxygen isotope fractionation factors in carbonate systems. *Geochimica et Cosmochimica Acta* 72, 3642-3660.
- Chakraborty, S., Ramesh, R., 1993. Monsoon-induced sea surface temperature changes recorded in Indian corals. *Terra Nova* 5, 545-551.
- Chan, P., Halfar, J., Norley, C.J.D., Pollmann, S.I., Adey, W., Holdsworth, D.W., 2017. Micro-computed tomography: applications for high-resolution skeletal density determinations: an example using annually banded crustose coralline algae. *Geochemistry Geophysics Geosystems* 18, 3542-3553.
- Charman, D.J., Blundell, A., Chiverrell, R.C., Hendon, D., Langdon, P.G., 2006. Compilation of non-annually resolved Holocene proxy climate records: stacked Holocene peatland palaeo-water table reconstructions from northern Britain. *Quaternary Science Reviews* 25, 336-350.
- Chave, K.E., 1954. Aspects of the biogeochemistry of magnesium 1. Calcareous marine organisms. *Journal of Geology* 62, 266-283.
- Chen, M., Tu, X., Zheng, F., Yan, W., Tang, X., Lu, J., Wang, B., Lu, M., 2000. Relations between sedimentary sequence and paleoclimatic changes during last 200 ka in the southern South China Sea. *Chinese Science Bulletin* 45, 1334-1340.

- Chenoweth, M., 1998. The early 19<sup>th</sup> century climate of the Bahamas and a comparison with 20<sup>th</sup> century averages. *Climate Change* 40, 577-603.
- Chollett, I., Muller-Karger, F.E., Heron, S.F., Skirving, W., Mumby, P.J., 2012a. Seasonal and spatial heterogeneity of recent sea surface temperature trends in the Caribbean Sea and southeast Gulf of Mexico. *Marine Pollution Bulletin* 64, 956-965.
- Chollett, I., Mumby, P.J., Muller-Karger, F.E., Hu, C., 2012b. Physical environments of the Caribbean Sea. *Limnology and Oceanography* 57, 1233-1244.
- Cleroux, C., Cortijo, E., Anand, P., Labeyrie, L., Bassinot, F., Caillon, N., Duplessy, J.C., 2008. Mg/Ca and Sr/Ca ratios in planktonic foraminifera: proxies for upper water column temperature reconstruction. *Paleoceanography* 23. doi:10.1029/2007PA001505.
- Cobb, K.M., Charles, C.D., Cheng, H., Kastner, M., Edwards, R.L., 2003. U/Th-dating living and young fossil corals from the central tropical Pacific. *Earth and Planetary Science Letters* 210, 91-103.
- Cochran, J.K., Kallenberg, K., Landman, N.H., Harries, P.J., Weinreb, D., Turekian, K.K., Beck, A.J., Cobban, W.A., 2010. Effect of diagenesis on the Sr, O, and C isotope composition of Late Cretaceous mollusks from the Western Interior Seaway of North America. *American Journal of Science* 310, 69-88.
- Cohen, A.L., McConnaughey, T.A., 2003. Geochemical perspectives on coral mineralization. In: Dove, P.M., Yorer, J.J.D., Weiner, S. (Eds.), *Biom mineralization*. Mineralogy Society of America, Washington, DC, pp. 37.
- Cohen, A.L., Gaetani, G.A., 2010. Ion partitioning and the geochemistry of coral skeletons: solving the mystery of the vital effect. In: Prieto, M., Stoll, H.M., *Mineralogy, European Mineralogy Union Notes in* (Eds.), *Ion partitioning in ambient-temperature aqueous systems*. European Mineralogy Union, Vienna, pp. 377-397.
- Cohen, A.L., Layne, G.D., Hart, S.R., Lobel, P.S., 2001. Kinetic control of skeletal Sr/Ca in a symbiotic coral: implications for the paleotemperature proxy. *Paleoceanography* 16, 20-26.

- Cohen, A.L., Owens, K.E., Layne, G.D., Shimizu, N., 2002. The effect of algal symbionts on the accuracy of Sr/Ca paleotemperatures from coral. *Science* 296, 331-333.
- Cole, J.E., Fairbanks, R.G., Shen, G.T., 1993. Variability in the Southern Oscillation: isotopic results from a Tarawa Atoll coral. *Science* 260, 1790-1793.
- Coplen, T.B., 2007. Calibration of the calcite-water oxygen-isotope geothermometer at Devils Hole, Nevada, a natural laboratory. *Geochimica et Cosmochimica Acta* 71, 3948-3957.
- Corderio, L.G.M.S., Belem, A.L., Rangel, B., Sifeddine, A., Capilla, R., Albuquerque, A.L.S., 2014. Reconstruction of southwestern Atlantic sea surface temperatures during the last century: Cabo Frio continental shelf (Brazil). *Palaeogeography, Palaeoclimatology, Palaeoecology* 415, 225-232.
- Correge, T., 2006. Sea surface temperature and salinity reconstruction from coral geochemical tracers. *Palaeogeography, Palaeoclimatology, Palaeoecology* 232, 408-428.
- Correge, T., Deleroix, T., Recy, J., Beck, W.C., Cabioch, G., Le Cornec, F., 2000. Evidence for stronger El Niño-Southern Oscillation (ENSO) events in a mid-Holocene massive coral. *Paleoceanography* 15, 465-470.
- Correge, T., Quinn, T., Delcroix, T., Le Cornec, F., Recy, J., Cabioch, G., 2001. Little Ice Age sea surface temperature variability in the southwest tropical Pacific. *Geophysical Research Letters* 28, 3477-3480.
- Correge, T., Gagan, M.K., Beck, J.W., Burr, G.S., Cabloch, G., Le Cornec, F., 2004. Interdecadal variation in the extent of South Pacific tropical waters during the Younger Dryas event. *Nature* 428, 927-929.
- Coyne, M.K., 2003. Transgressive-regressive cycles in the Ironshore Formation, Grand Cayman, British West Indies, Unpublished. M.Sc. Thesis, University of Alberta, Edmonton, Alberta, Canada, 98 pp.
- Coyne, M.K., Jones, B., Ford, D., 2007. Highstands during marine isotope stage 5: evidence from the Ironshore Formation of Grand Cayman, British West Indies. *Quaternary Science Reviews* 26, 536-559.

- Craig, H., 1965. The measurement of oxygen isotope paleotemperatures. In: E., Tongiorgi. (Ed.), Stable Isotopes in Oceanographic Studies and Paleotemperatures. Spoleto, Consiglio Nazionale delle Ricerche, Laboratorio de Geologica Nucleare, Pisa, pp. 161-182.
- Crann, C.A., Murseli, S., St-Jean, G., Zhao, X., Clark, I.D., Kieser, W.E., 2017. First status report on radiocarbon sample preparation techniques at the A.E. Lalonde AMS Laboratory (Ottawa, Canada). Radiocarbon 59, 695-704.
- Cronin, T.M., Hayo, K., Thunell, R.C., Dwyer, G.S., Saenger, C., Willard, D.A., 2010. The Medieval Climate Anomaly and Little Ice Age in Chesapeake Bay and the North Atlantic Ocean. Palaeogeography, Palaeoclimatology, Palaeoecology 291, 299-310.
- Cross, T.S., Cross, B.W., 1983. U, Sr, and Mg in Holocene and Pleistocene corals *A. palmata* and *M. annularis*. Journal of Sedimentary Petrology 53, 587-594.
- Crowley, T.J., Kim, K., 1994. Milankovitch forcing of the last Interglacial sea level. Science 265, 1566-1568.
- Crowley, T.J., Quinn, T.M., Hyde, W.T., 1999. Validation of coral temperature calibrations. Paleoceanography 14, 605-615.
- Cuiff, J., Dauphin, Y., 2004. Associated water and organic compounds in coral skeletons: quantitative thermogravimetry coupled to infrared absorption spectrometry. Geochemistry Geophysics Geosystems 5. doi:10.1029/2004GC000783.
- Cuiff, J., Dauphin, Y., 2005. The environment recording unit in coral skeletons- a synthesis of structural and chemical evidences for a biochemically driven, stepping-growth process in fibers. Biogeosciences 2, 61-73.
- Culver, S.J., 1990. Benthic foraminifera of Puerto Rican mangrove-lagoon systems: potential for paleoenvironmental interpretations. PALAIOS 5, 34-51.
- Dana, J.D., 1846. Structure and classification of zoophytes. U.S. Exploring Expedition 1838-1842, 7. Lea and Blanchard, Philadelphia, 740 pp.
- Day, M., 2010. Challenges to sustainability in the Caribbean karst. Geologia Croatia 63, 149-154.
- de Villiers, S., 1999. Seawater strontium and Sr/Ca variability in the Atlantic and Pacific oceans.

- Earth and Planetary Science Letters 171, 623-634.
- de Villiers, S., Shen, G.T., Nelson, B.K., 1994. The Sr/Ca-temperature relationship in coralline aragonite: influence of variability in  $(\text{Sr}/\text{Ca})_{\text{seawater}}$  and skeletal growth parameters. *Geochimica et Cosmochimica Acta* 58, 197-208.
- de Villiers, S., Nelson, B.K., Chivas, A.R., 1995. Biological controls on coral Sr/Ca and  $\delta^{18}\text{O}$  reconstructions of sea surface temperatures. *Science* 269, 1247-1250.
- DeCarlo, T.M., Gaetani, G.A., Holcomb, M., Cohen, A.L., 2015. Experimental determination of factors controlling U/Ca of aragonite precipitated from seawater: implications for interpreting coral skeleton. *Geochimica et Cosmochimica Acta* 162, 151-165.
- DeCarlo, T.M., Gaetani, G.A., Cohen, A.L., Foster, G.L., Alpert, A.E., Stewart, J.A., 2016. Coral Sr-U thermometry. *Paleoceanography* 31, 626-638.
- Delaney, M.L., Be, A.W.H., Boyle, E.A., 1985. Li, Sr, Mg, and Na in foraminiferal calcite shells from laboratory culture, sediment traps, and sediment cores. *Geochimica et Cosmochimica Acta* 49, 1327-1341.
- Delaney, M.L., Popp, B.N., Lepzelter, C.G., Anderson, T.F., 1989. Lithium-to-calcium ratios in modern, Cenezoic, and Paleozoic articulate brachiopod shells. *Paleoceanography* 4, 681-691.
- Delaney, M.L., Linn, L.J., Davies, P.J., 1996. Trace and minor element ratios in *Halimeda* aragonite from the Great Barrier Reef. *Coral Reefs* 15, 181-189.
- Delaney, J., Eichler, B.B., Duleba, W., Bonetti, C., Eichler-Colho, P., 1998. Water stratification in coastal lagoons: its influence on foraminiferal assemblages in two Brazilian lagoons. *Marine Micropaleontology* 35, 67-89.
- DeLong, K.L., Quinn, T.M., Taylor, F.W., 2007. Reconstructing twentieth-century sea surface temperature variability in the southwest Pacific: a replication study using multiple coral Sr/Ca records from New Caledonia. *Paleoceanography* 22. doi:10.1029/2007PA001444.
- DeLong, K.L., Quinn, T.M., Shen, C., Lin, K., 2010. A snapshot of climate variability at Tahiti at 9.5 ka using a fossil coral from IODP Expedition 310. *Geochemistry Geophysics*

Geosystems 11. doi:10.1029/2009GC002758.

- DeLong, K.L., Flannery, J.A., Maupin, C.R., Poore, R.Z., Quinn, T.M., 2011. A coral Sr/Ca calibration and replication study of two massive corals from the Gulf of Mexico. *Palaeogeography, Palaeoclimatology, Palaeoecology* 307, 117-128.
- DeLong, K.L., Quinn, T.M., Taylor, F.W., Shen, C., Lin, K., 2013. Improving coral-based paleoclimate reconstructions by replicating 350 years of coral Sr/Ca variations. *Palaeogeography, Palaeoclimatology, Palaeoecology* 373, 6-24.
- DeLong, K.L., Flannery, J.A., Poore, R.Z., Quinn, T.M., Maupin, C.R., Lin, K., She, C., 2014. A reconstruction of sea surface temperature variability in the southeastern Gulf of Mexico from 1734 to 2008 C.E. using cross-dated Sr/Ca records from the coral *Siderastrea siderea*. *Paleoceanography* 29, 403-422.
- deMenocal, P., Ortiz, J., Guilderson, T., Sarnthein, M., 2000. Coherent high and low-latitude climate variability during the Holocene warm period. *Science* 288, 2198-2202.
- Deng, W., Wei, G., Li, X., Yu, K., Zhao, J., Sun, W., Lui, Y., 2009. Paleoprecipitation record from coral Sr/Ca and  $\delta^{18}\text{O}$  during the mid Holocene in the northern South China Sea. *The Holocene* 19, 811-821.
- Deng, W., Liu, X., Wei, G., Zeng, T., Xie, L., Zhao, J., 2017. A comparison of the climates of the Medieval Climate Anomaly, Little Ice Age, and Current Warm Period reconstructed using coral records from the northern South China Sea. *Journal of Geophysical Research: Oceans* 122, 264-275.
- Diaz, M., Macario, K.D., Gomes, P.R.S., Alvarez-Lajonchere, L., Aguilera, O., Alves, E.Q., 2017. Radiocarbon marine reservoir effects on the northwestern coast of Cuba. *Radiocarbon* 59, 333-341.
- Dietzel, M., Gussone, N., Eisenhauer, A., 2004. Co-precipitation of  $\text{Sr}^{2+}$  and  $\text{Ba}^{2+}$  with aragonite by membrane diffusion of  $\text{CO}_2$  between 10 and 50°C. *Chemical Geology* 203, 139-151.
- Dodge, R.E., Thomason, J., 1974. The natural radiochemical and growth records in contemporary hermatypic corals from the Atlantic and Caribbean. *Earth and Planetary Science Letters*

23, 313-322.

- Doherty, O.M., Riemer, N., Hameed, S., 2012. Control of Saharan mineral dust transport to Barbados in winter by the Intertropical Convergence Zone over West Africa. *Journal of Geophysical Research* 117. doi:10.1029/2012JD017767.
- Donegan, B., 2019. Saharan dust surges into Caribbean- here's what that means during hurricane season, The Weather Channel. TWC Product and Technology LLC.
- Druffel, E.R.M., 1997. Pulses of rapid ventilation in the north Atlantic surface ocean during the past century. *Science* 275, 1454-1457.
- Dunbar, R.B., Wefer, G., 1984. Stable isotope fractionation in benthic foraminifera from the Peruvian Continental Margin. *Marine Geology* 59, 215-225.
- Dunbar, R.B., Wellington, G.M., 1981. Stable isotopes in a branching coral monitor seasonal temperature variation. *Nature* 293, 453-455.
- Dunbar, R.B., Wellington, G.M., Colgan, M.W., Glynn, P.W., 1994. Eastern Pacific sea surface temperature since 1600 A.D.: the  $\delta^{18}\text{O}$  record of climate variability in Galapagos corals. *Paleoceanography* 9, 291-315.
- Edmond, J.M., Measures, C., McDuff, R.E., Chan, L.H., Collier, R., Grant, B., Gordon, L.I., Corliss, J.B., 1979. Ridge crest hydrothermal activity and the balances of the major and minor elements in the ocean: the Galapagos data. *Earth and Planetary Science Letters* 46, 1-18.
- Elderfield, H., Bertram, C.J., Erez, J., 1996. Biomineralization model for the incorporation of trace elements into foraminiferal calcium carbonate. *Earth and Planetary Science Letters* 142, 409-423.
- Elderfield, H., Cooper, M., Ganssen, G., 2000. Sr/Ca in multiple species of planktonic foraminifera: implications for reconstructions of seawater Sr/Ca. *Geochemistry Geophysics Geosystems* 1. doi: 10.1029/1999GC000031.
- Elderfield, H., Ganssen, G., 2000. Past temperature and delta-18O of surface ocean waters inferred from foraminiferal Mg/Ca ratios. *Nature* 405, 442-445.

- Elderfield, H., Vautravers, M., Cooper, M., 2002. The relationship between shell size and Mg/Ca, Sr/Ca,  $\delta^{18}\text{O}$ , and  $\delta^{13}\text{C}$  of species of planktonic foraminifera. *Geochemistry Geophysics Geosystems* 3. doi: 10.1029/2001GC000194.
- Elderfield, H., Yu, J., Anand, P., Kiefer, T., Nyland, B., 2006. Calibrations for benthic foraminiferal Mg/Ca paleothermometry and the carbonate ion hypothesis. *Earth and Planetary Science Letters* 250, 633-649.
- Emery, K.O., 1981. Low marine terraces of Grand Cayman Island. *Estuarine, Coastal and Shelf Science* 12, 569-578.
- Enfield, D.B., Mestas-Nunez, A.M., Trimble, P.J., 2001. The Atlantic multidecadal oscillation and its relation to rainfall and river flows in the continental U.S. *Geophysical Research Letters* 28, 2077-2080.
- Enmar, R., Stein, M., Bar-Matthews, M., Sass, E., Katz, A., Lazar, B., 2000. Diagenesis in live corals from the Gulf of Aqaba. I. The effect on paleo-oceanography tracers. *Geochimica et Cosmochimica Acta* 64, 3123-3132.
- Epstein, S., Buchsbaum, R., Lowenstam, H., Urey, H.C., 1953. Revised carbonate-water isotopic temperature scale. *Geological Society of America Bulletin* 64, 1315-1325.
- Erez, J., 1977. Influence of symbiotic algae on the stable isotope composition of hermatypic corals: a radioactive tracer approach. In: Taylor, D.L. (Ed.), *Third International Coral Reef Symposium*. Rosenstiel School of Marine and Atmospheric Sciences, Miami, Florida, 564-569.
- Erez, J., 1978. Vital effect on stable-isotopes composition seen in foraminifera and coral skeletons. *Nature* 273, 199-202.
- Evans, M.N., Fairbanks, R.G., Rubenstone, J.L., 1999. The thermal oceanographic signal of El Nino reconstructed from a Kiritimati Island coral. *Journal of Geophysical Research* 104, 409-421.
- Evans, D., Erez, J., Oron, S., Muller, W., 2015. Mg/Ca-temperature and seawater-test chemistry relationships in the shallow-dwelling large benthic foraminifera *Operculina ammonoides*.



- Geochimica et Cosmochimica Acta 148, 325-342.
- Fahlquist, D.A., Davies, D.K., 1971. Fault block origin of the western Cayman Ridge, Caribbean Sea. *Deep Sea Research* 18, 243-253.
- Fairbanks, R.D., Dodge, R.E., 1979. Annual periodicity of the  $^{18}\text{O}/^{16}\text{O}$  and  $^{13}\text{C}/^{12}\text{C}$  ratios in the coral *Montastrea annularis*. *Geochimica et Cosmochimica Acta* 43, 1009-1020.
- Fallon, S.J., McCulloch, M., Alibert, C., 2003. Examining water temperature proxies in *Porites* corals from the Great Barrier Reef: a cross-shelf comparison. *Coral Reefs* 22, 389-404.
- Fallon, S.J., McCulloch, M., van Woesik, R., Sinclair, D.J., 1999. Corals at their latitudinal limits: laser ablation trace element systematics in *Porites* from Shirigai Bay, Japan. *Earth and Planetary Science Letters* 172, 221-238.
- Farfan, G.A., Cordes, E.E., Waller, R.G., DeCarlo, T.M., Hansel, C.M., 2018. Mineralogy of deep-sea coral aragonites as a function of aragonite saturation state. *Frontiers in Marine Science* 5. doi: 10.3389/fmars.2018.00473.
- Fegyveresi, J.M., Alley, R.B., Fitzpatrick, J.J., Cuffey, K.M., McConnell, J.R., Voigt, D.E., Spencer, M.K., Stevens, N.T., 2016. Five millennia of surface temperatures and ice core bubble characteristics from the WAIS Divide deep core, West Antarctica. *Paleoceanography* 31, 416-433.
- Felis, T., Patzold, J., Loya, Y., 2003. Mean oxygen-isotope signatures in *Porites* sp. corals: inter-colony variability and correction for extension-rate effects. *Coral Reefs* 22, 328-336.
- Felis, T., Lohmann, G., Kuhnert, H., Lorenz, S.J., Scholz, D., Patzold, J., Al-Rousan, S., Al-Moghrabi, S.M., 2004. Increased seasonality in Middle East temperatures during the last interglacial period. *Nature* 429, 164-168.
- Felis, T., Suzuki, A., Kuhnert, H., Dima, M., Lohmann, G., Kawahata, H., 2009. Subtropical coral reveals abrupt early-twentieth-century freshening in the western North Pacific Ocean. *Geology* 37, 527-530.
- Felis, T., Merkel, U., Asami, R., Deschamps, P., Hathorne, E., Kolling, M., Bard, E., Cabioch, G., Durand, N., Prange, M., 2012. Pronounced interannual variability in tropical South

- Pacific temperatures during Heinrich Stadial 1. National Communication 3. doi: 10.1038/ncomms1973.
- Felis, T., Giry, C., Scholz, D., Lohmann, G., Pfeiffer, M., Patzold, J., Kolling, M., Scheffers, S.R., 2015. Tropical Atlantic temperature seasonality at the end of the last interglacial. *Nature: Communications*, 6. doi: 10.1038/ncomms7159.
- Fensterer, C., Scholz, D., Hoffmann, D.L., Spotl, C., Pajon, J.M., Mangini, A., 2012. Cuban stalagmite suggests relationship between Caribbean precipitation and the Atlantic Multidecadal Oscillation during the past 1.3ka. *Holocene* 22, 1405-1412.
- Flannery, J.A., Poore, R.Z., 2013. Sr/Ca proxy sea-surface temperature reconstructions from modern and Holocene *Montastrea faveolata* specimens from the Dry Tortugas National Park, Florida, U.S.A. *Journal of Coastal Research* 63, 20-31.
- Flannery, J.A., Richey, J.N., Thirumalai, K., Poore, R.Z., Della-Marta, P., 2017. Multi-species coral Sr/Ca-based sea-surface temperature reconstruction using *Orbicella faveolata* and *Siderastrea siderea* from the Florida Straits. *Palaeogeography, Palaeoclimatology, Palaeoecology*. 466, 100-109.
- Flannery, J.A., Richey, J.N., Toth, L.T., Kuffner, I.B., Poore, R.Z., 2018. Quantifying uncertainty in Sr/Ca-based estimates of SST from the coral *Orbicella faveolata*. *Paleoceanography and Paleoclimatology* 33, 958-973.
- Fensterer, C., Scholz, D., Hoffmann, D.L., Spotl, C., Pajon, J.M., Mangini, A., 2012. Cuban stalagmite suggests relationship between Caribbean precipitation and the Atlantic Multidecadal Oscillation during the past 1.3ka. *Holocene* 22, 1405-1412.
- Fenner, D.P., 1993. Some reefs and corals of Roatan (Honduras), Cayman Brac, and Little Cayman. *Atoll Research Bulletin* 388, 1-32.
- Ferrier-Pages, C., Boisson, F., Allemand, D., Tambutte, E., 2002. Kinetics of strontium uptake in the scleractinian coral *Stylophora pistillata*. *Marine Ecology - Progress Series* 245, 93-100.
- Finch, A.A., Allison, N., 2003. Strontium in coral aragonite: 2. Sr coordination and the long-term

- stability of coral environmental records. *Geochimica et Cosmochimica Acta* 67, 4519-4527.
- Finch, A.A., Allison, N., 2008. Mg structural state in coral aragonite and implications for the paleoenvironmental proxy. *Geophysical Research Letters* 35. doi:10.1029/2008GL033543.
- Finkenbinder, M.S., Abbot, M.B., Steinman, B.A., 2016. Holocene climate change in Newfoundland reconstructed using oxygen isotope analysis of lake sediment cores. *Global and Planetary Change* 143, 251-261.
- Finne, M., Holmgren, K., Sundqvist, H.S., Weiberg, E., Lindblom, M., 2011. Climate in the eastern Mediterranean, and adjacent regions, during the past 6000 years- a review. *Journal of Archaeological Science* 38, 3153-3173.
- Fleming, K., Johnston, P., Zwart, D., Yokoyama, Y., Lambeck, K., Cchappell, J., 1998. Refining the eustatic sea-level curve since the Last Glacial Maximum using far- and intermediate-field sites. *Earth and Planetary Science Letters* 163, 327-342.
- Fowell, S.E., Sandford, K., Stewart, J.A., Castillo, K.D., Ries, J.B., Foster, G.L., 2016. Intrareef variations in Li/Mg and Sr/Ca sea surface temperature proxies in the Caribbean reef-building coral *Siderastrea siderea*. *Paleoceanography* 31, 1315-1329.
- Frich, P.L., Alexander, V., Della-Marta, P., Gleason, B., Haylock, M., Tank, A.K., Peterson, T.C., 2002. Global changes in climatic extremes during the 2<sup>nd</sup> half of the 20<sup>th</sup> century. *Climate Resources* 19, 193-212.
- Frisia, S., Borsato, A., Spotl, C., Villa, I., Cucchi, F., 2005. Climate variability in the SE Alps of Italy over the past 17 000 years reconstructed from a stalagmite record. *Boreas* 34, 445-455.
- Gaetani, G.A., Cohen, A.L., 2006. Element partitioning during precipitation of aragonite from seawater: a framework for understanding paleoproxies. *Geochimica et Cosmochimica Acta* 70, 4617-4634.
- Gaetani, G.A., Cohen, A.L., Wang, Z., Crusius, J., 2011. Rayleigh-based, multi-element coral

- thermometry: a biomineralization approach to developing climate proxies. *Geochimica et Cosmochimica Acta* 75, 1920-1932.
- Gagan, M.K., Dunbar, G.B., Suzuki, A., 2012. The effect of skeletal mass accumulation in *Porites* on coral Sr/Ca and  $\delta^{18}\text{O}$  paleothermometry. *Paleoceanography* 27. doi:10.1029/2011PA002215.
- Gagan, M.K., Chivas, A.R., Isdale, P.J., 1994. High-resolution isotopic records from corals using ocean temperature and mass-spawning chronometers. *Earth and Planetary Science Letters* 121, 549-558.
- Gagan, M.K., Ayliffe, L.K., Hopley, D., Cali, J.A., Mortimer, G.E., Chappell, J., McCulloch, M., Head, M.J., 1998. Temperature and surface-ocean water balance of the Mid-Holocene tropical western Pacific. *Science* 279, 1014-1018.
- Gagan, M.K., Ayliffe, L.K., Hopley, D., Cali, J.A., Mortimer, G.E., Chappell, J., McCulloch, M., Head, M.J., 1998. Temperature and surface-ocean water balance of the Mid-Holocene tropical western Pacific. *Science* 279, 1014-1018.
- Gagan, M.K., Ayliffe, L.K., Beck, J.W., Cole, J.E., Druffel, E.R.M., Dunbar, R.B., Schrag, D.P., 2000. New views of tropical paleoclimates from corals. *Quaternary Science Reviews* 19, 45-64.
- Gagnon, A.C., Adkins, J.F., Fernandez, D.P., Robinson, L.F., 2007. Sr/Ca and Mg/Ca vital effects correlated with skeletal architecture in a scleractinian deep-sea coral and the role of Rayleigh fractionation. *Earth and Planetary Science Letters* 261, 280-295.
- Gaillardet, J., Allegre, C.J., 1995. Boron isotopic composition of corals: seawater or diagenesis record? *Earth and Planetary Science Letters* 136, 665-676.
- Gallup, C.D., Olson, D.M., Edwards, L.R., Gruhn, L.M., Winter, A., Taylor, B., 2006. Sr/Ca-sea surface temperature calibration in the branching Caribbean coral *Acropora palmata*. *Geophysical Research Letters* 33. doi: 10.1029/2005GL024935.
- Gattuso, J.P., Frankignoulle, M., Bourge, I., Romaine, S., Buddemeier, R.W., 1998. Effect of calcium carbonate saturation of seawater on coral calcification. *Global and Planetary*

Change 18, 37-46.

- Giry, C., Felis, T., Kolling, M., Scholz, D., Wei, W., Lohmann, G., Scheffers, S.R., 2012. Mid- to late Holocene changes in tropical Atlantic temperature seasonality and interannual to multidecadal variability documented in southern Caribbean corals. *Earth and Planetary Science Letters* 331-332, 187-200.
- Giry, C., Felis, T., Kolling, M., Scheffers, S., 2010. Geochemistry and skeletal structure of *Diploria strigosa*, implications for coral-based climate reconstruction. *Paleogeography*. doi: 10.1016/j.palaeo.2010.10.022.
- Given, R.K., Wilkinson, B.H., 1985. Kinetic control of morphology, composition and mineralogy of abiogenic sedimentary carbonates. *Journal of Sedimentary Petrology* 55, 109-119.
- Glynn, P.W., 1992. Coral reef bleaching: ecological perspectives. *Coral Reefs* 12, 1-17.
- Gonnee, M.E., Paytan, A., Herrera-Silveira, J.A., 2004. Tracing organic matter sources and carbon burial in mangrove sediments over the past 160 years. *Estuarine, Coastal and Shelf Science* 61, 211-227.
- Gonnee, M.E., Cohen, A.L., DeCarlo, T.M., Charette, M.A., 2017. Relationship between water and aragonite barium concentrations in aquaria reared juvenile corals. *Geochimica et Cosmochimica Acta* 209, 123-134.
- Goodkin, N.F., Hughen, K.A., Cohen, A.L., Smith, S.R., 2005. Record of Little Ice Age sea surface temperatures at Bermuda using a growth-dependent calibration of coral Sr/Ca. *Paleoceanography* 20, doi:10.1029/2005PA001140.
- Goodkin, N.F., Hughen, K.A., Cohen, A.L., 2007. A multicoral calibration method to approximate a universal equation relating Sr/Ca and growth rate to sea surface temperature. *Paleoceanography* 22. doi:10.1029/2006PA001312.
- Goreau, T.J., Hayes, R.L., Clark, J.W., Basta, D.J., Robertson, C.N., 1992. Elevated satellite sea surface temperatures correlate with Caribbean coral reef bleaching. In: Geyer, R.A. (Ed.), *A Global Warming Forum: Scientific, Economic, and Legal Overview*. CRC Press, Florida, USA, pp. 225-255.

- Graham, D.W., Bender, M.L., Williams, D.F., Keigwin, L.D., 1982. Strontium-calcium ratios in Cenozoic planktonic foraminifera. *Geochimica et Cosmochimica Acta* 46, 1281-1292.
- Gregory, B.R.B., Peros, M., Reinhardt, E.G., Donnelly, J.P., 2015. Middle-late Holocene Caribbean aridity inferred from foraminifera and elemental data in sediment cores from two Cuban lagoons. *Palaeogeography, Palaeoclimatology, Palaeoecology* 426, 239-241.
- Grossman, E.L., 2012. Applying oxygen isotope paleothermometry in deep time. *Paleontological Society Papers* 18, 39-67.
- Grossman, E.L., Ku, T.L., 1986. Oxygen and carbon isotope fractionation in biogenic aragonite: temperature effects. *Chemical Geology* 59, 59-74.
- Grottoli, A.G., Eakin, C.M., 2007. A review of modern coral  $\delta^{18}\text{O}$  and  $\Delta^{14}\text{C}$  proxy records. *Earth Science Reviews* 81, 67-91.
- Grove, C.A., Brummer, G.A., Kasper, S., Zinke, J., Pfeiffer, M., Garbe-Schonberg, D., 2013. Confounding effects of coral growth and high SST variability on skeletal Sr/Ca: implications for coral paleothermometry. *Geochemistry, Geophysics, Geosystems* 14, 1277-1294.
- Guilderson, T.P., Fairbanks, R.D., Rubenstone, J.L., 1994. Tropical temperature variations since 20,000 years ago: modulating interhemispheric climate change. *Science* 263, 663-665.
- Haase-Schramm, A., Bohm, F., Eisenhauer, A., Dullo, W., Joachimski, M.M., Hansen, B., Reitner, J., 2003. Sr/Ca ratios and oxygen isotopes from sclerosponges: temperature history of the Caribbean mixed layer and thermocline during the Little Ice Age. *Paleoceanography* 10. doi:10.1029/2002PA000830.
- Hadden, C.S., Cherkinsky, A., 2015.  $^{14}\text{C}$  variations in pre-bomb nearshore habitats of the Florida panhandle USA. *Radiocarbon* 57, 469-491.
- Hall, J.M., Chan, L.H., 2004. Li/Ca in multiple species of benthic and planktonic foraminifera: thermocline, latitudinal, and glacial-interglacial variations. *Geochimica et Cosmochimica Acta* 66, 1955-1967.
- Hansen, J., Sato, M., Ruedy, R., K., L., Lea, D.W., Medina-Elizalde, M., 2006. Global

- temperature change. *Proceedings of the National Academy of Science of the USA* 106, 14288-14293.
- Hasen, J., Sato, M., Russell, G., Kharecha, P., 2018. Climate sensitivity, sea level and atmospheric carbon dioxide. *Philosophical Transactions of the Royal Society A*. doi: 371: 20120294.
- Hart, S.R., Cohen, A.L., 1996. An ion probe study of annual cycles of Sr/Ca and other trace elements in corals. *Geochimica et Cosmochimica Acta* 60, 3075-3084.
- Hathorne, E.C., Felis, T., Suzuki, A., H., K., Cabioch, G., 2013. Lithium in the aragonite skeletons of massive *Porites* corals: a new tool to reconstruct tropical sea surface temperatures. *Paleoceanography* 28, 143-152.
- Haug, G.H., Hughen, K.A., Sigman, D.M., Peterson, L.C., Rohl, U., 2001. Southward migration of the Intertropical Convergence Zone through the Holocene. *Science* 293, 1304-1310.
- Haug, G.H., Gunther, D., Peterson, L.C., Sigman, D.M., Hughen, K.A., Aeschlimann, B., 2003. Climate and collapse of Maya civilization. *Science* 299, 1731-1735.
- Hays, P.D., Grossman, E.L., 1991. Oxygen isotopes in meteoric calcite cements as indicators of continental paleoclimate. *Geology* 19, 441-444.
- Heiss, G.A., Camoin, G.F., Eisenhauer, A., Wischow, D., Dullo, W., Hasen, B., 1997. Stable isotopes and Sr/Ca-signals in corals from the Indian Ocean, 8th International Coral Reef Symposium, pp. 1713-1718.
- Helama, S., Jones, P.D., Briffa, K.R., 2017. Dark Ages Cold Period: a literature review and directions for future research. *The Holocene* 27, 1601-1606.
- Hemming, N.G., Hanson, G.N., 1992. Boron isotopic composition and concentration in modern marine carbonates. *Geochimica et Cosmochimica Acta* 56, 537-543.
- Hendy, E.J., Gagan, M.K., Albert, C.A., McCulloch, M.T., Lough, J.M., Isdale, P.J., 2002. Abrupt decrease in tropical Pacific sea surface salinity at the end of the Little Ice Age. *Science* 295, 1511-1514.
- Hendy, E.J., Gagan, M.K., Lough, J.M., McCulloch, M., deMenocal, P., 2007. Impact of skeletal dissolution and secondary aragonite on trace element and isotopic climate proxies in

- Porites* corals. *Paleoceanography* 22. doi: 10.1029/2007PA001462.
- Hershey, J.P., Fernandez, M., Milne, P.J., Millero, F.J., 1986. The ionization of boric acid in NaCl, Na-Ca-Cl and Na-Mg-Cl solutions at 25°C. *Geochimica et Cosmochimica Acta* 50, 143-148.
- Hetzinger, S., Pfeiffer, M., Dullo, W., Ruprecht, E., Garbe-Schonberg, D., 2006. Sr/Ca and  $\delta^{18}\text{O}$  in a fast-growing *Diploria strigosa* coral: evaluation of a new climate archive for the tropical Atlantic. *Geochemistry Geophysics Geosystems* 7. doi: 10.1029/2006GC001347.
- Hetzinger, S., Pfeiffer, M., Dullo, W., Garbe-Schonberg, D., Halfar, J., 2010. Rapid 20th century warming in the Caribbean and impact of remote forcing on climate in the northern tropical Atlantic as recorded in a Guadeloupe coral. *Palaeogeography, Palaeoclimatology, Palaeoecology* 296, 111-124.
- Highsmith, R.C., Lueptow, R.L., Schonberg, S.C., 1983. Growth and bioerosion of three massive corals in the Belize barrier reef. *Marine Ecology - Progress Series* 13, 261-271.
- Hinokidani, K., Nakanishi, Y., 2019. Dissolved iron elution from mangrove ecosystem associated with polyphenols and a herbivorous snail. *Ecology and Evolution* 9, 6772-6784.
- Hintz, C.J., Shaw, T.J., Bernhard, J.M., Chandler, G.T., McCorkle, D.C., Blanks, J.K., 2006. Trace/minor element:calcium ratios in cultured benthic foraminifera. Part I: inter-species and inter-individual variability. *Geochimica et Cosmochimica Acta* 70, 1952-1963.
- Hodell, D.A., Curtis, J.H., Jones, G.A., Higuera-Gundy, A., Brenner, M., Binford, M.W., Dorsey, K.T., 1991. Reconstruction of Caribbean climate change over the past 10,500 years. *Nature: Letters* 352, 790-794.
- Hodell, D.A., Curtis, J.H., Brenner, M., 1995. Possible role of climate in the collapse of Classic Maya civilization. *Letters to Nature* 375, 391-394.
- Hodell, D.A., Brenner, M., Curtis, J.H., Medina-Gonzalez, R., Can, E.I.C., Albornaz-Pat, A., Guilderson, T.A., 2005. Climate change on the Yucatan Peninsula during the Little Ice Age. *Quaternary Research* 63, 109-121.
- Holcomb, M., Cohen, A.L., Gabitov, R.I., Hutter, J.L., 2009. Compositional and morphological



- features of aragonite precipitated experimentally from seawater and biogenically by corals. *Geochimica et Cosmochimica Acta* 73, 4166-4179.
- Holmgren, K., Karlen, W., Lauritzen, S.E., Lee-Thorp, J.A., Partridge, T.C., Piketh, S., Repinshi, P., Stevenson, C., Svanered, O., Tyson, P.D., 1999. A 3000-year high-resolution stalagmite-based record of palaeoclimate for northeastern South Africa. *The Holocene* 9, 295-309.
- Horta-Puga, G., Carriquiry, J.D., 2012. Coral Ba/Ca molar ratios as a proxy of precipitation in the northern Yucatan Peninsula, Mexico. *Applied Geochemistry* 27, 1579-1586.
- Houck, J.E., Buddemeier, R.W., Smith, S.V., Jokiel, P.I., 1977. The response of coral growth rate and skeletal strontium content to light intensity and water temperature. In: Taylor, D.L. (Ed.), *Third International Coral Reef Symposium*, Rosenstiel School of Marine and Atmospheric Sciences. University of Miami, Miami, pp. 425-431.
- Hudson, J.H., Shinn, E.A., Halley, R.B., Lidz, B., 1976. Sclerochronology: tool for interpreting past environments. *Geology* 4, 361-364.
- Hudson, J.H., 1981. Growth rates in *Montastraea annularis*: a record of environmental change in Key Largo coral reef marine sanctuary, Florida. *Bulletin of Marine Science* 2, 444-459.
- Hudson, J.D., Anderson, T.F., 1989. Ocean temperatures and isotopic compositions through time. *Transactions of the Royal Society of Edinburgh: Earth Science* 80, 183-192.
- Hughen, K.A., Southon, J.R., Bertrand, C.J.H., Frantz, B., Zermeno, P., 2004. Cariaco Basin calibration update: revisions to calendar and <sup>14</sup>C chronologies for core PI07-58PC. *Radiocarbon* 46, 1161-1187.
- Hunter, I.G., Jones, B., 1988. Corals and paleogeography of the Pleistocene Ironshore Formation of Grand Cayman, *Proceedings of the Sixth International Coral Reef Symposium*, Townsville, Australia, pp. 431-435.
- Hunter, I.G., 1994. Modern and ancient coral association of the Cayman Islands, Unpublished Ph.D., University of Alberta, Edmonton, Alberta, Canada, 345 pp.
- Hunter, I.G., Jones, B., 1995. Coral associations of the Pleistocene Ironshore Formation, Grand

- Cayman. *Coral Reefs* 15, 249-267.
- Ichikuni, M., Kikuchi, K., 1972. Retention of boron by travertines. *Chemical Geology* 9, 13-21.
- Imbrie, J., McIntyre, A., 2006. SPECMAP time scale developed by Imbrie et al., 1984 based on normalized planktonic records (normalized O-18 vs time, specmap.017). PANGAEA. doi: 10.1594/PANGAEA.441706.
- Inoue, M., Suzuki, A., Nohara, M., Hibino, K., Kawhata, H., 2007. Empirical assessment of coral Sr/Ca and Mg/Ca ratios as climate proxies using colonies grown at different temperatures. *Geophysical Research Letters* 34. doi:10.1029/2007GL029628.
- IPCC, 2014. *Climate change 2014: synthesis report. Contribution of working groups I, II and III to the Fifth Assessment Report of the Intergovernmental Panel on Climate Change*, Geneva, Switzerland, 151 pp.
- IPCC, 2018. *Summery for policymakers*, World Meteorological Organization, Geneva, Switzerland, 32 pp.
- James, N.P., Jones, B., 2015. *Origin of carbonate sedimentary rocks*. Wiley, pp. 464.
- Jaume-Santero, F., Pickler, C., Beltrami, H., Mareschal, J., 2016. North American regional climate reconstruction from ground surface temperature histories. *Climate of the Past* 12, 2181-2194.
- Jones, B., 1994. *Geology of the Cayman Islands. The Cayman Islands: natural history and biogeography*. Kluwer Academic Publishers, The Netherlands, pp. 13-49.
- Jones, B., 2019. Diagenetic processes associated with unconformities in carbonate successions on isolated oceanic islands: case study of the Pliocene to Pleistocene sequence, Little Cayman, British West Indies. *Sedimentary Geology* 386, 9-30.
- Jones, B., Hunter, I.G., 1990. Pleistocene paleogeography and sea levels on the Cayman Islands, British West Indies. *Coral Reefs* 9, 81-91.
- Jones, B., Pemberton, S.P., 1989. Sedimentology and ichnology of a Pleistocene unconformity bounded, shallowing upward carbonate sequence: the Ironshore Formation, Salt Creek, Grand Cayman. *Palaios* 4, 343-355.

- Jones, J.P., Carricart-Ganivet, J.P., Prieto, R.I., Enriquez, S., Ackerson, M., Gabitov, R.I., 2015. Microstructural variation in oxygen isotopes and elemental calcium ratios in the coral skeleton of *Orbicella annularis*. *Chemical Geology* 419, 192-199.
- Kawamura, H., Holbourn, A., Kuhnt, W., 2006. Climate variability and land-ocean interactions in the Indo Pacific Warm Pool: a 460-ka palynological and organic geochemical record from the Timor Sea. *Marine Micropaleontology* 59, 1-14.
- Keigwin, L.D., Pickart, R.S., 1999. Slope water current over the Laurentian Fan on interannual to millennial time scales. *Science* 286, 520-252.
- Keith, M.L., Weber, J.N., 1965. Carbon and oxygen composition of selected limestones and fossils. *Geochimica et Cosmochimica Acta* 28, 1787-1816.
- Kele, S., Breitenbach, S.F.M., Capezzuoli, E., Meckler, A.N., Ziegler, M., Millan, I.M., Kluge, T., Deak, J., Hanselmann, K., John, C.M., Yan, H., Liu, Z., Bernasconi, S.M., 2015. Temperature dependence of oxygen- and clumped-isotope fractionation in carbonates: a study of travertines and tufas in the 6-95°C temperature range. *Geochimica et Cosmochimica Acta* 168, 172-192.
- Kemp, A.C., Horton, B.P., Donnelly, J.P., Mann, M.E., Vermeer, M., Rahmstorf, S., 2011. Climate related sea-level variations over the past two millennia. *Proceedings of the National Academy of Science of the USA* 108, 11017-11022.
- Kilbourne, K.H., Quinn, T.M., Taylor, F.W., 2004. A fossil coral perspective on western tropical Pacific climate ~350 ka. *Paleoceanography* 19. doi:10.1029/2003PA000944.
- Kilbourne, K.H., 2006. Tropical Atlantic and Caribbean climate variations during the past eight centuries, Unpublished. Ph.D., University of South Florida, Florida, USA, 188 pp.
- Kilbourne, K.H., Quinn, T.M., Guilderson, T.P., Webb, R.S., Taylor, F.W., 2007. Decadal-to interannual-scale source water variations in the Caribbean Sea recorded by Puerto Rican coral radiocarbon. *Climate Dynamics*, 29, 51-62.
- Kilbourne, K.H., Quinn, T.M., Webb, R., Guilderson, T., Nyberg, J., Winter, A., 2010. Coral windows onto seasonal climate variability in the northern Caribbean since 1479.

- Geochemistry Geophysics Geosystems 11. doi: 10.1029/2010GC003171.
- Kim, S., O'Neil, J.R., 1997. Equilibrium and nonequilibrium oxygen isotope effects in synthetic carbonates. *Geochimica et Cosmochimica Acta* 61, 3461-3475.
- Kim, S., O'Neil, J.R., Hillaire-Marcel, C., Mucci, A., 2007. Oxygen isotope fractionation between synthetic aragonite and water: influence of temperature and  $Mg^{2+}$  concentration. *Geochimica et Cosmochimica Acta* 71, 4704-4715.
- Kim, S., Coplen, T.B., Horita, J., 2015. Normalization of stable isotope data for carbonate minerals: implementation of IUPAC guidelines. *Geochimica et Cosmochimica Acta* 158, 276-289.
- Kinsman, D.J.J., 1969. Interpretation of  $Sr^{2+}$  concentrations in carbonate minerals and rocks. *Journal of Sedimentary Petrology* 39, 486-508.
- Kinsman, D.J.J., Holland, H.D., 1969. The co-precipitation of cations with  $CaCO_3$ -IV. The co-precipitation of  $Sr^{2+}$  with aragonite between 16 and 96°C. *Geochimica et Cosmochimica Acta* 33, 1-17.
- Kitano, Y., Kanamori, N., Oomori, T., 1971. Measurements of distribution coefficients of strontium and barium between carbonate precipitate and solution: abnormally high values of distribution coefficients measured at early stages of carbonate formation. *Geochemical Journal* 4, 183-206.
- Knowlton, N., Weil, E., Weigt, L.A., Guzman, H.M., 1992. Sibling species in *Montastrea annularis*, coral bleaching, and the coral climate record. *Science* 255, 330-333.
- Knutson, D.W., Buddermeier, R.W., Smith, S.V., 1972. Coral chronometers: seasonal growth bands in reef corals. *Science* 177, 270-272.
- Koeppenkastrop, D., DeCarlo, E.H., Roth, M., 1991. A method to investigate the interaction of rare earth elements in aqueous solution with metal oxides. *Journal of Radioanalytical and Nuclear Chemistry* 152, 337-346.
- Kolling, H.M., Stein, R., Fahl, K., Perner, K., Moros, M., 2017. Short-term variability in late Holocene sea ice cover on the East Greenland Shelf and its driving mechanisms.

- Palaeogeography, Palaeoclimatology, Palaeoecology 485, 336-350.
- Kristjansdottir, G.B., Lea, D.W., Jennings, A.E., Pak, D.K., Belanger, C., 2007. New spatial Mg/Ca-temperature calibrations for three Arctic, benthic foraminifera and reconstruction of north Iceland shelf temperature for the past 4000 years. *Geochemistry Geophysics Geosystems* 8. doi: 10.1029/2006GC001425.
- Kuffner, I.B., Jokiel, P.I., Rodgers, K.S., Anderson, A.J., Mackenzie, F.T., 2012. An apparent “vital effect” of calcification rate on the Sr/Ca temperature proxy in the reef coral *Montipora capitata*. *Geochemistry Geophysics Geosystems* 13. doi: 10.1029/2012GC004128.
- Kuffner, I.B., Lidz, B., Hudson, J.H., Anderson, J.S., 2015. A century of ocean warming on Florida Keys coral reefs: historic in situ observations. *Estuaries and Coasts* 38, 1085-1096.
- Kuffner, I.B., Roberts, H.H., Flannery, J.A., Morrison, J.M., Richey, J.N., 2017. Fidelity of Sr/Ca proxy in recording ocean temperature in the western Atlantic coral *Siderastrea siderea*. *Geochemistry Geophysics Geosystems* 18, 178-188.
- Kukla, G., McManus, J.F., Rousseau, D.D., Chuine, I., 1997. How long and how stable was the last interglacial? *Quaternary Science Reviews* 16, 605-612.
- Kuss, J., Garbe-Schonberg, C., Kremling, K., 2001. Rare earth elements in suspended particulate material of North Atlantic surface waters. *Geochimica et Cosmochimica Acta* 65, 187-199.
- Lachniet, M., Johnson, L., Asmerom, Y., Burns, S.J., Polyak, V., Patterson, W.P., Burt, L., Azouz, A., 2009. Late Quaternary moisture export across Central America and to Greenland: evidence for tropical rainfall variability from Costa Rican stalagmites. *Quaternary Science Reviews* 28, 3348-3360.
- Lahann, R.W., 1978. A chemical model for calcite crystal growth and morphology control. *Journal of Sedimentary Petrology* 48, 337-344.
- Land, L.S., Lang, J.C., Barnes, D.J., 1975. Extension rate: a primary control on the isotopic

- composition of West Indian (Jamaican) scleractinian reef coral skeletons. *Marine Biology* 33, 221-233.
- Lane, C.S., Horn, S.P., Mora, C.I., Orvis, K.H., 2009. Late-Holocene paleoenvironmental change at mid-elevation on the Caribbean slope of the Cordillera Central, Dominican Republic: a multi-site, multi-proxy analysis. *Quaternary Science Reviews* 28, 2239-2260.
- Lane, C.S., Horn, S.P., Orvis, K.H., Thomason, J.M., 2011. Oxygen isotope evidence of Little Ice Age aridity on the Caribbean slope of the Cordillera Central, Dominican Republic. *Quaternary Research* 75, 461-470.
- Langdon, P.G., Barber, K.E., Hughes, P.D.M., 2003. A 7500-year peat-based palaeoclimate reconstruction and evidence for an 1100-year cyclicity in bog surface wetness from Temple Hill Moss, Pentland Hills, southeast Scotland. *Quaternary Science Reviews* 22, 259-274.
- Lea, D.W., Shen, G.T., Boyle, E.A., 1989. Coralline barium records temporal variability in equatorial Pacific upwelling. *Nature* 340, 373-376.
- Lea, D.W., 1999. Trace elements in foraminiferal calcite. In: Sen Gupta, B.K. (Ed.), *Modern foraminifera*. Kluwer Academic Publishing, Dordrecht, pp. 259-277.
- Lear, C.H., Rosenthal, Y., Slowey, N., 2002. Benthic foraminiferal Mg/Ca paleothermometry: a revised core-top calibration. *Geochimica et Cosmochimica Acta* 66, 3375-3387.
- Lear, C.H., Elderfield, H., Wilson, P.A., 2003. A Cenozoic seawater Sr/Ca record from benthic foraminiferal calcite and its application in determining global weathering fluxes. *Earth and Planetary Science Letters* 208, 69-84.
- Leder, J.J., Swart, P.K., Szmant, A.M., Dodge, R.E., 1996. The origin of variations in the isotopic record of scleractinian corals: I. Oxygen. *Geochimica et Cosmochimica Acta* 60, 2857-2870.
- Lerche, D., Nozaki, Y., 1998. Rare earth elements of sinking particulate matter in the Japan Trench. *Earth and Planetary Science Letters* 159, 71-86.
- Li, R., Jones, B., 2013a. Temporal and spatial variations in the diagenetic fabrics and stable

- isotopes of Pleistocene corals from the Ironshore Formation of Grand Cayman, British West Indies. *Sedimentary Geology* 286-287, 58-72.
- Li, R., Jones, B., 2013b. Heterogeneous diagenetic patterns in Pleistocene Ironshore Formation of Grand Cayman, British West Indies. *Sedimentary Geology* 294, 251-265.
- Li, R., Jones, B., 2014. Calcareous crusts on exposed Pleistocene limestones: a case study from Grand Cayman, British West Indies. *Sedimentary Geology* 299, 88-105.
- Linsley, B.K., Wellington, G.M., Schrag, D.P., 2000. Decadal sea surface temperature in the subtropical South Pacific from 1726 to 1997 A.D. *Science* 290, 1145-1148.
- Linsley, B.K., Wellington, G.M., Schrag, D.P., Ren, L., Salinger, M.J., Tudhope, A.W., 2004. Geochemical evidence from corals for changes in the amplitude and spatial pattern of South Pacific interdecadal climate variability over the last 300 years. *Climate Dynamics* 22. doi: 10.1007/s00382-003-0364-y.
- Linsley, B.K., Kaplan, A., Gouriou, Y., Salinger, J., deMenocal, P.B., Wellington, G.M., Howe, S.S., 2006. Tracking the extent of the South Pacific Convergence Zone since the early 1600s. *Geochemistry Geophysics Geosystems* 7. doi:10.1029/2005GC001115.
- Linsley, B.K., Zhang, P., Kaplan, A., Howe, S.S., Wellington, G.M., 2008. Interdecadal-decadal climate variability from multicoral oxygen isotope records in the South Pacific Convergence Zone region since 1650 A.D. *Paleoceanography* 23. doi: 10.1029/2007PA001539.
- Ljungqvist, F.C., 2009. Temperature proxy records covering the last two millennia: a tabular and visual overview. *Swedish Society of Anthropology and Geography* 91, 11-29.
- Lough, J.M., 2004. A strategy to improve the contribution of coral data to high-resolution paleoclimatology. *Palaeogeography, Palaeoclimatology, Palaeoecology* 204, 115-143.
- Lowenstein, T.K., Li, J., Brown, C., Roberts, S.M., Ku, T., Luo, S., Yang, W., 1999. 200 k.y. paleoclimate record from Death Valley salt core. *Geology* 27, 3-6.
- Lynch-Stieglitz, J., Curry, W.B., Slowey, N., 1999. A geostrophic transport estimate for Florida Current from the oxygen isotope composition of benthic foraminifera. *Palaeogeography*

14, 360-373.

- MacDonald, K.C., Holcombe, T.L., 1978. Inversion of magnetic anomalies and sea-floor spreading in the Cayman Trough. *Earth and Planetary Science Letters* 40, 407-414.
- MacKinnon, L., 2000. Sedimentology of North Sound, Grand Cayman, British West Indies, Unpublished. M.Sc., University of Alberta, Edmonton, Alberta, Canada, 144 pp.
- MacKinnon, L., Jones, B., 2001. Sedimentological evolution of North Sound, Grand Cayman: a freshwater to marine carbonate succession driven by Holocene sea-level rise. *Journal of Sedimentary Research* 71, 568-580.
- Maeda, A., Fujita, K., Horikawa, K., Suzuki, A., Ohno, Y., Kawahata, H., 2018. Calibration between temperature and Mg/Ca and oxygen isotope ratios in high-magnesium calcite tests of asexually reproduced juveniles of large benthic foraminifers. *Marine Micropaleontology* 143, 63-69.
- Mahowald, N.M., Muhs, D.R., Levis, S., Rasch, P.J., Yoshioka, M., Zender, C.S., Luo, C., 2006. Change in atmospheric mineral aerosols in response to climate: last glacial period, preindustrial, modern, and double carbon dioxide climates. *Journal of Geophysical Research* 111. doi: 10.1029/2005JD006653.
- Marchitto, T.M., deMenocal, P., 2003. Late Holocene variability of upper North Atlantic Deep Water temperature and salinity. *Geochemistry Geophysics Geosystems* 4. doi: 10.1029/2003GC000598.
- Marchitto, T.M., Bryan, S.P., Curry, W.B., McCorkle, D.C., 2007. Mg/Ca temperature calibration for the benthic foraminifer *Cibicides lobatulus*. *Paleoceanography* 22. doi: 10.1029/2006PA001287.
- Marchitto, T.M., Bryan, S.P., Doss, W., McCulloch, M., Montagna, P., 2018. A simple biomineralization model to explain Li, Mg, and Sr incorporation into aragonitic foraminifera and corals. *Earth and Planetary Science Letters* 481, 20-29.
- Marco-Barba, J., Holmes, J.A., Mesquita-Joanes, F., Miracle, M.R., 2013. The influence of climate and sea-level change on the Holocene evolution of a Mediterranean coastal



- lagoon: evidence from ostracod palaeoecology and geochemistry. *Geobios* 46, 409-421.
- Marcott, S.A., Shakun, J.D., Clark, P.U., Mix, A.C., 2013. A reconstruction of regional and global temperature for the past 11,300 years. *Science* 339, 1198-1201.
- Markoff, A., 2012. Terror came to Cayman 80 years ago. *Cayman Compass*. Pinnacle Media Ltd., Cayman Islands, November 9, 2012.
- Markoff, A., 2015, Cayman's stormy hurricane history. <http://hurricanes.ky/caymans-stormy-hurricane-history/> (Accessed March 2016).
- Marriott, C.S., Henderson, G.H., Belshaw, N.S., Tudhope, A.W., 2004a. Temperature dependence of  $\delta^7\text{Li}$ ,  $\delta^{44}\text{Ca}$  and Li/Ca during growth of calcium carbonate. *Earth and Planetary Science Letters* 22, 615-624.
- Marriott, C.S., Henderson, G.H., Crompton, R., Staubwasser, M., Shaw, S., 2004b. Effect of mineralogy, salinity, and temperature on Li/Ca and Li isotope composition of calcium carbonate. *Chemical Geology* 212, 5-15.
- Marshall, J.F., McCulloch, M.T., 2002. An assessment of the Sr/Ca ratio in shallow water hermatypic corals as a proxy for sea surface temperature. *Geochimica et Cosmochimica Acta* 66, 3263-3280.
- Marshall, J.F., McCulloch, M., 2001. Evidence of El Nino and the Indian Ocean Dipole from Sr/Ca derived SSTs from modern corals at Christmas Island, eastern Indian Ocean. *Geophysical Research Letters* 28, 3453-3456.
- Martin, G.D., Wilkinson, B.H., Lohman, K.C., 1985. The role of skeletal porosity in aragonite neomorphism- *Strombus* and *Montastrea* from the Pleistocene Key Largo Limestone, Florida. *Journal of Sedimentary Petrology* 56, 194-203.
- Martin, P.A., Lea, D.W., Rosenthal, Y., Shackleton, N.J., Sarinthein, M., Papenfuss, T., 2002. Quaternary deep sea temperature histories derived from benthic foraminiferal Mg/Ca. *Earth and Planetary Science Letters* 198, 193-209.
- Matley, C.A., 1926. The geology of the Cayman Islands (British West Indies), and their relations to the Barlett Trough. *Quarterly Journal of the Geological Society of London* 82, 352-

386.

- Maupin, C.R., Quinn, T.M., Halley, R.B., 2008. Extracting a climate signal from the skeletal geochemistry of the Caribbean coral *Siderastrea siderea*. *Geochemistry Geophysics Geosystems* 9. doi: 10.1029/2008GC002106.
- Mavromatis, V., Goetschl, K.E., Grengg, C., Konrad, F., Purgstaller, B., Dietzel, M., 2018. Barium partitioning in calcite and aragonite as a function of growth rate. *Geochimica et Cosmochimica Acta* 237, 65-78.
- Mayewski, P.A., Rohling, E.J., Stager, J.C., Karlen, W., Maasch, K.A., Meeker, L.D., Meyerson, E.A., Gasse, F., van Kreveld, S., Holmgren, K., 2004. Holocene climate variability. *Quaternary Research* 62, 243-255.
- McConnaughey, T., 1988.  $^{13}\text{C}$  and  $^{18}\text{O}$  isotopic disequilibrium in biological carbonates: I. Patterns. *Geochimica et Cosmochimica Acta* 53, 151-162.
- McCulloch, M.T., Gagan, M.K., Mortimer, G.E., Chivas, A.R., Isdale, P.J., 1994. A high-resolution Sr/Ca and  $\delta^{18}\text{O}$  coral record from the Great Barrier Reef, Australia, and the 1982-1983 El Nino. *Geochimica et Cosmochimica Acta* 58, 2747-2754.
- McCulloch, M.T., Tudhope, A.W., Esat, T.M., Mortimer, G.E., Chappell, J., Pillans, B., Chivas, A.R., Omura, A., 1999. Coral record of equatorial sea-surface temperatures during the Penultimate Deglaciation at Huon Peninsula. *Science* 283, 202-204.
- McCulloch, M.T., Esat, T., 2000. The coral record of last interglacial sea levels and sea surface temperatures. *Chemical Geology* 169, 107-129.
- McCulloch, M., Fallon, S., Wyndham, T., Hendy, E., Lough, J., Barnes, D., 2003. Coral record of increased sediment flux to the inner Great Barrier Reef since European settlement. *Nature* 421, 727-730.
- McCulloch, M., Falter, J., Trotter, J., Montagna, P., 2012. Coral resilience to ocean acidification and global warming through pH up-regulation. *Nature Letters- Climate Change* 2, doi: 10.1038/NCLIMATE1473.
- McCrea, J.M., 1950. On the isotopic chemistry of carbonates and a paleotemperature scale.

- Journal of Chemical Physics 18, 849-859.
- McGregor, H.V., Gagan, M.K., 2003. Diagenesis and geochemistry of *Porites* corals from Papua New Guinea: implications for paleoclimate reconstruction. *Geochimica et Cosmochimica Acta* 67, 2147-2156.
- McGregor, H.V., Abram, N.J., 2008. Images of diagenetic textures in *Porites* corals from Papua New Guinea and Indonesia. *Geochemistry Geophysics Geosystems* 9, 1-17.
- McIntire, W.L., 1963. Trace element partition coefficients- a review of theory and applications to geology. *Geochimica et Cosmochimica Acta* 27, 1209-1264.
- McLennan, S.M., 1989. Rare earth elements in sedimentary rocks: influence of provenance and sedimentary processes. *Reviews in Mineralogy* 21, 169-200.
- McManus, J.F., Oppo, D.W., Cullen, J.L., 1999. A 0.5-million year record of millennial-scale climate variability in the North Atlantic. *Science* 283, 971-975.
- McWilliams, J.P., Cote, I.M., Gill, J.A., Sutherland, W.J., Watkinson, A.R., 2005. Accelerating impacts of temperature-induced coral bleaching in the Caribbean. *Ecology* 86, 2055-2060.
- Meibom, A., Stage, M., Wooden, J., Constantz, B.R., Dunbar, R.B., Owen, A., Grumet, N., Bacon, C.R., Chamberlin, C.P., 2003. Monthly strontium/calcium oscillations in symbiotic coral aragonite: biological effects limiting the precision of paleotemperature proxy. *Geophysical Research Letters* 30, doi 10.1029/2002GL016864.
- Meibom, A., Cuiff, J., Hillion, F., Constantz, B.R., Juillet-Leclerc, A., Dauphin, Y., Watanabe, T., Dunbar, R.B., 2004. Distribution of magnesium in coral skeleton. *Geophysical Research Letters* 31. doi:10.1029/2004GL021313.
- Meibom, A., Cuiff, J., Houlbreque, F., Mostefaoui, S., Dauphin, Y., Meibom, K.L., Dunbar, R.B., 2008. Compositional variations at ultra-structure length scales in coral skeleton. *Geochimica et Cosmochimica Acta* 72, 1555-1569.
- Meibom, A., Yurimoto, H., Cuiff, J., Domart-Coulon, I., Houlbreque, F., Constantz, B., Dauphin, Y., Tambutte, E., Tambutte, S., Allemand, D., Dunbar, R.B., 2006. Vital effects in coral

- skeletal composition display strict three-dimensional control. *Geophysical Research Letters* 33. doi: 10.1029/2006GL025968.
- Mekik, F., Francois, R., M, S., 2007. A novel approach to dissolution correction of Mg/Ca-based paleothermometry in the tropical Pacific. *Paleoceanography and Paleoclimatology* 22. doi: 10.1029/2007PA001504.
- Melo-Gonzalez, N.M., Muller-Karger, F.E., Cerdeira-Estrada, S., Perez de los Reyes, R., Victoria del Rio, I., Cardenas-Perez, P., Mitrani-Arenal, I., 2000. Near-surface phytoplankton distribution in the western Intra-Americas Sea: the influence of El Nino and weather events. *Journal of Geophysical Research* 105, 14029-14043.
- Meyers, W.J., Lohman, K.C., 1983. Isotope geochemistry of regionally extensive calcite cement zones and marine components in Mississippian limestones, New Mexico. In: Schneiderman, N., Harris, P.M. (Eds), *Carbonate Cements*. The Society of Economic Paleontologists and Mineralogists Special Publication 36, pp. 223-239.
- Milne, G.A., Long, A.J., Bassett, S.E., 2005. Modelling Holocene relative sea-level observations from the Caribbean and South America. *Quaternary Science Reviews* 24, 1183-1202.
- Min, G.R., Edwards, R.L., Taylor, F.W., Recy, J., Gallup, C.D., Beck, J.W., 1995. Annual cycles of U/Ca in coral skeletons and U/Ca thermometry. *Geochimica et Cosmochimica Acta* 59, 2025-2042.
- Mitsuguchi, T., Matsumoto, E., Abe, O., Uchida, T., Isdale, P.J., 1996. Mg/Ca thermometry in coral skeletons. *Science* 274, 961-963.
- Mitsuguchi, T., Uchida, T., Matsumoto, E., Isdale, P.J., Kawana, T., 2001. Variations in Mg/Ca, Na/Ca, and Sr/Ca ratios of coral skeletons with chemical pretreatments: implications for carbonate geochemistry. *Geochimica et Cosmochimica Acta* 65, 2865-2874.
- Mitsuguchi, T., Dang, P.X., Kitagawa, H., Uchida, T., Shibata, Y., 2008. Coral Sr/Ca and Mg/Ca records in Con Dao Island off the Mekong Delta: assessment of their potential for monitoring ENSO and East Asian monsoon. *Global and Planetary Change* 63, 341-352.
- Moore, W.S., Krishnaswami, S., 1974. Correlation of X-Radiography revealed banding in corals

- with radiometric growth rates. In: Cameron, A.M., Cambell, B.M., Cribb, A.B., Endean, R., Jell, J.S., Jones, O.A., Mather, P., Talbot, F.H. (Eds.), Proceeding of the Second International Coral Reef Symposium 2. Great Barrier Reef Committee, Brisbane, pp. 269-276.
- Montaggioni, L.F., Le Cornec, F., Correge, T., Cabioch, G., 2006. Coral barium/calcium record of mid-Holocene upwelling activity in New Caledonia, South-West Pacific. *Paleogeography, Paleoclimatology, Paleoecology* 237, 436-455.
- Montagna, P., McCulloch, M., Douville, E., Lopez Correa, M., Trotter, J., Rodolfo-Metalpa, R., Dissard, D., Ferrier-Pages, C., Frank, N., Freiwald, A., Goldstein, S., Mazzoli, C., Reynaud, S., Ruggeberg, A., Russo, S., Taviani, M., 2014. Li/Mg systematics in scleractinian corals: calibration of the thermometer. *Geochimica et Cosmochimica Acta* 132, 288-310.
- Moraetis, D., Mouslopoulou, V., 2013. Preliminary results of REE-Y sorption on carbonate rocks. *Bulletin of the Geological Society of Greece* 47, 843-851.
- Moreau, M., Correge, T., Dassies, E.P., Le Cornec, F., 2015. Evidence for the non-influence of salinity variability on the *Porites* coral Sr/Ca palaeothermometer. *Climate of the Past* 11, 523-532.
- Mortyn, P.G., Elderfield, H., Anand, P., Greavea, M., 2005. An evaluation of controls on planktonic foraminiferal Sr/Ca: comparison of water column and core-top data from a North Atlantic transect. *Geochemistry Geophysics Geosystems* 6. doi: 10.1029/2005GC001047.
- Muehlenbachs, K., Clayton, R.N., 1976. Oxygen isotope composition of the oceanic crust and its bearing on seawater. *Journal of Geophysical Research* 81, 4365-4369.
- Muhs, D.R., Budahn, J.R., 2009. Geochemical evidence for African dust and volcanic ash inputs to terra rossa soils on carbonate reef terraces, northern Jamaica, West Indies. *Quaternary International* 196, 13-35.
- Muhs, D.R., Budahn, J.R., Prospero, J.M., Carey, S.N., 2007. Geochemical evidence for African

- dust inputs to soils of western Atlantic islands: Barbados, the Bahamas, and Florida. *Journal of Geophysical Research* 112.
- Muhs, D.R., Crittenden, R.C., Rosholt, J.N., Bush, C.A., Stewart, K.C., 1987. Genesis of marine terrace soils, Barbados, West Indies: evidence from mineralogy and geochemistry. *Earth Surface processes and Landforms* 12, 605-618.
- Muller, A.D., Gagan, M.K., McCulloch, M.T., 2001. Early marine diagenesis in corals and geochemical consequences for paleoceanographic reconstructions. *Geophysical Research Letters* 28, 4471-4474.
- Mulitza, S., Donner, B., Fischer, G., Paul, A., Patzold, J., Ruhlemann, C., Segl, M., 2003. The South Atlantic oxygen isotope record of planktic foraminifera. In: Wefer, G., Mulitza, S., Ratmeyer, V. (Eds.), *The South Atlantic in the Late Quaternary*. Springer, Berlin, Heidelberg.
- Murty, S.A., Bernstein, W.N., Ossolinski, J.E., Davis, R.S., Goodkin, N.F., Hughen, K.A., 2018. Spatial and temporal robustness of the Sr/Ca-SST calibrations in Red Sea corals: evidence for influence of mean annual temperature on calibration slopes. *Paleoceanography and Paleoclimatology* 33, 443-456.
- Nesje, A., Kvamme, M., Rye, N., Lovlie, R., 1991. Holocene glacial and climate history of the Jostedaksbreen Region, Westerns Norway: evidence from lake sediments and terrestrial deposits. *Quaternary Science Reviews* 10, 87-114.
- Ng, K., 1990. Diagenesis of the Oligocene-Miocene Bluff Formation of the Cayman Islands: a petrographic and hydrogeological approach., Unpublished. Ph.D., University of Alberta, Edmonton, Alberta, Canada, 343 pp.
- NOAA, 2018, World Sea Temperatures. <https://www.seatemperature.org/>.
- NOAA, 2016, In what types of water do corals live? <https://oceanservice.noaa.gov/facts/coralwaters.html>.
- Nothdurft, L.D., Webb, G.E., 2007. Microstructure of common reef-building coral genera *Acropora*, *Pocillopora*, *Goniastrea* and *Porites*: constraints on spatial resolution in

- geochemical sampling. *Facies* 53. doi: 10.1007/s10347-006-0090-0.
- Nothdurft, L.D., Webb, G.E., Bostrom, T., Rintoul, L., 2007. Calcite-filled borings in the most recently deposited skeleton in live-collected *Porites* (Scleractinia): implications for trace element archives. *Geochimica et Cosmochimica Acta* 71, 5423-5438.
- Nothdurft, L.D., Webb, G.E., 2009. Earliest diagenesis in scleractinian coral skeletons: implications for palaeoclimate-sensitive geochemical archives. *Facies* 55, 161-201.
- Nozaki, Y., Zhang, J., Amakawa, H., 1997. The fractionation between Y and Ho in the marine environment. *Earth and Planetary Science Letters* 148, 329-340.
- Nurhati, I.S., Cobb, K.M., Charles, C.D., Dunbar, R.B., 2009. Late 20th century warming and freshening in the central tropical Pacific. *Geophysical Research Letters* 36. doi: 10.1029/2009GL040270.
- Nurhati, I.S., Cobb, K.M., Di Lorenzo, E., 2011. Decadal-scale SST and salinity variations in the central tropical Pacific: signatures of natural and anthropogenic climate change. *Journal of Climate* 24, 3294-3308.
- Nurse, L.A., Sem, G., 2001. Small island states. In: McCarth, J.J., Canziani, O.F., Leary, N.A., Dokken, D.J., White, K.S. (Ed.), *Climate change 2001: impacts, adaptations and vulnerability*. Cambridge University Press. pp. 843-875.
- Nyberg, J., Kuijpers, A., Malmgren, B.A., Kunzendorf, H., 2001. Late Holocene changes in precipitation and hydrography recorded in marine sediments from the northeastern Caribbean Sea. *Quaternary Science Reviews* 56, 87-102.
- Okumura, M., Kitano, Y., 1986. Coprecipitation of alkali metal ions with calcium carbonate. *Geochimica et Cosmochimica Acta* 50, 49-58.
- O'Neil, J.R., Clayton, R.N., Mayeda, T.K., 1969. Oxygen isotopes fractionation in divalent metal carbonates. *Journal of Chemical Physics* 51, 5547- 5560.
- Oomori, T., Kaneshima, K., Nakamura, Y., Kitano, Y., 1982. Seasonal variation of minor elements in coral skeletons. *Galaxea* 1, 77-86.
- Oppo, D.W., McManus, J.F., Cullen, J.L., 1998. Abrupt climate events 500,000 to 340,000 years

- ago: evidence from subpolar North Atlantic sediments. *Science* 279, 1335-1338.
- Osborn, G., Luckman, B.H., 1988. Holocene glacier fluctuations in the Canadian Cordillera (Alberta and British Columbia). *Quaternary Science Reviews* 7, 115-128.
- Osborne, A.H., Haley, B.A., Hathorne, E.C., Plancherel, Y., Frank, M., 2015. Rare earth element distribution in Caribbean seawater: continental inputs versus lateral transport of distinct REE compositions in subsurface water masses. *Marine Chemistry* 177, 172-183.
- Ourbak, T., Correge, T., Malaize, B., Le Cornec, F., Charlier, K., Peypouquet, J.P., 2006. A high-resolution investigation of temperature, salinity, and upwelling activity proxies in corals. *Geochemistry Geophysics Geosystems* 7. doi:10.1029/2005GC001064.
- Ourbak, T., DeLong, K.L., Correge, T., Malaize, B., Kilbourne, H., Cawuineau, S., Hollander, D., 2008. The significance of geochemical proxies in corals; does size (age) matter?, *Proceedings of the 11th International Coral Reef Symposium, Ft. Lauderdale, Florida*, pp. 82-86.
- Patterson, W.P., Smith, G.R., Lohmann, K.C., 1993. Continental paleothermometry and seasonality using the isotopic composition of aragonitic otoliths of freshwater fishes. In: Swart, P.K., Lohman, K.C., McKenzie, J., Savin, S. (Eds.), *Climate Change in Continental Isotopic Records. Geophysical Monograph Series. American Geophysical Union, Washington, D.C.*, 78, 191-202.
- Perfit, M.R., Heezen, B.C., 1978. The geology and the evolution of the Cayman Trench. *Geological Society of America Bulletin* 89, 1155-1174.
- Peros, M.C., Reinhardt, E.G., Schwarcz, H.P., Davis, A.M., 2007. High-resolution paleosalinity reconstruction from Laguna de la Leche, north coastal Cuba, using Sr, O, and C isotopes. *Palaeogeography, Palaeoclimatology, Palaeoecology* 245, 535-550.
- Peterson, T.C., Taylor, M.A., Demeritte, R., Duncombe, D.L., Burton, S., Thompson, F., Porter, A., Mercedes, M., Villegas, E., Fils, R.S., Tank, A.K., Martis, A., Warner, R., Joyette, A., Mills, W., Gleason, B., 2002. Recent changes in climate extremes in the Caribbean region. *Journal of Geophysical Research* 107, doi: 10.1029/2002JD002251.



- Pfeiffer, M., Timm, O., Dullo, W., Garbe-Schonberg, D., 2006. Paired coral Sr/Ca and  $\delta^{18}\text{O}$  records from the Chagos Archipelago: late twentieth century warming affects rainfall variability in the tropical Indian Ocean. *Geology* 34, 1069-1072.
- Pfeiffer, M., Dullo, W., Zinke, J., Garbe-Schonberg, D., 2009. Three monthly coral Sr/Ca records from the Chagos Archipelago covering the period of 1950-1995 A.D.: reproducibility and implication for quantitative reconstructions of sea surface temperature variations. *International Journal of Earth Sciences* 98, 53-66.
- Pingitore, N.E., 1976. Vadose and phreatic diagenesis: processes, products and their recognition in corals. *Journal of Sedimentary Petrology* 46, 985-1006.
- Pingitore, N.E., 1978. The behavior of  $\text{Zn}^{2+}$  and  $\text{Mn}^{2+}$  during carbonate diagenesis: theory and applications. *Journal of Sedimentary Petrology* 48, 799-814.
- Pingitore, N.E., Rangel, Y., Kwarteng, A., 1988. Barium variation in *Acropora palmata* and *Montastrea annularis*. *Coral Reefs* 8, 31-36.
- Politi, Y., Batchelor, D.R., Zaslansky, P., Chmelka, B.F., Weaver, J.C., Sagi, I., Weiner, S., Addadi, L., 2010. Role of magnesium ion stabilization of biogenic amorphous calcium carbonate: a structure-function investigation. *Chemistry of Materials* 22, 161-166.
- Porter, J.W., Fitt, W.K., Spero, H.J., Rogers, C.S., White, M.W., 1989. Bleaching in reef corals: physiological and stable isotopic responses. *Ecology* 86, 9342-9346.
- Prabhu, C.N., Shankar, R., Anupama, K., Taieb, M., Bonnefille, R., Vidal, L., Prasad, S., 2004. A 200-ka pollen and oxygen-isotopic record from two sediment cores from the eastern Arabian Sea. *Palaeogeography, Palaeoclimatology, Palaeoecology* 214, 309-321.
- Prospero, J.M., Bonatti, E., Schubert, C., Carlson, T.N., 1970. Dust in the Caribbean atmosphere traced to an African dust storm. *Earth and Planetary Science Letters* 9, 287-293.
- Prospero, J.M., Lamb, P.J., 2003. African droughts and dust transport to the Caribbean: climate change implications. *Science* 302, 1024-1029.
- Prospero, J.M., Mayol-Bracero, O.L., 2013. Understanding the transport and impact of African dust on the Caribbean Basin. *American Meteorological Society* 94, 1329-1338.

- Prospero, J.M., Mayol-Bracero, O.L., 2013. Understanding the transport and impact of African dust on the Caribbean Basin. *American Meteorological Society*, 1329-1338.
- Prouty, N.G., Field, M.E., Stock, J.D., Jupiter, S.D., McCulloch, M., 2010. Coral Ba/Ca records of sediment input to the fringing reef of the southshore of Moloka'i, Hawai'i over the last several decades. *Marine Pollution Bulletin* 60, 1822-1835.
- Quinn, T.M., Sampson, D.E., 2002. A multiproxy approach to reconstructing sea surface conditions using coral skeleton geochemistry. *Paleoceanography* 17, doi:10.1029/2000PA000528.
- Quinn, T.M., Taylor, F.W., 2006. SST artifacts in coral proxy records produced by early marine diagenesis in a modern coral from Rabaul, Papua New Guinea. *Geophysical Research Letters* 35. doi: 10.1029/2005GL024972.
- Raddatz, J., Liebetrau, V., Rüggeberg, A., Hathorne, E., Krabbenhoft, A., Eisenhauer, A., Böhm, F., Vollstaedt, H., Fietzke, J., Lopez Correa, M., Freiwald, A., Dullo, W., 2013. Stable Sr-isotope, Sr/Ca, Mg/Ca, Li/Ca and Mg/Li ratios in the scleractinian cold-water coral *Lophelia pertusa*. *Chemical Geology* 352, 143-152.
- Raja, R., Saraswati, P.K., Rogers, K., Iwao, K., 2005. Magnesium and strontium compositions of recent symbiont-bearing benthic foraminifera. *Marine Micropaleontology* 58, 31-44.
- Ramos, R.D., Goodkin, N.F., Siringan, F.P., Hughen, K.A., 2017. *Diploastrea heliopora* Sr/Ca and  $\delta^{18}\text{O}$  records from northeast Luzon, Philippines: an assessment of interspecies coral proxy calibrations and climate controls of sea surface temperature and salinity. *Paleoceanography* 32, 424-438.
- Rathburn, A.E., De Deckker, P., 1997. Magnesium and strontium compositions of recent benthic foraminifera from the Coral Sea, Australia and Prydz Bay, Antarctica. *Marine Micropaleontology* 32, 231-248.
- Rathmann, S., Hess, S., Kuhnert, H., Mulitza, S., 2004. Mg/Ca ratios of the benthic foraminifera *Oridorsalis umbonatus* obtained by laser ablation from core top sediments: relationship to bottom water temperature. *Geochemistry Geophysics Geosystems* 5. doi:

10.1029/2004GC000808.

- Reeder, R.J., Nugent, M., Lamble, G.M., Drew, C., Morris, D.E., 2000. Uranyl incorporation into calcite and aragonite: XAFS and luminescence studies. *Environmental Science Technology* 34, 634-644.
- Reghellin, D., Coxall, H.K., Dickens, G.R., Backman, J., 2015. Carbon and oxygen isotopes of bulk carbonate in sediment deposited beneath the eastern equatorial Pacific over the last 8 million years. *Paleoceanography*, 30, 1261-1287.
- Rehder, H.A., 1962. The Pleistocene molluscs of Grand Cayman Islands, with notes on the geology of the island. *Journal of Paleontology* 36, 583-585.
- Rehman, J., Jones, B., Hagan, T.H., Coniglio, M., 1994. The influence of sponge borings on aragonite-to-calcite inversion in Late Pleistocene *Strombus gigas* from Grand Cayman, British West Indies. *Journal of Sedimentary Research* 64, 174-179.
- Reimer, P.J., Bard, E., Bayliss, A., Beck, J.W., Blackwell, P.G., Ramsey, C.B., Buck, C.E., Cheng, H., Edwards, R.L., Friedrich, M., Grootes, P.M., Guilderson, T.P., Haffidason, H., Hajdas, I., Hatte, C., Heaton, T.J., Hoffmann, D.L., Hogg, A.G., Hughen, K.A., Kaiser, K.F., Kromer, B., Manning, S.W., Niu, M., Reimer, R.W., Richardson, D.A., Scott, E.M., Southon, J., Staff, R.A., Turney, C.S.M., van der Plicht, J., 2013. IntCal13 and Marine13 radiocarbon age calibration curves 0-50,000 years cal BP. *Radiocarbon* 55, 1869-1887.
- Ren, M., Jones, B., 2017. Spatial variations in the stoichiometry and geochemistry of Miocene dolomite from Grand Cayman: implications for the origins of island dolostone. *Sedimentary Geology* 348, 69-93.
- Reynaud, S., Ferrier-Pages, C., Meibom, A., Mostefaoui, S., Mortlock, R., Fairbanks, R., Allemand, D., 2007. Light and temperature effects on Sr/Ca and Mg/Ca ratios in the scleractinian coral *Acropora* sp. *Geochimica et Cosmochimica Acta* 71, 354-362.
- Ribaud-Laurenti, A., Hamelin, B., Montaggioni, L., Cardinal, D., 2001. Diagenesis and its impacts on Sr/Ca ratio in Holocene *Acropora* corals. *International Journal of Earth Sciences* 90, 438-451.

- Richey, J.N., 2007. A 1400-year multi-proxy record of climate variability from the northern Gulf of Mexico, Unpublished. M.Sc., University of South Florida, Florida, USA, 66 pp.
- Rigby, J.K., Roberts, H.H., 1976. Grand Cayman Island: geology, sediments, and marine communities. Brigham Young University Geology Studies: Special Publication, 4. Brigham Young University, Department of Geology, Utah, 122 pp.
- Rind, D., Overpeck, J.T., 1993. Hypothesized causes of decade-to-century climate variability: climate model results. *Quaternary Science Reviews* 12, 357-374.
- Roberts, H.H., Rouse, L.J., Walker, S.E., Hudson, J.H., 1982. Cold-water stress in Florida Bay and northern Bahamas: a product of winter cold-air outbreaks. *Journal of Sedimentary Research* 52, 145-155.
- Rodrigues, L.J., Grottoli, A.G., 2006. Calcification rate and the stable carbon, oxygen, and nitrogen isotopes in the skeleton, host tissue, and zooxanthellae of bleached and recovering Hawaiian corals. *Geochimica et Cosmochimica Acta* 70, 2781-2789.
- Rohling, E.J., Grant, K., Bolshaw, M., Roberts, A.P., Siddall, M., Hemleben, C., Kucera, M., 2009. Antarctic temperature and global sea level closely coupled over past five glacial cycles. *Nature Geoscience Letters* 2, 500-504.
- Rosenthal, Y., Boyle, E., Slowey, N., 1997. Temperature control on the incorporation of magnesium, strontium, fluorine and cadmium into benthic foraminiferal shells from Little Bahama Bank: prospects for thermocline paleoceanography. *Geochimica et Cosmochimica Acta* 61, 231-248.
- Rosenthal, Y., Lohman, K.C., 2002. Accurate estimation of sea surface temperatures using dissolution-corrected calibrations for Mg/Ca paleothermometry. *Paleoceanography* 17. doi: 10.1029/2001PA000749.
- Rosenthal, Y., Lear, C.H., Oppo, D.W., Linsley, B.K., 2006. Temperature and carbonate ion effects on Mg/Ca and Sr/Ca ratios in benthic foraminifera: the aragonite species *Hoeglundina elegans*. *Paleoceanography* 21. doi: 10.1029/2005PA001158.
- Rosenthal, Y., Linsley, B., 2006. Mg/Ca and Sr/Ca paleothermometry from calcareous marine

- fossils, Encyclopedia of Quaternary Sciences. Elsevier Ltd., 24 pp.
- Rothlisberger, F., 1986. 10000 Jahre Gletschergeschichte der Erde, mit einem Beitrag von M.A. Geyh. Sauerländer, Aarau und Frankfurt am Main, 416 pp.
- Runcorn, S.K., 1966. Corals as paleontological clocks. *Scientific America* 215, 26-33.
- Russell, A.D., Honish, B., Spero, H.J., Lea, D.W., 2004. Seawater carbonate chemistry, processes and elements during experiments with planktonic foraminifera *Orbulina universa*. *Geochimica et Cosmochimica Acta* 68, 4347-4361.
- Sadler, J., Webb, G.E., Nothdurft, L.D., Dechnik, B., 2014. Geochemistry-based coral paleoclimate studies and the potential of 'non-traditional' (non-massive *Porites*) coral: recent developments and future progression. *Earth Science Reviews* 139, 291-316.
- Sadler, J., Webb, G.E., Nothdurft, L.D., 2015. Structure and palaeoenvironmental implications of inter-branch coenosteum-rich skeleton in corymbose *Acropora* species. *Coral Reefs* 34, 201-213.
- Sadler, J., Nguyen, A.D., Leonard, N.D., Webb, G.E., Nothdurft, L.D., 2016a. *Acropora* interbranch skeleton Sr/Ca ratios: evaluation of a potential new high-resolution paleothermometer. *Paleoceanography* 31, 505-517.
- Sadler, J., Webb, G.E., Leonard, N.D., Nothdurft, L.D., Clark, T.R., 2016b. Reef core insights into mid-Holocene water temperatures of the southern Great Barrier Reef. *Paleoceanography* 31, 1395-1408.
- Saenger, C., Cohen, A.L., Oppo, D.W., Hubbard, D., 2008. Interpreting sea surface temperature from strontium/calcium ratios in *Montastrea* corals: link with growth rate and implications for proxy reconstructions. *Paleoceanography* 23. doi: 10.1029/2007PA001572.
- Saenger, C., Cohen, A.L., Oppo, D.W., Halley, R.B., Carilli, J.E., 2009. Surface-temperature trends and variability in the low-latitude North Atlantic since 1552. *Nature Geoscience Letters* 2, 492-946.
- Saha, N., Webb, G.E., Zhao, J., Nguyen, A.D., Lewis, S.E., Lough, J.M., 2019. Coral-based high-

- resolution rare earth element proxy for terrestrial sediment discharge affecting coastal seawater quality, Great Barrier Reef. *Geochimica et Cosmochimica Acta* 254, 173-191.
- Sauer, J.D., 1982. Cayman Islands seashore vegetation. A study in comparative biogeography. University of California Press, London, England. 25, 161 pp.
- Sayani, H.R., Cobb, K.M., Cohen, A.L., Elliott, W.C., Nurhati, I.S., Dunbar, R.B., Rose, K.A., Zaunbrecher, L.K., 2011. Effects of diagenesis on paleoclimate reconstructions from modern and young fossil corals. *Geochimica et Cosmochimica Acta* 75, 6361-6373.
- Schrag, D.P., 1999. Rapid analysis of high-precision Sr/Ca ratios in corals and other marine carbonates. *Paleoceanography* 14, 97-102.
- Scott, R.B., Holland, C.L., Quinn, T.M., 2010. Multidecadal trends in instrumental SST and coral proxy Sr/Ca records. *Journal of Climate* 23, 1017-1033.
- Seo, I., Lee, Y.I., Watanabe, T., Yamano, H., Shimamura, M., Yoo, C.M., Hyeong, K., 2013. A skeletal Sr/Ca record preserved in *Dipsastraea* (*Favia*) *speciosa* and implications for coral Sr/Ca thermometry in mid-latitude regions. *Geochemistry Geophysics Geosystems* 14, 2873-2885.
- Shackleton, N.J., 1974. Attainment of isotopic equilibrium between ocean water and the benthonic foraminifera genus *Uvigerina*: isotopic changes in the ocean during the last glacial. *Colloques Internationaux du Centre National de la Recherche Scientifique* 219, 203-210.
- Shackleton, N.J., Kennett, J.P., 1975a. Late Cenozoic oxygen and carbon isotopic changes at DSDP site 284: implications for glacial history of the northern hemisphere and Antarctica, Initial Reports of the Deep Sea Drilling Project. U.S. Government Printing Office, Washington, D.C., pp. 801.
- Shackleton, N.J., Kennett, J.P., 1975b. Paleotemperature history of the Cenozoic and the initiation of Antarctic glaciation: oxygen and carbon isotope analyses in DSDP sites 277, 279, 281, Initial Reports of the Deep Sea Drilling Project. U.S. Government Printing Office, Washington, D.C., pp. 743.

- Sharp, Z., 2007. Principles of stable isotope geochemistry. Pearson/Prentice Hall, Upper Saddle River, New Jersey, 334 pp.
- Shaw, T.J., Moore, W.S., Kloepfer, J., Sochaski, M.A., 1998. The flux of barium to the coastal waters of the southeaster USA: the importance of submarine groundwater discharge. *Geochimica et Cosmochimica Acta* 62, 3047-3054.
- Shen, G.T., Dunbar, R.B., 1995. Environmental controls on uranium in reef corals. *Geochimica et Cosmochimica Acta* 59, 2009-2024.
- Shen, C., Lee, T., Chen, C., Wang, C., Dai, C., Li, A., 1996. The calibration of  $D_{(Sr/Ca)}$  versus sea surface temperature relationship for *Porites* coral. *Geochimica et Cosmochimica Acta* 60, 3849-3858.
- Shen, C., Li, K., Sieh, K., Natawidjaja, D., Cheng, H., Wang, X., Edwards, R.L., Lam, D.D., Hsieh, Y., Fan, T., Meltzner, A.J., Taylor, F.W., Quinn, T.M., Chiang, H., Kilbourne, K.H., 2008. Variation of initial  $^{230}\text{Th}/^{232}\text{Th}$  and limits of high precision U-Th dating of shallow-water corals. *Geochimica et Cosmochimica Acta* 7, 4201-4223.
- Sholkovitz, E.R., Landing, W.M., Lewis, B.L., 1994. Ocean particle chemistry: the fractionation of rare earth elements between suspended particles and seawater. *Geochimica et Cosmochimica Acta* 58, 1567-1579.
- Siddall, M., Chappell, J., Potter, E.K., 2007. Eustatic sea level during past Interglacials. In: Sirocko, F., Claussen, M., Litt, T., Sanchez-Goni, M.F. (Eds.), *The Climate of Past Interglacials*. Elsevier Science, pp. 75-92.
- Siegel, F.R., 1960. The effects of strontium on the aragonite-calcite ratios of Pleistocene corals. *Journal of Sedimentary Petrology* 30, 297-304.
- Sinclair, D.J., 2005. Correlated trace element 'vital effects' in tropical corals: a new tool for probing biomineralization chemistry. *Geochimica et Cosmochimica Acta* 69, 3265-3284.
- Sinclair, D.J., Kinsley, L.P.J., McCulloch, M.T., 1998. High resolution analysis of trace elements in corals by laser ablation ICP-MS. *Geochimica et Cosmochimica Acta* 62, 1889-1901.
- Sinclair, D.J., McCulloch, M., 2004. Corals record low mobile barium concentrations in the

- Burdekin River during the 1974 flood: evidence for limited Ba supply to rivers?  
 Palaeogeography, Palaeoclimatology, Palaeoecology 214, 155-174.
- Sinclair, D.J., Williams, B., Risk, M., 2006. A biological origin for climate signals in corals-  
 trace element 'vital effects' are ubiquitous in scleractinian coral skeletons. Geophysical  
 Research Letters 33. doi: 10.1029/2006GL027183.
- Siriananskul, W., Pumijumnong, N., 2014. A preliminary study of Sr/Ca thermometry in Chang  
 Islands, Gulf of Thailand. Songklanakarin Journal of Science and Technology 36, 583-  
 589.
- Siriananskul, W., Pumijumnong, N., Mitsuguchi, T., Puchakarn, S., Boontanon, N., 2012. Mg/Ca  
 and Sr/Ca ratios in a coral from Koh Chuek, Surat Thani, Thailand. Journal of Coral Reef  
 Studies 14, 63-72.
- Skinner, L.C., Shackleton, N.J., Elderfield, H., 2003. Millennial-scale variability of deep-water  
 temperature and  $\delta^{18}\text{O}_{\text{dw}}$  indicating deep-water source variations in the Northeast Atlantic,  
 0-34 cal. ka BP. Geochemistry Geophysics Geosystems 4, 1098.
- Smith, S.R., Buddemeier, R.W., Redale, R., Houck, J.E., 1979. Strontium-calcium thermometry in  
 coral skeletons. Science 204, 404-406.
- Smith, J.M., Quinn, T.M., Helmle, K.P., Halley, R.B., 2006. Reproducibility of geochemical and  
 climatic signals in the Atlantic coral *Montastrea faveolata*. Paleoceanography 21, doi  
 10.1029/2005PA001187.
- Spero, H.J., Mielke, K.M., Kalve, E.M., Lea, D.W., Pak, D.K., 2003. Multispecies approach to  
 reconstructing eastern equatorial Pacific thermocline hydrography during the past 360  
 kyr. Paleoceanography 18. doi: 10.1029/2002PA000814.
- Stansell, N.D., Steinman, B.A., Abbot, M.B., Rubinov, M., Roman-Lacayo, M., 2013. Lacustrine  
 stable isotope record of precipitation changes in Nicaragua during the Little Ice Age and  
 Medieval Climate Anomaly. Geology 41, 151-154.
- Stephans, C.L., Quinn, T.M., Taylor, F.W., Correge, T., 2004. Assessing the  
 reproducibility of coral-based climate records. Geophysical Research Letters 31.



doi:10.1029/2004GL020343.

- Stoll, H.M., Schrag, D.P., Clemens, S.C., 1999. Are seawater Sr/Ca variations preserved in Quaternary foraminifera? *Geochimica et Cosmochimica Acta* 63, 3535-3547.
- Stoffyn-Egli, P., Mackenzie, F.T., 1984. Mass balance oceans of dissolved lithium. *Geochimica et Cosmochimica Acta* 48, 859-872.
- Storz, D., Gischler, E., Fiebig, J., Eisenhauer, A., Garbe-Schonberg, D., 2013. Evaluation of oxygen isotope and Sr/Ca ratios from a Maldivian scleractinian coral from reconstruction of climate variability in the Northwestern Indian Ocean. *Palaios* 28, 42-55.
- Strong, A.E., 1989. Greater global warming revealed by satellite-derived sea-surface temperature trends. *Nature* 338, 642-645.
- Stuiver, M., Reimer, P.J., Reimer, R.W., 2020. CALIB 7.10 {WWW program} at <http://calib.org>.
- Sun, Y., Sun, M., Lee, T., Nie, B., 2005. Influence of seawater Sr content on coral Sr/Ca and Sr thermometry. *Coral Reefs* 24, 23-29.
- Swart, P.K., 1981. The strontium, magnesium, and sodium composition of recent scleractinian coral skeletons as standards for palaeoenvironmental analysis. *Palaeogeography, Palaeoclimatology, Palaeoecology* 34, 115-136.
- Swart, P.K., Hubbard, J.A.E.B., 1982. Uranium in scleractinian coral skeletons. *Coral Reefs* 1, 13-19.
- Swart, P.K., 1983. Carbon and oxygen isotope fractionation in scleractinian corals: a review. *Earth-Science Reviews* 19, 51-80.
- Swart, P.K., Elderfield, H., Greaves, M.J., 2002. A high-resolution calibration of Sr/Ca thermometry using the Caribbean coral *Montastraea annularis*. *Geochemistry Geophysics Geosystems* 3. doi: 10.1029/2002GC000306.
- Switzer, A.D., Jones, B.G., 2008. Large-scale washover sedimentation in a freshwater lagoon from the southeast Australian coast: sea-level change, tsunami or exceptionally large storm? *The Holocene* 18, 787-803.
- Tachikawa, K., Vidal, L., Sonzogni, C., Brad, E., 2009. Glacial/interglacial sea surface

- temperature changes in the Southwest Pacific Ocean over the past 360 ka. *Quaternary Science Reviews* 28, 1160-1170.
- Tanaka, K., Holcomb, M., Takahashi, A., Kurihara, H., Asami, R., Shinjo, R., Sowa, K., Rankenburg, K., Watanabe, T., McCulloch, M., 2015. Response of *Acropora digitifera* to ocean acidification: constraints from  $\delta^{11}\text{B}$ , Sr, Mg, and Ba composition of aragonitic skeletons cultured under variable seawater pH. *Coral Reefs* 34, 1139-1149.
- Taylor, S.R., McLennan, S.M., 1985. *The continental crust: its composition and evolution*. Blackwell Scientific Publications, 312 pp.
- Team, R.C., 2013. R: a language and environment for statistical computing In: *Computing, R Foundation for Statistical (Ed.)*, Vienna, Austria.
- Thebault, J., Schone, B.R., Hallmann, N., Barth, M., Nunn, E.V., 2009. Investigation of Li/Ca variations in aragonitic shells of the ocean quahog *Arctica islandica*, northeast Iceland. *Geochemistry Geophysics Geosystems* 10. doi: 10.1029/2009GC002789.
- Thorrold, S.R., Campana, S.E., Jones, C.M., Swart, P.K., 1997. Factors determining  $\delta^{13}\text{C}$  and  $\delta^{18}\text{O}$  fractionation in aragonitic otoliths of marine fish. *Geochimica et Cosmochimica Acta* 61, 2909-2919.
- Tierney, J.E., Abram, N.J., Anchukaitis, K.J., Evans, M.N., Giry, C., Kilbourne, K.H., Saenger, C., Wu, H.C., Zinke, J., 2015. Tropical sea surface temperatures for the last four centuries reconstructed from coral archives. *Paleoceanography* 30, 226-252.
- Tipping, R., Davies, A., McCulloch, R., Tisdall, E., 2008. Response to late Bronze Age climate change of farming communities in north east Scotland. *Journal of Archaeological Science* 35, 2379-2386.
- Titelboim, D., Sadekov, A., Almogi-Labin, A., Herut, B., Kucera, M., Schmidt, C., Hyams-Kaphzan, O., Abramovich, S., 2017. Geochemical signatures of benthic foraminiferal shells from a heat-polluted shallow marine environment provide field evidence for growth and calcification under extreme warmth. *Global Change Biology* 23, 4346-4353.
- Toler, S.K., Hallock, P., Schijf, J., 2001. Mg/Ca ratios in stressed foraminifera, *Amphistegina*

- gibbosa*, from the Florida Keys. *Marine Micropaleontology* 43, 199-206.
- Toth, L.T., Cheng, H., Edwards, L.R., Ashe, E., Richey, J.N., 2017. Millennial-scale variability in the local radiocarbon reservoir age of south Florida during the Holocene. *Quaternary Geochronology* 42, 130-143.
- Toyofuku, T., Kitazato, H., 2005. Micromapping of Mg/Ca values in cultured specimens of the high-magnesium benthic foraminifera. *Geochemistry Geophysics Geosystems* 6. doi: 10.1029/2005GC000961.
- Toyofuku, T., Kitazato, H., Kawahata, H., Tsuchiya, M., Nohara, M., 2000. Evaluation of Mg/Ca thermometry in foraminifera: comparison of experimental results and measurements in nature. *Paleoceanography* 15, 456-464.
- Trapp, J.M., Millero, F.J., Prospero, J.M., 2010. Temporal variability of the elemental composition of African dust measured in trade wind aerosoles at Barbados and Maimi. *Marine Chemistry* 120, 71-82.
- Trenberth, K.E., Jones, P.D., Ambenje, P., Bojariu, R., Easterling, D., Klein Tank, A., Parker, D., Rahimzadeh, F., Renwick, J.A., Rusticucci, M., Soden, B., Zhai, P., 2007. Observations: surface and atmospheric climate change. In: Solomon, S., Qin, D., Manning, M., Chen, Z., Marquis, M., Averyt, K.B., Tignor, M., Miller, H.L. (Eds.), *Climate Change 2007: The Physical Science Basis. Contribution of Working Group I to the Fourth Assessment Report of the Intergovernmental Panel on Climate Change* Cambridge University Press, Cambridge, United Kingdom, 102 pp.
- Trouet, V., Diaz, H.F., Wahl, E.R., Viau, A.E., Graham, R., Graham, N., Cook, E.R., 2013. A 1500-year reconstruction of annual mean temperature for temperate North America on decadal-to-multidecadal time scales. *Environmental Research Letters* 8. doi:10.1088/1748-9326/8/2/024008.
- Tudhope, A.W., Lea, D.W., Shimmield, G.B., Chilcott, C.P., Head, S., 1996. Monsoon climate and Arabian Sea coastal upwelling recorded in massive corals from southern Oman. *PALAIOS* 11, 347-361.

- Turekian, K.K., Wedepohl, K.H., 1961. Distribution of the elements in some major units of the Earth's crust. *Geological Society of America Bulletin* 72, 175-192.
- Urey, H.C., 1947. The thermodynamic properties of isotopic substances. *Journal of the Chemical Society of London*, 562-581.
- van Hengstum, P.J., Donnelly, J.P., Kingston, A.W., Williams, B.E., Scott, D.B., Reinhardt, E.G., Little, S.N., Patterson, W.P., 2015. Low-frequency storminess signal at Bermuda linked to cooling events in the North Atlantic region. *Paleoceanography* 30, 52-76.
- Vaughan, T.W., 1918. Some shoal-water from Murray Island (Australia), Coco-Keelinh Islands, and Fanning Island, Papers Department of Marine Biology, Carnegie Institute of Washington, 9, pp. 49-234.
- Veizer, J., 1983. Chemical diagenesis of carbonates: theory and application of trace elements. In: Arthur, M.A. (Ed.), *Stable Isotopes in Sedimentary Geology*, 10, 100 pp.
- Vengosh, A., Kolodny, Y., Starinsky, A., Chivas, A.R., McCulloch, M.T., 1991. Coprecipitation and isotopic fractionation of boron in modern carbonates. *Geochimica et Cosmochimica Acta* 55, 2901-2910.
- Venn, A.A., Tambutte, E., Holcomb, M., Laurent, J., Allemand, D., Tambutte, S., 2013. Impact of seawater acidification on pH at the tissue-skeleton interface and calcification on coral reefs. *Geochimica et Cosmochimica Acta* 68, 1473-1488.
- Vežina, J.L., 1997. Stratigraphy and sedimentology of the Pleistocene Ironshore Formation at Rogers Wreck Point, Grand Cayman: a 400 ka record of sea-level highstands, Unpublished. M.Sc. Thesis, University of Alberta, Edmonton, Alberta, Canada, 131 pp.
- Vežina, J.L., Jones, B., Ford, D., 1999. Sea level highstands over the last 500,000 years: evidence from the Ironshore Formation on Grand Cayman, British West Indies. *Journal of Sedimentary Research* 69, 317-327.
- von Langen, P.J., Pak, D.K., Spero, H.J., Lea, D.W., 2005. Effects of temperature on Mg/Ca in neogloboquadrinid shells determined by living culturing. *Geochemistry Geophysics Geosystems* 6. doi: 10.1029/2005GC000989.

- Hetzinger, S., Garbe-Schonberg, D., Manfrino, C., Dullo, W., 2016. Impact of warming events on reef-scale temperature variability as captured in two Little Cayman coral Sr/Ca records. *Geochemistry Geophysics Geosystems* 17. doi: 10.1002/2015GC006194.
- Wahl, E.R., Diaz, H.F., Ohlwein, C., 2012. A pollen-based reconstruction of summer temperature in central North America and implications for circulation patterns during medieval times. *Global and Planetary Change* 84-85, 66-74.
- Wang, H., Chen, J., Zhang, S., Zhang, D.D., Wang, Z., Xu, Q., Chen, S., Wang, S., Hang, S., Chen, F., 2018. A chironomid-based record of temperature variability during the past 4000 years in northern China and its possible societal implications. *Climate of the Past* 14, 383-396.
- Wang, T., Surge, D., Mithen, S., 2012. Seasonal temperature variability of the Neoglacial (3300-2500 BP) and Roman Warm Period (2500-1600 BP) reconstructed from oxygen isotope ratios of limpet shells (*Patella vulgata*), Northwest Scotland. *Palaeogeography, Palaeoclimatology, Palaeoecology* 317-318, 104-113.
- Wang, T., Surge, D., Walker, K.J., 2013. Seasonal climate change across the Roman Warm Period/Vandal Minimum transition using isotope sclerochronology in archaeological shells and otoliths, southwest Florida, USA. *Quaternary International* 308-309, 230-241.
- Wanner, H., Solomina, O., Grosjean, M., Ritz, S.P., Jetel, M., 2011. Structure and origin of Holocene cold events. *Quaternary Science Reviews* 30, 3109-3123.
- Wassenburg, J.A., Immenhauser, A., Richter, D.K., Niedermayr, A., Riechelmann, S., Fietzke, J., Scholz, D., Jochum, K.P., Fohlmeister, J., Schroder-Ritzrau, A., Sabaoui, A., Riechelmann, D.F.C., Schneider, L., Esper, J., 2013. Moroccan speleothem and tree ring records suggest a variable positive state of the North Atlantic Oscillation during the Medieval Warm Period. *Earth and Planetary Science Letters* 375, 291-302.
- Watanabe, T., Winter, A., Oba, T., 2001. Seasonal changes in sea surface temperatures and salinity during the Little Ice Age in the Caribbean Sea deduced from Mg/Ca and  $^{18}\text{O}/^{16}\text{O}$  ratios in corals. *Marine Geology* 173, 21-35.

- Webb, G.E., Nothdurft, L.D., Kamber, B.S., Kloprogge, J.T., Zhao, J., 2009. Rare earth element geochemistry of scleractinian coral skeleton during meteoric diagenesis: a sequence through neomorphism of aragonite to calcite. *Sedimentology* 56, 1433-1463.
- Webb, G.E., Nothdurft, L.D., Zhao, J., Opdyke, B., Price, G., 2016. Significance of shallow core transects for reef models and sea-level curves, Heron Reef, Great Barrier Reef. *Sedimentology* 63, 1396-1424.
- Weber, J.N., 1973. Incorporation of strontium into reef coral skeletal carbonate. *Geochimica et Cosmochimica Acta* 37, 2173-2190.
- Weber, J.N., 1977. Use of corals in determining glacial-interglacial changes in temperature and isotopic composition of seawater: reef biota. In: Frost, S. H., Weiss, M. P., Saunders, J. B. (Eds.), *Reefs and Related Carbonates - Ecology and Sedimentology*. American Association of Petroleum Geologists Special Volumes, 4, pp. 289-295.
- Weber, J.N., White, E.W., Weber, P.H., 1975a. Correlation of density banding in reef coral skeletons with environmental parameters: the basis for interpretation of chronological records preserved in the coralla of corals. *Paleobiology* 1, 137-149.
- Weber, J.N., Deines, P., Weber, P.H., Baker, P.A., 1975b. Depth related changes in the  $^{13}\text{C}/^{12}\text{C}$  ratio of skeletal carbonate deposited by the Caribbean reef-frame building coral *Montastrea annularis*: further implications of a model from stable isotope fractionation by scleractinian corals. *Geochimica et Cosmochimica Acta* 40, 31-39.
- Weber, J.N., Woodhead, P.M.J., 1970. Carbon and oxygen isotope fractionation in the skeletal carbonate of reef-building corals. *Chemical Geology* 6, 93-117.
- Weber, J.N., Woodhead, P.M.J., 1972. Temperature dependence of oxygen-18 concentration in reef coral carbonates. *Journal of Geophysical Research* 77, 463-474.
- Webster, P.J., Moore, A.M., Loschnigg, J.P., Leben, R.R., 1999. Coupled ocean-atmosphere dynamics in the Indian Ocean during 1997-1998. *Nature* 401, 356-360.
- Wei, G., Sun, M., Li, X., Nie, B., 2000. Mg/Ca, Sr/Ca and U/Ca ratios of a *Porites* coral from Sanya Bay, Hainan Island, South China Sea and their relationship to sea surface

- temperature. *Palaeogeography, Palaeoclimatology, Palaeoecology* 162, 59-74.
- Weil, S.M., Buddemeier, R.W., Smith, S.V., Kroopnick, P.M., 1981. The stable isotopic composition of coral skeletons: control by environmental variables. *Geochimica et Cosmochimica Acta* 45, 1147-1153.
- Weil, E., Knowlton, N., 1994. A multi-character analysis of the Caribbean coral *Montastrea annularis* (Ellis and Solander, 1786) and its two sibling species, *M. faveolata* (Ellis and Solander, 1786) and *M. franksi* (Gregory, 1895). *Bulletin of Marine Science* 55, 151-175.
- Wejnert, K.E., Thunell, R.C., Astor, Y., 2013. Comparison of species-specific oxygen isotope paleotemperature equations: sensitivity analysis using planktonic foraminifera from the Cariaco Basin, Venezuela. *Marine Micropaleontology* 101, 76-88.
- Wellington, G.M., Dunbar, R.B., Merlen, G., 1996. Calibration of stable oxygen isotope signatures in Galapagos corals. *Paleoceanography* 11, 467-480.
- Wells, J.W., 1963. Coral growth and geochronometry. *Nature* 197, 948-950.
- White, R.M.P., Dennis, P.F., Atkinson, T.C., 1999. Experimental calibration and field investigation of the oxygen isotopic fractionation between biogenic aragonite and water. *Rapid Communications in Mass Spectrometry* 13, 1242-1247.
- Wignall, B., 1995. Sedimentology and diagenesis of the Cayman (Miocene) and Pedro Castle (Pliocene) Formations at Safe Haven, Grand Cayman. British West Indies, Edmonton, AB. M.Sc., University of Alberta, 110 pp.
- Winter, A., Appeldoorn, R.S., Bruckner, A., Williams, E.H., Goenaga, C., 1998. Sea surface temperatures and coral reef bleaching off La Parguera, Puerto Rico (northeastern Caribbean Sea). *Coral Reefs* 17, 377-382.
- Winter, A., Paul, A., Nyberg, J., Oba, T., Lundberg, J., Schrag, D.P., Taggart, B., 2003. Orbital control of low-latitude seasonality during the Eemian. *Geophysical Research Letters* 30. doi:10.1029/2002GL016275.
- Winter, A., Sammarco, P.W., 2010. Lunar banding in the scleractinian coral *Montastraea faveolata*: fine-scale structures and influences of temperature. *Journal of Geophysical*

Research 115. doi: 10.1029/2009JG001264.

- Winter, A., Paul, A., Nyberg, J., Oba, T., Lundberg, J., Schrag, D.P., Taggart, B., 2003. Orbital control of low-latitude seasonality during the Eemian. *Geophysical Research Letters* 30. doi:10.1029/2002GL016275.
- Woodroffe, C.D., Stoddart, D.R., Giglioli, M.E.C., 1980. Pleistocene patch reefs and Holocene swamp morphology, Grand Cayman Island, West Indies. *Journal of Biogeography* 7, 103-113.
- Worum, F.P., Carricart-Ganivet, J.P., Benson, L., Golicher, D., 2007. Simulation and observations of annual density banding in skeletons of *Montastrea* (Cnidaria: Scleractinia) growing under thermal stress associated with ocean warming. *Limnology and Oceanography* 52, 2317-2323.
- Wurtzel, J.B., Black, D.E., Thunell, R.C., Peterson, L.C., Tappa, E.J., Rahman, S., 2013. Mechanisms of southern Caribbean SST variability over the last two millennia. *Geophysical Research Letters* 40, 5954-5958.
- Xu, Y., Pearson, S., Kilbourne, K.H., 2015. Assessing coral Sr/Ca-SST calibration techniques using the species *Diploria strigosa*. *Palaeogeography, Palaeoclimatology, Palaeoecology* 440, 353-362.
- Yu, K., Zhao, J., Liu, T., Wei, G., Wang, P., Collerson, K.D., 2004. High-frequency winter cooling and reef coral mortality during the Holocene climatic optimum. *Earth and Planetary Science Letters* 224, 143-155.
- Yu, K., Zhao, J., Wei, G., Cheng, X., Chen, T., Felis, T., Wang, P., Liu, T., 2005.  $\delta^{18}\text{O}$ , Sr/Ca and Mg/Ca records of *Porites lutea* corals from Leizhou Peninsula, northern South China Sea, and their applicability as paleoclimatic indicators. *Palaeogeography, Palaeoclimatology, Palaeoecology* 218, 57-73.
- Yu, W., Tian, L., Risi, C., Yao, T., Ma, Y., Zhao, H., Zhu, H., He, Y., Xu, B., Zhang, H., Qu, D., 2016.  $\delta^{18}\text{O}$  records in water vapor and an ice core from the eastern Pamir Plateau: implications for paleoclimate reconstructions. *Earth and Planetary Science Letters* 456,



146-156.

Zinke, J., Dullo, W., Heiss, G.A., Eisenhauer, A., 2004. ENSO and Indian Ocean subtropical dipole variability is recorded in a coral record off southwest Madagascar for the period 1659 to 1995. *Earth and Planetary Science Letters* 228, 177-194.

**APPENDIX**

Supplementary Table 2.1. Sr/Ca geothermometers.

Reference	Sample type	Location	SST (°C)	Equation	n	r <sup>2</sup>	r	SST <sub>error</sub> (°C)
Weber (1973)	<i>Acropora</i>	Global	20 – 30	$K(\text{Sr}/\text{Ca}) = 1.0732 + 0.0024 * \text{SST} - 0.0175 * \text{ext}$	413	-	-	-
Houek et al. (1977)	<i>Pocillopora</i>	Lab grown	21 – 29	$\text{Sr}/\text{Ca} = 9.8 - 0.067 * \text{SST}$	51	-	-	-
	<i>damicornis</i>			$\text{Sr}/\text{Ca} = 11.2 - 0.108 * \text{SST}$	60			
	<i>Montipora</i> <i>verrucosa</i>			$\text{Sr}/\text{Ca} = 11.0 - 0.118 * \text{SST}$	44			
	<i>Porites lobata</i>							
Smith et al. (1979)	<i>Pollicipora</i>	Panama,	18 – 30	$\text{Sr}/\text{Ca} = 11.01 - 0.071 * \text{SST}$	32	0.77	-	-
	<i>damicornis</i>	Hawaii, Midway Atoll,		$\text{Sr}/\text{Ca} = 10.94 - 0.070 * \text{SST}$	22	0.71		
	<i>Porites</i>	Johnston Atoll,		$\text{Sr}/\text{Ca} = 11.64 - 0.089 * \text{SST}$	18	0.63		
	<i>Montipora</i> <i>verrucosa</i>	Enewetak Atoll, Guam		$\text{Sr}/\text{Ca} = 11.32 - 0.082 * \text{SST}$	72	0.60		
Beck et al. (1992) (corrected in 1994)	<i>Porites lobata</i>	Noumea	20 – 28	$\text{Sr}/\text{Ca} = 10.72 - 0.062 * \text{SST}$	17	-	-	0.5
		New Caledonia Tahiti		$\text{Sr}/\text{Ca} = 10.48 - 0.063 * \text{SST}$				
de Villiers et al. (1994)	<i>Porites lobata</i>	Hawaii	23 – 27	$\text{Sr}/\text{Ca} = 10.96 - 0.080 * \text{SST}$	26	0.95	-	-
	<i>Pocillopora</i> <i>eydouxii</i>	Galapagos Islands	19 – 25	$\text{Sr}/\text{Ca} = 11.00 - 0.076 * \text{SST}$	14	0.93		
	<i>Pavona clavus</i>			$\text{Sr}/\text{Ca} = 10.65 - 0.068 * \text{SST}$	29	0.64		

Reference	Sample type	Location	SST (°C)	Equation	<i>n</i>	<i>r</i> <sup>2</sup>	<i>r</i>	SST <sub>error</sub> (°C)
de Villiers et al. (1995)	<i>Panovia clavus</i>	Galapagos Islands	20 – 26	Sr/Ca= 10.25 – 0.042 * SST Sr/Ca= 10.11 – 0.034 * SST Sr/Ca= 9.92 – 0.033 * SST	70	-	0.89	-
Min et al. (1995)	<i>Porites</i>	New Caledonia, Tahiti	20 – 26	Sr/Ca= 8.94 – 0.053 * SST	-	-	-	-
Mitsuguchi et al. (1996)	<i>Porites lutea</i>	Japan	20 – 30	Sr/Ca= 10.50 – 0.061 * SST	112	0.73	-	-
Shen et al. (1996)	<i>Porites lobata</i> <i>Porites lutea</i>	Southern Taiwan	22 – 28	Sr/Ca= 10.27 – 0.051 * SST Sr/Ca= 10.32 – 0.053 * SST	36 36	0.91 0.96	-	-
Alibert and McCulloch (1997)	<i>Porites</i> sp.	Great Barrier Reef	23 – 29	Sr/Ca= 10.48 – 0.062 * SST	534	-	0.98	-
Bessat (1997)	<i>Porites</i> sp.	Muruoroa (French Polynesia)	23 – 29	Sr/Ca= 11.30 – 0.082 * SST	116	0.66	-	-
Boiseau et al. (1997)	<i>Acropora nobilis</i>	Mayotte Island	26 – 29	Sr/Ca= 18.20 – 0.330 * SST	15	-	0.8	-
Heiss et al. (1997)	<i>Porites lutea</i>	La Reunion	23 – 32	Sr/Ca= 10.58 – 0.061 * SST	73	0.84	-	-
Gagan et al. (1998)	<i>Porites lutea</i>	Great Barrier Reef	20 – 31	Sr/Ca= 10.73 – 0.064 * SST Sr/Ca= 10.78 – 0.066 * SST	84 79	-	0.98 0.80	-

Reference	Sample type	Location	SST (°C)	Equation	n	r <sup>2</sup>	r	SST <sub>error</sub> (°C)
Gagan et al. (1998)	<i>Porites lutea</i>	Great Barrier Reef Java Dampier Archipelago	20 – 31	Sr/Ca= 10.68 – 0.062 * SST	84	-	0.98	-
Sinclair et al. (1998)	<i>Porites myeri</i>	Great Barrier Reef	22 – 29	Sr/Ca= 10.80 – 0.070 * SST	36	0.82	-	-
Evans et al. (1999)	<i>Porites</i> sp.	Christmas Island	22 – 28	Sr/Ca= 0.010 – 0.061 * SST	59	-	0.77	-
Fallon et al. (1999)	<i>Porites lobata</i>	Japan	14 – 28	Sr/Ca= 10.76 – 0.063 * SST	425	-	-0.77	-
McCulloch et al. (1999)	<i>Porites</i> sp.	Huon peninsula	28 – 30	Sr/Ca= 10.70 – 0.062 * SST	100	-	-	2
Schrag (1999)	<i>Porites lutea</i>	Galapagos Islands	19 – 25	Sr/Ca= 10.55 – 0.051 * SST	155	-	-0.70	-
Correge et al. (2000)	<i>Porites lutea</i>	New Caledonia	20 – 26	Sr/Ca= 10.73 – 0.066 * SST	85	0.64	-	-
Linsley et al. (2000)	<i>Porites lutea</i>	Fiji Rarotonga	24 – 30 22 – 29	Sr/Ca= 10.65 – 0.053 * SST Sr/Ca= 11.12 – 0.065 * SST	175	0.77	-	-
McCulloch and Esat (2000)	<i>Porites</i>	Great Barrier Reef	21 – 29	Sr/Ca= 10.42 – 0.060 * SST	240	0.98	-	-
Wei et al. (2000)	<i>Porites</i> sp.	South China Sea	19 – 31	Sr/Ca= 210.20 – 19.83 * SST	120	-	0.75	-

Reference	Sample type	Location	SST (°C)	Equation	n	r <sup>2</sup>	r	SST <sub>error</sub> (°C)
Cardinal et al. (2001)	<i>Diploria labyrinthiformis</i>	Bermuda	19 – 28	Sr/Ca= 10.03 – 0.045 * SST	50	0.86	-	-
				Sr/Ca= 9.94 – 0.042 * SST	92	0.79		
Marshall and McCulloch (2001)	<i>Porites</i> sp.	Christmas Island	24 – 31	Sr/Ca= 10.38 – 0.059 * SST	350	0.69	-	-
Correge et al. (2001)	<i>Porites lobata</i>	New Caledonia	22 – 25	Sr/Ca= 10.73 – 0.066 * SST	85	-	0.79	-
Cohen et al. (2002)	<i>Astrangia poculata</i>	New England	6 – 29	Sr/Ca= 10.07 – 0.036 * SST	7	-	-	-
	<i>Porites</i>			Sr/Ca= 9.98 – 0.038 * SST	4			
Marshall and McCulloch (2002)	<i>Porites lutea</i>	Great Barrier Reef	23 – 29	Sr/Ca= 10.40 – 0.058 * SST	112	-	-	0.3
	<i>Porites</i> sp.			Sr/Ca= 10.40 – 0.059 * SST	66			
Quinn and Sampson (2002)	<i>Porites lutea</i>	New Caledonia	20 – 27	Sr/Ca= 10.07 – 0.052 * SST	212	0.84	-	-
				Sr/Ca= 10.12 – 0.057 * SST	212	0.84		
				Sr/Ca= 10.38 – 0.061 * SST	293	0.84		
				Sr/Ca= 10.52 – 0.067 * SST	293	0.84		
Swart et al. (2002)	<i>Montastrea annularis</i>	Florida	23 – 31	Sr/Ca= 10.17 – 0.047 * SST	98	-	0.62	-

Reference	Sample type	Location	SST (°C)	Equation	n	r <sup>2</sup>	r	SST <sub>error</sub> (°C)
Fallon et al. (2003)	<i>Porites</i>	Great Barrier Reef	22 – 31	Sr/Ca= 10.11 – 0.041 * SST	72	-	-0.50	-
				Sr/Ca= 10.62 – 0.065 * SST	108		-0.83	
				Sr/Ca= 10.23 – 0.052 * SST	48		-0.79	
				Sr/Ca= 10.39 – 0.060 * SST	84		-0.84	
				Sr/Ca= 10.73 – 0.071 * SST	84		-0.91	
				Sr/Ca= 10.42 – 0.057 * SST	108		-0.79	
				Sr/Ca= 10.35 – 0.060 * SST	36		-0.82	
Allison and Finch (2004)	<i>Porites lobata</i>	Hawaii	23 – 28	Sr/Ca= 10.97 – 0.067 * SST	8	0.87	-	-
				Sr/Ca= 10.86 – 0.080 * SST	8	0.92		
				Sr/Ca= 9.10 – 0.080 * SST	95	-		
				Sr/Ca= 9.23 – 0.110 * SST				
				Sr/Ca= 9.29 – 0.130 * SST				
Bagnato et al. (2004)	<i>Diploastrea heliopore</i>	Fiji	24 – 30	Sr/Ca= 10.08 – 0.034 * SST	20	-	0.84	-
Correge et al. (2004)	<i>Diploastrea heliopore</i>	Indonesia New Caledonia	22 – 30	Sr/Ca= 10.57 – 0.060 * SST	256	0.75	-	-

Reference	Sample type	Location	SST (°C)	Equation	n	r <sup>2</sup>	r	SST <sub>error</sub> (°C)
Felis et al. (2004)	<i>Porites</i>	Gulf of Aqaba	21 – 27	Sr/Ca= 10.78 – 0.060 * SST	588	0.78	-	-
Kilbourne et al. (2004)	<i>Porites lutea</i>	Vanuatu	26 – 29	Sr/Ca <sub>anomaly</sub> = - 0.050 * SST	1100	-	-0.78	-
Linsley et al. (2004)	<i>Porites lutea</i>	Fiji	24 – 30	Sr/Ca= 11.73 – 0.055 * *SST	175	0.70	-	-
		Rarotonga	22 – 29	Sr/Ca= 11.07 – 0.063 * SST		0.64		
Stephans et al. (2004)	<i>Porites lutea</i>	New Caledonia	20 – 26	Sr/Ca= 10.33 – 0.050 * SST	308	-	-0.93	-
Yu et al. (2004)	<i>Goniopora</i> sp.	South China Sea	18 – 30	Sr/Ca= 9.60 – 0.031 * SST	48	-	-0.99	-
Zinke et al. (2004)	<i>Porites lobata</i>	Madagascar	21 – 28	Sr/Ca= 10.01 – 0.037 * SST	48	0.74	-	-
				Sr/Ca= 10.48 – 0.054 * SST	168	0.90		
				Sr/Ca= 10.32 – 0.049 * SST	168	0.89		
				Sr/Ca= 10.40 – 0.053 * SST	264	0.38		
				Sr/Ca= 10.35 – 0.050 * SST	264	0.89		
				Sr/Ca= 10.32 – 0.050 * SST	216	0.61		
				Sr/Ca= 12.04 – 0.117 * SST	216	0.54		
Goodkin et al. (2005)	<i>Diploria</i> <i>labyrinthiformis</i>	Bermuda	18 – 29	Sr/Ca= 10.10 – 0.036 * SST	96	-	0.86	-
				Sr/Ca= 10.30 – 0.041 * SST			0.51	
				Sr/Ca= 10.40 – 0.048 * SST			0.21	
				Sr/Ca= 10.70 – 0.053 * SST – 0.0017 * ext			0.68	



Reference	Sample type	Location	SST (°C)	Equation	n	r <sup>2</sup>	r	SST <sub>error</sub> (°C)
Sun et al. (2005)	<i>Porites</i> sp.	Xisha Island (SCS)	19 – 30	Sr/Ca= 10.24 – 0.053 * SST	60	0.96	-	-
Yu et al. (2005)	<i>Porites lutea</i>	South China Sea	19 – 30	Sr/Ca= 9.85 – 0.042 * SST	134	-	-	0.4
Correge (2006)	<i>Porites</i> sp.	New Caledonia	22 – 28	Sr/Ca= 10.41 – 0.058 * SST	95	0.91	-	-
	Mean of 38 coral equations		18 – 32	Sr/Ca= 10.19 – 0.047 * SST	117	0.85		
Gallup et al. (2006)	<i>Acropora palmata</i>	Dominican Republic Puerto Rico	24 – 31	Sr/Ca= 11.30 – 0.071 * SST	85	0.79	-	-
				Sr/Ca= 11.32 – 0.063 * SST	30	0.62		
Hetzinger et al. (2006)	<i>Diploria strigosa</i>	Guadeloupe	22 – 30	Sr/Ca= 9.99 – 0.041 * SST	440	0.45	-	-
				Sr/Ca= 10.23 – 0.049 * SST		0.68		
				Sr/Ca= 10.90 – 0.074 * SST		0.35		
				Sr/Ca= 10.01 – 0.042 * SST		0.42		
				Sr/Ca= 10.26 – 0.050 * SST		0.62		
				Sr/Ca= 10.70 – 0.066 * SST		0.21		
				Sr/Ca= 9.58 – 0.027 * SST		0.43		
				Sr/Ca= 10.11 – 0.048 * SST		0.61		

Reference	Sample type	Location	SST (°C)	Equation	n	r <sup>2</sup>	r	SST <sub>error</sub> (°C)
Ourbak et al. (2006)	<i>Porites</i> sp.	New Caledonia	21 – 29	Sr/Ca= 10.25 – 0.054 * SST	220	-	-0.80	-
				Sr/Ca= 10.45 – 0.062 * SST				
Pfeiffer et al. (2006)	<i>Porites solida</i>	Peros Banhos Atoll (Indian Ocean)	27 – 29	Sr/Ca= 10.15 – 0.050 * SST	22	-	0.52	-
				Sr/Ca= 10.62 – 0.067 * SST				
				Sr/Ca= 10.33 – 0.056 * SST				
Smith et al. (2006)	<i>Montastrea faveolata</i>	Florida Keys	23 – 30	Sr/Ca= 9.96 – 0.028 * SST	494	-	-0.86	-
Calvo et al. (2007)	<i>Porites</i> sp.	NE Australia	24 – 29	Sr/Ca= 10.11 – 0.045 * SST	37	-	0.96	-
				Sr/Ca= 10.05 – 0.043 * SST				
				Sr/Ca= 10.31 – 0.052 * SST				
				Sr/Ca= 10.43 – 0.057 * SST				
DeLong et al. (2007)	<i>Porites lutea</i>	New Caledonia	21 – 26	Sr/Ca= 10.45 – 0.054 * SST	392	-	0.94	-
Goodkin et al. (2007)	<i>Diploria labyrinthiformis</i>	Bermuda	18 – 29	Sr/Ca= 10.1 – 0.036 * SST	96	0.86	-	-
				Sr/Ca= 10.1 – 0.038 * SST				
				Sr/Ca= 10.3 – 0.044 * SST				

Reference	Sample type	Location	SST (°C)	Equation	n	r <sup>2</sup>	r	SST <sub>error</sub> (°C)
Goodkin et al. (2007)	<i>Diploria labyrinthiformis</i>	Bermuda	18 – 29	Sr/Ca= 10.3 – 0.043 * SST	96	0.76	-	-
				Sr/Ca= 10.4 – 0.048 * SST		0.21		
				Sr/Ca= 11.2 – 0.084 * SST		0.31		
				Sr/Ca= 10.3 – 0.045 * SST		0.15		
				Sr/Ca= 10.7 – 0.053 * SST – 0.0017 * ext		0.68		
				Sr/Ca= 11.4 – 0.091 * SST – 0.0005 * ext		0.36		
				Sr/Ca= 10.4 – 0.050 * SST – 0.0005 * ext		0.18		
				Sr/Ca= 9.4 – 0.0002 * SST – 0.0019 * ext		0.14		
				Sr/Ca= – 0.0007 * IG * SST + 0.003 * AG * SST – 0.074 * SST + 10.8			0.51	
Inoue et al. (2007)	<i>Porites</i> sp.	Lab grown	21 – 29	Sr/Ca= 10.31 – 0.057 * SST	25	-	-0.83	-
Reynaud et al. (2007)	<i>Acropora palmata</i>	Lab grown	21 – 29	Sr/Ca= 0.007 * SST <sup>2</sup> – 0.393 * SST + 14.81	50	0.97	-	-
Alibert and Kinsley (2008)	<i>Porites</i>	Papua New Guinea	27 – 31	Sr/Ca= 0.23 – 0.016 * SST	400	-	-	0.5
				Sr/Ca= 0.17 – 0.014 * SST				
Cahyarini et al. (2008)	<i>Porites</i> sp.	Tahiti	26 – 29	Sr/Ca= 10.52 – 0.063 * SST	240	-	0.86	-
		Timor	28 – 30	Sr/Ca= 9.83 – 0.040 * SST	240		0.68	
Mitsuguchi et al. (2008)	<i>Porites</i> sp.	Con Don Island (Vietnam)	25 – 31	Sr/Ca= 10.11 – 0.045 * SST	43	0.95	-	-

Reference	Sample type	Location	SST (°C)	Equation	n	r <sup>2</sup>	r	SST <sub>error</sub> (°C)		
Saenger et al. (2008)	<i>Montastrea</i> <i>faveolata</i>	St. Croix	26 – 30	Sr/Ca= 11.82 – 0.092 * SST	276	-	-	1.4		
		Bermuda		Sr/Ca= 11.74 – 0.095 * SST						
	<i>Montastrea</i> <i>franski</i>				Sr/Ca= 10.98 – 0.077 * SST					
					Sr/Ca= 11.45 – 0.099 * SST					
					Sr/Ca= 10.60 – 0.075 * SST					
					Sr/Ca= 10.22 – 0.050 * SST					
Cahyarini et al. (2009)	<i>Porites</i>	Tahiti	26 – 29	Sr/Ca= 9.82 – 0.040 * SST	870	-	0.69	-		
				Sr/Ca= 10.14 – 0.050 * SST	1105		0.51			
						Sr/Ca= 10.21 – 0.060 * SST	259		0.73	
						Sr/Ca= 10.05 – 0.050 * SST	259		0.82	
						Sr/Ca= 10.09 – 0.040 * SST	259		0.83	
						Sr/Ca= 10.09 – 0.040 * SST	259		0.88	
						Sr/Ca= 11.18 – 0.080 * SST	259		0.28	
						Sr/Ca= 14.62 – 0.220 * SST	259		0.79	
						Sr/Ca= 10.27 – 0.050 * SST	259		0.21	
						Sr/Ca= 12.82 – 0.150 * SST	259		0.71	
						Sr/Ca= 11.17 – 0.090 * SST	259		0.55	
						Sr/Ca= 10.63 – 0.030 * SST	259		0.46	

Reference	Sample type	Location	SST (°C)	Equation	n	r <sup>2</sup>	r	SST <sub>error</sub> (°C)
Deng et al. (2009)	<i>Porites lutea</i>	Hainan Island (SCS)	21 – 31	$Sr/Ca = 9.82 - 0.043 * SST$	169	-	-	0.3
Nurhati et al. (2009)	<i>Porites</i> sp.	Palmyra Fanning Island Christmas Island	26 – 29	$Sr/Ca = 11.45 - 0.088 * SST$ $Sr/Ca = 10.78 - 0.065 * SST$ $Sr/Ca = 11.12 - 0.079 * SST$	155 225 145	-	-0.71 -0.79 -0.80	
Pfeiffer et al. (2009)	<i>Porites solida</i> <i>Porites lobata</i>	Chagos Archipelago	26 – 30	$Sr/Ca = 10.15 - 0.050 * SST$ $Sr/Ca = 11.08 - 0.083 * SST$ $Sr/Ca = 11.59 - 0.100 * SST$ $Sr/Ca = 10.94 - 0.077 * SST$ $Sr/Ca = 9.70 - 0.035 * SST$ $Sr/Ca = 10.81 - 0.076 * SST$ $Sr/Ca = 10.27 - 0.053 * SST$	620 583 639 1842 620 583 639	-	-0.52 -0.50 -0.68 -0.70 -0.63 -0.81 -0.64	-
DeLong et al. (2010)	<i>Porites</i>	SW Pacific	24 – 29	$Sr/Ca = 10.26 - 0.055 * SST$ $Sr/Ca = 11.37 - 0.089 * SST$	1842 13	-	-0.84 -0.99	-
Kilbourne et al. (2010)	<i>Montastrea</i> <i>faveolata</i>	Puerto Rico	24 – 33	$Sr/Ca = 10.62 - 0.058 * SST$ $Sr/Ca = 11.82 - 0.092 * SST - 0.147 * ext$	960	-	-	1.1

Reference	Sample type	Location	SST (°C)	Equation	n	r <sup>2</sup>	r	SST <sub>error</sub> (°C)
Armistead et al. (2011)	<i>Porites cylindrica</i>	Lab grown	22 – 30	Sr/Ca= 10.21 – 0.064 * SST	37	0.59	-	-
DeLong et al. (2011)	<i>Montastrea faveolata</i>	Florida	19 – 31	Sr/Ca= 9.89 – 0.027 * SST	115	-	-0.93	-
	<i>Siderastrea sidera</i>			Sr/Ca= 10.21 – 0.038 * SST	168		-0.91	
				Sr/Ca= 10.08 – 0.043 * SST	115		-0.97	
				Sr/Ca= 10.20 – 0.047 * SST	168		-0.96	
				Sr/Ca= 10.06 – 0.041 * SST	112		-0.97	
Nurhati et al. (2011)	<i>Porites</i>	Palmyra Island	21 – 32	Sr/Ca= 130.43 – 11.39 * SST	29	-	-0.97	-
Felis et al. (2012)	<i>Porites</i>	Tahiti	20 – 30	Sr/Ca= 10.53 – 0.057 * SST	85	0.69	-	-
Gagan et al. (2012)	<i>Porites</i>	Indo-Pacific	20 – 30	Sr/Ca= 11.28 – 0.084 * SST	-	-	-	0.6
Giry et al. (2012)	<i>Diploria strigosa</i>	Bonaire		Sr/Ca= 10.15 – 0.034 * SST	188	0.52	-	-
Siriananskul et al. (2012)	<i>Porites lutea</i>	Chueak Island (Thailand)	28 – 30	Sr/Ca= 11.83 – 0.098 * SST	65	-	0.96	-
Flannery and Poore (2013)	<i>Montastrea faveolata</i>	Florida	20 – 31	Sr/Ca= 10.21 – 0.039 * SST	645	-	0.97	-

Reference	Sample type	Location	SST (°C)	Equation	<i>n</i>	<i>r</i> <sup>2</sup>	<i>r</i>	SST <sub>error</sub> (°C)
Grove et al. (2013)	<i>Porites lutea</i>	Madagascar	23 – 29	Sr/Ca= 10.30 – 0.051 * SST	520	0.73	-	-
				Sr/Ca= 10.34 – 0.052 * SST		0.74		
				Sr/Ca= 9.95 – 0.045 * SST		0.72		
				Sr/Ca= 9.96 – 0.045 * SST		0.71		
				Sr/Ca= 10.13 – 0.048 * SST		0.82		
				Sr/Ca= 10.15 – 0.048 * SST		0.82		
				Sr/Ca= 8.62 – 0.013 * SST		0.01		
				Sr/Ca= 9.02 – 0.002 * SST		0.00		
				Sr/Ca= 10.25 – 0.056 * SST		0.19		
				Sr/Ca= 9.56 – 0.030 * SST		0.05		
				Sr/Ca= 9.43 – 0.022 * SST		0.06		
				Sr/Ca= 9.29 – 0.016 * SST		0.03		
				Sr/Ca= 10.64 – 0.064 * SST		0.91		
				Sr/Ca= 10.66 – 0.064 * SST		0.92		
				Sr/Ca= 10.20 – 0.055 * SST		0.92		
				Sr/Ca= 10.21 – 0.055 * SST		0.91		
				Sr/Ca= 10.38 – 0.057 * SST		0.96		
				Sr/Ca= 10.39 – 0.058 * SST		0.96		

Reference	Sample type	Location	SST (°C)	Equation	n	r <sup>2</sup>	r	SST <sub>error</sub> (°C)
Seo et al. (2013)	<i>Diploastrea speciose</i>	Japan	13 – 27	Sr/Ca = 10.18 – 0.041 * SST	38	0.97	-	-
Bolton et al. (2014)	<i>Porites</i>	Vietnam	26 – 30	Sr/Ca = 10.63 – 0.057 * SST	403	0.68	-	-
				Sr/Ca = 10.53 – 0.054 * SST	273	0.70		
				Sr/Ca = 10.57 – 0.055 * SST	407	0.75		
				Sr/Ca = 9.91 – 0.031 * SST	34	0.12		
				Sr/Ca = 10.50 – 0.052 * SST	68	0.77		
				Sr/Ca = 10.47 – 0.051 * SST	24	0.90		
Carilli et al. (2014)	<i>Porites</i>	Gilbert Islands	28 – 30	Sr/Ca = 135.3 – 11.90 * SST	240	-	0.68	-
DeLong et al. (2014)	<i>Siderastrea siderea</i>	Florida	19 – 31	Sr/Ca = 10.11 – 0.043 * SST	90	-	-0.95	-
Siriananskul and Pumijsunong (2014)	<i>Porites</i> sp.	Chang Island (Thailand)	26 – 29	Sr/Ca = 11.56 – 0.070 * SST	24	-	0.89	-
				Sr/Ca = 11.89 – 0.081 * SST	34		0.87	
Xu et al. (2015)	<i>Diploria strigosa</i>	Anegada (British Virgin Islands)	21 – 31	Sr/Ca <sub>anomaly</sub> = 0.046 – 0.16 * SST	688	-	-	0.0004
				Sr/Ca <sub>anomaly</sub> = 0.059 – 0.12 * SST				0.0012
				Sr/Ca <sub>anomaly</sub> = 0.063 – 0.095 * SST				0.004



Reference	Sample type	Location	SST (°C)	Equation	n	r <sup>2</sup>	r	SST <sub>error</sub> (°C)
Alpert et al. (2016)	<i>Porites lobata</i>	Jarvis Island	23 – 26	Sr/Ca= 11.60 – 0.090 * SST	95	-	-0.84	-
				Sr/Ca= 10.00 – 0.030 * SST	65		-0.58	
				Sr/Ca= 10.60 – 0.060 * SST	78		-0.70	
				Sr/Ca= 11.60 – 0.090 * SST	78		-0.81	
				Sr/Ca= 11.70 – 0.090 * SST	98		-0.72	
				Sr/Ca= 9.90 – 0.030 * SST	65		-0.47	
				Sr/Ca= 10.70 – 0.060 * SST	98		-0.69	
Sadler et al. (2016)	<i>Acropora</i>	Great Barrier Reef	22 – 31	Sr/Ca <sub>anomaly</sub> = -0.051 * SST <sub>anomaly</sub>	154	0.63	-	-
				Sr/Ca <sub>anomaly</sub> = -0.042 * SST <sub>anomaly</sub>	100	0.73		
				Sr/Ca <sub>anomaly</sub> = -0.048 * SST <sub>anomaly</sub>	254	0.65		
				Sr/Ca <sub>annual mean</sub> = -0.021 * SST <sub>annual mean</sub> + 20.16	254	0.14		
				Sr/Ca <sub>annual mean</sub> = -0.021 * SST <sub>annual mean</sub> + 20.16	254	0.14		
von Reumont et al. (2016)	<i>Diploria strigosa</i>	Little Cayman	24 – 32	Sr/Ca= 9.42 – 0.019 * SST	1218	0.45	-	-
				Sr/Ca= 9.50 – 0.021 * SST	0.69			
				Sr/Ca= 8.82 + 0.003 * SST	0.00			
				Sr/Ca= 10.24 – 0.040 * SST	0.49			
					0.66			

Reference	Sample type	Location	SST (°C)	Equation	<i>n</i>	<i>r</i> <sup>2</sup>	<i>r</i>	SST <sub>error</sub> (°C)
von Reumont et al. (2016)	<i>Diploria strigosa</i>	Little Cayman	24 – 32	Sr/Ca= 10.16 – 0.037 * SST	1218	0.03	-	-
Alpert et al. (2017)	<i>Porites</i> , <i>Orbicella</i> , <i>Siderastrea</i> , <i>Diploria</i> , <i>Pocillopora</i>	Caracao, Bermuda, Jarvis Island, Red Sea, Palmyra Atoll, Palau, Panama, Puerto Rico, St Croix, Yucatan	23 – 30	Sr/Ca= 12.42 – 0.124 * SST	19	0.63	-	-
Kuffner et al. (2017)	<i>Siderastrea sidera</i>	Florida Keys	20 – 31	Sr/Ca= 10.17 – 0.043 * SST	804	-	-	3.1
Ramos et al. (2017)	<i>Diploastrea helipora</i> <i>Porites</i>	Luzon	27 – 29	Sr/Ca= 10.66 – 0.057 * SST Sr/Ca= 10.79 – 0.068 * SST	365 365	0.74 0.84	-	-
Flannery et al. (2018)	<i>Orbicella faveolata</i>	Florida	19 – 31	Sr/Ca= 10.46 – 0.049 * SST	847	0.76	-	-

Reference	Sample type	Location	SST (°C)	Equation	<i>n</i>	<i>r</i> <sup>2</sup>	<i>r</i>	SST <sub>error</sub> (°C)
Murty et al. (2018)	<i>Porites</i> spp.	Red Sea	25 – 31	Sr/Ca= 10.60 – 0.054 * SST	387	0.84	-	-
				Sr/Ca= 10.63 – 0.053 * SST	461	0.69		
				Sr/Ca= 10.08 – 0.037 * SST	566	0.79		
				Sr/Ca= 10.47 – 0.049 * SST	552	0.83		
				Sr/Ca= 10.15 – 0.042 * SST	114	0.80		
				Sr/Ca= 10.61 – 0.055 * SST	829	0.72		
				Sr/Ca= 11.22 – 0.083 * SST	97	0.62		
				Sr/Ca= 11.16 – 0.074 * SST	97	0.73		
				Sr/Ca= 11.03 – 0.068 * SST	98	0.53		

Sr/Ca in mmol/mol

K= distribution coefficient

ext= linear extension/growth rate in mm/year

IG= interannual growth rate in mm/year

AG= annual growth rate in mm/year

**Supplementary Table 2.2.** Mg/Ca geothermometers.

Reference	Sample type	Location	SST range (°C)	Equation	n	r <sup>2</sup>	r	SST <sub>error</sub> (°C)
Mitsuguchi et al. (1996)	<i>Porites lutea</i>	Japan	20 – 30	Mg/Ca= 1.15 + 0.129 * SST	112	-	-	0.5
(modified in 2001)				Mg/Ca= 0.85 + 0.129 * SST				
Sinclair et al. (1998)	<i>Porites myeri</i>	Great Barrier Reef	22 – 29	Mg/Ca= 0.0 + 0.16 * SST	36	0.79	-	-
Fallon et al. (1999)	<i>Porites lobata</i>	Japan	14 – 28	Mg/Ca= 1.38 + 0.088 * SST	425	-	0.66	-
Wei et al. (2000)	<i>Porites</i> sp.	South China Sea	19 – 31	Mg/Ca= -14.13 + 8.846 * SST	120	-	0.97	-
Watanabe et al. (2001)	<i>Montastrea faveolata</i>	Puerto Rico	24 – 33	Mg/Ca= -3.24 + 0.280 * SST	70	-	0.92	-
Quinn and Sampson (2002)	<i>Porites lutea</i>	New Caledonia	20 – 27	Mg/Ca= 2.64 + 0.105 * SST	182	0.61	-	-
				Mg/Ca= 1.96 + 0.133 * SST	182	0.61		
				Mg/Ca= 1.94 + 0.125 * SST	266	0.55		
				Mg/Ca= 0.87 + 0.168 * SST	266	0.55		
Fallon et al. (2003)	<i>Porites</i>	Great Barrier Reef	22 – 30	Mg/Ca= 0.10 + 0.116 * SST	72	-	0.66	-
				Mg/Ca= -0.60 + 0.116 * SST	108		0.80	
				Mg/Ca= 0.10 + 0.112 * SST	48		0.73	

Reference	Sample type	Location	SST range (°C)	Equation	n	r <sup>2</sup>	r	SST <sub>error</sub> (°C)
				Mg/Ca= 0.13 + 0.089 * SST	84		0.47	
				Mg/Ca= 0.70 + 0.132 * SST	84		0.65	
				Mg/Ca= 3.73 + 0.007 * SST	108		0.04	
				Mg/Ca= 0.76 + 0.116 * SST	36		0.73	
Yu et al. (2005)	<i>Porites lutea</i>	South China Sea	19 – 30	Mg/Ca= 1.32 + 0.110 * SST	134	-	-	0.4
Ourbak et al. (2006)	<i>Porites</i>	New Caledonia	20 – 29	Mg/Ca= 0.14 + 0.218 * SST	220	-	0.81	-
Reynaud et al. (2007)	<i>Acropora palmata</i>	Lab grown	21 – 29	Mg/Ca= 0.90 + 0.138 * SST	50	0.98	-	-
Armud et al. (2011)	<i>Porites cylindrica</i>	Lab grown	22 – 30	Mg/Ca= 1.97 + 0.100 * SST	37	0.67	-	-
Siriananskul et al. (2012)	<i>Porites lutea</i>	Chueak Island (Thailand)	28 – 30	Mg/Ca= -1.72 + 0.0193 * SST	65	-	0.97	-
Hathorne et al. (2013)	<i>Porites</i>	Japan, Tahiti	18 – 29	Mg/Ca= 3.16 + 0.050 * SST	150	0.26	-	-

Mg/Ca in mmol/mol

**Supplementary Table 2.3.** U/Ca geothermometers

References	Sample type	Location	SST range (°C)	Equation	<i>n</i>	<i>r</i> <sup>2</sup>	<i>r</i>	SST <sub>error</sub> (°C)
Min et al. (1995)	<i>Porites</i>	New Caledonia, Tahiti	20 – 26	U/Ca= 2.23 – 0.047 * SST U/Ca= 2.27 – 0.047 * SST U/Ca= 2.11 – 0.043 * SST U/Ca= 2.45 – 0.054 * SST	52	-	-	0.5 – 1
Sinclair et al. (1998)	<i>Porites myeri</i>	Great Barrier Reef	22 – 29	U/Ca= 2.24 – 0.046 * SST	36	0.83	-	-
Fallon et al. (1999)	<i>Porites lobata</i>	Japan	14 – 28	U/Ca= 2.26 – 0.044 * SST	168	-	-0.84	-
Wei et al. (2000)	<i>Porites</i> sp.	South China Sea	19 – 31	U/Ca= 81.15 – 48.14 * SST	120	-	0.85	-
Quinn and Sampson (2002)	<i>Porites lutea</i>	New Caledonia	20 – 27	U/Ca= 1.85 – 0.029 * SST U/Ca= 2.19 – 0.044 * SST U/Ca= 1.95 – 0.032 * SST U/Ca= 2.31 – 0.046 * SST	200 200 284 284	0.44 0.44 0.47 0.47	- - - -	- - - -

References	Sample type	Location	SST range (°C)	Equation	n	r <sup>2</sup>	r	SST <sub>error</sub> (°C)
Fallon et al. (2003)	<i>Porites</i>	Great Barrier Reef	22 – 30	U/Ca= 2.17e-3 – 2.940e-5 * SST	72	-	-0.53	-
				U/Ca= 2.36e-3 – 4.310e-5 * SST	108		-0.79	
				U/Ca= 2.00e-3 – 3.510e-5 * SST	48		-0.78	
				U/Ca= 1.81e-3 – 2.860e-5 * SST	84		-0.6	
				U/Ca= 2.02e-3 – 3.980e-5 * SST	84		-0.78	
				U/Ca= 1.46e-3 – 1.469e-5 * SST	108		-0.37	
				U/Ca= 2.03e-3 – 3.640e-5 * SST	36		-0.79	
Ourbak et al. (2006)	<i>Porites</i>	New Caledonia	20 – 29	U/Ca= 1.93 – 0.033 * SST	220	-	-0.84	-
Felis et al. (2009)	<i>Porites</i>	Japan	22 – 25	U/Ca= 2.06 – 0.034 * SST	2640	0.68	-	-
Armistead et al. (2011)	<i>Porites cylindrica</i>	Lab grown	22 – 30	U/Ca= 1.49 – 0.021 * SST	37	0.78	-	-

U/Ca in μmol/mol

Supplementary Table 2.4. Sr-U geothermometers

Reference	Species	Location	SST range (°C)	Equation	<i>n</i>	<i>r</i> <sup>2</sup>	
DeCarlo et al. (2016)	<i>Porites</i> sp.	Red Sea, Palmyra	26 – 30	$T = -11 * (Sr-U-9) + 28.1$	14	0.93	
		Atoll, Jarvis		$T = -10 * (Sr-U_{parallel}^{-7.7}) + 28.8$		0.91	
Alpert et al. (2017)	<i>Porites</i> , <i>Orbicella</i> , <i>Siderastrea</i> , <i>Diploria</i> , <i>Pocillopora</i>	Island, Palau					
		Island					
		Caracao,	23 – 30	$T = -11 * (Sr-U) + 126.98$	19	0.91	
		Bermuda, Jarvis					
		Island, Red Sea,					
		Palmyra Atoll,					
		Palau Island,					
Panama, Puerto Rico, St Croix, Yucatan							



Supplementary Table 2.5. Li/Ca geothermometers.

Reference	Sample type	Location	SST range (°C)	Equation	n	r <sup>2</sup>
Marriott et al. (2004)	<i>Porites</i>	Jarvis Island	5 – 30	$0.01e^{0.049SST}$	14	-
			25 – 30			
Hathorne et al. (2013)	<i>Porites</i>	Japan, Tahiti	18 – 29	$9.97 - 0.12 * SST$	150	0.73
				$14.4 - 0.31 * SST$		0.45
				$4.30 - 0.10 * SST$		0.32
				$14.0 - 0.28 * SST$		0.68

Li/Ca in  $\mu\text{mol/mol}$

Supplementary Table 2.6. Li/Mg and Mg/Li geothermometers

Reference	Sample type	Location	SST range (°C)	Equation	<i>n</i>	<i>r</i> <sup>2</sup>
Hathorne et al. (2013)	<i>Porites</i>	Japan,	18 – 29	$\text{Li/Mg} = 2.76 - 0.05 * \text{SST}$	150	0.67
		Tahiti		$\text{Li/Mg} = 2.96 - 0.06 * \text{SST}$		0.64
				$\text{Mg/Li} = 0.19 + 0.18 * \text{SST}$		0.69
Fowell et al. (2016)	<i>Siderastrea siderea</i>	Belize	26 – 31	$\text{Mg/Li} = -0.40 + 0.04 * \text{SST}$		0.32
				$\text{Mg/Li} = -0.19 + 0.04 * \text{SST}$		0.65
				$\text{Li/Mg} = -0.10 * \text{SST} + 3.962$	26	0.71
	Multiple species	Globally	0 – 31	$\text{Li/Mg} = -0.03 * \text{SST} + 2.458$	30	0.40
				$\text{Li/Mg} = 5.405e^{-0.05\text{SST}}$	305	0.95

Li/Mg in mmol/mol

Mg/Li in mol/mmol

**Supplementary Table 2.7.** Ba/Ca geothermometers.

Reference	Sample type	Location	SST range (°C)	Equation	<i>n</i>	<i>r</i> <sup>2</sup>
Gonneea et al. (2017)	<i>Favia fragum</i>	Lab grown	22 – 28	$K(\text{Ba}/\text{Ca}) = 2.51 - 0.029 * \text{SST}$	100	-

Ba/Ca in mmol/mol

Supplementary Table 2.8. B<sup>11</sup>/Ca geothermometers.

Reference	Sample type	Location	SST range (°C)	Equation	n	r <sup>2</sup>	r
Sinclair et al. (1998)	<i>Porites myeri</i>	Great Barrier Reef	22 – 29	B <sup>11</sup> /Ca = 1000 – 20.60 * SST	36	0.91	-
Fallon et al. (1999)	<i>Porites lobata</i>	Japan	14 – 28	B <sup>11</sup> /Ca = 767 – 9.00 * SST	425	-	-0.74
Fallon et al. (2003)	<i>Porites</i>	Great Barrier Reef	22 – 30	B <sup>11</sup> /Ca = 5328 – 44.36 * SST	72	-	-0.37
				B <sup>11</sup> /Ca = 9093 – 17.07 * SST	108		-0.80
				B <sup>11</sup> /Ca = 8190 – 14.57 * SST	48		-0.79
				B <sup>11</sup> /Ca = 9247 – 10.85 * SST	84		-0.79
				B <sup>11</sup> /Ca = 1098 – 26.09 * SST	84		-0.89
				B <sup>11</sup> /Ca = 8952 – 16.50 * SST	108		-0.87
				B <sup>11</sup> /Ca = 7880 – 12.80 * SST	36		-0.83

B<sup>11</sup>/Ca in μmol/mol

**Table 3.1.** Subsamples collected from ER#30-C. Distance measured from the base of the coral upwards. Calculated temperatures are determined from the Cayman geothermometer,  $\delta^{18}\text{O}_{\text{water}}$  value of +0.8‰.

Subsample	Distance (cm)	$\delta^{13}\text{C}_{\text{VPDB}}$ (‰)	$\delta^{18}\text{O}_{\text{VPDB}}$ (‰)	$\delta^{18}\text{O}_{\text{VSMOW}}$ (‰)	Calculated Temperature (°C)
ER#30 a	0.4	-0.85	-3.83	+27.0	29.8
ER#30 b	0.6	-1.85	-2.96	+27.5	27.3
ER#30 c	0.8	-1.54	-2.79	+27.6	26.5
ER#30 d	1.0	-1.46	-3.59	+27.2	28.6
ER#30 e	1.2	-1.53	-3.00	+27.8	25.7
ER#30 f	1.4	-0.70	-3.60	+27.2	28.6
ER#30 g	1.6	-0.44	-3.17	+27.3	28.4
ER#30 h	1.8	-0.31	-3.65	+26.8	30.7
ER#30 i	2.0	-0.89	-3.64	+26.8	30.7
ER#30 j	2.3	-0.72	-3.72	+26.7	31.1
ER#30 k	2.5	-0.46	-3.69	+26.7	30.9
ER#30 l	2.7	-0.14	-3.58	+26.8	30.4
ER#30 m	3.0	-0.65	-3.63	+26.8	30.6
ER#30 n	3.3	-0.36	-3.45	+27.0	29.7
ER#30 o	3.6	-0.51	-3.48	+26.9	29.9
ER#30 p	3.9	-0.60	-3.66	+26.8	30.8
ER#30 q	4.1	-0.01	-3.58	+26.8	30.4
ER#30 r	4.5	-0.27	-3.56	+26.8	30.3
ER#30 s	4.8	-0.50	-3.38	+27.0	29.4
ER#30 t	5.0	-0.66	-4.05	+26.3	32.7
ER#30 u	5.3	-0.77	-3.85	+26.6	31.7
ER#30 v	5.5	-1.34	-3.74	+26.7	31.2

Subsample	Distance (cm)	$\delta^{13}\text{C}_{\text{VPDB}}$ (‰)	$\delta^{18}\text{O}_{\text{VPDB}}$ (‰)	$\delta^{18}\text{O}_{\text{VSMOW}}$ (‰)	Calculated Temperature (°C)
ER#30 w	5.7	-0.63	-3.54	+26.9	30.2
ER#30 x	6.0	-0.35	-3.23	+27.2	28.6
ER#30 y	6.2	-1.38	-4.49	+26.3	33.0
ER#30 z	6.5	-0.96	-2.94	+27.5	27.2
ER#30 aa	6.9	-1.35	-3.11	+27.3	28.1
ER#30 ab	7.2	-1.59	-3.05	+27.4	27.8
ER#30 ac	7.5	-0.95	-3.46	+27.0	29.8
ER#30 ad	7.7	-1.02	-2.94	+27.5	27.2
ER#30 ae	7.9	-1.14	-3.14	+27.3	28.2
ER#30 af	8.1	-1.87	-3.26	+27.2	28.8
ER#30 ag	8.4	-1.69	-3.25	+27.2	28.8
ER#30 ah	8.6	-1.64	-2.66	+27.8	25.9
ER#30 ai	9.0	-1.68	-2.94	+27.5	27.2
ER#30 aj	9.4	-1.86	-3.12	+27.3	28.1
ER#30 ak	9.7	-2.44	-3.41	+27.0	29.5
ER#30 al	10.1	-2.56	-3.04	+27.4	27.7
ER#30 am	10.5	-1.83	-3.22	+27.2	28.6
ER#30 an	10.8	-1.59	-2.83	+27.6	26.7
ER#30 ao	11.2	-1.51	-2.55	+27.9	25.3
ER#30 ap	11.5	-1.96	-2.89	+27.5	27.0
ER#30 aq	11.9	-2.19	-2.68	+27.8	26.0
ER#30 ar	12.2	-2.41	-2.66	+27.8	25.9
ER#30 as	12.4	-2.42	-2.81	+27.6	26.6
ER#30 at	12.6	-2.47	-3.75	+26.7	31.2
ER#30 au	12.9	-2.10	-2.77	+27.7	26.4

Subsample	Distance (cm)	$\delta^{13}\text{C}_{\text{VPDB}}$ (‰)	$\delta^{18}\text{O}_{\text{VPDB}}$ (‰)	$\delta^{18}\text{O}_{\text{VSMOW}}$ (‰)	Calculated Temperature (°C)
ER#30 av	13.2	-2.67	-3.24	+27.2	28.7
ER#30 aw	13.4	-2.29	-2.82	+27.6	26.6
ER#30 ax	13.6	-2.64	-3.51	+26.9	30.1
ER#30 ay	14.1	-2.13	-3.02	+27.4	27.6
ER#30 az	14.5	-1.86	-2.80	+27.6	26.5
ER#30 bb	14.8	-1.90	-2.59	+27.9	25.5
ER#30 bc	15.2	-1.11	-3.32	+27.1	29.1
ER#30 bd	15.6	-1.36	-2.93	+27.5	27.2
ER#30 be	15.9	-1.90	-2.48	+28.0	25.0
ER#30 bf	16.1	-1.93	-2.79	+27.6	26.5
ER#30 bg	16.5	-1.86	-2.54	+27.9	25.3
ER#30 bh	17.0	-1.92	-2.59	+27.9	25.5
ER#30 bi	17.5	-2.65	-3.17	+27.3	28.3
ER#30 bj	17.9	-2.29	-2.47	+28.0	24.9
ER#30 bk	18.1	-2.63	-2.69	+27.7	26.0
ER#30 bl	18.4	-3.00	-3.00	+27.4	27.6

**Table 3.2.** Subsamples collected from CB1-A. Distance measured from the base of the coral upwards. Calculated temperatures are determined from the Cayman geothermometer,  $\delta^{18}\text{O}_{\text{water}}$  value of 0.0‰.

Subsample	Distance (cm)	$\delta^{13}\text{C}_{\text{VPDB}}$ (‰)	$\delta^{18}\text{O}_{\text{VPDB}}$ (‰)	$\delta^{18}\text{O}_{\text{VSMOW}}$ (‰)	Calculated Temperature (°C)
CB1 a	0.5	+0.13	-3.44	+27.0	25.8
CB1 b	1.0	-0.22	-4.05	+26.3	28.8
CB1 c	1.3	+0.16	-3.75	+26.7	27.3
CB1 d	1.9	+0.40	-3.50	+26.9	26.1
CB1 e	2.2	-1.27	-3.75	+26.7	27.3
CB1 f	2.4	-0.10	-3.47	+26.9	26.0
CB1 g	2.8	-0.30	-3.64	+26.8	26.8
CB1 h	3.2	-1.41	-3.57	+26.8	26.5
CB1 i	3.5	-0.34	-3.55	+26.9	26.4
CB1 j	4.1	-0.42	-4.01	+26.4	28.7
CB1 k	4.5	-0.22	-3.42	+27.0	25.7
CB1 l	4.9	-1.23	-4.18	+26.2	29.5
CB1 m	5.5	-0.43	-3.83	+26.6	27.7
CB1 n	5.9	+0.47	-3.86	+26.5	27.9
CB1 o	6.3	-0.80	-3.93	+26.5	28.3
CB1 p	6.7	-0.77	-4.21	+26.2	29.6
CB1 q	7.0	-0.79	-4.15	+26.2	29.3
CB1 r	7.3	-1.42	-3.97	+26.4	28.4
CB1 s	7.7	+0.58	-3.62	+26.8	26.7
CB1 t	8.0	-0.28	-3.67	+26.7	27.0
CB1 u	8.4	+0.17	-3.68	+26.7	27.0
CB1 v	9.0	-0.13	-3.72	+26.7	27.2



Subsample	Distance (cm)	$\delta^{13}\text{C}_{\text{VPDB}}$ (‰)	$\delta^{18}\text{O}_{\text{VPDB}}$ (‰)	$\delta^{18}\text{O}_{\text{VSMOW}}$ (‰)	Calculated Temperature (°C)
CB1 w	9.4	-1.00	-3.96	+26.4	28.4
CB1 x	9.8	+0.05	-3.70	+26.7	27.1
CB1 y	10.0	+0.25	-3.36	+27.1	25.4
CB1 z	10.3	+0.44	-3.30	+27.1	25.1
CB1 aa	10.9	-1.03	-3.62	+26.8	26.7
CB1 ab	11.5	+0.60	-3.16	+27.3	24.5
CB1 ac	12.0	-1.20	-3.91	+26.5	28.1
CB1 ad	12.3	-0.69	-3.49	+26.9	26.1
CB1 ae	12.6	-0.83	-4.23	+26.2	29.7
CB1 af	12.9	-0.18	-3.69	+26.7	27.1
CB1 ag	13.4	-0.60	-3.86	+26.5	27.9
CB1 ah	13.9	-0.14	-3.82	+26.6	27.7
CB1 ai	14.25	-0.28	-3.51	+26.9	26.2
CB1 aj	14.6	+0.46	-4.19	+26.2	29.5
CB1 ak	14.9	-0.83	-4.10	+26.3	29.1
CB1 al	15.3	-0.68	-4.03	+26.4	28.7
CB1 am	15.75	-1.25	-4.15	+26.2	29.3
CB1 an	16.2	-0.33	-3.92	+26.5	28.2
CB1 ao	16.7	0.00	-3.35	+27.1	25.4
CB1 ap	17.2	-0.27	-4.13	+26.3	29.2
CB1 aq	17.7	-1.20	-4.18	+26.2	29.5
CB1 ar	18.0	-0.05	-3.30	+27.1	25.2
CB1 as	18.3	-1.60	-4.43	+26.0	30.7
CB1 at	18.7	-1.60	-4.04	+26.4	28.8
CB1 au	19.0	-0.27	-3.73	+26.7	27.2

Subsample	Distance (cm)	$\delta^{13}\text{C}_{\text{VPDB}}$ (‰)	$\delta^{18}\text{O}_{\text{VPDB}}$ (‰)	$\delta^{18}\text{O}_{\text{VSMOW}}$ (‰)	Calculated Temperature (°C)
CB1 av	19.3	-0.58	-3.85	+26.6	27.9
CB1 aw	19.7	-0.55	-4.17	+26.2	29.4
CB1 ax	20.2	-0.89	-3.92	+26.5	28.2
CB1 ay	20.6	-0.35	-3.61	+26.8	26.7
CB1 az	20.8	+0.18	-3.59	+26.8	26.6
CB1 ba	21.2	+0.14	-3.40	+27.0	25.6
CB1 bb	21.4	+0.36	-3.47	+26.9	26.0
CB1 bc	21.8	+0.02	-3.36	+27.1	25.4
CB1 bd	22.5	+0.82	-3.35	+27.1	25.4
CB1 be	23.0	+0.47	-3.25	+27.2	24.9
CB1 bf	23.5	-0.18	-3.67	+26.7	27.0
CB1 bg	23.8	-0.37	-3.63	+26.8	26.8
CB1 bh	24.0	-0.37	-4.20	+26.2	29.6
CB1 bi	24.3	+0.83	-3.24	+27.2	24.9
CB1 bj	24.8	+0.98	-3.17	+27.3	24.5
CB1 bk	25.3	+0.80	-3.27	+27.2	25.0
CB1 bl	25.8	-0.04	-3.53	+26.9	26.3
CB1 bm	26.4	+0.74	-3.21	+27.2	24.7
CB1 bn	27.0	-0.37	-3.51	+26.9	26.2
CB1 bo	27.5	-0.25	-3.84	+26.6	27.8
CB1 bp	28.1	-0.01	-3.36	+27.1	25.4
CB1 bq	28.6	+0.35	-3.43	+27.0	25.8
CB1 br	29.1	+0.22	-3.42	+27.0	25.7
CB1 bs	29.5	-1.28	-4.33	+26.1	30.2
CB1 bt	29.9	+0.77	-3.56	+26.8	26.4

Subsample	Distance (cm)	$\delta^{13}\text{C}_{\text{VPDB}}$ (‰)	$\delta^{18}\text{O}_{\text{VPDB}}$ (‰)	$\delta^{18}\text{O}_{\text{VSMOW}}$ (‰)	Calculated Temperature (°C)
CB1 bu	30.5	-0.06	-3.84	+26.6	27.8
CB1 bv	30.9	+0.57	-3.98	+26.4	28.5
CB1 bw	31.2	+0.33	-3.65	+26.8	26.9
CB1 bx	31.4	-0.31	-3.87	+26.5	28.0
CB1 by	31.7	-0.07	-4.07	+26.3	28.9
CB1 bz	32.0	-0.05	-3.97	+26.4	28.4
CB1 ca	32.3	+0.64	-3.78	+26.6	27.5
CB1 cb	32.8	+0.52	-3.57	+26.8	26.4
CB1 cc	33.3	-0.24	-4.06	+26.3	28.9
CB1 cd	33.8	+0.60	-3.35	+27.1	25.4
CB1 ce	34.5	+0.71	-3.47	+26.9	26.0
CB1 cf	34.9	+0.60	-3.47	+26.9	26.0
CB1 cg	35.3	+0.17	-3.69	+26.7	27.0
CB1 ch	35.6	+0.23	-3.81	+26.6	27.6
CB1 ci	35.9	+0.31	-3.34	+27.1	25.3
CB1 cj	36.4	+0.58	-3.41	+27.0	25.7
CB1 ck	36.8	-0.16	-3.58	+26.8	26.5
CB1 cl	37.4	+0.12	-3.49	+26.9	26.1
CB1 cm	38.1	-0.34	-4.06	+26.3	28.9
CB1 cn	38.6	+0.57	-3.22	+27.2	24.8
CB1 co	39.0	+0.17	-3.46	+27.0	25.9
CB1 cp	39.4	-0.36	-4.05	+26.3	28.8
CB1 cq	39.7	+0.89	-3.26	+27.2	24.9
CB1 cr	40.1	+1.99	-2.65	+27.8	22.0

Subsample	Distance (cm)	$\delta^{13}\text{C}_{\text{VPDB}}$ (‰)	$\delta^{18}\text{O}_{\text{VPDB}}$ (‰)	$\delta^{18}\text{O}_{\text{VSMOW}}$ (‰)	Calculated Temperature (°C)
CB1 cs	40.4	-0.38	-3.76	+26.6	27.4
CB1 ct	40.8	+0.74	-3.18	+27.2	24.5
CB1 cu	41.1	+0.56	-3.46	+27.0	25.9
CB1 cv	41.4	+1.00	-3.31	+27.1	25.2
CB1 cw	41.8	-0.64	-3.91	+26.5	28.1
CB1 cx	42.2	+0.76	-3.02	+27.4	23.8
CB1 cy	42.7	-0.38	-3.48	+26.9	26.1
CB1 cz	43.3	-0.30	-3.69	+26.7	27.1
CB1 da	44.4	-1.46	-3.70	+26.7	27.1
CB1 db	45.2	-0.41	-4.36	+26.0	30.4
CB1 dc	45.5	+0.20	-4.53	+25.8	31.2
CB1 de	46.2	+0.66	-4.14	+26.3	29.2
CB1 df	46.6	+0.54	-4.40	+26.0	30.6
CB1 dg	47.2	+1.00	-4.25	+26.1	29.8
CB1 dh	47.7	+1.32	-4.29	+26.1	30.0
CB1 di	47.9	+0.68	-4.39	+26.0	30.5
CB1 dj	48.2	+0.45	-4.15	+26.2	29.3
CB1 dk	48.7	+0.37	-4.48	+25.9	30.9
CB1 dl	49.0	-0.27	-4.33	+26.1	30.2
CB1 dm	49.3	-0.10	-4.40	+26.0	30.5
CB1 dn	49.6	-0.14	-4.51	+25.9	31.1
CB1 do	49.9	-0.82	-4.59	+25.8	31.5

**Table 3.3.** Subsamples collected from ER#32-A. Distance measured from the base of the coral upwards. Calculated temperatures are determined from the Cayman geothermometer,  $\delta^{18}\text{O}_{\text{water}}$  value of +0.8‰.

Subsample	Distance (cm)	$\delta^{13}\text{C}_{\text{VPDB}}$ (‰)	$\delta^{18}\text{O}_{\text{VPDB}}$ (‰)	$\delta^{18}\text{O}_{\text{VSMOW}}$ (‰)	Calculated Temperature (°C)
Left branch					
ER#32 a	5.1	-0.52	-4.22	+26.6	31.7
ER#32 b	5.5	-1.14	-2.93	+27.5	27.2
ER#32 c	5.7	-1.15	-3.39	+27.0	29.5
ER#32 D1	6.0	-1.36	-3.16	+27.3	28.3
ER#32 1	6.2	-2.06	-3.69	+26.7	30.9
ER#32 d	7.0	-1.99	-3.80	+26.6	31.5
ER#32 e	7.2	-1.47	-3.66	+26.7	30.8
ER#32 f	7.5	-1.50	-3.74	+26.7	31.2
ER#32 g	7.7	-1.26	-3.47	+26.9	29.8
ER#32 D2	8.2	-1.85	-3.33	+27.1	29.1
ER#32 h	8.5	-1.49	-3.52	+26.9	30.1
ER#32 i	9.0	-1.58	-4.14	+26.3	33.1
ER#32 j	9.4	-1.69	-3.71	+26.7	31.0
ER#32 2	9.7	-1.88	-3.58	+26.8	30.4
ER#32 k	10.1	-2.10	-3.81	+26.6	31.5
ER#32 l	10.3	-1.74	-3.80	+26.6	31.4
ER#32 m	10.6	-2.44	-3.95	+26.4	32.2
ER#32 n	10.9	-1.71	-3.60	+26.8	30.5
ER#32 D3	11.5	-0.85	-3.02	+27.4	27.6
ER#32 o	11.6	-2.04	-3.75	+26.7	31.2
ER#32 p	12.0	-2.17	-3.81	+26.6	31.5

Subsample	Distance (cm)	$\delta^{13}\text{C}_{\text{VPDB}}$ (‰)	$\delta^{18}\text{O}_{\text{VPDB}}$ (‰)	$\delta^{18}\text{O}_{\text{VSMOW}}$ (‰)	Calculated Temperature (°C)
ER#32 3	12.3	-1.72	-3.46	+27.0	29.8
ER#32 q	12.8	-1.80	-3.71	+26.7	31.0
ER#32 r	13.0	-1.61	-3.24	+27.2	28.7
ER#32 s	13.4	-2.59	-3.94	+26.5	32.2
ER#32 t	13.6	-2.72	-3.68	+26.7	30.9
ER#32 u	13.8	-1.78	-3.03	+27.4	27.7
ER#32 v	14.3	-1.78	-3.32	+27.1	29.1
ER#32 w	14.6	-1.45	-3.72	+26.7	31.1
ER#32 x	14.8	-2.32	-4.54	+26.2	33.2
ER#32 y	15.0	-2.69	-4.92	+25.8	35.1
ER#32 z	15.3	-2.10	-4.06	+26.3	32.7
ER#32 aa	15.6	-1.77	-3.90	+26.5	32.0
ER#32 ab	15.9	-2.59	-4.50	+25.9	34.9
ER#32 ac	16.1	-2.71	-4.40	+26.0	34.4
ER#32 ad	16.4	-1.77	-4.03	+26.4	32.6
ER#32 ae	16.8	-2.37	-3.57	+26.8	30.3
ER#32 af	17.1	-1.35	-3.60	+26.8	30.5
ER#32 ag	17.3	-1.74	-3.52	+26.9	30.1
ER#32 4	17.7	-2.20	-3.73	+26.7	31.1
ER#32 ah	18.1	-2.00	-3.68	+26.7	30.9
ER#32 ai	18.5	-2.57	-3.91	+26.5	32.0
ER#32 aj	18.8	-2.09	-3.48	+26.9	29.9
ER#32 ak	19.1	-3.29	-4.20	+26.2	33.4
ER#32 D4	19.5	-1.35	-2.91	+27.5	27.1
ER#32 al	19.9	-2.64	-3.19	+27.2	28.5

Subsample	Distance (cm)	$\delta^{13}\text{C}_{\text{VPDB}}$ (‰)	$\delta^{18}\text{O}_{\text{VPDB}}$ (‰)	$\delta^{18}\text{O}_{\text{VSMOW}}$ (‰)	Calculated Temperature (°C)
ER#32 am	20.2	-2.35	-2.83	+27.6	26.7
ER#32 an	20.5	-2.47	-3.60	+26.8	30.5
ER#32 ao	20.7	-2.45	-4.09	+26.3	32.9
ER#32 ap	21.1	-2.20	-3.25	+27.2	28.8
ER#32 aq	21.3	-2.31	-3.29	+27.1	28.9
ER#32 ar	21.6	-3.10	-3.36	+27.1	29.3
ER#32 as	21.8	-2.34	-3.90	+26.5	31.9
ER#32 at	22.3	-3.26	-3.88	+26.5	31.8
ER#32 D5	22.8	-1.65	-3.13	+27.3	28.2
ER#32 au	22.7	-2.46	-3.46	+27.0	29.8
ER#32 av	23.0	-2.98	-3.02	+27.4	27.6
ER#32 aw	23.3	-3.00	-3.29	+27.1	29.0
ER#32 ax	23.5	-1.13	-2.72	+27.7	26.1
ER#32 ay	24.0	-1.97	-3.04	+27.4	27.7
ER#32 az	24.3	-2.39	-3.30	+27.1	29.0
ER#32 bb	24.7	-2.88	-3.82	+26.6	31.5
ER#32 bc	25.0	-2.85	-3.29	+27.1	29.0
ER#32 bd	25.4	-2.77	-3.22	+27.2	28.6
ER#32 5	25.9	-2.12	-3.47	+26.9	29.9
ER#32 be	26.2	-2.56	-2.97	+27.5	27.4
ER#32 bf	26.6	-2.28	-3.24	+27.2	28.7
ER#32 bg	26.9	-3.33	-3.42	+27.0	29.6
<b>Right branch</b>					
ER#32 Ra	14.9	-1.91	-2.91	+27.9	25.2
ER#32 Rb	15.2	-1.35	-3.06	+27.8	26.0

Subsample	Distance (cm)	$\delta^{13}\text{C}_{\text{VPDB}}$ (‰)	$\delta^{18}\text{O}_{\text{VPDB}}$ (‰)	$\delta^{18}\text{O}_{\text{VSMOW}}$ (‰)	Calculated Temperature (°C)
ER#32 Rc	15.4	-2.15	-3.26	+27.6	26.9
ER#32 Rd	15.7	-2.20	-3.36	+27.4	27.4
ER#32 Re	15.9	-1.87	-3.21	+27.6	26.7
ER#32 Rf	16.9	-2.46	-3.19	+27.6	26.6
ER#32 Rg	17.9	-2.03	-3.32	+27.5	27.3
ER#32 Rh	18.9	-1.95	-3.15	+27.7	26.4
ER#32 Ri	19.9	-1.45	-3.13	+27.7	26.3
ER#32 Rj	20.9	-1.57	-3.07	+27.7	26.0
ER#32 Rk	21.9	-1.92	-3.06	+27.8	26.0
ER#32 Rl	22.9	-2.70	-3.12	+27.7	26.3
ER#32 Rm	23.9	-1.80	-3.14	+27.7	26.4
ER#32 Rn	24.9	-2.00	-3.05	+27.8	25.9
ER#32 Ro	25.9	-2.88	-3.79	+27.0	29.6
ER#32 Rp	26.9	-2.20	-3.11	+27.7	26.2
ER#32 Rq	27.9	-2.35	-3.51	+27.3	28.2
ER#32 Rr	28.9	-2.95	-3.67	+27.1	28.9
ER#32 Rs	29.9	-1.88	-2.88	+27.9	25.1
ER#32 Rt	30.9	-1.89	-3.18	+27.6	26.6
ER#32 Ru	31.9	-1.83	-3.11	+27.7	26.2
ER#32 Rv	32.9	-3.16	-3.51	+27.3	28.2
ER#32 Rw	33.9	-2.05	-2.87	+27.9	25.1
ER#32 Rx	34.9	-2.03	-2.56	+28.3	23.5
ER#32 Ry	35.9	-3.68	-3.40	+27.4	27.6
ER#32 Rz	36.9	-1.79	-2.71	+28.1	24.3
ER#32 Raa	37.9	-1.59	-2.64	+28.2	23.9



Subsample	Distance (cm)	$\delta^{13}\text{C}_{\text{VPDB}}$ (‰)	$\delta^{18}\text{O}_{\text{VPDB}}$ (‰)	$\delta^{18}\text{O}_{\text{VSMOW}}$ (‰)	Calculated Temperature (°C)
ER#32 Rab	38.9	-2.37	-2.95	+27.9	25.4
ER#32 Rac	39.9	-2.80	-3.08	+27.7	26.1
ER#32 Rad	40.9	-1.92	-2.83	+28.0	24.8
ER#32 Rae	41.9	-0.41	-2.31	+28.5	22.3
ER#32 Raf	42.9	-2.45	-2.98	+27.8	25.6
ER#32 Rag	43.9	-2.75	-3.29	+27.5	27.1
ER#32 Rah	44.9	-3.36	-3.50	+27.3	28.2
ER#32 Rai	45.9	-2.78	-3.26	+27.6	26.9
ER#32 Raj	46.9	-3.69	-3.56	+27.2	28.4
ER#32 Rak	47.9	-3.03	-3.43	+27.4	27.8
ER#32 Ral	48.9	-3.45	-3.42	+27.4	27.7
ER#32 Ram	49.9	-3.04	-3.19	+27.6	26.6
ER#32 Ran	50.9	-3.79	-3.35	+27.5	27.4
ER#32 Rao	51.9	-2.00	-3.07	+27.7	26.0
ER#32 Rap	52.9	-3.15	-3.84	+27.0	29.8
ER#32 Raq	53.9	-3.00	-3.22	+27.6	26.8
ER#32 Rar	54.9	-2.57	-3.41	+27.4	27.7
ER#32 Ras	55.9	-3.24	-3.45	+27.4	27.9
ER#32 Rat	56.9	-2.46	-3.09	+27.7	26.1

**Table 3.4.** Subsamples collected from ER#31-A. Distance measured from the base of the coral upwards. Calculated temperatures are determined from the Cayman geothermometer,  $\delta^{18}\text{O}_{\text{water}}$  value of +0.8‰.

Subsample	Distance (cm)	$\delta^{13}\text{C}_{\text{VPDB}}$ (‰)	$\delta^{18}\text{O}_{\text{VPDB}}$ (‰)	$\delta^{18}\text{O}_{\text{VSMOW}}$ (‰)	Calculated temperature (°C)
ER#31 a	1.7	-0.52	-3.26	+27.5	27.0
ER#31 b	2.0	-2.01	-3.47	+26.9	29.8
ER#31 c	2.5	-2.17	-3.19	+27.2	28.4
ER#31 d	2.8	-2.07	-3.12	+27.3	28.1
ER#31 e	3.3	-1.86	-3.45	+27.0	29.8
ER#31 f	3.9	-0.79	-3.26	+27.2	28.8
ER#31 l	4.3	-0.37	-2.87	+27.6	26.9
ER#31 g	4.7	-0.70	-2.66	+27.8	25.9
ER#31 h	5.0	-0.68	-3.22	+27.2	28.6
ER#31 i	5.4	-0.13	-2.52	+27.9	25.2
ER#31 j	5.6	-1.10	-3.60	+26.8	30.5
ER#31 k	6.0	-2.12	-3.64	+26.8	30.6
ER#31 l	6.5	-0.70	-2.47	+28.0	24.9
ER#31 m	6.9	-1.15	-3.16	+27.3	28.3
ER#31 n	7.3	-1.00	-2.47	+28.0	24.9
ER#31 o	7.7	-1.39	-3.01	+27.4	27.6
ER#31 p	8.2	-1.11	-2.68	+27.8	26.0
ER#31 D1	8.6	-0.91	-2.74	+27.7	26.3
ER#31 q	9.1	-1.12	-2.60	+27.8	25.6
ER#31 r	9.6	-1.06	-2.70	+27.7	26.1
ER#31 s	10.2	-1.10	-3.30	+27.1	29.0
ER#31 t	10.9	-1.17	-2.93	+27.5	27.2

Subsample	Distance (cm)	$\delta^{13}\text{C}_{\text{VPDB}}$ (‰)	$\delta^{18}\text{O}_{\text{VPDB}}$ (‰)	$\delta^{18}\text{O}_{\text{VSMOW}}$ (‰)	Calculated Temperature (°C)
ER#31 u	11.4	-1.70	-2.83	+27.6	26.7
ER#31 v	12.0	-1.12	-2.78	+27.7	26.4
ER#31 w	12.3	-0.81	-3.11	+27.3	28.1
ER#31 x	12.8	-0.70	-2.51	+27.9	25.1
ER#31 y	13.4	-1.06	-3.22	+27.2	28.6
ER# 31 2	13.9	-0.23	-2.61	+27.8	25.6
ER#31 z	14.4	-0.66	-2.15	+28.3	23.4
ER#31 aa	14.7	-1.08	-2.24	+28.2	23.8
ER#31 ab	14.9	-0.21	-2.22	+28.2	23.7
ER#31 ac	15.2	-1.57	-2.70	+27.7	26.1
ER#31 ad	15.6	-1.46	-2.26	+28.2	23.9
ER#31 ae	16.1	-1.32	-2.39	+28.1	24.5
ER#31 af	16.6	-0.47	-2.40	+28.4	22.7
ER#31 ag	16.9	-0.51	-2.16	+28.3	23.4
ER#31 ah	17.1	-0.76	-2.92	+27.5	27.1
ER#31 ai	17.2	-0.02	-2.12	+28.3	23.2
ER#31 aj	17.5	-1.77	-3.59	+26.8	30.4
ER#31 D2	18.1	+0.09	-2.25	+28.2	23.8
ER#31 ak	18.9	-2.40	-3.07	+27.4	27.9
ER#31 al	19.5	+0.29	-2.08	+28.4	23.0
ER#31 am	20.2	-1.24	-2.36	+28.1	24.4
ER#31 an	20.7	-1.14	-2.21	+28.2	23.6
ER#31 ao	21.5	-0.82	-2.42	+28.0	24.7
ER#31 ap	22.1	-2.20	-2.53	+27.9	25.2
ER#31 3	22.9	+0.12	-2.50	+27.9	25.1

Subsample	Distance (cm)	$\delta^{13}\text{C}_{\text{VPDB}}$ (‰)	$\delta^{18}\text{O}_{\text{VPDB}}$ (‰)	$\delta^{18}\text{O}_{\text{VSMOW}}$ (‰)	Calculated Temperature (°C)
ER#31 aq	23.3	-2.22	-3.07	+27.4	27.9
ER#31 ar	23.6	-0.86	-2.45	+28.0	24.8
ER#31 D3	24.6	-0.15	-2.36	+28.1	24.4
ER#31 as	24.7	-1.38	-2.57	+27.9	25.4
ER#31 4	25.4	-0.47	-2.80	+27.6	26.6
ER#31 at	26.0	-1.65	-2.77	+27.7	26.4
ER#31 au	26.4	-1.03	-2.70	+27.7	26.1
ER#31 av	26.6	-1.07	-3.71	+26.7	31.0
ER#31 D4	27.1	-1.18	-2.76	+27.7	26.3
ER#31 aw	27.5	-0.58	-3.24	+27.2	28.7
ER#31 ax	28.0	-1.65	-3.46	+26.9	29.8
ER#31 5	28.8	-1.29	-2.91	+27.5	27.1
ER#31 ay	29.4	-1.86	-3.79	+26.6	31.4
ER#31 az	30.0	-1.65	-3.16	+27.3	28.3
ER#31 D5	30.8	-1.62	-2.78	+27.7	26.4
ER#31 bb	31.4	-1.17	-3.14	+27.3	28.2
ER#31 bc	31.8	-1.61	-3.61	+26.8	30.5
ER#31 bd	32.1	-1.12	-3.38	+27.0	29.4
ER#31 be	32.4	-2.54	-3.35	+27.1	29.3
ER#31 bf	32.8	-0.98	-3.08	+27.4	27.9
ER#31 bg	33.1	-2.64	-3.61	+26.8	30.5
ER#31 6	33.9	-1.42	-3.13	+27.3	28.2
ER#31 bh	34.5	-1.23	-3.07	+27.4	27.9
ER#31 bi	34.9	-1.89	-3.49	+26.9	29.9
ER#31 bj	35.2	-2.25	-2.88	+27.5	27.0

---

Subsample	Distance	$\delta^{13}\text{C}_{\text{VPDB}}$	$\delta^{18}\text{O}_{\text{VPDB}}$	$\delta^{18}\text{O}_{\text{VSMOW}}$	Calculated
	(cm)	(‰)	(‰)	(‰)	Temperature (°C)
ER#31 bk	35.6	-1.57	-2.84	+27.6	26.8

---

**Table 3.5.** Subsamples collected from GW-A. Distance measured from the base of the coral upwards. Calculated temperatures are determined from the Cayman geothermometer,  $\delta^{18}\text{O}_{\text{water}}$  value of +0.8‰.

Subsamples	Distance (cm)	$\delta^{13}\text{C}_{\text{VPDB}}$ (‰)	$\delta^{18}\text{O}_{\text{VPDB}}$ (‰)	$\delta^{18}\text{O}_{\text{VSMOW}}$ (‰)	Calculated Temperatures (°C)
GW co	0.1	-0.68	-2.49	+28.3	23.1
GW cp	0.3	-0.59	-2.60	+28.2	23.7
GW cq	0.5	-0.65	-2.48	+28.4	23.1
GW cr	0.7	-1.08	-2.83	+28.0	24.8
GW cs	0.8	-1.03	-2.28	+28.6	22.1
GW ct	1.0	-0.49	-2.21	+28.6	21.7
GW cu	1.2	-0.36	-2.49	+28.3	23.1
GW cv	1.4	-0.67	-2.42	+28.4	22.8
GW cw	1.6	-0.98	-2.37	+28.5	22.5
GW cx	1.9	-0.49	-2.24	+28.6	21.9
GW cy	2.2	-0.51	-2.69	+28.1	24.1
GW cz	2.5	-0.56	-2.03	+28.8	20.9
GW da	2.8	-0.28	-2.41	+28.4	22.7
GW db	3.2	-0.62	-2.48	+28.4	23.1
GW dc	3.6	-0.26	-2.51	+28.3	23.2
GW dd	3.9	-0.86	-2.60	+28.2	23.7
GW de	4.1	-0.85	-2.89	+27.9	25.1
GW df	4.3	-1.16	-2.85	+28.0	24.9
GW dg	4.5	-0.76	-2.49	+28.3	23.1
GW dh	4.7	-0.60	-2.57	+28.3	23.5
GW di	4.9	-0.89	-2.74	+28.1	24.3
GW dj	5.2	-0.99	-2.75	+28.1	24.4

Subsamples	Distance (cm)	$\delta^{13}\text{C}_{\text{VPDB}}$ (‰)	$\delta^{18}\text{O}_{\text{VPDB}}$ (‰)	$\delta^{18}\text{O}_{\text{VSMOW}}$ (‰)	Calculated Temperatures ( $^{\circ}\text{C}$ )
GW dk	5.6	-0.39	-2.33	+28.5	22.4
GW dl	6.0	-0.78	-2.42	+28.4	22.8
GW dm	6.2	-0.37	-2.17	+28.7	21.6
GW dn	6.5	-0.58	-2.89	+27.9	25.1
GW do	6.8	-0.73	-2.36	+28.5	22.5
GW dp	7.1	-0.15	-2.22	+28.6	21.8
GW dq	7.5	-0.27	-2.51	+28.3	23.2
GW dr	8.0	-0.22	-2.48	+28.4	23.1
GW ds	8.6	-0.76	-2.38	+28.5	22.6
GW dt	9.1	-0.63	-2.60	+28.2	23.7
GW du	9.5	-0.51	-2.22	+28.6	21.8
GW dv	9.7	-0.67	-2.65	+28.2	23.9
GW dw	10.0	-0.94	-2.25	+28.6	22.0
GW dx	10.2	-0.69	-2.28	+28.6	22.1
GW dy	10.6	-0.13	-2.34	+28.5	22.4
GW dz	11.2	-0.69	-2.26	+28.6	22.0
GW ea	11.5	-0.78	-2.38	+28.5	22.6
GW eb	11.8	-0.28	-2.10	+28.7	21.2
GW ec	12.2	-0.04	-2.52	+28.3	23.3
GW ed	12.7	-0.51	-2.24	+28.6	21.9
GW ee	13.3	-0.91	-2.77	+28.1	24.5
GW ef	14.1	-0.59	-2.54	+28.3	23.3
GW eg	0.3	-0.63	-1.95	+28.9	20.5
GW eh	0.7	-0.80	-2.54	+28.3	23.4
GW ei	1.0	-0.83	-2.15	+28.7	21.5

Subsamples	Distance (cm)	$\delta^{13}\text{C}_{\text{VPDB}}$ (‰)	$\delta^{18}\text{O}_{\text{VPDB}}$ (‰)	$\delta^{18}\text{O}_{\text{VSMOW}}$ (‰)	Calculated Temperatures ( $^{\circ}\text{C}$ )
GW ej	1.5	-0.02	-1.99	+28.9	20.7
GW ek	1.9	-1.00	-2.70	+28.1	24.1
GW el	2.2	-0.64	-2.30	+28.5	22.2
GW em	2.5	-1.10	-2.26	+28.6	22.0
GW en	2.8	-0.49	-2.06	+28.8	21.0
GW eo	3.4	-0.54	-2.11	+28.7	21.3
GW ep	4.1	-0.51	-2.22	+28.6	21.8
GW eq	4.6	-0.98	-2.15	+28.7	21.5
GW er	5.2	-0.65	-2.78	+28.0	24.5
GW es	5.7	-0.46	-2.28	+28.6	22.1
GW et	6.0	-0.93	-2.10	+28.7	21.2
GW eu	6.3	-0.20	-2.33	+28.5	22.3
GW ev	6.5	-1.00	-2.28	+28.6	22.1
GW ew	6.8	-1.16	-2.34	+28.5	22.4
GW ex	7.0	-0.80	-1.99	+28.9	20.7
GW ey	7.3	-0.50	-2.79	+28.0	24.6
GW ez	7.5	-0.84	-2.42	+28.4	22.8
GW fa	7.8	-0.33	-2.39	+28.4	22.6
GW fb	8.1	-0.44	-2.74	+28.1	24.3
GW fc	8.3	-1.28	-3.50	+27.3	28.1
GW fd	8.6	-0.14	-2.64	+28.2	23.9
GW fg	8.9	-0.57	-2.71	+28.1	24.2
GW fh	9.2	-0.83	-2.54	+28.3	23.4
GW fi	9.6	-0.28	-2.46	+28.4	23.0
GW fj	9.9	-0.63	-2.26	+28.6	22.0



Subsamples	Distance (cm)	$\delta^{13}\text{C}_{\text{VPDB}}$ (‰)	$\delta^{18}\text{O}_{\text{VPDB}}$ (‰)	$\delta^{18}\text{O}_{\text{VSMOW}}$ (‰)	Calculated Temperatures ( $^{\circ}\text{C}$ )
GW fk	10.4	-0.76	-2.13	+28.7	21.3
GW fl	10.9	-0.55	-2.81	+28.0	24.7
GW fm	11.2	-0.31	-2.10	+28.7	21.2
GW fn	11.4	-0.57	-2.47	+28.4	23.0
GW fo	11.8	-0.52	-2.04	+28.8	20.9
GW fp	12.3	-0.18	-2.08	+28.8	21.1
GW fq	12.7	-0.43	-1.95	+28.9	20.5
GW fr	13.0	-0.87	-2.75	+28.1	24.4
GW fs	13.4	-0.91	-2.10	+28.7	21.2
GW ft	13.9	-0.49	-2.09	+28.8	21.2
GW fu	14.7	+0.01	-2.82	+28.0	24.8
GW fv	15.3	-0.17	-2.47	+28.4	23.0
GW fw	15.7	-0.60	-2.65	+28.2	23.9
GW fx	16.0	-0.04	-2.80	+28.0	24.6
GW fy	16.4	-0.18	-2.67	+28.2	24.0
GW fz	16.7	-0.45	-2.93	+27.9	25.3
GW ga	17.0	-0.39	-2.17	+28.7	21.6
GW gb	17.2	-0.24	-2.31	+28.5	22.3
GW gc	17.4	-0.54	-2.06	+28.8	21.0
GW gd	17.8	-0.46	-1.99	+28.9	20.7
GW ge	18.4	-0.98	-2.07	+28.8	21.0
GW gf	18.8	-0.79	-1.99	+28.9	20.7
GW gg	19.1	-0.84	-2.33	+28.5	22.3
GW gh	19.3	-0.69	-1.78	+29.1	19.6
GW gi	19.6	-0.49	-2.36	+28.5	22.5

Subsamples	Distance (cm)	$\delta^{13}\text{C}_{\text{VPDB}}$ (‰)	$\delta^{18}\text{O}_{\text{VPDB}}$ (‰)	$\delta^{18}\text{O}_{\text{VSMOW}}$ (‰)	Calculated Temperatures ( $^{\circ}\text{C}$ )
GW gj	19.9	-1.08	-2.29	+28.5	22.2
GW gk	20.1	-0.53	-1.96	+28.9	20.5
GW gl	20.5	-0.24	-2.30	+28.5	22.2
GW gm	20.7	-0.88	-2.19	+28.7	21.7
GW a	0.2	-0.61	-2.52	+28.3	23.3
GW b	0.6	-1.15	-2.78	+28.0	24.6
GW c	1.0	-0.69	-2.47	+28.4	23.0
GW d	1.2	-0.58	-2.68	+28.2	24.1
GW e	1.5	-0.85	-2.50	+28.3	23.2
GW f	1.7	-0.46	-2.84	+28.0	24.9
GW g	2.1	-0.90	-2.80	+28.0	24.7
GW h	2.3	-0.26	-2.62	+28.2	23.8
GW i	2.7	-0.84	-2.96	+27.9	25.4
GW j	3.0	-0.31	-2.55	+28.3	23.4
GW k	3.3	-0.98	-3.21	+27.6	26.6
GW l	3.6	-0.63	-2.54	+28.3	23.4
GW m	4.0	-0.73	-3.42	+27.4	27.7
GW n	4.4	-0.39	-2.73	+28.1	24.3
GW o	4.7	-1.03	-2.82	+28.0	24.8
GW p	5.0	-0.28	-2.67	+28.2	24.0
GW q	5.2	-0.80	-3.29	+27.5	27.1
GW r	5.4	-0.61	-2.80	+28.0	24.7
GW s	5.7	-0.50	-2.86	+28.0	24.9
GW t	6.1	-0.22	-3.05	+27.8	25.9
GW u	6.5	-0.67	-2.90	+27.9	25.1

Subsamples	Distance (cm)	$\delta^{13}\text{C}_{\text{VPDB}}$ (‰)	$\delta^{18}\text{O}_{\text{VPDB}}$ (‰)	$\delta^{18}\text{O}_{\text{VSMOW}}$ (‰)	Calculated Temperatures ( $^{\circ}\text{C}$ )
GW v	6.9	-0.85	-2.98	+27.8	25.5
GW w	7.2	-0.50	-2.98	+27.8	25.5
GW x	7.5	-0.50	-3.05	+27.8	25.9
GW y	8.0	-0.61	-2.95	+27.9	25.4
GW z	8.4	-0.49	-2.49	+28.3	23.1
GW aa	8.6	-0.81	-2.88	+28.0	25.0
GW ab	9.0	-0.06	-2.61	+28.2	23.7
GW ac	9.2	-0.91	-2.84	+28.0	24.8
GW ad	9.5	-0.31	-2.71	+28.1	24.2
GW ae	9.8	-0.88	-2.91	+27.9	25.2
GW af	10.0	-0.33	-3.17	+27.7	26.4
GW ag	10.2	-0.81	-3.12	+27.7	26.2
GW ai	10.6	-1.05	-3.43	+27.4	27.7
GW aj	10.9	-0.54	-2.40	+28.4	22.7
GW ak	11.1	-0.97	-2.69	+28.1	24.1
GW al	11.3	-0.80	-3.00	+27.8	25.6
GW am	11.5	+0.10	-2.62	+28.2	23.8
GW an	11.7	-1.36	-2.86	+28.0	24.9
GW ao	12.1	0.00	-2.79	+28.0	24.6
GW ap	12.3	-0.50	-3.68	+27.1	29.0
GW aq	12.6	-0.13	-3.51	+27.3	28.1
GW ar	12.8	-0.38	-4.00	+26.8	30.5
GW as	13.0	-0.45	-3.11	+27.7	26.2
GW at	13.2	-0.31	-3.08	+27.7	26.0
GW au	13.5	-0.82	-3.27	+27.5	26.9

Subsamples	Distance (cm)	$\delta^{13}\text{C}_{\text{VPDB}}$ (‰)	$\delta^{18}\text{O}_{\text{VPDB}}$ (‰)	$\delta^{18}\text{O}_{\text{VSMOW}}$ (‰)	Calculated Temperatures ( $^{\circ}\text{C}$ )
GW av	13.7	-0.17	-3.03	+27.8	25.8
GW aw	13.9	-0.52	-3.18	+27.6	26.5
GW ax	14.2	-0.20	-2.89	+27.9	25.1
GW ay	14.4	-0.91	-3.03	+27.8	25.8
GW az	14.6	-0.36	-3.83	+27.0	29.7
GW ba	14.8	-0.66	-3.31	+27.5	27.1
GW bb	15.0	-0.26	-2.87	+28.0	25.0
GW bc	15.2	-0.07	-3.26	+27.6	26.9
GW bd	15.5	-0.53	-3.18	+27.6	26.5
GW be	15.8	0.08	-3.02	+27.8	25.7
GW bf	16.2	-0.42	-2.63	+28.2	23.8
GW bg	16.4	-0.79	-2.61	+28.2	23.7
GW bh	16.6	-0.38	-2.06	+28.8	21.0
GW bi	16.8	-1.11	-2.58	+28.3	23.6
GW bj	17.1	-0.25	-1.96	+28.9	20.5
GW bk	17.3	-0.61	-2.20	+28.6	21.7
GW bl	17.6	-0.34	-2.46	+28.4	23.0
GW bm	17.8	-0.62	-2.13	+28.7	21.4
GW bn	18.2	-0.38	-2.53	+28.3	23.3
GW bo	18.4	-0.26	-2.24	+28.6	21.9
GW bp	18.6	-1.01	-2.56	+28.3	23.5
GW bq	18.9	-0.31	-2.45	+28.4	22.9
GW br	19.2	-0.59	-2.46	+28.4	23.0
GW bs	19.4	-1.20	-3.56	+27.2	28.4
GW bt	19.7	-0.58	-2.73	+28.1	24.3

Subsamples	Distance (cm)	$\delta^{13}\text{C}_{\text{VPDB}}$ (‰)	$\delta^{18}\text{O}_{\text{VPDB}}$ (‰)	$\delta^{18}\text{O}_{\text{VSMOW}}$ (‰)	Calculated Temperatures ( $^{\circ}\text{C}$ )
GW bu	20.0	-0.28	-2.50	+28.3	23.2
GW bv	20.1	-0.07	-2.17	+28.7	21.6
GW bw	20.4	-0.53	-2.76	+28.1	24.5
GW bx	20.6	-0.21	-2.27	+28.6	22.1
GW by	20.8	-1.02	-2.35	+28.5	22.5
GW bz	21.0	-0.21	-2.95	+27.9	25.4
GW ca	21.1	-0.97	-3.00	+27.8	25.7
GW cb	21.3	-0.74	-2.49	+28.3	23.1
GW cc	21.5	-0.06	-2.39	+28.4	22.6
GW cd	21.7	-0.65	-2.53	+28.3	23.3
GW ce	22.0	-0.56	-2.38	+28.5	22.6
GW cf	22.2	-1.02	-2.68	+28.1	24.1
GW cg	22.5	-0.28	-2.13	+28.7	21.4
GW ch	22.7	-0.29	-2.54	+28.3	23.4
GW ci	23.0	-0.58	-2.81	+28.0	24.7
GW cj	23.2	-0.21	-2.23	+28.6	21.8
GW ck	23.4	-0.98	-2.47	+28.4	23.0
GW cl	23.6	-0.53	-2.12	+28.7	21.3
GW cm	23.7	0.00	-1.99	+28.9	20.7
GW cn	24.0	-0.87	-2.30	+28.5	22.2

**Table 3.6.** Subsamples collected from coral DD-A. Distance measured from the base of the coral upwards. Calculated temperatures are determined from the Cayman geothermometer,  $\delta^{18}\text{O}_{\text{water}}$  value of +0.8‰.

Subsamples	Distance (cm)	$\delta^{13}\text{C}_{\text{VPDB}}$ (‰)	$\delta^{18}\text{O}_{\text{VPDB}}$ (‰)	$\delta^{18}\text{O}_{\text{VSMOW}}$ (‰)	Calculated Temperatures (°C)
DD a	4.1	+0.78	-2.86	+28.0	24.9
DD b	4.4	+0.54	-2.99	+27.8	25.6
DD c	4.7	-0.10	-2.65	+28.2	23.9
DD d	5.2	+0.46	-2.59	+28.2	23.6
DD e	5.8	+0.27	-3.31	+27.5	27.2
DD f	6.5	-0.09	-2.52	+28.3	23.3
DD g	7.0	+0.30	-2.56	+28.3	23.5
DD h	7.4	+0.30	-2.44	+28.4	22.9
DD i	7.9	-0.48	-2.42	+28.4	22.8
DD j	8.2	-0.44	-1.71	+29.2	19.3
DD k	8.5	-0.51	-2.07	+28.8	21.1
DD l	8.8	-0.51	-2.11	+28.7	21.2
DD m	9.2	-0.19	-1.80	+29.1	19.7
DD n	9.6	-0.58	-2.32	+28.5	22.3
DD o	10.0	-0.35	-2.18	+28.7	21.6
DD p	10.5	-0.04	-2.00	+29.9	20.2
DD q	11.0	-0.21	-2.30	+28.5	22.2
DD r	11.4	-0.30	-1.92	+28.9	20.3
DD s	11.9	-0.04	-2.75	+28.1	24.4
DD t	12.2	-0.03	-2.32	+28.5	22.3
DD u	12.5	+0.03	-2.64	+28.2	23.9
DD v	12.8	+0.21	-2.71	+28.1	24.2

Subsamples	Distance (cm)	$\delta^{13}\text{C}_{\text{VPDB}}$ (‰)	$\delta^{18}\text{O}_{\text{VPDB}}$ (‰)	$\delta^{18}\text{O}_{\text{VSMOW}}$ (‰)	Calculated Temperatures ( $^{\circ}\text{C}$ )
DD w	13.1	-0.24	-2.34	+28.5	22.4
DD x	13.4	+0.26	-2.82	+28.0	24.8
DD y	13.8	+0.18	-2.15	+28.7	21.5
DD z	14.1	+0.19	-2.25	+28.6	22.0
DD aa	14.4	+0.20	-2.23	+28.6	21.9
DD ab	15.1	-0.19	-2.38	+28.5	22.6
DD ac	15.4	+0.06	-2.49	+28.3	23.1
DD ad	15.8	+0.27	-2.67	+28.2	24.0
DD ae	16.2	+0.26	-2.04	+28.8	20.9
DD af	16.7	+0.15	-2.45	+28.4	22.9
DD ag	17.0	-0.03	-2.07	+28.8	21.1
DD ah	17.4	-0.09	-2.60	+28.2	23.7
DD ai	17.9	-0.16	-2.35	+28.5	22.5
DD aj	18.2	+0.34	-2.11	+28.7	21.3
DD ak	18.5	+0.11	-2.43	+28.4	22.8
DD al	18.8	+0.16	-2.26	+28.6	22.0
DD am	19.1	-0.04	-2.03	+28.8	20.9
DD an	19.7	-0.10	-2.03	+28.8	20.9
DD ao	20.1	-0.91	-2.04	+28.8	20.9
DD ap	20.4	-0.19	-2.01	+28.8	20.7
DD aq	20.8	-0.33	-2.39	+28.5	22.6
DD ar	21.2	+0.34	-2.43	+28.4	22.8
DD as	21.6	-0.27	-2.49	+28.4	23.1
DD at	22.1	+0.28	-2.73	+28.1	24.3
DD au	22.8	+0.23	-2.62	+28.2	23.8

Subsamples	Distance (cm)	$\delta^{13}\text{C}_{\text{VPDB}}$ (‰)	$\delta^{18}\text{O}_{\text{VPDB}}$ (‰)	$\delta^{18}\text{O}_{\text{VSMOW}}$ (‰)	Calculated Temperatures ( $^{\circ}\text{C}$ )
DD av	23.1	+0.12	-3.35	+27.5	27.4
DD aw	23.3	-0.54	-1.87	+29.0	20.1
DD ax	23.5	-0.23	-1.58	+29.3	18.6
DD ay	23.7	-0.26	-2.34	+28.5	22.4
DD az	23.9	-0.91	-2.24	+28.6	21.9
DD ba	24.2	+0.16	-2.39	+28.4	22.6
DD bb	24.6	-0.50	-2.73	+28.1	24.3
DD bc	24.9	-0.21	-1.89	+29.0	20.2
DD bd	25.2	-0.41	-2.08	+28.8	21.1
DD be	26.0	-0.47	-1.90	+29.0	20.2
DD bf	26.9	-0.16	-2.05	+28.8	21.0
DD bg	27.2	-0.58	-2.12	+28.7	21.3
DD bh	27.5	-0.08	-2.51	+28.3	23.2
DD bi	27.8	-0.35	-1.77	+29.1	19.6
DD bj	28.1	-0.43	-2.45	+28.4	22.9
DD bk	28.3	-0.31	-1.79	+29.1	19.7
DD bl	28.6	-0.12	-2.13	+28.7	21.4
DD bm	29.0	-0.53	-1.96	+28.9	20.5
DD bn	29.4	-0.33	-2.15	+28.7	21.4
DD bo	29.7	+0.15	-1.86	+29.0	20.1
DD bp	30.0	-0.73	-1.92	+28.9	20.3
DD bq	30.3	-0.29	-1.97	+28.9	20.6
DD br	30.8	-0.08	-2.11	+28.7	21.3
DD bs	31.2	-0.22	-1.93	+28.9	20.4
DD bt	31.5	-0.58	-2.26	+28.6	22.0



Subsamples	Distance (cm)	$\delta^{13}\text{C}_{\text{VPDB}}$ (‰)	$\delta^{18}\text{O}_{\text{VPDB}}$ (‰)	$\delta^{18}\text{O}_{\text{VSMOW}}$ (‰)	Calculated Temperatures ( $^{\circ}\text{C}$ )
DD bu	31.8	-0.21	-1.96	+28.9	20.5
DD bv	32.1	+0.08	-2.47	+28.4	23.0
DD bw	32.5	-0.39	-2.05	+28.8	20.9
DD bx	33.0	-0.68	-2.00	+28.8	20.7
DD by	33.3	-1.17	-2.26	+28.6	22.0
DD bz	33.5	-1.03	-1.79	+29.1	19.7
DD ca	33.7	+0.36	-2.47	+28.4	23.0
DD cb	34.1	-0.31	-2.59	+28.2	23.6
DD cc	34.4	+0.50	-2.68	+28.2	24.1
DD cd	34.7	+0.19	-2.53	+28.3	23.3
DD ce	35.1	+0.48	-2.47	+28.4	23.0
DD cf	35.3	+0.60	-2.54	+28.3	23.4
DD cg	35.7	-0.45	-2.57	+28.2	23.5
DD ch	36.1	-0.08	-2.88	+27.9	25.0
DD ci	36.5	-0.45	-1.48	+29.4	18.2
DD cj	37.0	-0.21	-2.68	+28.2	24.0
DD ck	37.5	+0.38	-2.62	+28.2	23.7
DD cl	37.8	+0.26	-3.02	+27.8	25.7
DD cm	38.2	-0.05	-2.43	+28.4	22.8
DD cn	38.5	+0.11	-2.75	+28.1	24.4
DD co	38.8	+0.14	-2.31	+28.5	22.2
DD cp	39.0	+0.60	-2.37	+28.5	22.6
DD cq	39.3	-0.06	-2.62	+28.2	23.8
DD cr	39.5	-0.14	-2.32	+28.5	22.3
DD cs	39.8	-0.08	-2.78	+28.0	24.6

Subsamples	Distance (cm)	$\delta^{13}\text{C}_{\text{VPDB}}$ (‰)	$\delta^{18}\text{O}_{\text{VPDB}}$ (‰)	$\delta^{18}\text{O}_{\text{VSMOW}}$ (‰)	Calculated Temperatures ( $^{\circ}\text{C}$ )
DD ct	40.1	0.00	-2.59	+28.2	23.6
DD cu	40.5	-1.04	-1.60	+29.3	18.8
DD cv	41.0	-0.43	-1.67	+29.2	19.1
DD cw	41.4	-0.02	-1.89	+29.0	20.2
DD cx	41.7	-0.54	-1.84	+29.0	19.9
DD cy	42.1	+0.19	-1.36	+29.5	17.6
DD da	42.6	+0.19	-1.52	+29.3	18.4
DD db	42.8	-0.38	-1.92	+28.9	20.3
DD dc	43.2	-0.45	-2.45	+28.8	22.9
DD dd	43.4	-0.23	-1.84	+29.0	20.0
DD de	43.8	+0.14	-1.87	+29.0	20.1
DD df	44.2	-0.52	-1.95	+28.9	20.5
DD dg	44.5	+0.28	-1.90	+29.0	20.3
DD dh	45.0	-0.28	-1.97	+28.9	20.6
DD di	45.4	+0.26	-1.75	+29.1	19.5
DD dj	45.8	-0.55	-1.89	+29.0	20.2
DD dk	46.2	+0.26	-1.77	+29.1	19.6
DD dl	46.6	-0.39	-1.76	+29.1	19.6
DD dm	47.0	-0.38	-1.85	+29.0	20.0
DD dn	47.3	-0.27	-1.69	+29.2	19.2
DD do	47.8	+0.23	-2.18	+28.7	21.6
DD dp	48.0	-0.87	-2.15	+28.7	21.5
DD dq	48.4	-0.08	-1.89	+29.0	20.2
DD dr	48.8	-0.31	-2.28	+28.6	22.1
DD ds	49.3	-0.39	-2.40	+28.4	22.7

Subsamples	Distance (cm)	$\delta^{13}\text{C}_{\text{VPDB}}$ (‰)	$\delta^{18}\text{O}_{\text{VPDB}}$ (‰)	$\delta^{18}\text{O}_{\text{VSMOW}}$ (‰)	Calculated Temperatures ( $^{\circ}\text{C}$ )
DD dt	49.7	-0.17	-2.17	+28.7	21.6
DD du	50.0	-0.05	-1.96	+28.9	20.5
DD dv	50.3	-0.41	-2.18	+28.7	21.6
DD dw	50.7	-0.28	-2.12	+28.7	21.3
DD dx	51.1	+0.13	-1.95	+28.9	20.5
DD dy	51.5	+0.06	-2.07	+28.8	21.0
DD dz	51.9	-0.52	-2.28	+28.6	22.1
DD ea	52.2	-0.86	-2.44	+28.4	22.9
DD eb	52.5	-0.66	-2.05	+28.8	21.0
DD ec	52.9	-0.09	-2.11	+28.7	21.3
DD ed	53.1	+0.04	-1.77	+29.1	19.6

**Table 3.7.** Subsamples collected from coral TA-C. Distance measured from the base of the coral upwards. Calculated temperatures are determined from the Cayman geothermometer,  $\delta^{18}\text{O}_{\text{water}}$  value of +1.4‰.

Subsamples	Distance (cm)	$\delta^{13}\text{C}_{\text{VPDB}}$ (‰)	$\delta^{18}\text{O}_{\text{VPDB}}$ (‰)	$\delta^{18}\text{O}_{\text{VSMOW}}$ (‰)	Calculated Temperatures (°C)
TA a	0.2	-1.43	-2.77	+28.1	27.4
TA b	0.6	-1.82	-2.38	+28.5	25.4
TA c	0.8	-0.94	-2.59	+28.2	26.5
TA d	1.1	-0.97	-2.16	+28.7	24.4
TA e	1.4	-0.83	-2.44	+28.4	25.8
TA f	1.7	-0.47	-1.74	+29.1	22.3
TA g	2.0	-1.43	-2.13	+28.7	24.2
TA h	2.2	-1.83	-2.54	+28.3	26.2
TA i	2.4	-0.91	-2.26	+28.6	24.8
TA j	2.5	-0.66	-2.26	+28.6	24.9
TA k	2.8	-0.84	-2.36	+28.5	25.4
TA l	3.1	-0.76	-2.53	+28.3	26.2
TA m	3.3	-0.30	-1.86	+29.0	22.9
TA n	3.5	-0.42	-1.58	+29.3	21.5
TA o	3.7	-1.04	-2.04	+28.8	23.8
TA p	4.0	-0.24	-2.44	+28.4	25.7
TA q	4.3	+0.05	-2.53	+28.3	26.2
TA r	4.8	-0.36	-2.82	+28.0	27.6
TA s	5.1	+0.04	-2.15	+28.7	24.3
TA t	5.5	-1.30	-2.79	+28.0	27.5
TA u	5.6	-0.51	-2.45	+28.4	25.8
TA v	5.8	-0.14	-2.68	+28.1	26.9

Subsamples	Distance (cm)	$\delta^{13}\text{C}_{\text{VPDB}}$ (‰)	$\delta^{18}\text{O}_{\text{VPDB}}$ (‰)	$\delta^{18}\text{O}_{\text{VSMOW}}$ (‰)	Calculated Temperatures (°C)
TA w	6.0	-0.47	-2.80	+28.0	27.5
TA x	6.1	-0.24	-2.83	+28.0	27.6
TA y	6.4	-0.20	-2.35	+28.5	25.3
TA z	6.6	+0.22	-2.52	+28.3	26.1
TA aa	6.8	-0.31	-2.31	+28.5	25.1
TA ab	7.2	-0.09	-2.47	+28.4	25.9
TA ac	7.5	-0.12	-2.54	+28.3	26.2
TA ad	7.8	+0.62	-2.39	+28.4	25.5
TA ae	8.0	-0.23	-2.49	+28.4	26.0
TA af	8.4	-0.07	-2.58	+28.3	26.4
TA ag	8.6	-0.51	-2.78	+28.1	27.4
TA ah	8.9	-0.11	-2.64	+28.2	26.7
TA ai	9.2	-0.09	-2.43	+28.4	25.7
TA aj	9.6	+0.16	-1.96	+28.9	23.4
TA ak	9.9	-0.65	-2.18	+28.7	24.5
TA al	10.2	-0.39	-2.55	+28.3	26.3
TA am	10.5	-0.87	-2.01	+28.8	23.6
TA an	10.9	-0.16	-2.18	+28.7	24.4
TA ao	11.2	-0.33	-2.83	+28.0	27.6
TA ap	11.5	-1.45	-2.08	+28.8	24.0
TA aq	11.8	-0.91	-2.18	+28.7	24.5
TA ar	12.1	-0.91	-2.23	+28.6	24.7
TA as	12.4	-1.31	-2.29	+28.6	25.0
TA at	12.9	-1.30	-2.10	+28.7	24.1
TA au	13.4	-0.52	-2.06	+28.8	23.9

Subsamples	Distance (cm)	$\delta^{13}\text{C}_{\text{VPDB}}$ (‰)	$\delta^{18}\text{O}_{\text{VPDB}}$ (‰)	$\delta^{18}\text{O}_{\text{VSMOW}}$ (‰)	Calculated Temperatures (°C)
TA av	13.9	+0.29	-1.48	+29.4	21.0
TA aw	14.3	-0.41	-1.63	+29.3	21.8
TA ax	14.6	-2.20	-2.03	+28.8	23.7
TA ay	15.0	-1.29	-2.35	+28.5	25.3
TA az	15.3	-1.74	-2.39	+28.4	25.5
TA ba	15.6	-1.12	-2.07	+28.8	23.9
TA bb	16.1	-0.59	-2.32	+28.5	25.2
TA bc	16.5	-0.84	-1.95	+28.9	23.3
TA bd	17.0	-0.53	-2.48	+28.4	25.9
TA be	17.2	-0.22	-2.60	+28.2	26.5
TA bf	17.4	-0.83	-2.39	+28.4	25.5
TA bg	17.7	-0.91	-2.45	+28.4	25.8
TA bh	18.0	-0.28	-2.01	+28.8	23.7
TA bi	18.3	+0.12	-2.49	+28.4	26.0
TA bj	18.6	-0.28	-2.23	+28.6	24.7
TA bl	19.1	-0.47	-2.12	+28.7	24.2
TA bm	19.4	-0.55	-2.23	+28.6	24.7
TA bn	19.8	-0.11	-1.94	+28.9	23.3
TA bo	20.3	-0.21	-2.16	+28.7	24.4
TA bp	20.8	-0.82	-2.39	+28.4	25.5
TA bq	21.0	-0.56	-2.06	+28.8	23.9
TA br	21.4	-0.32	-1.83	+29.0	22.7
TA bs	21.6	-0.37	-2.52	+28.3	26.1
TA bt	21.8	-0.71	-1.97	+28.9	23.4
TA bu	22.3	-0.56	-1.79	+29.1	22.5

Subsamples	Distance (cm)	$\delta^{13}\text{C}_{\text{VPDB}}$ (‰)	$\delta^{18}\text{O}_{\text{VPDB}}$ (‰)	$\delta^{18}\text{O}_{\text{VSMOW}}$ (‰)	Calculated Temperatures (°C)
TA bv	22.6	-0.74	-2.30	+28.5	25.1
TA bw	23.0	-0.73	-1.85	+29.0	22.9
TA bx	23.4	-1.12	-3.09	+27.7	28.9
TA by	23.9	0.00	-2.59	+28.2	26.5

**Table 3.8.** Published coral  $\delta^{18}\text{O}$  geothermometers

Reference	Coral type	Location	Temperature range (°C)	Equation
Weber, 1977	79 colonies of <i>Galaxea spp.</i>	Australian continental shelf	23.9 to 29.3, 26.6	$T = ((\delta^{18}\text{O}_c - \delta^{18}\text{O}_w) - 0.3348) - 0.1732$
Dunbar and Wellington, 1981	2 colonies of <i>Pocillopora damicornis</i>	Gulf of Panama	21.5 to 28.8, 25.2	$T = 7.0 - 3.6 * (\delta^{18}\text{O}_c - \delta^{18}\text{O}_w)$
Weil et al., 1981	3 colonies of <i>Pocillopora damicornis</i>	Hawaii Gulf of Panama	21.8 to 28.3, 25.1	$T = 3.76 - 4.29 * (\delta^{18}\text{O}_c - \delta^{18}\text{O}_w)$
McConnaughey, 1988	1 colony of <i>Porites lobata</i>	Ecuador	21.5 to 25.3, 23.3	$T = ((\delta^{18}\text{O}_c - \delta^{18}\text{O}_w) + 0.594) - 0.209$
Chakraborty and Ramesh, 1993	1 colony of <i>Porites</i>	Lakshadweep Archipelago	26.5 to 32.0, 28.0	$T = 3.0 - 4.68 * (\delta^{18}\text{O}_c - \delta^{18}\text{O}_w)$
Leder et al., 1996	4 colonies of <i>O. annularis</i>	Florida	22.5 to 30.7, 26.6	$T = 5.33 - 4.51 * (\delta^{18}\text{O}_c - \delta^{18}\text{O}_w)$
Wellington et al., 1996	1 colony of <i>Porites lobata</i>	Ecuador	20.5 to 28.0, 23.6	$T = 3.97 - 4.48 * (\delta^{18}\text{O}_c - \delta^{18}\text{O}_w)$
Cardinal et al., 2001	2 colonies of <i>Diploria labyrinthiformis</i>	Bermuda	19.3 to 27.5, 21.9	$T = -8.6 - 7.4 * (\delta^{18}\text{O}_c - \delta^{18}\text{O}_w)$
Watanabe et al., 2001	1 colony of <i>O. faveolata</i>	Puerto Rico	24.7 to 31.1, 27.9	$T = ((\delta^{18}\text{O}_c - \delta^{18}\text{O}_w) + 0.75) - 0.19$
Felis et al., 2004	1 colony of <i>Porites</i>	Gulf of Aqaba, Red Sea	18.5 to 33.0, 27.7	$T = ((\delta^{18}\text{O}_c - \delta^{18}\text{O}_w) - 0.801) - 0.1514$
Smith et al., 2006	2 colonies of <i>O. faveolata</i>	Florida	23.1 to 30.0, 26.6	$T = ((\delta^{18}\text{O}_c - \delta^{18}\text{O}_w) + 1.24) - 0.101$
Kilbourne et al., 2010	2 colonies of <i>O. faveolata</i>	Puerto Rico	24.7 to 31.1, 27.9	$T = ((\delta^{18}\text{O}_c - \delta^{18}\text{O}_w) - 0.85) - 0.18$



Supplementary Table 4.1. Published Sr/Ca geothermometers.

Reference	Sample type	Equation
Elderfield et al. (2000)	Foraminifera- <i>G. hirsuta</i>	$T = \frac{Sr/Ca - 1.00}{0.04}$
	<i>G. truncatulinoides</i>	$T = \frac{Sr/Ca - 0.98}{0.03}$
	<i>G. inflata</i>	$T = \frac{Sr/Ca - 1.20}{0.02}$
Mortyn et al. (2005)	Foraminifera- <i>Globorotaliids</i>	$T = \frac{Sr/Ca - 1.10}{0.03}$
Cleroux et al. (2008)	Foraminifera- <i>Globorotalia</i>	$T = \frac{Sr/Ca - 1.10}{0.02}$
	<i>G. Turncatulinoides</i> + <i>G. Inflata</i>	$T = \frac{Sr/Ca - 1.05}{0.02}$
	<i>G. Inflata</i>	$T = \frac{Sr/Ca - 1.12}{0.02}$
	<i>G. Turncatulinoides</i> (dextral)	$T = \frac{Sr/Ca - 0.81}{0.04}$
	<i>G. Turncatulinoides</i> (sinistral)	$T = \frac{Sr/Ca - 1.01}{0.04}$

## REFERENCES

- Cleroux, C., Cortijo, E., Anand, P., Labeyrie, L., Bassinot, F., Caillon, N., Duplessy, J.C., 2008. Mg/Ca and Sr/Ca ratios in planktonic foraminifera: proxies for upper water column temperature reconstruction. *Paleoceanography* 23. doi:10.1029/2007PA001505.
- Elderfield, H., Cooper, M., Ganssen, G., 2000. Sr/Ca in multiple species of planktonic foraminifera: implications for reconstructions of seawater Sr/Ca. *Geochemistry Geophysics Geosystems* 1. doi: 10.1029/1999GC000031.
- Mortyn, P.G., Elderfield, H., Anand, P., Greavea, M., 2005. An evaluation of controls on planktonic foraminiferal Sr/Ca: comparison of water column and core-top data from a North Atlantic transect. *Geochemistry Geophysics Geosystems* 6. doi: 10.1029/2005GC001047.

Supplementary Table 4.2. Published Mg/Ca geothermometers.

Reference	Sample type	Equation
Rathburn and De Deckker (1997)	Foraminifera- <i>C.</i> <i>wuellerstorfi</i>	$T = \frac{(Mg/Ca - 1.39)}{0.342}$
	<i>C. wuellerstorfi/C.</i> <i>refulgens</i>	$T = \frac{(Mg/Ca - 1.73)}{0.277}$
Rosenthal et al. (1997)	Foraminifera- <i>C.</i> <i>pachyderma</i>	$T = \frac{\ln\left(\frac{Mg/Ca}{1.36}\right)}{0.044}$
Lea (1999)	Foraminifer- <i>O. universa</i>	$T = \frac{\ln\left(\frac{Mg/Ca}{1.36}\right)}{0.085}$
	<i>G. bulloides</i>	$T = \frac{\ln\left(\frac{Mg/Ca}{0.53}\right)}{0.10}$
Elderfield and Ganssen (2000)	Foraminifera- 8 species	$T = \frac{\ln\left(\frac{Mg/Ca}{0.52}\right)}{0.01}$
Toyofuku et al. (2000)	Foraminifera- <i>P.</i> <i>opercularis</i>	$T = 0.4403 * (Mg/Ca) - 39.15$ $T = 2.22 * (Mg/Ca) - 89.69$
	<i>Q. yabi</i>	$T = 0.3431 * (Mg/Ca) - 22.54$ $T = 2.90 * (Mg/Ca) - 65.98$
Toler et al. (2001)	Foraminifera- <i>A. angulatus</i>	$T = \frac{Mg/Ca - 6.4}{0.21}$
Billups and Schrag (2002)	Foraminifera- <i>C.</i> <i>wuellerstorfi</i>	$T = \frac{Mg/Ca - 0.76}{0.32}$
Elderfield et al. (2002)	Foraminifera- 16 species	$T = \frac{\ln\left(\frac{Mg/Ca}{0.35}\right)}{0.09}$
		$T = \frac{\ln\left(\frac{Mg/Ca}{0.89}\right)}{0.05}$
Lear et al. (2002)	Foraminifera- <i>Cibicides</i>	$T = \frac{\ln\left(\frac{Mg/Ca}{0.867}\right)}{0.109}$
	<i>Uvigerina</i>	$T = \frac{\ln\left(\frac{Mg/Ca}{0.924}\right)}{0.061}$

Reference	Sample type	Equation
	<i>Planulina</i>	$T = \frac{\ln\left(\frac{Mg/Ca}{0.788}\right)}{0.119}$
	<i>P. ariminensis</i>	$T = \frac{\ln\left(\frac{Mg/Ca}{0.911}\right)}{0.062}$
	<i>O. umbonta</i>	$T = \frac{\ln\left(\frac{Mg/Ca}{1.008}\right)}{0.114}$
		$T = \frac{\ln\left(\frac{Mg/Ca}{1.006}\right)}{0.10}$
		$T = \frac{\ln\left(\frac{Mg/Ca}{1.010}\right)}{0.11}$
	<i>M. barleeanus/M. pompilioides</i>	$T = \frac{\ln\left(\frac{Mg/Ca}{0.982}\right)}{0.101}$
Martin et al. (2002)	Foraminifera- <i>C. pachyderma</i>	$T = \frac{\ln\left(\frac{Mg/Ca}{0.85}\right)}{0.11}$
	<i>C. wuellerstorfi</i>	$T = \frac{\ln\left(\frac{Mg/Ca}{1.22}\right)}{0.109}$
	<i>Uvigerina</i> spp	$T = \frac{\ln\left(\frac{Mg/Ca}{0.76}\right)}{0.15}$
Rosenthal and Lohman (2002)	Foraminifera- <i>G. ruber</i>	$T = \frac{\ln\left(\frac{Mg/Ca}{(0.025 * weight\%) + 0.11}\right)}{0.095}$
	<i>G. sacculifer</i>	$T = \frac{\ln\left(\frac{Mg/Ca}{(0.032 * weight\%) + 0.181}\right)}{0.095}$
Anand et al. (2003)	Foraminifera- Average	$T = \frac{\ln\left(\frac{Mg/Ca}{0.38}\right)}{0.09}$
	<i>G. ruber</i> (pink)	$T = \frac{\ln\left(\frac{Mg/Ca}{0.383}\right)}{0.09}$
	<i>G. ruber</i> (white)	$T = \frac{\ln\left(\frac{Mg/Ca}{0.395}\right)}{0.09}$

Reference	Sample type	Equation
	<i>G. sacculifer</i> (with sac)	$T = \frac{\ln\left(\frac{Mg/Ca}{0.377}\right)}{0.09}$
	<i>N. duterteri</i>	$T = \frac{\ln\left(\frac{Mg/Ca}{0.342}\right)}{0.09}$
	<i>P. obliquilocilata</i>	$T = \frac{\ln\left(\frac{Mg/Ca}{0.328}\right)}{0.09}$
	<i>G. conglobatus</i>	$T = \frac{\ln\left(\frac{Mg/Ca}{0.347}\right)}{0.09}$
	<i>G. inflata</i>	$T = \frac{\ln\left(\frac{Mg/Ca}{0.229}\right)}{0.09}$
	<i>G. truncatulinoides</i>	$T = \frac{\ln\left(\frac{Mg/Ca}{0.359}\right)}{0.09}$
	<i>G. hisuta</i>	$T = \frac{\ln\left(\frac{Mg/Ca}{0.409}\right)}{0.09}$
	<i>G. crassaformis</i>	$T = \frac{\ln\left(\frac{Mg/Ca}{0.339}\right)}{0.09}$
Marchitto and deMenocal (2003)	Foraminifera- <i>C. pachyderma</i>	$T = \frac{Mg/Ca - 0.35}{0.25}$
Skinner et al. (2003)	Foraminifera- <i>G. affinis</i>	$T = \frac{\ln\left(\frac{Mg/Ca}{2.91}\right)}{0.08}$
		$T = \frac{Mg/Ca - 3.0}{0.025}$
Rathmann et al. (2004)	Foraminifera- <i>O. umbonta</i>	$T = \frac{\ln\left(\frac{Mg/Ca}{1.528}\right)}{0.09}$
Russell et al. (2004)	Foraminifera- <i>O. universa</i>	$T = \frac{\ln\left(\frac{Mg/Ca}{0.85}\right)}{0.096}$
Raja et al. (2005)	Foraminifera- <i>M. kudakajimaensis</i>	$T = \frac{\ln\left(\frac{Mg/Ca}{143.18}\right)}{0.0317}$
		$T = \frac{\ln\left(\frac{Mg/Ca}{145.71}\right)}{0.0313}$

Reference	Sample type	Equation
Toyofuku and Kitazato (2005)	Foraminifera- <i>P. opercularis</i>	$T = \frac{Mg/Ca - 81.5}{1.6}$
von Langen et al. (2005)	Foraminifera- <i>N. pachyderma</i>	$T = \frac{\ln\left(\frac{Mg/Ca}{0.51}\right)}{0.10}$
Elderfield et al. (2006)	Foraminifera- <i>Cibicides</i>	$T = \frac{\ln\left(\frac{Mg/Ca}{0.9}\right)}{0.11}$
	<i>C. kullenbergi</i>	$T = \frac{Mg/Ca - 0.88}{0.11}$
	<i>C. wuellerstorfi</i>	$T = \frac{Mg/Ca - 0.10}{0.42}$
		$T = \frac{Mg/Ca - 0.33}{0.47}$
		$T = \frac{Mg/Ca - 0.34}{0.34}$
		$T = \frac{Mg/Ca - 0.91}{0.44}$
		$T = \frac{Mg/Ca - 0.45}{0.77}$
	<i>Uvigerina</i>	$T = \frac{Mg/Ca - 0.87}{0.075}$
	<i>U. peregrina</i>	$T = \frac{Mg/Ca - 0.91}{0.065}$
	<i>M. barleeanus</i>	$T = \frac{Mg/Ca - 1.29}{0.18}$
Hintz et al. (2006)	Foraminifera- <i>B. aculeata</i>	$T = \frac{\ln\left(\frac{Mg/Ca}{0.29}\right)}{0.104}$
Rosenthal et al. (2006)	Foraminifers- <i>H. elegans</i>	$T = \frac{Mg/Ca - 0.96}{0.034}$
Black et al. (2007)	Foraminifera- <i>G. bulloides</i>	$T = 5.78 * \log(Mg/Ca) + 17.56$
Kristjansdottir et al. (2007)	Foraminifer- <i>M. barleeanus</i>	$T = \frac{\ln\left(\frac{Mg/Ca}{0.658}\right)}{0.137}$

Reference	Sample type	Equation
	<i>I. norcrossi/I. helenae</i>	$T = \frac{\ln\left(\frac{Mg/Ca}{1.051}\right)}{0.06}$
	<i>C. neoteretis</i>	$T = \frac{\ln\left(\frac{Mg/Ca}{0.864}\right)}{0.082}$
Marchitto et al. (2007)	Foraminifera- <i>C. pachyderma</i>	$T = \frac{Mg/Ca - 1.2}{0.116}$
Mekik et al. (2007)	Foraminifera- <i>G. bulloides</i>	$T = 19.03 * (Mg/Ca)^{0.4}$
	<i>P. obliquiloculata</i>	$T = 21.97 * (Mg/Ca)^{0.25}$
	<i>G. tumida</i>	$T = 15.95 * (Mg/Ca)^{0.06}$
	<i>N. dutertrei</i>	$T = 18.26 * (Mg/Ca)^{0.45}$
Bryan and Marchitto (2008)	Foraminifera- <i>U. peregrina</i>	$T = \frac{Mg/Ca - 0.77}{0.079}$
	<i>P. ariminensis</i>	$T = \frac{Mg/Ca - 0.05}{0.17}$
	<i>P. foveleolata</i>	$T = \frac{Mg/Ca - 2.10}{0.04}$
	<i>H. elegans</i>	$T = \frac{Mg/Ca - 1.01}{0.03}$
	<i>C. pachyderma</i>	$T = \frac{Mg/Ca - 1.20}{0.12}$
Evans et al. (2015)	Foraminifera- <i>O. ammonoides</i>	$T = \frac{Mg/Ca - 81.3}{2.57}$
		$T = \frac{Mg/Ca - 84.2}{2.42}$
Titelboim et al. (2017)	Foraminifera- <i>P. calcariformata</i>	$T = \frac{Mg/Ca - 48.27}{3.20}$
	<i>Lachlanella</i>	$T = \frac{Mg/Ca - 56.88}{3.30}$
Maeda et al. (2018)	Foraminifera- Average	$T = \frac{Mg/Ca - 74.70}{2.73}$
	<i>N. calcar</i>	$T = \frac{Mg/Ca - 72.50}{2.84}$
	<i>B. sphaerulata</i>	$T = \frac{Mg/Ca - 68.40}{2.97}$
	<i>C. gaudichaudii</i>	$T = \frac{Mg/Ca - 84.00}{2.34}$

## REFERENCES

- Anand, P., Elderfield, H., Conte, M.H., 2003. Calibration of Mg/Ca thermometry in planktonic foraminifera from a sediment trap time series. *Paleoceanography* 18. doi:10.1029/2002PA000846.
- Billups, K., Schrag, D.P., 2002. Paleotemperatures and ice volume of the past 27 Myr revisited with paired Mg/Ca and  $^{18}\text{O}/^{16}\text{O}$  measurements on benthic foraminifera. *Paleoceanography* 17. doi: 10.1029/2000PA000567.
- Black, D.E., Abahazi, M.A., Thunell, R.C., Kaplan, A., Tappa, E.J., Peterson, L.C., 2007. An 8-century tropical Atlantic SST record from the Cariaco Basin: baseline variability, twentieth-century warming, and Atlantic hurricane frequency. *Paleoceanography* 22, 4023-4034.
- Bryan, S.P., Marchitto, T.M., 2008. Mg/Ca-temperature proxy in benthic foraminifera: new calibrations from the Florida Straits and a hypothesis regarding Mg/Li. *Paleoceanography* 23. doi: 10.1029/2000PA000567.
- Elderfield, H., Ganssen, G., 2000. Past temperature and delta-18O of surface ocean waters inferred from foraminiferal Mg/Ca ratios. *Nature* 405, 442-445.
- Elderfield, H., Vautravers, M., Cooper, M., 2002. The relationship between shell size and Mg/Ca, Sr/Ca,  $\delta^{18}\text{O}$ , and  $\delta^{13}\text{C}$  of species of planktonic foraminifera. *Geochemistry Geophysics Geosystems* 3. doi: 10.1029/2001GC000194.
- Elderfield, H., Yu, J., Anand, P., Kiefer, T., Nyland, B., 2006. Calibrations for benthic foraminiferal Mg/Ca paleothermometry and the carbonate ion hypothesis. *Earth and Planetary Science Letters* 250, 633-649.
- Evans, D., Erez, J., Oron, S., Muller, W., 2015. Mg/Ca-temperature and seawater-test chemistry relationships in the shallow-dwelling large benthic foraminifera *Operculina ammonoides*. *Geochimica et Cosmochimica Acta* 148, 325-342.
- Hintz, C.J., Shaw, T.J., Bernhard, J.M., Chandler, G.T., McCorkle, D.C., Blanks, J.K., 2006. Trace/minor element:calcium ratios in cultured benthic foraminifera. Part I: inter-species

- and inter-individual variability. *Geochimica et Cosmochimica Acta* 70, 1952-1963.
- Kristjansdottir, G.B., Lea, D.W., Jennings, A.E., Pak, D.K., Belanger, C., 2007. New spatial Mg/Ca-temperature calibrations for three Arctic, benthic foraminifera and reconstruction of north Iceland shelf temperature for the past 4000 years. *Geochemistry Geophysics Geosystems* 8. doi: 10.1029/2006GC001425.
- Lea, D.W., 1999. Trace elements in foraminiferal calcite. In: Sen Gupta, B.K. (Ed.), *Modern foraminifera*. Kluwer Academic Publishing, Dordrecht, pp. 259-277.
- Lear, C.H., Rosenthal, Y., Slowey, N., 2002. Benthic foraminiferal Mg/Ca paleothermometry: a revised core-top calibration. *Geochimica et Cosmochimica Acta* 66, 3375-3387.
- Maeda, A., Fujita, K., Horikawa, K., Suzuki, A., Ohno, Y., Kawahata, H., 2018. Calibration between temperature and Mg/Ca and oxygen isotope ratios in high-magnesium calcite tests of asexually reproduced juveniles of large benthic foraminifera. *Marine Micropaleontology* 143, 63-69.
- Marchitto, T.M., deMenocal, P., 2003. Late Holocene variability of upper North Atlantic Deep Water temperature and salinity. *Geochemistry Geophysics Geosystems* 4. doi: 10.1029/2003GC000598.
- Marchitto, T.M., Bryan, S.P., Curry, W.B., McCorkle, D.C., 2007. Mg/Ca temperature calibration for the benthic foraminifer *Cibicides pachyderma*. *Paleoceanography* 22. doi: 10.1029/2006PA001287.
- Martin, P.A., Lea, D.W., Rosenthal, Y., Shackleton, N.J., Sarinthein, M., Papenfuss, T., 2002. Quaternary deep sea temperature histories derived from benthic foraminiferal Mg/Ca. *Earth and Planetary Science Letters* 198, 193-209.
- Mekik, F., Francois, R., M, S., 2007. A novel approach to dissolution correction of Mg/Ca-based paleothermometry in the tropical Pacific. *Paleoceanography and Paleoclimatology* 22. doi: 10.1029/2007PA001504.
- Raja, R., Saraswati, P.K., Rogers, K., Iwao, K., 2005. Magnesium and strontium compositions of recent symbiont-bearing benthic foraminifera. *Marine Micropaleontology* 58, 31-44.



- Rathburn, A.E., De Deckker, P., 1997. Magnesium and strontium compositions of recent benthic foraminifera from the Coral Sea, Australia and Prydz Bay, Antarctica. *Marine Micropaleontology* 32, 231-248.
- Rathmann, S., Hess, S., Kuhnert, H., Mulitza, S., 2004. Mg/Ca ratios of the benthic foraminifera *Oridorsalis umbonatus* obtained by laser ablation from core top sediments: relationship to bottom water temperature. *Geochemistry Geophysics Geosystems* 5. doi: 10.1029/2004GC000808.
- Rosenthal, Y., Lohman, K.C., 2002. Accurate estimation of sea surface temperatures using dissolution-corrected calibrations for Mg/Ca paleothermometry. *Paleoceanography* 17. doi: 10.1029/2001PA000749.
- Rosenthal, Y., Boyle, E., Slowey, N., 1997. Temperature control on the incorporation of magnesium, strontium, fluorine and cadmium into benthic foraminiferal shells from Little Bahama Bank: prospects for thermocline paleoceanography. *Geochimica et Cosmochimica Acta* 61, 231-248.
- Rosenthal, Y., Lear, C.H., Oppo, D.W., Linsley, B.K., 2006. Temperature and carbonate ion effects on Mg/Ca and Sr/Ca ratios in benthic foraminifera: the aragonite species *Hoeglundina elegans*. *Paleoceanography* 21. doi: 10.1029/2005PA001158.
- Russell, A.D., Honish, B., Spero, H.J., Lea, D.W., 2004. Seawater carbonate chemistry, processes and elements during experiments with planktonic foraminifera *Orbulina universa*. *Geochimica et Cosmochimica Acta* 68, 4347-4361.
- Skinner, L.C., Shackleton, N.J., Elderfield, H., 2003. Millennial-scale variability of deep-water temperature and  $\delta^{18}\text{O}_{\text{dw}}$  indicating deep-water source variations in the Northeast Atlantic, 0-34 cal. ka BP. *Geochemistry Geophysics Geosystems* 4, 1098.
- Titelboim, D., Sadekov, A., Almogi-Labin, A., Herut, B., Kucera, M., Schmidt, C., Hyams-Kaphzan, O., Abramovich, S., 2017. Geochemical signatures of benthic foraminiferal shells from a heat-polluted shallow marine environment provide field evidence for growth and calcification under extreme warmth. *Global Change Biology* 23, 4346-4353.

- Toler, S.K., Hallock, P., Schijf, J., 2001. Mg/Ca ratios in stressed foraminifera, *Amphistegina gibbosa*, from the Florida Keys. *Marine Micropaleontology* 43, 199-206.
- Toyofuku, T., Kitazato, H., 2005. Micromapping of Mg/Ca values in cultured specimens of the high-magnesium benthic foraminifera. *Geochemistry Geophysics Geosystems* 6. doi: 10.1029/2005GC000961.
- Toyofuku, T., Kitazato, H., Kawahata, H., Tsuchiya, M., Nohara, M., 2000. Evaluation of Mg/Ca thermometry in foraminifera: comparison of experimental results and measurements in nature. *Paleoceanography* 15, 456-464.
- von Langen, P.J., Pak, D.K., Spero, H.J., Lea, D.W., 2005. Effects of temperature on Mg/Ca in neogloboquadrinid shells determined by living culturing. *Geochemistry Geophysics Geosystems* 6. doi: 10.1029/2005GC000989.

Supplementary Table 4.33. Published  $\delta^{18}\text{O}$ -geothermometers.

Reference	Sample type	Equation
McCrea (1950)	Abiogenic carbonate	$T = 16.0 + (5.1 * (\delta^{18}\text{O}_{\text{carb}} - \delta^{18}\text{O}_{\text{water}}) + 0.9 * (\delta^{18}\text{O}_{\text{carb}} - \delta^{18}\text{O}_{\text{water}})^2)$
Epstein et al. (1953)	Biogenic calcite	$T = 16.5 - (4.34 * (\delta^{18}\text{O}_{\text{carb}} + 0.27) + 0.14 * (\delta^{18}\text{O}_{\text{carb}} + 0.27)^2)$
Craig (1965)	Abiogenic carbonate	$T = 16.9 - (4.2 * (\delta^{18}\text{O}_{\text{carb}} - \delta^{18}\text{O}_{\text{water}}) + 0.13 * (\delta^{18}\text{O}_{\text{carb}} - \delta^{18}\text{O}_{\text{water}})^2)$
O'Neil et al. (1969)	Abiogenic carbonate	$T = \sqrt{\frac{1000 \ln a(\delta^{18}\text{O}_{\text{carb}} - \delta^{18}\text{O}_{\text{water}}) - 3.9}{2.78}} - 273.15$
Shackleton (1974)	Biogenic calcite	$T = 16.9 - (4.32 * (\delta^{18}\text{O}_{\text{carb}} + 0.2) + 0.13 * (\delta^{18}\text{O}_{\text{carb}} + 0.2)^2)$
Aharon and Chappell (1983)	Biogenic aragonite	$T = 21.3 - (4.42 * (\delta^{18}\text{O}_{\text{carb}} - \delta^{18}\text{O}_{\text{water}}))$
Anderson and Arthur (1983)	Biogenic calcite	$T = 16.0 - (4.14 * \delta^{18}\text{O}_{\text{carb}} - \delta^{18}\text{O}_{\text{water}}) + 0.13 * (\delta^{18}\text{O}_{\text{carb}} - \delta^{18}\text{O}_{\text{water}})^2)$
Erez and Luz (1983)	Foraminifera- <i>G. sacculifer</i>	$T = 17.0 - (4.52 * (\delta^{18}\text{O}_{\text{carb}} - \delta^{18}\text{O}_{\text{water}}) + 0.03 * (\delta^{18}\text{O}_{\text{carb}} - \delta^{18}\text{O}_{\text{water}})^2)$
Dunbar and Wefer (1984)	Biogenic calcite	$T = 3.73 * ((\delta^{18}\text{O}_{\text{carb}} - \delta^{18}\text{O}_{\text{water}}) - 5.1)$
Bouvier-Soumagnac and Duplessy (1985)	Foraminifera- <i>O. universa</i>	$T = 16.4 - (4.67 * (\delta^{18}\text{O}_{\text{carb}} - \delta^{18}\text{O}_{\text{water}}))$
	<i>G. menardii</i>	$T = 15.4 - (4.81 * (\delta^{18}\text{O}_{\text{carb}} - \delta^{18}\text{O}_{\text{water}}))$
	<i>N. dutertrei</i>	$T = 14.6 - (5.03 * (\delta^{18}\text{O}_{\text{carb}} - \delta^{18}\text{O}_{\text{water}}))$
Grossman and Ku (1986)	Biogenic aragonite	$T = 10.5 - (6.58 * (\delta^{18}\text{O}_{\text{carb}} - \delta^{18}\text{O}_{\text{water}}))$
		$T = \frac{(\frac{1000 \ln a(\delta^{18}\text{O}_{\text{carb}} - \delta^{18}\text{O}_{\text{water}}) - 31.08}{18.07})}{10^3} - 273.15$
Hudson and Anderson (1989)	Biogenic aragonite	$T = 19.7 - (4.34 * (\delta^{18}\text{O}_{\text{carb}} - \delta^{18}\text{O}_{\text{water}}))$
Hays and Grossman (1991)	Biogenic calcite	$T = 15.7 - (4.36 * (\delta^{18}\text{O}_{\text{carb}} - \delta^{18}\text{O}_{\text{water}}) + 0.12 * (\delta^{18}\text{O}_{\text{carb}} - \delta^{18}\text{O}_{\text{water}})^2)$
Patterson et al. (1993)	Biogenic aragonite	$T = \frac{(\frac{1000 \ln a(\delta^{18}\text{O}_{\text{carb}} - \delta^{18}\text{O}_{\text{water}}) - 33.49}{18.56})}{10^3} - 273.15$
Kim and O'Neil (1997)	Abiogenic carbonate	$T = \frac{(\frac{1000 \ln a(\delta^{18}\text{O}_{\text{carb}} - \delta^{18}\text{O}_{\text{water}}) - 32.42}{18.03})}{10^3} - 273.15$
Thorrold et al. (1997)	Biogenic aragonite	$T = \frac{18560}{1000 \ln a(\delta^{18}\text{O}_{\text{carb}} - \delta^{18}\text{O}_{\text{water}}) + 32.543} - 273.15$

Reference	Sample type	Equation
Bemis et al. (1998)	Foraminifera- <i>O. universa</i>	$T = 16.5 - (4.80 * (\delta^{18}O_{carb} - \delta^{18}O_{water}))$ $T = 14.9 - (4.80 * (\delta^{18}O_{carb} - \delta^{18}O_{water}))$ $T = 13.2 - (4.89 * (\delta^{18}O_{carb} - \delta^{18}O_{water}))$ $T = 16.1 - (4.76 * (\delta^{18}O_{carb} + 0.27))$ $T = 21.4 - (4.83 * (\delta^{18}O_{carb} - \delta^{18}O_{water}))$ 18450 $T = \frac{1000 \ln a(\delta^{18}O_{carb} - \delta^{18}O_{water}) + 32.54}{17400} - 273.15$
Lynch-Stieglitz et al. (1999)	<i>G. bulloides</i>	
White et al. (1999)	Biogenic calcite	
Bohm et al. (2000)	Biogenic aragonite	
Mulitza et al. (2003)	Foraminifera- <i>G. sacculifer</i>	
	<i>G. bulloides</i>	
	<i>C. gaudichaudii</i>	
	<i>N. calcar</i>	
Spero et al. (2003)	Foraminifera- <i>G. bulloides</i>	
	<i>O. universa</i>	
	<i>G. menardii</i>	
	<i>G. sacculifer</i>	
Coplen (2007)	Abiogenic carbonates	$T = \frac{17400}{1000 \ln a(\delta^{18}O_{carb} - \delta^{18}O_{water}) + 28.6} - 273.15$
Kim et al. (2007)	Abiogenic carbonate	$T = \frac{17880}{1000 \ln a(\delta^{18}O_{carb} - \delta^{18}O_{water}) + 31.14} - 273.15$
Chacko and Deines (2008)	Abiogenic carbonate	Computer program
Grossman (2012)	Abiogenic carbonates	$T = 13.7 - (4.54 * (\delta^{18}O_{carb} - \delta^{18}O_{water}) + (\delta^{18}O_{carb} - \delta^{18}O_{water})^2)$
Kele et al. (2015)	Abiogenic carbonate	20000 $T = \frac{1000 \ln a(\delta^{18}O_{carb} - \delta^{18}O_{water}) + 36.0}{17400} - 273.15$
Maeda et al. (2018)	<i>B. sphaerulata</i>	$T = 16.1 - (5.10 * (\delta^{18}O_{carb} - \delta^{18}O_{water}))$

## REFERENCES

- Aharon, P., Chappell, J., 1983. Carbon and oxygen isotope probes of reef environment histories. In: Barnes, D.J. (Ed.), *Perspectives on coral reefs*. Australian Institute of Marine Science, pp. 1-10.
- Anderson, T.F., Arthur, M.A., 1983. Stable isotopes of oxygen and carbon and their application to sedimentological and paleoenvironmental problems. *Stable Isotopes in Sedimentary Geology*. SEPM Short Course 10, 1-151.
- Bemis, B.E., Spero, H.J., Bijma, J., Lea, D.W., 1998. Reevaluation of the oxygen isotopic composition of planktonic foraminifera: experimental results and revised paleotemperature equations. *Paleoceanography* 13, 150-160.
- Bohm, F., Joachimski, M.M., Dullo, W., Eisenhauer, A., Lehnert, H., Reitner, J., Worheide, G., 2000. Oxygen isotope fractionation in marine aragonite of coralline sponges. *Geochimica et Cosmochimica Acta* 64, 1695-1703.
- Bouvier-Soumagnac, Y., Duplessy, J.C., 1985. Carbon and oxygen isotopic composition of planktonic foraminifera from laboratory culture, planktonic tows and recent sediment: implications for the reconstruction of paleoclimatic conditions and of the global carbon cycle. *Journal of Foraminiferal Research* 15, 302-320.
- Chacko, T., Deines, P., 2008. Theoretical calculation of oxygen isotope fractionation factors in carbonate systems. *Geochimica et Cosmochimica Acta* 72, 3642-3660.
- Coplen, T.B., 2007. Calibration of the calcite-water oxygen-isotope geothermometer at Devils Hole, Nevada, a natural laboratory. *Geochimica et Cosmochimica Acta* 71, 3948-3957.
- Craig, H., 1965. The measurement of oxygen isotope paleotemperatures. In: E., Tongiorgi. (Ed.), *Stable Isotopes in Oceanographic Studies and Paleotemperatures*. Spoleto, Consiglio Nazionale delle Ricerche, Laboratorio de Geologica Nucleare, Pisa, pp. 161-182.
- Dunbar, R.B., Wefer, G., 1984. Stable isotope fractionation in benthic foraminifera from the Peruvian Continental Margin. *Marine Geology* 59, 215-225.
- Epstein, S., Buchsbaum, R., Lowenstam, H., Urey, H.C., 1953. Revised carbonate-water isotopic

- temperature scale. *Geological Society of America Bulletin* 64, 1315-1325.
- Erez, J., Luz, B., 1983. Experimental paleotemperature equation for planktonic foraminifera. *Geochimica et Cosmochimica Acta* 47, 1025-1031.
- Grossman, E.L., 2012. Applying oxygen isotope paleothermometry in deep time. *Paleontological Society Papers* 18, 39-67.
- Grossman, E.L., Ku, T.L., 1986. Oxygen and carbon isotope fractionation in biogenic aragonite: temperature effects. *Chemical Geology* 59, 59-74.
- Hays, P.D., Grossman, E.L., 1991. Oxygen isotopes in meteoric calcite cements as indicators of continental paleoclimate. *Geology* 19, 441-444.
- Hudson, J.D., Anderson, T.F., 1989. Ocean temperatures and isotopic compositions through time. *Transactions of the Royal Society of Edinburgh: Earth Science* 80, 183-192.
- Kele, S., Breitenbach, S.F.M., Capezzuoli, E., Meckler, A.N., Ziegler, M., Millan, I.M., Kluge, T., Deak, J., Hanselmann, K., John, C.M., Yan, H., Liu, Z., Bernasconi, S.M., 2015. Temperature dependence of oxygen- and clumped-isotope fractionation in carbonates: a study of travertines and tufas in the 6-95°C temperature range. *Geochimica et Cosmochimica Acta* 168, 172-192.
- Kim, S., O'Neil, J.R., 1997. Equilibrium and nonequilibrium oxygen isotope effects in synthetic carbonates. *Geochimica et Cosmochimica Acta* 61, 3461-3475.
- Kim, S., O'Neil, J.R., Hillaire-Marcel, C., Mucci, A., 2007. Oxygen isotope fractionation between synthetic aragonite and water: influence of temperature and  $Mg^{2+}$  concentration. *Geochimica et Cosmochimica Acta* 71, 4704-4715.
- Lynch-Stieglitz, J., Curry, W.B., Slowey, N., 1999. A geostrophic transport estimate for Florida Current from the oxygen isotope composition of benthic foraminifera. *Palaeogeography* 14, 360-373.
- Maeda, A., Fujita, K., Horikawa, K., Suzuki, A., Ohno, Y., Kawahata, H., 2018. Calibration between temperature and Mg/Ca and oxygen isotope ratios in high-magnesium calcite tests of asexually reproduced juveniles of large benthic foraminifers. *Marine*

- Micropaleontology 143, 63-69.
- McCrea, J.M., 1950. On the isotopic chemistry of carbonates and a paleotemperature scale. *Journal of Chemical Physics* 18, 849-859.
- Mulitza, S., Donner, B., Fischer, G., Paul, A., Patzold, J., Ruhlemann, C., Segl, M., 2003. The South Atlantic oxygen isotope record of planktic foraminifera. In: Wefer, G., Mulitza, S., Ratmeyer, V. (Eds.), *The South Atlantic in the Late Quaternary*. Springer, Berlin, Heidelberg.
- O'Neil, J.R., Clayton, R.N., Mayeda, T.K., 1969. Oxygen isotopes fractionation in divalent metal carbonates. *Journal of Chemical Physics* 51, 5547- 5560.
- Patterson, W.P., Smith, G.R., Lohmann, K.C., 1993. Continental paleothermometry and seasonality using the isotopic composition of aragonitic otoliths of freshwater fishes. In: Swart, P.K., Lohman, K.C., McKenzie, J., Savin, S. (Eds.), *Climate Change in Continental Isotopic Records*. Geophysical Monograph Series. American Geophysical Union, Washington, D.C., 78, pp. 191-202.
- Shackleton, N.J., 1974. Attainment of isotopic equilibrium between ocean water and the benthonic foraminifera genus *Uvigerina*: isotopic changes in the ocean during the last glacial. *Colloques Internationaux du Centre National de la Recherche Scientifique* 219, 203-210.
- Spero, H.J., Mielke, K.M., Kalve, E.M., Lea, D.W., Pak, D.K., 2003. Multispecies approach to reconstructing eastern equatorial Pacific thermocline hydrography during the past 360 kyr. *Paleoceanography* 18. doi: 10.1029/2002PA000814.
- Thorrold, S.R., Campana, S.E., Jones, C.M., Swart, P.K., 1997. Factors determining  $\delta^{13}\text{C}$  and  $\delta^{18}\text{O}$  fractionation in aragonitic otoliths of marine fish. *Geochimica et Cosmochimica Acta* 61, 2909-2919.
- White, R.M.P., Dennis, P.F., Atkinson, T.C., 1999. Experimental calibration and field investigation of the oxygen isotopic fractionation between biogenic aragonite and water. *Rapid Communications in Mass Spectrometry* 13, 1242-1247.

**Table 5.1.** Subsamples collected from Unit D of the Ironshore Formation, corals RWP-D, IS1, and GTH-D. Distance measured from the base of the coral upwards. Calculated temperatures are determined from the geothermometer of Booker et al. (2019),  $\delta^{18}\text{O}_{\text{water}}$  value of +0.1‰.

Unit D	Distance (cm)	$\delta^{13}\text{C}_{\text{VPDB}}$ (‰)	$\delta^{18}\text{O}_{\text{VPDB}}$ (‰)	$\delta^{18}\text{O}_{\text{VSMOW}}$ (‰)	Calculated Temperatures (°C)
RWP-D Piece 1					
a	0.2	+1.23	-2.89	+27.9	21.6
b	0.3	+0.99	-3.09	+27.7	22.6
c	0.5	+1.59	-2.79	+28.0	21.1
d	0.7	+1.87	-2.66	+28.2	20.4
e	0.8	+1.62	-2.66	+28.2	20.4
f	1.0	+0.03	-3.31	+27.5	23.6
g	1.2	+0.55	-3.41	+27.4	24.1
h	1.4	-0.01	-3.76	+27.0	25.8
i	1.5	+0.79	-3.36	+27.4	23.9
j	1.7	-0.10	-3.53	+27.3	24.7
k	1.9	+0.26	-3.54	+27.3	24.8
l	2.1	0.00	-3.65	+27.1	25.3
m	2.3	+0.68	-3.96	+26.8	26.8
n	2.5	+0.52	-4.07	+26.7	27.4
o	2.6	+1.86	-3.19	+27.6	23.1
p	2.7	+1.37	-3.63	+27.2	25.2
q	2.9	+1.70	-3.91	+26.9	26.6
r	3.1	+0.09	-3.48	+27.3	24.5
s	3.2	+0.83	-4.35	+26.4	28.8
t	3.4	+1.41	-4.14	+26.6	27.7



Unit D	Distance (cm)	$\delta^{13}\text{C}_{\text{VPDB}}$ (‰)	$\delta^{18}\text{O}_{\text{VPDB}}$ (‰)	$\delta^{18}\text{O}_{\text{VSMOW}}$ (‰)	Calculated Temperatures (°C)
u	3.5	+1.23	-4.13	+26.7	27.7
v	3.7	+0.62	-3.99	+26.8	27.0
w	3.9	+0.22	-4.10	+26.7	27.5
x	4.1	+0.22	-4.16	+26.6	27.8
y	4.3	-0.12	-4.10	+26.7	27.5
z	4.4	-0.52	-4.18	+26.6	27.9
aa	4.6	-0.02	-4.07	+26.7	27.4
ab	4.8	+0.10	-3.92	+26.9	26.6
ac	4.9	-0.10	-4.05	+26.7	27.3
ad	5.1	-0.78	-4.19	+26.6	28.0
ae	5.2	-0.05	-3.91	+26.9	26.6
af	5.5	-0.04	-3.70	+27.1	25.6
ag	5.7	+0.23	-3.66	+27.1	25.3
ah	5.9	-0.24	-4.03	+26.8	27.2
ai	6.0	-0.42	-4.17	+26.6	27.9
aj	6.2	-0.15	-3.52	+27.3	24.7
ak	6.3	-0.07	-3.49	+27.3	24.5
al	6.4	-0.41	-3.70	+27.1	25.5
am	6.5	-0.41	-3.90	+26.9	26.5
an	6.6	-0.77	-3.89	+26.9	26.5
ao	6.8	-0.34	-3.57	+27.2	24.9
ap	6.9	-0.28	-3.71	+27.1	25.6
aq	7.1	-0.90	-3.82	+27.0	26.1
ar	7.3	+0.12	-3.42	+27.4	24.2
as	7.6	+0.24	-3.35	+27.5	23.8

Unit D	Distance (cm)	$\delta^{13}\text{C}_{\text{VPDB}}$ (‰)	$\delta^{18}\text{O}_{\text{VPDB}}$ (‰)	$\delta^{18}\text{O}_{\text{VSMOW}}$ (‰)	Calculated Temperatures (°C)
Piece 2					
at	0.2	+0.41	-3.68	+27.1	25.4
au	0.4	+0.33	-3.60	+27.2	25.1
av	0.5	+0.25	-3.54	+27.3	24.8
aw	0.7	+0.56	-3.55	+27.2	24.8
ax	0.9	+0.28	-3.98	+26.8	26.9
ay	1.1	-0.62	-3.74	+27.1	25.8
az	1.3	-0.31	-3.81	+27.0	26.1
ba	1.5	-0.24	-4.63	+26.1	30.1
bb	1.8	+0.39	-4.01	+26.8	27.1
bc	2.0	-0.11	-4.18	+26.6	27.9
bd	2.3	+0.29	-4.01	+26.8	27.0
be	2.6	+0.39	-4.32	+26.5	28.6
bf	2.8	-0.41	-3.94	+26.8	26.7
bg	3.1	+0.01	-4.15	+26.6	27.8
bh	3.3	+0.39	-4.02	+26.8	27.1
bi	3.5	-0.36	-4.24	+26.5	28.2
bj	3.7	+0.32	-3.84	+26.9	26.3
bk	3.9	-1.67	-4.97	+25.8	31.8
bl	4.2	-0.68	-3.92	+26.9	26.6
bm	4.5	+0.40	-3.60	+27.2	25.1
bn	4.8	+0.39	-4.23	+26.5	28.2
bo	5.0	-0.74	-4.80	+26.0	31.0
bp	5.2	-0.58	-4.23	+26.6	28.1
bq	5.5	+0.04	-4.40	+26.4	29.0

Unit D	Distance (cm)	$\delta^{13}\text{C}_{\text{VPDB}}$ (‰)	$\delta^{18}\text{O}_{\text{VPDB}}$ (‰)	$\delta^{18}\text{O}_{\text{VSMOW}}$ (‰)	Calculated Temperatures (°C)
br	5.7	-0.54	-4.33	+26.4	28.6
bs	6.0	+0.54	-4.09	+26.7	27.4
bt	6.3	-0.53	-4.53	+26.2	29.6
bu	6.5	+0.27	-4.06	+26.7	27.3
bv	6.7	+0.46	-4.54	+26.2	29.7
bw	7.1	-0.31	-4.48	+26.3	29.4
bx	7.3	+1.10	-4.19	+26.6	28.0
by	7.5	+0.04	-4.62	+26.2	30.0
bz	7.7	+0.41	-3.92	+26.9	26.6
ca	8.0	+0.65	-4.38	+26.4	28.9
cb	8.2	-0.77	-4.51	+26.3	29.5
cc	8.4	+0.55	-4.22	+26.6	28.1
cd	8.7	-0.65	-4.45	+26.3	29.3
ce	8.9	+0.29	-3.93	+26.9	26.7
cf	9.1	-0.74	-4.03	+26.8	27.2
<hr/>					
IS1					
<hr/>					
a	1.0	+0.25	-3.84	+26.9	26.2
b	1.2	+0.45	-4.32	+26.5	28.6
c	1.5	0.00	-4.38	+26.4	28.9
d	1.8	-0.48	-4.33	+26.4	28.7
e	2.3	-0.10	-3.91	+26.9	26.6
f	2.	-0.50	-5.04	+25.7	32.1
g	2.9	-0.03	-4.74	+26.0	30.6
h	3.1	-0.18	-4.19	+26.6	28.0
i	3.3	-0.90	-4.63	+26.1	30.1

Unit D	Distance (cm)	$\delta^{13}\text{C}_{\text{VPDB}}$ (‰)	$\delta^{18}\text{O}_{\text{VPDB}}$ (‰)	$\delta^{18}\text{O}_{\text{VSMOW}}$ (‰)	Calculated Temperatures (°C)
j	3.6	-0.24	-3.79	+27.0	26.0
k	3.8	-0.24	-4.11	+26.7	27.6
l	3.9	+0.34	-3.96	+26.8	26.8
m	4.1	-0.35	-4.70	+26.1	30.5
n	4.3	-1.08	-4.41	+26.4	29.0
o	4.6	-0.31	-4.02	+26.8	27.1
p	4.8	+0.02	-3.89	+26.9	26.5
q	5.2	-0.73	-4.34	+26.4	28.7
r	5.5	-0.66	-3.65	+27.1	25.3
s	5.8	-0.87	-4.17	+26.6	27.9
t	6.0	-0.69	-4.28	+26.5	28.4
u	6.2	-0.24	-3.81	+27.0	26.1
v	6.4	-1.06	-4.34	+26.4	28.7
w	6.6	-0.20	-4.45	+26.3	29.2
x	6.8	+0.49	-3.63	+27.2	25.2
y	7.0	+0.28	-3.94	+26.8	26.7
z	7.4	-0.56	-4.26	+26.5	28.3
aa	7.7	-0.07	-3.84	+26.9	26.3
ab	7.9	-0.27	-4.05	+26.7	27.3
ac	8.1	-1.17	-4.38	+26.4	28.9
ad	8.3	-0.18	-3.67	+27.1	25.4
ae	8.6	-0.94	-4.17	+26.6	27.9
af	8.8	-0.02	-3.56	+27.2	24.9
ag	9.0	+0.06	-3.88	+26.9	26.4
ah	9.1	+0.05	-3.98	+26.8	26.9

Unit D	Distance (cm)	$\delta^{13}\text{C}_{\text{VPDB}}$ (‰)	$\delta^{18}\text{O}_{\text{VPDB}}$ (‰)	$\delta^{18}\text{O}_{\text{VSMOW}}$ (‰)	Calculated Temperatures (°C)
ai	9.4	-0.30	-3.86	+26.9	26.3
aj	9.6	+0.37	-3.71	+27.1	25.6
ak	9.9	-1.12	-4.80	+26.0	30.9
al	10.1	-0.86	-3.96	+26.8	26.8
am	10.3	-0.25	-3.87	+26.9	26.4
an	10.5	-0.71	-4.24	+26.5	28.2
ao	10.8	-0.15	-3.86	+26.9	26.3
ap	11.1	+0.22	-3.75	+27.0	25.8
aq	11.3	-0.34	-3.92	+26.9	26.6
ar	11.6	+0.27	-3.59	+27.2	25.0
as	11.8	-0.29	-3.95	+26.8	26.8
at	12.1	-0.68	-3.86	+26.9	26.3
au	12.3	+0.43	-4.31	+26.5	28.6
av	12.5	-0.27	-4.63	+26.1	30.1
aw	12.7	+0.97	-3.76	+27.0	25.8
ax	13.0	+0.16	-3.66	+27.1	25.3
ay	13.4	+0.86	-3.80	+27.0	26.0
az	13.6	+1.08	-4.06	+26.7	27.3
ba	13.8	-0.94	-4.43	+26.3	29.1
bb	14.1	-0.45	-3.98	+26.8	26.9
bc	14.3	-0.59	-3.80	+27.0	26.0
bd	14.5	-0.75	-4.01	+26.8	27.1
be	14.8	-0.40	-3.41	+27.4	24.1
GTH-D					

Unit D	Distance (cm)	$\delta^{13}\text{C}_{\text{VPDB}}$ (‰)	$\delta^{18}\text{O}_{\text{VPDB}}$ (‰)	$\delta^{18}\text{O}_{\text{VSMOW}}$ (‰)	Calculated Temperatures (°C)
a	0.9	-0.52	-2.69	+28.1	20.6
b	1.1	-0.88	-2.56	+28.3	19.9
c	1.3	-0.03	-3.21	+27.6	23.1
d	1.6	-0.66	-2.89	+27.9	21.6
e	1.9	-0.60	-2.63	+28.2	20.3
f	2.1	-0.64	-2.94	+27.9	21.8
g	2.3	-0.49	-2.89	+27.9	21.6
h	2.8	-0.51	-3.23	+27.6	23.2
i	3.3	-0.64	-2.81	+28.0	21.2
j	3.7	-0.34	-2.65	+28.2	20.4
k	3.8	-0.30	-3.07	+27.7	22.4
l	4.0	+0.61	-2.76	+28.1	20.9
m	4.4	+0.34	-2.93	+27.9	21.8
n	4.9	+1.05	-2.60	+28.2	20.1
o	5.3	+0.22	-2.83	+28.0	21.3
p	5.7	-0.49	-3.45	+27.4	24.3
q	5.9	+0.09	-2.96	+27.9	21.9
r	6.2	+0.57	-2.56	+28.3	20.0
s	6.8	+0.19	-2.61	+28.2	20.2
t	7.2	+0.46	-2.72	+28.1	20.7
u	7.5	+0.61	-2.80	+28.0	21.1
v	7.8	+0.86	-2.72	+28.1	20.8
w	8.3	+0.23	-2.68	+28.2	20.5
x	8.8	+0.23	-3.04	+27.8	22.3
y	9.5	+0.11	-3.00	+27.8	22.1

Unit D	Distance (cm)	$\delta^{13}\text{C}_{\text{VPDB}}$ (‰)	$\delta^{18}\text{O}_{\text{VPDB}}$ (‰)	$\delta^{18}\text{O}_{\text{VSMOW}}$ (‰)	Calculated Temperatures (°C)
z	9.8	-0.67	-3.35	+27.5	23.8
aa	10.1	+0.17	-2.52	+28.3	19.7
ab	10.3	+0.09	-2.48	+28.4	19.6
ac	10.6	-0.36	-3.13	+27.7	22.7
ad	11.1	-0.24	-1.92	+28.9	16.8
ae	11.4	-0.09	-2.46	+28.4	19.5
af	11.7	0.00	-2.85	+28.0	21.4
ag	12.0	-0.36	-3.06	+27.8	22.4
ah	12.2	+0.64	-2.86	+28.0	21.4
ai	12.7	-0.04	-3.61	+27.2	25.1
aj	13.0	+1.00	-2.74	+28.1	20.9
ak	13.4	+0.96	-2.90	+27.9	21.6
al	13.7	+0.32	-3.33	+27.5	23.7
am	14.1	+0.05	-3.37	+27.4	23.9
an	14.6	-0.03	-3.74	+27.1	25.7
ao	14.8	-0.39	-2.57	+28.3	20.0
ap	15.2	+0.34	-2.53	+28.3	19.8
aq	15.7	-0.29	-2.68	+28.2	20.5
ar	16.3	+0.52	-3.02	+27.8	22.2
as	17.5	-0.12	-1.90	+29.0	16.7

**Table 5.2.** Subsamples collected from Unit E of the Ironshore Formation, coral GTH-E.

Distance measured from the base of the coral upwards. Calculated temperatures are determined from the geothermometer of Booker et al. (2019),  $\delta^{18}\text{O}_{\text{water}}$  value of  $-0.4\text{‰}$ .

GTH-E	Distance (cm)	$\delta^{13}\text{C}_{\text{VPDB}}$ (‰)	$\delta^{18}\text{O}_{\text{VPDB}}$ (‰)	$\delta^{18}\text{O}_{\text{VSMOW}}$ (‰)	Calculated Temperatures (°C)
a	0.4	-1.69	-2.45	+28.4	17.3
b	0.8	-0.73	-2.69	+28.1	18.4
c	1.1	-0.84	-2.85	+28.0	19.2
d	1.3	-0.95	-2.55	+28.3	17.8
e	1.6	-1.25	-2.99	+27.8	19.9
f	1.8	-0.82	-3.13	+27.7	20.6
g	2.1	-0.45	-2.82	+28.0	19.1
h	2.4	-1.56	-3.48	+27.3	22.3
i	2.7	-0.62	-2.83	+28.0	19.1
j	2.9	-1.03	-3.40	+27.4	21.9
k	3.1	-0.20	-2.64	+28.2	18.2
l	3.3	-1.09	-2.85	+28.0	19.2
m	3.5	-1.06	-3.36	+27.4	21.7
n	3.7	-1.24	-2.80	+28.0	19.0
o	3.9	-1.55	-3.28	+27.5	21.3
p	4.1	-1.18	-2.57	+28.3	17.8
q	4.3	-1.25	-2.09	+28.8	15.5
r	4.5	-1.58	-2.72	+28.1	18.6
s	4.8	-0.80	-2.56	+28.3	17.8
t	5.0	-0.78	-2.09	+28.8	15.5
u	5.2	-1.57	-2.82	+28.0	19.1
v	5.4	-0.83	-2.57	+28.3	17.9



GTH-E	Distance (cm)	$\delta^{13}\text{C}_{\text{VPDB}}$ (‰)	$\delta^{18}\text{O}_{\text{VPDB}}$ (‰)	$\delta^{18}\text{O}_{\text{VSMOW}}$ (‰)	Calculated Temperatures (°C)
w	5.6	-1.01	-3.56	+27.2	22.7
x	5.8	-0.44	-2.22	+28.6	16.1
y	6.1	-0.88	-2.91	+27.9	19.5
z	6.3	-0.35	-2.33	+28.5	16.7
aa	6.5	-1.01	-2.61	+28.2	18.0
ab	6.7	-1.23	-2.70	+28.1	18.5
ac	6.9	-0.50	-2.20	+28.6	16.0
ad	7.1	-0.50	-2.16	+28.7	15.9
ae	7.3	-0.99	-2.55	+28.3	17.7
af	7.6	-0.22	-2.57	+28.3	17.9
ag	7.8	-0.68	-2.67	+28.2	18.3
ah	8.0	-0.42	-2.27	+28.6	16.4
ai	8.2	-1.27	-2.08	+28.8	15.4
aj	8.3	-1.23	-1.93	+28.9	14.7
ak	8.5	-0.93	-1.97	+28.9	14.9
al	8.8	-1.57	-2.82	+28.0	19.1
am	9.0	-1.88	-2.58	+28.3	17.9
an	9.2	-1.82	-2.57	+28.3	17.9
ao	9.4	-0.42	-2.37	+28.5	16.9
ap	9.6	-0.61	-2.01	+28.8	15.1
aq	9.8	-1.34	-2.68	+28.1	18.4
ar	10.1	-1.29	-3.09	+27.7	20.4
as	10.4	-0.45	-1.98	+28.9	15.0
at	10.7	-0.59	-3.07	+27.7	20.3
au	10.9	-0.13	-2.22	+28.6	16.1

GTH-E	Distance (cm)	$\delta^{13}\text{C}_{\text{VPDB}}$ (‰)	$\delta^{18}\text{O}_{\text{VPDB}}$ (‰)	$\delta^{18}\text{O}_{\text{VSMOW}}$ (‰)	Calculated Temperatures (°C)
av	11.2	+0.09	-2.45	+28.4	17.3
aw	11.4	-0.56	-2.79	+28.0	18.9
ax	11.6	+0.10	-1.99	+28.9	15.0
ay	11.8	-0.45	-2.43	+28.4	17.2
az	12.1	-0.59	-2.65	+28.2	18.2
ba	12.4	-0.85	-2.14	+28.7	15.7
bb	12.6	-0.66	-2.24	+28.6	16.2
bc	12.8	+0.03	-1.73	+29.1	13.7
bd	13.1	-0.02	-2.11	+28.7	15.6
be	13.3	-0.03	-2.45	+28.4	17.2
bf	13.6	-0.77	-2.32	+28.5	16.6
bg	13.8	-0.61	-2.24	+28.6	16.2
bh	14.0	-0.64	-2.15	+28.7	15.8
bi	14.3	-1.12	-2.39	+28.4	17.0
bj	14.5	-0.58	-2.37	+28.5	16.9
bk	14.7	+0.16	-2.31	+28.5	16.6
bl	14.9	-0.67	-2.85	+28.0	19.3
bm	15.1	-0.43	-2.81	+28.0	19.1
bn	15.3	-0.53	-2.69	+28.1	18.4
bo	15.5	-0.47	-2.47	+28.4	17.4
bp	15.6	-0.35	-2.36	+28.5	16.8
bq	15.8	-1.44	-2.26	+28.6	16.4
br	16.1	-1.18	-2.54	+28.3	17.7
bs	16.4	-0.40	-2.27	+28.6	16.4
bt	16.6	-0.14	-2.38	+28.5	16.9

GTH-E	Distance (cm)	$\delta^{13}\text{C}_{\text{VPDB}}$ (‰)	$\delta^{18}\text{O}_{\text{VPDB}}$ (‰)	$\delta^{18}\text{O}_{\text{VSMOW}}$ (‰)	Calculated Temperatures (°C)
bu	16.8	-0.64	-2.35	+28.5	16.8
bv	17.1	-0.52	-2.49	+28.3	17.4
bw	17.3	-0.03	-1.93	+28.9	14.7
bx	17.6	-1.00	-2.36	+28.5	16.8
by	18.0	-0.36	-2.27	+28.6	16.4
bz	18.3	-0.63	-2.44	+28.4	17.2
ca	18.7	-0.93	-2.68	+28.1	18.4
cb	19.0	-0.58	-2.30	+28.5	16.5
cc	19.3	-0.62	-2.51	+28.3	17.6
cd	19.6	-0.84	-2.09	+28.8	15.5
ce	20.3	-1.03	-2.62	+28.2	18.1
cf	20.5	-0.33	-2.59	+28.2	18.0
cg	20.7	-0.36	-2.23	+28.6	16.2
ch	20.9	-0.53	-2.74	+28.1	18.7
ci	21.2	-0.56	-2.47	+28.4	17.3
cj	21.4	+0.15	-2.17	+28.7	15.9

**Table 5.3.** Subsamples collected from Unit F of the Ironshore Formation, coral GTH-F.

Distance measured from the base of the coral upwards. Calculated temperatures are determined from the geothermometer of Booker et al. (2019),  $\delta^{18}\text{O}_{\text{water}}$  value of +0.9‰.

GTH-F	Distance (cm)	$\delta^{13}\text{C}_{\text{VPDB}}$ (‰)	$\delta^{18}\text{O}_{\text{VPDB}}$ (‰)	$\delta^{18}\text{O}_{\text{VSMOW}}$ (‰)	Calculated Temperatures (°C)
a	1.5	+0.36	-2.74	+28.1	24.7
b	1.7	+0.24	-3.07	+27.7	26.3
c	2.1	+0.18	-3.13	+27.7	26.6
d	2.5	-0.52	-3.32	+27.5	27.5
e	2.7	+0.24	-1.79	+29.1	20.0
f	2.9	-0.91	-3.30	+27.5	27.4
g	3.1	-0.14	-2.81	+28.0	25.0
h	3.3	+0.22	-3.24	+27.6	27.1
i	3.7	+0.12	-2.90	+27.9	25.5
j	4.0	-0.27	-3.06	+27.8	26.2
k	4.3	-0.92	-3.16	+27.6	26.8
l	4.6	-0.20	-2.91	+27.9	25.5
m	5.0	-0.61	-3.46	+27.3	28.2
n	5.4	+0.31	-2.83	+28.0	25.1
o	5.6	-1.16	-3.01	+27.8	26.0
p	5.9	+0.31	-2.42	+28.4	23.1
q	6.2	-0.02	-2.68	+28.1	24.4
r	6.5	-0.68	-2.83	+28.0	25.1
S	6.9	-0.71	-2.42	+28.4	23.1
t	7.2	-0.69	-2.58	+28.3	23.9
u	7.4	-0.37	-2.16	+28.7	21.8

GTH-F	Distance (cm)	$\delta^{13}\text{C}_{\text{VPDB}}$ (‰)	$\delta^{18}\text{O}_{\text{VPDB}}$ (‰)	$\delta^{18}\text{O}_{\text{VSMOW}}$ (‰)	Calculated Temperatures ( $^{\circ}\text{C}$ )
v	7.7	-0.46	-2.81	+28.0	25.0
w	7.9	-0.37	-2.30	+28.5	22.6
x	8.4	-0.90	-2.94	+27.9	25.7
y	9.0	-0.67	-3.21	+27.6	27.0
z	9.4	-0.32	-2.98	+27.8	25.8
aa	9.7	-0.15	-2.68	+28.1	24.4
ab	10.0	-0.54	-3.56	+27.2	28.7
ac	10.3	-0.14	-2.93	+27.9	25.6
ad	10.5	-0.57	-3.10	+27.7	26.5
ae	10.7	-1.29	-3.61	+27.2	29.0
af	11.1	+0.02	-3.73	+27.1	29.5
ag	11.3	-1.53	-3.30	+27.5	27.5
ah	11.5	+0.07	-2.00	+28.8	21.1
ai	11.7	-1.73	-3.13	+27.7	26.6
aj	12.0	-1.59	-2.99	+27.8	25.9
ak	12.3	-0.20	-2.62	+28.2	24.1
al	12.7	+0.25	-2.39	+28.4	23.0
am	13.0	-0.72	-2.62	+28.2	24.1
an	13.2	+0.27	-2.63	+28.2	24.2
ao	13.4	-0.72	-3.56	+27.2	28.7
ap	13.7	+0.45	-2.53	+28.3	23.7
aq	14.0	-0.44	-3.36	+27.4	27.7
ar	14.1	-0.74	-2.53	+28.3	23.6
as	14.4	-0.74	-2.71	+28.1	24.5
at	14.8	+0.18	-2.83	+28.0	25.2

GTH-F	Distance (cm)	$\delta^{13}\text{C}_{\text{VPDB}}$ (‰)	$\delta^{18}\text{O}_{\text{VPDB}}$ (‰)	$\delta^{18}\text{O}_{\text{VSMOW}}$ (‰)	Calculated Temperatures ( $^{\circ}\text{C}$ )
au	15.3	+0.23	-2.47	+28.4	23.4
av	15.5	-0.23	-2.64	+28.2	24.2
aw	15.7	-0.14	-2.58	+28.3	23.9
ax	16.0	+0.36	-2.77	+28.1	24.8
ay	16.3	-0.71	-2.95	+27.9	25.7
az	16.5	-0.01	-2.89	+27.9	25.4
ba	16.8	-0.34	-2.60	+28.2	24.0
bb	17.1	-0.63	-2.40	+28.4	23.0
bc	17.3	-1.05	-2.66	+28.2	24.3
bd	17.5	+0.25	-2.72	+28.1	24.6
be	17.7	-0.77	-2.57	+28.3	23.8
bf	18.0	+0.20	-2.58	+28.2	23.9
bg	18.3	-0.54	-2.56	+28.3	23.8
bh	18.6	+0.35	-2.46	+28.4	23.3
bi	18.8	-1.03	-3.06	+27.8	26.2
bj	19.0	+0.16	-2.72	+28.1	24.6
bk	19.2	-0.08	-2.52	+28.3	23.6
bl	19.6	-0.19	-2.50	+28.3	23.5
bm	19.9	-0.36	-2.74	+28.1	24.7
bn	20.2	-0.98	-2.66	+28.2	24.3
bo	20.5	-0.44	-2.66	+28.2	24.3
bp	20.7	+0.31	-2.47	+28.4	23.4
bq	21.0	-0.08	-2.44	+28.4	23.2
br	21.5	+0.02	-2.83	+28.0	25.2
bs	21.8	+0.21	-2.36	+28.5	22.8

GTH-F	Distance (cm)	$\delta^{13}\text{C}_{\text{VPDB}}$ (‰)	$\delta^{18}\text{O}_{\text{VPDB}}$ (‰)	$\delta^{18}\text{O}_{\text{VSMOW}}$ (‰)	Calculated Temperatures ( $^{\circ}\text{C}$ )
bt	22.0	-0.95	-2.93	+27.9	25.6
bu	22.3	+0.47	-2.79	+28.0	24.9
bv	22.5	-0.89	-2.89	+27.9	25.4
bw	22.8	-0.65	-2.72	+28.1	24.6
bx	23.2	+0.28	-2.70	+28.1	24.5
by	23.5	-0.50	-2.51	+28.3	23.6
bz	23.8	-0.53	-2.46	+28.4	23.3
ca	24.0	+0.21	-2.30	+28.5	22.5
cb	24.2	-0.55	-2.59	+28.2	24.0
cc	24.5	+0.03	-2.26	+28.6	22.3
cd	24.7	+0.42	-2.67	+28.2	24.3
ce	25.0	-0.45	-2.43	+28.4	23.2
cf	25.7	+0.12	-2.80	+28.0	25.0
cg	25.5	-0.24	-2.69	+28.1	24.4
ch	25.7	-0.24	-3.12	+27.7	26.6
ci	25.9	-0.27	-2.55	+28.3	23.7
cj	26.1	+0.62	-2.62	+28.2	24.1
ck	26.2	-0.74	-2.94	+27.9	25.7
cl	26.3	+0.03	-2.26	+28.6	22.3
cm	26.4	-1.13	-3.04	+27.8	26.2
cn	26.5	-0.21	-2.61	+28.2	24.0
co	26.7	-0.71	-2.88	+27.9	25.4
cp	27.0	-1.08	-2.80	+28.0	25.0
cq	27.4	-0.03	-2.63	+28.2	24.1

GTH-F	Distance (cm)	$\delta^{13}\text{C}_{\text{VPDB}}$ (‰)	$\delta^{18}\text{O}_{\text{VPDB}}$ (‰)	$\delta^{18}\text{O}_{\text{VSMOW}}$ (‰)	Calculated Temperatures ( $^{\circ}\text{C}$ )
cr	27.6	+0.21	-2.51	+28.3	23.5
cs	28.0	-0.60	-2.69	+28.1	24.4
ct	28.5	+0.15	-2.98	+27.8	25.9
cu	28.6	+0.42	-2.76	+28.1	24.8
cv	28.8	-0.20	-2.79	+28.0	24.9
cw	29.1	-0.35	-2.57	+28.3	23.8
cx	29.3	+0.37	-2.86	+28.0	25.3
cy	29.5	+0.07	-3.10	+27.7	26.5
cz	29.7	-0.52	-3.01	+27.8	26.0
da	29.8	-0.23	-2.76	+28.1	24.8
db	30.1	+0.14	-2.72	+28.1	24.6
dc	30.6	-0.19	-2.54	+28.3	23.7
dd	31.1	+0.05	-2.57	+28.3	23.9
de	31.4	+0.50	-3.01	+27.8	26.0
df	31.6	-1.08	-3.13	+27.7	26.6
dg	31.8	-0.05	-2.64	+28.2	24.2
dh	32.1	+0.08	-2.65	+28.2	24.2
di	32.3	+0.02	-2.64	+28.2	24.2
dj	32.6	+0.33	-2.74	+28.1	24.7
dk	32.9	-0.24	-2.64	+28.2	24.2
dl	33.1	-0.10	-3.19	+27.6	26.9
dm	33.5	-0.37	-2.64	+28.2	24.2
dn	33.6	+0.12	-2.55	+28.3	23.8
do	33.8	+0.20	-2.62	+28.2	24.1
dp	34.3	+0.31	-2.76	+28.1	24.8



GTH-F	Distance (cm)	$\delta^{13}\text{C}_{\text{VPDB}}$ (‰)	$\delta^{18}\text{O}_{\text{VPDB}}$ (‰)	$\delta^{18}\text{O}_{\text{VSMOW}}$ (‰)	Calculated Temperatures ( $^{\circ}\text{C}$ )
dq	34.9	-0.04	-2.97	+27.9	25.8
dr	35.5	-0.02	-2.92	+27.9	25.6
ds	36.0	+0.50	-2.92	+27.9	25.6
dt	36.4	-0.09	-3.18	+27.6	26.9
du	36.8	+0.23	-2.82	+28.0	25.1
dv	37.1	+0.09	-2.98	+27.8	25.9
dw	37.3	+0.44	-3.24	+27.6	27.1
dx	37.5	+0.07	-3.03	+27.8	26.1
dy	37.7	+0.69	-3.15	+27.7	26.7
dz	37.9	-0.66	-3.23	+27.6	27.1
ea	38.1	+0.61	-3.28	+27.5	27.4
eb	38.4	+0.65	-2.75	+28.1	24.8
ec	38.6	-0.21	-3.06	+27.8	26.2
ed	38.9	+0.16	-2.71	+28.1	24.5
ee	39.4	+0.06	-2.86	+28.0	25.3
ef	39.8	-0.95	-2.84	+28.0	25.2
eg	40.2	-0.62	-3.38	+27.4	27.8
eh	40.4	-0.18	-3.02	+27.8	26.0
ei	40.7	-0.16	-3.04	+27.8	26.1
ej	41.2	-0.57	-3.29	+27.5	27.4
ek	41.6	+0.02	-3.20	+27.6	26.9
el	42.0	-0.23	-3.08	+27.7	26.3
em	42.3	+0.18	-3.29	+27.5	27.4
en	42.6	-0.73	-3.41	+27.4	28.0

GTH-F	Distance (cm)	$\delta^{13}\text{C}_{\text{VPDB}}$ (‰)	$\delta^{18}\text{O}_{\text{VPDB}}$ (‰)	$\delta^{18}\text{O}_{\text{VSMOW}}$ (‰)	Calculated Temperatures ( $^{\circ}\text{C}$ )
eo	42.8	+0.18	-2.59	+28.2	23.9
ep	43.0	-0.05	-3.03	+27.8	26.1
eq	43.2	-0.06	-2.62	+28.2	24.1
er	43.4	-0.16	-2.52	+28.3	23.6
es	43.7	-0.19	-2.56	+28.3	23.8
et	44.2	-0.33	-2.52	+28.3	23.6
eu	44.6	+0.05	-2.56	+28.3	23.8
ev	44.9	-0.25	-2.53	+28.3	23.7
ew	45.2	-0.24	-2.56	+28.3	23.8
ex	45.5	+0.23	-2.49	+28.3	23.5
ey	45.7	-0.48	-2.71	+28.1	24.5
ez	46.1	-0.37	-2.38	+28.5	22.9
fa	46.4	+0.09	-2.31	+28.5	22.6
fb	46.7	-0.20	-2.27	+28.6	22.4
fc	47.1	-0.28	-2.21	+28.6	22.1
fd	47.4	-0.28	-2.42	+28.4	23.1
fe	48.5	-0.40	-2.42	+28.4	23.1
ff	48.7	-0.41	-2.35	+28.5	22.8
fg	49.3	-0.39	-2.29	+28.5	22.5
fh	49.6	-0.59	-1.96	+28.9	20.9
fi	49.9	-0.36	-2.28	+28.6	22.5
fj	50.1	-0.44	-2.28	+28.6	22.4